NASA Reference Publication 1050

Classical Aerodynamic Theory

DECEMBER 1979

NASA

NASA Reference Publication 1050

Classical Aerodynamic Theory

Compiled by R. T. Jones
Ames Research Center
Moffett Field, California

National Aeronautics
and Space Administration

**Scientific and Technical
Information Branch**

1979

Page intentionally left blank

PREFACE

Aerodynamic theory was not prepared to offer assistance in the early development of the airplane. The scientific community, most qualified for action at the forefront of human endeavor, often turns out in practice to be surprisingly conservative. It is recorded that Lord Rayleigh expressed "not the smallest molecule of faith in aerial navigation, except by balloon." It was not until experiments such as those of Lilienthal and Langley and the successful powered flights of the Wright brothers that correct theories for the aerodynamic action of wings were developed.

Following the successful demonstrations of the Wright brothers, aerodynamic theory developed rapidly, primarily in European laboratories. These developments we associate with the names Joukowsky, Kutta, Prandtl and his students, Munk, Betz, and Von Karman. It should not be forgotten that the writings of F. W. Lanchester provide many of the physical insights that were elaborated in these mathematical theories.

Throughout World War I, these developments in aerodynamic theory remained virtually unknown in the U.S. However, in the early 1920's, the U.S. National Advisory Committee for Aeronautics undertook to translate or otherwise make available important works on aerodynamic theory in the form of NACA Technical Reports, Notes, and Memoranda, and to encourage similar effort in its own laboratory.

At the present time, many of these old NACA documents are no longer readily available and it seems worthwhile to collect the most important early works under the title "Classical Aerodynamics." In most cases, the theories are explained in the author's own words and often with a degree of clarity unequalled in later interpretations.

R. T. Jones
Senior Staff Scientist
NASA-Ames Research Center
June 18, 1979

Page intentionally left blank

TABLE OF CONTENTS

		Page
PREFACE		iii
TR 116	APPLICATIONS OF MODERN HYDRODYNAMICS TO AERONAUTICS *L. Prandtl*	1
	THE MECHANISM OF FLUID RESISTANCE *Th. v. Kármán and H. Rubach*	57
TM 336	PRESSURE DISTRIBUTION ON JOUKOWSKI WINGS *Otto Blumenthal*	67
	GRAPHIC CONSTRUCTION OF JOUKOWSKI WINGS *E. Trefftz*	84
TR 121	THE MINIMUM INDUCED DRAG OF AEROFOILS *Max M. Munk*	95
TR 184	THE AERODYNAMIC FORCES ON AIRSHIP HULLS *Max M. Munk*	111
TR 191	ELEMENTS OF THE WING SECTION THEORY AND OF THE WING THEORY *Max M. Munk*	127
TN 196	REMARKS ON THE PRESSURE DISTRIBUTION OVER THE SURFACE OF AN ELLIPSOID, MOVING TRANSLATIONALLY THROUGH A PERFECT FLUID *Max M. Munk*	151
TR 164	THE INERTIA COEFFICIENTS OF AN AIRSHIP IN A FRICTIONLESS FLUID *H. Bateman*	161
TR 253	FLOW AND DRAG FORMULAS FOR SIMPLE QUADRICS *A. F. Zahm*	175
TR 323	FLOW AND FORCE EQUATIONS FOR A BODY REVOLVING IN A FLUID *A. F. Zahm*	197
TM 713	BEHAVIOR OF VORTEX SYSTEMS *A. Betz*	237

Page

TR 452 GENERAL POTENTIAL THEORY OF ARBITRARY WING SECTIONS 257
T. Theodorsen and I. E. Garrick

TR 496 GENERAL THEORY OF AERODYNAMIC INSTABILITY AND THE MECHANISM OF FLUTTER 291
Theodore Theodorsen

REPORT No. 116.

APPLICATIONS OF MODERN HYDRODYNAMICS TO AERONAUTICS.

By L. PRANDTL.

PART I.

FUNDAMENTAL CONCEPTS AND THE MOST IMPORTANT THEOREMS.

1. All actual fluids show internal friction (viscosity), yet the forces due to viscosity, with the dimensions and velocities ordinarily occurring in practice, are so very small in comparison with the forces due to inertia, for water as well as for air, that we seem justified, as a first approximation, in entirely neglecting viscosity. Since the consideration of viscosity in the mathematical treatment of the problem introduces difficulties which have so far been overcome only in a few specially simple cases, we are forced to neglect entirely internal friction unless we wish to do without the mathematical treatment.

We must now ask how far this is allowable for actual fluids, and how far not. A closer examination shows us that for the interior of the fluid we can immediately apply our knowledge of the motion of a nonviscous fluid, but that care must be taken in considering the layers of the fluid in the immediate neighborhood of solid bodies. Friction between fluid and solid body never comes into consideration in the fields of application to be treated here, because it is established by reliable experiments that fluids like water and air never slide on the surface of the body; what happens is, the final fluid layer immediately in contact with the body is attached to it (is at rest relative to it), and all the friction of fluids with solid bodies is therefore an internal friction of the fluid. Theory and experiment agree in indicating that the transition from the velocity of the body to that of the stream in such a case takes place in a thin layer of the fluid, which is so much the thinner, the less the viscosity. In this layer, which we call the boundary layer, the forces due to viscosity are of the same order of magnitude as the forces due to inertia, as may be seen without difficulty.[1] It is therefore important to prove that, however small the viscosity is, there are always in a boundary layer on the surface of the body forces due to viscosity (reckoned per unit volume) which are of the same order of magnitude as those due to inertia. Closer investigation concerning this shows that under certain conditions there may occur a reversal of flow in the boundary layer, and as a consequence a stopping of the fluid in the layer which is set in rotation by the viscous forces, so that, further on, the whole flow is changed owing to the formation of vortices. The analysis of the phenomena which lead to the formation of vortices shows that it takes place where the fluid experiences a retardation of flow along the body. The retardation in some cases must reach a certain finite amount so that a reverse flow arises. Such retardation of flow occurs regularly in the rear of blunt bodies; therefore vortices are formed there very soon after the flow begins, and consequently the results which are furnished by the theory of nonviscous flow can not be applied. On the other hand, in the rear of very tapering bodies the retardations are often so small that there is no noticeable formation of vortices. The principal successful results of hydrodynamics apply to this case. Since it is these tapering bodies which offer specially small resistance and which, therefore, have found special consideration in aeronautics under similar applications, the theory can be made useful exactly for those bodies which are of most technical interest.

[1] From this consideration one can calculate the approximate thickness of the boundary layer for each special case.

20167—23——11

For the considerations which follow we obtain from what has gone before the result that in the interior of the fluid its viscosity, if it is small, has no essential influence, but that for layers of the fluid in immediate contact with solid bodies exceptions to the laws of a nonviscous fluid must be allowable. We shall try to formulate these exceptions so as to be, as far as possible, in agreement with the facts of experiment.

2. A further remark must be made concerning the effect of the compressibility of the fluid upon the character of the flow in the case of the motion of solid bodies in the fluid. All actual fluids are compressible. In order to compress a volume of air by 1 per cent, a pressure of about one one-hundredth of an atmosphere is needed. In the case of water, to produce an equal change in volume, a pressure of 200 atmospheres is required; the difference therefore is very great. With water it is nearly always allowable to neglect the changes in volume arising from the pressure differences due to the motions, and therefore to treat it as absolutely incompressible. But also in the case of motions in air we can ignore the compressibility so long as the pressure differences caused by the motion are sufficiently small. Consideration of compressibility in the mathematical treatment of flow phenomena introduces such great difficulties that we will quietly neglect volume changes of several per cent, and in the calculations air will be looked upon as incompressible. A compression of 3 per cent, for instance, occurs in front of a body which is being moved with a velocity of about 80 m./sec. It is seen, then, that it appears allowable to neglect the compressibility in the ordinary applications to technical aeronautics. Only with the blades of the air screw do essentially greater velocities occur, and in this case the influence of the compressibility is to be expected and has already been observed. The motion of a body with great velocity has been investigated up to the present, only along general lines. It appears that if the velocity of motion exceeds that of sound for the fluid, the phenomena are changed entirely, but that up close to this velocity the flow is approximately of the same character as in an incompressible fluid.

3. We shall concern ourselves in what follows only with a nonviscous and incompressible fluid, about which we have learned that it will furnish an approximation sufficient for our applications, with the reservations made. Such a fluid is also called "the ideal fluid."

What are the properties of such an ideal fluid? I do not consider it here my task to develop and to prove all of them, since the theorems of classical hydrodynamics are contained in all textbooks on the subject and may be studied there. I propose to state in what follows, for the benefit of those readers who have not yet studied hydrodynamics, the most important principles and theorems which will be needed for further developments, in such a manner that these developments may be grasped. I ask these readers, therefore, simply to believe the theorems which I shall state until they have the time to study the subject in some textbook on hydrodynamics.

The principal method of description of problems in hydrodynamics consists in expressing in formulas as functions of space and time the velocity of flow, given by its three rectangular components, u, v, w, and in addition the fluid pressure p. The condition of flow is evidently completely known if u, v, w, and p are given as functions of x, y, z, and t, since then u, v, w, and p can be calculated for any arbitrarily selected point and for every instant of time. The direction of flow is defined by the ratios of u, v, and w; the magnitude of the velocity is $\sqrt{u^2+v^2+w^2}$. The "streamlines" will be obtained if lines are drawn which coincide with the direction of flow at all points where they touch, which can be accomplished mathematically by an integration. If the flow described by the formulas is to be that caused by a definite body, then at those points in space, which at any instant form the surface of the body, the components of the fluid velocity normal to this surface must coincide with the corresponding components of the velocity of the body. In this way the condition is expressed that neither does the fluid penetrate into the body nor is there any gap between it and the fluid. If the body is at rest in a stream, the normal components of the velocity at its surface must be zero; that is, the flow must be tangential to the surface, which in this case therefore is formed of stream lines.

4. In a stationary flow—that is, in a flow which does not change with the time, in which then every new fluid particle, when it replaces another particle in front of it, assumes its velocity, both in magnitude and in direction and also the same pressure—there is, for the fluid particles lying on the same stream line, a very remarkable relation between the magnitude of the velocity, designated here by V, and the pressure, the so-called Bernouilli equation—

$$p+\frac{\rho}{2}V^2=\text{const.} \tag{1}$$

(ρ is the density of the fluid, i. e., the mass of a unit volume). This relation is at once applicable to the case of a body moving uniformly and in a straight line in a fluid at rest, for we are always at liberty to use for our discussions any reference system having a uniform motion in a straight line. If we make the velocity of the reference system coincide with that of the body, then the body is at rest with reference to it, and the flow around it is stationary. If now V is the velocity of the body relative to the stationary air, the latter will have in the new reference system the velocity V upon the body (a man on an airplane in flight makes observations in terms of such a reference system, and feels the motion of flight as "wind").

The flow of incident air is divided at a blunt body, as shown in figure 1. At the point A the flow comes completely to rest, and then is again set in motion in opposite directions, tangential to the surface of the body. We learn from equation (1) that at such a point, which we shall call a "rest-point," the pressure must be greater by $\frac{\rho}{2}V^2$ than in the undisturbed fluid. We shall call the magnitude of this pressure, of which we shall make frequent use, the "dynamical pressure," and shall designate it by q. An open end of a tube facing the stream produces a rest point of a similar kind, and there arises in the interior of the tube, as very careful experiments have shown, the exact dynamical pressure, so that this principle can be used for the measurement of the velocity, and is in fact much used. The dynamical pressure is also well suited to express the laws of air resistance. It is known that this resistance is proportional to the square of the velocity and to the density of the medium; but $q=\frac{\rho}{2}V^2$; so the law of air resistance may also be expressed by the formula

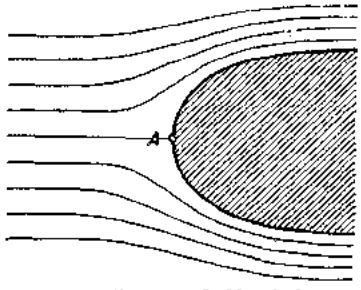

FIG. 1.—Flow around a blunt body.

$$W=c\,.\,F\,.\,q \tag{2}$$

where F is the area of the surface and c is a pure number. With this mode of expression it appears very clearly that the force called the "drag" is equal to surface times pressure difference (the formula has the same form as the one for the piston force in a steam engine). This mode of stating the relation has been introduced in Germany and Austria and has proved useful. The air-resistance coefficients then become twice as large as the "absolute" coefficients previously used.

Since V^2 can not become less than zero, an increase of pressure greater than q can not, by equation (1), occur. For diminution of pressure, however, no definite limit can be set. In the case of flow past convex surfaces marked increases of velocity of flow occur and in connection with them diminutions of pressure which frequently amount to $3q$ and more.

5. A series of typical properties of motion of nonviscous fluids may be deduced in a useful manner from the following theorem, which is due to Lord Kelvin. Before the theorem itself is stated, two concepts must be defined. 1. The circulation: Consider the line integral of the velocity $\int V\cos(V, ds)\,.\,ds$, which is formed exactly like the line integral of a force, which is called "the work of the force." The amount of this line integral, taken over a path which returns on itself is called the circulation of the flow. 2. The fluid line: By this is meant a line which is always formed of the same fluid particles, which therefore shares in the motion of the

fluid. The theorem of Lord Kelvin is: In a nonviscous fluid the circulation along every fluid line remains unchanged as time goes on. But the following must be added:

(1) The case may arise that a fluid line is intersected by a solid body moving in the fluid. If this occurs, the theorem ceases to apply. As an example I mention the case in which one pushes a flat plate into a fluid at rest, and then by means of the plate exerts a pressure on the fluid. By this a circulation arises which will remain if afterwards the plate is quickly withdrawn in its own plane. See figure 2.

(2) In order that the theorem may apply, we must exclude mass forces of such a character that work is furnished by them along a path which returns on itself. Such forces do not ordinarily arise and need not be taken into account here, where we are concerned regularly only with gravity.

(3) The fluid must be homogeneous, i. e., of the same density at all points. We can easily see that in the case of nonuniform density circulation can arise of itself in the course of time if we think of the natural ascent of heated air in the midst of cold air. The circulation increases continuously along a line which passes upward in the warm air and returns downward in the cold air.

Frequently the case arises that the fluid at the beginning is at rest or in absolutely uniform motion, so that the circulation for every imaginable closed line in the fluid is zero. Our theorem then says that for every closed line that can arise from one of the originally closed lines the circulation remains zero, in which we must make exception, as mentioned above, of those lines which are cut by bodies. If the line integral along every closed line is zero, the line integral for an open curve from a definite point O to an arbitrary point P is independent of the selection of the line along which the integral is taken (if this were not so, and if the integrals along two lines from O to P were different, it is evident that the line integral along the closed curve OPO would not be zero, which contradicts our premise). The line integral along the line OP depends, therefore, since we will consider once for all the point O as a fixed one, only on the coordinates of the point P, or, expressed differently, it is a function of these coordinates. From analogy with corresponding considerations in the case of fields of force, this line integral is called the "velocity potential," and the particular kind of motion in which such a potential exists is called a "potential motion." As follows immediately from the meaning of line integrals, the component of the velocity in a definite direction is the derivative of the potential in this direction. If the line-element is perpendicular to the resultant velocity, the increase of the potential equals zero, i. e., the surfaces of constant potential are everywhere normal to the velocity of flow. The velocity itself is called the gradient of the potential. The velocity components u, v, w are connected with the potential Φ by the following equations:

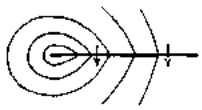

FIG. 2.—Production of circulation by introduction and withdrawal of flat plate.

$$u=\frac{\partial\phi}{\partial x},\quad v=\frac{\partial\phi}{\partial y},\quad w=\frac{\partial\phi}{\partial z} \tag{3}$$

The fact that the flow takes place without any change in volume is expressed by stating that as much flows out of every element of volume as flows in. This leads to the equation

$$\frac{\partial u}{\partial x}+\frac{\partial v}{\partial y}+\frac{\partial w}{\partial z}=0 \tag{4}$$

In the case of potential flow we therefore have

$$\frac{\partial^2\phi}{\partial x^2}+\frac{\partial^2\phi}{\partial y^2}+\frac{\partial^2\phi}{\partial z^2}=0 \tag{4a}$$

as the condition for flow without change in volume. All functions $\Phi(x, y, z, t)$, which satisfy this last equation, represent possible forms of flow. This representation of a flow is specially convenient for calculations, since by it the entire flow is given by means of the one function Φ. The most valuable property of the representations is, though, that the sum of two, or of as many as one desires, functions Φ, each of which satisfies equation (4a), also satisfies this equation, and therefore represents a possible type of flow ("superposition of flows").

6. Another concept can be derived from the circulation, which is convenient for many considerations, viz, that of rotation. The component of the rotation with reference to any axis is obtained if the circulation is taken around an elementary surface of unit area in a plane perpendicular to the axis. Expressed more exactly, such a rotation component is the ratio of the circulation around the edge of any such infinitesimal surface to the area of the surface. The total rotation is a vector and is obtained from the rotation components for three mutually perpendicular axes. In the case that the fluid rotates like a rigid body, the rotation thus defined comes out as twice the angular velocity of the rigid body. If we take a rectangular system of axes and consider the rotations with reference to the separate axes, we find that the rotation can also be expressed as the geometrical sum of the angular velocities with reference to the three axes.

The statement that in the case of a potential motion the circulation is zero for every closed fluid line can now be expressed by saying the rotation in it is always zero. The theorem that the circulation, if it is zero, remains zero under the conditions mentioned, can also now be expressed by saying that, if these conditions are satisfied in a fluid in which there is no rotation, rotation can never arise. An irrotational fluid motion, therefore, always remains irrotational. In this, however, the following exceptions are to be noted: If the fluid is divided owing to bodies being present in it, the theorem under consideration does not apply to the fluid layer in which the divided flow reunites, not only in the case of figure 2 but also in the case of stationary phenomena as in figure 3, since in this case a closed fluid line drawn in front of the body can not be transformed into a fluid line that intersects the region where the fluid streams come together. Figure 3 shows four successive shapes of such a fluid line. This region is, besides, filled with fluid particles which have come very close to the body. We are therefore led to the conclusion from the standpoint of a fluid with very small but not entirely vanishing viscosity that the appearance of vortices at the points of reunion of the flow in the rear of the body does not contradict the laws of hydrodynamics. The three components of the rotation ξ, η, ζ are expressed as follows by means of the velocity components u, v, w.

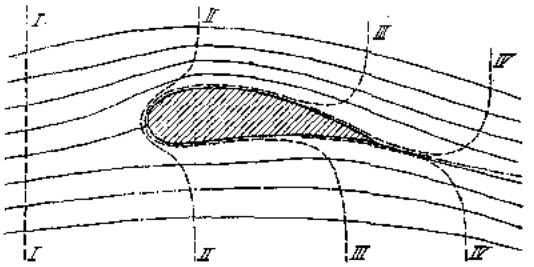

FIG. 3.—Successive positions of a fluid line in flow around a solid body.

$$\xi=\frac{\partial w}{\partial y}-\frac{\partial v}{\partial z},\ \eta=\frac{\partial u}{\partial z}-\frac{\partial w}{\partial x},\ \zeta=\frac{\partial v}{\partial x}-\frac{\partial u}{\partial y} \tag{5}$$

If the velocity components are derived from a potential, as shown in equation (2), the rotation components, according to equation (5) vanish identically, since $\frac{\partial^2\Phi}{\partial z\partial y}=\frac{\partial^2\Phi}{\partial y\partial z}$

7. Very remarkable theorems hold for the rotation, which were discovered by v. Helmholtz and stated in his famous work on vortex motions. Concerning the geometrical properties of the rotation the following must be said:

At all points of the fluid where rotation exists the direction of the resultant rotation axes can be indicated, and lines can also be drawn whose directions coincide everywhere with these axes, just as the stream lines are drawn so as to coincide with the directions of the velocity. These lines will be called, following Helmholtz, "vortex lines." The vortex lines through the points of a small closed curve form a tube called a "vortex tube." It is an immediate consequence of the geometrical idea of rotation as deduced above that through the entire extent of a vortex tube its strength—i. e., the circulation around the boundary of the tube—is constant. It is seen, in fact, that on geometrical grounds the space distribution of rotation quite independently of the special properties of the velocity field from which it is deduced is of the same nature as the space distribution of the velocities in an incompressible fluid. Consequently a vortex tube, just like a stream line in an incompressible fluid, can not end anywhere in the interior of the fluid; and the strength of the vortex, exactly like the quantity of fluid passing per second through the tube of stream lines, has at one and the same instant the same value

throughout the vortex tube. If Lord Kelvin's theorem is now applied to the closed fluid line which forms the edge of a small element of the surface of a vortex tube, the circulation along it is zero, since the surface inclosed is parallel to the rotation axis at that point. Since the circulation can not change with the time, it follows that the element of surface at all later times will also be part of the surface of a vortex tube. If we picture the entire bounding surface of a vortex tube as made up of such elementary surfaces, it is evident that, since as the motion continues this relation remains unchanged, the particles of the fluid which at any one time have formed the boundary of a vortex tube will continue to form its boundary. From the consideration of the circulation along a closed line inclosing the vortex tube, we see that this circulation—i. e., the strength of our vortex tube—has the same value at all times. Thus we have obtained the theorems of Helmholtz, which now can be expressed as follows, calling the contents of a vortex tube a "vortex filament": "The particles of a fluid which at any instant belong to a vortex filament always remain in it; the strength of a vortex filament throughout its extent and for all time has the same value." From this follows, among other things, that if a portion of the filament is stretched, say, to double its length, and thereby its cross section made one-half as great, then the rotation is doubled, because the strength of the vortex, the product of the rotation and the cross section, must remain the same. We arrive, therefore, at the result that the vector expressing the rotation is changed in magnitude and direction exactly as the distance between two neighboring particles on the axis of the filament is changed.

8. From the way the strengths of vortices have been defined it follows for a space filled with any arbitrary vortex filaments, as a consequence of a known theorem of Stokes, that the circulation around any closed line is equal to the algebraic sum of the vortex strengths of all the filaments which cross a surface having the closed line as its boundary. If this closed line is in any way continuously changed so that filaments are thereby cut, then evidently the circulation is changed according to the extent of the strengths of the vortices which are cut. Conversely we may conclude from the circumstance that the circulation around a closed line (which naturally can not be a fluid line) is changed by a definite amount by a certain displacement, that by the displacement vortex strength of this amount will be cut, or expressed differently, that the surface passed over by the closed line in its displacement is traversed by vortex filaments whose strengths add up algebraically to the amount of the change in the circulation.

The theorems concerning vortex motion are specially important because in many cases it is easier to make a statement as to the shape of the vortex filaments than as to the shape of the stream lines, and because there is a mode of calculation by means of which the velocity at any point of the space may be determined from a knowledge of the distribution of the rotation. This formula, so important for us, must now be discussed. If Γ is the strength of a thin vortex filament and ds an element of its medial line, and if, further, r is the distance from the vortex element to a point P at which the velocity is to be calculated, finally if α is the angle between ds and r, then the amount of the velocity due to the vortex element is

$$dv = \frac{\Gamma}{4\pi} \frac{ds \sin \alpha}{r^2}; \tag{6}$$

the direction of this contribution to the velocity is perpendicular to the plane of ds and r. The total velocity at the point P is obtained if the contributions of all the vortex elements present in the space are added. The law for this calculation agrees then exactly with that of Biot-Savart, by the help of which the magnetic field due to an electric current is calculated. Vortex filaments correspond in it to the electric currents, and the vector of the velocity to the vector of the magnetic field.

As an example we may take an infinitely long straight vortex filament. The contributions to the velocity at a point P are all in the same direction, and the total velocity can be determined by a simple integration of equation (6). Therefore this velocity is

$$v = \frac{\Gamma}{4\pi} \int_{-\infty}^{+\infty} \frac{ds \cdot \sin \alpha}{r^2}$$

As seen by figure 4, $s = h \operatorname{ctg} \alpha$, and by differentiation, $ds = -\frac{h}{\sin^2\alpha} d\alpha$. Further $r = \frac{h}{\sin \alpha}$; so that

$$v = \frac{\Gamma}{4\pi h}\int_0^{\pi} \sin \alpha d\alpha = -\frac{\Gamma}{4\pi h}[\cos \alpha]_0^{\pi} = \frac{\Gamma}{2\pi h} \tag{6a}$$

This result could be deduced in a simpler manner from the concept of circulation if we were to use the theorem, already proved, that the circulation for any closed line coincides with the vortex strength of the filaments which are inclosed by it. The circulation for every closed line which goes once around a single filament must therefore coincide with its strength. If the velocity at a point of a circle of radius h around our straight filament equals v then this circulation equals "path times velocity" $= 2\pi h \cdot v$, whence immediately follows $v = \frac{\Gamma}{2\pi h}$. The more exact investigation of this velocity field shows that for every point outside the filament (and the formula applies only to such points) the rotation is zero, so that in fact we are treating the case of a velocity distribution in which only along the axis does rotation prevail, at all other points rotation is not present.

For a finite portion of a straight vortex filament the preceding calculation gives the value

$$v = \frac{\Gamma}{4\pi h}(\cos \alpha_1 - \cos \alpha_2) \tag{6b}$$

This formula may be applied only for a series of portions of vortices which together give an infinite or a closed line. The velocity field of a single portion of a filament would require rotation also outside the filament, in the sense that from the end of the portion of the filament vortex lines spread out in all the space and then all return together at the beginning of the portion. In the case of a line that has no ends this external rotation is removed, since one end always coincides with the beginning of another portion of equal strength, and rotation is present only where it is predicated in the calculation.

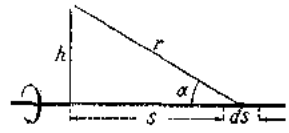

FIG. 4.—Velocity-field due to infinite rectilinear vortex.

9. If one wishes to represent the flow around solid bodies in a fluid, one can in many cases proceed by imagining the place of the solid bodies taken by the fluid, in the interior of which disturbances of flow (singularities) are introduced, by which the flow is so altered that the boundaries of the bodies become streamline surfaces. For such hypothetical constructions in the interior of the space actually occupied by the body, one can assume, for instance, any suitably selected vortices, which, however, since they are only imaginary, need not obey the laws of Helmholtz. As we shall see later, such imaginary vortices can be the seat of lifting forces. Sources and sinks also, i. e., points where fluid continuously appears, or disappears, offer a useful method for constructions of this kind. While vortex filaments can actually occur in the fluid, such sources and sinks may be assumed only in that part of the space which actually is occupied by the body, since they represent a phenomenon which can not be realized. A contradiction of the law of the conservation of matter is avoided, however, if there are assumed to be inside the body both sources and sinks, of equal strengths, so that the fluid produced by the sources is taken back again by the sinks.

The method of sources and sinks will be described in greater detail when certain practical problems are discussed; but at this point, to make the matter clearer, the distribution of velocities in the case of a source may be described. It is very simple, the flow takes place out from the source uniformly on all sides in the direction of the radii. Let us describe around the point source a concentric spherical surface, then, if the fluid output per second is Q, the velocity at the surface is

$$v = \frac{Q}{4\pi r^2}; \tag{7}$$

the velocity therefore decreases inversely proportional to the square of the distance. The flow is a potential one, the potential comes out (as line-integral along the radius)

$$\Phi = \text{const.} - \frac{Q}{4\pi r} \tag{7a}$$

If a uniform velocity toward the right of the whole fluid mass is superimposed on this velocity distribution—while the point source remains stationary—then a flow is obtained which, at a considerable distance from the source, is in straight lines from left to right. The fluid coming out of the source is therefore pressed toward the right (see fig. 5); it fills, at some distance from the source, a cylinder whose diameter may be determined easily. If V is the velocity of the uniform flow, the radius r of the cylinder is given by the condition $Q = \pi r^2 \cdot V$. All that is necessary now is to assume on the axis of the source further to the right a sink of the same strength as the source for the whole mass of fluid from the source to vanish in this, and the flow closes up behind the sink again exactly as it opened out in front of the source. In this way we obtain the flow around an elongated body with blunt ends.

10. The special case when in a fluid flow the phenomena in all planes which are parallel to a given plane coincide absolutely plays an important rôle both practically and theoretically. If the lines which connect the corresponding points of the different planes are perpendicular to the planes, and all the streamlines are plane curves which lie entirely in one of those planes, we speak of a uniplanar flow. The flow around a strut whose axis is perpendicular to the direction of the wind is an example of such a motion.

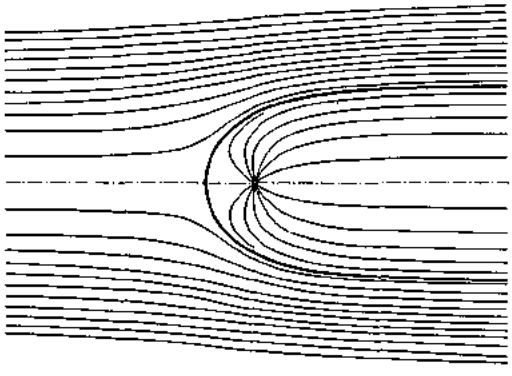

FIG. 5.—Superposition of uniform flow and that caused by a source.

The mathematical treatment of plane potential flow of the ideal fluid has been worked out specially completely more than any other problem in hydrodynamics. This is due to the fact that with the help of the complex quantities $(x+iy$, where $i=\sqrt{-1}$, is called the imaginary unit) there can be deduced from every analytic function a case of flow of this type which is incompressible and irrotational. Every real function, $\Phi(x, y)$ and $\Psi(x, y)$, which satisfies the relation

$$\Phi + i\Psi = f(x+iy), \tag{8}$$

where f is any analytic function, is the potential of such a flow. This can be seen from these considerations: Let $x+iy$ be put $=z$, where z is now a "complex number." Differentiate equation (8) first with reference to x and then with reference to y, thus giving

$$\frac{\partial \Phi}{\partial x} + i\frac{\partial \Psi}{\partial x} = \frac{df}{dz}\frac{\partial z}{\partial x} = \frac{df}{dz}$$

$$\frac{\partial \Phi}{\partial y} + i\frac{\partial \Psi}{\partial y} = \frac{df}{dz}\frac{\partial z}{\partial y} = i\frac{df}{dz} = i\frac{\partial \Phi}{\partial x} - \frac{\partial \Psi}{\partial y}$$

In these the real parts on the two sides of the equations must be equal and the imaginary parts also. If Φ is selected as the potential, the velocity components u and v are given by

$$u = \frac{\partial \Phi}{\partial x} = \frac{\partial \Psi}{\partial y}; \quad v = \frac{\partial \Phi}{\partial y} = -\frac{\partial \Psi}{\partial x} \tag{9}$$

If now we write the expressions $\frac{\partial u}{\partial x} + \frac{\partial v}{\partial y}$ (continuity) and $\frac{\partial v}{\partial x} - \frac{\partial u}{\partial y}$ (rotation) first in terms of Φ and then of Ψ, they become

$$\left.\begin{aligned} \frac{\partial u}{\partial x}+\frac{\partial v}{\partial y}&=\frac{\partial^2\Phi}{\partial x^2}+\frac{\partial^2\Phi}{\partial y^2}=\underbrace{\frac{\partial^2\Psi}{\partial y\partial x}-\frac{\partial^2\Psi}{\partial x\partial y}}_{=0}\\ \frac{\partial v}{\partial x}-\frac{\partial u}{\partial y}&=\underbrace{\frac{\partial^2\Phi}{\partial y\partial x}-\frac{\partial^2\Phi}{\partial x\partial y}}_{=0}=-\frac{\partial^2\Psi}{\partial x^2}-\frac{\partial^2\Psi}{\partial y^2} \end{aligned}\right\} \tag{10}$$

It is seen therefore that not only is the motion irrotational (as is self-evident since there is a potential), but it is also continuous. The relation $\frac{\partial^2\Phi}{\partial x^2}+\frac{\partial^2\Phi}{\partial y^2}=o$ besides corresponds exactly to our equation (4a). Since it is satisfied also by Ψ, this can also be used as potential.

The function Ψ, however, has, with reference to the flow deduced by using Φ as potential, a special individual meaning. From equation (8) we can easily deduce that the lines $\Psi=$ const. are parallel to the velocity; therefore, in other words, they are streamlines. In fact if we put

$$d\Psi=\frac{\partial\Psi}{\partial x}dx+\frac{\partial\Psi}{\partial y}dy=o, \text{ then } \frac{dy}{dx}=-\frac{\frac{\partial\Psi}{\partial x}}{\frac{\partial\Psi}{\partial y}}=\frac{v}{u}$$

which expresses the fact of parallelism. The lines $\Psi=$ const. are therefore perpendicular to the lines $\Phi=$ const. If we draw families of lines, $\Phi=$ const. and $\Psi=$ const. for values of Φ and Ψ which differ from each other by the same small amount, it follows from the easily derived equation $d\Phi+id\Psi=\frac{df}{dz}(dx+idy)$ that the two bundles form a square network; from which follows that the diagonal curves of the network again form an orthogonal and in fact a square network. This fact can be used practically in drawing such families of curves, because an error in the drawing can be recognized by the eye in the wrong shape of the network of diagonal curves and so can be improved. With a little practice fairly good accuracy may be obtained by simply using the eye. Naturally there are also mathematical methods for further improvement of such networks of curves. The function Ψ, which is called the "stream function," has another special meaning. If we consider two streamlines $\Psi=\Psi_1$ and $\Psi=\Psi_2$, the quantity of fluid which flows between the two streamlines in a unit of time in a region of uniplanar flow of thickness 1 equals $\Psi_2-\Psi_1$. In fact if we consider the flow through a plane perpendicular to the X-axis, this quantity is

$$Q=\int_{y_1}^{y_2}udy=\int_{y_1}^{y_2}\frac{\partial\Psi}{\partial y}dy=\int_{y_1}^{y_2}d\Psi=\Psi_2-\Psi_1.$$

The numerical value of the stream function coincides therefore with the quantity of fluid which flows between the point x, y and the streamline $\Psi=o$.

As an example let the function

$$\Phi+i\Psi=A(x+iy)^n$$

be discussed briefly. It is simplest in general to ask first about the streamline $\Psi=o$. As is well known, if a transformation is made from rectangular coordinates to polar ones r, φ, $(x+iy)^n=r^n(\cos n\varphi+i\sin n\varphi)$. The imaginary part of this expression is $ir^n\sin n\varphi$. This is to be put equal to $i\Psi$. $\Psi=o$ therefore gives $\sin n\varphi=o$, i. e., $n\varphi=o, \pi, 2\pi$, etc. The streamlines $\Psi=o$ are therefore straight lines through the origin of coordinates, which make an angle $\alpha=\frac{\pi}{n}$ with each other, the flow is therefore the potential flow between two plane walls making the angle α with each other. The other streamlines satisfy the equation $r^n\sin n\varphi=$ const. The velocities can be obtained by differentiation, e. g., with reference to x:

$$\frac{\partial\Phi}{\partial x}+i\frac{\partial\Psi}{\partial x}=u-iv=An(x+iy)^{n-1}=Anr^{n-1}\{\cos(n-1)\varphi+i\sin(n-1)\varphi\}$$

For $r=o$ this expression becomes zero or infinite, according as n is greater or less than 1, i. e., according as the angle α is less or greater than $\pi(=180°)$. Figures 6 and 7 give the streamlines for $\alpha=\frac{\pi}{4}=45°$ and $\frac{3}{2}\pi=270°$, corresponding to $n=4$ and $\frac{2}{3}$. In the case of figure 7 the velocity, as just explained, becomes infinite at the corner. It would be expected that in the case of the actual flow some effect due to friction would enter. In fact there are observed at such corners, at the beginning of the motion, great velocities, and immediately thereafter the formation of vortices, by which the motion is so changed that the velocity at the corner becomes finite.

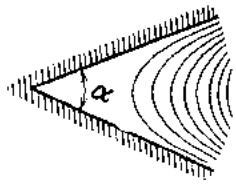

FIG. 6.—Uniplanar flow between plane walls making an angle $\alpha=45°$ with each other.

It must also be noted that with an equation

$$p+iq=\varphi(x+iy) \tag{11}$$

the x–y plane can be mapped upon the p–q plane, since to every pair of values x,y a pair of values p,q corresponds, to every point of the x–y plane corresponds a point of the p–q plane, and therefore also to every element of a line or to every curve in the former plane a linear element and a curve in the latter plane. The transformation keeps all angles unchanged, i. e., corresponding lines intersect in both figures at the same angle.

By inverting the function φ of equation (11) we can write

$$x+iy=\chi\ (p+iq)$$

and therefore deduce from equation (8) that

$$\Phi+i\Psi=f\ [\chi(p+iq)]=F\ (p+iq) \tag{12}$$

Φ and Ψ are connected therefore with p and q by an equation of the type of equation (8), and hence, in the p–q plane, are potential and stream functions of a flow, and further of that flow which arises from the transformation of the Φ, Ψ network in the x–y plane into the p–q plane.

This is a powerful method used to obtain by transformation from a known simple flow new types of flow for other given boundaries. Applications of this will be given in section 14.

11. The discussion of the principles of the hydrodynamics of nonviscous fluids to be applied by us may be stopped here. I add but one consideration, which has reference to a very useful theorem for obtaining the forces in fluid motion, namely the so-called "momentum theorem for stationary motions."

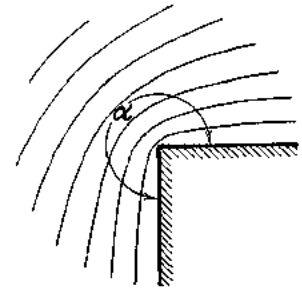

FIG. 7.—Uniplanar flow around plane walls making an angle 270° with each other.

We have to apply to fluid motion the theorem of general mechanics, which states that the rate of change with the time of the linear momentum is equal to the resultant of all the external forces. To do this, consider a definite portion of the fluid separated from the rest of the fluid by a closed surface. This surface may, in accordance with the spirit of the theorem, be considered as a "fluid surface," i. e., made up always of the same fluid particles. We must now state in a formula the change of the momentum of the fluid within the surface. If, as we shall assume, the flow is stationary, then after a time dt every fluid particle in the interior will be replaced by another, which has the same velocity as had the former. On the boundary, however, owing to its displacement, mass will pass out at the side where the fluid is approaching, and a corresponding mass will enter on the side away from which the flow takes place. If dS is the area of an element of surface, and v_n the component of the velocity in the direction of the outward drawn normal at this element, then at this point $dm=\rho dS\ .\ v_n\ dt$. If we wish to derive the component of the "impulse"—defined as the time rate of the change of momentum—for any direction s, the contribution to it of the element of surface is

$$dJ_s=v_s\frac{dm}{dt}=\rho dS\ .\ v_n v_s \tag{13}$$

With this formula we have made the transition from the fluid surface to a corresponding solid "control surface."

The external forces are compounded of the fluid pressures on the control surface and the forces which are exercised on the fluid by any solid bodies which may be inside of the control surface. If we call the latter P, we obtain the equation

$$\Sigma P_s = \iint p \cdot \cos(n, s) \cdot dS + \rho \iint v_n v_s dS \tag{14}$$

for the s component of the momentum theorem. The surface integrals are to be taken over the entire closed control surface. The impulse integral can be limited to the exit side, if for every velocity v_s on that side the velocity v_s' is known with which the same particle arrives at the approach side. Then in equation (13) dJ is to be replaced by

$$dJ - dJ' = (v_s - v_s') \frac{dm}{dt} = \rho dS v_n (v_s - v_s') \tag{13a}$$

The applications given in Part II will furnish illustrations of the theorem.

REPORT No. 116.

APPLICATIONS OF MODERN HYDRODYNAMICS TO AERONAUTICS.

By L. PRANDTL.

PART II.

APPLICATIONS.

A. DISTRIBUTION OF PRESSURE ON AIRSHIP BODIES.

12. The first application of hydrodynamical theory to be tested by experiment in the Göttingen Laboratory referred to the distribution of pressure over the surface of models of airships. We can construct mathematically the flow for any number of varieties of sectional forms of bodies of revolution of this kind if we place along an axis parallel with the direction of the air current any suitable distribution of sources and sinks, taking care that the total strength of the sources and sinks are the same. According to the intensity of the uniform motion which is superimposed upon the flow from the sources, we obtain from the same system of sources and sinks bodies of different thicknesses. In order to obtain the smoothest possible shapes, the sources and sinks are generally distributed continuously along the axis, although single-point sources are allowable.

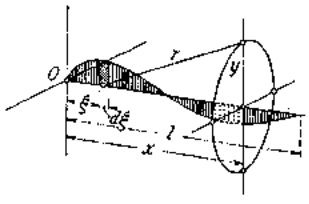

FIG. 8.—Explanation of quantities used in calculation of streamline shapes.
Abscissae: Position of source.
Ordinates: Intensity of source per unit length, i. e. $f(\xi)$.

In the case of continuously distributed sources and sinks the method of procedure is briefly this: The abscissas of the single sources are denoted by ξ, the intensity of the source per unit of length by $f(\xi)$, in which positive values of $f(\xi)$ denote sources, negative values sinks. The condition that makes the stream from the sources self-contained is expressed by the equation

$$\int_0^l f(\xi)\,d\xi = 0.$$

By simply adding the potentials due to the single elementary sources $f(\xi)\,d\xi$, i. e., in this case by integrating them, the total flow due to the sources will be given by the potential defined by the following formula

$$\Phi_1(x,y) = -\frac{1}{4\pi}\int_0^l \frac{f(\xi)\,d\xi}{r} \tag{15}$$

in which $r=\sqrt{(x-\xi)^2+y^2}$, and y is the perpendicular distance from the axis of the point for which the potential is calculated, x is the abscissa along the axis measured from the same origin as ξ. (See fig. 8.) There must be added to this potential that due to the uniform flow with the velocity V, viz, $\Phi_2 = Vx$. The total potential is then $\Phi=\Phi_1+\Phi_2$; and therefore the velocity parallel to the axis is $u=\frac{\partial\Phi}{\partial x} = V+\frac{\partial\Phi_1}{\partial x}$ and the sidewise (radial) velocity is $v=\frac{\partial\Phi}{\partial y}=\frac{\partial\Phi_1}{\partial y}$

In order to calculate the streamlines one could perform an integration of the direction given by u and v. These lines are obtained more conveniently, in this case also, by means of the stream function. (See sec. 10.) In the case of flow symmetrical with reference to the axis, such as is here discussed, one can take as stream function the quantity of fluid flowing inside the circle drawn through the point x, y in a plane perpendicular to the axis and having its center

on the axis. The amount of fluid delivered by the sources which lie up the stream is purposely deducted from this. It is not difficult to see that all points of the $X-Y$ plane, through whose parallel circles the same amount of fluid flows per second—after deduction of the sources—must lie on one and the same streamline, for evidently there is no flow, either in or out, through the surface formed by the streamlines drawn through the points of any one parallel circle (since the flow is along the surface); therefore the quantity of fluid flowing within this surface is constant, so far as it is not increased by the sources. From the meaning of the stream function, to determine which the velocity must be integrated over a surface, it follows that the stream function of a flow due to two or more causes is at every point the sum of the stream functions of the several partial flows. For a continuous distribution of sources therefore the stream function ψ is obtained by an integration exactly as was the potential. According to our premise the surface of the body is designated simply by the value $\psi = o$. The formulas are obtained as follows:

The flow from a simple source through a circle passing through a point lying to the right of the source is, writing $r = \sqrt{x^2 + y^2}$,

$$\Psi' = \int_o^y u.2\pi y dy = \int_o^y \frac{Qx}{4\pi r^3}\, 2\pi y dy = \frac{Qx}{2}\int_o^y \frac{y dy}{r^3} = \frac{Q}{2}\left(1 - \frac{x}{r}\right)$$

From this, in accordance with what has been said, the quantity Q must be subtracted, so that

$$\Psi = \Psi' - Q = -\frac{Q}{2}\left(1 + \frac{x}{r}\right) \tag{16}$$

For points lying to the left of the source we obtain from the integral

$$\Psi'' = -\frac{Q}{2}\left(1 + \frac{x}{r}\right)$$

which coincides with formula (16); this holds, then, everywhere.

For the assumed continuous distribution of sources we obtain

$$\Psi_1 = -\frac{1}{2}\int_o^l f(\xi)\left(1 + \frac{x-\xi}{r}\right) d\xi \tag{17}$$

in which $r = \sqrt{(x-\xi)^2 + y^2}$. To this stream function of the sources must now be added that due to the parallel flow

$$\Psi_2 = V\pi y^2 \tag{18}$$

Putting the total stream function $\Psi_1 + \Psi_2 = \Psi$ equal to zero, gives the equation of the surface of the body around which the flow takes place. Putting $\Psi_1 + \Psi_2 = C$ gives any other streamline. It is evident that, with the same distribution of sources, a whole group of body surfaces can be obtained, depending upon the choice of the ratio of the intensity of the sources to the strength of the parallel flow.

The determination is best made practically by graphical methods, for instance, by laying off the curves $x = \text{const.}$ in a system of coordinates consisting of y and $-\Psi$, which can be obtained at once from a calculation by tables for the stream function Ψ_1. If we intersect these curves by parabolas corresponding to the equation $-\Psi = V\pi y^2 - C$, we obtain at once a contour (for $C = o$), or some external or internal streamline (for $C > o$ or $C < o$). The parabola may be drawn upon transparent paper, and then by displacing the parabola along the Ψ axis we can at once obtain from figure 9 the values of y corresponding to any x.

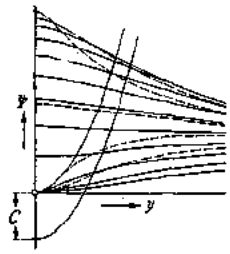

FIG. 9.—The curves are for different values of $x =$ const.

In this manner a former colleague of mine, who unfortunately fell immediately at the beginning of the war, Dr. G. Fuhrmann, calculated the shapes of bodies corresponding to a series of source distributions, and on the one hand he determined the distribution of pressure over the surface of these bodies by means of the Bernouilli equation (see sec. 4)

$$p = p_0 + \frac{\rho}{2}\{V^2 - (u^2 + v^2)\}^1 \tag{19}$$

[1] The velocities u and v may be obtained from the potential, but also from the stream function ψ; for $u = \frac{1}{2\pi y}\frac{\partial \psi}{\partial y}$ and $v = -\frac{1}{2\pi y}\frac{\partial \psi}{\partial x}$.

and on the other he constructed models according to these drawings and measured the pressure distribution over them when placed in a wind tunnel. The agreement was altogether surprisingly good, and this success gave us the stimulus to seek further relations between theoretical hydronamics and practical aeronautics. The work of Fuhrmann was published in Jahr-b. der Motorluftschiff-Studien Gesellsch., Volume V, 1911–12 (Springer, Berlin), and contains a large number of illustrations. Four of the models investigated are shown here. The upper halves of figures 10 to 13 show the streamlines for a reference system at rest with reference to the undisturbed air, the lower halves the streamlines for a reference system attached to the body. The distribution of the source intensities is indicated on the axis. The pressure distributions are shown in figures 14 to 17. The calculated pressure distributions are indicated by the lines which are drawn full, the individual observed pressures by tiny circles.[2]

It is seen that the agreement is very complete; at the rear end, however, there appears a characteristic deviation in all cases, since the theoretical pressure distribution reaches the full dynamical pressure at the point where the flow reunites again, while actually this rise in pressure, owing to the influence of the layer of air retarded by friction, remains close to the surface.

As is well known there is no resistance for the theoretical flow in a nonviscous fluid. The actual drag consists of two parts, one resulting from all the normal forces (pressures) acting on the surface of the body, the other from all the tangential forces (friction). The pressure resistance, which in this case can be obtained by integration of the pressure distribution over the surface of the body, arises in the main from the deviation mentioned at the rear end, and is, as is known, very small. Fuhrmann's calculations gave for these resistances a coefficient, with reference to the volume of the body, as shown in the following table:[3]

Model	I	II	III	IV
k_1 =	0.0170	0.0123	0.0131	0.0145

This coefficient is obtained from the following formula:

$$\text{Drag } w_i = k_1 \, U^{2/3} \, q$$

where U designates the volume and q the dynamical pressure.

The total resistance (drag) was obtained for the four models by means of the balance; the difference between the two quantities then furnishes the frictional resistance. The total drag coefficients were:[3]

Model	I	II	III	IV
k =	0.0340	0.0220	0.0246	0.0248

With greater values of VL than were then available for us, the resistance coefficients become nearly 30 per cent smaller. For purposes of comparison with other cases it may be mentioned that the "maximum section" was about 2/5 of $U^{2/3}$. The surface was about seven times $U^{2/3}$; from which can be deduced that the total resistance of the good models was not greater than the friction of a plane surface having the same area. The theoretical theorem that in the ideal fluid the resistance is zero receives in this a brilliant confirmation by experiment.

B. THEORY OF LIFT.

13. The phenomena which give rise to the lift of an aerofoil may be studied in the simplest manner in the case of uniplanar motion. (See sec. 10.) Such a uniplanar flow would be expected obviously in the case that the wing was unlimited at the sides, therefore was "infinitely

[2] In the wind tunnel there was a small pressure drop in the direction of its length. In order to eliminate the effect of this, the pressures toward the fore had to be diminished somewhat and those aft somewhat increased.

[3] After deduction of the horizontal buoyancy.

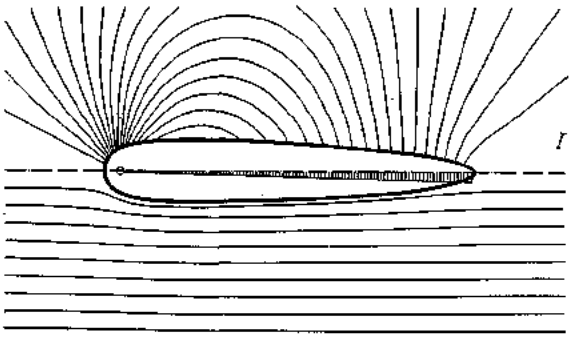

FIG. 10.

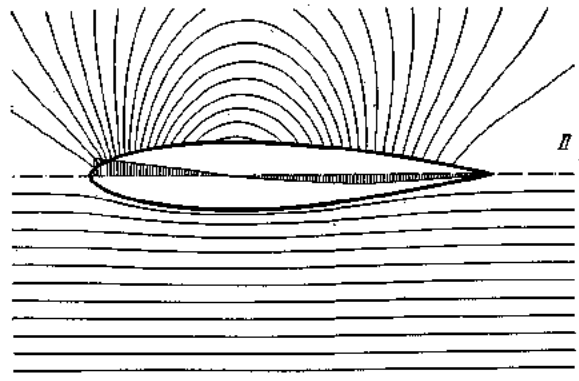

FIG. 11.

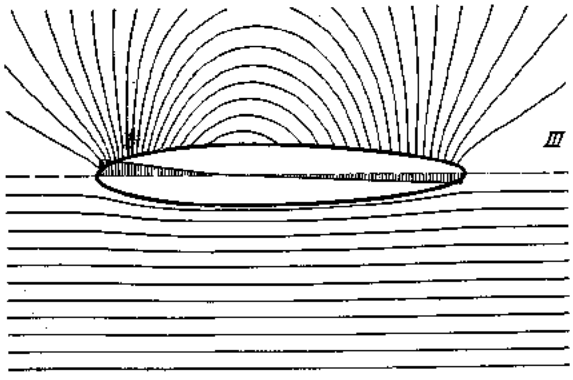

FIG. 12.

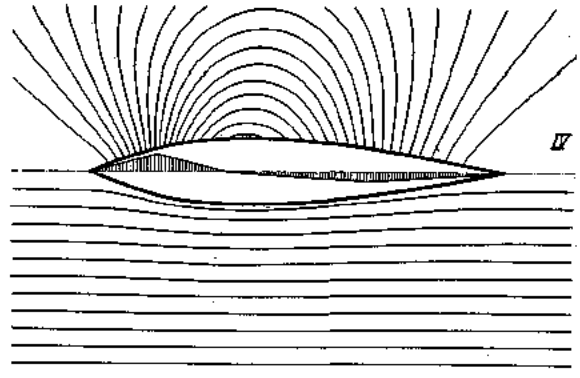

FIG. 13.

Four airship models as derived by Fuhrmann by combination of sources and uniform flow. Distribution of sources indicated on axis. Upper half: Streamlines relative to undisturbed air. Lower half: Streamlines relative to airship.

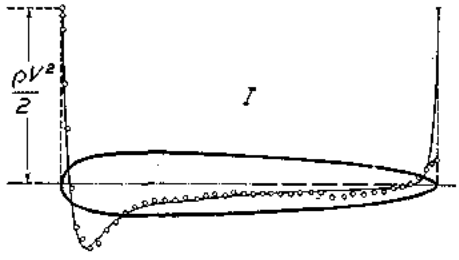

FIG. 14.

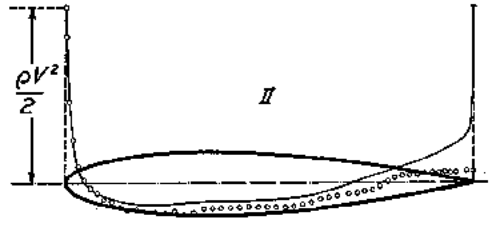

FIG. 15.

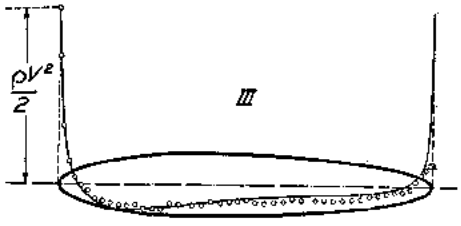

FIG. 16.

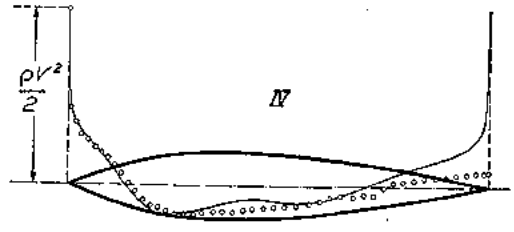

FIG. 17.

Pressure distribution over airships of figures 10 to 13. Full lines represent calculated values; small circles, points as found by observation in a wind-tunnel.

long," and throughout exhibited the same profile and the same angle of attack. In this case all the sections will be alike in all respects and each one can be considered as a plane of symmetry. The infinitely long wing plays an important part therefore in the considerations of the theoretical student. It is not possible to realize it in free air, and marked deviations from the infinitely long wing are shown even with very long wings, e. g., those having an aspect ratio of 1:10. In laboratories, however, the infinitely long wing, or uniplanar flow, may be secured with good approximation, if a wing having a constant profile is placed between plane walls in a wind tunnel, the walls running the full height of the air stream. In this case the wing must extend close to the walls; there must be no gap through which a sensible amount of air can flow. We will now discuss such experiments, and first we shall state the fundamental theory of uniplanar flow.

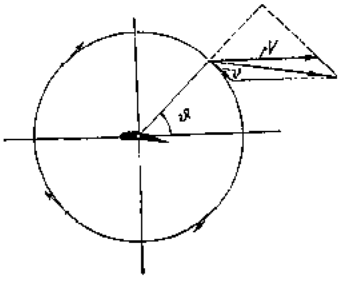

FIG. 18.—Deduction of the Kutta formula, uniplanar flow around infinite wing.

Since, as explained in section 4, in a previously undisturbed fluid flow, the sum of the static and dynamic pressures is constant: $p+\frac{\rho}{2}V^2=\text{const.}$, in order to produce lift, for which the pressure below the surface must be increased and that above diminished, such arrangements must be made as will diminish the velocity below the wing and increase it above. The other method of producing such pressure differences, namely, by causing a vortex region above the surface placed like a kite oblique to the wind, by which a suction is produced, does not come under discussion in practical aeronautics owing to the great resistance it sets up. Lanchester has already called attention to the fact that this lifting current around the wing arises if there is superimposed upon a simple potential flow a circulating flow which on the pressure side runs against the main current and on the suction side with it. Kutta (1902) and Joukowski (1906) proved, independently of each other, the theorem that the lift for the length l of the wing is

$$A=\rho\Gamma Vl \tag{20}$$

in which Γ is the circulation of the superimposed flow. It may be concluded from this formula that in a steady fluid flow lift is not possible unless there is motion giving rise to a circulation. In uniplanar flow in an ideal fluid this lift does not entail any drag.

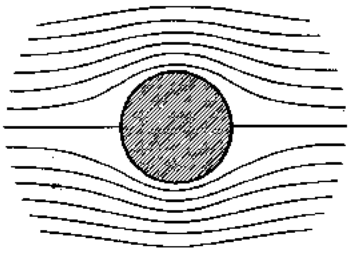
FIG. 19.—Uniplanar uniform flow around circular cylinder.

The proof of the Kutta-Joukowski formula is generally deduced by applying the momentum theorem to a circular cylinder of large radius whose axis is the medial line of the wing. The circulatory motion, which could be obtained numerically close to the wing only by elaborate mathematical processes, is reduced at a great distance from the wing to a motion which agrees exactly with the flow around a rectilinear vortex filament (see sec. 8), in which, therefore, the single particles describe concentric circles. The velocity around a circle of radius R is, then, $v=\frac{\Gamma}{2\pi R}$. For an element of surface $l.\ Rd\theta$ (see fig. 18) the normal component of the velocity is $V\cos\theta$, the mass flowing through per second $dm=\rho lRV\cos\theta d\theta$. If we wish to apply the momentum theorem for the vertical components, i. e., those perpendicular to the direction of V, then this component of the velocity through the element of surface must be taken. This, obviously, is $v\cos\theta$, taken positive if directed downward; the total impulse, then, is

$$J=\int v\cos\theta dm=\rho lRVv\int_0^{2\pi}\cos^2\theta d\theta.$$

The integral equals π, and therefore introducing the value of v

$$J=\frac{1}{2}\rho V\Gamma l.$$

Since the resulting impulse is directed downward (the upward velocity in front of the wing is changed into a downward one behind the wing), this means that the reaction of the fluid against the wing is a lift of the wing upward. The amount of the impulse furnishes, as is seen by referring to formula (20), only half the lift. The other half comes from the pressure differences on the control surfaces. Since, for a sufficiently large R, v can always be considered small compared with V, neglecting $\frac{\rho}{2} v^2$, the pressure p is given, according to the ernouilli equation, by

$$p = p_0 + \frac{\rho}{2} V^2 - \frac{\rho}{2}\left\{(V + v \sin\theta^2 + v^2 \cos^2\theta\right\} \cong p_0 - \rho V \sin\theta.$$

A component of this, obtained by multiplying by $\sin\theta$, acts vertically on the surface element $lRd\theta$. The resulting force D is, then,

$$D = \rho l R V v \int_0^{2\pi} \sin^2\theta d\theta.$$

This integral also equals π, so that here also

$$D = \frac{1}{2} \rho V \Gamma l$$

its direction is vertically up. The total lift, then, is

$$A = J + D = \rho V \Gamma .$$

14. For the more accurate analysis of the flow around wings the complex functions (see sec. 10) have been applied with great success, following the procedure of Kutta. Very different

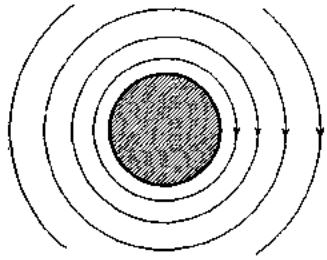

FIG. 20.—Uniplanar flow around circular cylinder considered as a columnar vortex of strength Γ.

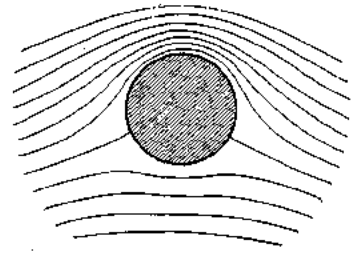

FIG. 21.—Superposition of two preceding flows.

methods have been used. Here we shall calculate only one specially simple case, in which the flow will be deduced first around a circular cylinder and then calculated for a wing profile by a transformation of the circular cylinder and its flow, using complex functions.

The flow around a circular cylinder has long been known. If the coordinates in the plane of the circle are p and q, and if we write $p + iq = t$, the potential and stream functions for the ordinary symmetrical flow around the circular cylinder are given by the very simple formula

$$\Phi_1 + i\Psi_1 = V\left(t + \frac{a^2}{t}\right)^5 \tag{21}$$

It is easily seen by passing to polar coordinates that, for $r = a$, $\psi_1 = o$, and that therefore the circle of radius a is a streamline. Further, for the p axis, $\psi_1 = o$, i. e., this is also a streamline. The whole flow is that shown in figure 19. To this flow must be added the circulation flow expressed by the formula

$$\Phi_1 + i\Psi_2 = \frac{i\Gamma}{2\pi} \log t^6 \tag{22}$$

which, as shown in figure 20, is simply a flow in concentric circles with the velocity $\frac{\Gamma}{2\pi r}$. The combination of the two flows, i. e., the flow for the sum of the expressions in equations (21) and (22), is shown in figure 21. It is seen that the rest point is moved down an amount de. By a suitable choice of the circulation this can be brought to any desired point.

---

[5] $t + \frac{a^2}{t} = \left(r + \frac{a^2}{r}\right)\cos\vartheta + i\left(r - \frac{a^2}{r}\right)\sin\vartheta$ [6] $i \log t = -\vartheta + i \log r$.

We must now discuss the transformation of this flow to a wing profile. For this purpose manifold means are possible. The simplest is furnished by a transformation according to the equation

$$z = x + iy = t + \frac{b^2}{t},$$

By this the circle of diameter $AB = 2b$ in the t plane (as we shall for brevity's sake call the p, q plane) is transformed into a straight line $A'B'$ of the length $4b$ along the X axis, and concen-

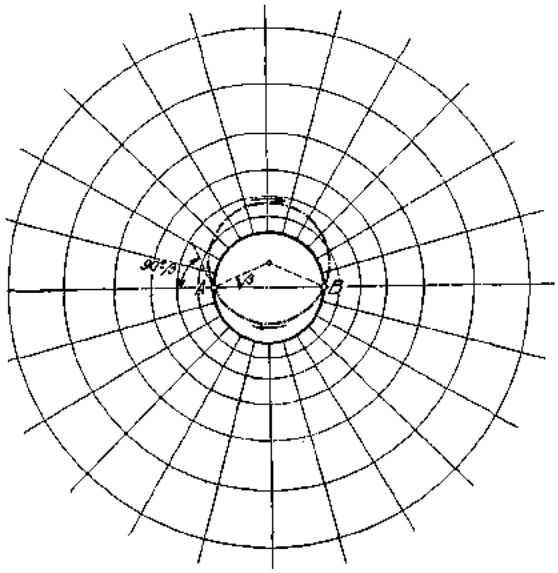

FIG. 22.

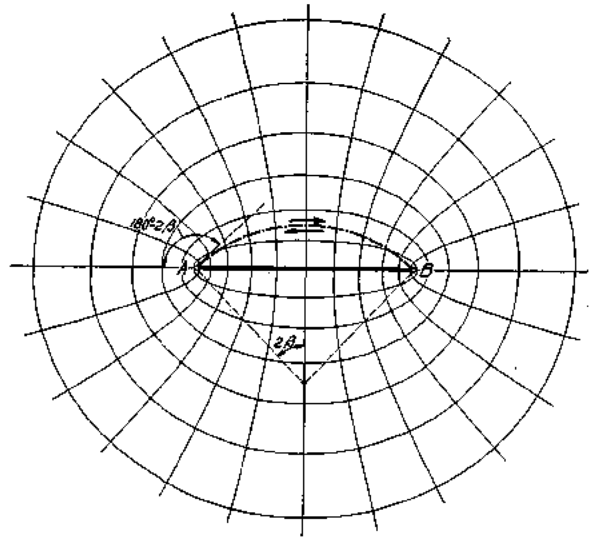

FIG. 23.

Conformal transformation of z plane into t plane by $z = t + \frac{b^2}{t}$.

tric circles around the former become ellipses, the radii become hyperbolas. All the ellipses and hyperbolas have their foci at the ends of the straight line, this forming a confocal system. Figures 22 and 23 illustrate the transformation. It may be mentioned, in addition, that the interior of the circle in figure 22 corresponds to a continuation of the meshwork in figure 23 through the slit $A'B'$, whose form agrees with the meshwork as drawn. Any circle through the points AB is thereby transformed into an arc of a circle passed over twice, having an angle subtended at the center equal to 4β.

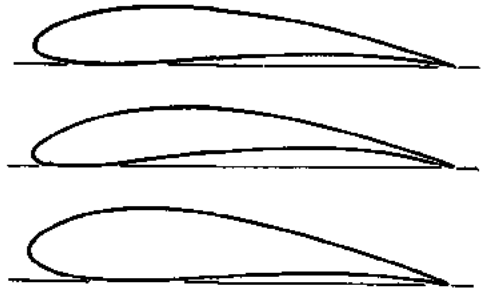

FIG. 24.—Illustrations of Joukowski sections.

Many different results may now be obtained by means of this mapping, according to the position which the circle, around which the flow takes place according to equations (21) and (22), bears to the diameter AB of the circle of figure 22. If the diameter AB is made to coincide with any oblique diameter of the circular section of the cylinder, we obtain a flow around an oblique plate whose angle of attack coincides with the inclination of the line AB. If the diameter AB is selected somewhat smaller, so that both points lie inside the circle symmetrically on the diameter, the flow around ellipses is obtained. If, however, the diameter AB coincides with a chord of the circle around which the original flow was, which, for example, may lie below the center, the flow around a curved plate forming an arc of a circle is obtained. By selection of various points in the interior of the original circle forms of diverse shapes are obtained. The recognition of the fact that among these forms very beautiful winglike profiles may be found we

owe to Joukowski. These are obtained if the point B is selected on the boundary of the original circle and the point A inside, and somewhat below the diameter through the point B. Figure 24 gives illustrations of such Joukowski profiles.

In order that the flow may be like the actual one, in the cases mentioned the circulation must always be so chosen that the rear rest point coincides with the point B, or, respectively, with the point on the original circle which lies nearest this point. In this case there will be, after mapping on the z plane, a smooth flow away from the trailing edge, as is observed in practice. It is therefore seen that the circulation must be taken greater according as the angle of attack is greater, which agrees with the observation that the lift increases with increasing angle of attack.

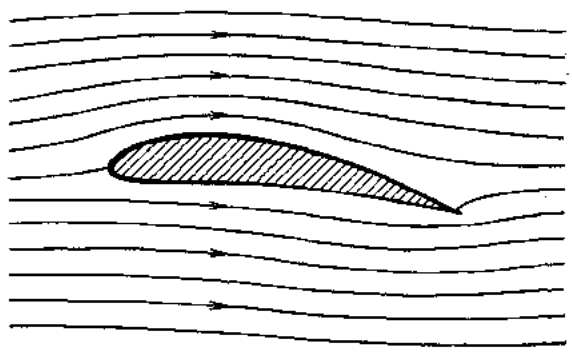

FIG. 25.—Transformation of simple potential flow, figure 19.

The transformation of the flows shown in figures 19 to 21 into wing profiles gives illustrations of streamlines as shown in figures 25 to 27—figure 25, simple potential flow; figure 26, circulation flow; figure 27, the actual flow around a wing obtained by superposition of the two previous flows.

We are, accordingly, by the help of such constructions, in the position of being able to calculate the velocity at every point in the neighborhood of the wing profile, and with it the pressure. In particular, the distribution of pressure over the wing itself may be calculated.

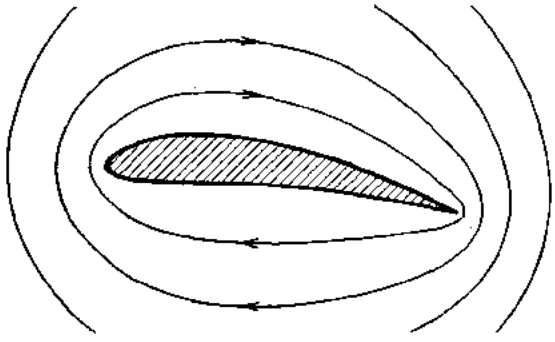

FIG. 26.—Transformation of circulatory flow, figure 20.

My assistant, Dr. A. Betz, in the year 1914 worked out the pressure distribution for a Joukowski wing profile, for a series of angles of attack, and then in a wind tunnel measured the pressure distribution on a hollow model of such a wing made of sheet metal, side walls of the height of the tunnel being introduced so as to secure uniplanar flow The results of the measurements agreed in a very satisfactory manner with the calculations, only—as could be well explained as due to friction—the actual circulation was always slightly less than that calculated for the same angle of attack. If the pressure distributions would be compared, not for the same angles of attack, but for the same amount of circulation, the agreement would be noticeably better. The pressure distributions are shown in figures 28 to 30, in which again the full curves correspond to the measurements and the dashes to the calculated pressures. Lift and drag for the wing were also obtained by the wind-tunnel balance. In order to do this, the middle part of the wing was isolated from the side parts, which were fastened to the walls of the tunnel by carefully designed labyrinths, so that within a small range it could move without friction. The result of the experiment is shown in figure 31. The theoretical drag is zero, that obtained by measurement is very small for that region where the wing is "good," but sensibly larger for too large and too small angles of attack. The lift is correspondingly in agreement

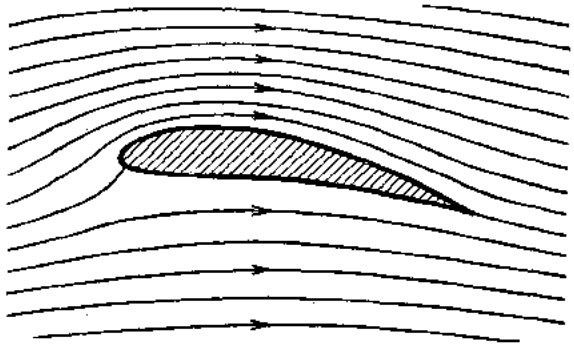

FIG. 27.—Transformation of superposition of the two flows, figure 21.

with the theoretical value in the good region, only everywhere somewhat less. The deviations of drag as well as of lift are to be explained by the influence of the viscosity of the fluid. The agreement on the whole is as good as can be expected from a theory which neglects completely the viscosity.

For the connection between the angle of incidence α and the circulation which results from the condition discussed above calculations give the following result for the lift:

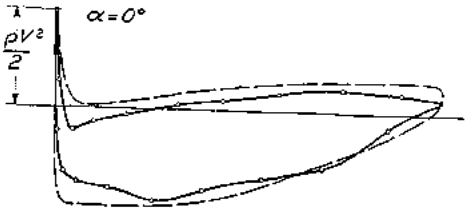

FIG. 28.

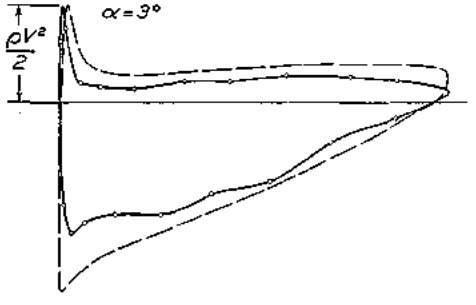

FIG. 29.

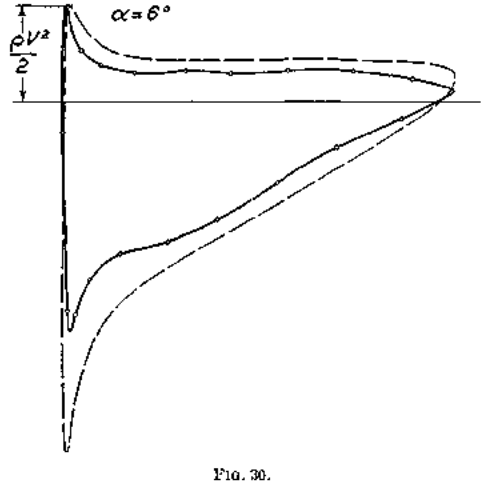

FIG. 30.

Pressure distribution over a Joukowski wing, different angles of attack. Full lines give results of wind-tunnel tests; dashed lines, calculated values.

(1) The Kutta theory gives for the thin plane plate the formula

$$A = bt.\pi\rho V_\infty^2 \sin\alpha \tag{23}$$

The lift coefficient C_a is defined by the equation

$$C_a = \frac{A}{Fq} \text{ where } q = \frac{1}{2}\rho V^2$$

and therefore

$$C_a = 2\pi \sin\alpha \tag{24}$$

(2) For the circularly curved plates having an angle of arc 4β subtended at the center (see figure 23) we have, according to Kutta, if α is the angle of attack of the chord,

$$C_a = 2\pi \frac{\sin(\alpha+\beta)}{\cos\beta} \tag{25}$$

which, for small curvatures, becomes $2\pi \sin(\alpha+\beta)$; this can be expressed by saying that the lift of the circularly curved plate is the same as that of a plane which touches the former at a point three-fourths of the distance around the arc from its leading edge.

For the Joukowski profiles and for others the formulas are less simple. v. Mises showed in 1917 that the increase of C_a with the angle of attack, i. e., $\frac{dC_a}{d\alpha}$, is greater for all other profiles than for the flat plate, and is the greater the thicker the profile. But the differences are not marked for the profiles occurring in practice.

The movement of the center of pressure has also been investigated theoretically. With the plane plate, in the region of small angles, it always lies at one-fourth of the width of the plate; with circularly curved thin plates its position for small angles is given by the following law:

$$x_o = -\frac{t}{4}\frac{\tan\alpha}{\tan\alpha+\tan\beta} \tag{26}$$

in which t is the chord of the plate, and x_o is the distance measured from the center of the plate. The fact that the movement of the center of pressure in the case of "good" angles of attack of the profiles agrees with theory is proved by the agreement of the actual pressure distribution with that calculated. In the case of thin plates a less satisfactory agreement as respects pressure distribution is to be expected because with them in practice there is a formation of vortices at the sharp leading edges, while theory must assume a smooth flow at this edge.

15. That a circulatory motion is essential for the production of lift of an aerofoil is definitely established. The question then is how to reconcile this fact with the proposition that

the circulation around a fluid line in a nonviscous fluid remains constant. If, before the motion begins, we draw a closed line around the wing, then, so long as everything is at rest, the circulation certainly is zero. Even when the motion begins, it can not change for this line. The explanation of why, in spite of this, the wing gains circulation is this: At the first moment of the motion there is still no circulation present, the motion takes place approximately according to figure 25, there is a flow at high velocity around the trailing edge. (See sec. 10.) This motion can not, however, continue; there is instantly formed at the trailing edge a vortex of increasing intensity, which, in accordance with the Helmholtz theorem that the vortex is always made up of the same fluid particles, remains with the fluid as it passes on. (See fig. 32.) The circulation around the wing and vortex, taken together, remains equal to zero; there remains then around the wing a circulation equal and opposite to that of the vortex which has gone off with the current. Therefore vortices will be given off until the circulation around the wing is of such a strength as to make the fluid flow off smoothly from the trailing edge. If by some alteration of the angle of attack the condition for smooth flow is disturbed, vortices are again given off until the circulation reaches its new value. These phenomena are completed in a comparatively short distance, so the full lift is developed very quickly.

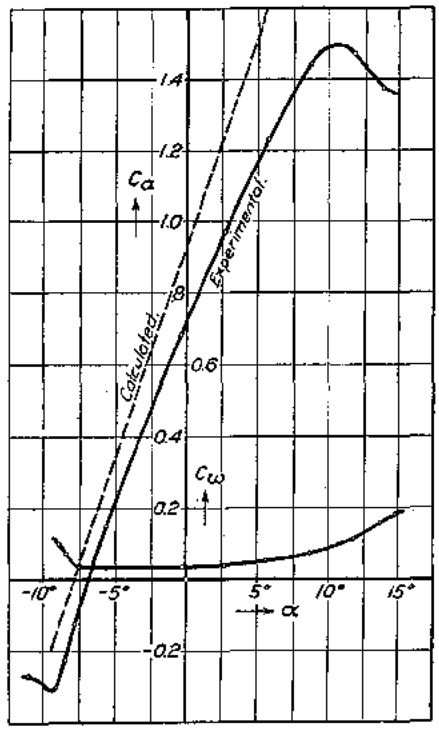

FIG. 31.—Values of lift and drag coefficients of a Joukowski wing as obtained in wind-tunnel tests and by theory.

In the pictures of flow around a wing, e. g., figure 27, one sees that the air in front of the wing flows upward against the reaction of the lift. The consideration of momentum has shown that half of the impulse is due to the oncoming ascending current. This fact needs some further explanation. The best answer is that given by Lanchester,[7] who shows that for the production of lift the air mass at any time below the wing must be given an acceleration downward. The question he asks is: What kind of a motion arises if for a short time the air below the wing is accelerated downward, then the wing is moved forward a bit without pressure, then the air is again accelerated, and so on? The space distribution of the accelerations is known for the case of a plane plate, infinitely extended at the sides, accelerated from rest; the pattern of the acceleration direction is given in figure 33. It is seen that above and below the plate the acceleration is downward, in front of and behind the plate it is upward opposite to the acceleration of the plate, since the air is escaping from the plate. Lanchester asks now about the velocities which arise from the original uniform velocity relative to the plate owing to the fact that the plate, while it gives rise to the accelerations as shown in figure 33, gradually comes nearer the air particle considered, passes by it, and finally again moves forward away from it. The picture of the velocities and streamlines which Lanchester obtained in this way and reproduced in his book was, independently of him, calculated exactly by Kutta. It is reproduced in figure 34. It is seen that as the result of the upward accelerations of the flow away from the wing

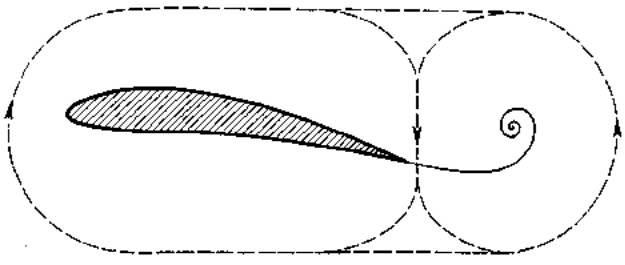

FIG. 32.—Production of circulation around a wing due to vortices leaving trailing edge.

[7] Aerodynamics I, § 110–118.

there is an upward velocity in front of the plate, a uniform downward acceleration at the plate itself due to which the upward velocity is changed into a downward one, and finally behind the plate a gradual decrease of the downward velocity on account of the acceleration upward.

C. THE FINITE WING.

16. It has been known for a long time that the aspect ratio of an aerofoil had a great effect on its properties. One could therefore have expected that, on account of the vanishing of pressure at the side edges, the intensity of the lift must decrease toward the edge, so that its average value for the same angle of attack must be smaller for small values of the aspect ratio than for large ones. But the observed influence of aspect ratios is sensibly greater than could be explained in this way. We must therefore investigate whether an explanation of this phenomenon can be found, if we apply to the finite aerofoil in some proper manner the results which are known to hold for uniplanar flow.

FIG. 33.—Acceleration diagram around an infinitely long flat plate accelerated at right angle to its surface.

It is easily seen that vortices in the free fluid must here be taken into account. For it is certain that circulation is present around the middle of the wing, because no lift is possible without circulation. If a closed line drawn around the middle of the wing, around which, therefore, there is circulation, is displaced sideways over the end of a wing, it will certainly no longer show circulation here when it is beyond the wing. From the theorem that the circulation along a closed line only changes if it cuts vortex filaments, and that the amount of the change of the circulation equals the sum of the strengths of the vortex filaments cut (see sec. 8), we must conclude that from each half of a wing vortex filaments whose strengths add up to Γ must proceed, which are concentrated mainly near the ends of the wing. According to the Helmholtz theorem we know further that every vortex produced in the fluid continues to move with the same fluid particles. We may look upon the velocities produced by the wing as small compared with the flight velocity V, so that as an approximation we may assume that the vortices move away from the wing backwards with the rectilinear velocity V. (If it is wished, we can also improve the considerations based upon such an assumption if the motion of the vortices of themselves relative to the air is taken into account. This will, however, be seen to be unnecessary for practical applications of the theory.)

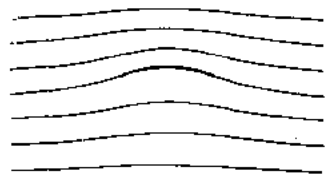

FIG. 34.—Streamlines around an infinitely long curved plate.

In order now to obtain the simplest possible scheme, we shall assume that the lift is uniformly distributed over the wing; then the total circulation will arise only at the ends, and continue rearwards as free vortices. The velocity field of an infinitely long wing, as we saw, was the same at great distances as that of a rectilinear vortex filament instead of the wing. We shall assume that the corresponding statement holds for the finite wing. We thus obtain, for the velocity field around a finite wing, a picture which is somewhat crude, it is true, if we take for it the velocity distribution due to a vortex filament of corresponding shape.

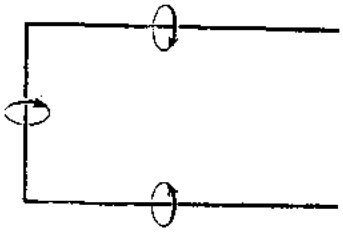

FIG. 35.—A finite wing, considered as due to vortices replacing the wing.

It may be mentioned here that, on account of there being the same laws for the velocity field of a vortex filament and the magnetic field of an electric current (see sec. 8), the velocity near a finite wing can also be investigated numerically by calculating the direction and intensity of the magnetic field produced near an electrical conductor shaped as shown in figure 35 due to an electrical current flowing in it.

The principles for the calculation of this velocity field have been stated in section 8; the total velocity is made up out of three partial velocities which are caused by the three rectilinear vortex portions. As is seen without difficulty, for the region between the vortices the flow is downward, outside it is upward.

17. This approximation theorem is specially convenient if the conditions at great distances from the wing are treated. With its help we can explain how the weight of an airplane is transferred to the ground. In order to make the flow satisfy the condition that at the ground components of velocity normal to it are impossible, we apply a concept taken from other branches of physics and superimpose the condition of an image of the airplane, taking the earth as the mirror. On account of symmetry, then, all velocity components normal to the earth's surface will vanish. If we use as our system of coordinates one attached to the airplane, we have then the case of stationary motion. If we take the X axis in the direction of the span of the wing, the Y axis horizontal in the direction of flight and the Z axis vertically down, and if u, v, w are the components of the additional velocity due to the vortices, then calling p_0 the undisturbed pressure and p' the pressure difference from p_0, and neglecting the weight of the air, Bernouilli's equation gives us

$$p_0 + p' + \frac{\rho}{2}[u^2 + (v - V)^2 + w^2] = p_0 + \frac{\rho}{2} V^2$$

If this is expanded and if u^2, v^2, and w^2 are neglected as being small of a higher order, there remains the simple equation

$$p' = \rho\, V v \qquad (27)$$

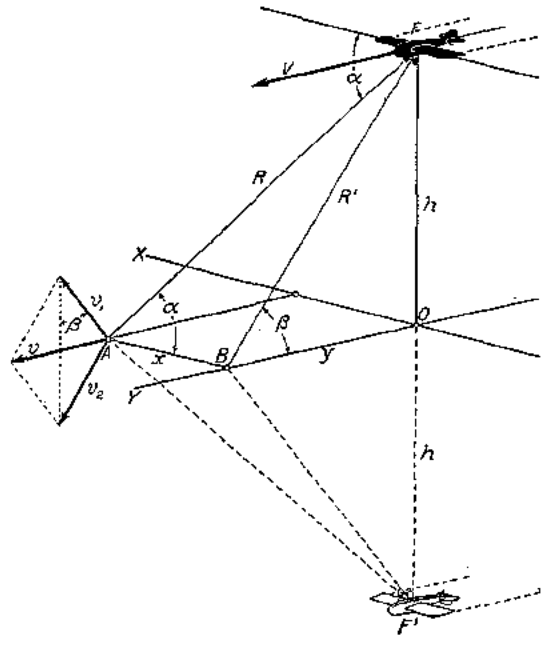

FIG. 36.—Application of method of images to airplane flying near the ground.

For the determination of the pressure distribution on the ground we must now calculate the value of v. Let us assume the vortices run off the wing in an exactly horizontal direction (actually, their path inclines downward slightly), in which case they do not contribute to v. There remains then only the "transverse vortex" of the length l (effective span) and the circulation Γ. We will assume that the span of the wing is small in comparison with the distance h of the airplane from the ground. In that case we can treat the transverse vortex as if it were a single vortex element. We obtain, then—see figure 36—at a point A, with the coordinates x and y, a velocity perpendicular to the plane ABF, of the amount

$$v_1 = \Gamma\, l\, \frac{\sin \alpha}{4\, \pi\, R^2}$$

The image of the airplane furnishes an equal amount perpendicular to the plane ABF' If β is the angle between the plane ABF and the XY plane, then the actual velocity at the ground, as far as it is due to the transverse vortex, will be the resultant of v_1 and v_2. It is therefore $v = 2v_1 \sin \beta$, or, if we write $\sin \alpha = \frac{R'}{R}$, $\sin \beta = \frac{h}{R'}$ (see fig. 36)

$$v = \frac{\Gamma\, l\, h}{2\, \pi\, R^3} \qquad (28)$$

If we take into account the fact that, according to the Kutta-Joukowski formula (20), $\rho\, \Gamma\, V\, l = A$, equations (27) and (28) lead to the relation

$$p' = \frac{A\, h}{2\, \pi\, R^3} \qquad (29)$$

If this is integrated over the whole infinite ground surface, it is seen that the resultant force due to the pressures on the ground has exactly the amount A. It is thus proved that the

pressure distribution due to the circulation motion transfers to the ground exactly the weigh of the airplane. The distribution of the pressure, which according to formula (29) is axially symmetrical with reference to the foot of the vertical line drawn from the airplane, is shown in figure 37. The pressure maximum is $p_1=\frac{A}{2\pi h^2}$. Its amount, even for low heights of flight, is very small, since the surface over which the pressure is distributed is very large.

18. Applications of an entirely different kind may be made of the velocity field which belongs to the vortex of figure 35. For instance, an estimate may be made as to the magnitude of the downward velocity component at any point of the tail surfaces, and in this manner the influence of the wings upon the tail surfaces may be calculated. If in accordance with the Kutta-Joukowski formula the lift is written $A=\rho\Gamma Vl$, in which, taking account of the fact that a

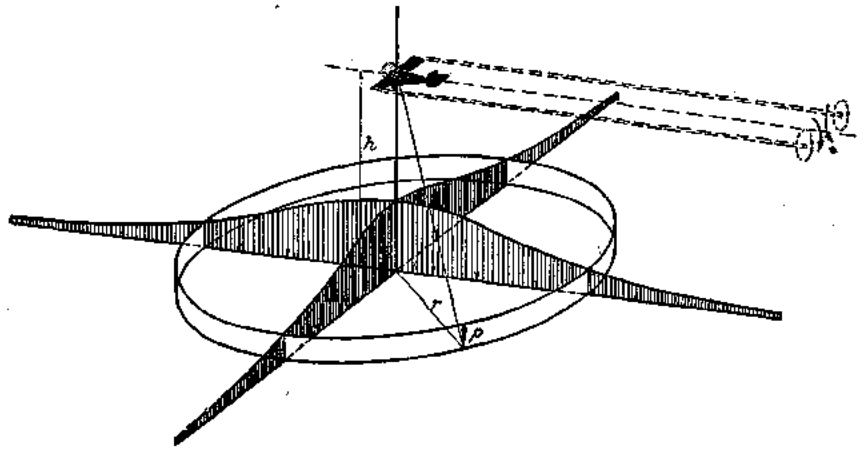

FIG. 37.—Distribution of pressure on ground caused by airplane flying near it.

portion of the vortices flow off within the ends of the wing, l, can be taken somewhat less than the actual span b, then at a distance d, behind the wing, the velocity component downward is

$$w=2\frac{\Gamma}{4\pi}\left\{\frac{1}{\frac{l}{2}}\left(1+\frac{d}{a}\right)+\frac{1}{d}\frac{l/2}{a}\right\}=\frac{\Gamma}{\pi l}\left(1+\frac{a}{d}\right) \tag{30}$$

in which $a=\sqrt{\left(\frac{l}{2}\right)^2+d^2}$.

If the flight velocity is V, this gives for the inclination of the downward sloping air-current $\tan\varphi=\frac{w}{V}$. We proved this relation in the year 1911 and found an approximate agreement with observation.

The principle made use of above has been applied with profit to the calculation of the influence of one wing of a biplane upon the other wing and has given a method for the calculation of the properties of a biplane from the properties of a single wing as found by experiments. The fundamental idea, which is always applied in such calculations, is that, owing to the vortex system of one wing, the velocity field near the wing is disturbed, and it is assumed that a wing experiences the same lift as in an undisturbed air stream if it cuts the streamlines of the flow disturbed by the other wing in the same manner as a monoplane wing cuts the straight streamlines of the undisturbed flow. As is easily seen, the wing profile must in general be slightly turned and its curvature slightly altered, as is shown in figures 38 and 39. By the rotation of the wing the direction of the resultant air force acting on it is turned through an equal angle. If the magnitude of the velocity as well as its direction is also changed, this must be expressed by a corresponding change in the resultant air force.

As an illustration we will treat briefly the case of a biplane without stagger. The most important component of the disturbance velocity w is again the vertical one; in the plane of the mean lift lines of the biplane it is affected only by the pair of vortices running off the wings, since the transverse vortex of one wing causes only an increase (or decrease) of the velocity of flow at the other wing. We are concerned here only with the calculation of that downward disturbance velocity due to the vortices from the wing not under investigation, since the other vortex system is present with the monoplane and its influence has already been taken into account in the experiments on a monoplane.

The total velocity due to a portion of a vortex proceeding to infinity in one direction, in the plane perpendicular to the vortex at its end, is, as may be deduced easily from the formula in section 8, exactly half of the corresponding velocity in the neighborhood of a rectilinear vortex filament extending to infinity in both directions. This can also be easily seen from the fact that two vortex filaments, each extending to infinity in only one direction—but oppositely in the two cases—form, if combined, a single filament extending to infinity in both directions. The total velocity caused at the point P by the vortex A, see figure 40, is $\frac{\Gamma_1}{4\pi r}$, where $r=\sqrt{x^2+h^2}$; its vertical component is

$$w_A=\frac{\Gamma_1}{4\pi r}\cdot\frac{x}{r}.$$

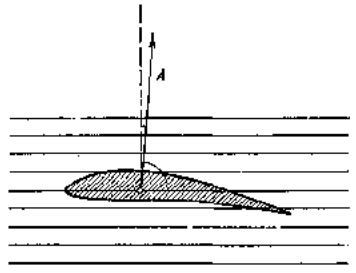

FIG. 38.

The vertical component due to the vortex B is

$$w_B=\frac{\Gamma_1}{4\pi r'}\cdot\frac{l_1-x}{r'}$$

where $r'=\sqrt{(l_2-x)^2+h^2}$.

Therefore the vertical component due to both vortices is

$$w=\frac{\Gamma}{4\pi}\left(\frac{x}{r^2}+\frac{l_1-x}{r'^2}\right) \qquad (31)$$

If we assume that the lift is uniformly distributed over the effective span l_2, which again we shall take as somewhat less than the actual span, then, since every element of the wing must be turned through the angle φ according to the formula $\tan\varphi=\frac{w}{V}$, the direction of the air force must be turned also, which means a negligible change in the lift, but an increase in the drag of this wing which must be taken into account.

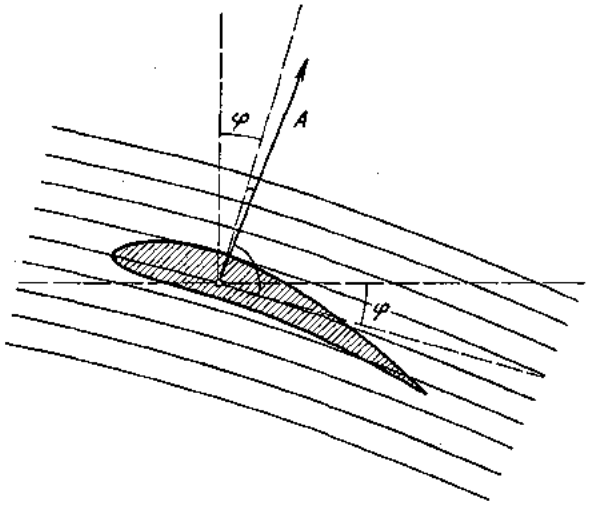

FIG. 39.

Influence of one wing of a biplane upon the other; rotation of wing profile, alteration of its curvature.

It is essential then in this calculation that we pass from a condition for a monoplane to one in which the wing when part of a biplane has the same lift as when considered as a monoplane. The angle of attack for which this condition will arise can be estimated afterwards from the average of the angles φ.

19. The contribution of vortex A to the increase of the drag of the upper wing in figure 40 is evidently

$$W'=\int_0^{l_2}\frac{w}{V}\frac{A_2}{l_2}dx=\frac{A_2}{l_2}\frac{\Gamma}{4\pi V}\int_0^{l_2}\frac{xdx}{r^2}=\frac{A_2}{l_2}\frac{\Gamma}{4\pi V}\log\frac{r_2}{r_1}$$

The contribution of vortex B is, by symmetry, the same. In accordance with equation (20), we can put $\Gamma=\frac{A_1}{l_1\rho V}$ and thus obtain for the increase of the drag of the upper wing

$$W_{12}=\frac{A_1A_2}{l_1\,l_2}\,\frac{\log r_2/r_1}{2\pi\rho V^2} \tag{32}$$

By the symbol W_{12} is meant that it is the drag produced by wing 1 upon wing 2. One can convince himself easily that the drag W_{21} which wing 2 produces upon wing 1 has the same magnitude. Therefore the total increase of drag due to the fact that two monoplanes which produce the lifts A_1 and A_2 are combined to form a biplane, the two lifts remaining unchanged (the angles of incidence of course being changed), is

$$W_{12}+W_{21}=2\,W_{12}=\frac{A_1A_2}{2\pi l_1\cdot\ l_2q}\log\frac{r_2}{r_1} \tag{33}$$

in which, as always $q=\frac{1}{2}\rho V^2$.)[8]

Upon the change in the magnitude of the velocity, which in accordance with the approximation used depends only upon the disturbance velocity v in the direction of flight, only the transverse vortex of the other wing has an influence. For any point this influence, according to our formula, is given by

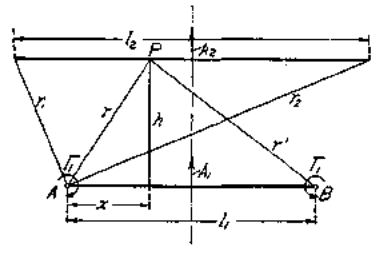

FIG. 40.—Velocity at a point P due to the tip vortices.

$$v=\frac{\Gamma}{4\pi h}\left(\frac{x}{r}+\frac{l-x}{r'}\right) \tag{34}$$

in which r and r' have the same meaning as before. The upper wing experiences due to the lower an increase in velocity, the lower one experiences due to the upper a decrease in velocity, to which correspond, respectively, an increase or a decrease in lift as shown by the usual formulæ. If we wish to keep the lifts unchanged, as required in the treatment given above, it is necessary to change the angles of attack correspondingly.

The effective change in the curvature[9] of the wing profile will, for simplicity's sake, be discussed here only for the medial plane of the biplane, i. e., for $x=\frac{l_1}{2}$. It is obtained in the simplest manner by differentiating the angle of inclination of the air current disturbed by the other wing, which is, remembering that $\tan\varphi=\frac{w}{V}$,

$$\frac{1}{R}=\frac{d}{dy}\left(\tan\beta\right)=\frac{1}{V}\frac{dw}{dy} \tag{35}$$

Outside of the vertical plane, owing to the disturbing wing, three vortices contribute to the magnitude of w. A side vortex contributes, at a point at the height h and the distance y in front of the transverse plane, a velocity v' perpendicular to r'' of the amount $\frac{\Gamma_1}{4\pi r}\left(1-\frac{y}{r''}\right)$, and therefore its share of w is

$$w_1=\frac{\Gamma_1 x}{4\pi r^2}\left(1-\frac{y}{r''}\right)=\frac{\Gamma_1 l_1}{8\pi r^2}\left(1-\frac{y}{r''}\right)$$

The transverse vortex contributes

$$w_2=-\frac{\Gamma_1}{4\pi r}\cdot\frac{l_1}{r''r'''}\,y$$

in which the meaning of r'' and r''' may be seen from figure 41. The total w is, accordingly,

$$w=2w_1+w_2=\frac{\Gamma l_1}{4\pi}\left(\frac{1}{r^2}-\frac{y}{r^2r''}-\frac{y}{r''r'''^2}\right)$$

[8] The mutual action of two wings placed side by side can also be calculated from the considerations stated above, and results in a decrease of the drag. This decrease is of a similar kind to that which arises in the theory of a monoplane by an increase in the aspect ratio.

[9] By change in curvature of the wing is meant that if the flow were to be kept straight and the curvature changed, the forces on the wing would be changed exactly as they are on the actual wing owing to the change in the flow.—Tr.

The differential of this with reference to y, for the value of $y=o$, is, since then $r''=r$ and $r'''=h$

$$\left(\frac{dw}{dy_0}\right)=-\frac{\Gamma l_1}{4\pi r}\left(\frac{1}{r^2}+\frac{1}{h^2}\right).$$

the curvature sought is, then, according to equation (35),

$$\frac{1}{R}=\frac{\Gamma}{4\pi V}\frac{l_1}{r}\left(\frac{1}{r^2}+\frac{1}{h^2}\right) \tag{36}$$

Calculations of the preceding nature were made in 1912 by my assistant, A. Betz, so as to compare experiments with monoplanes and biplanes and to study the influence of different angles of attack and different degrees of stagger of the two wings of a biplane upon each other. The influence upon the drag was not known to us at that time, and the calculation was carried out so as to obtain the changes in the lift due to w, to v and to the curvature of the streamlines. In this connection the change of the lift of a monoplane when flying near the earth's surface was also deduced, by calculating the influence of the "mirrored wing" exactly as was that of the other wing of a biplane. All that was necessary was to change some algebraic signs, because the mirrored wing had negative lift. The theory of these calculations was given by Betz in the Z. F. M., 1914, page 253.

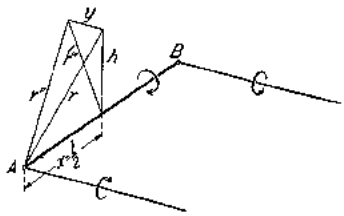

FIG. 41.—Curvature of wing-profile at its middle point due to velocities caused by transverse and tip vortices.

The results of the theory of Betz, from a more modern standpoint, such as adopted here, were given in the Technische Berichte, volume I, page 103 et seq. There one can find the discussion requisite for the treatment of the most general case of a biplane having different spans of the two wings and with any stagger. In the case of great stagger it appears, for example, that the forward wing is in an ascending air current caused by the rear wing; the latter is in an intensified descending current due to the forward wing and the vortices flowing off from it. Corresponding to this, if the angle of attack is unchanged, the lift of the forward wing is increased, and that of the rear one weakened; at the same time the ratio $\frac{\text{Drag}}{\text{Lift}}$ experiences a decrease for the forward wing and a marked increase for the rear one.

For a wing in the neighborhood of the ground, owing to the influence of v there is a decrease of lift, and conversely there is an increase of lift due to the influence of w, provided the angle of attack is kept constant, but as the result an evident decrease in the ratio $\frac{\text{Drag}}{\text{Lift}}$. Owing to this last it is seen why in the early days of aeronautics many machines could fly only near the ground and could not rise far from it. Their low-powered engines were strong enough to overcome the diminished drag near the ground but not that in free air.

D. THEORY OF THE MONOPLANE.

20. If we extend the principles, which up to this point have been applied to the influence of one wing upon another, to the effect upon a single wing of its own vortices, it can be said in advance that one would expect to find in that case effects similar to those shown in the influence of one wing of a biplane upon the other, i. e., the existence of lift presupposes a descending flow in the neighborhood of the wing, owing to which the angle of attack is made greater and the drag is increased, both the more so the closer to the middle the vortices flowing off at the ends are, i. e., the smaller the aspect ratio is. One might propose to apply the theory previously given for biplanes by making in the formulas of this theory the gap equal to zero. Apart from the fact that the formulas developed do not hold for the immediate neighborhood of the vortex-producing wing, but must be replaced by more accurate ones, this certainly is not the proper path to follow, for, in the earlier treatment, we have taken the undisturbed monoplane as the object with which other cases are to be compared and have asked what drag, what change in angle of attack, etc., are caused by adding a second wing to this monoplane. To proceed

according to the same method, we must seek for the theory of monoplanes another suitable object of comparison. As such, the infinitely long wing will serve. Where the discussion previously was about change of angle of attack, increase of drag, etc., we intend now to refer these to the infinitely long wing as a starting point. Since in the theoretical nonviscous flow the infinitely long wing experiences no drag, the total drag of such a wing in such a fluid must be due to vortices amenable to our calculations, as the following treatment will show. In a viscous fluid drag will arise for both wings, infinitely long or not, which for those angles of attack for which the profile is said to be "good" is, according to the results of experiment, of the order of magnitude of the frictional resistance of a plane surface.

The carrying out of this problem is accompanied with greater difficulties than the calculation for a biplane as given. In order to obtain the necessary assistance for the solution of the problem, we shall first be obliged to improve the accuracy of our picture of the vortex system.

The density of the lift (lift per unit length) is not constant over the whole span, but in general falls off gradually from a maximum at the middle nearly to zero at the ends. In accordance with what has been proved, there corresponds to this a circulation decreasing from within outward. Therefore, according to the theorem that by the displacement of the closed curve the circulation Γ can change only if a corresponding quantity of vortex filaments are cut, we must assume that vortex filaments proceed off from the trailing edge wherever Γ changes. For a portion of this edge of length dx the vortex strength is therefore to be written $\frac{d\Gamma}{dx}dx$, and hence per unit length of the edge is $\frac{d\Gamma}{dx}$. These vortex filaments flowing off, closely side by side, form, taken as a whole, a surface-like figure, which we shall call a "vortex ribbon."

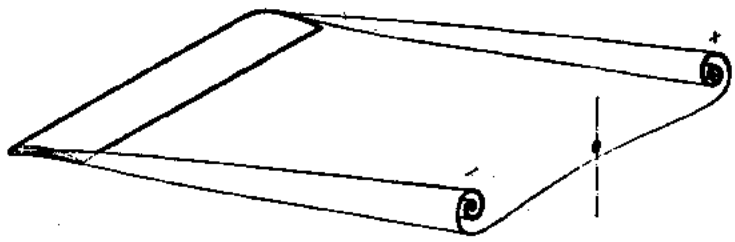

FIG. 42.—Change in shape of vortex ribbons at great distances behind the wing.

For an understanding of this vortex ribbon we can also approach the subject from an entirely different side. Let us consider the flow in the immediate neighborhood of the surface of the wing. Since the excess in pressure below the wing and the depression above it must vanish as one goes beyond the side edges of the wing in any manner, there must be a fall in pressure near these edges, which is directed outward on the lower side of the wing and inward on the upper. The oncoming flow, under the action of this pressure drop, while it passes along the wing, will receive on the lower side an additional component outward, on the upper side, one inward, which does not vanish later. If we assume that at the trailing edge the flow is completely closed again, as is the case in nonviscous flow, we will therefore have a difference in direction between the upper and lower flow; the upper one has a relative velocity inward with reference to the lower one, and this is perpendicular to the mean velocity, since on account of the Bernouilli equation in the absence of a pressure difference between the two layers the numerical values of their velocities must be the same. This relative velocity of the two flows is exactly the result of the surface distribution of vortices mentioned above (as the vortex theory proves, a surface distribution of vortices always means a discontinuity of velocity between the regions lying on the two sides of the surface). The relative velocity is the greater, the greater the sidewise pressure drop, i. e., the greater the sidewise change in lift. The picture thus obtained agrees in all respects with the former one.

21. The strengths of our vortex ribbon remain unchanged during the whole flight, yet the separate parts of the ribbon influence each other, and there takes place, somewhat as is shown in figure 42, a gradual rolling up of the ribbon, as a closer examination proves. An exact theoretical investigation of this phenomenon is not possible at this time; it can only be said that the two halves of the vortex ribbon become concentrated more and more, and that finally at great distances from the wing there remain a pair of vortices with rather weak cores.

For the practical problem, which chiefly concerns us, namely, to study the reaction of the vortices upon the wing, it is not necessary to know these changes going on at a great distance, for the parts of the vortex system nearest the wing will exercise the greatest influence. We shall therefore not consider the gradual transformation of the vortex ribbon, and, in order to make the matter quite simple, we shall make the calculation as if all the vortex filaments were running off behind in straight lines opposite to the direction of flight. It will be seen that, with this assumption, the calculations may be carried out and that they furnish a theory of the monoplane which is very useful and capable of giving assistance in various ways.

If we wish to establish the method referred to with greater mathematical rigor, we can proceed as follows: Since the complete problem is to be developed taking into account all circumstances, we shall limit ourselves to the case of a very small lift and shall systematically carry through all calculations in such a manner that only the lowest power of the lift is retained, all higher powers being neglected. The motion of the vortex ribbon itself is proportional to the total circulation, therefore also proportional to the lift; it is therefore small if the lift is small. If the velocities caused by the vortex ribbon are calculated, first for the ribbon in its actual form, then for the ribbon simplified in the manner mentioned, the difference for the two distributions will be small compared with the values of the velocity, therefore small of the second order, i. e., small as the square of the circulation. We shall therefore neglect the difference. Considerations of this kind are capable of deciding in every case what actions should be taken into account and what ones may be neglected. By our simplifications we have therefore made the problem linear, as a mathematician says, and by this fact we have made its solution possible. It must be considered a specially fortunate circumstance that, even with the greatest values of the lift that actually occur with the usual aspect ratios, the independent motion of the vortex ribbon is still fairly small, so that, in the sense of this theory, all lifts which are met in practice may still be regarded as small. For surfaces having large chords, as, for instance, a square, this no longer holds. In this case there are, in addition, other reasons which prove that our theory is no longer sufficiently accurate. This will be shown in the next paragraph.

It has already been mentioned that the infinitely long wing will serve as an object of comparison for the theory of the monoplane. We shall formulate this now more exactly by saying: Every separate section of the wing of length dx shall bear the same relation to the modified flow due to the vortex system as does a corresponding element of an infinitely long wing to the rectilinear flow. The additional velocities caused by the vortex system vary from place to place and also vary in the direction of the chord of the wing, so that again we have to do with an influence of curvature. This influence is in practice not very great and will for the sake of simplicity be neglected. This is specially allowable with wings whose chords are small in comparison with their spans, i. e., with those of large aspect ratio. If one wishes to express with mathematical exactness this simplifying assumption, it can be said that the theory of an actual wing of finite chord is not developed, but rather that of a "lifting line." It is clear that a wing of aspect ratio 1:6 may be approximated by a lifting line, specially if one considers that actually the lift is concentrated for the greatest part in a region nearer the leading edge. It is easily seen, however, that a surface in the form of a square can be approximated only poorly by a lifting line.

If we assume a straight lifting line, which lies in a plane perpendicular to the direction of flight, the flow due to the vortices, which according to the Biot-Sarvart law, is caused by its own elements, will not produce any velocities at the lifting line itself except the circulation flow around it, which would also be present for an infinitely long lifting line having the same circulation as at the point observed. All disturbance velocities at a point of the lifting line, which are to be looked upon as deviations from the infinitely long lifting line, are due therefore to the vortices which run off and hence can be calculated easily by an integration.

A qualitative consideration of the distribution to be expected for the disturbance velocities along our lifting line shows at once that—just as was the case for a biplane—the chief thing is the production of a descending current of air by the vortices. If we wish to retain the lift of the same intensity as with the infinite wing, the angle of attack must be increased, since the descend-

ing air stream added to the wind due to flight causes a velocity obliquely downward. In addition, the air force, as before, must be turned through the same angle, so that a drag results. The rotation will be the greater, the greater the lift and the closer to the middle of the wing the main production of vortices is. The drag must therefore increase both with increasing lift and with decreasing span.

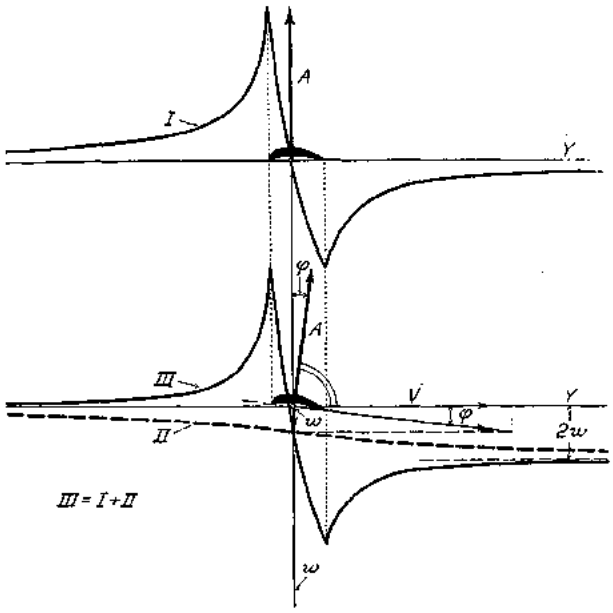

FIG. 43.—Wing having finite, but small, chord. Distribution of vertical velocity component along a line parallel to direction of flight.
I. Infinitely long wing.
II. The downward velocity produced by vortices flowing off.
III. Finite wing, sum of I and II.

A picture of what occurs with a wing of finite but small chord is given in figure 43. There the change is shown of the vertical velocity component along a straight line parallel to the direction of flight through the middle of the wing; in the upper part of the diagram, for the infinitely long wing, in the lower part, for the finite wing. We see from Curve I the rising flow in front of the wing, its transformation into a descending one at the wing itself and the gradual damping of the descending component due to the upward pressure drop behind the wing. (See sec. 15.) The corresponding curve for the finite wing is Curve III. It is derived from I by adding to the latter the descending velocity II. We recognize the rotation of the profile as well as that of the lifting force, which was originally perpendicular, through the angle φ where $\tan \varphi = \frac{w}{v}$ and w is the velocity downward at the location of the center of pressure (i. e., at the lifting line). If we follow the method of Lanchester, as described in section 15, the downward velocity w can also be looked upon as a diminution of the ascending flow at the leading edge of the wind due to the absence of the sidewise prolongation of the wing, i. e., to the deviation from an infinitely long wing which was the basis of the treatment in section 15. Discussions very similar to this are given in Lanchester, Volume I, section 117.

It may be seen from the figure that at great distances behind the wing the descending velocity is $2w$, which agrees with the relation already mentioned that the velocities due to a straight vortex filament extending to infinity in both directions are twice those due to a filament extending to infinity in one direction only, for points in the plane perpendicular to this vortex passing through its end point.

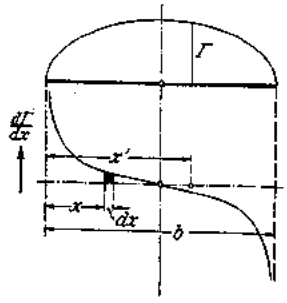

FIG. 44.—Velocity at a point x' due to vortex leaving wing at point x.

22. The mathematical processes involved in carrying out the theory outlined above become the most simplified if one considers as known the law, according to which the lift is distributed over the wing. We shall call this the "first problem." The calculation is made as follows: The distribution of lift is the circulation expressed as a function of the abscissa x. The strength of the vortex filament leaving an infinitely small section dx is then $\frac{d\Gamma}{dx} \cdot dx$. This produces at a point x', according to what has been already explained, a vertical velocity downward or upward of the amount

$$dw = \frac{1}{4\pi} \cdot \frac{d\Gamma}{dx} \cdot \frac{dx}{x' - x}$$

In this $x'-x$ takes the place of r in section 8. If the circulation falls to zero at the ends of the wing, as is actually the case, then all the vortices leaving the wing are of this kind. The whole added velocity at the position x', assuming that the function $\Gamma(x)$ is everywhere continuous, is

$$w=\frac{1}{4\pi}\int_0^b \frac{d\Gamma}{dx}\cdot\frac{dx}{x'-x} \tag{37}$$

We must take the so-called "chief value" of the integral, which is indeterminate at the point $x=x'$, i. e., the limiting value

$$\lim_{\epsilon\to 0}\left(\int_0^{x'-\epsilon}+\int_{x'+\epsilon}^b\right)$$

must be formed, as a closer examination shows. We can do this by calculating, instead of the value of the velocity at the lifting line, which is determined by the preponderating influence of the nearest elements, the value of w for a point a little above or below the lifting line. It is seen that this last is not indeterminate and that by passing to a zero distance from the lifting line it reaches the above limit. Concerning this excursus, important in itself, the preceding brief remarks may be sufficient.

After the calculation of the integral of (37), the downward velocity is known as a function of the abscissa x' (which we later shall call x). We then also know the inclination of the resultant air flow, $\tan\varphi=\frac{w}{V}$; the lift $dA=\rho\,\Gamma V\,dx'$, acting on the section dx', therefore contributes to the value of the drag

$$dW=\tan\varphi\cdot dA=\rho\Gamma(x')\cdot w(x')\,dx'$$

since it is inclined backward by the small angle φ. The total drag is therefore

$$W=\rho\int_0^b \Gamma(x')\cdot w(x')\cdot dx'=\frac{\rho}{4\pi}\int_0^b\int_0^b \frac{\Gamma(x')\frac{d\Gamma}{dx}dx\,dx'}{x'-x} \tag{38}$$

For a long time it was difficult to find suitable functions to express the distribution of lift, from which a plausible distribution of w would be obtained by equation (37). After various attempts it was found that a distribution of lift over the span according to a half ellipse gave the desired solution. According to this, if the origin of coordinates is taken at the center of the wing,

$$\Gamma=\Gamma_0\sqrt{1-\left(\frac{x}{b/2}\right)^2},\ \text{hence}\ \frac{d\Gamma}{dx}=\frac{-\Gamma_0 x}{\frac{b}{2}\sqrt{\left(\frac{b}{2}\right)^2-x^2}}$$

The "chief value" of the integral

$$\int^{+} \frac{t\,dt}{(t'-t)\sqrt{1-t^2}}\ \text{is equal to}\ \pi$$

and therefore the integral of equation (37) is equal to $\frac{\Gamma_0\pi}{b/2}$, and thus is independent of x' and constant over the whole span. Hence

$$w=\frac{\Gamma_0}{2b}$$

The value of Γ_0 is obtained from

$$A=\rho V\int_{-b/2}^{+b/2}\Gamma dx=\rho V\Gamma_0\int_{-b/2}^{+b/2}\sqrt{1-\frac{x}{b/2}}\cdot dx=\rho V\,\Gamma_0\frac{\pi}{4}\,b,$$

giving

$$\Gamma_0=\frac{4A}{\pi\rho V b}.$$

Hence

$$w=\frac{2A}{\pi\rho V b^2} \tag{39}$$

Since w is constant there is no need of calculating the drag by an integral, for it is simply

$$W=\frac{w}{V}A=\frac{2A^2}{\pi\rho V^2 b^2}=\frac{A^2}{\pi q b^2} \tag{40}$$

The calculation can also be performed for distributions of circulation given by the following general formula:

$$\Gamma = \sqrt{1-\xi^2}\ (\Gamma_0 + \Gamma_2 \xi^2 + \Gamma_4 \xi^4 + \ldots) \tag{41}$$

in which $\xi = \frac{x}{b/2}$.

According to the calculations of A. Betz

$$w = \frac{1}{2b} \Sigma n \left\{ \Gamma_{2n} \sum_{m=0}^{m=n} \xi^{2m} [(2n+1)\, p_{n-m} - 2n p_{n-m-1}] \right\} \tag{42}$$

and

$$W = \frac{\pi \rho}{4} \Sigma_i\ \Sigma_k \left\{ \Gamma_{2i}\ \Gamma_{2k} \sum_{m=0}^{m=k} q_{i+m} [(2k+1)\ p_{k-m} - 2k p_{k-m-1}] \right\} \tag{43}$$

in which the numbers p and q have the meaning

$$p_n = \frac{1.3 \ldots .(2n-1)}{2.4 \ldots . 2n};\quad q_n = \frac{p_n}{2_n+2},\quad p_0 = 1,\ p_{-1} = o$$

The elliptical distribution of lift, apart from its simplicity, has obtained a special meaning from the fact that the drag as calculated from equation (40) proved to be the smallest drag that is imaginable for a monoplane having given values of the total lift, the span and the velocity. The proof of this will be given later.

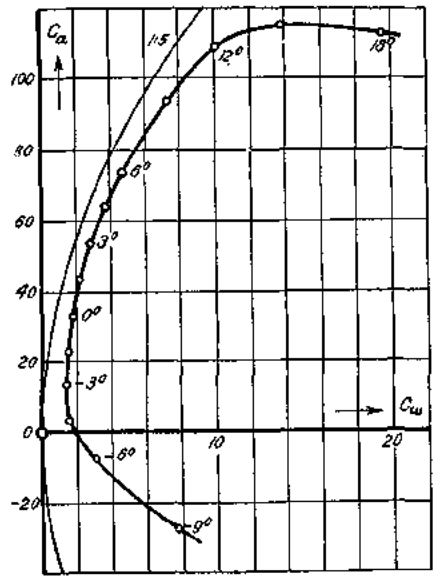

FIG. 45.—Polar diagram showing theoretical drag and observed drag.

It was desirable to compare this theoretical minimum drag with the drags actually obtained. As far back as 1913 this was done, but, on account of the poor quality of the profiles then investigated, all that was done was to establish that the actual drag was greater than the theoretical. Later (1915) it was shown, upon the investigation of good profiles, that the theoretical drag corresponds very closely to the relation giving the change of the observed drag as a function of the lift. If we plot in the usual manner the theoretical drag, as given in formula (40) as a function of the corresponding lift, we obtain a parabola, which runs parallel with the measured "polar curve" through the entire region for which the profile is good. (See fig. 45.)

This process was repeated for wings of different aspect ratios, and it was proved that for one and the same profile the difference between the measured and the theoretical drags for one and the same value of the lift coefficient had almost identically the same value in all cases.

This part of the drag depends, however, upon the shape of the profile, and we have therefore called it "profile drag." The part of the drag obtained from theory is called "edge drag," since it depends upon the phenomena at the edges of the wings. More justifiably the expression "induced drag" is used, since in fact the phenomena with the wings are to a high degree analogous to the induction phenomena observed with electric conductors.

Owing to this fact that the profile drag is independent of the aspect ratio, it became possible from a knowledge of the actual drag for one aspect ratio to calculate it for another. To do this, we pass from the formula (40) for the drag to the dimensionless lift and drag coefficients, by letting $\frac{A}{Fq} = c_a$ and $\frac{W}{Fq} = c_w$: we obtain then for the coefficient of the induced drag the relation

$$c_{wi} = \frac{c_a^2 F}{\pi b^2} \tag{44}$$

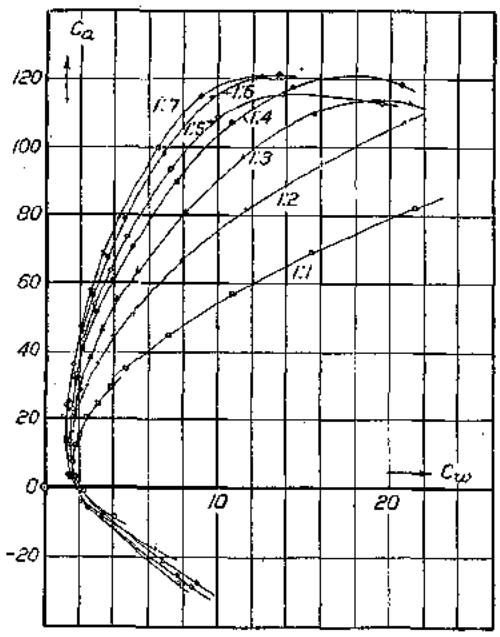

FIG. 46.—Polar diagrams for seven wings, aspect ratios 1:7, 1:6, etc., 1:1.

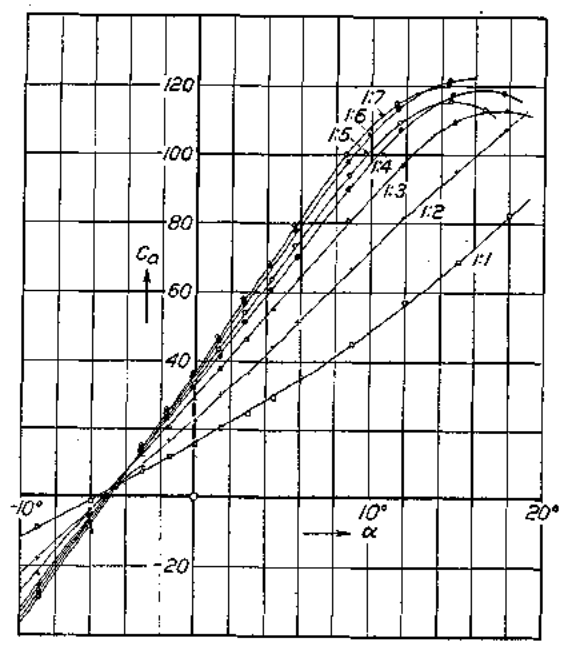

FIG. 47.—Lift coefficients plotted as function of angle of attack for aspect ratios 1:7 to 1:1.

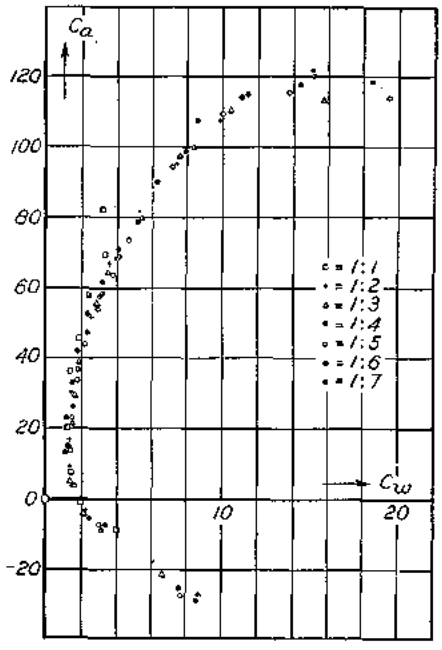

FIG. 48.—Polar diagrams reduced from observations on aspect ratio 1:5.

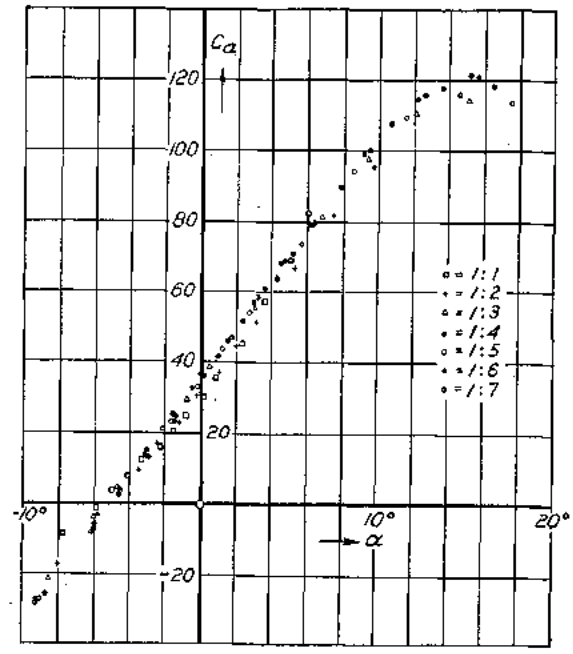

FIG. 49.—Lift coefficients as function of angle of attack, reduced for aspect ratio 1:5.

20167—23——13

The profile drag may then be written $c_{wo}=c_w-c_{wi}$. If this drag coefficient depends only upon the lift coefficient, then it would be evident, since it would be the difference between the measured and the theoretical drag coefficients, that, for the polar curves of two different wings having $c_{a1}=c_{a2}=c_a$,

$$c_{w1}-\frac{c_a^2F_1}{\pi b_1^2}=c_{w2}-\frac{c_a^2F_2}{\pi b_2^2},$$

and therefore

$$c_{w2}=c_{w1}+\frac{c_a^2}{\pi}\left(\frac{F_2}{b_2^2}-\frac{F_1}{b_1^2}\right) \tag{45}$$

In a similar manner a calculation for the angle of attack may be made if we presuppose an elliptical distribution of lift. According to our assumption there is a close connection between the lift of the separate elements of the wing and the "effective" angle of attack, which is the same as the angle of attack of an infinitely long wing. This effective angle of attack, according to our earlier considerations, is the angle of attack of the chord with reference to the resultant air current. It is therefore $\alpha'=\alpha-\phi$. If we substitute $\tan\phi=\frac{w}{V}$ for ϕ, and introduce in equation (39) again the lift coefficient, instead of using the lift, we obtain for the comparison of two wings, expressing the fact that the effective angle of attack is to be the same for two equal lift coefficients, the relation

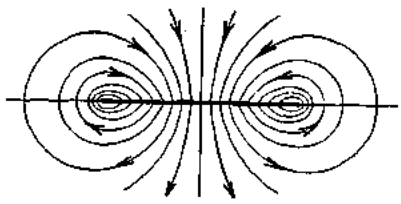

FIG. 40a.—Uniplanar flow in case of elliptic distribution of lift on a lifting line.

$$\alpha_1-\frac{c_a}{\pi}\frac{F_1}{b_1^2}=\alpha_2-\frac{c_a}{\pi}\frac{F_2}{b_2^2},$$

which leads to the transformation formula

$$\alpha_2=\alpha_1+\frac{c_a}{\pi}\left(\frac{F_2}{b_2^2}-\frac{F_1}{b_1^2}\right) \tag{46}$$

These formulas have been found to hold for distributions of lift which do not deviate too much from elliptical ones, although strictly speaking they apply only to the latter. The fact that the type of distribution does not have a marked effect is based upon the consideration that both in the calculation of drag and in that of the mean effective angles of attack we are concerned with average results. For the calculation of the drag one can also introduce the thought that no quantity varies much in the neighborhood of its minimum. Closer investigation of the square cornered wing has shown that, if the aspect ratio is not too small, the lift distribution does not deviate greatly from the elliptic type, and that the theoretical drag for usual aspect ratios at the most is 5 per cent greater than for the elliptic distribution. As an example of these formulas we shall take four figures from the book published by the Göttingen Institute (Ergebnisse der Aerodynamischen Versuchsanstalt, 1, Lieferung, 1921). The first and second figures show the polar curves, and the connection between lift coefficient and angle of incidence for seven wings of aspect ratio[10] 1:7 to 1:1. The last two figures give the results of calculating these experimental quantities from the results for the wing having the aspect ratio 1:5. It is seen that, apart from the aspect ratios 1:1 and 1:2 practically no deviations are present. The fact that the square can not be correctly deduced from the aspect ratio 1:5 need not excite surprise, since the theory was developed from the concept of the lifting line, and a square or a wing of aspect ratio 1:2 can scarcely be properly approximated by a lifting line. On the other hand it is a matter of surprise that an aspect ratio of 1:3 can be sufficiently approximated by the imaginary construction of a lifting line. The deviations in the case of the square are moreover in the direction one would expect from a lift distribution expanded over the chord. A quantitative theory is not available in any case at the present time.

23. If the lift distribution is not given, but, for example, the downward velocity, then the method of treatment followed hitherto may be used, by developing the downward velocity in a power series and determining the constants of the series given above for the lift from the constants

[10] The American practice is to define aspect ratio as the ratio of span to chord, which would involve taking the reciprocals of the ratios given in the text. Tr.

of this power series, by the solution of linear equations. By this the lift distribution and everything else are known.

Another method for the solution of this "second problem" will be obtained by the following consideration: The velocities at a distance behind the wing, on account of the connection mentioned so often between a vortex filament extending to infinity in one direction only and one extending to infinity in both directions, are twice as great as those in the cross section of the lifting line, if we do not take into account the change in shape of the vortex ribbon. We therefore have here, neglecting this change in shape, an illustration of a two-dimensional fluid flow (uniplanar flow), for which the vertical velocity components at the point where the wing is reached are specified. For the simple case that the vertical velocity w is constant, as was found to be true for the elliptical lift distribution, the shape of the flow that arises has been known for a long time. It is given in figure 49a. It is the same as that already considered, in another connection, in section 15. The picture of the streamlines show clearly the velocity discontinuity between the upper and lower sides of the vortex ribbon, indicated by the nick in the streamlines, and also the vortical motion around the two extreme points of the vortex ribbon, corresponding to the ends of the wing.

Any problems of this kind can therefore be solved by means of the methods provided by the potential theory for the corresponding problem of two-dimensional fluid flow. We can not go into these matters more closely at this time; by a later opportunity some special relations will be discussed, however.

A "third problem" consists in determining the lift distribution for a definite wing having a given shape and given angle of attack. This problem, as may be imagined, was the first we proposed; its solution has taken the longest, since it leads to an integral which is awkward to handle. Dr. Betz in 1919 succeeded after very great efforts in solving it for the case of a square-cornered wing having everywhere the same profile and the same angle of attack. The way the solution was obtained may be indicated briefly here. We start, as before, from the relation

$$\alpha = \alpha' + \phi \cong \alpha' + \frac{w}{V}$$

By equation (37) w is expressed in terms of the circulation. The effective angle of attack α' can be expressed in terms of Γ, since, according to the assumptions made before the lift, distribution, which is proportional to Γ, depends directly upon α'. The relation between α' and Γ can be assumed to be given sufficiently exactly for our purposes by a linear expression

$$\Gamma = Vt\,(c_1\,\alpha' + c_2) \tag{47}$$

in which t is the length of the chord (measured in the direction of flight). By the introduction of the factor Vt, c_1 and c_2 are made pure numbers. The numerical value of c_1, which is the more important, can be expressed, if c_{a_∞} is the lift coefficient for the infinitely long wing at the angle of attack α', by the relation

$$c_1 = \frac{1}{2}\,\frac{dc_{a_\infty}}{d\alpha'}$$

In fact

$$c_{a_\infty} = \frac{A}{Fq} = \frac{\rho\,\Gamma V l}{lt \cdot \frac{1}{2}\,\rho\,V^2} = \frac{2\Gamma}{Vt} = 2\,(c_1\alpha' + c_2)$$

For a flat-plate theory proves that $c_1 = \pi$, for curved wings it has a slightly greater value.

If, according to what has gone before, we express α' by Γ and w by $\frac{d\Gamma}{dx}$ and write

$$\frac{d\Gamma}{dx} = f(x) \text{ and therefore } \Gamma = \int_0^x f(x)\,dx$$

we obtain after a simple calculation the integral equation

$$\int_0^x f(x)\,dx + \frac{c_1 t}{4\pi}\int_0^b \frac{f(x')\,dx'}{x - x'} = Vt\,(c_1\alpha + c_2) = \text{const.} \tag{48}$$

A solution of this equation can be obtained by expanding Γ as in equation (41) and developing then all the expressions in power series of $\xi=\frac{x}{b/2}$. For every power of ξ there is then a linear equation between the quantities Γ_0, Γ_2, etc. There is a system of equations, then, with an indefinite number of equations for an infinite number of unknowns, the solution of which in this form is not yet possible. The aspect ratio of the wing appears in these equations as a parameter, and it is clear that the solution for a small aspect ratio, i. e., $\frac{b}{t}$ is easier than for a large one. Dr. Betz proved that a development in powers can be made for the unknowns in terms of a parameter containing the aspect ratio. The calculations which are contained in the dissertation[11] of Dr. Betz (1919) are very complicated and can not be reproduced here; but certain results will be mentioned. The Betz parameter L has the meaning

$$L=\frac{2b}{c_1 t}=\frac{4b}{t}\frac{d\alpha'}{dc_{a\infty}}$$

In the application to surfaces which are investigated in wind tunnels the value $\frac{dc_a}{d\alpha}$ is known, not $\frac{dc_{a\infty}}{d\alpha'}$. For this case theory gives a relation which can be expressed approximately

$$L\cong 3.85\,\frac{b}{t}\,\frac{d\alpha}{dc_a}-1.3.$$

We can thus obtain the value of $\frac{d\alpha'}{dc_{a\infty}}$ from the connection mentioned.

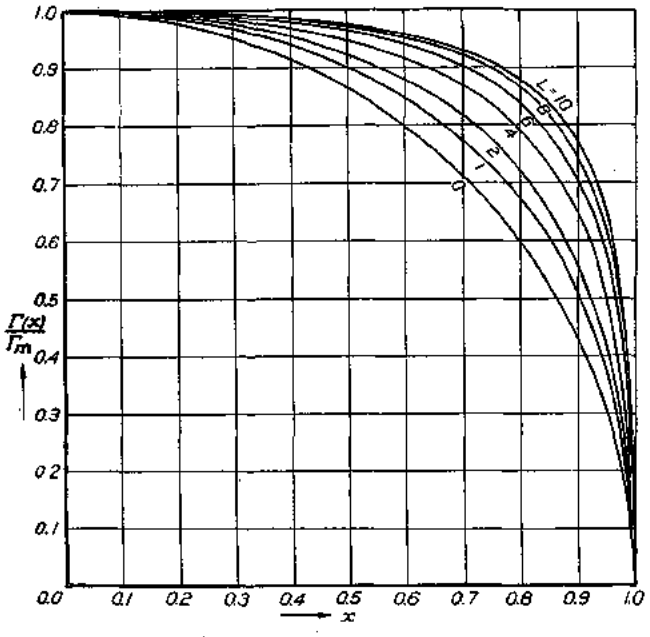

FIG. 50.—Change in distribution of lift, as a function of L, the parameter of Betz.

The distribution of lift density ever the span is elliptical for very small aspect ratios and for greater ratios becomes more and more uniform; for very elongated wings it approaches gradually a rectangular distribution. Figure 50 shows this change in the distribution depending upon L.

The drag of the wing with the rectangular distribution is greater naturally than with the elliptic distribution, since this gives the minimum of drag, yet the differences are not very great; for instance, for $L=4$, $\left(\frac{b}{t}\cong 6\right)$ it is about 5 per cent greater than that of the elliptical distribution. An approximation formula, according to the values obtained by Betz, is

$$W\cong\frac{A^2}{\pi q b^2}(0.99+0.015\,L).$$

This is applicable for values of L between 1 and 10.

The distribution of lift, downward velocity, and drag upon a very elongated wing is shown qualitatively in figure 51. It is seen that the downward velocity and the drag gradually accumulate at the ends of the wing. This gives also the correct transition to an infinitely long wing, with which for interior positions the lift is constant, and the downward velocity and the drag are equal to zero, while, as we know, near the ends these last quantities always assume finite values.

[11] Printed in extracts in Heft 2 of the "Berichte u. Abhl. der Wiss. Ges. f. Luftf." Munich, 1920 (R. Oldenbourg).

E. IMPROVED THEORY OF AIRPLANES HAVING MORE THAN ONE WING.

24. The knowledge obtained in the theory of a monoplane can be applied also to multiplanes and furnishes here a series of remarkable theorems. We shall limit ourselves to the theory of the first order, as designated in the theory of monoplanes, therefore we shall neglect the influences of v. Further, we shall not take into account the effect of curvature—i. e., we shall consider the separate wings replaced by "lifting lines." For the sake of simplicity we shall limit ourselves to multiplanes with wings which are straight and parallel to each other. The generalization of the theorems for nonparallel wings, corresponding to the deduction given in "Wing theory II," will then be stated without proof.

Let us first solve the introductory problem of calculating the vertical velocity w produced by a lifting line at a point A which lies off the lifting line. At the beginning let us assume that this point lies in the same "transverse plane" (plane perpendicular to the direction of flight). According to our assumption as to the location of A, the action of the transverse vortex is zero. With reference to the longitudinal vortices it is to be remembered that the velocity $\frac{1}{4\pi}\frac{d\Gamma}{dx}\cdot\frac{dx}{a}$ produced by a longitudinal vortex of strength $\frac{d\Gamma}{dx}dx$ is perpendicular to the line a (see fig. 52), and therefore must be multiplied by $\sin\beta$ to obtain the vertical component. We arrive at the downward velocity, therefore, by integrating over the lifting line, viz:

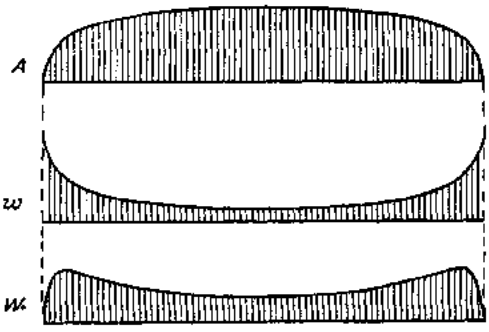

FIG. 51.—Distribution of lift, down-wash and drag for a long wing.

$$w=-\frac{1}{4\pi}\int_0^b\frac{d\Gamma}{dx}\left(\frac{\sin\beta}{a}\right)dx \tag{49}$$

This relation can be brought into another form by a partial integration. Since at both wing ends $\Gamma=o$, we have

$$w=\frac{1}{4\pi}\int_0^b\Gamma\frac{d}{dx}\left(\frac{\sin\beta}{a}\right)dx$$

But

$$\frac{d}{dx}\left(\frac{\sin\beta}{a}\right)=\frac{d}{dx}\left(\frac{z}{a^2}\right)=\frac{a^2-2x^2}{a^4}=\frac{1-2\sin^2\beta}{a^2}=\frac{\cos 2\beta}{a^2}$$

so that we have

$$w=\frac{1}{4\pi}\int_0^b\Gamma\frac{\cos 2\beta}{a^2}dx \tag{50}$$

With the aid of this relation we can write down immediately the value of the drag which arises owing to a second wing being under the influence of the disturbance caused by the first wing lying in the same transverse plane. Let us call w_{12} the disturbance velocity at a point A on the second wing. According to the results of section 22, the drag then is

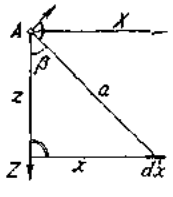

FIG. 52.—Velocity at a point A off the lifting line, but in the transverse plane, due to the vortex system.

$$W_{12}=\rho\int_0^{b_2}\Gamma_2 w_{12}dx$$

or, if the value of w_{12} as given by equation (50) is substituted,

$$W_{12}=\frac{\rho}{4\pi}\int_0^{b_1}\int_0^{b_2}\Gamma_1\Gamma_2\frac{\cos 2\beta}{a^2}dx_1dx_2 \tag{51}$$

The double integral, as one sees, is perfectly symmetrical in the quantities associated with both wings 1 and 2. We conclude from this that the drag which wing 1 experiences owing to the presence of wing 2 is of the same amount as the drag calculated here, that, therefore,

$$W_{12}=W_{21}.$$

In the more general case of two curved lifting lines lying in a transverse plane, a formula is obtained which differs from equation (51) only in having cos $(\beta_1+\beta_2)$ in place of cos 2β in which β_1 and β_2 are the angles which the line a makes with the normals on the two lifting elements connected by a, and in having $ds_1 ds_2$ in place of $dx_1 dx_2$. The relation $W_{12}=W_{21}$ therefore holds in this case also. This mutual relation, which was discovered in a different manner by my assistant, Dr. Munk, is of importance in various applications. Since it plainly is not necessary for the lifting elements taken as a whole to belong to a single surface, the theorem may be stated:

If, out of a lifting system all of whose elements lie in a transverse plane any two groups are selected, the portion of the drag experienced by group 1 due to the velocity field of group 2 is exactly of the same amount as that experienced by group 2 due to the velocity field of group 1.

We can interpret the partial integration performed above by saying that the velocity w appears by it as built up out of the contributions by merely infinitesimal wings having the length dx and the circulation Γ, while previously we have always built it up out of the actions of the separate vortices $\frac{d\Gamma}{dx}dx$. The integrand of equation (50) in fact agrees with the velocity which is caused by two vortex lines of equal but opposite strengths Γ lying at a distance dx apart. The double integral in equation (51) can, from this point of view, be looked upon as the sum of the actions of the vortex strips of all the elements dx_1 on all the lifting elements dx_2.

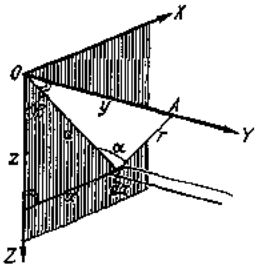

FIG. 53.—Velocity at a point A not in the transverse plane, due to the vortex system.

The objection might be raised that equations (50) and (51) cease to be applicable if the value $a=o$ appears, since this gives an expression of the form $\infty-\infty$. They are not, therefore, suited for the calculation of the velocity w at the wing itself. In this case we must return to equation (49), and take the "chief value" of the integral; or, the value of w_{12} and of W_{12} for a lifting line that lies very close must be calculated, and then we can obtain our final result by passing to the limit for coinciding lifting lines. As is seen from this, the relations $W_{12}=W_{21}$ hold also for lifting lines coinciding in space, which, besides, may have any arbitrary lift distribution.

The mutual drag need not, as has already been mentioned, always be positive. For instance, it is negative for two wings placed side by side, since then each wing is in an ascending current caused by the other, and the total drag is therefore less than the sum of the mutual drags which each of the wings would have at a greater distance apart. The behavior of certain birds which in a common flight space themselves in a regular phalanx can be explained by reference to this.

25. In order to be able to treat the case of staggered wing systems, the next problem is to calculate the velocity field due to a lifting element of the length dx together with its pair of vortices at a point A which may now lie off the transverse plane, and at a distance y from it. (See fig. 53.) The origin of coordinates will be taken at the projection of the point A upon the transverse plane, and the X axis parallel to the direction of the element. Using the abbreviations

$$a^2=x^2+z^2,\ r^2=a^2+y^2,$$

the velocity produced at the point A by one of the two vortices, by formula (6b), is given by $\frac{\Gamma}{4\pi a}\left(1+\frac{y}{r}\right)$; the component in the direction of the Z axis, to which we here again limit ourselves, is, then, putting $\sin\beta=\frac{x}{a}$.

$$w_1=\frac{\Gamma x}{4\pi a^2}\left(1+\frac{y}{r}\right)$$

The pair of vortices produces then a velocity which may be written as the difference of the effects of two vortices which are close together:

$$dw_1=\frac{\partial w_1}{\partial x}dx=\frac{\Gamma dx}{4\pi}\left[\left\{\frac{a^2-2x^2}{a^4}\left(1+\frac{y}{r}\right)-\frac{x^2y}{a^2r^3}\right\}\right]$$

To this must be added the contribution of the transverse vortex

$$dw_2 = \frac{\Gamma dx \cdot y}{4\pi r^3}$$

The sum of these two velocities, if the two angles defined in figure 53 are introduced, amounts to

$$dw = \frac{\Gamma dx}{4\pi}\left\{\frac{\cos 2\beta}{a^2}(1+\sin\alpha)+\frac{\sin\alpha \cdot \cos^2\beta}{r^2}\right\} \tag{52}$$

With the help of this formula we can now calculate at once the drag experienced by a lifting element situated at the point A and parallel to the former, whose length is dx_2 and circulation Γ_2. If the first element is given the index 1, this drag is

$$d^2 W_{12} = \frac{\rho \Gamma_1 \Gamma_2 dx_1 dx_2}{4\pi}\left[\left\{\frac{\cos 2\beta}{a^2}(1+\sin\alpha)+\frac{\sin\alpha\cos^2\beta}{r^2}\right\}\right] \tag{53}$$

As is easily seen, the drag produced on the lifting element 1 by the lifting element 2 is obtained if in place of α and β the values $\alpha+\pi$ and $\beta+\pi$ are introduced. Therefore it is

$$d^2 W_{21} = \frac{\rho \Gamma_2 \Gamma_1 dx_2 dx_1}{4\pi}\left[\left\{\frac{\cos 2\beta}{a^2}(1-\sin\alpha)-\frac{\sin\alpha\cos^2\beta}{r^2}\right\}\right] \tag{53a}$$

It is seen from this that the two parts of the drag are equal only if $a=0$, that is if the two elements lie in the same transverse plane. Yet in the general case the sum $d^2 W_{12}+d^2 W_{21}$ is independent of a, therefore independent of the amount of stagger. The sum of the two mutual drags leads thus to the same formula as that already derived for nonstaggered wings. If we again pass to the general case of nonparallel lifting lines, in which again ds_1 and ds_2 are to be written in place of dx_1 and dx_2, we obtain as may be proved by performing the calculation, the relation

$$W_{12}+W_{21} = \frac{\rho}{2\pi}\int\int \frac{\Gamma_1 \Gamma_2 ds_1 ds_2 \cos(\beta_1+\beta_2)}{a^2} \tag{54}$$

As is evident, this sum remains unchanged if the two lifting groups are displaced in the direction of flight. Since the total drag of a lifting system is composed of such mutual drags as calculated above and of the proper drags of the separate wings, which likewise are not changed by a displacement of the wing in the direction of flight, the following theorem may be stated:

The total drag of any lifting system remains unchanged if the lifting elements are displaced in the direction of flight without changing their lift forces.

This "stagger theorem" was likewise proved by Munk. For a proper understanding of this theorem it must be mentioned expressly that, in the displacement of the separate lifting elements, their angles of attack must so be changed that the effective angles of attack and therefore the lifting forces remain unaltered.

This theorem, which at first sight is surprising, may also be proved from considerations of energy. Let us remember that, by the overcoming of the drag, work is done, and that in a nonviscous fluid, such as we everywhere assume, this work can not vanish. Its equivalent is, in fact, the kinetic energy that remains behind in the vortex motions in the rear of the lifting system. This energy depends only upon the character of these vortices, not upon the way in which they are produced. If we neglect, as we have throughout, any change in shape of the vortex system, then, in fact, the staggering of the separate parts of the lifting system can not have any influence upon the total drag.

26. For the practical calculation of the total drag of a multiplane, we have then the following: The total drag consists of the sum of all the separate drags and of as many mutual drags as there are combinations of the wings in twos. If the nature of the lift distribution over all the separate wings is specified, then the proper drags are proportional to the square of the separate lifts; the mutual drags, to the product of the lifts of the two wings in question. If the coefficients of this mixed quadratic expression are all known, then one can solve without difficulty the problem: For a specified total lift, to determine the distribution of lift over the separate wings which will make the total drag a minimum.

In order to know these coefficients to a certain degree I calculated them for the case of two straight lifting lines whose middle points lie in the same plane of symmetry, with the assumption that the lift over each separate wing is distributed according to a half ellipse. The results are given in my paper "The induced drag of multiplanes" in Volume III, part 7 of the Technische Berichte. For this purpose the velocity w for the entire neighborhood of a wing in the transverse plane was first calculated by formula (49), and then the integrals for the mutual drags were obtained by planimetry. To show the analogy with equation (40) this may now be expressed by the formula

$$W_{12}=\sigma\frac{A_1 A_2}{\pi q b_1 b_2} \tag{55}$$

by means of which the numerical factor σ can be expressed as a function of the two variables $\frac{h}{\frac{1}{2}(b_1+b_2)}$ and $\frac{b_2}{b_1}$. Calculation gave the following table:

TABLE I.—*Values of* σ

$\frac{2h}{b_1+b_2}$		0	0.05	0.1	0.15	0.2	0.3	0.4	0.5
$\frac{b_2}{b_1}=$	1.0	0.780	0.655	0.561	0.485	0.370	0.290	0.230
	.8	.690	.600	.523	.459	.355	.282	.225
	.6	.540	.485	.437	.394	.315	.255	.210

The curve of the function σ is given in figure 54. For the most important case, viz, for two wings of equal span, I have developed an approximation formula which is

$$\sigma=\frac{1-0.66\frac{h}{b}}{1.055+3.7\frac{h}{b}} \tag{56}$$

It may be used from $\frac{h}{b}=0.05$ to 0.5.

The total induced drag of a biplane is then, if b_1 is the greater span and if the ratio $\frac{b_2}{b_1}$ is designated by μ

$$W=W_{11}+2W_{12}+W_{22}=\frac{1}{\pi q b^2}(A_1^2+2\sigma\mu A_1 A_2+\mu^2 A_2^2) \tag{57}$$

Simple calculation shows that for a given A_1+A_2 this drag is a minimum for

$$A_2 : A_1=(\mu-\sigma) : \left(\frac{1}{\mu}-\sigma\right) \tag{58}$$

The value of the minimum is fouud to be

$$W_{\min}=\frac{(A_1+A_2)^2}{\pi q b_1^2}\cdot\frac{1-\sigma^2}{1-2\sigma\mu+\mu^2} \tag{59}$$

The first factor of this formula is the drag of a monoplane having the span b_1 and the lift A_1+A_2. Since $\sigma<\mu$, the second factor of the formula is always less than 1, i. e., the induced drag of a biplane is less than that of a monoplane which in the same span carries the same load. For a "tandem," i. e., an arrangement of two wings one behind the other, the stagger theorem shows an equivalence with two coinciding wings, i. e., a monoplane. Among the different biplanes having prescribed span b_1 and prescribed gap h, that one is the most favorable in which the second wing also has the span b_1. The most favorable ratio of the two lifts is then 1 : 1 and the second factor of equation (59) becomes equal to $\frac{1}{2}(1+\sigma)$.

These statements must not, however, be misunderstood; they refer only to the comparison of such wing systems as have the same value for the greatest span. Naturally, for every biplane a monoplane may be found with somewhat greater span than that of the biplane, which at the same total lift has the same induced drag as the biplane.

This last remark leads us to apply also to the biplane the deduction formulas obtained for monoplanes. All that is necessary is to replace the biplane of span b_1 by a monoplane of a somewhat greater span kb_1, which with reference to the drag—and, on the whole, with reference to the angle of attack—is equivalent to the biplane. If again we pass from the lift and drag to their coefficients c_a and c_w, the formula connecting the drags of any two lifting systems 1 and 2 is

$$c_{w_1} - c_{w_2} = \frac{c_a^2}{\pi}\left(\frac{F_1}{(k_1 b_1)^2} - \frac{F_2}{(k_2 b_2)^2}\right) \tag{60}$$

in which, as is easily seen, the factor k, for a biplane having the most favorable distribution of lift, is the reciprocal of the square root of the second factor in formula (59).

The tests of this formula with biplanes have shown that, when by giving a special shape to the wing the lift distribution was made elliptical, there was good agreement with the calculations from monoplane experiments; with biplanes having the usual square-cornered wings, on the other hand, there was a discrepancy, which is to be attributed to the fact that the lift distribution on these biplanes deviates too far from an elliptic one. We can, however, retain the same transformation formula if the factor k is determined empirically for every wing system; it is found to be somewhat smaller than according to the theory given above. The experiments on this point are not yet completed, so more accurate values can not as yet be given. The earlier Göttingen experiments were worked up by Dr. Munk, to whom this last idea is due, in the paper "Contribution to the aerodynamics of the lifting parts of airplanes" in the Technische Berichte, Volume II, page 187.

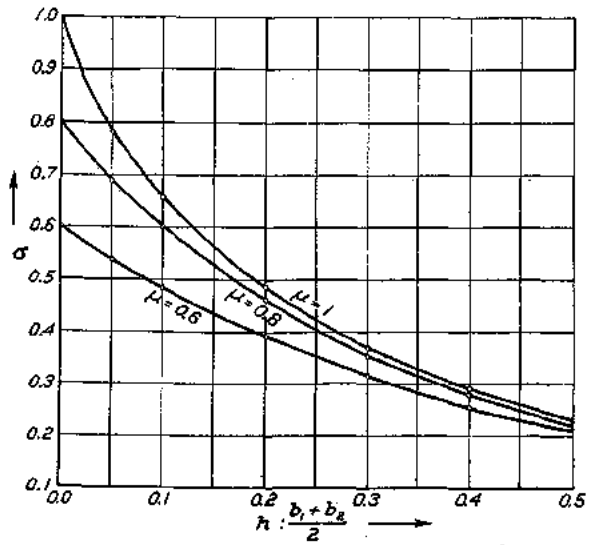

FIG. 54.—Curve of the function σ for biplanes whose span ratio, $\mu = \frac{b_2}{b_1}$, is varied.

27. In the previous section I have treated the problem of finding the minimum of the induced drag of a multiplane, under very definite assumptions concerning the distribution of lift over each separate wing. The strict minimum problem is however different, viz:

To determine for a given front view of a lifting system that distribution of lift over all the lifting elements which will make the induced drag a minimum for a specified total lift.

In this statement of the problem the expression "a given front view"—i. e., more exactly stated, a given projection of the lifting system upon a plane perpendicular to the direction of flight—is used to mean that the wing chord is of secondary consideration, and does not need to be determined until later when the selection of suitable angles of attack is made.

The general solution of this problem was also given by Dr. Munk. It will be deduced here in a simpler manner than that given in Munk's dissertation, where the solution was obtained by the calculus of variations. By means of the stagger theorem mentioned in section 25 the wing system will be referred back to the corresponding nonstaggered system. For this, as we showed, the relation $W_{12} = W_{21}$ holds. We shall now introduce—with the simplifying assumption that all the lifting elements are parallel to each other—a variation of the lift distribution by adding at any one place a lift δA and at the same time taking away an equal amount at some other place, so that on the whole the lift, which is prescribed, remains unchanged. We must now consider the change in the induced drag caused by this variation. If there is superimposed upon the lift distribution an additional air force δA distributed over a short portion dx, there arises therefrom, in addition to the drag proper of the added lift—which, however, if sufficiently small is of the second order—a mutual drag, because on the one hand the added lift finds itself

in a flow having the downward velocity w, which is due to the lifting system, and on the other the lifting system is in the velocity field of the added lift. The first of these two drags, as is easily seen, is $\delta A\frac{w}{V}$; the other part, according to our theorem, has the same value; so the total drag is twice this. What condition, now, must be satisfied by the sum of the mutual drags caused by our twofold change of the lift distribution in order to obtain the absolute minimum of the induced drag? The answer is, evidently, that we will have the minimum only if by no change of this kind can the drag be further diminished. The sum of the induced drags, therefore, can in no case be negative; also it may not be positive, because in that case by a reversal of the signs of the changes which we selected we could make the sum negative. Only the value zero is therefore allowable. Hence, if w is the vertical velocity at point 1 and w_2 that at point 2, we have the relation

$$\delta A_1\frac{w_1}{V}+\delta A_2\frac{w_2}{V}=o$$

and, therefore, since $\delta A_1=-\delta A_2$,

$$w_1=w_2.$$

Since this holds for all the lifting elements, we have obtained the answer. The lift distribution which in the given wing system, for a specified total lift, causes a minimum of drag is that which leads to the same downward velocity at all the lifting elements. With monoplanes the elliptical lift distribution leads to a constant downward velocity w. We recognize from this that the elliptical distribution in fact is that distribution of lift which causes the least drag for a monoplane.

The theorem can, besides, be extended easily to the case of nonparallel lifting elements lying in a transverse plane. If w_n is the velocity in the transverse plane perpendicular to the lifting element and ϵ is the angle between the direction of w_n and that of the given total lift, then, as may be shown without difficulty, $w_n=w_o\cos\epsilon$ for all the elements. (If $\epsilon=o$, and hence $\cos\epsilon=1$, the statement made above again appears.)

28. A way to solve the problem of finding the lift distribution for a prescribed distribution of the vertical velocity has been indicated already in section 23. The velocity field left behind in the air by the lifting surface is, approximately, according to the remark made before, a uniplanar flow around the vortex system produced by the lifting system in its motion, and this vortex system may be regarded, as a first approximation, as a solid body in the fluid. In the minimum case this figure, according to the results of section 27, moves like a *rigid* body, not alone in the case of parallel lifting elements, but also in the general case, for the general minimum condition, $w_n=w_o\cos\epsilon$, expresses directly that the normal velocity of the fluid at an element of the rigid figure moving in the direction of the lift coincides with the normal component of the velocity w_o of the rigid figure itself. The problem is thus reduced to a perfectly definite one treated in the hydrodynamics of uniplanar fluid motion.

This uniplanar flow can be brought into relation, in a specially clear manner, with the pressure distribution existing on the wing system. The wing system, during its motion along its path, imparts to one portion of the air after the other the velocities which we have learned to know as the result of the vortices flowing off from the wings. This transmission of velocity is the result of the spreading out of the pressure field of the wing system over the air particles one after another. In order to simplify the phenomenon for ourselves we can now imagine that these velocities are produced at the same moment by a sort of impulse phenomenon over the whole path of the lifting system. To produce this impulse it is necessary to have a solid figure of the shape of the geometrical region passed over by the lifting system (i. e., of the shape of the vortex surfaces which it leaves behind). If we are concerned with a system of least drag, this figure moves as a rigid body; otherwise it would also experience a change of shape due to the impulse. The final velocity w^* of the figure coincides with the motion of the vortex surfaces at a great distance from the lifting system, and is therefore to be put equal to $2w$. For a monoplane having elliptical distribution our figure is therefore an infinitely long flat plate of the breadth b.

By the production of the velocity during the impulselike acceleration an increase in the pressure p_1 arises below the plate (in the case of multiplanes, under each of the plates corresponding to the separate wings) and at the same time a decrease in pressure p_2 above the plate (or the plates). We can now compare in a very simple manner the total action of the pressure differences at each point of a plate during the time of the impulse with the total action of the pressure differences of the wing in its forward movement at the point of the medium in question. If the resulting motion is the same in both cases, then the pressure differences integrated through the proper times must have the same values. If in the impulse phenomenon lasting a time τ a portion of the fluid of length l is considered, and if therefore the action of the lift $\frac{dA}{dx}dx$ in the time $t=\frac{l}{V}$ required to pass over the length l is to be compared, the following relation must hold for the conditions on a strip of width dx:

$$ldx\int_0^\tau (p_1-p_2)dt=\frac{dA}{dx}dx\cdot\frac{l}{V} \tag{61}$$

A formula connected with our previous relations can be obtained by a transformation of the left-hand term. According to a known extension of the Bernouilli equation for accelerated motion we have

$$\rho\frac{\partial\Phi}{\partial t}+\frac{\rho v^2}{2}+p=f(t).$$

For our impulse phenomenon the arbitrary time function $f(t)$ is a constant, since at the points of the fluid lying far away from the impinging plate the pressure does not change. If the impulse is sufficiently quick, then during the short time of impulse τ the acceleration and the pressure differences will be very large, and therefore the term $\frac{\rho v^2}{2}$ may be neglected in comparison with the other two, since it itself does not exceed moderate values. We obtain therefore the simplified relation

$$\rho\frac{\partial\Phi}{\partial t}+p=\text{const.}=p_0$$

which, if at the beginning everything is at rest, ($\Phi_0=o$) may be integrated to

$$\rho\Phi=\int_0^\tau (p_0-p)dt \tag{62}$$

we can therefore write, in equation (61), the expression $\rho(\Phi_2-\Phi_1)$ in place of $\int_0^\tau (p_1-p_2)dt$. The potential differences $\Phi_2-\Phi_1$ which here appears is, according to the connection between potential and circulation (see sec. 5), nothing but the circulation Γ for a closed curve which passed around one edge of the vortex ribbon and intersects our vortex ribbon at x, the point considered. This circulation is again nothing but the circulation around the wing at the point x. If the factor ldx is omitted from both sides of equation (61), it takes, as a result of this transformation, the form

$$\frac{dA}{dx}=\rho(\Phi_2-\Phi_1)V=\rho V\Gamma \tag{63}$$

We have thus proved in an entirely independent way, as we see, the Kutta-Joukowski theorem for a wing element, which previously we took over, without proof, from the infinitely long wing.

The relations deduced in the previous paragraphs permit, in the case of a constant w, the formation of general theorems for w and W in place of (39) and (40). By integration of (63) the total lift is at once obtained

$$A=\rho V\Sigma\int(\Phi_2-\Phi_1)dx \tag{64}$$

The values of Φ in this formula are proportional to the velocity w^* of the vortex ribbon, that is, are dependent upon A. Quantities which are independent of A are derived if the potentials Φ are divided by w*. In this way we obtain the potentials for a velocity of the vortex

ribbon equal to 1. The potential, being the line integral of the velocity, has the dimension velocity times length; the potential ϕ for $w^*=1$ has therefore the dimension of a length, and hence

$$\Sigma\int(\phi_2-\phi_1)dx$$

is a surface, which will in what follows be called F', which depends only upon the geometrical properties of the projection of the wing system upon a plane perpendicular to the direction of flight, therefore upon the front view of the wing system; and which evidently for geometrically similar front views is proportional to the square of the span. By introducing F' into equation (64) we have, since $\Phi=\phi w^*$,

$$A=\rho V w^* F' \tag{65}$$

From this we may immediately deduce w^*, and thereby also the downward velocity at the point of the wing system

$$w=\frac{1}{2}w^*=\frac{A}{2\rho V F'} \tag{66}$$

If this value is introduced into the relation $W=\frac{w}{V}A$, we have

$$W=\frac{A^2}{2\rho V^2 F'}=\frac{A^2}{4qF'} \tag{67}$$

The evaluation in the manner of the flow of figure 49 gives a potential Φ, if the span of the wing is set equal to b, which has the value $\sqrt{(b/2)^2-x^2}$ at the plate. The geometrical expression of this value gives a circle having the span b as diameter, therefore $F'=\frac{\pi b^2}{4}$. Using this value formula (67) passes over in fact into formula (40).

It may also be noted that a uniform velocity can be superimposed upon the uniplanar flow here discussed, whose discontinuity in potential at the rigid figure representing the vortex ribbon causes the surface F', without thereby changing the relation for F', for the potential discontinuity between the lower and upper sides, with which we are here concerned, is not changed by the superimposed uniform motion. We may now choose the velocity of the uniform motion exactly opposite and equal to the velocity w^* of the rigid figure, and thereby secure the condition that in the new flow the rigid figure is at rest and is surrounded by a flow which at infinity has the velocity w. The forces which the rigid figure experiences by the production of this motion, and which are connected intimately with the so-called "apparent mass," are what we have here set in parallel with the wing-lift.

The surface F' supplies in addition a very simple mechanical connection between the velocity w on the one hand and the lift and drag on the other. According to equation (65)

$$A=\rho F' V w^*$$

$$WV=Aw=\rho F' V\frac{w^{*2}}{2}$$

where in the second equation use has again been made of the relation $w^*=2w$. Now $\rho F' V$ is the mass of air flowing per second through the section F'. If in order to simplify the whole problem it is once assumed that all the air particles within the section F' experience the full deviation w^* but that all outside are entirely undeviated, then exactly the correct lift and the correct work due to drag are obtained by application of the impulse theorem and the energy theorem. For the lift is now equal to the mass of the fluid deviated per second times the vertical velocity imparted to it, therefore equal to the impulse imparted to the medium. Also, in the same manner, the work done per second by the drag WV is the product of the mass of the fluid passing per second times the half square of the deflection velocity, and therefore equal to the kinetic energy left behind in the medium. This relation is indeed best suited to establish the phenomena of the theory of airplanes in a course for students who are only slightly skilled in mathematics. The fact that for a monoplane the circle having a diameter equal to the span comes out as the surface F' is one that will appear most plausible to the laity.

29. Of the theory pictured in the preceding section, according to which the determination of the induced drag in the case of the most favorable lift distribution is reduced to a problem of the potential theory, manifold applications have already been made. Especially, Dr. Grammel and K. Pohlhausen have treated, at my instigation, the case of the biplane made up of two straight monoplanes of the same span, and also, on the other hand, that of a monoplane having a longitudinal slot. The calculations in both cases are solved by means of elliptic integrals. I have given the formulas in my Wing Theory II. It may be sufficient here to state the practical final result, which is referred to the magnitude of the surfaces F'. These surfaces are best expressed for biplanes in terms of the corresponding surfaces of the monoplane having the same span. In fact, the ratio $F' : \frac{\pi}{4} b^2$, as is easily seen, equals the square of the factor k, introduced in section 26, by which the span must be increased in order to have a monoplane of the same induced drag. The values of k^2 for the biplane are obtained from the following table. The gap of the biplane, i. e., the distance apart of the two wings, is designated by h.

TABLE 2.

Values of $k^2 = F' : \frac{\pi}{4} b^2$

h/b — ...	0.	0.05	0.10	0.15	0.2	0.3	0.4	.....	0.5	∞
k^2 — ...	1.000	1.156	1.212	1.289	1.352	1.461	1.550	.....	1.625	2.000

The values given in the table may be expressed by the approximation formula

$$k^2 \cong \frac{1.027 + 3.84 h/b}{1 + 1.63 h/b} \tag{68}$$

In the case of the monoplane having a slot a suitable comparison wing is obtained by shoving the two halves of the monoplane together until the slot is closed. If b is the original span and d is the width of the slot, this monoplane has evidently the span $d - d$. We shall therefore form the ratio $F' : \frac{\pi}{4} (b - d)^2$ and again designate it by k^2. Calculations gave the following values:

TABLE 3.

Values of $k^2 = F' : \frac{\pi}{4} (b-d)^2$.

$\frac{d}{b}$	0.000	0.001	0.010	0.0316	0.100	0.250	0.500	1.000
k^2	1.000	0.762	0.676	0.6200	0.568	0.528	0.506	0.500

It is seen that even very narrow slots produce an important increase in the induced drag. For a very wide opening k^2 falls to one-half, as may be deduced easily from the fact that now, instead of one monoplane, we have two monoplanes of half the span. The values given in the table may be expressed by the approximation formula

$$k^2 = 1 - \frac{1}{2\sqrt{1 + 0.35 (\log_{10} b/d)^2}} \tag{69}$$

Figures 55–57 show, at the left, the uniplanar $w^* -$flow and, at the right, the surfaces F', for a monoplane, a biplane, and a monoplane with a slot.

F. AEROFOILS IN A TUBE OR IN A FREE JET.

30. To draw conclusions from the experimental results obtained in a tube bounded by solid walls or in a free jet from a nozzle, it is very useful to know the influence of the neighboring walls and of the boundaries of the jet upon the phenomena at the aerofoil. We wish indeed to know the behavior of the aerofoil in an air space infinitely extended in all directions; and the problem therefore arises to introduce a method for passing by calculation from the case which prevails in the experiments to that of the unlimited air space. For this purpose we shall next state clearly the boundary conditions which exist at solid walls parallel to the direction of the

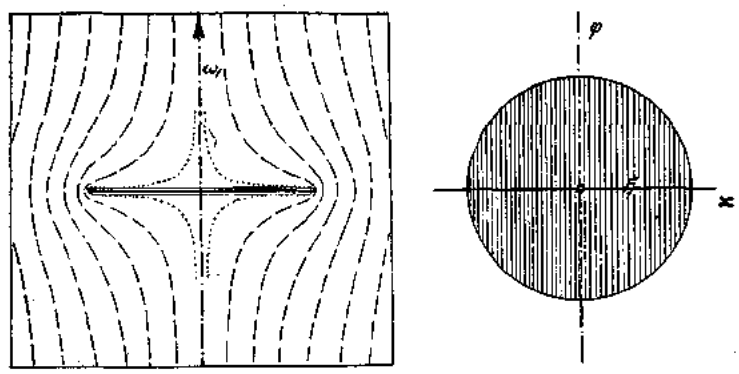

FIG. 55.

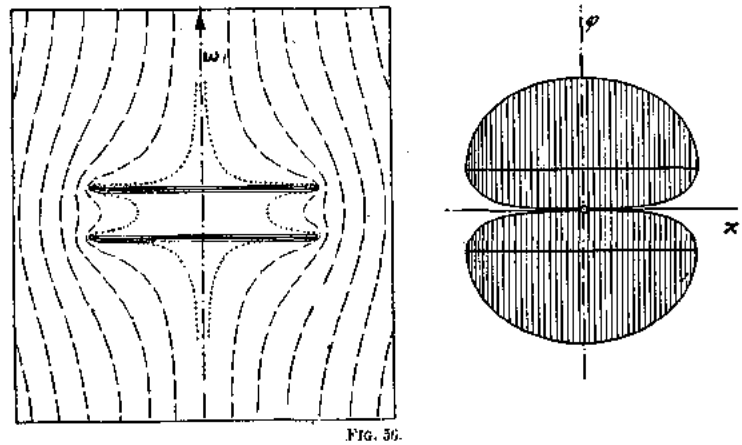

FIG. 56.

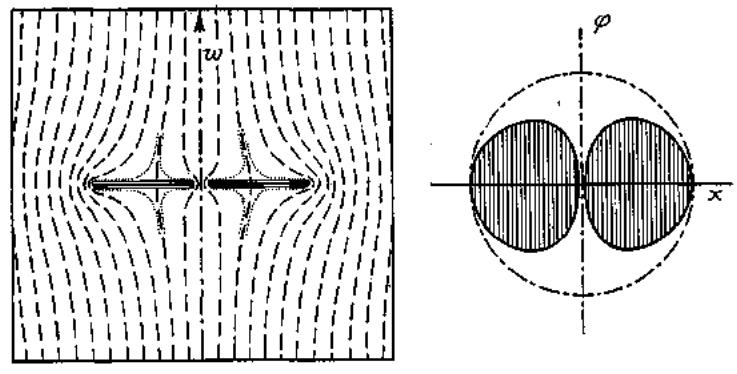

FIG. 57.

Left: Flow behind a monoplane, a biplane, and a monoplane with a slot, with reference to an observer moving downwards with the velocity W^* of the vortex system.
Right: Corresponding surfaces F_1.

wind and at the free boundary of a jet. At solid walls, the velocity components normal to the wall, w_n, must equal zero; on a free jet boundary, on the other hand, the pressure is to be put equal to that of the surrounding quiescent air layer, and therefore is constant. We can transform these last relations as follows, keeping within our theory of the first order. According to the Bernouilli theorem, if V is the undisturbed wind velocity, and u, v, and w are the additional velocities

$$p+\frac{\rho}{2}\left[u^2+(V+v)^2+w^2\right]=p_o+\frac{\rho}{2}V^2$$

or, since $p=p_o$,

$$u^2+v^2+w^2+2Vv=o.$$

If we neglect the squares of the disturbance velocities as being small of the second order, we have as the approximate initial condition for the free jet $v=o$. We proceed a step farther upon the path indicated to us by the approximation theory of the first order if we prescribe the value $v=o$, not for the actual jet boundary, but for that cylinder which is given by the surface of the undeviated jet. By doing this the boundary condition for the free jet becomes very similar, in a formal way, to that for the solid walls.

The two problems can now be solved in the following manner: We consider first the velocity field for the unlimited air space, according to the exposition previously given. This field offers, both in the case of the tube and in that of the free jet, contradictions with our boundary conditions at the walls or the jet boundary. We must superimpose a velocity field which in the interior of the region considered is free of singularities and which on the boundaries has velocities opposite to those velocity components, the vanishing of which is prescribed by the boundary condition. It is easily seen that by the superposition of this second velocity field on the original one the boundary conditions are satisfied exactly. The influence of this second field upon the aerofoil is now exactly that influence which we are seeking, and which we can calculate from the results of the theory of aerofoils as soon as this second field is known.

The additional velocity field corresponds to a pure potential motion; we have, therefore, the problem of determining its potential Φ. In the case of solid walls we are thus led to the problem of finding the potential for a given region (the interior of the tube) when the normal component w_n of the flow is given at the boundary of the region. This is the so-called "second boundary value problem" of the potential theory. The corresponding problem for a jet, as we shall see at once, leads to the "first boundary value problem," in which at the boundary the values of the potential itself are prescribed. According to what has been said above our region is a cylinder whose generating lines are parallel to the velocity V, hence, parallel to the Y axis, and for each point on the boundary the relation $\frac{\partial\Phi}{\partial y}=-\bar{v}$ (in which the dashes indicate boundary values) is prescribed. Integrating this relation for each generating line gives

$$\bar{\Phi}(y)=-\int_{-\infty}^{y}\bar{v}dy$$

If we go sufficiently far upstream every influence of the aerofoil vanishes; therefore for $y=-\infty$, $\Phi=o$; and hence $y=-\infty$ is taken as the lower limit of the integral. By this, then, we obtain the boundary values of the potential $\bar{\Phi}(y)$.

The complete calculation of the added potential Φ for the entire interior of the tube or jet is fairly difficult. If we concern ourselves, however, only with our main problem, to determine the corrections which must be applied to our experimental results, then we can again assume that the velocity components perpendicular to the axis of the tube in the plane of our aerofoil are half as large as at a great distance behind it. This consideration, which proceeded from the comparison of a vortex filament proceeding to infinity in one direction only with one proceeding to infinity in both directions, holds here exactly as well as in the cases discussed previously. We can therefore pass here as before from the space problem to a uniplanar one if we calculate the phenomena far behind the aerofoil. Our boundary conditions for the uniplanar problem are, for the tube, $\bar{w}_n=o$, for the free jet, $\bar{\Phi}=\text{const.}$ The last condition may be interpreted specially

conveniently if use is made of the method of treatment of section 28. Since in this, for the end of the impulse phenomenon, $\Phi = \int_0^\tau (p_0 - p)\, dt$, $\Phi = \text{const.}$ means simply that $\overline{p} = \text{const.}$, which, indeed, was the original boundary condition for the free jet.

31. The conditions stated in the preceding section can be secured most easily for a jet, or tube, of a circular cross section. In this case the added motion is obtained very simply by assuming for every vortex flowing off an equally strong one outside the circle, at the point outside corresponding to the one inside according to the reciprocal radii. If the direction of rotation of the external vortex is taken the same as that of the interior one, then at the points of the circle the boundary condition for a free jet is obtained; and, if opposite directions of rotations are taken, then the boundary condition for a tube is satisfied. This may be expressed by saying that there is combined with the aerofoil another obtained by reflexion according to reciprocal radii, whose circulation at corresponding points is the same in absolute value as that of the actual aerofoil, and for the jet it has the same sign, but for the tube the opposite sign.

The exact calculation has been made for a straight monoplane in the middle of the jet, assuming the lift to be distributed according to a half ellipse. If b is the span of the monoplane and D the diameter of the jet, then the disturbance velocity w' caused by the jet boundary at the distance x from the middle of the jet is

$$w' = \frac{A}{\pi D^2 \rho V}\left(1 + \frac{3}{4}\xi^2 + \frac{5}{8}\xi^4 + \frac{35}{128}\xi^6 + \text{etc.}\right) \tag{70}$$

in which $\xi = 2xb/D^2$.

The added drag calculated from this velocity according to equation (38) is found to be

$$W' = \frac{A^2}{\pi D^2 \rho V^2}\left[1 + \frac{3}{16}\left(\frac{b}{D}\right)^4 + \frac{5}{64}\left(\frac{b}{D}\right)^8 + \cdots\right] \tag{71}$$

A similar calculation for a uniform lift distribution gave for the first term in the formula for the drag the same value as in equation (71). It appears that the other terms of the series have but little importance with the usual ratios, so that we can limit ourselves to the first term. An approximation treatment shows, further, that any small wing system, in the middle of the circular jet gives rise to the same expression. We can therefore write for the total induced drag of the wing system in a jet of cross section F_0, if the surface F' is again introduced from section 28,

$$W = \frac{A^2}{4q}\left(\frac{1}{F'} + \frac{1}{2F_0}\right) \tag{72}$$

For a tube of circular cross section the same disturbance effect is found, but with the opposite sign; and therefore we have the approximation formula for the drag

$$W = \frac{A^2}{4q}\left(\frac{1}{F'} - \frac{1}{2F_0}\right) \tag{72a}$$

The correction, owing to the consideration of the finite cross section of the jet, is for the ratios ordinarily used not small. For $\frac{b}{D} = \frac{1}{2}$, it is already one-eighth of the induced drag. Formula (71) gives 0.1262 instead of 0.125; the corresponding formula for uniform distribution gives 0.127. It is seen, therefore, that the differences are not great, and that the approximation formula (72) is satisfactory for most cases.

For a tube of rectangular cross section the calculations would have to be made in such a manner that the aerofoil was mirrored at all the walls an infinite number of times, like a checkerboard. Further development of the calculation leads to elliptic functions. It has not yet been carried through. One can assume, however, that for a tube having a square cross section the influence of the walls will be of about the same magnitude as for the circle having an equal area.

G. APPLICATION OF THE THEORY OF AEROFOILS TO THE SCREW PROPELLER.

32. The fundamental ideas of the aerofoil theory can be applied step by step to the screw propeller. For the elements of the blades the Kutta-Joukowski formula holds, viz, that the air force is perpendicular to the velocity c of the element with reference to the air and that, per unit length of the blade, it has the value $\rho\Gamma c$. Corresponding to what has gone before, vortices will arise at the blade, having a vortex strength per unit length equal to $\frac{d\Gamma}{dx}$. If we wish again to construct a theory of the first order, that is, if we agree to consider as small the air forces and the velocities produced by them, then again the proper motion of the vortices will be small and therefore in a first approximation may again be neglected. The vortices then have the shape of screw lines and form vortex ribbons which—if for the sake of simplicity we assume straight radial blades—have the shape of ordinary screw surfaces.

The calculation of the velocity field of a screw vortex is markedly more complicated than that of a rectilinear vortex and leads to functions which thus far have not been studied in detail. In spite of this it is possible, as Dr. Betz has shown, to prove a series of general theorems very similar to those of Munk for multiplanes. Since the velocity c is not the same at the separate blade elements, we must speak of the "work lost" where Munk speaks of drag. The work applied for the motion of the propeller is composed of two parts—useful work + work lost. The latter in our ideal case, where friction is excluded, is transformed completely into kinetic energy of the air. The kinetic energy stands again in close connection with the vortex system produced by the propeller. Betz proved, among others, the following theorems:

(1) If two elements of a propeller blade lie upon the same radius at distances x and ξ from the axis, then the work lost at the point ξ due to the disturbance velocity caused by the air force at the point x is equal to the work lost at the point x owing to the disturbance velocity caused by the air force at the point ξ.

(2) This theorem must be somewhat modified for two elements which do not lie on the same radius. It reads: The work lost at the point ξ due to the disturbance velocity caused by the air force at the point x is of the same amount as the work which would be lost at the point x if the screw vortex proceeding from the element at ξ were to pass out forward in the prolongation of the actual vortex instead of going backward.[12]

(3) This last theorem leads at once to the following relation for the sum of the two amounts of work lost: The total work lost due to the mutual action of the air forces by two blade elements at points x and ξ is the same as the work which would be lost at one point alone if the screw vortex proceeding from the other point were to extend to infinity both forward and backward.

It is easily seen that this theorem is perfectly analogous to the stagger theorem of section 25, for if the vortex of the inducing element extends in both directions, then the position of the element itself on its own vortex strip is immaterial as far as the velocity field produced is concerned.[13] It is therefore true of screws that nothing is changed in the total energy-loss if blade elements are displaced in any way, without change of their air forces, along the relative streamlines passing through them (i. e., in this case, screw lines). This naturally is connected again with the fact that the total amount of the energy loss depends only upon the final distribution of the vortex systems, not upon the relative position of the places where the separate vortices arise.

Theorem No. 3 will be of use to us also in what follows. It can be made clearer by the following consideration. The field of the vortex ribbon of a lifting element dies away very quickly forward of the element, but in the rear it extends over the entire length of the path traversed. If the sum is formed of the two mutual losses in work of two elements at the points x and ξ, we can proceed, owing to the stagger theorem, to displace one of the two elements along its screw line so far backward that its velocity field is no longer appreciable at the position of the other

[12] In this the sense of rotation of the transverse vortex is to be reversed.

[13] The transverse vortex in this case cancels out completely in the determination of the velocity field, since it appears twice with opposite senses of circulation.

20167—23——14

undisplaced element. At the same time, however, the influence of the latter element upon the first is increased since its vortex ribbon, viewed from the new position of the first element, extends as far forward as backward. The sum of the two mutual losses in work is reduced in this manner to the loss which the velocity field of the front element produces upon the displaced one.[14]

(4) The most important of Betz's theorems, from a practical standpoint, furnishes the complete analogy to Munk's theorem concerning the wing system having the least drag, and, corresponding perfectly to the statements in sections 27 and 28, may be expressed thus: The flow behind a propeller having the least loss in energy is as if the screw surfaces passed over by the propeller blades were solidified into a solid figure and this were displaced backward in the nonviscous fluid with a given small velocity. The potential difference between the front and rear sides of a screw surface at one and the same point furnishes, then, again the circulation Γ of the corresponding point of the propeller blade.

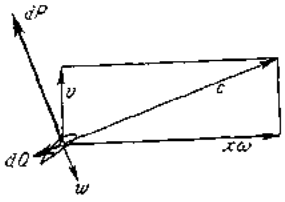

FIG. 58.—Velocity field near a blade of a screw-propeller.

A short proof of theorem 4 will be given. For this purpose the principal equations for the action of a screw must first be deduced. The screw is imagined to be displaced with the velocity v relative to the air, and to rotate at the same time with the angular velocity ω. A blade element at the distance x from the axis has then, with reference to the air which in the theory of the first order may be assumed to be at rest, the velocity c, with the components v and $x\omega$. (See fig. 58.)

If no vortex were produced, then, with the assumption of a nonviscous fluid, an air force dP would arise, which, according to the Kutta-Joukowski theorems, would be perpendicular to the velocity c and would have the value, for a blade element of length dx,

$$dP = \rho \Gamma c\, dx \tag{73}$$

The force dP is decomposed into two components, of which the one in the direction of v interests us specially, since it is applied to the screw. This component is

$$dS = dP \cdot \cos \epsilon = \rho \Gamma x \omega\, dx \tag{74}$$

The total thrust, if there are n blades, is then

$$S = \rho \omega \sum_{1}^{n} \int_{0}^{r} \Gamma\, x\, dx \tag{75}$$

The other component

$$dT = dP \sin \epsilon = \rho \Gamma v\, dx \tag{76}$$

furnishes a contribution as a torque to the rotation moment. It is seen at once that $dS \cdot v = dT \cdot x\omega$, i. e., the useful thrustwork is equal to the work done by the torque hitherto used in our calculations. This depends immediately upon our assumption that the force dP is perpendicular to the velocity c. But the screw blades actually produce a vortex system and we must ask as to the reaction of the vortex system upon the phenomena of a screw. We shall assume, exactly as in the aerofoil theory, that we turn the blade profile in such a manner that the lifting forces desired by us actually come into play. Since we are interested here merely in the loss in work caused by the vortex system, we have to do only with the drag components caused by the vortex system. This depends, exactly as before, upon the velocity component perpendicular to the velocity of motion of the element, which in this case equals c. We shall again designate it by w. The added velocity component w furnishes a drag in the direction of motion equal to

$$dQ = dP \frac{w}{c} = \rho \Gamma w\, dx \tag{77}$$

The loss of work per second is therefore

$$dQ \cdot c = \rho \Gamma dx \cdot w \cdot c \; (= dP \cdot w)$$

[14] This process of thought can be applied, naturally, in the same way to aerofoils and furnishes a convenient deduction for the sum of the drags $W_{12} + W_{21}$.

If now, according to figure 58, we put $c = v/\sin E$, our problem is to make a minimum the total loss of work

$$L = \rho v \sum_{1}^{n} \int_{0}^{l} \frac{\Gamma w dx}{\sin \epsilon} \tag{78}$$

The variation of this quantity must therefore be put equal to zero. We shall proceed, for this purpose, similarly to the way Munk's theorem was deduced in section 27. We shall change by small amounts the circulation at two places, which may reach from x_1 to $x_1 + dx_1$ and from x_2 to $x_2 + dx_2$, in such a manner that the total thrust remains unchanged. According to equation (75) we must make

$$\delta\Gamma_1 \cdot x_1 dx_1 + \delta\Gamma_2 \cdot x_2 dx_2 = o \tag{79}$$

Exactly as before the condition for the minimum is obtained if the loss of energy due to our added circulation remains unchanged. In order to calculate the loss, let us make use of theorem No. 3 and assume that the added wing forces are brought into action far behind the propeller so that the loss is merely the product of the added air force by the velocity w^* which arises from the vortices of the propeller, and therefore for the first element is equal to $\rho v \delta\Gamma_1 \frac{w_1^*}{\sin \epsilon} dx_1$. Omitting the constant factor, we obtain as the minimum condition—

$$\delta\Gamma_1 \frac{w_1^*}{\sin \epsilon_1} dx_1 + \delta\Gamma_2 \frac{w_2^*}{\sin \epsilon_2} dx_2 = o,$$

from which is derived, making use of equation (79)

$$\frac{w_1^*}{x_1 \sin \epsilon_1} = \frac{w_2^*}{x_2 \sin \epsilon_2} = \text{const.} \tag{80}$$

We must compare this condition with that obtained for the velocity components normal to a rigid screw surface, when this surface is moved backward with the velocity w'. We then have (see fig. 59):

$$w_n = w' \cos \epsilon.$$

But on a screw surface the pitch h is connected with the angle of pitch ϵ and the radius x by the relation $h = 2\pi x \tan \epsilon$.

Multiplying this last equation with that for w_n, and solving, we get

$$w_n = \frac{2\pi w' x \sin \epsilon}{h},$$

and therefore

$$\frac{w_n}{x \sin \epsilon} = \text{const.} \tag{81}$$

On comparing (81) with (80) it is seen that by a suitable choice of w' the value of w_n can always be made to agree with that of w^*, which proves Betz' theorem.

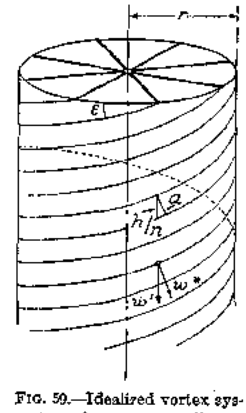

FIG. 59.—Idealized vortex system of a screw-propeller.

33. In order to learn more accurately the nature of the distribution of circulation which we are seeking, we shall proceed as if the velocity field at great distances from the screw is produced by having the velocity w' in the direction of the axis imparted impulsively to the rigid figure composed of the screw surfaces. In a purely qualitative way one can see that with any system of screw surfaces having a small pitch the air in the interior of the system is actually accelerated backward, with, of course, the appearance of tangential velocity components whose intensity is a function of the angle ϵ and is greatest for $\epsilon = 45°$. At the axis itself there is neither an axial nor a tangential acceleration. Less simple are the conditions near the outer boundary of the screw surface where a flow around the edges of the surfaces occurs.

In order to obtain a quantitative statement, we shall for simplicity's sake next think of a screw having a large number of blades. Our rigid figure consists, then, of a very large number

of screw surfaces, lying close together, and therefore the air is led with difficulty into the interior. When the impulse occurs it escapes in the direction of the normals to the screw surface. The radial velocity components w_r will be appreciable only in the neighborhood of the outer boundary of the screw surfaces; further in, we may put it equal to zero approximately. For the tangential components w_t and the axial components w_a, the relations hold, as is easily seen,

$$w_t = w^* \sin \epsilon = w' \cos \epsilon \sin \epsilon$$

$$w_a = w^* \cos \epsilon = w' \cos^2 \epsilon.$$

The angle may be expressed by writing

$$\tan \epsilon = \frac{h}{2\pi x} = \frac{v}{x\omega} = \frac{r'}{x} \tag{82}$$

In this, for brevity's sake, $\frac{h}{2\pi} = \frac{v}{\omega}$ is put equal to r' (r' is that radius for which the pitch of the screw, $\tan \epsilon$, $= 1$). Then

$$\sin \epsilon = \frac{r'}{\sqrt{r'^2 + x^2}} \text{ and } \cos \epsilon = \frac{x}{\sqrt{r'^2 + x^2}} \tag{83}$$

and hence

$$w_t = w' \cdot \frac{r'x}{r'^2 + x^2} \text{ and } w_a = w' \frac{x^2}{r'^2 + x^2} \tag{84}$$

We must now determine the circulation around the separate blades as a function of the radius x. For a screw with n blades the total circulation of the vortices inside the circle of radius x coincides with the line integral for the closed circle of radius x; this circulation must evidently equal $n\Gamma$, where Γ is the circulation of one of the screw blades at the point x. From this we have

$$\Gamma = \frac{2\pi x \cdot w_t}{n} = \frac{2\pi r' w'}{n} \cdot \frac{x^2}{r'^2 + x^2} \left(= \frac{h w_a}{n} \right) \tag{85}$$

The curve for Γ according to equation (85) is shown in curve I of figure 62.

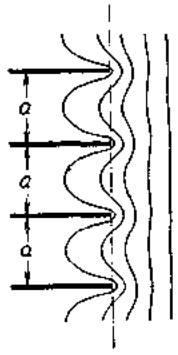

FIG. 60.—Conformal transformation $z = \frac{a}{\pi} \log \frac{1}{2} \left(t + \frac{1}{t} \right)$.

At the ends of the blades we would expect to have a decrease of the circulation of the same character as found for aerofoils. An approximate treatment can be devised in the following way: We imagine an infinite series of aerofoils which have a distance apart a and are not staggered and which extend infinitely far toward the left. We inquire what is the most favorable distribution of lift near the ends of these aerofoils. The distance a is then to be made equal to the perpendicular distance apart of the edges of two consecutive blades of the screw, i. e., according to figure 59,

$$a = \frac{h}{n} \cos \epsilon_1 = \frac{2\pi r'}{n} \cdot \frac{r^2}{r'^2 + r^2} \tag{86}$$

The problem now, according to the procedure of section 28, may be solved by seeking the potential flow around the edges of the corresponding family of planes and by determining the discontinuity of potential at the planes. This problem may be solved without difficulty by means of conformal representations. (See sec. 10.) It can be shown that the plane with the straight cuts as shown in figure 60, which we shall call the z plane, may be transformed into the unit circle (t plane) by the formula

$$z = \frac{a}{\pi} \log \frac{1}{2} \left(t + \frac{1}{t} \right) \tag{87}$$

The flow of figure 58 is transformed thereby into circulation flow around the unit circle; in fact

$$\Phi + i\Psi = iC \log t$$

After a short calculation, by elimination of t, we have

$$z = \frac{a}{\pi} \log \cos \frac{\Phi + i\Psi}{C} \tag{88}$$

For the surface around which the flow takes place, and which is given by the streamline $\psi = o$, we have, therefore,

$$x = \frac{a}{\pi} \log \cos \frac{\Phi}{C}$$

or

$$\Phi = \pm C \cos^{-1} e^{\frac{x\pi}{a}} \tag{89}$$

which gives the real values for negative values of x. The potentials thus obtained or the velocity equal to 1 of the free flow $\left(\text{to obtain which } C \text{ must be put equal to } \frac{a}{\pi}\right)$, which, according to what has gone before, give us the surface F', form a picture such as is shown in figure 61. By means of this one can form a definite judgment as to how the circulation, and with it the thrust also, decreases at the blade tips. We can replace the shaded portions of Figure 61 by a straight line, having an equal area below it which, in accordance with the integration performed, must lie behind the blade tips at the distance

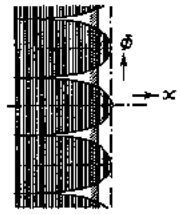

Fig. 61.—Potential obtained by the flow of figure 60.

$$a' = a \log \frac{2}{\pi} = 0.2207a \tag{90}$$

We conclude from this that, with screws also, the decrease of circulation at the blade tips has about the same effect as if the screw had a radius diminished by $0.2207a$, and then the air would be considered uniform in every circle of radius x (as would be the case for a screw having an infinite number of blades).

The properties found for the inner portion of the screw and for its edge may be combined into a single formula, which can be applied as an approximation formula also for screws having a small number of blades. This formula is obtained by multiplying the value in equation (85) by the expression $\frac{2}{\pi} \cos^{-1} e^{\frac{-\pi(r-x)}{a}}$, which for large values of $\frac{r-x}{a}$ takes the value 1. (For $-x$ of formula (89) $r-x$ is here substituted, as is obvious.) Thus we obtain the formula

$$\Gamma = \frac{4w'r'}{n} \cdot \frac{x^2}{r'^2+x^2} \cdot \cos^{-1} e^{\frac{-\pi(r-x)}{a}} \tag{91}$$

The curve of Γ according to equation (91) is given in figure 62, for a 4-blade screw and for $r' : r = 1 : 5$, which correspond to average conditions in practice.

The whole deduction holds, as has already been remarked, for screws which are not heavily loaded. For screws with heavy loads an improvement can be introduced by calculating the pitch of the screw surfaces formed by the vortices, corresponding to the state of flow prevailing in the circular plane of the screw. Instead of writing $\tan \xi = \frac{v}{x\omega}$, we must write, more exactly, $\tan \xi = \frac{V + \frac{w_a}{2}}{x\omega - \frac{w_t}{2}}$, in which V is the velocity of flight, since in the screw disk plane half of the final disturbance velocities is already present. A useful approximation is obtained if, retaining our formulae, v is put equal to $V + \frac{w'}{2}$, and therefore r' is put equal to $\frac{V + \frac{w'}{2}}{\omega}$.

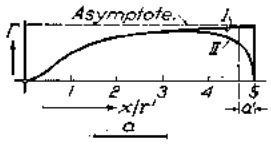

Fig. 62.—Distribution of circulation. I. Infinite number of blades. II. Four blades a is the distance of two vortices. (See Fig. 59.)

After the circulation is known, the distribution of thrust and torque may be calculated easily by means of equations (74) and (76), and thus, following the method used in the aerofoil theory, the requisite widths of the blades and angles of attack may be determined in order that for a given working condition (i. e., r' and w' given), in which the screw is to have the most favorable performance, all the information may be deduced from the theory. By taking into

account the more exact velocity relations in the propeller-disk plane this information may be improved.

The aerofoil theory has numerous further applications. An investigation of curved flights specially of the moment—important in discussions of stability—around the longitudinal axis in the case of a wing moved in a circle, is at present being made, also the calculation of the moment of a warped wing. A series of not unimportant single questions must wait for a further improvement of the theory, e. g., various conclusions specially concerning properties of profiles, influence of curvature, etc., can be reached, if we pass from the lifting line to the case of a load distributed also along the chord; for the treatment of a wing set oblique to the direction of flight the assumption of a load distributed along the chord is necessary since in this case the conditions contradict the "lifting line." Investigations of this kind, which can be accomplished only by very comprehensive numerical calculations, were begun during the war but since then, owing to a lack of fellow workers, have had to remain unfinished. A similar statement also applies to the calculations of a flapping wing already begun, in which one is likewise forced to assume the lift distributed along the chord, since otherwise the result is indefinite. Therefore much remains to be done.

MOST IMPORTANT SYMBOLS.

ρ =density.
V =velocity of the airplane.
u, v, w=velocity components in the X, Y, Z directions. (In the case of an airplane X is in the direction of the span of the wings, Y is in the direction of flight, Z is vertical.)
$q=\frac{\rho V^2}{2}$=dynamical pressure.
b =span of a wing ("Breite").
t =chord of a wing ("Tiefe").
h =gap of a biplane ("Höhe").
F =area of surface (=b . t) ("Fläche").
A =lift ("Auftrieb").
W =drag ("Widerstand").
$c_a=\frac{A}{Fq}$=lift coefficient (=2 K_y "absolute").
$c_w=\frac{W}{Fq}$=drag coefficient (=2 K_x "absolute").
α =angle of attack.
Γ =circulation.
Φ =velocity potential.
ψ =stream function.

LIST OF THE MOST IMPORTANT LITERATURE.

Abbreviations: Z. F. M.=Zeitschrift für Flugtechnik und Motorluftschiffahrt.
TB =Technische Berichte der Flugzeugmeisterei.

A. GÖTTINGEN PUBLICATIONS.

L. Prandtl: Tragflügeltheorie I. und II. Mitteilung. Nachr. von der Kgl. Gesellschaft der Wissenschaften. Math.-phys. Klasse 1918, S. 451, u. 1919, S. 107. (Aerofoil Theory, I and II Communications. Nachr. Kgl. Gesellschaft der Wissenschaft. Math.-phys. Classe, Göttingen, 1918, p. 451, and 1919, p. 107.)

—— Tragflächen-Auftrieb und -Widerstand in der Theorie. Jahrb. der Wissenschaftlichen Gesellschaft f. Luftfahrt, V. 1920, S. 37. (Aerofoil Lift and Drag in Theory. Jahrb. d. Wissens. Gesells. f. Luftfahrt, V. 1920, p. 37.)

—— Der induzierte Widerstand von Mehrdeckern. TB Bd. III, S. 309. (The Induced Drag of Multiplanes. TB. Vol. III, p. 309.)

G. Fuhrmann: Theoretische und experimentelle Untersuchungen an Ballonmodellen. Jahrbuch 1911/12 der Motorluftschiff-Studiengesellschaft, S. 65. (Theoretical and Experimental Investigations of Models of Airship Bodies. Jahrb. 1911/12 d. Motor Luftschiff-Studiengesells, p. 65.)

A. BETZ: Die gegenseitige Beeinflussung zweier Tragflächen. Z. F. M., 1914, S. 253. (The Mutual Influence of Two Aerofoils. Z. F. M., 1914, p. 253.)

—— Untersuchung einer Joukowski'schen Tragfläche. Z. F. M., 1915, S. 173. (Investigation of a Joukowski Aerofoil. Z. F. M., 1915, p. 173.)

—— Einfluss der Spannweite und Flächenbelastung auf die Luftkräfte von Tragflächen. TB, Bd. I, S. 98. (Influence of Span and Wing-Loading upon the Air forces of Aerofoils. TB, Vol. I, p. 98.)

—— Beiträge zur Tragflügeltheorie mit besonderer Berücksichtigung des einfachen rechteckigen Flügels. Dissertation, Göttingen, 1919. Auszug in Beiheft II der Z. F. M., 1920, S. 1. (Contributions to the Theory of Aerofoils with Special Reference to the Simple Rectangular Wing. Dissertation, Göttingen, 1919. Extract in Beiheft. II Z. F. M., 1920, p. 1.)

—— Schraubenpropeller mit geringstem Energieverlust, mit einem Zusatz von L. Prandtl, Nachr. v. d. Kgl. Gesellschaftder Wissenschaften, Math.-phys. Klasse 1919, S. 193. (The Screw Propeller having the Least Loss of Energy, with an Appendix by L. Prandtl. Nachr. Kgl. Gesellschaft der Wissenschaft, Math.-phys. Class, Göttingen, 1919, p. 193.)

—— Eine Erweiterung der Schraubenstrahltheorie. Z. F. M., 1920, S. 105. (An Extension of the Theory of Screw Jets. Z. F. M., 1920, p. 105.)

M. MUNK: Beitrag zur Aerodynamik der Flugzeugtragorgane. TB, Bd. II, S. 187. (Contribution to the Aerodynamics of Lifting Airplane Members. TB., Vol. II, p. 187.)

—— Isoperimetrische Aufgaben aus der Theorie des Fluges. Dissertation, Göttingen, 1919. (Isoperimetric problems from the Theory of Flight. Dissertation, Göttingen, 1919.)

C. WIESELSBERGER: Beitrag zur Erklärung des Winkelfluges einiger Zugvögel. Z. F. M., 1914, S. 225. (Contribution to the Explanation of the Formation Flight of Migratory Birds. Z. F. M., 1914, p. 225.)

—— Experimentelle Prüfung der Umrechnungsformeln. In "Ergebnisse der Aerodynamischen Versuchsanstalt 1. Lieferung," München, 1921, S. 50. (Experimental Examination of the Formulae for Relations between Aerofoils. In "Ergebnisse der Aerodynamischen Versuchsanstalt," Part I, Munich, 1921, p. 50.)

B. WORKS ON THE TWO DIMENSIONAL PROBLEM.

W. M. KUTTA: "Auftriebskräfte in strömenden Flüssigkeiten." Illustr. aeronaut. Mitteilungen, 1902, S. 133. Ausführlichere Abhandlungen in den Sitzungsber. der Bayr. Akad. d. Wiss., Math.-Phys. Klasse 1910, 2. Abh. und 1911, S. 65. (Forces of Lift in Flowing Fluids. Illustr. aeronaut. Mitteilungen, 1902, p. 133. More detailed papers in the reports of the proceedings of the Bavarian Acad. of Sciences, Math.-Phys. Class 1910, 2d report, and 1911, p. 65.)

N. JOUKOWSKI: Ueber die Konturen der Tragflächen der Drachenflieger. Z. F. M., 1910, S. 281. "Aerodynamique" aus dem Russischen übersetzt von Drzewiecki, Paris, 1916. (On the Contours of Airplane Wings. Z. F. M., 1910, p. 281. "Aerodynamics" translated from the Russian by Drzewiecki, Paris, 1916.

R. GRAMMEL: "Die hydrodynamischen Grundlagen des Fluges." Braunschweig, 1917. (The Hydrodynamic Principles of Flight. Brunswick, 1917.)

R. v. MISES: Zur Theorie des Tragflächenauftriebs. Z. F. M., 1917, S. 157, 1920, S. 68 und 87. (The Theory of Lift of Wings. Z. F. M., 1917, p. 157, 1920, pp. 68 and 87.)

After this memoir was written, two papers, by R. Fuchs and E. Trefftz, on the theory of aerofoils appeared, both of which discuss the theory of a monoplane and that of airplanes of least drag. These papers are published in the "Zeitschrift für Angewandte Mathematik und Mechanik," 1921, Heft 2 u. 3, Berlin.

The Mechanism of Fluid Resistance.[1]

By Th. v. Kármán and H. Rubach.

The resistance of a solid body moving with a uniform velocity in an unlimited fluid can be calculated theoretically only in the limiting cases of very slow motion of small bodies or of very high fluid viscosity. We are brought in such cases to a resistance proportional to the first power of the velocity, to the viscosity constant, and, for geometrically similar systems, to the linear dimensions of the body. To the domain of this "linear resistance"—which has aroused much interest, especially within recent years, on account of some important experimental applications—has to be opposed the limiting domain of comparatively large velocities, for which the so-called "velocity square law" holds with very good approximation. In this latter domain, which embraces nearly all the important technical applications, the resistance is nearly independent of fluid viscosity, and is proportional to the fluid density, the square of the velocity, and—again for geometrically similar systems—to a surface dimension of the body. In this domain of the "square law" is included the important case of air resistance, because it is easy to verify, by the calculation of the largest density variations which can occur for the speeds we meet in aeronautics and airscrews, that the air compression can be neglected without any sensible error. The influence of the compression first becomes important for velocities of the order of the velocity of sound. In fact, experiments show that the air resistance, in a broad range from the small speeds at which the viscosity plays a role up to the large speeds comparable to the velocity of sound, is proportional to the square of the velocity with very good approximation.[3] In general, fluid resistance depends upon the form and the orientation of the body in such a complicated way that it is extraordinarily difficult to predetermine the flow to a degree sufficient for the evaluation of the resistance of a body of given form, by a process of pure calculation, as can be done by aid of the Stokes formula in the case of very slow motions. We also will not succeed in this paper in reaching such a solution, but will still make the attempt to give a general view of the *mechanism of fluid resistance within the limits of the square law.*

We can state the problem of fluid resistance in the following somewhat more exact way.

Since the time of the fundamental considerations of *Osborne Reynolds* on the mechanical similitude of flow phenomena of incompressible viscous fluids of different density and viscosity and—under geometrical similitude—for different sizes of the system considered, it is known that the resistance phenomenon depends upon a single parameter which is a certain ratio of the above-mentioned quantities. Thus the fluid resistance of a body moving with the uniform velocity U in an incompressible unlimited fluid may be expressed by a formula of the form [4]

$$W=\mu l U f\left(\frac{U l \rho}{\mu}\right) \tag{I}$$

where

μ is the viscosity constant

ρ the fluid density

l a definite but arbitrarily chosen linear dimension of the body, and $f\left(\frac{U l \rho}{\mu}\right)$ a function of the single variable $R=\frac{U \rho l}{\mu}$. We will call "Reynolds' parameter" the quantity R which has a zero dimension.

Theory and experiment show that for very small values of R—that is, for low velocities, or small bodies, or great viscosity—the function $f(R)$ is very nearly constant; the resistance coefficient of the Stokes formula corresponds to the limiting case of $f(R)$ for $R=0$. The square law corresponds to the limiting case of $R=\infty$. We approach this latter case the more nearly the smaller the viscosity μ, so that in the limiting case of $R=\infty$, the fluid can be considered as frictionless. And we can ask ourselves, *to what limiting configuration does the flow of the viscous fluid around a solid body tend when we pass to the limiting case of a perfect fluid?* This is, according to our view, the fundamental point of the resistance problem.

The fact that we obtain in this case a resistance nearly independent of the viscosity constant—since according to formula (I) this corresponds to the square law—allows us to conjecture that in this limiting case the resistance is determined by flow types such as can occur in a perfect fluid.

---

[1] Translation of the paper of Th. v. Kármán and H. Rubach published in "Physikalische Zeitschrift," Jan. 15, 1912.

It is now certain that neither the so-called "continuous" potential flow, nor the "discontinuous" potential flow discovered by *Kirchhoff* and *v. Helmholtz*, can express properly this limiting case. Continuous potential flow does not cause any resistance in the case of uniform motion of a body, as may be shown directly by aid of the general momentum theorem; the theory of the discontinuous potential flow, which, in relation to the resistance problem has been discussed principally by Lord Rayleigh,[1] leads to a resistance which is proportional to the square of the velocity; the calculated values do not, however, agree with the observed ones. And, independent of the insufficient agreement between the numerical values, the hypothesis of the "dead water," which, according to this theory ought to move with the body, is in contradiction to nearly all observations. It is easy to see by aid of the simplest experiments that the flow, when referred to a system of coordinates moving with the body, is not stationary, as assumed in this theory. Furthermore, in the theory of discontinuous potential motion, the suction effect behind the body is totally missing, while in the dead water, which extends to infinity, we have everywhere the same pressure as in the undisturbed fluid at a great distance from the body. But according to recent measurements, in many cases the suction effect is of first importance for the resistance, and in any case contributes a sensible part of the last.

The reason why in a perfect fluid the discontinuous potential flow, although hydrodynamically possible, is not realized is without any doubt the instability of the surfaces of discontinuity, as has already been recognized by v. Helmholtz and specially mentioned by Lord Kelvin.[2] A surface of discontinuity can be considered as a vortex sheet; and it can be shown in a quite general way that such a sheet is always unstable. This can also be observed directly; observation shows that vortex sheets have a tendency to roll themselves up; that is, we see the concentration around some points of the vortex intensity of the sheet originally between them. This observation leads to the question: Can there exist

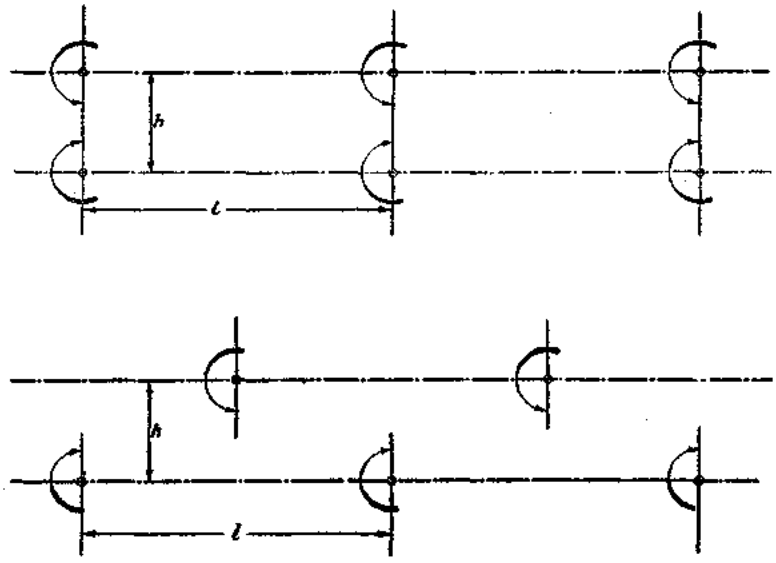

FIG. 1.

stable arrangements of isolated vortex filaments, which can be considered as the final product of decomposed vortex sheets? This question forms the starting point of the following investigations; it will, in fact, appear that at least for the simplest case of uniplanar flow, to which we will limit ourselves, we will be led to a "flow picture" which in all respects corresponds quite well to reality.

THE INVESTIGATION OF STABILITY.

We will investigate the question whether or not two parallel rows of rectilinear infinite vortices, of equal strength but of inverse senses, can be so arranged that the whole system, while maintaining an invariable configuration, will have a uniform translation and be stable at the same time. It is easy to see that there exist two kinds of arrangements for which two parallel vortex rows can move with a uniform and rectilinear velocity. The vortices may be placed one opposite the other (arrangement a, fig. 1), or the vortices of one row may be placed opposite the middle points of the spacing of the vortices of the other row (arrangement b). In the case of equality of spacing of the vortices in both rows, as a consequence of symmetry for the two arrangements a and b, it appears that each vortex has the same velocity in the sense of the X axis, and that the velocity in the sense of the Y axis is equal to zero. We have to answer the question, which of these two arrangements is stable?

To illustrate first by a simple example the method of the investigation of stability, we will start with the consideration of an infinite row of infinite vortices disposed at equal distances l and having the intensity ζ, and will study

[1] On the resistance of fluids, Mathematical and Physical Papers, Vol. I, p. 287.

[2] Mathematical and Physical Papers, Vol. IV, p. 215. This paper contains a detailed critique of the theory of discontinuous motion.

the stability of such a system. If we designate by x_p, y_p, the coordinates of the $p-th$ vortex, and by x_q, y_q the coordinates of the $q-th$ the velocity impressed on the latter vortex by the former is given by the formulæ

$$u_{pq}=\frac{\zeta}{2\pi}\cdot\frac{y_p-y_q}{(x_p-x_q)^2+(y_p-y_q)^2}$$

$$v_{pq}=-\frac{\zeta}{2\pi}\cdot\frac{x_p-x_q}{(x_p-x_q)^2+(y_p-y_q)^2}$$

These formulæ express the fact that each vortex communicates to the other a velocity which is normal to the line joining them and is inversely proportional to their distance apart. Therefore the resultant velocity of the $q-th$ vortex due to all the vortices is equal to

$$\frac{dx_q}{dt}=\frac{\zeta}{2\pi}\sum_{p=-\infty}^{\infty}{}'\frac{y_p-y_q}{(x_p-x_q)^2+(y_p-y_q)^2}$$

$$\frac{dy_q}{dt}=-\frac{\zeta}{2\pi}\sum_{p=-\infty}^{\infty}{}'\frac{x_p-x_q}{(x_p-x_q)^2+(y_p-y_q)^2}$$

where $p=q$ is excluded from the summation. If now the vortices are disturbed from their equilibrium position, the small displacements being ξ_p, η_p, the vortex velocities can be developed in terms of these quantities, and we will be brought to a system of differential equations for the disturbances ξ_p, η_p, i. e., for small oscillations of the system.

Let us accordingly put

$$x_p=pl+\xi_p$$
$$y_p=\eta_p$$

and, neglecting the small quantities of higher orders, we will get

$$\frac{d\xi_q}{dt}=\frac{\zeta}{2\pi}\sum_{p=-\infty}^{\infty}{}'\frac{\eta_p-\eta_q}{(p-q)^2l^2}$$

$$\frac{d\eta_q}{dt}=\frac{\zeta}{2\pi}\sum_{p=-\infty}^{\infty}{}'\frac{\xi_p-\xi_q}{(p-q)^2l^2}$$

The differential equations so obtained, which are infinite in number, are reduced to two equations by the substitution

$$\xi_p=\xi_o e^{ip\varphi};\ \eta_p=\eta_o e^{ip\varphi}$$

These two equations are

$$\frac{d\xi_o}{dt}=\eta_o\frac{\zeta}{2\pi}\sum_{p=-\infty}^{\infty}{}'\frac{e^{ip\varphi}-1}{p^2l^2}$$

$$\frac{d\eta_o}{dt}=\xi_o\frac{\zeta}{2\pi}\sum_{p=-\infty}^{\infty}{}'\frac{e^{ip\varphi}-1}{p^2l^2}$$

with $p\neq o$

The physical meaning of this substitution is easy to see: we consider a disturbance in which each vortex undergoes the same motion only with a different phase φ. Under such conditions we have to do with a wave disturbance and the system will be called stable, when for any value of φ, that is, for any phase difference between two consecutive vortices, the amplitude of the disturbance does not increase with the time.

Let us introduce the notation

$$\kappa(\varphi)=\frac{\zeta}{2\pi}\sum_{p=-\infty}^{\infty}{}'\frac{e^{ip\varphi}-1}{p^2l^2}=\frac{\zeta}{\pi l^2}\sum_{p=1}^{\infty}\frac{\cos(p\varphi)-1}{p^2}$$

The foregoing equations then take the form

$$\frac{d\xi_o}{dt}=\kappa(\varphi)\eta_o$$

$$\frac{d\eta_o}{dt}=\kappa(\varphi)\xi_o$$

Let us put ξ_o and η_o proportional to $e^{\lambda t}$; we will then find for each value of φ two values for λ, that is

$$\lambda=\pm\kappa(\varphi)$$

It follows that the vortex system considered is unstable for any periodic disturbance, because there is always present a positive real value of λ, that is, the disturbance is of increasing amplitude.

Applying this method in the case of two vortex rows we will find that the arrangement a, that is, the symmetrical arrangement, is likewise unstable, but that for the arrangement b there exists a value of the ratio h/l (h is the distance between the two rows, l is the distance between the vortices in the row) for which the system is stable.

In both cases λ can be brought to the form

$$\frac{\pi}{\zeta}\lambda=\pm i(B\pm\sqrt{C^2-A^2})$$

where A, B, C are functions of the phase difference φ. The system will be stable if (C^2-A^2) is positive for any value of φ.

For the symmetrical arrangement a, the functions A, B, C are expressed by the formulæ:

$$A(\varphi)=\frac{1}{2h^2}-\sum_{p=1}^{\infty}\frac{p^2l^2-h^2}{(p^2l^2+h^2)^2}+\sum_{p=1}^{\infty}\frac{1-\cos p\varphi}{p^2l^2}$$

$$B(\varphi)=\sum_{p=1}^{\infty}\frac{p^2l^2-h^2}{(p^2l^2+h^2)^2}\sin(p\varphi)$$

$$C(\varphi)=\frac{1}{2h^2}-\sum_{p=\lambda}^{\infty}\frac{p^2l^2-h^2}{(p^2l^2+h^2)^2}\cos(p\varphi)$$

But for $\varphi=\pi$ we get

$$A(\pi)=\frac{\pi^2}{8l^2}\left[\operatorname{ctgh}^2\left(\frac{h\pi}{l}\right)-\operatorname{tgh}^2\left(\frac{h\pi}{l}\right)\right]$$

$$C(\pi)=\frac{\pi^2}{8l^2}\left[\operatorname{ctgh}^2\left(\frac{h\pi}{l}\right)-\operatorname{tgh}^2\left(\frac{h\pi}{l}\right)\right]$$

so that this arrangement is unstable for any values of h and l.

For the unsymmetrical arrangement b we find

$$A(\varphi)=-\sum_{p=0}^{\infty}\frac{(p+\frac{1}{2})^2l^2-h^2}{[(p+\frac{1}{2})^2l^2+h^2]^2}+\sum_{p=1}^{\infty}\frac{1-\cos(p\varphi)}{p^2l^2}$$

$$B(\varphi)=\sum_{p=0}^{\infty}\frac{(p+\frac{1}{2})^2l^2-h^2}{[(p+\frac{1}{2})^2l^2+h^2]^2}\sin(p+\tfrac{1}{2})\varphi$$

$$C(\varphi)=\sum_{p=0}^{\infty}\frac{(p+\frac{1}{2})^2l^2-h^2}{[(p+\frac{1}{2})^2l^2+h^2]^2}\cos(p+\tfrac{1}{2})\varphi$$

We see now that $C(\pi)=0$, so that in the place where $\varphi=\pi$, A must also be equal to zero, because, on account of the double sign, λ takes a positive real value. This brings us to the condition

$$\sum_{p=0}^{\infty}\frac{(p+\frac{1}{2})^2l^2-h^2}{[(p+\frac{1}{2})^2l^2+h^2]^2}=\sum_{p=0}^{\infty}\frac{2}{(2p+1)^2l^2}$$

But

$$\sum_{p=0}^{\infty}\frac{[(p+\frac{1}{2})^2l^2-h^2}{[(p+\frac{1}{2})^2l^2+h^2]^2}=\frac{\pi^2}{2l^2\cosh^2\frac{\pi h}{l}}$$

and

$$\sum_{p=0}^{\infty}\frac{2}{(2p+1)^2l^2}=\frac{\pi^2}{4l^2}$$

so that, as the necessary condition of stability we find the relation

$$\cosh\frac{h\pi}{l}=\sqrt{2}$$

and for the ratio h/l we find the value

$$h/l=0{,}283\ldots.$$

For a certain value of the wave length of the disturbance, corresponding to $\varphi=\pi$, we get $\lambda=o$, that is, the system is in a neutral state. But it can be shown by calculation that our system is stable for all other disturbances. This unique disturbance has to be tested by further investigations. It can, however, be seen that a zero value for λ must appear, because only one stable configuration exists. If this were not so, we would find for l/h a finite domain of stability.[1]

THE "FLOW PICTURE."

The consideration of the question of stability has brought us to the result that there exists a particular configuration of two vortex rows which is stable. The vortices of both rows have then such an arrangement that the vortices of one row are placed opposite the middle of the interval between the vortices of the other row, and the ratio of the distance h between the two rows to the distance l between the vortices of the same row has the value

$$\frac{h}{l}=\frac{1}{\pi}\ \text{arc cosh}\ \sqrt{2}=0{,}283$$

The whole system has the velocity

$$u=\frac{\zeta}{\pi}\sum_{p=o}^{\infty}\frac{h}{(p+\frac{1}{2})^2l^2+h^2}$$

which can also be written

$$u=\frac{\zeta}{2l}\text{tg h}\frac{\pi h}{l}$$

or, introducing the value of h/l found by the stability investigation, we get

$$u=\frac{\zeta}{l\sqrt{8}}$$

The flow is given by the complex potential (φ potential, ψ flow function)

$$\chi=\varphi+i\psi=\frac{i\zeta}{2\pi}\,lg\,\frac{\sin\,(z_o-z)\frac{\pi}{l}}{\sin\,(z_o+z)\frac{\pi}{l}}$$

where

$$z_o=\frac{l}{4}+\frac{hi}{2}$$

By aid of this formula we have calculated the corresponding streamlines and have represented them in Fig. 2. We see that some of the streamlines are closed curves around the vortices, while the others run between the vortices.

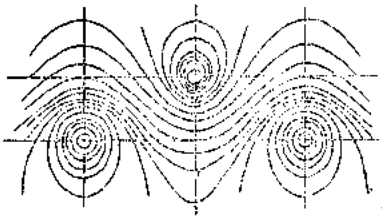

FIG. 2.

On the other hand, we have tried to make visible the flow picture behind a body, e. g., a flat plate or circular cylinder, moved through immobile water, by aid of lycopodium powder sifted on the surface of the water, and to fix these pictures photographically (exposure one-tenth of a second).

The regularly alternated arrangement of the vortices can not be doubted. In most cases the vortex centers can also be well determined; sometimes the picture is disturbed by small "accidental vortices" produced in all probability by small vibrations of the body, which in our provisional experiments could not be avoided. We had a narrow tank whose floor was formed by a band running on two rolls, and the bodies tested were simply put on the moving band and carried by it. It is to be expected that by aid of an arrangement especially made for the purpose much more regular flow pictures could be obtained, while in the actual experiments the flow was disturbed on the one hand by the vibrations of the body and on the other by the water flow produced by the moving band itself.

The alternated arrangement of the vortices rotating to the right and to the left can only be obtained when the vortices periodically run off first from one side of the body, then from the other, and so on, so that behind the body there appears a periodic motion, oscillating from one side to the other, but with such a regularity, however, that the frequency of this oscillation can be estimated with sufficient exactness. The periodic character of the motion in the so-called "vortex wake" has often been observed. Thus, Bernard [2] has remarked that the flow picture behind a narrow obstacle can be decomposed into vortex fields with alternated rotations. Also for the flow of water around balloon models the oscillation of the vortex field has been observed.[3] Finally, v. d. Borne [4] has observed and photographed recently the alternated formation of vortices in the case of air flowing around different obstacles. The

[1] From a mathematical standpoint our stability investigation may be considered as a direct application of the theorems of Mr. O. Toplitz on Cyclanten with an infinite number of elements, which he has in part published in two papers (Gottingen Nachrichten, 1907, p. 110; Math. Annalen 1911. p. 351), and in part been so kind as to communicate personally to us.

[2] Comptes Rendus, Paris, 148, 839, 1908.

[3] Technical report of the Advisory Committee for Aeronautics (British), 1910-11.

[4] Undertaken on the initiative of the representatives of aeronautical science in Gottingen, November, 1911.

phenomenon could not be explained until now; according to our stability investigation the periodic variations appear as a natural consequence of the instability of the symmetrical flow.[1]

It is also very interesting to observe how the stable configuration is established. When, for example, a body is set in motion from rest (or conversely, the stream is directed onto the body) some kind of "separation layer" is first formed, which gradually rolls itself up, at first symmetrically on both sides of the body, till some small disturbance destroys the symmetry, after which the periodic motion starts. The oscillatory motion is then maintained corresponding to the regular formation of left hand and right hand vortices.

We have also made a second series of photographs for the case of a body placed at rest in a uniform stream of water. For this case the flow picture can be obtained from Fig. 2 by the superposition of a uniform horizontal velocity. We will then see on the lines drawn through the vortex centers perpendicular to the stream direction, some ebbing point where the stream lines intersect and the velocity is equal to zero. However, in the same way as the motion is affected by the vibrations of the experimental body in the case of the motion of a body in the fluid, so in this case the turbulence of the water stream gives rise to disturbances.

As to the quantitative agreement attained by the theory, it must be noted that our stability conditions refer to infinite vortex rows, so that an agreement of the ratio h/l with the measured values is to be expected only at a certain distance from the body. The measurements on the photographs show that the distance l between vortices in a row is very regular, so that l may be measured satisfactorily, but per contra the distance h is much more variable, because the disturbance of the vortices takes place principally in the direction normal to the rows, that is, the latter undergo in the main transverse oscillations. The best way to determine the mean positions of the centers of the vortices would be by aid of cinematography, but we can also, without any special difficulty, find by comparison the mean direction of each vortex row directly from photographs. So in the case of the photograph of a circular cylinder 1.5 cm. in diameter, when making measurements beyond the first two or three vortex pairs we have found the following mean values for h and l

$$h=1.8 \text{ cm.}; \quad l=6.4 \text{ cm.}$$

So that for the ratio h/l we obtain the value

$$h/l=0.28.$$

For the flow around a plate of 1.75 cm. breadth we found

$$h=3 \text{ cm.}; \quad l=9.8 \text{ cm.}$$

Accordingly

$$h/l=0.305.$$

The agreement with the theoretical value 0.283 is entirely satisfactory.

For the first vortex pair behind the body, h/l comes out sensibly larger, somewhere near $h/l=0.35$. But in the first investigation of Kármán, mentioned at the beginning of this paper, the stability of the vortex system was investigated in such a way that all the vortices with the exception of one pair were maintained at rest and the free vortex pair considered oscillating in the velocity field of the others. Under such assumptions it was found that $h/l=1/\pi \operatorname{arc\,cosh} \sqrt{3} = 0.36$. We therefore think that the conclusion can be drawn, that in the neighborhood of the body, where the vortices are even more limited in their displacements, the ratio h/l is greater than 0.283 and approaches rather the value of 0.36.

APPLICATION OF THE MOMENTUM THEOREM TO THE CALCULATION OF FLUID RESISTANCE.

Let us assume that at a certain distance behind the body there exists a flow differing but slightly from the one of stable configuration which we have established theoretically in the foregoing, but that at a distance in front of the body, which is great in comparison with the size of the body, the fluid is at rest—as it is quite natural to assume. We will then be brought by the application of the momentum theorem to a quite definite expression for the resistance which a body moving with a uniform velocity in a fluid must experience. Practically, by such a calculation for the uniplanar problem, we will obtain the resistance of a unit of length of an infinite body placed normally to the plane of the flow.

We will use a system of coordinates moving with the same speed u as the vortex system behind the body. In this coordinate system, according to our assumptions, at a sufficient distance from the body the vortex motion behind the body as well as the fluid state in front of the body will be steady, and we will have, when referred to this system of coordinates, a uniform flow of speed $-u$ in front of the body, but behind the body the velocity components will be expressed by

$$-u+\frac{\partial \psi}{\partial y} \text{ and } -\frac{\partial \psi}{\partial x}$$

where ψ is the real part of the complex potential

$$\chi=\varphi+i\psi=\frac{i\zeta}{2\pi} lg \frac{\sin (z_0+z)\frac{\pi}{l}}{\sin (z_0-z)\frac{\pi}{l}}$$

[1] The tone that is emitted by a stick rapidly displaced in air is fixed by this periodicity, to which Prof. C. Runge has already drawn our attention.

The body itself has, relative to this system of coordinates, the velocity $U-u$, where U is the absolute velocity of the body. If we designate by l the distance between the vortices of one row, there must take place, as a consequence of the displacement of the body, in the time $T=l/(U-u)$, the formation of a vortex on each side of the body. We will calculate the increment of the momentum, along the X axis, in this time interval T (that is, between two instants of time of identical flow state) and for a part of the flow plane, which we define in the following way (see fig. 3). On the sides the plane portion considered is limited by the two parallel straight lines $y=\pm\eta$; in front and behind, by two straight lines $x=$Const. disposed at distances from the body which are great in comparison with the size of the body, the line behind the body being drawn so as to pass through the point half way between two vortices having inverse rotation. When the boundary lines are sufficiently far from the body we can consider the fluid velocities at those lines as having the values indicated in the foregoing.

For a space with the boundaries indicated above the relation must exist that the momentum imparted to the body $\int_0 W dt$ (where W is the resultant fluid resistance) is equal to the difference between the momentum contained in the space considered at the times $t=\tau$ and $t=\tau+T$ and the sum of the inflow momentum and the time integral of the pressure along the boundary lines. If we thus consider as exterior forces the force $-W$ and the pressure, which act on the whole system of fluid and solid, they must then correspond to the increment of the momentum—that is, to the excess of momentum after the time T less the inflow momentum.

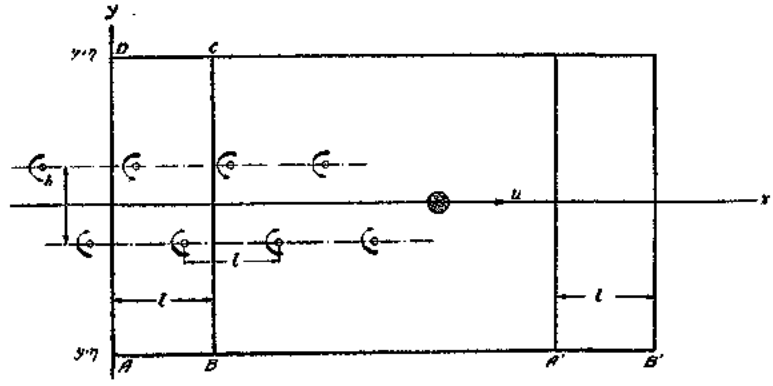

FIG. 3.

We will calculate these momentum parts separately. The excess of momentum after the time T is equal to the difference of the values that the double integral $\rho\iint u\,(x,\,y)\,dx\,dy$ takes at the times $t=\tau$ and $t=\tau+T$. But the time interval has been chosen in such a way that the state of flow is identical, with the difference that the body has been displaced through the distance $l=(U-u)\,T$. The double integral reduces thus to the difference of the integrals taken over the strips $ABCD$ and $A'B'C'D'$ both of breadth l. For the strip $A'B'C'D'$ the fluid speed can be taken equal to $-u$ for the strip $ABCD$ equal to $-u+\frac{\partial\psi}{\partial y}$ so that we get

$$I_1=\rho\int_0^l\int_{-\eta}^{\eta}\frac{\partial\psi}{\partial y}dx\,dy$$

If we pass to side boundaries having $\eta=\infty$, we obtain for I_1 the very simple expression

$$I_1=\rho\Gamma h$$

which can also be obtained directly by the application of the general momentum theorem to vortex systems.

We will unite in one single term the inflow momentum and the time integral of the pressure, because in such a way we will be led to more simple results. If we consider a uniplanar steady fluid motion with the velocity components $u\,(x,\,y)$ and $v\,(x,\,y)$ and consider a fixed contour in the plane, the inflow momentum in a unit of time in the direction of X is expressed by the closed integral $\rho\int(\overline{u}^2dy-\overline{uv}dx)$ where $\overline{u}$, $\overline{v}$ are the velocities on the contour. The pressure gives the resultant $\int\overline{p}\,dy$ along the X axis, but since for a steady flow the relation

$$p=\text{Const}-\rho\frac{\overline{u}^2+\overline{v}^2}{2}$$

must hold, we thus obtain for the sum of both integrals, multiplied by T

$$I_2=T\int\rho(\overline{u}^2dy-\overline{uv}dx)+T\int p\,dy$$
$$=T\rho\int\left(\frac{\overline{u}^2-\overline{v}^2}{2}dy-\overline{uv}dx\right)$$

Or, introducing the complex quantity,

$$\overline{w}=\overline{u}-i\overline{v}=\frac{\partial(\varphi+i\psi)}{\partial(x+iy)}=\frac{\partial\chi}{\partial z}$$

we get

$$I_2=\rho\ Im\int\left(\overline{w}^2dz\right)$$

where Im is to be understood as the complex part of the integral.

If we put for the contour

$$\overline{u}=-u+u'$$
$$\overline{v}=v'$$

then the terms in u^2 will at once be eliminated, and also the terms in u on account of the equality of the inflow and outflow; and there will remain only the terms in u'^2 and $u'v'$. The latter will give a finite value only for the boundary line passing through the vortex system (AD in fig. 3). Passing to $\eta=\infty$, we get

$$I_2=T\rho\,Im\left[\int_{-i\infty}^{+i\infty}\left(\frac{d\chi}{dz}\right)^2dz\right]$$

and integrating along AD we get

$$I_2=T\rho Im\left[\int_{\chi(-i\infty)}^{\chi(i\infty)}\frac{d\chi}{dz}d\chi\right]$$

But

$$w=\frac{d\chi}{dz}=-\frac{\zeta}{l}\operatorname{tgh}\frac{h\pi}{l}\frac{i\zeta\cos\frac{2\pi\chi}{\zeta}}{l\cosh\frac{h\pi}{l}}$$

so that, integrating and introducing the values

$$\chi(iw)=\frac{\zeta}{4}-i\frac{h\zeta}{2l}$$

$$\chi(-iw)=-\frac{\zeta}{4}+i\frac{h\zeta}{2l}$$

$$I_2=T\rho\left[\frac{\zeta uh}{l}-\frac{\zeta^2}{2\pi l}\right]$$

where u again has been written for $\frac{\zeta}{2l}\operatorname{tgh}\frac{\pi h}{l}$.

Thus the total momentum imparted to the body is

$$\int_o^T Wdt=\rho\zeta h-T\rho\left(\frac{\zeta uh}{l}-\frac{\zeta^2}{2\pi l}\right)$$

If for the mean value of $\frac{1}{T}\int_o^T Wdt$ we write W (as the time mean value of the resistance) we will obtain with $T=l/(U-u)$ the final formula

$$W=\rho\zeta\frac{h}{l}(U-2u)+\rho\frac{\zeta^2}{2\pi l} \tag{II}$$

The fluid resistance appears here expressed by the three characteristic constants ζ, h, l of the vortex configuration (as u is expressed by the last). In the deduction of this last formula we did not take account of the stability conditions, so that this formula applies to any value of the ratio h/l. If we assume the vortices in the row to be brought all close together so that they are uniformly distributed along the row, but in such a way that the vortex intensity per unit of length remains finite, we thus pass to the case of continuous vortex sheets. In this case $\zeta/l=U$, but $\zeta^2/l=0$ and $u=\frac{U}{2}$, so that the fluid resistance disappears. The discontinuous potential flow of v. Helmholtz thus does not give any resistance when the depth of the dead water remains finite, as can also be shown from general theorems.

THE FORMULAE FOR FLUID RESISTANCE.

Let us now apply to our special case the general formula we have just found, introducing the relations between ζ and u, and h and l according to the stability conditions. For the speed u we have

$$u=\frac{\zeta}{l\sqrt{8}}$$

further,

$$h/l=0{,}283$$

so that we get

$$W=\rho l\left[0{,}283\sqrt{8}.u\,(U-2u)+\frac{4}{\pi}u^2\right]$$

If we introduce, as is ordinarily done, the resistance coefficient according to the formula

$$W=\psi_w\,\rho\,d\,U^2$$

where d is a chosen characteristic dimension of the body, to which we refer the resistance, we will obtain ψ_w expressed by the two ratios u/U and l/d in the following way

(III) $$\Psi_w=\left[0{,}799\frac{u}{U}-0{,}323\left(\frac{u}{U}\right)^2\right]\frac{l}{d}$$

We have thus obtained the resistance coefficient—which before could be observed only by resistance measurements—expressed by two quantities which can be taken directly from the flow phenomenon, viz, the ratio

$$\frac{u}{U}=\frac{\text{Velocity of the vortex system}}{\text{Velocity of the body}}$$

and

$$\frac{l}{d}=\frac{\text{Distances apart of the vortices in one row}}{\text{Reference dimension of the body}}$$

Both quantities, corresponding to the similitude of the phenomenon, within the limits of validity of the square law can depend only upon the dimension of the body.

These two quantities can be observed very easily experimentally. The ratio l/d can be taken directly from photographs, while the ratio u/U can be found easily by counting the number of vortices formed. If we designate by T the time between two identical flow states we can then introduce the quantity $l_o=UT$, which is the distance the body moves in the period T. This quantity must be independent of velocity for the same body, and the ratio l/l_o for similar bodies must also be independent of the dimensions of the body but determined by the shape of the body. Remembering that $T=l/(U-u)$, we then find between u/U and l/l_o the simple relation

$$\frac{u}{U}=1-\frac{l}{l_o}$$

By some provisional measurements we have proved the similitude rule and afterwards calculated the resistance coefficient for a flat plate and a cylinder disposed normal to the stream, for the purpose of seeing if the calculated values agreed with the air resistance measurements, at least in order of magnitude.

Our measurements were made first on two plates of width 1.75 and 2.70 cm. and 25 cm. length, and we have measured the period T and calculated the quantity $l_o=UT$ for two different velocities. We have used a chronograph for time measurements and the period was observed for each vortex row independently. Thus was found for the narrower plate

U=10.0 *cm/sec*	15.1 *cm/sec*
T=1.26 *sec*	0.805 *sec*
UT=12.6 *cm*	12.1 *cm*

for the wider plate

U=9.6 *cm/sec*	15.5 *cm/sec*
T=1.99 *sec.*	1.20 *sec.*
UT=19.1 *sec.*	18.6 *sec.*

Mean value UT=18.8 *cm*

The ratio of the plate width is equal to

$$\frac{2.\,70}{1.\,75}=1.54$$

and the ratio of the quantities $l_o=UT$ is equal to

$$\frac{18.\,8}{12.\,3}=1.52$$

So that the similitude rule is in any case confirmed.

A circular cylinder of 1.5 cm. diameter was also teasted at two speeds. We found the values

U=11.0 *cm/sec*	15.8 *cm/sec*
T=0.66 *sec.*	0.48 *sec.*
UT=7.3 *cm*	7.5 *cm*

Mean value UT=7.4 *cm*

Knowing the values of $l_0 = UT$ we can calculate for the plate and the cylinder the speed ratio u/U. Thus,

for the plate $u/U = 0.20$.
for the cylinder $u/U = 0.14$

and with the values of l indicated before we have

for the plate $l/d = 5.5$
for the cylinder $l/d = 4,3$

where d is the plate width or cylinder diameter. We thus find the resistance coefficients

for the plate $\psi_w = 0.80$
for the cylinder $\psi_w = 0.46$

The resistance measurements of Foppl[1] have given for a plate with an aspect ratio of 10:1 the resistance coefficient $\psi_w = 0.72$ and the Eiffel[2] measurements, for an aspect ratio of 50:1; that is, for a nearly plane flow, the value $\psi_w = 0.78$. Further, Foppl has found for a long circular cylinder $\psi_w = 0.45$, so that the agreement between the calculated and measured resistance coefficients must be considered as fully satisfactory.

The theoretical investigations here developed ought to be extended and completed in two directions. First, we have limited ourselves to the uniplanar problem; that is, to the limiting case of a body of great length in the direction normal to the flow. It is to be expected that by the investigation of stable vortex configurations in space we will also be brought to a better understanding of the mechanism of fluid resistance. However, the problem is rendered difficult by the fact that the translation velocity of curved vortex filaments is not any longer independent of the size of the vortex section, because to an infinitely thin filament would correspond an infinitely great velocity. Nevertheless, it must not be considered that the extension of the theory to the case of space would bring unsurmountable difficulties.

Much more difficult appears the extension of the theory in another direction, which really would first lead to a complete understanding of the theory of fluid resistance, namely, the evaluation by pure calculation of the ratios l/d and u/U, which we have found from flow observations, and which determine the fluid resistance. This problem can not be solved without investigation of the process of vortex formation. An apparent contradiction is brought out by the fact that we have used only the theorems established for perfect fluids, which in such a fluid (frictionless fluid) no vortices can be formed. This contradiction is explained by the fact that we can everywhere neglect friction except at the surface of the body. It can be shown that the friction forces tend to zero when the friction coefficient decreases, but the vortex intensity remains finite. If we thus consider the perfect fluid as the limiting case of a viscous fluid, then the law of vortex formation must be limited by the condition that only those fluid particles can receive rotation which have been in contact with the surface of the body.

This idea appear first, in a perfectly clear way, in the Prandtl theory of fluids having small friction. The Prandtl theory investigates those phenomena which take place in a layer at the surface of the body, and the way in which the separation of the flow from the surface of the body occurs. It we could succeed in bringing into relation these investigations on the method of separation of the stream from the wall with the calculation of stable configuration of vortex films formed in any way whatever, as has been explained in the foregoing pages, then this would evidently mean great progress. Whether or not this would meet with great difficulties can not at the present time be stated.

---

[1] See the work of O. Foppl already mentioned.
[2] G. Eiffel, "La Resistance de l'Air et l'Aviation," p. 47, Paris, 1910.

TECHNICAL MEMORANDUMS

NATIONAL ADVISORY COMMITTEE FOR AERONAUTICS

No. 336

PRESSURE DISTRIBUTION ON JOUKOWSKI WINGS

By Otto Blumenthal

and

GRAPHIC CONSTRUCTION OF JOUKOWSKI WINGS

By E. Trefftz

Zeitschrift für Flugtechnik und Motorluftschiffahrt
May 31, 1913

Washington
October, 1925

NATIONAL ADVISORY COMMITTEE FOR AERONAUTICS.

TECHNICAL MEMORANDUM NO. 336.

PRESSURE DISTRIBUTION ON JOUKOWSKI WINGS.*

By Otto Blumenthal.

In the winter semester of 1911-12, I described, in a lecture on the hydrodynamic bases of the problem of flight, the potential flow about a Joukowski wing.** In connection with this lecture, Karl Toepfer and Erich Trefftz computed the pressure distribution on several typical wings and plotted their results. I now publish these diagrams accompanied by a qualitative discussion of the pressure distribution, which sufficiently indicates the various possible phenomena. For a quicker survey, I have divided the article into two parts, the first part dealing with the more mathematical and hydrodynamic aspects and the second part, which is comprehensible in itself, taking up the real discussion from the practical standpoint.

---

* From "Zeitschrift für Flugtechnik und Motorluftschiffahrt," May 31, 1913.

** See above magazine, Vol. I (1910), p. 281.

I

We obtain the entire number of all Joukowski wings of the length $2l$ with the trailing edge at the point $x = -l$, by laying, in a $\zeta = \xi + i\eta$ plane through the point $\zeta = l/2$, the cluster of all the circles which contain the point $\zeta = l/2$, either inside or on their circumference, and plotting these circles by means of the formula

$$z = \zeta + \frac{l^2}{4\zeta} \qquad (1)$$

on the $z = x + i\,y$ plane. The circles, which contain the point $\zeta = l/2$ on their circumference, thus become doubly intersected arcs and, in particular, the circle, which has the distance $(-l/2, +l/2)$ for its diameter, becomes the rectilinear distance of the length $2l$. The circles which contain the point $\zeta = l/2$ inside, furnish the real Joukowski figures. The point $\zeta = -l/2$ passes every time into the sharp trailing edge. The individual Joukowski wings are characterized by the following quantities (Fig. 1). The center M of the circle K is connected with the point H, $\zeta = -l/2$, and the point of intersection of this connecting line with the η axis is designated by M'. The distance OM' on the η axis is equal to half the height of the arc produced by describing the circle about M' as its center and is therefore designated by $f/2$, as half the camber of the Joukowski wing, f being its first characteristic dimension. We have chosen as the

second characteristic dimension, the radii difference $MM' = \delta$. This gives a measurement for the thickness of the Joukowski wing.

We will now consider the determination of the velocity and pressure distribution which produce an air flow along the wing, in infinity, with the velocity V at an angle of $\pi-\beta$ with the positive x axis, β being the angle of attack of the wing.

The absolute velocity q of this flow is calculated thus: If $\kappa(\xi,\eta)$ is the absolute velocity of the air flow, of velocity V and angle of attack β, around the circle K in the ζ plane, then

$$q(x,y) = \frac{\kappa(\xi,\eta)}{\left|\frac{dz}{d\zeta}\right|}.$$

It is, however,

$$\left|\frac{dz}{d\zeta}\right| = \frac{1}{\sigma^2}\sqrt{\left(\sigma^2 - \frac{l^2}{4}\right)^2 + l^2\eta^2}, \quad \sigma^2 = \xi^2 + \eta^2,$$

and along the circle K

$$\kappa(\xi,\eta) = \frac{1}{\frac{\sqrt{l^2 + f^2}}{2} + \delta}\left|2V(\xi\sin\beta + \eta\cos\beta) + c\right|,$$

where $2\pi c$ is the circulation. This constant is determined according to Kutta, by the condition that the velocity at the trailing edge is finite and therefore, since $dz/d\zeta$ there disappears, κ must also disappear at the point H. Thus we obtain

$$\left.\begin{aligned} \kappa(\xi,\eta) &= \frac{1}{\frac{\sqrt{l^2+f^2}}{2}+\delta}\,2\left|\left(\xi+\frac{l}{2}\right)\sin\beta+\eta\cos\beta\right|, \\ \frac{q}{V} &= \frac{\sigma^2}{\frac{\sqrt{l^2+f^2}}{2}+\delta}\,\frac{2\left|\left(\xi+\frac{l}{2}\right)\sin\beta+\eta\cos\beta\right|}{\sqrt{\left(\sigma^2-\frac{l^2}{4}\right)^2+l^2\eta^2}} \\ \sigma^2 &= \xi^2+\eta^2. \end{aligned}\right\} \quad (2)$$

This rather involved expression is simplified by the introduction of a new variable, the angle ω at the center of the circle K, measured from the radius MH. In this angle, the coordinates ξ,η and the quantities connected with them are expressed as follows: For abbreviation, we designate the radius of the circle K with $r = \frac{\sqrt{l^2+f^2}}{2}+\delta$ and introduce the angle A by

$$\cos A = \frac{l}{\sqrt{l^2+f^2}}, \qquad \sin A = \frac{f}{\sqrt{l^2+f^2}}.$$

The geometric significance of A and ω is obvious from Fig. 1. By simple calculations we now obtain

$$\left.\begin{aligned} \xi &= -\frac{l}{2}+2\,r\sin\frac{\omega}{2}\sin\left(\frac{\omega}{2}+A\right), \\ \eta &= -2\,r\sin\frac{\omega}{2}\cos\left(\frac{\omega}{2}+A\right), \end{aligned}\right\} \quad (3)$$

$$\left.\begin{aligned} \sigma^2 &= \frac{l^2}{4}-2l\,r\sin\frac{\omega}{2}\sin\left(\frac{\omega}{2}+A\right)+4\,r^2\sin^2\frac{\omega}{2} \\ &= \frac{l^2}{4}+4\,r\sin\frac{\omega}{2}\left[\delta\sin\frac{\omega}{2}-\frac{f}{2}\cos\left(\frac{\omega}{2}+A\right)\right] \end{aligned}\right\} \quad (4)$$

Formula 2 for q is simplified by the introduction of the angle ω, to

$$\left.\begin{aligned}\left|\frac{q}{V}\right| &= \frac{\sigma^2}{r\,\frac{l}{2}} \\ &\cdots\cdots\cdots \frac{\left|\cos\left(\frac{\omega}{2}+A+\beta\right)\right|}{\sqrt{\cos^2\left(\frac{\omega}{2}+A\right)+\frac{4}{l^2}\left[\delta\sin\frac{\omega}{2}-\frac{f}{2}\cos\left(\frac{\omega}{2}+A\right)\right]^2}} \cdots\cdots\cdots \\ &= \frac{\sigma^2}{r\,\frac{l}{2}}\,F\end{aligned}\right\} \quad (5)$$

From this we next derive a few general results which hold good for all the quantities f, δ, β.

a) On the trailing edge $\frac{q}{V} = \frac{l}{2r}\cos(A+\beta)$.

b) On top of the wing, there is always a portion along which the velocity $q > V$, hence where there is a negative pressure. As proof of this, we will consider the center of the upper side, the point $\omega = \frac{3\pi}{2} - A$. At this point $\sigma > r$, as can easily be seen geometrically (Fig. 1) or from formula 4. However, if we put $\omega = \frac{3\pi}{2} - A$ in formula 5, it then becomes

$$\left|\frac{q}{V}\right| = \frac{\sigma^2}{r\,\frac{l}{2}}\,\frac{\cos\left(\frac{\pi}{4}-\frac{A}{2}-\beta\right)}{\cos\left(\frac{\pi}{4}-\frac{A}{2}\right)}\,\frac{1}{\sqrt{1+\frac{4}{l^2}\left(\delta+\frac{f}{2}\right)^2}}$$

$$> \frac{\cos\left(\frac{\pi}{4}-\frac{A}{2}-\beta\right)}{\cos\left(\frac{\pi}{4}-\frac{A}{2}\right)}\,\frac{r}{\sqrt{\frac{l^2}{4}+\left(\delta+\frac{f}{2}\right)^2}} > \frac{\cos\left(\frac{\pi}{4}-\frac{A}{2}-\beta\right)}{\cos\left(\frac{\pi}{4}-\frac{A}{2}\right)}$$

c) The velocity is zero at the point $\omega = \pi - 2A - 2\beta$, which is always located on the lower side. At this point the streamline enters the wing. Further general conclusions (i.e., applying to all f, δ, β) can hardly be drawn. We obtain considerably more accurate expressions in the especially interesting practical case where, in the vicinity of the leading edge, a pronounced velocity maximum and consequently a strong suction is produced. We will confine ourselves to this case in all that follows. Hereby we can, in formula 5, first of all disregard the slight fluctuation of the factor σ^2 for small values of f and δ and consider only the factor F, which must be alone decisive for the great changes in velocity. This factor, however, enables a simple explanation.

For this purpose, we introduce the angle $\psi = \frac{\omega}{2} + A + \beta$. The entering point of the streamline then lies at $\psi = \pi/2$, where F disappears. In general, we have

$$\left.\begin{aligned} \frac{1}{F^2} &= (a^2 + \sin^2\beta)\tan^2\psi - 2(ab - \sin\beta\cos\beta)\tan\psi + \\ &\quad + (b^2 + \cos^2\beta), \\ a &= \frac{2}{l}\left(\delta\cos(A+\beta) - \frac{f}{2}\sin\beta\right), \\ b &= \frac{2}{l}\left(\delta\sin(A+\beta) + \frac{f}{2}\cos\beta\right). \end{aligned}\right\} \qquad (6)$$

Consequently, F attains its maximum value at the angle ψ_o, which is given by the formula

$$\tan\psi_o = \frac{ab - \sin\beta\cos\beta}{a^2 + \sin^2\beta} \qquad (7)$$

and this value is

$$F_{max} = \frac{\sqrt{\left(\delta \cos (A + \beta) - \frac{f}{2} \sin\beta\right)^2 + \frac{l^2}{4} \sin^2\beta}}{\delta \cos A} \qquad (7')$$

We now make the assumption, corresponding to the already announced purpose of our investigation, that F has a high maximum in relation to the value of $\cos (A + \beta)$ on the trailing edge. We require, e.g., that F_{max} shall equal or exceed $\sqrt{2}$. This is mathematically the most favorable. Formula 7', with the aid of a rough estimate, then gives

$$\frac{\sqrt{l^2 + f^2}}{2} \sin\beta \geq \delta \cos (A + \beta) \left(1 + \frac{f}{\sqrt{l^2 + f^2}}\right)$$

$$= \delta \cos (A + \beta) (1 + \sin A) \ldots . \qquad (8)$$

With this insertion, the numerator of $\tan \psi_o$ is smaller than

$$- \frac{4\delta}{l^2} \cos (A + \beta) \left[\frac{\sqrt{l^2 + f^2}}{2} \cos\beta - \delta \sin (A + \beta) (1 - \sin A)\right]$$

For small f, δ and β, this value is always negative and therefore the maximum value of F is assumed to be at a point located between the entering point and the trailing edge on the portion of the surface belonging to the upper side.* On the

* Generally the point is located on the upper side. It lies between the entering point and the leading edge, only when δ is very small in comparison with f. For $\delta = 0$, it lies on the leading edge.

other hand, it can be shown that the maximum is located not far from the entering point. In fact the greatly preponderating member in the numerator of $\tan \psi_0$, on account of formula 8, is $\cos\beta \sin\beta$. The case is not quite so simple with the denominator, which is

$$a^2 + \sin^2\beta =$$

$$= \frac{4}{l^2}\left[\delta^2 \cos^2 (A + \beta) - \delta f \cos (A + \beta)\sin\beta + \frac{l^2 + f^2}{4} \sin^2\beta\right].$$

If we introduce into the first member, on the right side of formula 8, the above limit for δ, the denominator is then smaller than $2 \frac{l^2 + f^2}{l^2} \sin^2\beta$. Hence $\tan \psi_0$ is either smaller or at most only unessentially* greater than $-\frac{1}{2}\cot\beta$, which shows that ψ is either smaller or at most only slightly greater than $\frac{\pi}{2} + 2\beta$. The point ω, at which F assumes its maximum value, is located between the entering point of the streamline and the upper side and, at most, only slightly farther than 4β from the entering point.

Lastly, it may be remarked that in formula 6 for $\frac{1}{F^2}$, both the powers, $\tan^2\psi$ and $\tan\psi$, appear to be multiplied by small coefficients. Both these members therefore assume quite large values for large values of $\tan\psi$, i.e., in the immediate vicinity of the entering point and the leading edge. Hence F differs but little over the whole surface, with the exception of the specified region, from the value $\cos (A + \beta)$ on the trailing edge and therefore only slightly from unity.

* "Unessentially" means that the deviations are of the order of magnitude f/l, δ/l.

II

The results of the computations in I are as follows: A Joukowski wing is characterized by the three dimensions, namely, the length $2l$, the camber f and the radii difference δ, which is expressed in the thickness of the wing. To these is added the angle of attack β. The points on the surface are most conveniently computed with the aid of a variable ω of the angle at the center of the circle in Fig. 1. The formulas for the coordinates will not be given here. In practice, a graphic process is employed which is explained in the accompanying note by E. Trefftz (pages 130-131 of this same volume of "Zeitschrift für Flugtechnik und Motorluftschiffahrt.") We require only the following data: $\omega = 0$ gives the trailing edge; $\omega = \pi - 2A$ $(\tan A = \frac{f}{l})$ gives the leading edge and the intermediate values of ω correspond to the lower surface of the wing. $\omega = \pi - 2A - 2\beta$ gives the entering point, i.e., the point where the air flow strikes the surface and hence where the velocity is zero.

The ratio of the absolute velocity q of the air flow on the wing to the velocity V in infinity is given by

$$\frac{q}{V} = \frac{\sigma^2}{r \frac{l}{2}} F \qquad (5)$$

$r = \frac{\sqrt{l^2 + f^2}}{2} + \delta$ is the radius of the circle in Fig. 1 and

σ the distance OB in the same figure. Both factors, σ and F, depend on ω. For small f and δ, the value of the factor $\frac{\sigma^2}{r\frac{l}{2}}$ differs but little from unity. The properties of the factor F, as obtained by the calculations of I, can be summarized as follows.

On the trailing edge, F has the value $\cos(A + \beta)$ and decreases at the customary angles of attack (about 6°), from the leading edge to the entering point, where it becomes zero. For small f and δ, the decrease takes place very slowly throughout most of the lower side and first becomes rapid in the immediate vicinity of the entering point.

From the entering point, F increases rapidly and attains near the leading edge, a maximum of the order of magnitude $\beta l/2\delta$. This is approximately also the maximum value of the velocity ratio q : V. For this maximum value, the ratio of the angle of attack to the thickness of the wing is therefore decisive, the camber having, in the first order, no effect on it. In constructive wing shapes, where δ and β are of the same order of magnitude, the velocity at the leading edge is accordingly not very great. This result is important because it explains the effect of rounding the leading edge. The result is still more striking when we consider the radius of curvature ρ of the leading edge. It is, namely, with unessential omissions $\frac{\rho}{l} = 16\,\frac{\delta^2}{l^2}\left(1 - 4\,\frac{\delta}{l}\right)$. The radius of curvature therefore diminishes rapidly with decreasing δ, the rounding

off of the leading edge being very slight, and the maximum velocity remains within moderate bounds. The negative pressure on the leading edge, which, according to Bernoulli's equation, is proportional to q^2/V^2, is computed by the introduction of the radius of curvature in the first approximation, to $4\beta^2 \frac{l}{\rho}$. I consider this simple formula worthy of attention.

The course of F along the top of the wing can finally be characterized as follows: At some distance from the leading edge, F changes but slowly. If, therefore, the maximum value of F is much greater than unity, it falls abruptly at first and then gradually approaches the value at the trailing edge.

Only in the vicinity of the leading edge does the factor F give us sufficiently accurate information concerning the course of the velocity q. Everywhere else we need to know the course of σ. This can be easily found geometrically from Fig. 1. On the leading edge σ has the value of $l/2$. From the triangle HMO, it follows that σ assumes its minimum value for the angle ω_{min}, which is given by

$$\frac{\sin \omega_{min}}{\sin A} = \frac{\frac{l}{2}}{\sqrt{\delta^2 \cos^2 A + r^2 \sin^2 A}}$$

Hence

$$\sin \omega_{min} = \frac{1}{\sqrt{\frac{4\delta^2}{f^2} + \frac{4r^2}{l^2}}}$$

For the angle $2\omega_{min}$, we again have $\sigma = \frac{l}{2}$ and then σ

increases further, up to the angle $\omega_{max} = \omega_{min} + \pi$. The value of ω_{min} increases with f/δ. For $\frac{f}{\delta} = 0$, $\omega_{min} = 0$, hence the value of σ is smallest on the trailing edge and greatest on the leading edge. Conversely, for $\frac{\delta}{f} = 0$, $\omega_{min} = (\pi/2) - A$ and is therefore situated in the middle of the lower surface. In general, with increasing f/δ, the minimum value of σ moves from the trailing edge to the middle of the lower surface; the point where $\sigma = \frac{1}{2}$ again from the trailing edge to the leading edge, while the maximum value of σ moves simultaneously from the leading edge to the middle of the upper surface.

In order to get an idea of the course of the velocity, we must now estimate the mutual effect of the factors F and σ^2. I will proceed with this discussion in close connection with the diagrams, which I must first explain. Their arrangement is the same as for the diagrams in Eiffel's "Resistance de l'air." Each figure has, at the bottom, an accurate outline of the wing section. Vertically above each point of the wing, there is plotted from a zero line on the vertical the ratio q^2/V^2, the upper curve corresponding to the upper side and the lower curve to the lower side of the wing section. The dashed line shows the unit distance from the zero line. The area enclosed by the q^2/V^2 curve gives, when multiplied by $\frac{\gamma}{2g} V^2$, the lift of a unit width of the wing. The chosen angle of attack is $6^\circ(\beta = 0.1)$, the air flow being horizontal.

I am dividing the discussion into several paragraphs.

1. The strong suction on the greater portion of the upper surface is common to all the figures. This is indeed the chief source of the lift, while the pressure on the lower surface contributes only a small increment. This can be easily verified from the general laws. In fact, as already stated, F diminishes very slowly along the under surface from the trailing edge almost to the entering point. Hence F differs but little, on most of the lower surface, from the value $\cos(A + \beta)$, which it has on the trailing edge, and therefore only a little from unity. Since also the factor $\frac{\sigma^2}{r\frac{l}{2}}$ falls only slightly below 1, up to the vicinity of the entering point, q/V is certainly not much smaller than one and hence there is only a slight pressure.

2. Fig. 2 ($f = 0$ and $\frac{\sigma}{l} = \frac{1}{10}$) indeed shows a suction effect along a portion of the under side. Since the values of f are here less than unity, such a suction effect can only be very small. Its appearance is due to relatively large values of σ^2 and depends essentially on the ratio $f : \delta$. Between the trailing edge and $\omega = 2\omega_{min}$ no suction can occur, because σ is here smaller than $l/2$. Any suction effect can therefore be expected for only small values of $f : \delta$, where ω_{min} is small. For $\delta = 0$ any suction effect is entirely impossible, since $2\omega_{min}$ then corresponds to the leading edge.

The suction effect has also been experimentally determined by Eiffel on the wing "en aile d'oiseau" which probably alone of all the surfaces tested by him can be compared with a Joukowski wing section.*

3. Even on the upper side, the course of the velocity is characteristically affected by the ratio $f : \delta$. This is clearly shown by Figs. 3-4. f/δ is expressed on the upper surface in the position of the angle $\omega_{max} = \omega_{min} + \pi$, for which σ has its maximum value. The fact that σ continues to increase from the leading edge as far as ω_{max} causes the maximum value of q to move farther from the leading edge than the maximum of F and the fall in velocity to be less rapid. We differentiate "slightly cambered" wings $(f/\delta < 3)$, in which ω_{max} in near the leading edge, and "highly cambered" wings $(f/\delta > 3)$, in which ω_{max} lies nearer the middle of the upper surface. Fig. 3, with $f = 0$, is a typical example of a slightly cambered wing. Here the maximum value of σ is situated in the leading edge and the values of F and σ therefore decrease

* Eiffel, "Resistance de l'air," 1911, Table XII; also p. 105 and "Complement," p. 122 ("aile Nieuport"). The Eiffel figures show that the suction effect increases on the under side with decreasing angle of attack. This is in agreement with our theory, for the factor F increases, as shown by formula 6, at every point on the under side with decreasing β. Another suction effect, which Eiffel finds on the trailing edge of nearly all wings, is doubtless due to the formation of vortices.

simultaneously, thus producing a very pronounced maximum velocity, although the maximum velocity is not important in itself. On the other hand, Fig. 4 ($f/l = 1/5$, $\delta/l = 1/20$) shows, in spite of a twice as large maximum velocity, a remarkably slow velocity decrease toward the upper side. In fact, in these experiments, the maximum of σ is situated at about 1/3 of the upper side and a more rapid velocity decrease accordingly first begins behind this point. We note also the small intermediate maximum on the upper side, which is caused by the increase of σ^2 in spite of the simultaneous decrease in F. The mean between Fig. 2 and Fig. 4 is held by Fig. 3, with $f/l = 1/10$ and $\delta/l = 1/20$. Here ω_{max} does not lie very far from the leading edge, about 1/6 of the upper side, the increase in σ^2 vanishes under the decrease in F and along the greater portion of the upper side we note a uniform falling off in velocity, due to the simultaneous decrease in the factors F and σ^2.

These relations were also found in Eiffel's experiments with the wing "en aile d'oiseau." Even the intermediate maximum of q on highly cambered wings is found on his figures.*

Lastly, I wish to call attention to the fact that the measurements of Fig. 4 appear to me to be worthy of commendation, on account of the very uniform stressing of the upper side.

* On Eiffel's figures, it appears that, with decreasing β, the maximum velocity moves backward from the leading edge on the upper side. This also agrees with the theoretical conclusions.

4. Fig. 5 has a very slight rounding ($\delta/l = 1/50$) at $f/l = 1/5$. Therefore $\frac{l}{2}\frac{\beta}{\delta} = 3.5$ and hence the very high velocity maximum on the leading edge. We have already seen that the high maxima must decrease very rapidly toward the upper side. The region of this steep decline corresponds to an angle of about the size β. During the drop, however, there is in the figure a long space of almost constant velocity. This is explained, as in paragraph 3, by the fact that the maximum value of σ is located at about 1/2.5 of the upper side. Only behind this point is there again a rapid decline to the trailing edge. This behavior is generally characteristic for highly cambered wings of slight rounding and occurs also on Eiffel's diagrams.

As regards the production of the diagrams, it may be noted, in conclusion, that they were drawn according to the very convenient method of E. Trefftz, as set forth in the accompanying note. Wherever it appeared necessary, the plotting was verified by calculation.

GRAPHIC CONSTRUCTION OF JOUKOWSKI WINGS.*

By E. Trefftz.

In plotting the cross-sectional outline (or profile) of a Joukowski wing, we proceed as follows (Fig. 6).

We first plot an xy system of coordinates with the origin O such that the x axis forms the angle β with the horizontal direction of the wing and mark on the x axis the point L, for which $x = -l$, and on the y axis the point F, for which $y = f$.

We now describe two circles and label them K_1 and K_2. The center M_1 of the first circle is situated on the straight line LF at a distance 2δ from the point F (beyond the section LF). The circle, moreover, passes through the point L. The second circle likewise passes through the point L and its center M_2 is likewise on LF, the position of M on LF being determined by the following condition. If OV_1 is the portion of the positive x axis cut off by the circle K_1 and OV_2 the portion cut off by the circle K_2, then $OV_1 \times OV_2 = l^2$.

We now draw, from the point O, the two lines OA_1 and OA_2, so as to form equal angles with the x axis, A_1 being the point of intersection of the first line with the circle K_1 and A_2 the intersection of the second line with the circle

* From "Zeitschrift für Flugtechnik und Motorluftschiffahrt," May 31, 1913, pp. 130 and 131.

K_2. Then the center P of the line $A_1 A_2$ is the point sought on the Joukowski wing profile.

In plotting the preceding figures, 24 points were found in this manner for each one, by shifting the first line from the point L 15° each time and drawing the second line symmetrically with reference to the x axis.

In order to determine the pressure on each point of the profile, when the wing is exposed to a horizontal wind having the velocity V, we must know the velocity q at which the air flows by each point of the profile. The pressure on each unit area of the wing surface is then proportional to q^2.

We can now find the values of q in a very simple manner. For this purpose, we draw a horizontal line through the point L. If we designate by h the distance of the point A_1 (of the circle K_1) from this horizontal line, we obtain, for any desired point P of the figure, the corresponding value of q in the following manner. We take from the diagram the distance between the points A_1 and A_2, at the middle of which we had found the point P, and also the distances of the point A_1 from the origin O, from the center M_1 of the circle K_1 and from the horizontal line passing through L. We then have

$$q = V \frac{O A_1}{A_1 A_2} \frac{2 h}{M_1 A_1}$$

The mathematical proof for the given constructions is simple. As already mentioned, the profile of a Joukowski wing

can be constructed by describing on the z plane, with the aid of the formula $z = \zeta + \frac{l^2}{4\zeta}$, the circle K, determined by the camber and radii difference. This circle passes through the point $\zeta = -\frac{l}{2}$.

The systems of coordinates are plotted both in the ζ plane and in the z plane in such manner that the ξ axis and the x axis form the angle β with the horizontal wind direction.

If we now describe, in the z plane, both circles, which we obtain from the given circle K in the ζ plane by employing the two conversion formulas

$$z_1 = 2\zeta \quad \text{and} \quad z_2 = \frac{l^2}{2\zeta}$$

then these are the same two circles we designated above by K_1 and K_2.

The point A_1 has the coordinate z_1 and the point A_2 has the coordinate z_2, hence the center of $A_1 A_2$ has the coordinate $z = \frac{1}{2}(z_1 + z_2) = \zeta + \frac{l^2}{4\zeta}$, as desired. P is therefore an actual point on the Joukowski curve.

The following formula holds good for the velocity q at which the air flows by every point on the Joukowski figure.

$$q = \frac{K(\xi, \eta)}{\left|\frac{dz}{d\zeta}\right|}$$

From $z = \zeta + \frac{l^2}{4\zeta}$ it follows that

$$\frac{dz}{d\zeta} = 1 - \frac{l^2}{4\zeta^2} = \frac{1}{2\zeta}\left(2\zeta - \frac{l^2}{2\zeta}\right) = \frac{z_1 - z_2}{z_1}$$

whence we obtain

$$\left|\frac{dz}{d\zeta}\right| = \frac{A_1 A_2}{O A_1}$$

since the absolute value of $z_1 - z_2$ equals the distance $A_1 A_2$ and the absolute value of z_1 = the distance OA_1.

For $\kappa(\xi,\eta)$, we obtain, from formula 2 of the preceding article, $\kappa = \frac{2Vh}{M_1 A_1}$, in which h is the distance of the point A_1 from the horizontal line passing through L. In the expression there given for the numerator, it is equal to h and the denominator is equal to $\frac{1}{2}(M_1 A_1)$, as may be easily verified. We thus obtain

$$q = V \frac{2h}{M_1 A_1} \frac{O A_1}{A_1 A_2}$$

which is just the formula given above for q.

Translation by Dwight M. Miner,
National Advisory Committee
for Aeronautics.

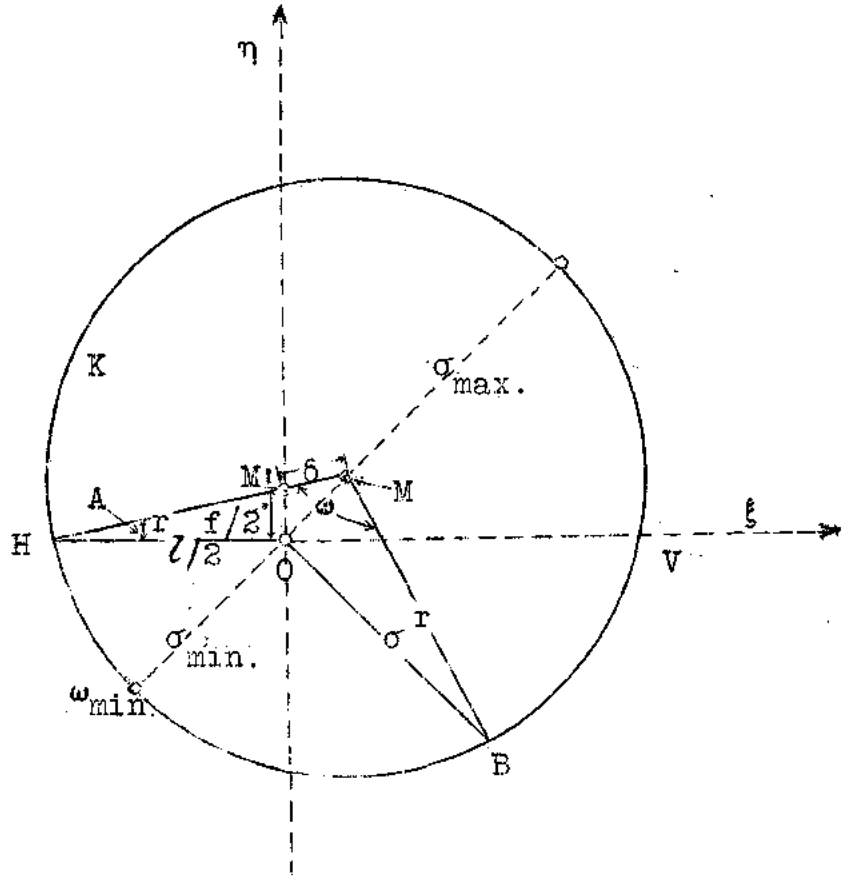

Fig.1

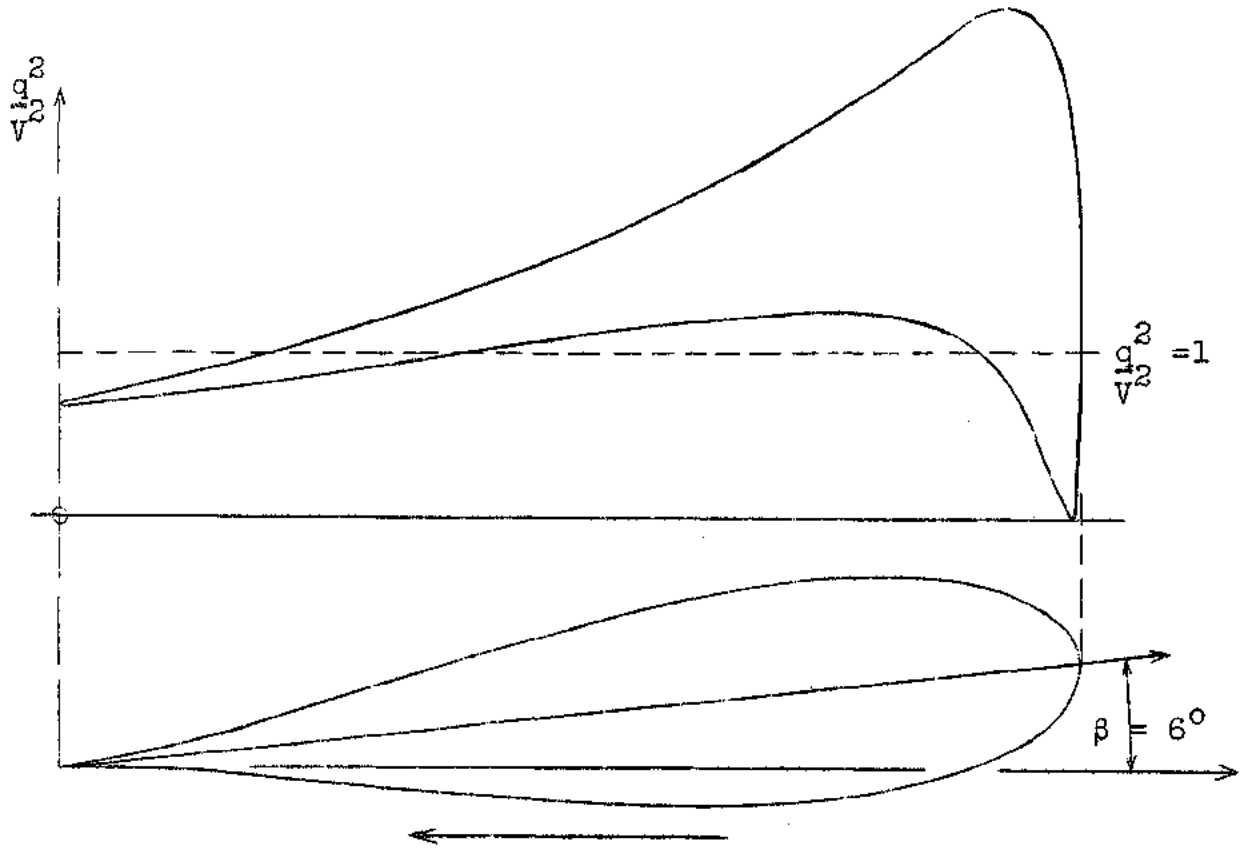

Fig.2: f = 0, $\delta/l = \frac{1}{10}$

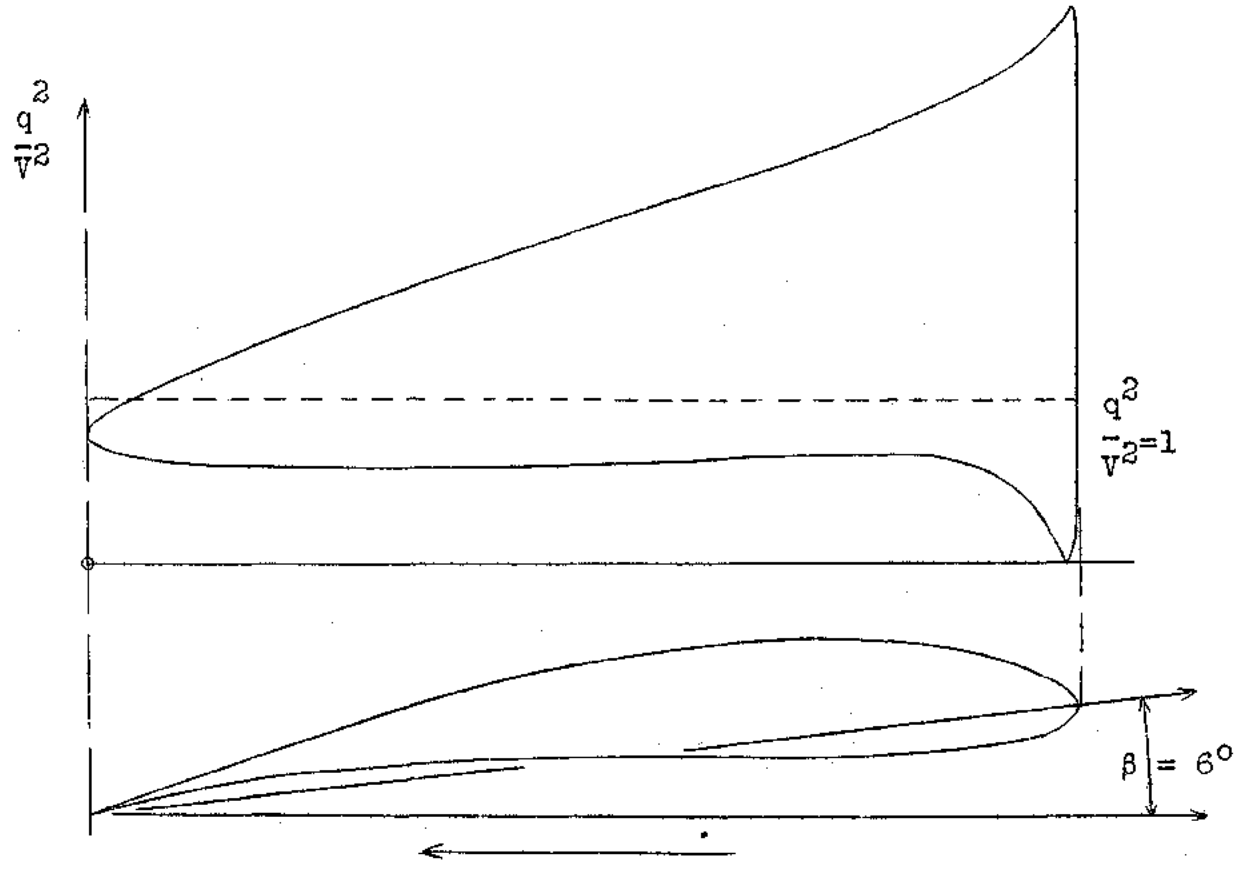

Fig.3: $f/l = \frac{1}{10}$, $\delta/l = \frac{1}{20}$

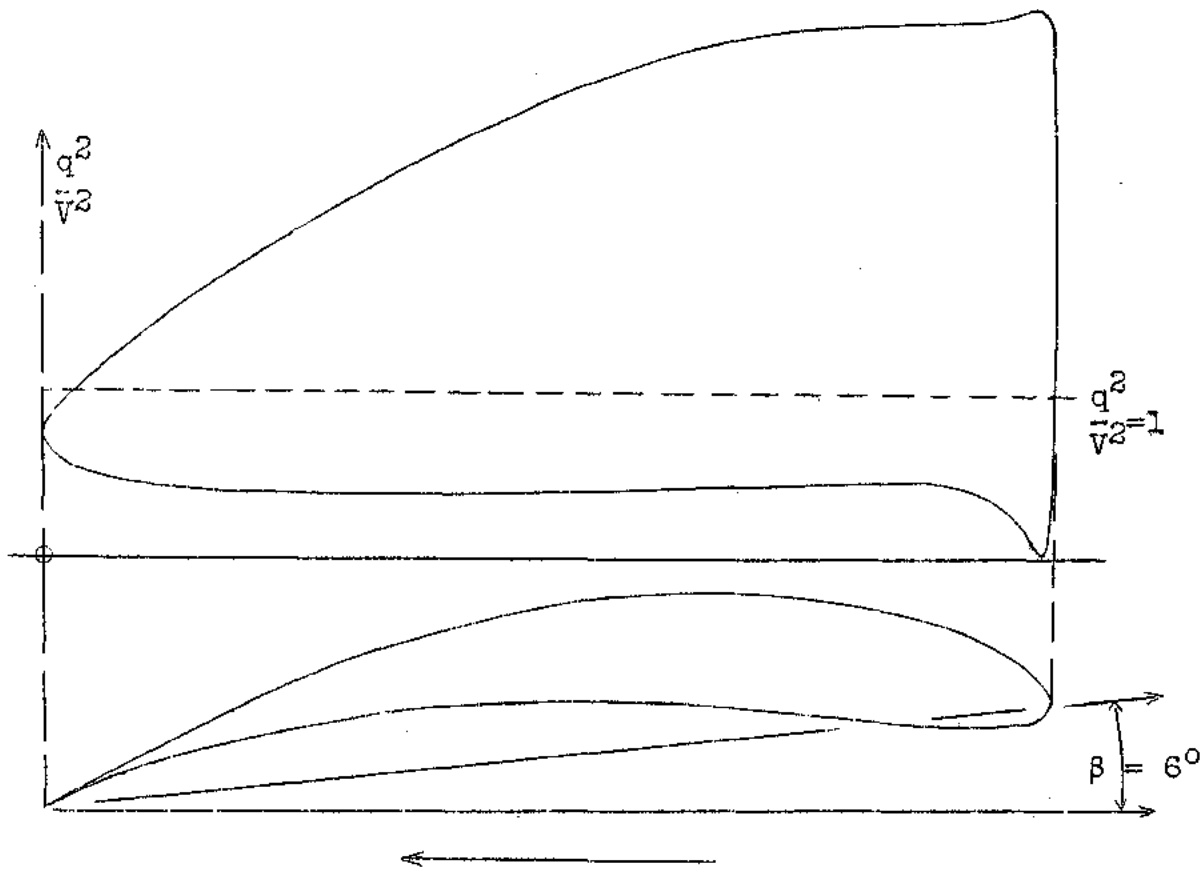

Fig.4: $f/l = \frac{1}{5}$, $\delta/l = \frac{1}{20}$

Fig.5: $f/l = \frac{1}{5}$, $\delta/l = \frac{1}{50}$

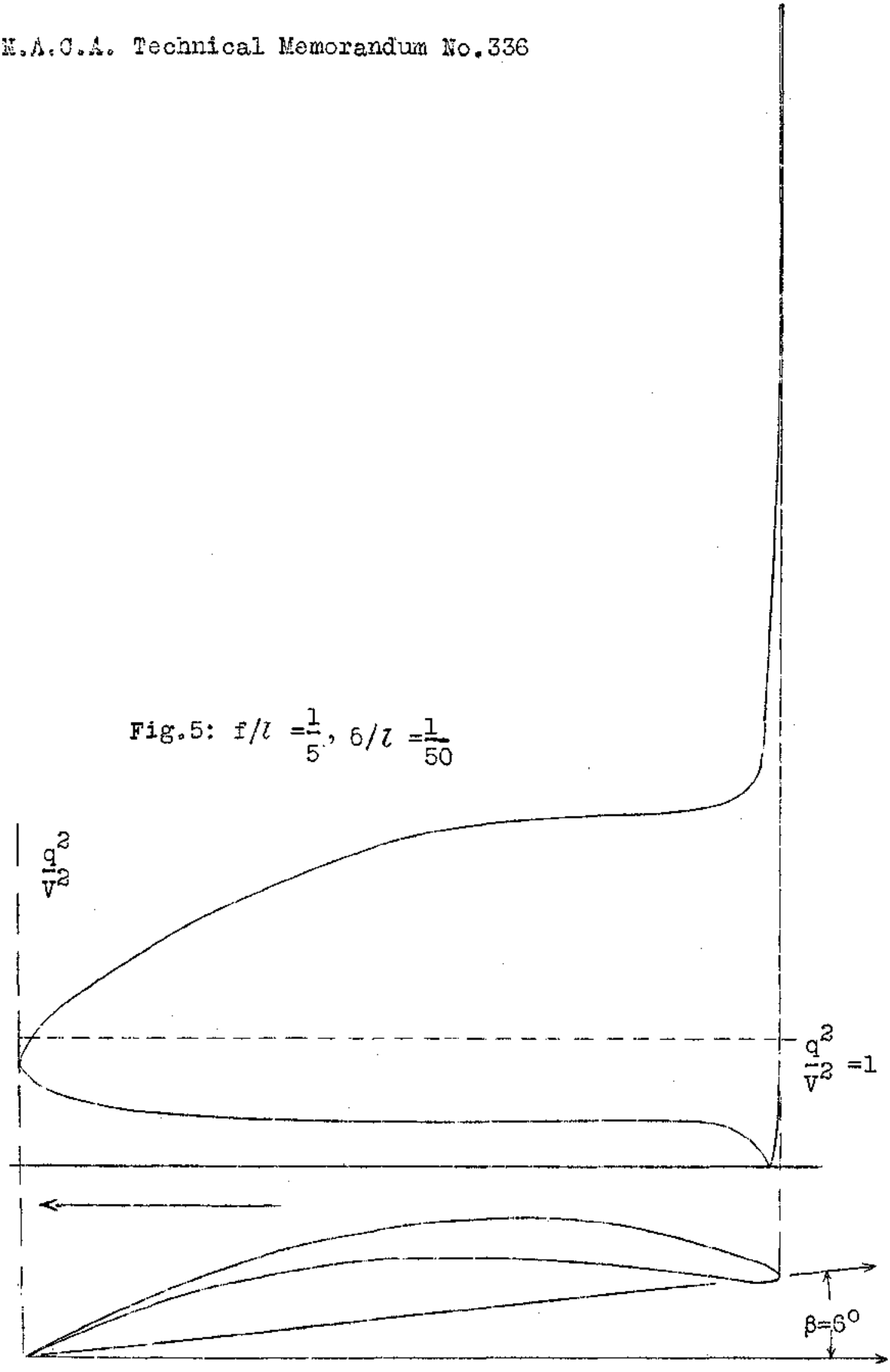

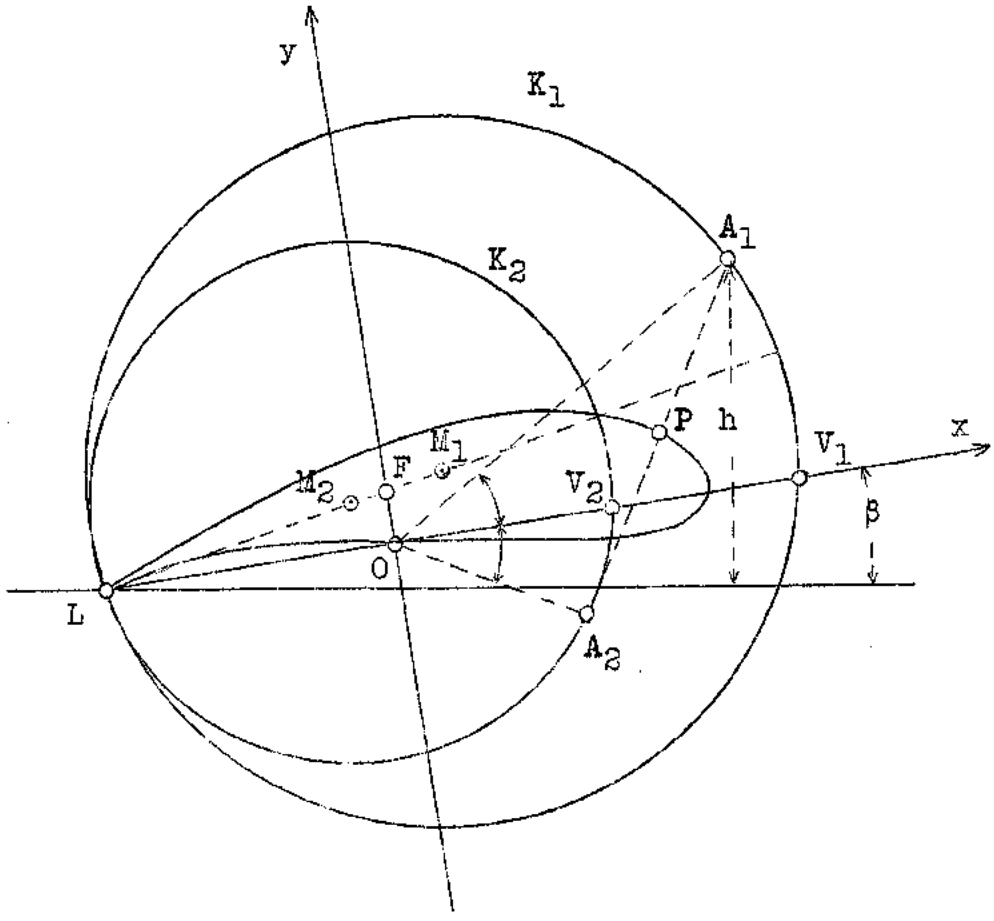

Fig.6

REPORT No. 121.

THE MINIMUM INDUCED DRAG OF AEROFOILS.

By Max M. Munk.

INTRODUCTION.

The following paper is a dissertation originally presented by the author to the University of Goettingen. It was intended principally for the use of mathematicians and physicists. The author is pleased to note that the paper has aroused interest in other circles, to the end that the National Advisory Committee for Aeronautics will make it available to a larger circle in America. The following introduction has been added in order to first acquaint the reader with the essence of the paper.

In the following development all results are obtained by integrating some simple expressions or relations. For our purposes it is sufficient, indeed, to prove the results for a pair of small elements. The qualities dealt with are integrable, since, under the assumptions we are allowed to make, they can not be affected by integrating. We have to consider only the relations between any two lifting elements and to add the effects. That is to say, in the process of integrating each element occurs twice—first, as an element producing an effect, and, second, as an element experiencing an effect. In consequence of this the symbols expressing the integration look somewhat confusing, and they require so much space in the mathematical expression that they are apt to divert the reader's attention from their real meaning. We have to proceed up to three dimensional problems. Each element has to be denoted twice (by a Latin letter and by a Greek letter), occurring twice in a different connection. The integral, therefore, is sixfold, six symbols of integration standing together and, accordingly, six differentials (always the same) standing at the end of the expression, requiring almost the fourth part of the line. The meaning of this voluminous group of symbols, however, is not more complicated and not less elementary than a single integral or even than a simple addition.

In section 1 we consider one aerofoil shaped like a straight line and ask how all lifting elements, which we assume to be of equal intensity, must be arranged on this line in order to offer the least drag.

If the distribution is the best one, the drag can not be decreased or increased by transferring one lifting element from its old position (a) to some new position (b). For then either the resulting distribution would be improved by this transfer, and therefore was not best before, or the transfer of an element from (b) to (a) would have this effect. Now, the share of one element in the drag is composed of two parts. It takes share in producing a downwash in the neighborhood of the other lifting elements and, in consequence, a change in their drag. It has itself a drag, being situated in the downwash produced by the other elements.

Fig. 1

Considering only two elements, Fig. 1 shows that in the case of the lifting straight line the two downwashes, each produced by one element in the neighborhood of the other, are equal. For this reason the two drags of the two elements each produced by the other are equal, too, and hence the two parts of the entire drag of the wings due to one element. The entire drag

produced by one element has twice the value as the drag of that element resulting from the downwash in its environs. Hence, the entire drag due to one element is unchanged when the element is transferred from one situation to a new one of the same downwash, and the distribution is the best only if the downwash is constant over the whole wing.

In sections 2 to 6 it is shown that the two parts of the drag change by the same value in all other cases, too. If the elements are situated in the same transverse plane, the two parts are equal. A glance at Fig. 2 shows that the downwash produced by (1) at (2), (3), (4), and (5)

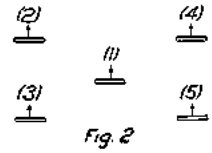

Fig. 2

is equal. But then it also equals the downwash due to (4), say, produced at (1). This holds true even for the component of the downwash in the direction of the lift if the elements are normal to each other (Fig. 3.); for this component is proportional $x.y/r^3$, according to the symbols

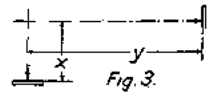

Fig. 3.

of the figure. Hence, it is proved for lift of any inclination, horizontal and vertical elements being able, by combination, to produce lift in any direction.

There remains only the question whether the two parts of the drag are also equal if the elements are situated one behind the other—that is to say, in different longitudinal positions. They are not; but their sum is independent of the longitudinal distance apart. To prove this, add in Fig. 4 to the lifting element (2) a second inverse lifting element (3) with inverse

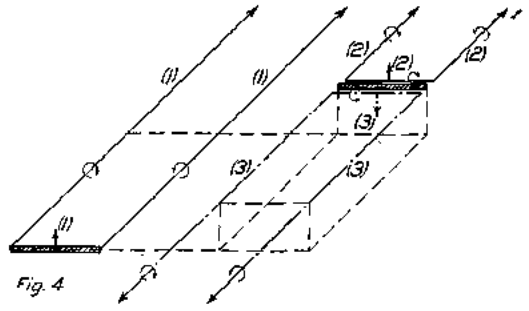

Fig. 4

linear longitudinal vortices in the inverse direction. The reader observes that the transverse vortices (2) and (3) neutralize each other; the longitudinal linear vortices, however, have the same sign, and all four vortices form a pair of vortices running from infinity to infinity. The drag, produced by the combination of (1) and this pair, is obviously independent of the longitudinal positions of (1) and (2). But the added element (3) has not changed the drag, for (1) and (3) are situated symmetrically and produce the same mutual downwash. The direction of the lift, however, is inverse, and therefore the two drags have the inverse sign, and their sum is zero.

If the two lifting elements are perpendicular to each other (chapter 5), a similar proof can be given.

Sections 6 and 7 contain the conclusions. The condition for a minimum drag does not depend upon the longitudinal coordinates, and in order to obtain it the downwash must be assumed to be constant at all points in a transverse plane of a corresponding system of aerofoils. This is not surprising; the wings act like two dimensional objects accelerating the air passing in an infinite transverse plane at a particular moment. Therefore the calculation leads to the consideration of the two dimensional flow about the projection of the wings on a transverse plane.

Section 8 gives the connection between the theory in perfect fluids and the phenomenon in true air. It is this connection that allows the application of the results to practical questions.

1. THE LIFTING STRAIGHT LINE.

A system of aerofoils moving in an incompressible and frictionless fluid has a drag (in the direction of its motion) if there is any lift (perpendicular to the direction of its motion). The magnitude of this drag depends upon the distribution of the lift over the surface of the aerofoils. Although the dimensions of the given system of aerofoils may remain unchanged, the distribution of the lift can be radically altered by changes in details, such as the aerofoil section or the angle of attack. The purpose of the investigation which is given in the following pages is to determine (*a*) the distribution of lift which produces the least drag, and (*b*) the magnitude of this minimum drag.

Let us first consider a single aerofoil of such dimensions that it may be referred to with sufficient exactness as a lifting straight line, which is at right angles to the direction of its flight. The length or span of this line may be denoted by l. Let the line coincide with the horizontal, or x axis of a rectangular system of coordinates having its origin at the center of the aerofoil. The density of the lift

$$A' = \frac{dA}{dx} \tag{1}$$

where A, the entire lift from the left end of the wing up to the point x, is generally a function of x and may be denoted by $f(x)$. Let the velocity of flight be v_0.

The modern theory of flight[1] allows the entire drag to be expressed as a definite double integral, if certain simplifying assumptions are made. In order to find this integral, it is necessary to determine the intensity of the longitudinal vortices which run from any lifting element to infinity in a direction opposite to the direction of flight. These vortices are generally distributed continuously along the whole aerofoil, and their intensity per unit length of the aerofoil is

$$\Gamma' = \frac{1}{v_0 \cdot \rho} \cdot \frac{dA'}{dx} \tag{2}$$

where ρ is the density of the fluid. Now, for each lifting element dx, we shall calculate the downwash w, which, in accordance with the law of Biot-Savart, is produced at it by all the longitudinal vortices. A single vortex, beginning at the point x, produces at the point $x=\xi$ the downwash

$$dw = \frac{1}{4\pi\rho v_0} \cdot dA' \cdot \frac{1}{\xi - x} \tag{3}$$

Therefore the entire downwash at the point ξ is

$$w = \frac{1}{4\pi\rho v_0} \int_{-\frac{l}{2}}^{+\frac{l}{2}} \frac{dA'}{dx} \cdot \frac{1}{\xi - x} dx \tag{4}$$

The integration is to be performed along the aerofoil; and the principal value of the integral is to be taken at the point $x=\xi$. This rule also applies to all of the following integrals. Hence it follows that the drag according to the equation

$$\frac{dW}{dx} = W' = \frac{w}{v_0} \cdot A' \tag{5}$$

is

$$W = \frac{1}{4\pi v_0^2 \rho} \int_{-\frac{l}{2}}^{+\frac{l}{2}} \left\{ \int_{-\frac{l}{2}}^{+\frac{l}{2}} \frac{dA'}{dx} \cdot \frac{1}{\xi - x} dx \right\} \cdot A' d\xi \tag{6'}$$

[1] See L. Prandtl, Tragflügeltheorie, I. Mitteilung. Nachrichten der Ges. d. Wiss. zu Göttingen, 1918.

or, otherwise expressed,

$$W=\frac{1}{4\pi v_0^2\rho}\int_{-\frac{l}{2}}^{+\frac{l}{2}}\int_{-\frac{l}{2}}^{+\frac{l}{2}}\frac{f'(x)\cdot f(\xi)}{\xi-x}dxd\xi \tag{6}$$

f' here signifies the derivative of f with respect to x or ξ. The entire lift is represented by

$$A=\int_{-\frac{l}{2}}^{+\frac{l}{2}}f(x)\,dx \tag{7}$$

Hence the solution of the problem to determine the best distribution of lift depends upon the determination of the function f so that the double integral

$$J_1=\int_{-\frac{l}{2}}^{+\frac{l}{2}}\int_{-\frac{l}{2}}^{+\frac{l}{2}}\frac{f'(x)\cdot f(\xi)}{\xi-x}\,dxd\xi \tag{8}$$

shall have a value as small as possible; while at the same time the value of the simple integral

$$J_2=\int_{-\frac{l}{2}}^{+\frac{l}{2}}f(x)dx=\text{const.} \tag{9}$$

is fixed.

The first step towards the solution of this problem is to form the first variation of J_1

$$\delta J_1=\int_{-\frac{l}{2}}^{+\frac{l}{2}}\left\{\delta f(x)\,dx\int_{-\frac{l}{2}}^{+\frac{l}{2}}\frac{f'(\xi)}{\xi-x}d\xi\right\}+\int_{-\frac{l}{2}}^{+\frac{l}{2}}\left\{\delta f'(\xi)d\xi\int_{-\frac{l}{2}}^{+\frac{l}{2}}\frac{f(x)}{\xi-x}dx\right\} \tag{10}$$

The second integral on the right side of (10) can be reduced to the first. By exchanging the symbols x and ξ and by partial integration with respect to x, considering $f'(\xi)$ as the integrable factor, there is obtained

$$\int_{-\frac{l}{2}}^{+\frac{l}{2}}\left\{\delta f'(\xi)d\xi\int_{-\frac{l}{2}}^{+\frac{l}{2}}\frac{f(x)}{\xi-x}dx\right\}=-\int_{-\frac{l}{2}}^{+\frac{l}{2}}\left\{\delta f(x)dx\cdot\frac{d}{dx}\int_{-\frac{l}{2}}^{+\frac{l}{2}}\frac{f(\xi)}{x-\xi}d\xi\right\} \tag{11}$$

The second member disappears since $f=0$ at the limits of integration.[2] Further, the right hand part of (11)

$$\frac{d}{dx}\int_{-\frac{l}{2}}^{+\frac{l}{2}}\frac{f(x)}{x-\xi}d\xi$$

upon substitution of the new variables x and $t=x-\xi$ for x and ξ, is transformed into

$$\frac{d}{dx}\int_{x+\frac{l}{2}}^{x-\frac{l}{2}}\frac{f(x-t)}{t}\,dt$$

[2] If this were not true, there would be infinite velocities at these points.

Now

$$\frac{d}{dx}\int_{x+\frac{l}{2}}^{x-\frac{l}{2}}\frac{f(x-t)}{t}\,dt=\frac{f\left(\frac{l}{2}\right)}{x=\frac{l}{2}}-\frac{f\left(-\frac{l}{2}\right)}{x+\frac{l}{2}}+\int_{x+\frac{l}{2}}^{x-\frac{l}{2}}\frac{f'(x-t)}{t}dt$$

or, since f disappears at the limits of integration,

$$\frac{d}{dx}\int_{x+\frac{l}{2}}^{x-\frac{l}{2}}\frac{f(x-t)}{t}\,dt=\int_{x+\frac{l}{2}}^{x-\frac{l}{2}}\frac{f'(x-t)}{t}\,dt$$

which, upon the replacement of the original variables, becomes

$$\int_{-\frac{l}{2}}^{+\frac{l}{2}}\frac{f'(\xi)}{x-\xi}\,d\xi$$

so that, finally,

$$\int_{-\frac{l}{2}}^{+\frac{l}{2}}\left\{\delta f'(\xi)\,d\xi\int_{-\frac{l}{2}}^{+\frac{l}{2}}\frac{f(x)}{\xi-x}dx\right\}=\int_{-\frac{l}{2}}^{+\frac{l}{2}}\left\{\delta f(x)\,dx\int_{-\frac{l}{2}}^{+\frac{l}{2}}\frac{f'(\xi)}{\xi-x}\,d\xi\right\} \tag{12}$$

Substituting this in (10) there finally results

$$\delta J_1=2\int_{-\frac{l}{2}}^{+\frac{l}{2}}\delta f(x)dx\int_{-\frac{l}{2}}^{+\frac{l}{2}}\frac{f'(\xi)}{\xi-x}d\xi \tag{13}$$

From which the condition for the minimum amount of drag, taking into consideration the second condition (9), is

$$\int_{-\frac{l}{2}}^{+\frac{l}{2}}\frac{f'(\xi)}{\xi-x}\,d\xi+\lambda=0 \tag{14}$$

or, when equation (4) is taken into consideration

$$w=\text{const.}=w_0 \tag{15}$$

The necessary condition for the minimum of drag for a lifting straight line is that the downwash produced by the longitudinal vortices be constant along the entire line.

That this necessary consideration is also sufficient results from the obvious meaning of the second variation, which represents the infinitesimal drag produced by the variation of the lift if it alone is acting, and therefore it is always greater than zero.

2. PARALLEL LIFTING ELEMENTS LYING IN A TRANSVERSE PLANE.

The method just developed may be applied at once to problems of a more general nature. If, instead of a single aerofoil, there are several aerofoils in the same straight line perpendicular to the direction of flight, only the limits of integration are changed in the development. The integration in such cases is to be performed along all of the aerofoils. However, this is nonessential for all of the equations and therefore the condition for the minimum drag (equation 15) applies to this entire system of aerofoils.

Let us now discard the condition that all of the lifting lines are lying in the same straight line, but retain, however, the condition that they are parallel to each other, perpendicular to the line of flight as before, and that they are all lying in a plane perpendicular to the line of flight. Let the height of any lifting line be designated by z or ζ. Equation (3) transforms into a similar one which gives the downwash produced at the point x, z by the longitudinal vortex beginning on the lifting element at the point ζ:

$$dw = \frac{1}{4\pi\rho v_0} dA' \frac{\xi - x}{(\xi - x)^2 + (\zeta - z)^2} \tag{3a}$$

The expression, which must now be a minimum, is

$$J_1 = \int\int \left[\frac{d}{dx} f(x, z)\right] \cdot f(\xi, \zeta) \frac{\xi - x}{(\xi - x)^2 + (\zeta - z)^2} d\xi\, dx \tag{8a}$$

with the unchanged secondary condition

$$J_2 = \int f(x, z)\, dx = \text{const.} \tag{9a}$$

These integrals are to be taken over all of the aerofoils.

This new problem may be treated in the same manner as the first.

$$\frac{\xi - x}{(\xi - x)^2 + (\zeta - z)^2}$$

is always to be substituted for $\frac{1}{\xi - x}$. It may be shown that this substitution does not affect the correctness of equations (10) to (15). Therefore

$$w = \text{const.} = w_0 \tag{15a}$$

is again obtained as the necessary condition for the minimum of the entire drag.

Finally, this also holds true for the limiting case in which, over a limited portion of the transverse plane, the individual aerofoils, like venetian blinds, lie so closely together that they may be considered as a continuous lifting part of a plane. Including all cases which have been considered so far, the condition for a minimum of drag can be stated:

Let the dimensions of a system of aerofoils be given, those in the direction of flight being small in comparison with those in other directions. Let the lift be everywhere directed vertically. Under these conditions, the downwash produced by the longitudinal vortices must be uniform at all points on the aerofoils in order that there may be a minimum of drag for a given total lift.

3. THREE DIMENSIONAL PARALLEL LIFTING ELEMENTS.

The three-dimensional problem may be based upon the two-dimensional one. Let now the dimensions in the direction of flight be considerable and let the lifting elements be distributed in space in any manner. Let y or η be the coordinates of any point in the direction of flight. For the time being, all lifting forces are assumed to be vertical.

The calculation of the density of drag for this case is somewhat more complicated than in the preceding cases. Consideration must be given not only to the longitudinal vortices, which are treated as before, but also to the transverse vortices which run perpendicular to the lift at any point and to the direction of flight. Their intensity at any point where there is a lifting element is

$$\Gamma = A' \cdot \frac{1}{v_0 \cdot \rho} = f(x, y, z) \cdot \frac{1}{v_0 \rho}.$$

The density of drag, W' now has two components, W_1 and W_2, the first being due to the transverse vortices and the second to the longitudinal vortices.

For the solution of the present problem only the total drag of all lifting elements

$$W=\int W'dx$$

is to be considered. In the first place it will be shown that the integral of those parts of the density resulting from the transverse vortices

$$W_1=\int W_1'dx$$

does not contribute to the total drag. A small element of one transverse vortex of the length dx at the point (x, y, z) produces at the point (ξ, η, ζ) the downwash

$$dw=\frac{1}{4\pi\rho v_0}\frac{\eta-y}{r^3}f(x, y, z)\cdot dx \tag{16}$$

where

$$r^2=(\xi-x)^2+(\eta-y)^2+(\zeta-z)^2.$$

Therefore

$$W_1=\frac{1}{4\pi\rho v_0^2}\int\int f(x, y, z)\cdot f(\xi, \eta, \zeta)\frac{\eta-y}{r^3}dxd\xi. \tag{17}$$

This integration is to be extended over all the aerofoils. It is possible to write this expression in such a manner that it holds for a continuous distribution of lift over parts of surfaces or in space. This is true, moreover, for most of the expressions in this paper. Now, exchanging the variables x, y, z, for ξ, η, ζ, in equation (17) does not change the value of the integral, since the symbols for the variables have no influence on the value of a definite integral. On the other hand, the factor $(\eta-y)$, and therefore the integral also, changes its sign. Hence

$$W_1=-W_1=0 \tag{18}$$

and, as stated,

$$W=W_2. \tag{19}$$

Therefore the entire drag may be calculated without taking into consideration the transverse vortices.

The method of calculating the effect of the longitudinal vortices can be greatly simplified. At the point (ξ, η, ζ) that part of the density of drag resulting from a longitudinal vortex beginning at the point (x, y, z) is

$$W_2'=\frac{1}{v_0^2\rho}\int f(\xi, \eta, \zeta)f'(x, y, z)\cdot\psi dx \tag{20}$$

where

$$f'=\frac{d}{dx}f, \text{ resp. } \frac{d}{d\xi}f$$

and

$$\psi=\frac{1}{4\pi}\int_s^\infty\frac{\xi-x}{t^3}ds;\ t^2=(\xi-x)^2+(\eta-s)^2+(\zeta-z)^2. \tag{21}$$

The entire drag is

$$W=\int W_2'dx=\frac{1}{v_0^2\rho}\int\int f(\xi, \eta, \zeta)f'(x, y, z)\psi d\xi dx. \tag{22}$$

Now, in the double integral (22) the variables x, y, z may be exchanged with ξ, η, ζ, as before, without affecting the value of the definite integral. Partial integration may then be performed twice, first with respect to ξ and then with respect to x. The substitution results in

$$W=\frac{1}{v_0^2\rho}\int\int f(x, y, z)f'(\xi, \eta, \zeta)\bar{\psi}dxd\xi \tag{23}$$

$\bar{\psi}$ is obtained from ψ upon the exchange of variables. Its value is therefore

$$\bar{\psi}=\frac{1}{4\pi}\int_{y}^{\infty}\frac{x-\xi}{\bar{t}^3}\,ds;\ \bar{t}^2=(\xi-x)^2+(s-y)^2+(\zeta-z)^2. \tag{24}$$

When partially integrating with respect to $d\xi$, the integrable factor is $f'(\xi, \eta, \zeta)$

$$W=-\frac{1}{v_0^2\rho}\int\int f(\xi, \eta, \zeta)\,\frac{d}{d\xi}\bar{\psi}\cdot f(x, y, z)\,dxd\xi \tag{25}$$

In the subsequent partial integration with respect to dx, the integrable factor is $\frac{d}{d\xi}\bar{\psi}=-\frac{d}{dx}\bar{\psi}$.

$$W=-\frac{1}{v_0^2\rho}\int\int f(\xi, \eta, \zeta)\cdot f'(x, y, z)\,\bar{\psi}dxd\xi. \tag{26}$$

Finally, by addition of (22) and (26), there is obtained

$$2W=\frac{1}{v_0^2\rho}\int\int f(\xi, \eta, \zeta)\,f'(x, y, z)\,(\psi-\bar{\psi})\,dxd\xi. \tag{27}$$

$s=y+\eta-s$ may now be substituted in (24) for the variable of integration s. Then $\bar{t}$ changes to t, and with the exception of the sign the integrand in (21) agrees with the resulting one in (22)

$$\bar{\psi}=-\frac{1}{4\pi}\int_{y}^{-\infty}\frac{x-\xi}{t^3}ds \tag{28}$$

Subtracting (28) from (21) there results finally

$$\psi-\bar{\psi}=\frac{1}{4\pi}\int_{-\infty}^{+\infty}\frac{\xi-x}{t^3}ds. \tag{29}$$

Hence, $\psi-\bar{\psi}$ and therefore the entire right side of equation (22) is seen to be independent of the longitudinal coordinates y of the lifting elements.

Therefore the entire resistance of a three-dimensional system of aerofoils with parallel lifting elements does not depend upon the longitudinal positions of the lifting elements.

4. LIFTING ELEMENTS ARRANGED IN ANY DIRECTIONS IN A TRANSVERSE PLANE.

The problem considered in section 2 can also be generalized in another way. For the present the condition that all lifting elements be in one transverse plane may remain. However, they need no longer be parallel, and the lift may be due to not only a great number of infinitesimal lifts dA but also to similar transverse forces dB. In the first place let the direction of all lifting elements be arbitrary, but such that there is a minimum drag, and let this direction be an unknown quantity to be determined.

In the present problem it is desirable to consider a continuous distribution of lift over given areas instead of lines. The last case can be deduced from the first at any time by passing to the limit.

Let $A'=f(x, z)$ be the density of the vertical lift per unit area, and $B'=F(x, z)$ the density of the lateral force per unit area. The lateral force is considered positive when acting in the positive direction of the X-axis. Then the density of the transverse vortices has the components $\frac{1}{v_0\rho}\cdot A'$ and $-\frac{1}{v_0\rho}B'$. The density of the longitudinal vortex is the divergence of the density of the transversal vortex, or $\frac{1}{v_0\rho}\left(\frac{dA'}{dx}-\frac{dB'}{dz}\right)$. The longitudinal vortices beginning

at the point (x, z) therefore produce at the point (ξ,ζ) the downwash and the transverse velocity

$$dw=\frac{1}{4\pi v_o\rho}\left(\frac{dA'}{dx}-\frac{dB'}{dz}\right)dxdz\,\frac{\xi-x}{r^2} \tag{3b}$$

$$du=\frac{1}{4\pi v_o\rho}\left(\frac{dA'}{dx}-\frac{dB'}{dz}\right)dxdz\,\frac{z-\zeta}{r^2} \tag{3c}$$

According to the above, the density of the drag is

$$d\,W=A'\frac{w}{v_o}dxdz+B'\frac{u}{v_o}dxdz \tag{5b}$$

With these symbols there results for the total drag the expression

$$W=\frac{1}{4\pi v^2\rho}\Big\{\int\int\int\int f'\,(x,z)\,f\,(\xi,\zeta)\,\frac{\xi-x}{r^2}\,dxdzd\xi d\zeta-\int\int\int\int F'\,(x,z)\;F\,(\xi,\zeta)\frac{z-\zeta}{r^2}dxdzd\xi d\zeta+ \tag{30}$$
$$\int\int\int\int f'\,(x,z)\;F\,(\xi,\zeta)\,\frac{z-\zeta}{r^2}\,dxdzd\xi d\zeta-\int\int\int\int F'\,(x,z)\,f\,(\xi,\zeta)\,\frac{\xi-x}{r^2}\,dxdzd\xi d\zeta\Big\}$$

All of these integrals are to be taken over all of the lifting surfaces. Now the first two integrals have forms corresponding to the integral in (8), and therefore there is a possibility of substituting (12) for these. A similar relation also holds for the last two integrals. For example, the variation of the third integral is

$$\delta\int\int\int\int f'\,(x,z)\;F\,(\xi,\zeta)\,\frac{z-\zeta}{r^2}\,dxdzd\xi d\zeta=$$
$$\int\int\int\int\Big[\delta f'\,(x,z)\cdot F\,(\xi,\zeta)\,\frac{z-\zeta}{r^2}+f'\,(x,z)\;\delta F\,(\xi,\zeta)\,\frac{z-\zeta}{r^2}\Big]dxdzd\xi d\zeta \tag{31}$$

Now in the first term on the right-hand side the variables x and z may be exchanged with ξ and ζ. It may then be partially integrated with respect to $d\xi$, the integrable factor being $df'(\xi,\zeta)$. This gives

$$\int\int\int\int\delta f'\,(x,z)\cdot F\,(\xi,\zeta)\,\frac{z-\zeta}{r^2}\,dxdzd\xi d\zeta=-\int\int\int\int\delta f\,(\xi,\zeta)\cdot\frac{d}{d\xi}\;F\,(x,z)\,\frac{\zeta-z}{r^2}\,dxdzd\xi d\zeta \tag{32}$$

This may be partially integrated with respect to dz, the integrable factor being

$$\frac{d}{d\zeta}\,\frac{\zeta-z}{r^2}=-\frac{d}{dz}\,\frac{\xi-x}{r^2}$$

$$\int\int\int\int\delta f'\,(x,z)\;F\,(\xi,\zeta)\,\frac{z-\zeta}{r^2}\,dxdzd\xi d\zeta=-\int\int\int\int\delta f\,(\xi,\zeta)\cdot F'\,(x,z)\,\frac{\xi-x}{r^2}\,dxdzd\xi d\zeta \tag{33}$$

Hence the first term of the variation of the third integral of (30) can be transformed into the second term of the variation of the fourth integral of this equation. In a similar manner the two other terms may be transformed into each other. It is therefore demonstrated that the variation of the entire drag may be written

$$\delta\,W=2\int\int\delta f\cdot w\cdot dxdz+2\int\int\delta F\cdot u\cdot dxdz \tag{13b}$$

Two problems of variation can now be stated. In the first place limited parts of the surfaces may be at our disposal, over which the vertical lift A and the horizontal transversal force B may have any distribution. Only the total lift

$$A = \iint f(x,z)\, dxdz = \text{const.} \tag{9b}$$

will be given in this case.

Then

$$w = \text{const.} = w_0;\ u = o \tag{15b}$$

is the condition for the least drag.

If, however, the lifting parts are similar to lines, there is generally one other condition to fulfill. It is then required that the lift disappear everywhere along the direction of the aerofoils. That is to say,

$$f \sin\beta - F\cos\beta = o \tag{34}$$

where β is the angle of inclination of the aerofoil to the horizontal X-axis. In order to add the new requirement (34) a second Lagrange constant μ is introduced. The condition for the least drag is now

$$w + \lambda + \frac{\mu}{\cos\beta} = o,\ u - \frac{\mu}{\sin\beta} = o \tag{34a}$$

and after the elimination of μ

$$w\cos\beta + u\sin\beta = w_o\cos\beta \tag{15c}$$

the constant 2λ being replaced by $-w_0$, as before. In words:

If all lifting elements are in one transverse plane, the component of the velocity perpendicular to the wings, produced by the longitudinal vortices, must be proportional, at all lifting elements, to the cosine of the angle of lateral inclination.

5. LIFT DISTRIBUTED AND DIRECTED IN ANY MANNER.

The results obtained previously can be generalized not only for lifting elements distributed in a transverse plane but also for lifting elements distributed in any manner in space. That part of the total drag resulting from the transverse vortices is, in the general case

$$\begin{aligned} W_1 = \frac{1}{4\pi\rho v^2}\Big[&\int\int\int\int\int\int f(x,y,z)\, f(\xi,\eta,\zeta)\, \frac{n-y}{r^3}\, dxdydzd\xi d\eta d\zeta \\ &+ \int\int\int\int\int\int F(x,y,z)\, F(\xi,\eta,\zeta)\, \frac{n-y}{r^3}\, dxdydzd\xi d\eta d\zeta \Big] \end{aligned} \tag{17a}$$

Both terms have the same form as the integral in (17). The demonstration for (17) therefore applies to both. In the general case also the total drag can be calculated from the longitudinal vortices without taking into consideration the transverse vortices.

$$\begin{aligned} W = \frac{1}{4\pi\rho v^2}\Big[&\int\int\int\int\int\int f(x,y,z)\, f(\xi,\eta,\zeta)\, \psi_1\, dxdydzd\xi d\eta d\zeta \\ &+ \int\int\int\int\int\int F'(x,y,z)\, F(\xi,\eta,\zeta)\, \psi_2\, dxdydzd\xi d\eta d\zeta \\ &- \int\int\int\int\int\int f(x,y,z)\, F'(\xi,\eta,\zeta)\, \psi_1\, dxdydzd\xi d\eta d\zeta \\ &- \int\int\int\int\int\int F(x,y,z)\, f'(\xi,\eta,\zeta)\, \psi_2\, dxdydzd\xi d\eta d\zeta \Big] \end{aligned} \tag{22a}$$

In this as in (20),

$$\psi_1 = \frac{1}{4\pi}\int_y^\infty \frac{\xi - x}{t^3}\, ds;\ t^2 = (\xi-x)^2 + (\eta-s)^2 + (\zeta-z)^2$$

$$\psi_2 = \frac{1}{4\pi}\int_y^\infty \frac{\zeta - z}{t^3}\, ds$$

The first two terms in (22a) have the same form as the right-hand side of (22), and the same conclusions are therefore valid for each. It can be proved directly for (22a) as for (22) that each of the two double integrals is independent of the longitudinal coordinates of the lifting elements. This proof can now be extended over the last two integrals of equation (22a).

The third integral, after changing the variables, becomes

$$\iiiiiii f(x, y, z)\ F'(\xi, \eta, \zeta)\ \psi_1\, dxdydzd\xi d\eta d\zeta = \iiiiiii f(\xi, \eta, \zeta)\ F'(x, y, z)\ \psi_1\, d\xi d\eta d\zeta dxdydz \tag{35}$$

where

$$\bar{\psi}_1 = -\frac{1}{4\pi}\int_y^\infty \frac{\xi - x}{t^3}\, ds;\quad t^2 = (\xi - x)^2 + (s - y)^2 + (\zeta - z)^2$$

Now, let F' be chosen as the integrable factor and be partially integrated with respect to z.

$$\iiiiiii f(x, y, z)\ F'(\xi, \eta, \zeta)\ \psi_1 dxdydzd\xi d\eta d\zeta = \iiiiiii f(\xi, \eta, \zeta)\ F(x, y, z)\ \frac{d}{dz}\bar{\psi}_1 d\xi d\eta d\zeta dxdydz. \tag{36}$$

As in the previous cases, the second integral to be expected vanishes since f as well as F disappear at the limits of the integration. Next $\frac{d}{dz}\bar{\psi}_1 = -\frac{d}{d\xi}\bar{\psi}_2$ is chosen as the integrable factor and partially integrated with respect to x. By $\bar{\psi}_2$, by analogy, is meant

$$\bar{\psi}_2 = -\frac{1}{4\pi}\int_y^\infty \frac{\zeta - z}{t^3}\, ds$$

$$\iiiiiii f(x, y, z)\ F'(\xi, \eta, \zeta)\ \psi_1 dxdydzd\xi d\eta d\zeta = \iiiiiii f'(\xi, \eta, \zeta)\ F(x, y, z)\ \bar{\psi}_2 d\xi d\eta d\zeta dxdydz. \tag{37}$$

Now $\bar{\psi}_2$ may be transformed, the variable s in the defining equation being replaced by $\eta + y - s$. The result is that

$$\bar{\psi}_2 = \frac{1}{4\pi}\int_y^{-\infty} \frac{\xi - z}{t^3}\, ds,\ t^2 = (\xi - x)^2 + (\eta - s)^2 + (\zeta - z)^2.$$

It is seen that the integrand agrees with that of the defining integral ψ_2. Therefore, and since the right-hand side of (37) contains the same function under the double integral as the fourth turn in (22a), this fourth term can be combined with the transformed third member. This gives

$$\iiiiiii f(x, y, z)\ F'(\xi, \eta, \zeta)\ \psi_1 dxdydzd\xi d\eta d\zeta + \iiiiiii F(x, y, z)\ f'(\xi, \eta, \zeta)\cdot\psi_2 dxdydzd\xi d\eta d\zeta = \iiiiiii F(x, y, z)\ f'(\xi, \eta, \zeta)\ (\psi_2 - \bar{\psi}_2)\ dxdydzd\xi d\eta d\zeta \tag{38}$$

where

$$\psi_2 - \bar{\psi}_2 = \frac{1}{4\pi}\int_{-\infty}^{+\infty} \frac{z - \xi}{t^3}\, ds;$$

$\psi_2 - \bar{\psi}_2$ and therefore the two sides of (38) are independent of y. This is therefore demonstrated for the whole right-hand side of (22a).

20167—23——25

In general it can therefore be said:

The total resistance is always independent of the longitudinal coordinates of the lifting elements.

And further:

The most favorable distribution of the lift, with reference to the total drag, occurs when this is also the case for the projection of the lifting elements on a transverse plane.

That is to say, all of the lifting elements are projected on a plane perpendicular to the direction of flight, and any element so obtained has a lift equal to the sum of the lifts of all lifting elements projected onto it.

6. DETERMINATION OF THE SOLUTIONS.

The previous demonstrations show that the investigation for the distribution of lift which causes the least drag is reduced to the solution of the problem for systems of aerofoils which are situated in a plane perpendicular to the direction of flight. In addition, the condition for least drag (15c), which becomes the condition of uniform downwash (15) if the lift is vertical, leads to a problem which has often been investigated in the theory of two-dimensional flow with a logarithmic potential. The flow produced within the lifting transverse plane by the longitudinal vortices originating in it is, indeed, of this type. Each such vortex produces a distribution of velocity such as is produced by a two-dimensional vortex of half its intensity, and the whole distribution of velocity is obtained by adding the distributions produced by the longitudinal vortices. The potential flow sought is determined by the condition of (15c). Let it be combined with the flow of constant vertical upward motion $\omega = -\omega_0$. The resulting flow satisfies the condition at the boundaries

$$\omega \cos \beta + \mu \sin \beta = 0 \tag{39}$$

and there results, for the case of lifting lines:

The two dimensional potential flow is of the type that encircles the lifting lines, and at a great distance the velocity is directed upwards and has the value $w = -w_0$.

Within lifting surfaces the velocity is zero according to the condition (15b), and the fluid therefore flows around the contour.

The intensity of the longitudinal vortices at any point is twice the rotation of the two dimensional flow. In the case of the lifting lines, therefore, the density of the longitudinal vortices is double the discontinuity of velocity from one side to the other. The intensity of the transversal vortices is determined by integrating the longitudinal vortices along the aerofoils and therefore equals twice the difference of the velocity-integral produced on the two sides of the aerofoil. Now the integral of the velocity produced is identical with the potential and hence it appears:

The density of the lift perpendicular to the lifting line is proportional to the discontinuity of potential $\varphi_2 - \varphi_1$, *and has the value*

$$\sqrt{A'^2 + B'^2} = 2v_0\rho(\varphi_2 - \varphi_1) \tag{40}$$

Hence the total lift obtained by integrating over all aerofoils is

$$A = 2v_0\rho \int (\varphi_2 - \varphi_1)dx \tag{41}$$

Sometimes a transformation of this equation is useful. In order to obtain it, suppose that all of the lifting lines are divided into small parts. Then, on the two ends of each lifting element there begin two inverse longitudinal vortices, the effect of which on a distant point is that of a double vortex. Their velocity-potential φ and their stream function ψ may be combined in the complex function $\psi + i\varphi$, and, not considering the existence of a parallel flow, which is without any importance in the calculation, this complex function has the form for a lifting line,

$$d(\psi + i\varphi) = \frac{dA + idB}{z - z_0} \tag{42}$$

where z represents $x+iy$ and $z_0=x_0+iy_0$, x_0 and y_0 being the coordinates of the lifting elements of the line. For a lift distributed over areas a similar equation can be formed. The integration of (42) gives

$$\psi+i\varphi=\int\frac{dA+idB}{z-z_0} \tag{42a}$$

Now the residuum of the integrand at infinity is $dA+idB$ and therefore the residuum of the integral is $A+iB$. Therefore the expression can be written.

$$A=2v_0\rho R\,[\mathrm{Res}(\psi+i\varphi)] \tag{41a}$$

where the last part means the real part of the residuum of $\psi+i\varphi$ at infinity. In the most important case of horizontal aerofoils the residuum itself is real and can be used directly to calculate the lift. The density of drag at any point is proportional to the perpendical component of the density of lift and is $W'=\frac{w_0}{v_0}\cdot A'$, from which results $W=\frac{w_0}{v_0}\cdot A$. Making use of (41) one obtains

$$W=A^2\frac{1}{2v_0^2\rho}\frac{1}{\int\left(\frac{\varphi_2-\varphi_1}{w_0}\right)dx} \tag{43}$$

$$W=A^2\frac{1}{2v_0^2\rho}\frac{w_0}{R\,[\mathrm{Res}\,(\psi+i\varphi)]} \tag{43a}$$

The integral in the denominator of (43) represents an area characteristic of the system of aerofoils investigated. Frequently the easiest method of calculation is to assume from the beginning the velocity w_0 at infinity to be unity.

The case of the lift continuously distributed over single parts of areas is derived from the preceding one by passing to the limit. Since the vertical velocity w disappears at all points in the lifting surfaces, the velocity is zero at all points and the rotation vanishes.

Therefore, in the case of the most favorable distribution of lift, all of the longitudinal vortices from the continuously lifting areas begin at the boundaries of the areas.

Equations (43) and (43a) remain. The distribution of lift is indeterminate to a certain extent. On the other hand, it is possible to connect the points of the contour having the same potential φ by strips of any form, and it is only necessary that the lift be always perpendicular to the strip and its density have a constant value along the whole strip. According to equation (40) this equals the difference of the potential at the contour between the two borders of the strip. Worthy of note is the special case in which all of the strips run along the contour, thus coming again to the case of lifting lines. It appears that:

Closed lines have the same minimum of drag as the enclosed areas when continuously loaded.

Especially important are those symmetrical contours which are cut by horizontal lines in only two points. With such the limitation to vertical lift does not involve an increase of the minimum drag. For this case it appears that:

The density of the vertical lift per unit area must be proportional to the vertical component of the velocity of the two-dimensional flow at the point of the contour of the same height z. It is

$$\frac{dA}{dF}=2v_0\rho\frac{d\varphi}{dz} \tag{44}$$

The corresponding density of drag is

$$\frac{dW}{dF}=2w_0\rho\frac{d\varphi}{dz} \tag{45}$$

7. EXAMPLES OF CALCULATIONS.

Examples of calculation of the previous demonstrations can be based on any calculated two-dimensional potential flow around parts of lines or areas. The simplest flow of the first kind is that around a single horizontal line. It leads to the problem investigated at the beginning of this paper.

In this case the potential is the real part of $\sqrt{p^2-1}$, where p denotes $x+iz$. The lifting line joins the two points $z=0$, $x=-1$ and $z=0$, $x=+1$, and has the length 2. The velocity at infinity is $w=1$. The discontinuity of potential along the lifting line is $\varphi_2-\varphi_1=2\sqrt{1-x^2}$. The density of lift is distributed according to the same law, therefore if plotted over the span the density of lift would be represented by the half of an ellipse.

The minimum drag is

$$W=A^2\frac{1}{v_0^2\rho/_2}\frac{1}{4\pi} \tag{46}$$

If, instead of the value 2, the span had the general value b, the minimum drag would be

$$W=A^2\cdot\frac{1}{v^2\rho/_2}\frac{1}{\pi b^2} \tag{47}$$

This same result has been obtained by Prof. Prandtl by another method.[3]

The simplest example for a lifting vertical area is the circle. Let its center coincide with the origin of the system of coordinates. Then the potential of the flow around this circle is

$$\varphi=\frac{z}{r^2}+z \tag{48}$$

where $r=\sqrt{x^2+z^2}$. At infinity $W_0=1$. Under the condition of and according to equation (40) the density of lift is

$$A'=2v_0\rho\frac{d}{dz}\left(\frac{z}{r^2}+z\right)_{r=1} \tag{49}$$

This results in a constant density of lift of $A'=2$. Therefore the drag is

$$W=A^2\cdot\frac{1}{2v_0^2\rho}\cdot\frac{1}{\iint 2dxdz}=A^2\frac{1}{v_0^2\rho/_2\cdot 8\pi} \tag{50}$$

The double integral is to be taken over the circle. If the general case for the diameter equal to D be considered, then the least drag is

$$W=A^2\cdot\frac{1}{v^2\rho/_2}\cdot\frac{1}{D^2 2\pi} \tag{51}$$

Hence in respect to the minimum drag the circle is equivalent to a lifting line having a length $\sqrt{2}$ times the diameter.

A lifting circular line would have the same minimum drag as the circular area.

This result was also obtained by Prof. Prandtl by another method.[4] A reduction of the original problem of variation to the two-dimensional flow sometimes enables a survey of the result to be made without calculation. For instance, let a third aerofoil be added between the two aerofoils of a biplane having a small gap. (The gap may be about one-sixth of the span.) Then, in order to find the most favorable distribution of lift, the double line about which the flow occurs is to be replaced by three lifting lines. Now, in the region of the middle lifting line the velocity is small, even before this line is introduced. Therefore the discontinuity of the potential along the middle line is very much smaller than that along the others. Hence it results that the middle aerofoil of a triplane should lift less than the other two.

[3] First communication concerning this in Zeitschrift für Flugtechnik und Motorl. 1914. S. 239, in a note by Betz.

[4] See Technische Berichte der Flugzeugmeisterei Bd. II Heft 3.

8. PROCEDURE FOR THE CASE OF FLUIDS WITH SMALL VISCOSITY.

The preceding results do not apply so much to the calculation of the most favorable distribution of lift as to the calculation of the least drag. For it appears, and the results are checked by calculation, that even considerable variations from the condition of most favorable distribution of lift do not increase the drag to any great extent. Usually the minimum drag can be considered as the real drag of the system of aerofoils and in order to allow for the effect of friction of the air it is sufficient to make an addition. This addition depends chiefly upon the aerofoil section; it also depends, omitting the Reynolds Number, only upon the area of the wings and on the dynamical pressure. It is independent of the dimensions of the system of wings themselves. It may be useful to have a name for that part of the density of drag, independent of the friction of the air, which results from the theory developed in this paper. It is called the "induced drag." Generally it is not the drag itself but an absolute coefficient which is considered. This coefficient is defined by

$$c_{wi}=\frac{W_i}{q\cdot F} \tag{52}$$

where W_i is the drag previously denoted by W, q is the dynamical pressure $v_0^2\cdot\rho/2$, and F is the total area of the wings. Equation (43) can now be written

$$c_{wi}=\frac{c_a^2\cdot F}{\pi(k\cdot b)^2} \tag{53}$$

where c_a is the lift coefficient $\frac{A}{F\cdot q}$ corresponding to c_w. The greatest horizontal span b of the system of wings perpendicular to the direction of flight is arbitrarily chosen as a length characteristic of the proportions of the system, k is a factor characteristic of the system of aerofoils and has, according to the preceding, the value.

$$k=\sqrt{\frac{4}{\pi}\cdot\frac{1}{b^2}\int\frac{\varphi_2-\varphi_1}{w_0}dx} \tag{54}$$

It has a special physical significance.

Under the same conditions a single aerofoil with a span of k times the maximum span of a system of aerofoils has the same induced minimum resistance as the system.

9. REFINEMENT OF THE THEORY.

The demonstrations given rest on the assumption that the velocities produced by the vortices are small in comparison with the velocity of flight. The next assumption, more accurate, would be that only powers higher than the first power could be neglected.

In this case the solutions just found for lifting elements in a transverse plane can be considered as the first step towards the calculation of more exact solutions. The following steps must be taken: The exact density of drag is $W'=A'\frac{w}{v_0+v}$ where v is the horizontal velocity produced at the lifting elements by the transverse vortices. It can be calculated exactly enough from the first approximation. Now, the condition of least drag is

$$w\cdot\cos\beta+\mu\sin\beta=w_0\cos\beta\left(1+\frac{v}{v_0}\right) \tag{15d}$$

and the flow of potential, according to this condition at the boundary, is to be found. Compared with the first approximation the density below is in general somewhat increased and the density above is somewhat decreased. The minimum drag changes only by quantities of the second order.

If the lifting elements are distributed in three dimensions a similar refinement can easily be found. In this case there is to be taken into consideration a second factor which always comes in if the differences of the longitudinal coordinates of the lifting elements are considerable. The direction of the longitudinal vortices do not agree exactly with the direction of flight, but they coincide with the direction of the velocity of the fluid around the aerofoil. They are therefore somewhat inclined downwards. A better approximation is obtained by projecting the lifting elements not in the direction of flight but in a direction slightly inclined upwards from the rear to the front. This inclination is about $\frac{2w_0}{v_0}$. Except for this, the method of calculation remains unchanged.

REPORT No. 184.

THE AERODYNAMIC FORCES ON AIRSHIP HULLS.

By Max M. Munk.

SUMMARY

This report describes the new method for making computations in connection with the study of rigid airships, which was used in the investigation of Navy's *ZR–1* by the special subcommittee of the National Advisory Committee for Aeronautics appointed for this purpose. It presents the general theory of the air forces on airship hulls of the type mentioned, and an attempt has been made to develop the results from the very fundamentals of mechanics, without reference to some of the modern highly developed conceptions, which may not yet be thoroughly known to a reader uninitiated into modern aerodynamics, and which may perhaps for all times remain restricted to a small number of specialists.

I. GENERAL PROPERTIES OF AERODYNAMIC FLOWS.

The student of the motion of solids in air will find advantage in first neglecting the viscosity and compressibility of the latter. The influence of these two properties of air are better studied after the student has become thoroughly familiar with the simplified problem. The results are then to be corrected and modified; but in most cases they remain substantially valid.

Accordingly I begin with the discussion of the general properties of aerodynamic flows produced by the motion of one or more solid bodies within a perfect fluid otherwise at rest. In order to be able to apply the general laws of mechanics to fluid motion I suppose the air to be divided into particles so small that the differences of velocity at different points of one particle can be neglected. This is always possible, as sudden changes of velocity do not occur in actual flows nor in the kind of flows dealt with at present. The term "flow" denotes the entire distribution of velocity in each case.

With aerodynamic flows external volume forces (that is, forces uniformly distributed over the volume) do not occur. The only force of this character which could be supposed to influence the flow is gravity. It is neutralized by the decrease of pressure with increasing altitude, and both gravity and pressure decrease can be omitted without injury to the result. This does not refer to aerostatic forces such as the buoyancy of an airship, but the aerostatic forces are not a subject of this paper.

The only force acting on a particle is therefore the resultant of the forces exerted by the adjacent particles. As the fluid is supposed to be nonviscous, it can not transfer tensions or forces other than at right angles to the surface through which the transfer takes place. The consideration of the equilibrium of a small tetrahedron shows, then, that the only kind of tension possible in a perfect fluid is a pressure of equal magnitude in all directions at the point considered.

In general this pressure is a steady function of the time t and of the three coordinates of the space, say x, y, and z, at right angles to each other. Consider now a very small cube with the edges dx, dy, and dz. The mean pressure acting on the face $dy\,dz$ may be p. The mean pressure on the opposite face is then $p+\partial p/\partial x dx$. The X-component of the resultant volume force is the difference of these two mean pressures, multiplied by the area of the faces $dydz$,

hence, it is $-\frac{\partial p}{\partial x}dx\ dy\ dz$. Per unit volume it is $-\frac{\partial p}{\partial x}$, as the volume of the cube is dx, dy, dz. It can be shown in the same way that the other two components of the force per unit volume are $-\frac{\partial p}{\partial y}$ and $-\frac{\partial p}{\partial z}$. Such a relation as existing between the pressure distribution and the force produced by it is generally described as the force being the "gradient" of the pressure, or rather the negative gradient. Any steady distribution of pressure has a gradient at each point, but if a distribution of forces (or of other vectors) is given, it is not always possible to assign a quantity such that the forces are its gradient.

We denote the density of air by ρ; that is, the mass per unit volume, assumed to be constant. $d\tau$ may denote the small volume of a particle of air. The mass of this particle is then $\rho d\tau$. The components of the velocity V of this particle parallel to x, y, and z may be denoted by u, v, and w. Each particle has then the kinetic energy $dT=\frac{\rho}{2}d\tau(u^2+v^2+w^2)$ and the component of momentum, say in the X direction, is $\rho d\tau u$. The kinetic energy of the entire flow is the integral of that of all particles.

$$T=\frac{\rho}{2}\int(u^2+v^2+w^2)d\tau \quad \text{.....(1)}$$

Similarly, the component of momentum in the X-direction is the integral

$$\rho\int u d\tau \quad \text{.....(2)}$$

and two similar equations give the components for the two other directions. These integrals will later be transformed to make them fit for actual computation of the energy and the momentum.

It is sometimes useful to consider very large forces, pressures, or volume forces acting during a time element dt so that their product by this time element becomes finite. Such actions are called "impulsive." Multiplied by the time element they are called impulses, or density of impulse per unit area or unit volume as the case may be.

After these general definitions and explanations, I proceed to establish the equations which govern an aerodynamic flow. Due to the assumed constant density, we have the well-known equation of continuity

$$\frac{\partial u}{\partial x}+\frac{\partial v}{\partial y}+\frac{\partial w}{\partial z}=O \quad \text{.....(3)}$$

We turn now to the fact that for aerodynamic problems the flow can be assumed to be produced by the motion of bodies in air originally at rest. As explained above, the only force per unit volume acting on each particle is the gradient of the pressure. Now, this gradient can only be formed and expressed if the pressure is given as a function of the space coordinates x, y, and z. The laws of mechanics, on the other hand, deal with one particular particle, and this does not stand still but changes its space coordinates continually. In order to avoid difficulties arising therefrom, it is convenient first to consider the flow during a very short time interval dt only, during which the changes of the space coordinates of the particles can be neglected as all velocities are finite. The forces and pressures, however, are supposed to be impulsive, so that during the short interval finite changes of velocity take place. Suppose first the fluid and the bodies immersed therein to be at rest. During the creation of the flow the density of impulse per unit area may be P, i. e., $P=\int p dt$. The principles of mechanics give then

$$u\rho=-\frac{\partial P}{\partial x}$$

$$u=\frac{\partial}{\partial x}\left(-\frac{P}{\rho}\right)$$

and similarly in the two other directions

$$v=\frac{\partial}{\partial y}\left(-\frac{P}{\rho}\right)$$
$$w=\frac{\partial}{\partial z}\left(-\frac{P}{\rho}\right) \quad \text{.....(4)}$$

Hence the velocity thus created is the gradient of $\left(-\frac{P}{\rho}\right)$. At this state of investigation the value of $\frac{P}{\rho}$ is not yet known. But the important result is that the flow thus created is of the type having a distribution of velocity which is a gradient of some quantity, called the velocity potential Φ. Φ is the impulse density which would stop the flow, divided by the density ρ. According to (4)

$$u=\frac{\partial\Phi}{\partial x},\ v=\frac{\partial\Phi}{\partial y},\ w=\frac{\partial\Phi}{\partial z} \quad \text{.....(5)}$$

from which follows

$$\Phi=\int(udx+vdy+wdz) \quad \text{.....(6)}$$

A second differentiation of (5) gives

$$\frac{\partial u}{\partial y}=\frac{\partial v}{\partial x},\ \text{etc.} \quad \text{.....(7)}$$

since both are equal to $\frac{\partial^2\Phi}{\partial x\partial y}$. The substitution of (5) into the equation of continuity (3) gives

$$\frac{\partial^2\Phi}{\partial x^2}+\frac{\partial^2\Phi}{\partial y^2}+\frac{\partial^2\Phi}{\partial z^2}=0 \quad \text{.....(8)}$$

(Laplace's equation), which is the desired equation for the potential Φ. The sum of any solutions of (8) is a solution of (8) again, as can easily be seen. This is equivalent to the superposition of flows; the sum of the potential, of the impulsive pressures, or of the velocity components of several potential flows give a potential flow again.

All this refers originally to the case only that the flow is created by one impulsive pressure from rest. But every continuous and changing pressure can be replaced by infinitely many small impulsive pressures, and the resultant flow is the superposition of the flows created by each impulsive pressure. And as the superposition of potential flows gives a potential flow again, it is thus demonstrated that all aerodynamic flows are potential flows.

It can further be shown that for each motion of the bodies immersed in the fluid, there exists only one potential flow. For the integral (6) applied to a stream line (that is, a line always parallel to the velocity) has always the same sign of the integrant, and hence can not become zero. Hence a stream line can not be closed, as otherwise the integral (6) would give two different potentials for the same point, or different impulsive pressures, which is not possible. On the contrary, each stream line begins and ends at the surface of one of the immersed bodies. Now suppose that two potential flows exist for one motion of the bodies. Then reverse one of them by changing the sign of the potential and superpose it on the other. The resulting flow is characterized by all bodies being at rest. But then no stream line can begin at their surface, and hence the flow has no stream lines at all and the two original flows are demonstrated to be identical.

It remains to compute the pressure at each point of a potential flow. The acceleration of each particle is equal to the negative gradient of the pressure, divided by the density of the fluid. The pressure is therefore to be expressed as a function of the space coordinates, and so is the acceleration of a particle. Each component of the acceleration, say $\frac{du}{dt}$, has to be expressed by the local rate of change of the velocity component at a certain point $\frac{\partial u}{\partial t}$ and

by the velocity components and their local derivatives themselves. This is done by the equation

$$\frac{du}{dt}=\frac{\partial u}{\partial t}+u\frac{\partial u}{\partial x}+v\frac{\partial u}{\partial y}+w\frac{\partial u}{\partial z} \quad \text{(9)}$$

For during the unit of time the particle changes its coordinates by u, v, and w, respectively, and therefore reaches a region where the velocity is larger by $u\frac{\partial u}{\partial x}$, etc. This increase of velocity has to be added to the rate of change per unit time of the velocity at one particular point.

The general principles of mechanics, applied to a particle of unit volume, give therefore

$$\frac{du}{dt}=\frac{\partial u}{\partial t}+u\frac{\partial u}{\partial x}+v\frac{\partial u}{\partial y}+w\frac{\partial u}{\partial z}=-\frac{1}{\rho}\frac{\partial p}{\partial x} \quad \text{(10)}$$

Substituting equation (7) in the last equation, we have

$$\frac{\partial u}{\partial t}+u\frac{\partial u}{\partial x}+v\frac{\partial v}{\partial x}+w\frac{\partial w}{\partial x}=-\frac{1}{\rho}\frac{\partial p}{\partial x} \quad \text{(11)}$$

Integrating this with respect to dx gives

$$\rho\frac{\partial\Phi}{\partial t}+\frac{\rho}{2}(u^2+v^2+w^2)=-\frac{1}{\rho}p \quad \text{(12)}$$

The equations for the two other components of the acceleration would give the same equation.

Hence it appears that the pressure can be divided into two parts superposed. The first part, $-\rho\frac{\partial\Phi}{\partial t}$, is the part of the pressure building up or changing the potential flow. It is zero if the flow is steady; that is, if

$$\frac{\partial\Phi}{\partial t}=0 \quad \text{(13)}$$

The second part,

$$-V^2\frac{\rho}{2} \quad \text{(14)}$$

if the pressure necessary to maintain and keep up the steady potential flow. It depends only on the velocity and density of the fluid. The greater the velocity, the smaller the pressure. It is sometimes called Bernouilli's pressure. This pressure acts permanently without changing the flow, and hence without changing its kinetic energy. It follows therefore that the Bernouilli's pressure (14) acting on the surface of a moving body, can not perform or consume any mechanical work. Hence in the case of the straight motion of a body the component of resultant force parallel to the motion is zero.

Some important formulas follow from the creation of the flow by the impulsive pressure $-\Phi\rho$. I will assume one body only, though this is not absolutely necessary for a part of the results. The distribution of this impulsive pressure over the surface of the bodies or body is characterized by a resultant impulsive force and a resultant impulsive moment. As further characteristic there is the mechanical work performed by the impulsive pressure during the creation of the flow, absorbed by the air and contained afterwards in the flow as kinetic energy of all particles.

It happens sometimes that the momentum imparted to the flow around a body moving translatory is parallel to the motion of the body. Since this momentum is proportional to the velocity, the effect of the air on the motion of the body in this direction is then taken care of by imparting to the body an apparent additional mass. If the velocity is not accelerated, no force is necessary to maintain the motion. The body experiences no drag, which is plausible, as no dissipation of energy is assumed. A similar thing may happen with a rotating body, where

then the body seems to possess an apparent additional moment of momentum. In general, however, the momentum imparted to the fluid is not parallel to the motion of the body, but it possesses a lateral component. The body in general possesses different apparent masses with respect to motions in different directions, and that makes the mechanics of a body surrounded by a perfect fluid different from that of one moving in a vacuum.

The kinetic energy imparted to the air is in a simple relation to the momentum and the velocity of the body. During the generation of the flow the body has the average velocity $\frac{V}{2}$ during the time dt, hence it moves through the distance $\frac{V}{2}dt$. The work performed is equal to the product of the component of resultant force of the creating pressure in the direction of motion, multiplied by this path, hence it is equal to half the product of the velocity and the component of the impulsive force in its direction.

The same argument can be used for the impulsive pressure acting over the surface of the body. Let dn be a linear element at right angles to the surface of the body drawn outward. The velocity at right angles to the surface is then, $-d\Phi/dn$ and the pressure $-\rho\Phi$ acts through the distance $-\frac{d\Phi/dn}{2}dt$. The work performed all over the surface is therefore

$$T=\int\frac{\rho}{2}\Phi\frac{d\Phi}{dn}dS \qquad (15)$$

which integral is to be extended over the entire surface of the body consisting of all the elements dS. The expression under the integral contains the mass of the element of fluid displaced by the surface element of the body per unit of time, each element of mass multiplied by the velocity potential. The Bernouilli pressure does not perform any work, as discussed above, and is therefore omitted.

The apparent mass of a body moving in a particular direction depends on the density of the fluid. It is more convenient therefore to consider a volume of the fluid having a mass equal to the apparent mass of the body. This volume is

$$K=\frac{T}{V^2\frac{\rho}{2}} \qquad (16)$$

and depends only on the dimensions and form of the body.

The kinetic energy of the flow relative to a moving body in an infinite fluid is of course infinite. It is possible, however, to consider the diminution of the kinetic energy of the air moving with constant velocity brought about by the presence of a body at rest. This diminution of energy has two causes. The body displaces fluid, and hence the entire energy of the fluid is lessened by the kinetic energy of the displaced fluid. Further, the velocity of the air in the neighborhood of the body is diminished on the average. The forces between the body and the fluid are the same in both cases, whether the air or the body moves. Hence this second diminution of kinetic energy is equal to the kinetic energy of the flow produced by the moving body in the fluid otherwise at rest.

II. THE AERODYNAMIC FORCES ON AIRSHIP HULLS.

An important branch of theoretical aerodynamics deals with moments on bodies moving through the air while producing a potential flow. Wings produce a flow different from a potential flow, in the strict meaning of the word. The wings have therefore to be excluded from the following discussion.

Consider first bodies moving straight and with constant velocity V through air extending in all directions to infinity. There can not then be a drag, as the kinetic energy of the flow remains constant and no dissipation of energy is supposed to take place. Nor can there be a

lift in conformity with the remarks just made. Hence the air pressures can at best produce a resultant pure couple of forces or resultant moment. The magnitude and direction of this moment will depend on the magnitude of the velocity V and on the position of the body relative to the direction of its motion. With a change of velocity all pressures measured from a suitable standard, change proportional to the square of the velocity, as follows from equation (14). Hence the resultant moment is likewise proportional to the square of the velocity. In addition it will depend on the position of the body relative to the direction of motion. The study of this latter relation is the chief subject of this section. At each different position of the body relative to the motion the flow produced is different in general and so is the momentum of the flow, possessing different components in the direction of and at right angles to the direction of motion. By no means, however, can the relation between the momentum and the direction of motion be quite arbitrarily prescribed. The flow due to the straight motion in any direction can be obtained by the superposition of three flows produced by the motions in three particular directions. That restricts the possibilities considerably. But that is not all, the moments can not even arbitrarily be prescribed in three directions. I shall presently show that there are additional restrictions based on the principle of conservation of energy and momentum.

Let there be a component of the momentum lateral to the motion, equal to $K_2 V\rho$, where ρ denotes the density of the air. Since the body is advancing, this lateral component of the momentum has continually to be annihilated at its momentary position and to be created anew in its next position, occupied a moment later. This process requires a resultant moment

$$M = K_2 V^2 \rho \qquad (17)$$

about an axis at right angles to the direction of motion and to the momentum. In other words, the lateral component of the momentum multiplied by the velocity gives directly the resultant moment. Conversely, if the body experiences no resultant moment and hence is in equilibrium, the momentum of the air flow must be parallel to the motion.

Now consider a flow relative to the body with constant velocity V except for the disturbance of the body and let us examine its (diminution of) kinetic energy. If the body changes its position very slowly, so that the flow can still be considered as steady, the resultant moment is not affected by the rotation but is the same as corresponding to the momentary position and stationary flow. This moment then performs or absorbs work during the slow rotation. It either tends to accelerate the rotation, so that the body has to be braked, or it is necessary to exert a moment on the body in order to overcome the resultant moment. This work performed or absorbed makes up for the change of the kinetic energy of the flow. That gives a fundamental relation between the energy and the resultant moment.

There are as many different positions of the body relative to its motion as a sphere has radii. The kinetic energy of the flow is in general different for all directions, the velocity V and density ρ supposed to be constant. It has the same value, however, if the motion of the immersed solid is reversed, for then the entire flow is reversed. Therefore each pair of directions differing by 180° has the same kinetic energy. This energy moreover is always positive and finite. There must therefore be at least one pair of directions, where it is a minimum and one where it is a maximum. Moving parallel to either of these directions the body is in equilibrium and experiences no resultant moment. This follows from the consideration that then a small change in the direction of motion does not give rise to a corresponding change of the kinetic energy; the moment does not perform any work, and hence must be zero. The equilibrium is stable if the diminution of energy of the entire flow is a maximum and unstable if it is a minimum. It can be proved that in addition there must be at least one other axis of equilibrium. This is the position "neutral" with respect to the stable direction and at the same time neutral with respect to the unstable one. I call these directions "main axes."

I proceed to demonstrate that the three main axes of equilibrium are always at right angles to each other. Consider first the motion parallel to a plane through one of the main axes and

only the components of the momentum parallel to this plane. The direction of motion of the body may be indicated by the angle α in such a way that $\alpha = O$ is one motion of equilibrium, and hence without lateral component of momentum. The component of momentum in the direction of the motion may then (that is, when $\alpha = O$) be $K_1 \rho V$. When moving at the angle of $\alpha = 90°$, the momentum may be supposed to possess the components $K_2 \rho V$ parallel and $K_3 \rho V$ at right angles to the motion, and we shall prove at once that the only momentum is the former.

The kinetic energy for any direction α can be written in the general form

$$T = V^2 \frac{\rho}{2} (K_1 \cos^2 \alpha + K_2 \sin^2 \alpha + K_3 \cos \alpha \sin \alpha)$$

and hence the resultant moment is

$$M = dT/d\alpha = V^2 \frac{\rho}{2} \left[(K_2 - K_1) \sin 2\alpha + K_3 \cos 2\alpha \right] \quad \ldots\ldots\ldots\ldots\ldots\ldots (18)$$

This resultant moment was supposed to be zero at $\alpha = O$. Hence $K_3 = O$, and it follows that $\alpha = 90°$ is a position of equilibrium for motions in the plane considered. As for other motions, it is to be noticed that the third component of the momentum, at right angles to the plane, changes if the plane rotates around the axis of equilibrium. It necessarily changes its sign during a revolution, and while doing it M is zero. Thus it is demonstrated that there are at least two axes at right angles to each other where all lateral components of the momentum are zero, and hence the motion is in equilibrium. And as this argument holds true for any pair of the three axes of equilibrium, it is proved that there are always at least three axes of equilibrium at right angles to each other.

Resolving the velocity V of the body into three components, u, v, w, parallel to these three main axes, the kinetic energy can be expressed

$$\frac{\rho}{2} (K_1 u^2 + K_2 v^2 + K_3 w^2)$$

The differential of the energy

$$\rho (K_1 u du + K_2 v dv + K_3 w dw)$$

is identically zero in more than three pairs of positions only if at least two of the K's are equal. Then it is zero in an infinite number of directions, and there are an infinite number of directions of equilibrium. The body is in equilibrium in all directions of motion only if all three K's are equal; that is, if the apparent mass of the body is the same in all directions. That is a special case.

In all other cases the body experiences a resultant moment if moving with the velocity components u, v, and w parallel to the three main axes. The component of this resultant moment is determined by the momentary lateral momentum and its components, as stated in equation 17.

In most practical problems the motion occurs in a main plane; that is, at right angles to a main axis. Then the entire resultant moment is according to (17) the product of the velocity and the component of momentum at right angles to it, giving

$$M = V^2 \frac{\rho}{2} (K_2 - K_1) \sin 2\alpha \quad \ldots\ldots\ldots\ldots\ldots\ldots\ldots\ldots\ldots\ldots (19)$$

In general, the three main momenta of the flow, parallel to the respective motion, do not pass through one center. Practical problems occur chiefly with bodies of revolution. With them as well as with bodies with a center of symmetry—that is, such as have three planes of symmetry—the relation between the motion and the momenta is simple. It follows then from symmetry that the body possesses an aerodynamic center through which the three main momenta pass. This means that the body can be put into any straight motion by applying a force at a fixed

center. The force, however, is not parallel to the motion except in the main directions. The center where the force has to be applied coincides with the aerodynamic center, if the center of gravity of the body does so or if the mass of the body itself can be neglected compared with any of the three main additional masses.

Airship hulls are often bounded by surfaces of revolution. In addition they are usually rather elongated, and if the cross sections are not exactly round, they are at least approximately of equal and symmetrical shape and arranged along a straight axis. Surfaces of revolution have, of course, equal transverse apparent masses; each transverse axis at right angles to the axis of revolution is a main direction. For very elongated surfaces of revolution a further important statement may be made regarding the magnitude of the longitudinal and transverse apparent mass. When moving transversely the flow is approximately two-dimensional along the greatest part of the length. The apparent additional mass of a circular cylinder moving at right angles to its axis will be shown to be equal to the mass of the displaced fluid. It follows therefore that the apparent transverse additional mass of a very elongated body of revolution is approximately equal to the mass of the displaced fluid. It is slightly smaller, as near the ends the fluid has opportunity to pass the bow and stern. For cross sections other than circular the two main apparent masses follow in a similar way from the apparent mass of the cross section in the two-dimensional flow.

The longitudinal apparent additional mass, on the other hand, is small when compared with the mass of the displaced fluid. It can be neglected if the body is very elongated or can at least be rated as a small correction. This follows from the fact that only near the bow and the stern does the air have velocities of the same order of magnitude as the velocity of motion. Along the ship the velocity not only is much smaller but its direction is essentially opposite to the direction of motion, for the bow is continually displacing fluid and the stern makes room free for the reception of the same quantity of fluid. Hence the fluid is flowing from the bow to the stern, and as only a comparatively small volume is displaced per unit of time and the space is free in all directions to distribute the flow, the average velocity will be small.

It is possible to study this flow more closely and to prove analytically that the ratio of the apparent mass to the displaced mass approaches zero with increasing elongation. This proof, however, requires the study or knowledge of quite a number of conceptions and theorems, and it seems hardly worth while to have the student go through all this in order to prove such a plausible and trivial fact.

The actual magnitudes of the longitudinal and transverse masses of elongated surfaces of revolution can be studied by means of exact computations made by H. Lamb (reference 5), with ellipsoids of revolutions of different ratio of elongation. The figures of k_1 and k_2, where $K=k\times$ volume, obtained by him are contained in Table I of this paper, and k_1-k_2 is computed. For bodies of a shape reasonably similar to ellipsoids it can be approximately assumed that (k_1-k_2) has the same value as for an ellipsoid of the same length and volume; that is, if Vol/L^3 has the same value.

The next problem of interest is the resultant aerodynamic force if the body rotates with constant velocity around an axis outside of itself. That is now comparatively simple, as the results of the last section can be used. The configuration of flow follows the body, with constant shape, magnitude, and hence with constant kinetic energy. The resultant aerodynamic force, therefore, must be such as neither to consume nor to perform mechanical work. This leads to the conclusion that the resultant force must pass through the axis of rotation. In general it has both a component at right angles and one parallel to the motion of the center of the body.

I confine the investigation to a surface of revolution. Let an airship with the apparent masses $K_1\rho$ and $K_2\rho$ and the apparent moment of inertia $K'\rho$ for rotation about a transverse axis through its aerodynamic center move with the velocity V of its aerodynamic center around an axis at the distance r from its aerodynamic center and let the angle of yaw ϕ be measured between the axis of the ship and the tangent of the circular path at the aerodynamic center. The ship is then rotating with the constant angular velocity V/r. The entire motion can be obtained by superposition of the longitudinal motion $V\cos\phi$ of the aerodynamic center, the

tranverse velocity $V \sin \phi$, and the angular velocity V/r. The longitudinal component of the momentum is $V\rho . \cos \phi . k_1 . \text{vol}$, and the tranverse component of the momentum is $V\rho \sin \phi . k_2 . \text{vol}$. Besides, there is a moment of momentum due to the rotation. This can be expressed by introducing the apparent moment of inertia $K'\rho = k'J\rho$ where J is the moment of inertia of the displaced air; thus making the angular momentum

$$k'J\rho\left(\frac{V}{r}\right)$$

As it does not change, it does not give rise to any resultant aerodynamic force or moment during the motion under consideration.

The momentum remains constant, too, but changes its direction with the angular velocity V/r. This requires a force passing through the center of turn and having the tranverse component

$$F_t = K_1\rho \cos \phi V^2/r \quad \ldots\ldots (20)$$

and the longitudinal component

$$F_l = K_2\rho \sin \phi V^2/r \quad \ldots\ldots (21)$$

The first term is almost some kind of centrifugal force. Some air accompanies the ship, increasing its longitudinal mass and hence its centrifugal force. It will be noticed that with actual airships this additional centrifugal force is small, as k_1 is small. The force attacking at the center of the turn can be replaced by the same force attacking at the aerodynamic center and a moment around this center of the magnitude.

$$M = \tfrac{1}{2}(K_2 - K_1)\rho \sin 2\phi V^2 \quad \ldots\ldots (22)$$

This moment is equal in direction and magnitude to the unstable moment found during straight motion under the same angle of pitch or yaw. The longitudinal force is in practice a negative drag as the bow of the ship is turned toward the inside of the circle. It is of no great practical importance as it does not produce considerable structural stresses.

It appears thus that the ship when flying in a curve or circle experiences almost the same resultant moment as when flying straight and under the same angle of pitch or yaw. I proceed to show, however, that the transverse aerodynamic forces producing this resultant moment are distributed differently along the axis of the ship in the two cases.

The distribution of the transverse aerodynamic forces along the axis can conveniently be computed for very elongated airships. It may be supposed that the cross section is circular, although it is easy to generalize the proceeding for a more general shape of the cross section.

The following investigation requires the knowledge of the apparent additional mass of a circular cylinder moving in a two-dimensional flow. I proceed to show that this apparent additional mass is exactly equal to the mass of the fluid displaced by the cylinder. In the two-dimensional flow the cylinder is represented by a circle.

Let the center of this circle coincide with the origin of a system of polar coordinates R and ϕ, moving with it, and let the radius of the circle be denoted by r. Then the velocity potential of the flow created by this circle moving in the direction $\phi = O$ with the velocity v is $\Phi = vr^2 (\cos \phi)/R$. For this potential gives the radial velocity components

$$\frac{d\Phi}{dR} = -v\frac{r^2}{R^2}\cos \phi$$

and at the circumference of the circle this velocity becomes $v \cos \phi$. This is in fact the normal component of velocity of a circle moving with the velocity v in the specified direction.

The kinetic energy of this flow is now to be determined. In analogy to equation (15), this is done by integrating along the circumference of the circle the product of (*a*) the elements of half the mass of the fluid penetrating the circle $\left(\frac{\rho}{2}\cos \phi vrd\phi\right)$ and (*b*), the value of the veloc-

ity potential at that point ($-v \cos \phi . r$). The integral is therefore

$$\frac{\rho}{2}\int_0^{2\pi} \cos^2 \phi v^2 r^2 d\phi$$

giving the kinetic energy $r^2 \pi v^2 \frac{\rho}{2}$.

This shows that in fact the area of apparent mass is equal to the area of the circle.

I am now enabled to return to the airship.

If a very elongated airship is in translatory horizontal motion through air otherwise at rest and is slightly pitched, the component of the motion of the air in the direction of the axis of the ship can be neglected. The air gives way to the passing ship by flowing around the axis of the ship, not by flowing along it. The air located in a vertical plane at right angles to the motion remains in that plane, so that the motion in each plane can be considered to be two-dimensional. Consider one such approximately vertical layer of air at right angles to the axis while the ship is passing horizontally through it. The ship displaces a circular portion of this layer, and this portion changes its position and its size. The rate of change of position is expressed by an apparent velocity of this circular portion, the motion of the air in the vertical layer is described by the two-dimensional flow produced by a circle moving with the same velocity. The momentum of this flow is $Sv\rho dx$, where S is the area of the circle, and v the vertical velocity of the circle, and dx the thickness of the layer. Consider first the straight flight of the ship under the angle of pitch ϕ. The velocity v of the displaced circular portion of the layer is then constant over the whole length of the ship and is $V \sin \phi$, where V is the velocity of the airship along the circle. Not so the area S; it changes along the ship. At a particular layer it changes with the rate of change per unit time,

$$V \cos \phi \cdot \frac{dS}{dx}$$

where x denotes the longitudinal coordinate.

Therefore the momentum changes with the rate of change

$$V^2 \frac{\rho}{2} \sin 2\phi \frac{dS}{dx} dx$$

This gives a down force on the ship with the magnitude

$$dF = dx V^2 \frac{\rho}{2} \sin 2\phi \frac{dS}{dx} \qquad (23)$$

Next, consider the ship when turning, the angle of yaw being ϕ. The momentum in each layer is again

$$vS\rho dx$$

The transverse velocity v is now variable, too, as it is composed of the constant portion $V \sin \phi$, produced by the yaw, and of the variable portion $V \frac{x}{r} \cos \phi$, produced by the turning. $x = O$ represents the aerodynamic center. Hence the rate of change of the momentum per unit length is

$$V^2 \frac{\rho}{2} \sin 2\phi \frac{dS}{dx} + \rho \frac{V^2}{r} \cos \phi \frac{d}{dx}(xS)$$

giving rise to the transverse force per unit length

$$V^2 \frac{\rho}{2} \sin 2\phi \frac{dS}{dx} + V^2 \frac{\rho}{r} \cos \phi \left(S + x \frac{dS}{dx}\right)$$

or otherwise written

$$dF = dx\left(V^2 \frac{\rho}{2} \sin 2\phi \frac{dS}{dx} + V^2 \frac{\rho}{r} \cos \phi \, S + V^2 \frac{\rho}{r} \cos \phi \cdot x \frac{dS}{dx}\right) \qquad (24)$$

The first term agrees with the moment of the ship flying straight having a pitch ϕ. The direction of this transverse force is opposite at the two ends, and gives rise to an unstable moment. The ships in practice have the bow turned inward when they fly in turn. Then the transverse force represented by the first term of (24) is directed inward near the bow and outward near the stern.

The sum of the second and third terms of (24) gives no resultant force or moment. The second term alone gives a transverse force, being in magnitude and distribution almost equal to the transverse component of the centrifugal force of the displaced air, but reversed. This latter becomes clear at the cylindrical portion of the ship, where the two other terms are zero. The front part of the cylindrical portion moves toward the center of the turn and the rear part moves away from it. The inward momentum of the flow has to change into an outward momentum, requiring an outward force acting on the air, and giving rise to an inward force reacting this change of momentum.

The third term of (24) represents forces almost concentrated near the two ends and their sum in magnitude and direction is equal to the transverse component of the centrifugal force of the displaced air. They are directed outward.

Ships only moderately elongated have resultant forces and a distribution of them differing from those given by the formulas (23) and (24). The assumption of the layers remaining plane is more accurate near the middle of the ship than near the ends, and in consequence the transverse forces are diminished to a greater extent at the ends than near the cylindrical part when compared with the very elongated hulls. In practice, however, it will often be exact enough to assume the same shape of distribution for each term and to modify the transverse forces by constant diminishing factors. These factors are logically to be chosen different for the different terms of (24). For the first term represents the forces giving the resultant moment proportional to (k_2-k_1), and hence it is reasonable to diminish this term by multiplying it by (k_2-k_1). The second and third terms take care of the momenta of the air flowing transverse with a velocity proportional to the distance from the aerodynamic center. The moment of inertia of the momenta really comes in, and therefore it seems reasonable to diminish these terms by the factor k', the ratio of the apparent moment of inertia to the moment of inertia of the displaced air.

The transverse component of the centrifugal force produced by the air taken along with the ship due to its longitudinal mass is neglected. Its magnitude is small; the distribution is discussed in reference (3) and may be omitted in this treatise.

The entire transverse force on an airship, turning under an angle of yaw with the velocity V and a radius r, is, according to the preceding discussion,

$$dF=dx\left[(k_2-k_1)\frac{dS}{dx}V^2\frac{\rho}{2}\sin 2\phi+k'V\frac{\rho}{r}S\cos\phi+k'V^2\frac{\rho x}{r}\frac{dS}{dx}\cos\phi\right]\text{.....(25)}$$

This expression does not contain of course the air forces on the fins.

In the first two parts of this paper I discussed the dynamical forces of bodies moving along a straight or curved path in a perfect fluid. In particular I considered the case of a very elongated body and as a special case again one bounded by a surface of revolution.

The hulls of modern rigid airships are mostly surfaces of revolution and rather elongated ones, too. The ratio of the length to the greatest diameter varies from 6 to 10. With this elongation, particularly if greater than 8, the relations valid for infinite elongation require only a small correction, only a few per cent, which can be estimated from the case of ellipsoids for which the forces are known for any elongation. It is true that the transverse forces are not only increased or decreased uniformly, but also the character of their distribution is slightly changed. But this can be neglected for most practical applications, and especially so since there are other differences between theoretical and actual phenomena.

Serious differences are implied by the assumption that the air is a perfect fluid. It is not, and as a consequence the air forces do not agree with those in a perfect fluid. The resulting air force by no means gives rise to a resulting moment only; it is well known that an airship

hull model without fins experiences both a drag and a lift, if inclined. The discussion of the drag is beyond the scope of this paper. The lift is very small, less than 1 per cent of the lift of a wing with the same surface area. But the resulting moment is comparatively small, too, and therefore it happens that the resulting moment about the center of volume is only about 70 per cent of that expected in a perfect fluid. It appears, however, that the actual resulting moment is at least of the same range of magnitude, and the contemplation of the perfect fluid gives therefore an explanation of the phenomenon. The difference can be explained. The flow is not perfectly irrotational, for there are free vortices near the hull, especially at its rear end, where the air leaves the hull. They give a lift acting at the rear end of the hull, and hence decreasing the unstable moment with respect to the center of volume

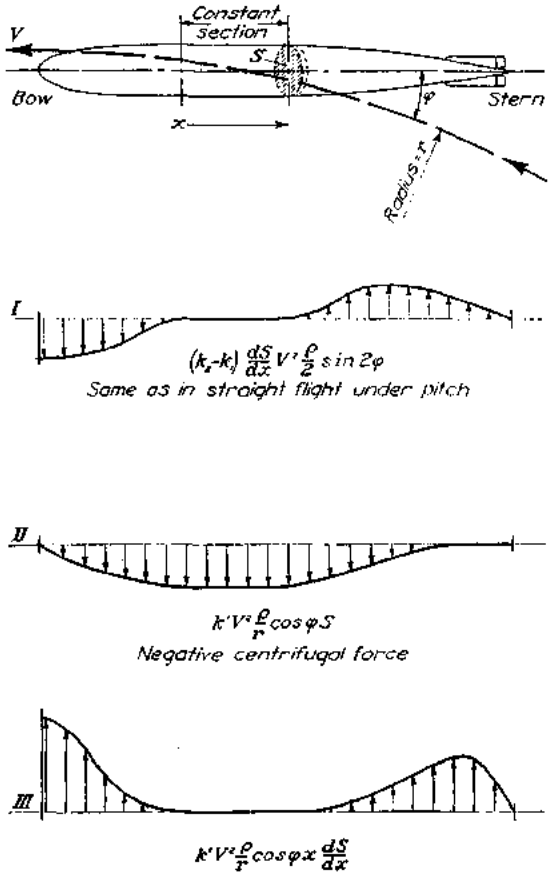

FIG. 1.—Diagram showing the direction of the transverse air forces acting on an airship flying in a turn. The three terms are to be added together.

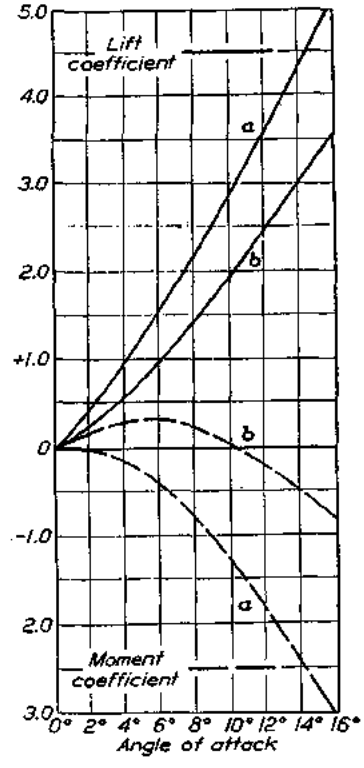

FIG. 2.

What is perhaps more important, they produce a kind of induced downwash, diminishing the effective angle of attack, and hence the unstable moment.

This refers to airship hulls without fins, which are of no practical interest. Airship hulls with fins must be considered in a different way. The fins are a kind of wings; and the flow around them, if they are inclined, is far from being even approximately irrotational and their lift is not zero. The circulation of the inclined fins is not zero; and as they are arranged in the rear of the ship, the vertical flow induced by the fins in front of them around the hull is directed upward if the ship is nosed up. Therefore the effective angle of attack is increased, and the influence of the lift of the hull itself is counteracted. For this reason it is to be expected that the transverse forces of hulls with fins in air agree better with these in a perfect fluid. Some model tests to be discussed now confirm this.

These tests give the lift and the moment with respect to the center of volume at different angles of attack and with two different sizes of fins. If one computes the difference between the observed moment and the expected moment of the hull alone, and divides the difference by the observed lift, the apparent center of pressure of the lift of the fins results. If the center of pressure is situated near the middle of the fins, and it is, it can be inferred that the actual flow of the air around the hull is not very different from the flow of a perfect fluid. It follows, then, that the distribution of the transverse forces in a perfect fluid gives a good approximation of the actual distribution, and not only for the case of straight flight under consideration, but also if the ship moves along a circular path.

The model tests which I proceed to use were made by Georg Fuhrmann in the old Goettingen wind tunnel and published in the Zeitschrift für Flugtechnik und Motorluftschiffahrt, 1910. The model, represented in Figure 3, had a length of 1,145 millimeters, a maximum diameter of 188 millimeters, and a volume of 0.0182 cubic meter. Two sets of fins were attached to the hull, one after another; the smaller fins were rectangular, 6.5 by 13 centimeters, and the larger ones, 8 by 15 centimeters. $(\text{Volume})^{2/3} = 0.069$ square meter. In Figure 3 both fins are shown. The diagram in Figure 2 gives both the observed lift and the moment expressed by means of absolute coefficients. They are reduced to the unit of the dynamical pressure, and also the moment is reduced to the unit of the volume, and the lift to the unit of $(\text{volume})^{2/3}$.

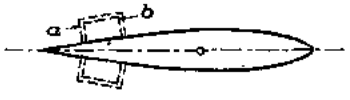

FIG. 3.—Airship model.

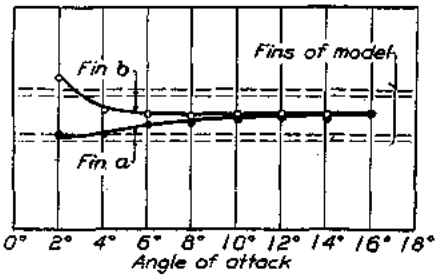

FIG. 4.—Center of pressure of fin forces.

Diagram Figure 4 shows the position of the center of pressure computed as described before. The two horizontal lines represent the leading and the trailing end of the fins. It appears that for both sizes of the fins the curves nearly agree, particularly for greater angles of attack at which the tests are more accurate. The center of pressure is situated at about 40 per cent of the chord of the fins. I conclude from this that the theory of a perfect fluid gives a good indication of the actual distribution of the transverse forces. In view of the small scale of the model, the agreement may be even better with actual airships.

III. SOME PRACTICAL CONCLUSIONS.

The last examination seems to indicate that the actual unstable moment of the hull in air agrees nearly with that in a perfect fluid. Now the actual airships with fins are statically unstable (as the word is generally understood, not aerostatically of course), but not much so, and for the present general discussion it can be assumed that the unstable moment of the hull is nearly neutralized by the transverse force of the fins. I have shown that this unstable moment is $M = (\text{volume})\ (k_2 - k_1)\ V^2 \frac{\rho}{2} \sin 2\phi$, where $(k_2 - k_1)$ denotes the factor of correction due to finite elongation. Its magnitude is discussed in the first part of this paper. Hence the transverse force of the fins must be about $\frac{M}{a}$, where a denotes the distance between the fin and the center of gravity of the ship. Then the effective area of the fins—that is, the area of a wing giving the same lift in a two-dimensional flow—follows:

$$\frac{(\text{Volume})(k_2 - k_1)}{a_n}$$

Taking into account the span b of the fins—that is, the distance of two utmost points of a pair of fins—the effective fin area S must be

$$\frac{(\text{Volume})(k_2-k_1)}{a}\times\frac{1+2\frac{S}{b^2}}{\pi}$$

This area S, however, is greater than the actual fin area. Its exact size is uncertain, but a far better approximation than the fin area is obtained by taking the projection of the fins and the part of the hull between them. This is particularly true if the diameter of the hull between the fins is small.

If the ends of two airships are similar, it follows that the fin area must be proportional to $(k_2-k_1)(\text{volume})/a$. For rather elongated airships (k_2-k_1) is almost equal to 1 and constant, and for such ships therefore it follows that the fin area must be proportional to $(\text{volume})/a$, or, less exactly, to the greatest cross section, rather than to $(\text{volume})^{2/3}$. Comparatively short ships, however, have a factor (k_2-k_1) rather variable, and with them the fin area is more nearly proportional to $(\text{volume})^{2/3}$.

This refers to circular section airships. Hulls with elliptical section require greater fins parallel to the greater plan view. If the greater axis of the ellipse is horizontal, such ships are subjected to the same bending moments for equal lift and size, but the section modulus is smaller, and hence the stresses are increased. They require, however, a smaller angle of attack for the same lift. The reverse holds true for elliptical sections with the greater axes vertical.

If the airship flies along a circular path, the centrifugal force must be neutralized by the transverse force of the fin, for only the fin gives a considerable resultant transverse force. At the same time the fin is supposed nearly to neutralize the unstable moment. I have shown now that the angular velocity, though indeed producing a considerable change of the distribution of the transverse forces, and hence of the bending moments, does not give rise to a resulting force or moment. Hence, the ship flying along the circular path must be inclined by the same angle of yaw as if the transverse force is produced during a rectilinear flight by pitching. From the equation of the transverse force

$$\text{Vol}\,\rho\frac{V^2}{r}=\frac{\text{Vol}(k_2-k_1)\,V^2\frac{\rho}{2}\sin 2\phi}{a}$$

it follows that the angle is approximately

$$\phi\sim\frac{a}{r}\frac{1}{k_2-k_1}$$

This expression in turn can be used for the determination of the distribution of the transverse forces due to the inclination. The resultant transverse force is produced by the inclination of the fins. The rotation of the rudder has chiefly the purpose of neutralizing the damping moment of the fins themselves.

From the last relation, substituted in equation (25), follows approximately the distribution of the transverse forces due to the inclination of pitch, consisting of

$$\frac{dS}{dx}V^2\frac{\rho}{2}\frac{2a}{r}dx \qquad (26)$$

This is only one part of the transverse forces. The other part is due to the angular velocity; it is approximately

$$k'\frac{2x\,dS}{r\,dx}V^2\frac{\rho}{2}dx+k'\frac{V^2\rho}{r}Sdx \qquad (27)$$

The first term in (27) together with (26) gives a part of the bending moment. The second term in (27), having mainly a direction opposite to the first one and to the centrifugal force, is almost neutralized by the centrifugal forces of the ship and gives additional bending moments not very considerable either. It appears, then, that the ship experiences smaller bending moments when creating an air force by yaw opposite to the centrifugal force than when creating the same

transverse force during a straight flight by pitch. For ships with elliptical sections this can not be said so generally. The second term in (27) will then less perfectly neutralize the centrifugal force, if that can be said at all, and the bending moments become greater in most cases.

Most airship pilots are of the opinion that severe aerodynamic forces act on airships flying in bumpy weather. An exact computation of the magnitude of these forces is not possible, as they depend on the strength and shape of the gusts and as probably no two exactly equal gusts occur. Nevertheless, it is worth while to reflect on this phenomenon and to get acquainted with the underlying general mechanical principles. It will be possible to determine how the magnitude of the velocity of flight influences the air forces due to gusts. It even becomes possible to estimate the magnitude of the air forces to be expected, though this estimation will necessarily be somewhat vague, due to ignorance of the gusts.

The airship is supposed to fly not through still air but through an atmosphere the different portions of which have velocities relative to each other. This is the cause of the air forces in bumpy weather, the airship coming in contact with portions of air having different velocities. Hence, the configuration of the air flow around each portion of the airship is changing as it always has to conform to the changing relative velocity between the portion of the airship and the surrounding air. A change of the air forces produced is the consequence.

Even an airship at rest experiences aerodynamical forces in bumpy weather, as the air moves toward it. This is very pronounced near the ground, where the shape of the surrounding objects gives rise to violent local motions of the air. The pilots have the impression that at greater altitudes an airship at rest does not experience noticeable air forces in bumpy weather. This is plausible. The hull is struck by portions of air with relatively small velocity, and as the forces vary as the square of the velocity they can not become large.

It will readily be seen that the moving airship can not experience considerable air forces if the disturbing air velocity is in the direction of flight. Only a comparatively small portion of the air can move with a horizontal velocity relative to the surrounding air and this velocity can only be small. The effect can only be an air force parallel to the axis of the ship which is not likely to create large structural stresses.

There remains, then, as the main problem the airship in motion coming in contact with air moving in a transverse direction relative to the air surrounding it a moment before. The stresses produced are severer if a larger portion of air moves with that relative velocity. It is therefore logical to consider portions of air large compared with the diameter of the airship; smaller gusts produce smaller air forces. It is now essential to realize that their effect is exactly the same as if the angle of attack of a portion of the airship is changed. The air force acting on each portion of the airship depends on the relative velocity between this portion and the surrounding air. A relative transverse velocity u means an effective angle of attack of that portion equal to u/V, where V denotes the velocity of flight. The airship therefore is now to be considered as having a variable effective angle of attack along its axis. The magnitude of the superposed angle of attack is u/V, where u generally is variable. The air force produced at each portion of the airship is the same as the air force at that portion if the entire airship would have that particular angle of attack.

The magnitude of the air force depends on the conicity of the airship portion as described in section 2. The force is proportional to the angle of attack and to the square of the velocity of flight. In this case, however, the superposed part of the angle of attack varies inversely as the velocity of flight. It results, then, that the air forces created by gusts are directly proportional to the velocity of flight. Indeed, as I have shown, they are proportional to the product of the velocity of flight and the transverse velocity relative to the surrounding air.

A special and simple case to consider for a closer investigation is the problem of an airship immersing from air at rest into air with constant transverse horizontal or vertical velocity. The portion of the ship already immersed has an angle of attack increased by the constant amount u/V. Either it can be assumed that by operation of the controls the airship keeps its course or, better, the motion of an airship with fixed controls and the air forces acting on it under these conditions can be investigated. As the fins come under the influence of the increased

transverse velocity later than the other parts, the airship is, as it were, unstable during the time of immersing into the air of greater transverse velocity and the motion of the airship aggravates the stresses.

In spite of this the actual stresses will be of the same range of magnitude as if the airship flies under an angle of pitch of the magnitude u/V, for in general the change from smaller to greater transverse velocity will not be so sudden and complete as supposed in the last paragraph. It is necessary chiefly to investigate the case of a vertical transverse relative velocity u, for the severest condition for the airship is a considerable angle of pitch, and a vertical velocity u increases these stresses. Hence it would be extremely important to know the maximum value of this vertical velocity. The velocity in question is not the greatest vertical velocity of portions of the atmosphere occurring, but differences of this velocity within distances smaller than the length of the airship. It is very difficult to make a positive statement as to this velocity, but it is necessary to conceive an idea of its magnitude, subject to a correction after the question is studied more closely. Studying the meteorological papers in the reports of the British Advisory Committee for Aeronautics, chiefly those of 1909–10 and 1912–13, I should venture to consider a sudden change of the vertical velocity by 2 m./sec. (6.5 ft./sec.) as coming near to what to expect in very bumpy weather. The maximum dynamic lift of an airship is produced at low velocity, and is the same as if produced at high velocity at a comparatively low angle of attack, not more than 5°. If the highest velocity is 30 m./sec. (67 mi./hr.), the angle of attack u/V, repeatedly mentioned before, would be $\frac{57.3 \times 2}{30} = 3.8°$. This is a little smaller than 5°, but the assumption for u is rather vague. It can only be said that the stresses due to gusts are of the same range of magnitude as the stresses due to pitch; but they are probably not larger.

A method for keeping the stresses down in bumpy weather is by slowing down the speed of the airship. This is a practice common among experienced airship pilots. This procedure is particularly recommended if the airship is developing large dynamic lift, positive or negative, as then the stresses are already large.

Length (diameters).	K_1 (longitudinal).	K_2 (transverse).	$K_2 - K_1$.	K′ (rotation).
1	0.500	0.500	0	0
1.50	.305	.621	.316	.094
2.00	.209	.702	.493	.240
2.51	.156	.763	.607	.367
2.99	.122	.803	.681	.465
3.99	.082	.860	.778	.608
4.99	.059	.895	.836	.701
6.01	.045	.918	.873	.764
6.97	.038	.933	.897	.805
8.01	.029	.945	.916	.840
9.02	.024	.954	.930	.865
9.97	.021	.950	.939	.883
∞	.000	1.000	1.000	1.000

REFERENCES.

1. MAX M. MUNK. The minimum induced drag of airfoils. National Advisory Committee for Aeronautics. Report No. 121.

2. MAX M. MUNK. The drag of Zeppelin airships. National Advisory Committee for Aeronautics. Report No. 117.

3. MAX M. MUNK. Notes on aerodynamic forces. National Advisory Committee for Aeronautics. Technical Notes Nos. 104–106.

4. HORACE LAMB. Hydrodynamics. Cambridge, 1916.

5. HORACE LAMB. The inertia coefficients of an ellipsoid. British Advisory Committee for Aeronautics. R. and M. No. 623.

6. Dr. W. N. SHAW. Report on vertical motion in the atmosphere. British Advisory Committee for Aeronautics. 1909–10.

7. J. S. DINES. Fourth report on wind structures. British Advisory Committee for Aeronautics. 1912–13.

REPORT No. 191.

ELEMENTS OF THE WING SECTION THEORY AND OF THE WING THEORY.

By MAX M. MUNK.

SUMMARY.

The following paper, prepared for the National Advisory Committee for Aeronautics, contains those results of the theory of wings and of wing sections which are of immediate practical value. They are proven and demonstrated by the use of the simple conceptions of "kinetic energy" and "momentum" only, familiar to every engineer; and not by introducing "isogonal transformations" and "vortices," which latter mathematical methods are not essential to the theory and better are used only in papers intended for mathematicians and special experts.

REFERENCES.

1. Max M. Munk. The Aerodynamic Forces on Airship Hulls. N. A. C. A. Report No. 184.
2. Max M. Munk. The Minimum Induced Drag of Aerofoils. N. A. C. A. Report No. 121.
3. Max M. Munk. General Theory of Thin Wing Sections. N. A. C. A. Report No. 142.
4. Max M. Munk. Determination of the Angles of Attack of Zero Lift and of Zero Moment, Based on Munk's Integrals. N. A. C. A. Technical Note No. 122.
5. Horace Lamb. Hydrodynamics.

I. THE COMPLEX POTENTIAL FUNCTION.

1. I have shown in the paper, reference 1, how each air flow, considered as a whole, possesses as characteristic quantities a kinetic energy and a momentum necessary to create it. Many technically important flows can be created by a distribution of pressure and they then have a "velocity potential" which equals this pressure distribution divided by the density of the fluid with the sign reversed. It is further explained in the paper referred to how the superposition of several "potential flows" gives a potential flow again.

The characteristic differential equation for the velocity potential Φ was shown to be

$$\frac{\partial^2\Phi}{\partial x^2}+\frac{\partial^2\Phi}{\partial y^2}+\frac{\partial^2\Phi}{\partial z^2}=0 \quad \text{(Lagrange's equation)} \tag{1}$$

where x, y, and z are the coordinates referred to axes mutually at right angles to each other. The velocity components in the directions of these axes are

$$u=\frac{\partial\Phi}{\partial x};\ v=\frac{\partial\Phi}{\partial y};\ w=\frac{\partial\Phi}{\partial z}.$$

I assume in this paper the reader to be familiar with paper reference 1, or with the fundamental things contained therein.

2. The configurations of velocity to be superposed for the investigation of the elementary technical problems of flight are of the most simple type. It will appear that it is sufficient to study two-dimensional flows only, in spite of the fact that all actual problems arise in three-dimensional space. It is therefore a happy circumstance that there is a method for the study of two-dimensional aerodynamic potential flows which is much more convenient for the investigation of any potential flow than the method used in reference 1 for three-dimensional flow.

The method is more convenient on account of the greater simplicity of the problem, there being one coordinate and one component of velocity less than with the three-dimensional flow. But the two-dimensional potential is still a function of two variables and it represents a distribution of velocity equivalent to a pair of functions of two variables. By means of introducing the potential a great simplification of the problem has been accomplished, reducing the number of functions to one. This simplification can now be carried on by also reducing the number of variables to one, leaving only one function of one variable to be considered. This very remarkable reduction is accomplished by the use of complex numbers.

The advantage of having to do with one function of one variable only is so great, and moreover this function in practical cases becomes so much simpler than any of the functions which it represents, that it pays to get acquainted with this method even if the student has never occupied himself with complex numbers before. The matter is simple and can be explained in a few words.

The ordinary or real numbers, x, are considered to be the special case of more general expressions $(x+iy)$ in which y happens to be zero. If y is not zero, such an expression is called a complex number. x is its real part, iy is its imaginary part and consists of the product of y, any real or ordinary number, and the quantity i, which is the solution of

$$i^2 = -1;\ i.\ e.,\ i = \sqrt{-1}$$

The complex number $(x+iy)$ can be supposed to represent the point of the plane with the coordinates x and y, and that may be in this paragraph the interpretation of a complex number. So far, the system would be a sort of vector symbolism, which indeed it is. The real part x is the component of a vector in the direction of the real x-axis, and the factor y of the imaginary part iy is the component of the vector in the y-direction. The complex numbers differ, however, from vector analysis by the peculiar fact that it is not necessary to learn any new sort of algebra or analysis for this vector system. On the contrary, all rules of calculation valid for ordinary numbers are also valid for complex numbers without any change whatsoever.

The addition of two or more complex numbers is accomplished by adding the real parts and imaginary parts separately.

$$(x+iy)+(x'+iy')=(x+x')+i(y+y')$$

This amounts to the same process as the superposition of two forces or other vectors. The multiplication is accomplished by multiplying each part of the one factor by each part of the other factor and adding the products obtained. The product of two real factors is real of course. The product of one real factor and one imaginary factor is imaginary, as appears plausible. The product of $i \times i$ is taken as -1, and hence the product of two imaginary parts is real again. Hence the product of two complex numbers is in general a complex number again

$$(x+iy)\ (x'+iy')=(xx'-yy')+i(xy'+x'y).$$

There is now one, as I may say, trick, which the student has to know in order to get the advantage of the use of complex numbers. That is the introduction of polar coordinates. The distance of the point (x,y) from the origin $(0,0)$ is called R and the angle between the positive real axis and the radius vector from the origin to the point is called φ, so that $x=R\cos\varphi$; $y=R\sin\varphi$. Multiply now

$$(R_1\cos\varphi_1+i\,R_1\sin\varphi_1)\ (R_2\cos\varphi_2+i\,R_2\sin\varphi_2).$$

The result is

$$R_1R_2\cos\varphi_1\cos\varphi_2-R_1R_2\sin\varphi_1\sin\varphi_2+i(R_1R_2\cos\varphi_1\sin\varphi_2+R_1R_2\sin\varphi_1\cos\varphi_2)$$

or, otherwise written

$$R_1R_2\,[\cos(\varphi_1+\varphi_2)+i\sin(\varphi_1+\varphi_2)]$$

That is: The radius R of the product is the product of the radii R_1 and R_2 of the two factors, the angle φ of the product is the sum of the angles φ_1 and φ_2 of the two factors. Further, as is well known, we may write

$$z = R(\cos\varphi + i\sin\varphi) = R\,e^{\varphi i}$$

where e denotes the base of the natural logarithms.

As a particular case

$$(e^{\varphi i})^n = (\cos\varphi + i\sin\varphi)^n = \cos n\varphi + i\sin n\varphi = e^{n\varphi i}$$

This is Moivre's formula.

I proceed now to explain why these complex numbers can be used for the representation of a two-dimensional potential flow. This follows from the fact that a function of the complex numbers, that is in general a complex number again different at each point of the plane, can be treated exactly like the ordinary real function of one real variable, given by the same mathematical expression. In particular it can be differentiated at each point and has then one definite differential quotient, the same as the ordinary function of one variable of the same form. The process of differentiation of a complex function is indeterminate, in so far as the independent variable $(x+iy)$ can be increased by an element $(dx+idy)$ in very different ways, viz, in different directions. The differential quotient is, as ordinarily, the quotient of the increase of the function divided by the increase of the independent variable. One can speak of a differential quotient at each point only if the value results the same in whatever direction of $(dx+idy)$ the differential quotient is obtained. It has to be the same, in particular, when dx or dy is zero.

The function to be differentiated may be

$$F(x+iy) = R(x, y) + iT(x, y)$$

where both R and T are real functions of x and y. The differentiation gives

$$\frac{\partial F}{\partial x} = \frac{\partial R}{\partial x} + i\frac{\partial T}{\partial x}$$

or again

$$\frac{\partial F}{i\partial y} = -i\frac{\partial R}{\partial y} + \frac{\partial T}{\partial y}$$

These two expressions must give identical results and hence are equal. That is, both the real parts and both the imaginary parts are equal:

$$\frac{\partial R}{\partial y} = -\frac{\partial T}{\partial x};\quad \frac{\partial R}{\partial y} = -\frac{\partial T}{\partial x}.$$

Differentiating these equations with respect to dx and dy

$$\frac{\partial^2 R}{\partial x\partial y} = \frac{\partial^2 T}{\partial y^2} = -\frac{\partial^2 T}{\partial x^2},\ i.\,e.,\ \frac{\partial^2 T}{\partial x^2} + \frac{\partial^2 T}{\partial y^2} = 0$$

or again

$$\frac{\partial^2 T}{\partial x\partial y} = \frac{\partial^2 R}{\partial y^2} = -\frac{\partial^2 R}{\partial x^2},\ i.\,e.,\ \frac{\partial^2 R}{\partial x^2} + \frac{\partial^2 R}{\partial y^2} = 0$$

Hence, it appears that the real part as well as the imaginary part of any analytical complex function complies with equation (1) for the potential of an aerodynamic flow, and hence can be such a potential. If the real part is this potential, I shall call the complex function the "potential function" of the flow. It is not practical, however, to split the potential function in order to find the potential and to compute the velocity from the potential. The advantage of having only one variable would then be lost. It is not the potential that is used for the computation of the velocity, but instead of it the potential function directly. It is easy to find the velocity directly from the potential function. Differentiate $F(x+iy) = F(z)$. It is seen that

$$\frac{dF(z)}{dz} = \frac{\partial R}{\partial x} + i\frac{\partial T}{\partial x}$$

But it was shown before that

$$\frac{\partial T}{\partial x} = -\frac{\partial R}{\partial y}$$

Hence

$$\frac{dF(z)}{dz} = \frac{\partial R}{\partial x} - i\frac{\partial R}{\partial y}$$

The velocity has the components $\frac{\partial R}{\partial x}$ and $\frac{\partial R}{\partial y}$. Written as a complex vector, it would be $\frac{\partial R}{\partial x} + i\frac{\partial R}{\partial y}$. It appears therefore:

Any analytical function $F(z)$ can be used for the representation of a potential flow. The potential of this flow is the real part of this potential function, and its differential quotient $\frac{dF}{dz}$, called the "velocity function," represents the velocity at each point "turned upside down." That means that the component of the velocity in the direction of the real axis is given directly by the real part of the velocity function $\frac{dF}{dz}$, and the component of the velocity at right angles to the real axis is equal to the reversed imaginary part of $\frac{dF}{dz}$. The absolute magnitude of the velocity is equal to the absolute magnitude of $\frac{dF}{dz}$.

3. I proceed now to the series of two-dimensional flows which are of chief importance for the solution of the aerodynamic problems in practice. They stand in relation to the straight line. The privileged position of the straight line rests on the fact that both the front view and the cross section of a monoplane are approximately described by a straight line. The different types of flow to be discussed in this section have in common that at the two ends of a straight line, but nowhere else, the velocity may become infinite. At infinity it is zero. This suggests the potential function $\sqrt{z^2-1}$ which has discontinuities at the points ± 1 only, but it does not give the velocity zero at infinity.

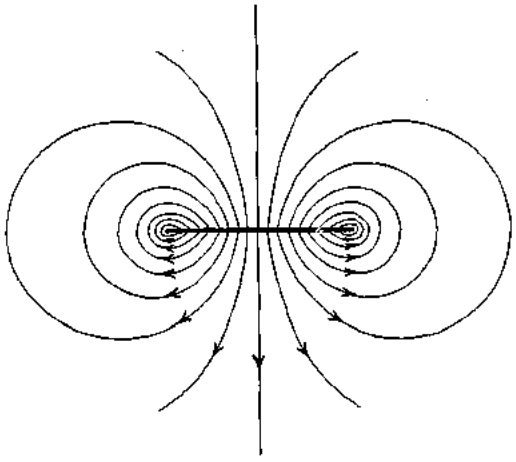

FIG 1.—Transverse flow, produced by a moving straight line.

$$F = \sqrt{z^2-1} - z$$

gives rise to an infinite velocity at the points $z = \pm 1$ which may be regarded as the ends of the straight line, and in addition the velocity becomes zero at infinity. A closer examination shows that indeed the potential function

$$F = i(z - \sqrt{z^2-1}) \qquad (2)$$

represents the flow produced by the straight line extending between the points $z = \pm 1$, moving transversely in the direction of the negative imaginary axis with the velocity 1 in the fluid otherwise at rest. For its velocity function is

$$F' = i - \frac{zi}{\sqrt{z^2-1}}$$

giving for points on the line a transverse velocity -1. This flow may be called "transverse flow." The velocity potential at the points of the line, i. e., for $y=0$ is $\sqrt{1-x^2}$. This gives the kinetic energy of the flow (half the integral of the product of potential, density and normal velocity component, taken around the line (reference 1)).

$$T=\frac{\rho}{2}\cdot 2\int_{-1}^{+1}\sqrt{1-x^2}\,dx=\frac{\rho}{2}\pi \tag{3}$$

giving an apparent mass of the straight line moving transversely equal to the mass of the fluid displaced by a circle over the straight line as diameter. This reminds us of the apparent additional mass of the circle itself, which is the same (ref. 1, sec. 6). It can be proved that the additional mass of any ellipse moving at right angles to a main axis is equal to the mass of the fluid displaced by a circle over this main axis as diameter (reference 6).

The flow around the straight line just discussed can be considered as a special case of a series of more general flows, represented by the potential function

$$F=i(z-\sqrt{z^2-1})^n \tag{4}$$

where n is any positive integer. $n=1$ gives the transverse flow considered before. For n different from 1 the component of the transverse velocity along the straight line is no longer constant, but variable and given by a simple law. Such a flow, therefore, can not be produced by a rigid straight line moving, but by a flexible line, being straight at the beginning and in the process of distorting itself.

It is helpful to introduce as an auxiliary variable the angle δ defined by $z=\cos\delta$. Then the potential function is

$$F=i\,(\cos n\delta-i\sin n\delta)=i\,e^{-in\delta}$$

where δ is, of course, complex. The potential along the line is

$$\Phi=\sin n\delta \tag{5}$$

where now δ is real. The velocity function is

$$F'=\frac{dF}{dz}=\frac{dF}{d\delta}\cdot\frac{d\delta}{dz}=-\frac{n\,e^{-in\delta}}{\sin\delta}=-\frac{n}{\sin\delta}\,(\cos n\delta-i\sin n\delta)$$

giving at points along the line the transverse component

$$u=-\frac{n\sin n\delta}{\sin\delta} \tag{6}$$

and the longitudinal component

$$v=-\frac{n\cos n\delta}{\sin\delta} \tag{7}$$

This becomes infinite at the two ends. The kinetic energy of the flow is

$$T=\frac{1}{2}\,n\rho\int_0^{2\pi}\frac{\sin^2 n\delta}{\sin\delta}\sin\delta\,d\delta=n\pi\,\frac{\rho}{2} \tag{8}$$

This impulse is given by the integral

$$\rho\int\Phi\,dx$$

to be taken along both sides of the straight lines, since the velocity potential times ρ represents the impulsive pressure necessary to create the flow. This integral becomes

$$\int_0^{2\pi}\sin n\delta\sin\delta\,d\delta$$

for the nth term. This is zero except for $n=1$.

By the superposition of several or infinitely many of the flows of the series discussed

$$F=i[A_1(z-\sqrt{z^2-1})+A_2(z-\sqrt{z^2-1})^2+\ldots+A_n(z-\sqrt{z^2-1})^n], \tag{9}$$

with arbitrary intensity, infinitely many more complicated flows around the straight line can be described. There is even no potential flow of the described kind around the straight line existing

which can not be obtained by such superposition. The kinetic energy of the flow obtained by superposition stands in a very simple relation to the kinetic energy of the single flows which relation by no means is self-evident. It is the sum of them. This follows from the computation of the kinetic energy by integrating the product of the transverse component of velocity and the potential along the line. This kinetic energy is

$$T=\frac{\rho}{2}\int_0^{2\pi}(A_1\sin\delta+A_2\sin 2\delta+\ldots)\ (A_1\sin\delta+2A_2\sin 2\delta+\ldots)d\delta \tag{10}$$

But the integral

$$\int_0^{\pi}\sin n\delta\sin m\delta\,d\delta=0\ (n\neq m) \tag{11}$$

is zero if m and n are different integers. For integrating two times partially gives the same integral again, multiplied by $(m/n)^2$. In the same way it can be proved that

$$\int_0^{\pi}\cos n\delta\cos m\delta\,d\delta=0\ (n\neq m) \tag{12}$$

Only the squares in integral (10) contribute to the energy and each of them gives just the kinetic energy of its single term (equation (8)).

It may happen that the distribution of the potential Φ along the line is given, and the flow determined by this distribution is to be expressed as the sum of flows (equation (9)). The condition is, for points on the line, a known function of x is given,

$$\Phi=A_1\sin\delta+A_2\sin 2\delta+\ldots+A_n\sin n\delta+\ldots \tag{13}$$

and the coefficients A are to be determined. The right-hand side of equation (13) is called a Fourier's series, and it is proved in the textbooks that the coefficients A can always be determined as to conform to the condition if Φ has reasonable values. At the ends $\delta=0$ or π, hence Φ has to be zero there as then all sines are zero.

Otherwise expressed equation (4) gives enough different types of flow to approximate by means of superposition any reasonable distribution of the potential over a line, with any exactness desired. This being understood, it is easy to show how the coefficients A can be found.

Integrate

$$\int_0^{\pi}(A_1\sin\delta+A_2\sin 2\delta\ldots)\sin n\delta\,d\delta$$

According to equation (11) all integrals become zero with the exception of

$$A_n\int_0^{\pi}\sin^2 n\delta\,d\delta=\frac{\pi}{2}\cdot A_n$$

Hence

$$A_n=\frac{2}{\pi}\int_0^{\pi}\Phi\sin n\delta\,d\delta \tag{14}$$

These values may be introduced into equation (9), and thus the potential function F is determined.

Another problem of even greater practical importance is to determine the potential functions, equation (4), which superposed give a desired distribution of the transverse component of velocity. The condition is now

$$u=A_1\frac{\sin\delta}{\sin\delta}+2A_2\frac{\sin 2\delta}{\sin\delta}+\ldots \tag{15}$$

That means, now, $u\sin\delta$, a known function, is to be expanded into a Fourier's series

$$u\sin\delta=B_1\sin\delta+B_2\sin 2\delta+\ldots+B_n\sin n\delta \tag{16}$$

The B's may be determined by an equation like (14), and then the A's may be deduced, since

$$A_n = B_n/n \tag{16a}$$

This is always possible if the velocity component is finite along the line. These values may then be introduced in equation (9).

The value of the potential function F as given by series (13) with the values of A_n substituted from (16) may be transformed into a definite integral which sometimes is more convenient for application. Let u_0 be a function of the coordinate z_0, a point on the line joining $z = -1$ and $z = +1$, and let $f(z, z_0)$ be a function to be determined so that

$$F = \int_{-1}^{+1} f(z, z_0) \cdot u_0 \cdot dz_0$$

I have found that this is satisfied by making

$$f = \frac{1}{\pi} [\log (e^{i\delta} - e^{i\delta_0}) - \log (e^{i\delta_0} - e^{-i\delta_0})] \tag{17}$$

and this leads to a physical interpretation of u_0.

Hence, the velocity function

$$F' = \frac{dF}{dz} = \int_{-1}^{+1} \frac{df}{dz} u_0 \, dz_0$$

The potential function and the velocity function are both thought of, then, as being the summation of functions due to "elementary flows." An element gives rise to a potential function $f(z, z_0) u_0 dz_0$ and to the velocity function $\frac{df}{dz} u_0 dz_0$ (18)

$$f' = \frac{df}{dz} = \frac{1}{\pi} \frac{\sin \delta_0}{\sin \delta} \frac{1}{\cos \delta - \cos \delta_0} = \pm \frac{1}{\pi} \frac{1}{z - z_0} \sqrt{\frac{1 - z_0^2}{1 - z^2}}$$

where the plus sign is to be taken for points on the positive side of the line, and the negative sign for those on the opposite side. In this elementary flow, then, the velocity is parallel to the line at all points of the line excepting the point z_0, being directed away from this point on the positive side of the line and toward it on the other side. For points close to z_0,

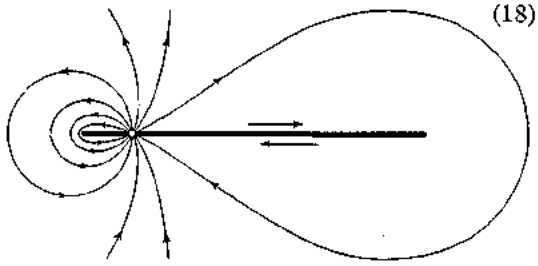

FIG. 2.—Flow around a straight line created by one element of the wing section.

$$f' \, u_0 \, dz_0 = \frac{u_0 \, dz_0}{\pi} \frac{1}{z - z_0}$$

from which the value of the velocity of the flow may be deduced. If a *small* circle is drawn around the point z_0, it is seen that there is a flow out from the point z_0 of amount $u_0 \, dz_0$ per second on the positive side and an inflow of an equal amount on the other side; so that this is equivalent to there being a transverse velocity u_0 at points along the element dz_0, positive on one side, negative on the other. The total flow around the line due to $f(z, z_0) u_0 dz_0$ is illustrated in Figure 2.

Substituting the value of f' in F'

$$F' = \pm \int_{-1}^{+1} \frac{1}{\pi} \frac{u_0 \, dz_0}{z - z_0} \sqrt{\frac{1 - z_0^2}{1 - z^2}}$$

Therefore, for any point on the real axis, the transverse velocity is u_0 and the longitudinal velocity

$$v_x = \pm \int_{-1}^{+1} \frac{1}{\pi} \frac{u_0 \, dz_0}{z - z_0} \sqrt{\frac{1 - z_0^2}{1 - z^2}}$$

Or, interchanging symbols, writing z for z_0 and *vice versa*

$$v_0 = \mp \int_{-1}^{+1} \frac{1}{\pi} \frac{u dz}{z - z_0} \sqrt{\frac{1 - z^2}{1 - z_0^2}} \tag{19}$$

For a point near the edge on the positive side, write $z_0 = 1 - \epsilon$

$$v_{edge} = -\frac{1}{\pi \sqrt{2\epsilon}} \int_{-1}^{+1} u dz \sqrt{\frac{1+z}{1-z}}$$

or, substituting $\sqrt{2\epsilon} = \sin \delta_{edge}$

$$v_{edge} = -\frac{1}{\pi \sin \delta_{edge}} \int_{-1}^{+1} u dz \sqrt{\frac{1+z}{1-z}} \tag{19a}$$

For the discussion of the elements of the wing theory, in addition to the flows mentioned, there is one flow which needs a discussion of its own. This is given by the potential function

$$F = A_0 \sin^{-1} z \tag{20}$$

The velocity function of this flow is

$$F' = \frac{A_0}{\sqrt{1 - z^2}}$$

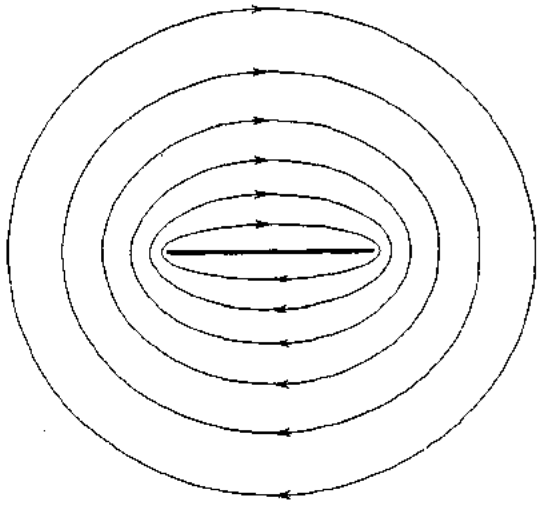

FIG. 3.—Circulation flow around a straight line.

I shall call this flow "circulation flow" as it represents a circulation of the air around the line. The transverse component of the velocity at points along the line is identically zero.

The circulation flow does not quite fit in with the other ones represented by equation (4), because the potential function (20) is a multiple valued one, the values at any one point differing by 2π or multiples thereof. All this indicates that the flow is a potential flow, it is true, but it does not conform to the condition of a potential flow when considered as in equation (4).

This is in accordance with the physical consideration, that it is impossible to produce this flow by an impulsive pressure over the straight line. Such a pressure would not perform any mechanical work, as the transverse components of velocity at points along the line are zero. The kinetic energy of this flow, on the other hand, is infinite, and hence this flow can not even be completely realized. Still it plays the most important part in aerodynamics.

The best way to understand this flow and its physical meaning is to suppose the line to be elongated at one end, out to infinity. On the one side the potential may be considered zero. Then it is constant and will be equal to 2π on the other side. The transverse velocity component is finite. Hence the flow can be produced by a constant impulsive pressure difference along this line extending from the edge $z = 1$ to infinity. This pressure difference makes the fluid circulate around the original straight line, the pressure along the line itself being given by the potential function (20) and not performing any work.

A pressure difference along an infinite line does never actually occur. At least t does not occur simultaneously along the whole line. A very similar thing, however, occurs very often which has the same effect. That is a constant momentum being transferred to the air at right angles to an infinite straight line at one point only, but the point traveling along the line, so that the final effect is the same as if it had occurred simultaneously. This is the fundamental case of an airplane flying along that infinitely long line. During the unit of time it may cover the length V and transfer to the air the momentum L, equal to the lift of the airplane. Then the impulse of the force, per unit of length of the line, is L/V, and hence the potential difference is $\frac{L}{V\rho}$. That makes A_0 in equation (20) $A_0=\frac{L}{2V\rho\pi}$. If the airplane has traveled long enough, the flow in the neighborhood of the wing, or rather one term of the flow, is described by the circulation flow, provided that the airplane is two-dimensional, that is, has an infinite span.

The velocity at the end of the wing $z=+1$ due to this circulation flow

$$F=A_0 \sin^{-1} z,$$

where

$$A_0=\frac{L}{2\pi\rho V} \tag{21}$$

is

$$V_{edge}=\left(\frac{A_0}{\sin\delta}\right)_{\delta=0}=\frac{L}{2\pi\rho V(\sin\delta)_{\delta=0}} \tag{21a}$$

II. THEORY OF WING SECTION.

4. The investigation of the air flow around wings is of great practical importance in view of the predominance of heavier-than-air craft. It is necessary to divide this problem into two parts, the consideration of the cross section of one or several wings in a two-dimensional flow, and the investigation of the remaining effect. This chapter is devoted to the first question.

All wings in practice have a more or less rounded leading edge, a sharp trailing edge and the section is rather elongated, being as first approximation described by a straight line. The application of the aerodynamic flows around a straight line for the investigation of the flow around a wing section suggests itself. I have shown in section (3) how the potential flow around a straight line is determined, for instance, from the transverse components of velocity along this line. Only one type of flow, the circulation flow, is excepted. This flow does not possess any transverse components at the points of the line and hence can be superposed on a potential flow of any magnitude without interfering with the condition of transverse velocity. I have shown, on the other hand, that it is just this circulation flow not determined so far, which gives rise to the chief quantity, the lift. It is, therefore, necessary to find some additional method for determining the magnitude of the circulation flow.

This magnitude of the circulation flow is physically determined by the fact that the air is viscous, no matter how slightly viscous it is. The additional condition governing the magnitude of the circulation flow can be expressed without any reference to the viscosity and was done so in a very simple way by Kutta. The condition is very plausible, too. Kutta's condition simply states that the air does not flow with infinite velocity at the sharp, rear edge of the wing section. On the contrary, the circulation flow assumes such strength that the air leaves the section exactly at its rear edge flowing there along the section parallel to its mean direction. The wing as it were acts as a device forcing the air to leave the wing flowing in a particular direction.

Consider, for instance, the wing section which consists merely of a straight line of the length 2. The angle of attack may be α. The flow produced by this line moving with the velocity V is then represented by the potential function

$$F=V\sin\alpha\cdot i\,e^{-\delta i}$$

which gives a constant transverse component of velocity along the wing, as shown in equation (6) for $n=1$. The real axis is parallel to the straight line, its origin is at the center of the line.

The infinite longitudinal velocity at the rear end is

$$-V \sin \alpha \cdot \frac{1}{(\sin \delta)_{\delta=0}}$$

The angle of attack may now be assumed to be small and I change slightly the way of representing the flow, turning the real axis of coordinates into the direction of motion. Instead of referring the flow to the line really representing the wing section I consider the straight line between $z = \pm 1$, which differs only slightly from the wing and is parallel to the motion. The transverse components of the flow relative to this line are approximately equal to the transverse velocity relative to the wing section at the nearest point and therefore constant again and equal to $V \sin \alpha$. Therefore, this way of proceeding leads to the same flow as the more exact way before. It also gives the same infinite velocity at the rear end.

This velocity determines the magnitude of the circulation flow

$$F = A_0 \sin^{-1} z \tag{21}$$

by the condition that the sum of their infinite velocities at the edge is zero.

$$V \sin \alpha \frac{1}{(\sin \delta)_{\delta=0}} - A_0 \frac{1}{(\sin \delta)_{\delta=0}} = 0$$

and hence $A_0 = V \sin \alpha$. The lift is therefore

$$L = 2\pi \ V^2 \rho \sin \alpha.$$

The lift coefficient, defined by $C_L = \frac{L}{S \ V^2 \frac{\rho}{2}}$, since the chord $= 2$, is therefore,

$$C_L = 2\pi \sin \alpha, \text{ or approximately } 2\pi\alpha \tag{22}$$

and

$$L = V^2 \frac{\rho}{2} S \ 2\pi\alpha \tag{23}$$

where S denotes the area of the wing.

The representation of the flow just employed is approximately correct and gives the same result as the exact method. This new method now can be generalized so that the lift of any wing section, other than a straight line, can be computed in the same way, too. The section can be replaced with respect to the aerodynamic effect by a mean curve, situated in the middle between the upper and lower curves of the section and having at all points the same mean direction as the portion of the wing section represented by it. The ordinates of this mean wing curve may be ξ, the abscissa x, so that the direction of the curve at each point is $\frac{d\xi}{dx}$. This direction can be considered as the local angle of attack of the wing, identifying the sine and tangent of the angle, with the angle itself. Accordingly it is variable along the section. Since the velocity of the air relative to the wing is approximately equal to the velocity of flight, the component at right angles to the x-axis is $\frac{V d\xi}{dx}$. As before, the infinite velocity at the rear edge is to be found. It is, according to equation (19a)

$$\frac{-V}{\pi (\sin \delta)_{\delta=0}} \int_{-1}^{+1} \frac{d\xi}{dx} \sqrt{\frac{1+x}{1-x}} \, dx \tag{24}$$

At the rear edge $x=1$. The mean apparent angle of attack, that is the angle of attack of the straight line giving the same lift as the wing section, is found by the condition that this infinite value must be the same as that deduced for a straight line; viz, $-\frac{V \sin \alpha}{\sin \delta}$. Hence, replacing $\sin \alpha$ by α

$$\alpha' = -\frac{1}{\pi}\int_{-1}^{+1} \frac{d\xi}{dx}\sqrt{\frac{1+x}{1-x}}\,dx \quad \text{length} = 2 \tag{25}$$

$$\alpha' = -\frac{2}{\pi}\int_{-1/2}^{+1/2} \frac{d\xi}{dx}\sqrt{\frac{1+2x}{1-2x}}\,dx \,\text{length} = 1 \tag{25a}$$

This formula holds true for any small angle of attack of the section. The integral can now be transformed into one containing the coordinate ξ rather than the inclination $\frac{d\xi}{dx}$ of the wing curve, provided that the trailing edge is situated at the x-axis, that is, if ξ is zero at the end $x=+1$. This transformation is performed by partial integration, considering $\frac{d\xi}{dx}\,dx$ as a factor to be integrated. It results

$$\alpha' = \frac{1}{\pi}\int_{-1}^{+1} \frac{dx\xi}{(1-x)\sqrt{1-x^2}} \quad \text{length} = 2 \tag{26}$$

$$\alpha' = \frac{4}{\pi}\int_{-1/2}^{+1/2} \frac{dx\xi}{(1-2x)\sqrt{1-4x^2}} \,\text{length} = 1 \tag{26a}$$

The important formula (26) gives the mean apparent angle of attack directly from the coordinates of the shape of the wing section. The mean height ξ of the section has to be integrated along the chord after having been multiplied by a function of the distance from the leading edge, the same for all wing sections. This integration can always be performed, whether the section be given by an analytical expression, graphically or by a table of the coordinates. In the latter case a numerical integration can be performed by means of Table II, taken from reference 4. The figures in the first column give the distance from the leading edge in per cent of the chord. The second column of figures gives factors for each of these positions. The height ξ of the mean curve of the section over its chord, measured in unit of the chord terms, is to be multiplied by the factors, and all products so obtained are to be added. The sum gives the apparent angle of attack in degrees.

5. The lift of a wing section as computed in section (4) is caused by the circulation flow symmetrical with respect to the straight line representing the wing. Hence the pressure creating this lift is located symmetrically to the wing, its center of pressure is at 50 per cent of the chord, it produces no moment with respect to the middle of the wing. This lift is the entire lift produced by the wing. It is not, however, the entire resultant air force. The remaining aerodynamic flow in general exerts a resultant moment (couple of forces) and this moment removes the center of pressure from its position at 50 per cent.

If the wing section is a straight line of the length 2, its apparent transverse mass is $\pi\rho$, as seen in section (4). The longitudinal mass is zero. Hence, according to reference 1, the resultant moment is

$$M = V^2 \frac{\rho}{2} \pi \sin 2\alpha \quad \text{length} = 2 \tag{27}$$

$$M \sim V^2 \frac{\rho}{2} 2\,\pi\alpha \quad \text{length} = 2 \tag{28}$$

Both the exact and the approximate expressions give the constant center of pressure 25 per cent of the chord from the leading edge, as results by dividing the moment by the lift (23).

The straight sections considered have a constant center of pressure, independent of the angle of attack. The center of pressure does not travel. This is approximately true also for symmetrical sections with equal upper and lower curves, where the center of pressure is also at 25 per cent. If, however, the upper and lower curves are different and hence the mean section

52201—25——11

curve is no longer a straight line, the potential flow produced at the angle of attack zero of the chord not only gives rise to the circulation flow and thus indirectly to a lift, but also creates a moment of its own. It is simple to compute this moment from the potential flow, which is represented in equation (9) as a superposition of the flows, equation (4).

The longitudinal velocity relative to the line is, according to equation (7),

$$v=-\left(A_1\frac{\cos\delta}{\sin\delta}+A_2\frac{2\cos 2\delta}{\sin\delta}+\cdot\ \cdot\ \cdot+A_n\frac{n\cos n\delta}{\sin\delta}\right)+V$$

As the section is supposed to be only slightly curved, $\frac{d\xi}{dx}$ is always small, so are, therefore, the coefficients A_n when compared to V, so that they may be neglected when added to it. The pressure at each point along the line, according to reference 1, is

$$p=\frac{\rho}{2}v^2$$

The present object is the computation of the resultant moment. When really forming the square of the bracket in the last expression, the term with V^2 indicates a constant pressure and does not give any resultant moment. The squares of the other terms are too small and can be neglected. There remains only the pressure,

$$p=-\rho V\left(A_1\frac{\cos\delta}{\sin\delta}+A_2\frac{2\cos 2\delta}{\sin\delta}\ \cdot\ \cdot\ \cdot\ \cdot\ \cdot\ \cdot\right)$$

giving the resultant moment about the origin

$$M=2\ V\rho\int_0^\pi\left(A_1\frac{\cos\delta}{\sin\delta}+A_2\frac{2\cos\ 2\delta}{\sin\delta}\ \cdot\ \cdot\ \cdot\ \cdot\ \cdot\right)\cos\delta\sin\delta\,d\delta,$$

since the density of lift is twice the density of pressure, the pressure being equal and opposite on both sides of the wing. But according to (12)

$$\int^\pi\cos n\delta\cos m\delta\,d\delta=0 \tag{12}$$

if m and n are different integers. Hence there remains only one term. The resultant moment is

$$M=2\rho\ V\ A_1\frac{\pi}{2}$$

A_1 was found according to equation (14) by means of the integral

$$A_1=\frac{2}{\pi}\int_0^\pi V\frac{d\xi}{dx}\sin^2\delta\,d\,\delta$$

Hence the moment is

$$M=2\rho V^2\int_0^\pi\frac{d\xi}{dx}\sin^2\delta\,d\,\delta$$

or, expressed by x

$$M=2\rho V^2\int_{-1}^{+1}\frac{d\xi}{dx}\sqrt{1-x^2}\,dx \tag{29}$$

By the same method as used with integral (25) this integral can be transformed into

$$M=2\rho V^2\int_{-1}^{+1}\frac{x\,dx\,\xi}{\sqrt{1-x^2}} \tag{30}$$

It has been shown that for a chord of length 2, the center of pressure has a lever arm $\frac{1}{2}$ and the lift is $V^2\frac{\rho}{2} \cdot 2\pi\alpha \cdot 2$, giving a moment $V^2\rho\pi\alpha$; so that an angle of attack corresponds to a moment $V^2\rho\pi\alpha$. Consequently the resultant moment is the same as if the angle of attack is increased by the angle

$$\alpha'' = \frac{2}{\pi}\int_{-1}^{+1}\frac{x\,dx\,\xi}{\sqrt{1-x^2}} \quad \text{length} = 2 \tag{31}$$

$$\alpha'' = \frac{16}{\pi}\int_{-1/2}^{+1/2}\frac{x\,dx\,\xi}{\sqrt{1-4x^2}} \quad \text{length} = 1 \tag{32}$$

It is readily seen that this angle is zero for sections with section curves equal in front and in rear. Hence such sections have the center of pressure 50 per cent at the angle of attack zero of the mean curve, that is, for the lift (24) produced by the shape of the section only. The additional lift produced at any other angle of attack of the chord and equal to the lift as produced by the straight line at that angle of attack has the center of pressure at 25 per cent. Hence a travel of the center of pressure takes place toward the leading edge when the angle of attack is increased, approaching the point 25 per cent without ever reaching it. The same thing happens for other sections with the usual shape. At the angle of attack zero of the chord the lift produced was seen to be $2\pi V^2\rho\alpha'$, i. e., from (26)

$$L = V^2\frac{\rho}{2}\,4\int_{-1}^{+1}\frac{dx\,\xi}{(1-x)\sqrt{1-x^2}}$$

and the moment, see equation (30),

$$M = 2\rho V^2\int_{-1}^{+1}\frac{x\,\xi\,dx}{\sqrt{1-x^2}} \tag{30}$$

giving the center of pressure at the distance from the middle

$$\frac{\int_{-1}^{+1}\frac{x\,\xi\,dx}{\sqrt{1-x^2}}}{\int_{-1}^{+1}\frac{dx\,\xi}{(1-x)\sqrt{1-x^2}}} \quad \text{length} = 2$$

The lift produced by the angle of attack of the chord, equation (23) as before has the center of pressure 25 per cent. The travel of the center of pressure can easily be obtained from this statement. The moment about the point 25 per cent is independent of the angle of attack.

The center of pressure in ordinary notation at the angle of attack zero is

$$CP = 50\% - 50\,\frac{\int_{-1}^{+1}\frac{x\,\xi\,dx}{\sqrt{1-x^2}}}{\int_{-1}^{+1}\frac{dx\,\xi}{(1-x)\sqrt{1-x^2}}}\,\%$$

The computation of the mean apparent angle of attack with respect to the moment is done in the same way as that of the angle with respect to the lift. Table II, gives the coefficients for numerical integration, by means of two ordinates only, to be used as the other figures in Table II. The final sum is the mean apparent angle in degrees.

6. The problem of two or even more wing sections, combined to a biplane or multiplane and surrounded by a two-dimensional flow can be treated in the same way as the single wing section. The two sections determine by their slope at each point a distribution of transverse velocity components along parallel lines. The distribution determines a potential flow with a resultant moment. According to Kutta's condition of finite velocity near the two rear edges, the potential flow in its turn determines a circulation flow giving rise to a lift and moment. The physical aspect of the question offers nothing new, it is a purely mathematical problem.

This mathematical problem has not yet been solved in this extension. I have attacked the problem within a more narrow scope (reference 4). The method followed by me amounts to the following considerations:

Equation (13) represents different types of flow around one straight line, consisting in a motion of the air in the vicinity of the straight line only. Now the motion of the flows with high order n is more concentrated in the immediate neighborhood of the straight line than the flows of low order n. The transverse velocity components along the line, determining the flow, change their sign $(n-1)$ times along the line. With large n, positive and negative components follow each other in succession very rapidly so that their effect is neutralized even at a moderate distance.

Hence the types of flow of high order n around each of a pair of lines will practically be the same as if each line is single. The flows of high order do not interfere with those of a second line in the vicinity even if the distance of this second line is only moderate. It will chiefly be the types of flow of low order, the circulation flow $n=0$, the transverse flow $n=1$, or it may be the next type $n=2$ which differ distinctly whether the wing is single or in the vicinity of a second wing. Accordingly, I computed only the flows of the order $n=0$ and $n=1$, the circulation flow and the transverse flow for the biplane and used the other flows as found for the single section.

The results are particularly interesting for biplanes with equal and parallel wings without stagger. Their lift is always diminished when compared with the sum of the lifts produced by the two wings when single. The interference is not always the same. If the sum of the angle of attack and the mean apparent angle of attack with respect to the moment is zero, or otherwise expressed, at the angle of attack where the center of pressure is at 50 per cent, it is particularly small. The lift produced at the angle of attack zero is diminished only about half as much as the remaining part of the lift produced by an increase of this angle of attack.

This second part of the lift does not have its point of application exactly at 25 per cent of the chord, although its center of pressure is constant, too. This latter is quite generally valid for any two-dimensional flow. At any angle of attack zero arbitrarily chosen, the configuration of wing sections produces a certain lift acting at a certain center. The increase of the angle of attack produces another lift acting at another fixed point. Hence the moment around this second center of pressure does not depend on the angle of attack; and the center of pressure at any angle of attack can easily be computed if the two centers of pressures and the two parts of the lift are known.

The resultant moment of the unstaggered biplane consisting of portions of equal and parallel straight lines is again proportional to the apparent transverse mass, as the longitudinal mass is zero (reference 1). This mass is of use for the considerations of the next chapter, too. Therefore, I wish to make some remarks concerning its magnitude. If the two straight lines are very close together, the flow around them is the same as around a line of finite thickness and is almost the same as around one straight line. Its apparent mass is the same, too, but in addition there is the mass of the air inclosed in the space between the two lines and practically moving with them. Hence the mass is approximately

$$b(b\frac{\pi}{4}+h)\rho$$

where b is the length of the lines and h their distance apart, if the distance h of the lines is small. For great distance, on the other hand, the flow around each of the lines is undisturbed, the apparent mass is twice that of the flow around each line if single. It is therefore

$$2b^2\frac{\pi}{4}\rho$$

For intermediate cases the apparent mass has to be computed. Particulars on this computation are given in reference 4. Table I gives the ratio of the apparent mass of a pair of lines to that of one single line for different values of $\frac{h}{b}$. This ratio, of course, is always between 1 and 2.

These few remarks on the theory of biplane sections seem to be sufficient in this treatise on the elements of wing theory. The student will find full information on the subject in my paper on biplanes, reference 4. The remarks laid down here, I hope, will assist him in understanding the leading principles of the method there employed.

III. AERODYNAMIC INDUCTION.

7. The last chapter does not give correct information on the aerodynamic wing forces, since the flow in vertical longitudinal planes was supposed to be two-dimensional. The vertical layers of air parallel to the motion were supposed to remain plane and parallel and only the distortion of the two other planes at right angles to it was investigated. This is a very incomplete and arbitrary proceeding, for the vertical longitudinal layers do not remain plane, as little as any other layers remain plane. It is therefore necessary to complete the investigation and to assume now another set of layers, parallel to the lift, to remain plane, thus studying the distortion of the vertical longitudinal layers. Accordingly, I will now assume that all vertical layers of air at right angles to the motion remain plane and parallel, so that the air only moves at right angles to the direction of flight. Hence, I have now to consider two-dimensional transverse vertical flows. This consideration, it will appear, gives sufficient information on the motion of the air at large, whereas the preceding investigation gives information on the conditions of flow in the vicinity of the wing. Both, the longitudinal two-dimensional flow studied before and the two-dimensional flow to be studied presently, possess vertical components of velocity. Both flows and in particular these vertical components are to be superposed, and thus one can determine the final aerodynamic pressures and resultant forces.

The transverse vertical layer of air is at rest originally. The wings, first approaching it, then passing through it and at last leaving it behind them, gradually build up a two-dimensional flow in each layer. The distribution of impulse creating this flow is identical with the distribution of the lift over the longitudinal projection of the wings. It is immaterial for the final effect whether all portions of the wings at every moment have transferred the same fraction of the momentum to a particular layer or not. The final effect and hence the average effect is the same as if they always have. They actually have if all wings are arranged in one transverse plane—that is, if the airplane is not staggered. It may be assumed at present that at each moment each layer has received the same fraction of the impulse from every portion of the wings and it follows then that the shape of the configuration of the two-dimensional flow is always the same and that it is built up gradually by increasing its magnitude while not changing its shape, beginning with the magnitude zero at a great distance in front of the wing and having obtained its final magnitude at a great distance behind the wings.

The potential of the final two-dimensional flow long after the wings have passed through the layer is easy to find, for the impulsive pressure creating it is known along the longitudinal projection of the wings. It is identical with the distribution of the lift over this projection, acting as long as the airplane stays in the layer. This is the unit of time, if the thickness of the layer is equal to the velocity of flight. Hence the potential difference along the longitudinal projection of the wings is equal to the density of the lift along this projection divided by the product of the density of air and the velocity of flight, since the velocity potential is equal to the impulse of the pressure creating the flow, divided by the density. In general the longitudinal projections of the wings can be considered as lines. The density of lift per unit length of these lines is then equal to the difference of pressure on both sides, and hence the density of the lift is proportional to the difference of the potential on both sides. This statement determines completely the final two-dimensional flow in the transverse vertical layer, and nothing remains unknown if the distribution of the lift over the wings is given. The actual determination of the flow is then a purely mathematical process.

For the present purpose, however, not the final transverse flow but the vertical flow at the moment of the passage of the wings is of interest. It is this flow that is to be superposed on the longitudinal flow in order to determine the actual air forces. It has already been mentioned that this flow can be supposed to differ from the final flow in magnitude only. It remains therefore only to find the ratio of momentum already transferred while the wing passes through the layer, to the momentum finally to be imparted.

The fraction ½ seems to me more plausible than any other fraction. The effect of the wing on the layer is the same at equal distances from the layer, whether in front or back of it and this would involve the factor ½. It is not necessary, however, to have recourse to a mere assumption in this question, however plausible it may be. It can be proved that the assumption of ½ is the only one which does not lead to a contradiction with the general principles of mechanics. I proceed at once to demonstrate this.

If the transverse flow in the plane of the wings is found, only the vertical component downward u', called the induced downwash, is used for the computation. This downwash can be positive or negative, but in general is positive. Such downwash in the neighborhood of a portion of wing changes the motion of the air surrounding the wing portion relative to it. The induced downwash is always small when compared with the velocity of flight. Hence, its superposition on the velocity of flight at right angles to it does not materially change the magnitude of the relative motion between the wing and the air in its vicinity. It changes, however, the direction of this relative velocity, which is no longer parallel to the path of the wing but inclined toward the path by the angle whose tangent is u'/V. This has two important consequences.

The flow produced and hence the air force no longer correspond to the angle of attack between the wing and the path of flight but to the angle given by the motion of the wing relative to the surrounding portion of the air. In most cases the angle of attack is decreased and the effective angle of attack, smaller than the geometric angle of attack between path and wing, determines now the flow and the air forces. Hence, the lift in general is smaller than would be expected from the geometric angle of attack. The angle of attack in the preceding chapter on the wing section is not identical with the geometric angle between the chord and the direction of flight but with the effective angle of attack, smaller in general, as there is an induced downwash motion in the vicinity of the wing. Therefore the geometrical angle of attack is decreased by

$$\alpha_i = \frac{u'}{V} \tag{34}$$

That is not all. The lift is not only decreased but its direction is changed, too. It is no longer at right angles to the path of flight, but to the relative motion between wing and adjacent portion of air. It is generally turned backward through an angle equal to the induced angle of attack. The turning backward of the lift by itself does not materially change the magnitude of the lift, as the angle is always small; the vertical component of the lift remains almost the same, but the effective angle of attack has to be decreased. In addition to this the air force has now a component in the direction of the motion. The wing experiences an "induced" drag, in addition to the drag caused by the viscosity of the air, not discussed in this paper, and the induced drag is often much larger than the viscous drag. The density of the induced drag is $dL\frac{u'}{V}$ where dL is the density of lift, as can be directly seen from Figure 4.

$$dD_i = dL\frac{u'}{V} \tag{35}$$

The existence of a drag could have been anticipated, as there must be a source of energy for the creation of the transverse flow under consideration. The final kinetic energy of this flow in a layer of thickness V is

$$\int \frac{1}{2} dL\, u$$

and this energy is to be delivered by the wing per unit of time, as during this unit of time another layer has been put into motion in the way discussed. On the other hand the energy delivered by the wings is the integral over the drag multiplied by the velocity, that is, $\int dL\, u'$. From which follows immediately $u' = \frac{1}{2} u$, and it is thus confirmed that the transverse flow is only half formed when the wings are passing through the vertical layer.

8. The problem is thus solved in general if the shape of the wings and the distribution of lift over the wings is known. Before passing to special wing arrangements and distributions of lift, in particular to the simple monoplane, there is one general problem to be discussed. The longitudinal projection of the wings being given, as well as the entire lift, the induced drag depends on the distribution of the lift over the projection. The drag is desired to be as small as possible. The question arises, What is the distribution of lift giving the smallest induced drag? The importance of this question is at once obvious.

The entire lift and the entire induced drag of the wings are found again as important characteristics of the final transverse flow, discussed in the last section. The resultant lift is equal to the resultant vertical momentum of this flow for the thickness of the layer equal to the velocity V. and the induced drag is equal to the kinetic energy in the same layer divided by V. The problem is therefore to find such a two-dimensional flow produced by impulsive pressure over the longitudinal projection of the wings as possesses a given magnitude of the vertical momentum, and the kinetic energy of which is a minimum.

It is sufficient for elementary questions to consider only arrangements of wing symmetrical with respect to a vertical longitudinal plane, giving moreover horizontal lines in the longitudinal projections. The results are valid for all conditions (reference 1). It is then easy to find the solution. The momentum of several flows superposed on each other is the sum of their single momenta. The flow is of the desired kind if the superposition of any other flow with the resultant vertical momentum zero increases the kinetic energy of the flow.

The velocity of the superposed flow can be assumed to be small, for instance, so that its own kinetic energy, containing the square of the velocity, can be neglected. The impulsive pressure along the projection of the wings necessary to create the superposed flow acts along a path determined by the magnitude of the downwash at the same points. The increase of kinetic energy is

$$\frac{1}{2} \rho \int u' \Phi \, dx$$

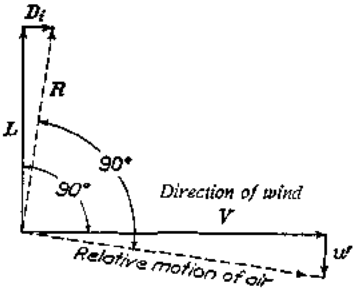

FIG. 4.—Diagram showing the creation of the induced drag.

where $\int \Phi \, dx = 0$.

It is readily seen that the first expression can be identically zero for any distribution of the potential Φ restricted by the second condition only if the downwash u' is constant over the entire projection of the wings. Only then a transfer of a portion of lift from one point to another with smaller downwash is impossible, whereas this proceeding in all other cases would lead to a diminution of the induced drag. It is thus demonstrated:

The induced drag is a minimum, if the transverse two-dimensional flow has a constant vertical component of velocity along the entire projection of the wings.

For wings without stagger it follows then that the induced angle of attack u'/V is constant over all wings.

The magnitude of the minimum induced drag of a system of wings is easily found from the apparent mass ρK of their longitudinal projection in the two-dimensional transverse flow. For the vertical momentum equal to the lift is $uV\rho K = L$ where u is the constant downwash of the final flow. This gives

$$u = \frac{L}{V \rho K}$$

The induced drag is equal to the kinetic energy divided by V

$$D_i = w^2 \frac{\rho}{2} K$$

It follows therefore that the minimum induced drag is

$$D_i = \frac{L^2}{4V^2 \frac{\rho}{2} K} \tag{36}$$

and the constant or at least average induced angle of attack is

$$\alpha_i = \frac{w'}{V} = \frac{L}{4V^2 \frac{\rho}{2} K} \tag{37}$$

K is a constant area determined by the longitudinal projection of the wings. It is the area of the air in the two-dimensional flow having a mass equal to the apparent mass of the projection of the wings.

The results (36) and (37) show that the minimum induced drag can be obtained from the consideration that the lift is produced by constantly accelerating a certain mass of air downward from the state of rest. The apparent mass accelerated downward is at best equal to the apparent mass of the longitudinal projection of the airplane in a layer of air passed by the airplane in the unit of time.

In practical applications the actual induced drag can be supposed to be equal to the minimum induced drag, and the average induced angle of attack equal to (37). It is, of course, slightly different, but the difference is not great as can be expected since no function changes its value much in the neighborhood of its minimum.

I proceed now to the application of the general theory of induction to the case of the monoplane without dihedral angle, giving in longitudinal projection a straight line of the length b. Consider first the distribution of lift for the minimum induced drag. It is characterized by the transverse potential flow with constant vertical velocity component along this straight line. This flow has repeatedly occurred in the earlier parts of this paper. For the length 2 of the line, it is the transverse flow given by equation (2) or by equation (4) and $n=1$. The potential function for the length b is

$$F = A_1 i\left[\frac{2z}{b} - \sqrt{\left(\frac{2z}{b}\right)^2 - 1}\right] \tag{38}$$

giving the constant vertical velocity component along the line

$$w = A_1 \frac{2}{b}$$

The density of the lift per unit length of the span is equal to the potential difference of the final flow on both sides of the line, multiplied by $V\rho$.

$$\frac{dL}{dx} = 2\, V\rho A_1 \sqrt{1 - \left(\frac{2x}{b}\right)^2} = 2\, A_1 V\rho \sin\delta = \frac{4\, L \sin\delta}{b\pi} * \tag{39}$$

where $\cos\delta = \frac{2x}{b}$. Plotted against the span, the density of lift per unit length of the span is represented by half an ellipse, the multiple of $\sin\delta$ being plotted against $\cos\delta$. The lift therefore is said to be elliptically distributed.

$$* L = \int_{-b/2}^{+b/2} \frac{dL}{dx} dx = \int_{-b/2}^{+b/2} 2\, V\rho A_1 \sqrt{1 - \left(\frac{2z}{b}\right)^2}\, dz = V\rho A_1 \pi \frac{b}{2}$$

Hence

$$A_1 = \frac{2L}{V\rho\pi b}$$

The apparent mass of the line with the length b according to equation (3) is equal to

$$\rho K = b^2 \frac{\pi}{4} \rho$$

Hence, with this distribution of lift, the minimum induced drag is, according to equation (36)

$$D_i = \frac{L^2}{b^2 V^2 \frac{\rho}{2} \pi} \tag{40}$$

and the constant induced angle of attack according to equation (37) is

$$\alpha_i = \frac{L}{b^2 V^2 \frac{\rho}{2} \pi} \tag{41}$$

The density of lift (39) per unit length of the span together with the chord c, different in general along the span, and with equation (22) determines the effective angle of attack at each point, including the apparent mean angle of attack of the section. Namely, from equation (39),

$$\alpha_e = \frac{\text{density of lift}}{2\pi \text{ chord } V^2 \frac{\rho}{2}} = \frac{\frac{dL}{dx}}{2\pi c V^2 \frac{\rho}{2}} = \frac{2L \sin \delta}{b\pi^2 c V^2 \frac{\rho}{2}} \tag{42}$$

The geometric angle of attack is greater by the constant induced angle of attack, and hence

$$\alpha_g = \frac{2L \sin \delta}{b\pi^2 c V^2 \frac{\rho}{2}} + \frac{L}{b^2 \pi V^2 \frac{\rho}{2}} = \alpha_e \left(1 + \frac{\pi c}{2b \sin \delta}\right) \tag{43}$$

Equation (40) indicates the importance of a sufficiently large span in order to obtain a small induced drag.

Any distribution of lift $\frac{dL}{dx}$ over the span other than the elliptical distribution is less simple to investigate, as then the induced downwash is variable. The distribution of lift gives directly the distribution of the potential difference along the two-dimensional wing projection.

$$\Delta\Phi = \frac{\frac{dL}{dx}}{V\rho} \tag{44}$$

The transverse two-dimensional flow can now be obtained by superposition of types of flow given by equation (4) with $z = \frac{2x}{b}$, as now the length of the line is not 2 but b. The condition that the superposition of such flows gives the required potential difference, viz,

$$\frac{1}{2} \Delta\Phi = \frac{\frac{dL}{dx}}{2 V\rho} = A_1 \sin \delta + A_2 \sin 2\delta + \cdots + A_n \sin n\delta + \tag{45}$$

Hence, the distribution of the density of lift, divided by $2\ V\rho$ is to be expanded into a Fourier's series. The induced angle of attack results then, according to equation (15),

$$\alpha_i = \frac{1}{bV \sin \delta} (A_1 \sin \delta + 2A_2 \sin 2\delta + \cdots + n\ A_n \sin n\delta + , \cdots) \tag{46}$$

and the entire induced drag, being the integral of the product of the induced angle of attack and the density of lift with respect to the element of the span is

$$D_i=\int_{-b/2}^{+b/2}\frac{dL}{dx}\alpha_i\,dx=\rho\frac{\pi}{2}A_1^2+2A_2^2+\cdots n\,A_n^2\cdots) \tag{47}$$

As mentioned before, the induced drag for any reasonable distribution of lift agrees practically with the minimum induced drag, given by equation (40). A_1 is the main coefficient and all other A's are then small when compared with it. It is, therefore, exact enough for practical problems to apply equation (40) indiscriminately, whether the distribution of lift is exactly elliptical or only within a certain approximation. In the same way, equation (41) for the constant induced angle of attack can be used generally for the average induced angle of attack.

9. In practice the reversed problem is more often met with. Not the distribution of the lift but the shape of the wing is known, viz, the magnitude of its chord and the angle of attack at each point. The air forces are to be determined.

The solution of this problem in full generality is barred by great mathematical difficulties. There is, however, one particular plan view of the wing which can be treated comparatively simply and which gives very interesting results. That is the elliptical wing; that is, a wing with such a plan view that the chord plotted against the span is represented by half an ellipse.

A possible way to investigate a wing with a given plan view would be to look for particular distributions of the angle of attack such that the solution for them can be found. It would be particularly easy to use such special solutions for the solution of the general problem, if it is possible to determine those particular special solutions, for which the induced angle of attack is proportional to the effective angle of attack and hence to the geometric angle of attack, too. These functions found, the distribution of the angle of attack arbitrarily given has to be expanded as a series of such functions, that is, as a sum of them. It is then easy to find from this series the induced angle of attack or the effective angle of attack, as this can be done for each term separately by the mere multiplication with a certain constant. Hence, a new series for the effective angle of attack is readily obtained from the series of geometric angles of attack.

That sounds simple, but it is extremely difficult to find such distributions of the angle of attack of a given plan view. It suggests itself, therefore, to try the other way and to begin with simple distributions of the angle of attack and to try to find a plan view which can be conveniently investigated by means of them. The only distributions discussed in this paper are those represented by the flows equation (4). It suggests itself to begin by considering their induced angle of attack and effective angle of attack. For one special term, as follows from equations (42), (45), and (46), the effective angle of attack is

$$\alpha_e=\frac{2A_n\sin n\delta}{\pi c\,V} \tag{48}$$

and the induced angle of attack is

$$\alpha_i=\frac{n\,A_n\sin n\delta}{b\,V\sin\delta} \tag{49}$$

It is at once seen that these two angles become proportional to each other if the chord c becomes proportional to $\sin\delta$. For circles and ellipses

$$c=\frac{S}{b\frac{\pi}{4}}\sin\delta, \tag{50}$$

and therefore this is taken as applying to other shapes also. Hence,

$$\alpha_e=\frac{A_n\sin n\delta}{V\,b\sin\delta\,\frac{2S}{b^2}}$$

where S denotes the entire area of the wing. The ratio of the two angles of attack becomes then

$$\frac{\alpha_i}{\alpha_e}=\frac{2n\,S}{b^2} \tag{51}$$

This plan view is called elliptical.

With an elliptical wing, all equations found for any monoplane become particularly simple. Equation (43) can be written

$$\alpha_g=\alpha_e\left(1+\frac{2S}{b^2}\right) \tag{52}$$

The geometric angle of attack follows from equations (48) and (49) for the effective and induced angles of attack, valid for a special n, by taking the sum of all such expressions. The condition for the coefficient A, if the geometric angle of attack α_g is given, is therefore

$$\frac{2VS}{b}\alpha_g\sin\delta=A_1\sin\delta\left(1+\frac{2S}{b^2}\right)+A_2\sin 2\delta\left(1+\frac{4S}{b^2}\right)+\;+A_n\sin n\delta\left(1+\frac{2nS}{b^2}\right)+\cdots\cdots \tag{53}$$

That is, $2V\alpha_g\sin\delta\,\frac{S}{b^2}$ is to be expanded into a Fourier's series

$$2V\alpha_g\sin\delta\,\frac{S}{b^2}=B_1\sin\delta+B_2\sin 2\delta+B_n\sin n\delta+\;\cdots \tag{54}$$

and the coefficients A_n are then

$$A_n=\frac{B_n}{1+\frac{2nS}{b^2}} \tag{55}$$

The distribution of the lift follows then from equation (44)

$$\frac{dL}{dx}=2V\rho\,(A_1\sin\delta+A_2\sin 2\delta+\;\cdots\;+A_n\sin n\delta+) \tag{56}$$

and the distribution of the induced angle of attack is given by equation (46). The entire induced drag is given by equation (47).

The entire lift is $\int_{-b/2}^{+b/2}\frac{dL}{dx}\,dx$ and only the first term of series (56) contributes to it in view of formula (11), since $dx=-\sin\delta\,d\,\delta$. Hence, the entire lift is

$$L=2V\rho\,A_1\int_{-b/2}^{+b/2}\sin\delta\,dx$$

or, transformed by introducing α_g, and using (54) and (55)

$$L=V^2\frac{\rho}{2}\,\frac{1}{1+\frac{2S}{b^2}}\,\frac{2}{\pi}\int_{-b/2}^{+b/2}\alpha_g\,c\,dx \tag{57}$$

That is to say, the entire lift of an elliptic wing can be obtained by supposing the effective angle of attack equal to the geometric angle of attack divided by $\left(1+\frac{2S}{b^2}\right)$. Otherwise expressed the aerodynamic induction reduces the entire lift of the elliptical wing in the ratio

$$\frac{1}{1+\frac{2S}{b^2}}$$

however the wing may be twisted.

This is not so plausible as it sounds. The distribution of the lift itself is by no means obtained by a mere diminution of the angle of attack in a constant ratio; only the entire lift can be computed that way. Nor does this theorem hold true for any other plan view but the elliptical. It may, however, be applied to shapes approximately elliptical so as to gain approximate results.

The rolling moment of the lift can be found by means of quite an analogous theorem. Only the second term in (56) gives a contribution to the rolling moment in view of formula (11). This is therefore as a consequence of formulas (56), (55), (54), and (50),

$$M = \frac{V^2 \frac{\rho}{2} 2\pi}{1 + \frac{4S}{b^2}} \int_{-b/2}^{+b/2} c \alpha x \, dx \tag{58}$$

Hence, the entire rolling moment is obtained by taking as the effective angle of attack, the geometric angle of attack times $\frac{1}{1+\frac{4S}{b^2}}$. The induction decreases the rolling moment in the ratio $\frac{1}{1+\frac{4S}{b^2}}$. This is of interest for the computation of the effect of a displacement of ailerons.

It will be noticed that this factor of decrease is a different one for the entire lift and for the entire rolling moment. The induced angle of attack is not proportional to the geometric angle of attack except when all factors but A_1 are zero. This is the case in the main case $n=1$ where the constant angle of attack is decreased by a constant induced angle of attack, as we have seen before.

Equation (58) may also be applied approximately to shapes differing from elliptical plan forms. The error involved in this proceeding is probably greater in general than for the determination of the entire lift, as the rolling moment is more influenced by the ends of the wing and there the deviation from the elliptical shape will be particularly pronounced.

10. The biplane, represented by two parallel lines in the longitudinal projection, gives rise to the same considerations as for the monoplane. The apparent mass of the pair of lines is always greater than that of one line. Therefore, the minimum induced drag of a biplane is always smaller than the induced drag of a monoplane of the same span under the same conditions. It is

$$D = \frac{L^2}{4K V^2 \frac{\rho}{2}} \tag{59}$$

It is equal to that of a monoplane of equal area and of greater span. The span of the monoplane with the same induced drag as the biplane has to be kb where $k^2 = \frac{K}{b^2 \frac{\pi}{4}}$. The magnitude of K is given in Table II.

I have discussed the subject at full length in my paper on the biplane (reference 4). This paper contains also the discussion of the influence of the induction on the stability of staggered biplanes. It can easily be seen that the induced angle of attack of a staggered biplane is greater at the rear wing, this wing being in a layer of air having received more than 50 per cent of the impulse, whereas the front wing is in a layer having received less than that. Hence, the center of pressure is moved toward the front wing.

A theory of a particularly shaped biplane when the angle of attack is given, in analogy to the theory of the elliptical wing as given by me in the last section is not yet written. Even less is written on triplanes and other multiplanes. The number of variables to be considered and the general mathematical difficulties increase with the number of wings, and at the same time

the results become less important as they are more seldom used. This refers to the exact numerical information. The general physical problem is as easily understood as with the monoplane.

TABLE I.

APPARENT MASS OF A PAIR OF STRAIGHT LINES.

$\frac{\text{gap}}{\text{span}}$	$K=b^2\frac{\pi}{4}\cdot\frac{c}{c}$	$k=\frac{i}{\sqrt{c}}$
0.60	1.000	1.000
.05	1.123	.962
.10	1.212	.909
.15	1.289	.881
.20	1.353	.860
.30	1.462	.827
.40	1.550	.803
.50	1.626	.784
∞	2.000	.707

TABLE II.

COMPUTING THE ANGLE OF ATTACK OF ZERO LIFT AND OF ZERO MOMENT

ZERO LIFT.

Per cent of chords.	Factor.
2 points:	
$X_1=89.185$	$f_1=284.9$
$X_2=10.815$	$f_2=32.1$
4 points:	
$X_1=99.548$	$f_1=1125.24$
$X_2=87.426$	$f_2=109.048$
$X_3=50.000$	$f_3=32.5959$
$X_4=12.574$	$f_4=15.6838$
$X_5=.542$	$f_5=5.97817$

ZERO MOMENT.

$X_1=95.74$	$f_1=f_2=62.634$
$X_2=4.26$	

TECHNICAL NOTES

NATIONAL ADVISORY COMMITTEE FOR AERONAUTICS

No. 196

REMARKS ON THE PRESSURE DISTRIBUTION OVER THE SURFACE OF AN ELLIPSOID, MOVING TRANSLATIONALLY THROUGH A PERFECT FLUID

By Max M. Munk

Washington

June 1924

NATIONAL ADVISORY COMMITTEE FOR AERONAUTICS.

TECHNICAL NOTE NO. 196.

REMARKS ON THE PRESSURE DISTRIBUTION OVER THE SURFACE OF AN ELLIPSOID, MOVING TRANSLATIONALLY THROUGH A PERFECT FLUID.

By Max M. Munk.

Summary

This note, prepared for the National Advisory Committee for Aeronautics, contains a discussion of the pressure distribution over ellipsoids when in translatory motion through a perfect fluid. An easy and convenient way to determine the magnitude of the velocity and of the pressure at each point of the surface of an ellipsoid of rotation is described.

The knowledge of such pressure distribution is of great practical value for the airship designer. The pressure distribution over the nose of an airship hull is known to be in such good agreement with the theoretical distribution as to permit basing the computation of the nose stiffening structure on the theoretical distribution of pressure.

References

1. Horace Lamb - "Hydrodynamics," Chapter V.

2. Max M. Munk - "The Aerodynamic Forces on Airship Hulls," N.A.C.A. Technical Report No. 184.

3. R. Jones & D. H. Williams - "The Distribution of Pressure Over the Surface of Airship Model N 721," Reports and Memoranda No. 600.

Experiments have shown that the knowledge of the pressure disbribution over the surface of ellipsoids, moving translationally through a perfect fluid, is often of considerable practical interest. This pressure distribution is of a simple description; it can easily and quickly be determined by analytical methods. To the best of my knowledge this has never been brought out clearly in any publication. The mathematical theory of the flow created by an ellipsoid is given by H. Lamb in his "Treatise on Hydrodynamics," Chapter V. It requires considerable mathematical training to grasp the full meaning of the results as given by Lamb. E. G. Gallop (Ref. 3) has given some comments on the nature of the resulting distribution of the velocity and pressure, for the special case of an ellipsoid of revolution. A part of this holds true for all ellipsoids, including those with three different principal axes. Mr. Gallop does not, however, for the special case of spheroids make the distribution of the pressure sufficiently plain for immediate computation or for the practical application of this interesting analysis.

The knowledge of one simple lemma on the potential flow around ellipsoids, implicitly contained in Lamb's result (Third Edition, Equation (114 (8)),) is sufficient for the deduction of all the following theorems and for the determination of the pressure distribution. This lemma is:

If an ellipsoid is moving with uniform velocity parallel to one of its principal axes, say parallel to the x-axis, the velocity

potential at any point of the surface can be written in the form

$$\Phi = A'x \qquad (1)$$

where A' is constant for a given flow and a given ellipsoid. This theorem is the key to all the relations referring to the distribution of velocity and of pressure.

If the velocity of flow is not parallel to a principal axis, but has components in the direction of each of them, the resulting flow is the superposition of three flows analogous to the one just considered. Hence, at all points of the surface, the potential is a linear function of the Cartesian coordinates x, y, and z again, and can be written in the form

$$\Phi = A'x + B'y + C'z \qquad (2)$$

where the coordinate axes are chosen to coincide with the axes of the ellipsoid. Hence the curves of equal potential Φ are situated on parallel planes.

Now, suppose first the ellipsoid to be at rest and the fluid to be moving relative to it, as in a wind tunnel or as with an airship moored in a gale. The change from the ellipsoid moving through the fluid otherwise at rest to the fluid passing by the stationary ellipsoid does not affect the validity of Equation (2) except giving the constants A', B', and C' other values, say A'', B'', and C''. In the latter case (the body at rest) the velocity of the fluid at all points of the surface is parallel to the surface. Consider first the elements of surface containing a

line element at right angles to the planes of constant potential, i.e. at the points of the ellipsoid where the plane $A''x + B''y + C''z = 0$ meets the surface. It is apparent from (2) that at all these points the velocity has the components A'', B'', and C''. This is evidently the maximum velocity.

At all other points of the ellipsoid the elements of surface are inclined towards the direction of maximum velocity, say by the angle ε. Then the elements of distance on the surface, Δs, between curves of equal potential are increased in the ratio $\frac{1}{\cos \varepsilon}$, when compared with the actual distances between the planes of equal potential. Accordingly, the velocity, being equal to $\frac{\delta \Phi}{\delta s}$ is decreased inversely, its magnitude is $A'' \cos \varepsilon$. It will be noted in particular that the velocity is equal at surface elements which are inclined by the same angle ε. It is equal to the projection of the maximum velocity at right angles to the surface element. Hence the velocity cannot exceed the one rightly denoted by "maximum velocity," having the components A'', B'', and C''.

Returning to the case when the direction of flow is parallel to a principal axis, it can be shown that the maximum velocity A'' stands in a very simple relation to the kinetic energy of the flow, and hence to the apparent additional mass of the ellipsoid. We have now to suppose the fluid to be at rest and the ellipsoid to move, say with the velocity U, parallel to a principal axis,

e.g., the x-axis. The kinetic energy of the flow set up is equal to $-\frac{1}{2}\rho\int\Phi\frac{d\phi}{dn}dS$, i.e., the volume of fluid displaced by an element of the surface per unit of time, multiplied by the potential at the point of displacement and by $\frac{\rho}{2}$ where ρ denotes the density of the fluid. Now, the volume displaced by a surface element per unit time is equal to the projection of this element perpendicular to the direction of x, multiplied by the velocity U. The potential being A'x the integrand becomes $A' Ux \frac{\rho}{2} dy\,dz$. $\int xdy\,dz$ is the volume of the ellipsoid, hence the integral gives $\overline{\text{Volume}}\ A'U\frac{\rho}{2}$. This is the kinetic energy, usually expressed by $\overline{\text{Volume}}\ k_1 U^2\frac{\rho}{2}$, where k_1 denotes the factor of apparent mass. It follows that

$$\frac{A'}{U} = k_1.$$

A", referring to the case when the ellipsoid is stationary, is connected with A" by the equation

$$A'' = A' + U_1$$

as the latter flow results from the former by the superposition of the constant velocity U. Hence it appears that

$$\frac{A''}{U} = k_1 + 1 = A.$$

A is the maximum velocity corresponding to a flow having unit velocity along the x-axis. It is a constant for a given ellipsoid.

It equals the sum of 1 and of the factor of apparent mass k_1 as is confirmed for two special cases, where the factor A is well known. With a sphere, the maximum velocity is 1.5 times

the velocity of flow, and the additional apparent mass is one-half the mass of the displaced fluid. With a circular cylinder, moving at right angles to its axis, the maximum velocity is twice the velocity of flow, and the apparent additional mass is equal to the mass of the displaced fluid.

The ratios $A = \frac{A''}{U}$, $B = \frac{B''}{V}$, $C = \frac{C''}{W}$ are independent of the velocities U,V, and W and hence only depend on the ratio of the three semi-axes of the ellipsoid a, b, and c. Lamb gives the method to compute them. Compute first the integral

$$\alpha = abc\int_0^\infty \frac{dx}{\sqrt{(a^2 + x)\ \ (a^2 + x)(b^2 + x)(c^2 + x)}}$$

and the analogous integrals β and γ for the axes b and c. The factors of apparent mass are then

$$k_1 = \frac{\alpha}{2 - \alpha}, \text{ etc.}$$

There are no tables for A, B, C, or for k_1, k_2, k_3, published yet. The integrals for α etc., can be numerically evaluated in each case, and I will assume at present that A,B, and C, are therefore known. For the special case b = c, that is, for ellipsoids of revolution, k_1 and k_2 have been computed for a series of elongation ratios, and are reprinted in a small table in Ref. 3. They are connected by the relation $k_1 = \frac{1 - k_2}{2\ k_2}$. The determination of the velocity at any point is thus reduced to a simple geometric problem. The maximum velocity, whose components are AU, BV, and CW, has to be projected onto the plane tangent

to the ellipsoid at the point considered, i.e. it has to be multiplied by the cosine of the angle between the normals to the surface at this point and at the point where the velocity is a maximum.

In the most interesting case of an ellipsoid of revolution, this can be done analytically in a very convenient way. The formula is most easily arrived at by the application of elementary vector analysis. First compute the component of the maximum velocity in a direction normal to the surface at a given point. The longitudinal component of the maximum velocity is AU, and the lateral component of the maximal velocity is BV.

Let the angle between the normal and the longitudinal axis be η, and let the dihedral angle between the plane containing this axis and the line of velocity of flow and the plane containing the axis and the point in question be β. Then $\cos \eta$ is the longitudinal component and $\sin \eta \cos \beta$ the lateral component of the normal of unit length. Hence the component of the maximum velocity in a direction perpendicular to the element of surface is

$$V_2 = (1 + k_1)\, U \cos \eta + (1 + k_2)\, V \sin \eta \cos \beta .$$

Let V_1 denote the component parallel to the surface element. Then

$$V_1^2 + V_2^2 = V_{max}^2, \text{ and hence}$$

$$V_1 = \sqrt{V_{max}^2 - V_2^2}$$

$$= \sqrt{(1+k_1)^2 U^2 + (1+k_2)^2 V^2 - \left[(1+k_1) U \cos\eta + (1+k_2) V \sin\eta \cos\beta\right]^2}$$

This is the desired formula for the velocity of flow along the surface. The pressure is computed directly from the velocity at the points of the ellipsoid, now supposed to be stationary in the flowing fluid. For this is a steady flow and hence Bernouilli's equation for the pressure holds true, viz.: $p + \frac{1}{2} \rho V_1^2 = \text{const.}$ That is, the pressure is equal to an arbitrary constant pressure minus $V_1^2 \frac{\rho}{2}$, where V_1 denotes the velocity. The points of greatest velocity are those of smallest pressure or of greatest section. The curves of equal velocity are also the curves of equal pressure.

In practice, we are chiefly interested in rather elongated ellipsoids of rotation, and the angle α between the principal axis and the direction of motion is small. With very elongated ellipsoids, k_1 is about 1 and k_2 is very small. Hence A is about 2 and B is about 1, and the angle between the direction of the line of maximum velocity and the axis is about twice as large as the angle between the direction of motion and the axis. The maximum velocity is always greater than the velocity of motion. The difference between the largest negative pressure and the presure in the undisturbed atmosphere is

$$V^2\left\{\frac{\rho}{2} (1 + k_1)^2 \cos^2 \alpha + (1 + k_2)^2 \sin^2 \alpha - 1\right\}$$

REPORT No. 164.

THE INERTIA COEFFICIENTS OF AN AIRSHIP IN A FRICTIONLESS FLUID.

By H. Bateman.

SUMMARY.

The following investigation of the apparent inertia of an airship hull was made at the request of the National Advisory Committee for Aeronautics. The exact solution of the aerodynamical problem has been studied for hulls of various shapes and special attention has been given to the case of an ellipsoidal hull. In order that the results for this last case may be readily adapted to other cases, they are expressed in terms of the area and perimeter of the largest cross section perpendicular to the direction of motion by means of a formula involving a coefficient K which varies only slowly when the shape of the hull is changed, being *0.637* for a circular or elliptic disk, *0.5* for a sphere, and about *0.25* for a spheroid of fineness ratio 7. For rough purposes it is sufficient to employ the coefficients, originally found for ellipsoids, for hulls otherwise shaped. When more exact values of the inertia are needed, estimates may be based on a study of the way in which K varies with different characteristics and for such a study the new coefficient possesses some advantages over one which is defined with reference to the volume of fluid displaced.

The case of rotation of an airship hull has been investigated also and a coefficient has been defined with the same advantages as the corresponding coefficient for rectilinear motion.

I. INTRODUCTION.

It follows from Green's analysis that when an ellipsoidal body moves in an infinite incompressible inviscid fluid in such a way that the flow is everywhere of the irrotational, continuous Eulerian type, the kinetic energy of the fluid produces an apparent increase in the mass and moments of inertia of the body. The terms mass and moment of inertia are used here in a generalized sense because it appears that the apparent mass is generally different for different directions of motion and the apparent moment of inertia different for different axes of spins For this reason it seems better to speak of inertia coefficients, these being the constant coefficients in the expression for the kinetic energy in terms of the component linear and angular velocities relative to axes fixed in the body.

The idea of inertia coefficients may be extended to bodies of any shape and to cases in which there is more than one body or in which the fluid is limited by a boundary. Generalized coefficients may be defined, too, for cases in which there is circulation round some of the bodies or boundaries and values can eventually be obtained which should correspond closely to the values of the inertia coefficients for the motion of a body in a viscous fluid.

The inertia coefficients of airship hulls are useful for the interpretation of running tests and in fact for a dynamical study of any type of motion of an airship, whether steady or unsteady. The coefficients are needed, for instance, in the study of the stability of an airship by the method of small oscillations [1] and for a computation of the resulting momenta in various types of steady motion.

For the case of motion of translation with velocity U the kinetic energy, T, of the fluid is usually expressed in the form

$$T = \tfrac{1}{2} k m U^2$$

where m is the mass of the fluid displaced by the body and k is a numerical coefficient whose value is known in certain cases. A value of k for an airship hull is generally found by choos-

[1] For the literature on this subject reference may be made to a paper by R. Jones and D. H. Williams, British Aeronautical Research Committee, R. M. 751. June, 1921.

ing an ellipsoid with nearly the same form as the hull and calculating the value of k for the ellipsoid. This method is to some extent unsatisfactory because the coefficient k varies considerably with the shape, being infinite for a circular disk, *0.5* for a sphere, and *0.045* for a prolate spheroid of fineness ratio *6*. For this reason an alternative method is proposed in which the kinetic energy of the fluid is expressed in terms of quantities relating to the master section of the hull by means of a formula involving a numerical coefficient K which varies only slowly with other characteristics such as the fineness ratio. The proposed expression is

$$T=\tfrac{4}{3}K\rho\frac{S^2U^2}{l}$$

where S denotes the area and l the perimeter of the greatest cross section of the hull by a plane perpendicular to the direction of motion; ρ is the density of the fluid and K the new coefficient which is apparently greatest for a circular or elliptic disk.

In the case of a spheroid moving in the direction of its axis of symmetry the way in which k and K vary with the fineness ratio is shown in Figure 1. In Figure 2 the corresponding curves have been drawn for a hull bounded by portions of two spheres cutting each other orthogonally. The high value of K when the two spheres are equal is undoubtedly caused by the presence of

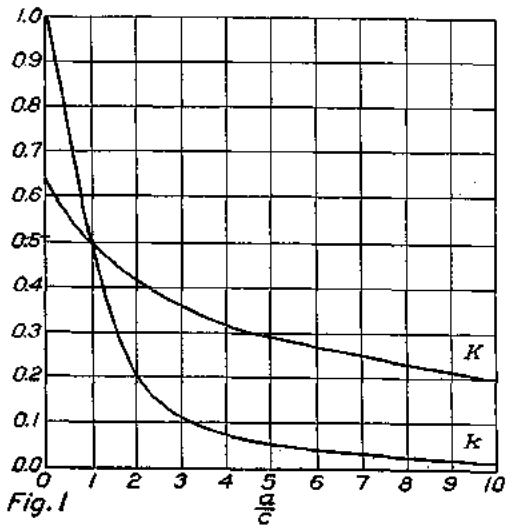

Fig. 1

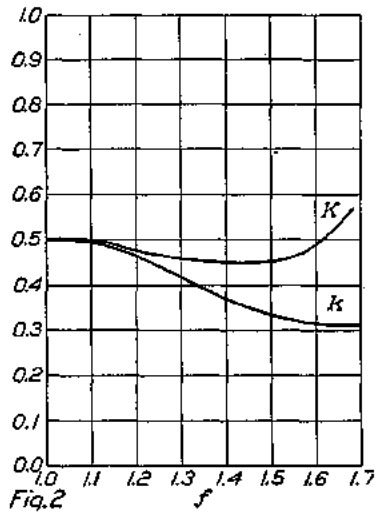

Fig. 2

the narrow waist, while the sudden drop in value indicates the effect of a lack of fore and aft symmetry. The curves for K have an advantage over those for k in indicating more clearly the effect of a change in shape. The effect of a flattening of the nose of the hull has been studied by considering the case of a surface of revolution whose meridian curve is a limacon. The effect is only slight, as is seen from the table in Section IV. In the case of an airship hull spinning about a central axis in a plane of symmetry the kinetic energy can also be expressed in terms of general characteristics by using a formula involving a coefficient K, which varies only slowly with the shape. The proposed formula is

$$T=\frac{64}{45}K'\rho R_x^2\frac{(S_z-S_y)^2}{l}\omega_x^2$$

where ω_x is the angular velocity about the axis of spin, which we take as the axis of x, R_x is the maximum radius of gyration of a meridian section about the axis of x, S_y and S_z are the areas of central sections perpendicular to the axes of y and z and l is the perimeter of the meridian section with the greatest perimeter, a meridian section being cut out by a plane through the axis of spin.

This formula has been constructed from the known formula for an ellipsoid with the axes of coordinates as principal axes. To adapt it to a hull of a different shape a suitable set of axes must be chosen. The principal axes of inertia at the center of gravity may, perhaps, be used with advantage.

The coefficients k, K and K' will now be computed in some cases in which the aerodynamical problem is soluble. In particular they will be computed for the following cases:

(1) Disk moving axially.
(2) Prolate spheroid moving longitudinally.
(3) Prolate spheroid moving laterally.
(4) Oblate spheroid moving in the direction of its axis of symmetry.
(5) Oblate spheroid moving at right angles to its axis of symmetry.
(6) Solid formed by two orthogonal spheres.
(7) Solid formed by the revolution of a limaçon about is axis of symmetry.

II, THE INERTIA COEFFICIENTS FOR AN ELLIPSOID.

When the viscosity of the fluid is neglected and the motion is treated as irrotational there is no scale effect. This means that if we increase the velocity of the body in the ratio $s:1$, keeping its size constant, the velocity at any point of the fluid changes in the same proportion. A similar remark applies to the case in which the body is spinning about an axis instead of moving with a simple motion of translation and in the more general case in which a body has motions of both translation and rotation the kinetic energy, T, can be expressed in the form[2]

$$2T = Au^2 + Bv^2 + Cw^2 + 2A'vw + 2B'wu + 2C'uv + Pp^2 + Qq^2 + Rr^2 + 2P'qr + 2Q'rp + 2R'pq + 2p(Fu + Gv + Hw) + 2q(F'u + G'v + H'w) + 2r(F''u + G''v + H''w),$$

where (u, v, w) are the component velocities of a point fixed in the body and (p, q, r) are the angular velocities of the body about axes through this point that are likewise fixed in the body. The coefficients $A, B, C, A', B', C', P, Q, R, P', Q', R', F, G, H, F', F'', G', G'', H', H''$ are constants which are called the *inertia-coefficients* of the body relative to these axes. This expression for the kinetic energy has been used also in cases in which the velocities are variable and the determination of the inertia coefficients is evidently a matter of some importance.

The inertia coefficients are usually found by writing down the velocity potential or stream-line function which specifies the flow and calculating the kinetic energy by means of an integral of type

$$2T = -\rho \int \phi \frac{d\phi}{dn} dS$$

over the surface of the body, ϕ being the velocity potential, ρ the density of the fluid and dn denotes an element of the normal to the surface dS drawn into the fluid. A different integral may be used when the stream-line function is known, but in many cases integration is unnecessary, for Munk[3] has remarked that in the case of a simple velocity of translation the fluid motion may be supposed to arise from a series of doublets and that the sum of the moments of all these doublets has a component in the direction of motion which is proportional to the sum of the kinetic energy of the fluid and the kinetic energy which the fluid displaced would have if it moved like a rigid body with the same velocity as the body. The sum of the masses of the fluid and the fluid displaced has been called the *complete mass*.

The inertia-coefficients are well known for the case of an ellipsoid with semiaxes a, b, c when the axes of reference are the principal axes of the ellipsoid. We have in fact[2]

$$A = \frac{\alpha_0}{2 - \alpha_0} m, \quad P = \frac{(b^2 - c^2)^2(\gamma_0 - \beta_0)}{2(b^2 - c^2) + (b^2 + c^2)(\beta_0 - \gamma_0)} \frac{m}{5}, \text{ etc.}$$

$$m = \frac{4}{3}\pi\rho abc, \quad A' = B' = C' = P' = Q' = R' = F = F' = F'' = G = G' = G'' = H = H' = H'' = 0.$$

where

$$\alpha_0 = abc \int_0^\infty \frac{d\lambda}{(a^2 + \lambda)\Delta}, \quad \beta_0 = abc \int_0^\infty \frac{d\lambda}{(b^2 + \lambda)\Delta}, \quad \gamma_0 = abc \int_0^\infty \frac{d\lambda}{(c^2 + \lambda)\Delta}, \quad \Delta = [(a^2 + \lambda)(b^2 + \lambda)(c^2 + \lambda)]^{\frac{1}{2}}.$$

[2] See Lamb's hydrodynamics.
[3] Technical Note No. 104, National Advisory Committee for Aeronautics. July, 1922.

The complete coefficients of inertia for motion of translation are

$$A^*=\frac{2m}{2-\alpha_0},\quad B^*=\frac{2m}{2-\beta_0},\quad C^*=\frac{2m}{2-\gamma_0}.$$

The coefficient k defined by the equation

$$k=\frac{\alpha_0}{2-\alpha_0}$$

has been tabulated by Professor Lamb in a number of cases.[4] We have extended his tables and have also tabulated the coefficient K defined in I. The different special cases of an ellipsoid will now be discussed.

1. *Elliptic disk.*—In this case k is infinite but the kinetic energy is finite. To find an expression for K we write

$$\alpha_0=\int_0^\infty\frac{abc\,d\lambda}{(a^2+\lambda)\Delta}=\sum_{n=0}^{\infty}\frac{1\cdot3\cdots(2n-1)}{2\cdot4\cdots2n}(c^2-b^2)^n\int_0^\infty\frac{abc\,d\lambda}{(a^2+\lambda)^{\frac{1}{2}}(c^2+\lambda)^{n+1}}$$

$$\int_0^\infty\frac{d\lambda}{(a^2+\lambda)^{\frac{1}{2}}(c^2+\lambda)}=\frac{2}{\sqrt{c^2-a^2}}\left[\frac{\pi}{2}-\tan^{-1}\frac{a}{\sqrt{c^2-a^2}}\right]=\frac{\pi}{c}-\frac{2a}{c^2}+\frac{\pi}{2}\frac{a^2}{c^3}-\cdots$$

when a is small. Differentiating once with respect to a and n times with respect to c^2, we get

$$(-1)^n\,n!\int_0^\infty\frac{a\,d\lambda}{(a^2+\lambda)^{\frac{1}{2}}(c^2+\lambda)^{n+1}}=\frac{2}{c^{2n+2}}(-1)^n\,n!-\frac{\pi a}{c^{2n+3}}(-1)^n\frac{3\cdot5\cdots(2n+1)}{2^n}+\cdots$$

Hence

$$\alpha_0=\frac{2b}{c}\left[1+\frac{1}{2}\frac{c^2-b^2}{c^2}+\frac{1\cdot3}{2\cdot4}\left(\frac{c^2-b^2}{c^2}\right)^2+\cdots\right]-\frac{\pi ab}{c^2}\left[1+\frac{1\cdot3}{2^2}\frac{c^2-b^2}{c^2}+\frac{1\cdot3^2\cdot5}{2^2\cdot4^2}\left(\frac{c^2-b^2}{c^2}\right)^2+\cdots\right]$$

$$=2\left[1-abc\int_0^{\frac{\pi}{2}}\frac{d\theta}{(c^2\cos^2\theta+b^2\sin^2\theta)^{\frac{1}{2}}}+\text{higher powers of a}\right]=2\left[1-\frac{al}{4bc}\right]$$

approximately, where l is the perimeter of the ellipse with semiaxes b and c. Hence finally we obtain

$$2T=\frac{16}{3\pi}\frac{\rho\,U^2S^2}{l},\quad S=\pi bc$$

and[5]

$$K=\frac{2}{\pi}=0.637$$

The distribution of doublets may be found from the well-known expression for the potential We have for an ellipsoid

$$\phi=\frac{abc\,x\,U}{2-\alpha_0}\int_{\lambda_0}^\infty\frac{d\lambda}{(a^2+\lambda)\Delta},\quad\frac{x^2}{a^2+\lambda_0}+\frac{y^2}{b^2+\lambda_0}+\frac{z^2}{c^2+\lambda_0}=1$$

As $a\to0$ we have

$$\phi=\frac{2b^2c^2}{l}\,x\,U\int_{\lambda_0}^\infty\frac{d\lambda}{\lambda^{\frac{1}{2}}(b^2+\lambda)^{\frac{1}{2}}(c^2+\lambda)^{\frac{1}{2}}},\quad\frac{x^2}{\lambda_0}+\frac{y^2}{b^2+\lambda_0}+\frac{z^2}{c^2+\lambda_0}=1$$

Putting $\lambda=x^2s$ and making $x\to0$ we find that the value of ϕ on the disk is

$$\phi_+=\frac{4bc}{l}\,U\sqrt{1-\frac{y^2}{b^2}-\frac{z^2}{c^2}}$$

[4] British Advisory Committee for Aeronautics, R. & M. No. 823, October (1918).

[5] In the case of an infinitely long strip bounded by two parallel lines the value of K is 0.589.

This must be equal to the 2π times the moment per unit area of the doublets in the neighborhood of the point (O, y, z) of the disk. Hence the expression for the potential is equivalent to

$$\phi = \frac{2bc}{\pi l}\, Ux \int\int \frac{\left[1-\frac{y_0^2}{b^2}-\frac{z_0^2}{c^2}\right]^{\frac{1}{2}} dy_0 dz_0}{[x^2+(y-y_0)^2+(z-z_0)^2]^{\frac{1}{2}}}$$

and this formula shows the way in which the potential arises from the doublets. The complete energy is in this case

$$T = \frac{8}{3\pi}\frac{\rho U^2\pi^2 b^2 c^2}{l} = 2\pi\rho U\left[\frac{2bc}{\pi l}U\int\int\left[1-\frac{y_0^2}{b^2}-\frac{z_0^2}{c^2}\right]^{\frac{1}{2}} dy_0 dz_0\right.$$

in accordance with Munk's theorem. To verify this result we put

$$y_0 = bs\cos\omega,\ z_0 = cs\sin\omega$$

then

$$\int\int\left[1-\frac{y_0^2}{b^2}-\frac{z_0^2}{c^2}\right]^{\frac{1}{2}} dy_0 dz_0 = bc\int_0^1 s\sqrt{1-s^2}ds\int_0^{2\pi} d\omega = \frac{2\pi}{3}bc.$$

With the above substitution the expression for the potential may be written in the form

$$\phi = \frac{2bc}{\pi l}\, Ux\int_0^1 s\sqrt{1-s^2}ds\int_0^{2\pi}\frac{d\omega}{R^3},$$

$$R^2 = x^2+(y-bs\cos\omega)^2+(z-cs\sin\omega)^2$$

and may be compared with the corresponding expression for the oblate spheroid. For the case of the circular disk $(b=c)$ the stream-line function may be obtained by replacing x in the above formula by $-(y^2+z^2)$. When an elliptic disk spins about the axis of y the kinetic energy is given by

$$2T = \frac{4}{15}\pi\rho c^2\Omega_y^2\int_0^{\frac{\pi}{2}}\frac{(1+\cos^2\theta)d\theta}{(c^2\cos^2\theta+b^2\sin^2\theta)^{\frac{1}{2}}}$$

where Ω_y is the angular velocity. In the case of a circular disk the kinetic energy is

$$\frac{8}{45}\rho c^5\Omega_y^2$$

The coefficient K' thus has the value

$$K' = \frac{1}{\pi} = 0.318.$$

2. *Prolate spheroid.*—In the case of a prolate spheroid moving in the direction of its axis of symmetry, we have (Lamb, loc. cit.)

$$\alpha_0 = \frac{2(1-e^2)}{e^3}\left\{\frac{1}{2}\log\frac{1+e}{1-e}-e\right\}$$

where e is the eccentricity of the meridian section and so

$$b = c = a\sqrt{1-e^2}$$

The velocity potential is

$$\phi_a = \frac{ab^2 Ux}{2-\alpha_0}\int_\lambda^\infty \frac{d\lambda}{(a^2+\lambda)^{\frac{3}{2}}(b^2+\lambda)}$$

where

$$\frac{x^2}{a^2+\lambda}+\frac{y^2+z^2}{b^2+\lambda}=1$$

By introducing the spheroidal coordinates

$$x=h\,\mu\zeta,\ y=\omega\cos w,\ z=\omega\sin w,\ \omega=h\,(1-\mu^2)^{\frac{1}{2}}(\zeta^2-1)^{\frac{1}{2}},\ h=ae$$

we may write this in the form

$$\phi_s=A\,P_1(\mu)\,Q_1(\zeta)=A\,\mu\left\{\frac{1}{2}\zeta\,log\frac{\zeta+1}{\zeta-1}-1\right\}$$

where

$$A\left\{\frac{1}{1-e^2}-\frac{1}{2e}\log\frac{1+e}{1-e}\right\}=a\,U.$$

The velocity potential may also be expressed as a definite integral

$$\phi_s=\frac{1}{2}\,Ah\int_{-1}^{+1}\frac{sds}{[(x-hs)^2+y^2+z^2]^{\frac{1}{2}}}$$

which indicates the way in which it may be imagined to arise from a row of sources and sinks on the line joining the foci. This result may be obtained by writing

$$\mu\left\{\frac{1}{2}\zeta\,\log\frac{\zeta+1}{\zeta-1}-1\right\}=\frac{1}{2}h\int_{-1}^{+1}\frac{f(s)ds}{[(x-hs)^2+y^2+z^2]^{\frac{1}{2}}}$$

and determining $f(s)$ from the integral equation

$$Q_1(\zeta)=\frac{1}{2}h\int_{-1}^{+1}\frac{f(s)ds}{h(\zeta-s)}$$

which is obtained by putting $y=z=O$. The integral equation is solved most conveniently by using the well-known expansion

$$\frac{1}{\zeta-s}=\sum_0^\infty\,(2n+1)\,P_n(s)Q_n(\zeta)$$

and the integral formula

$$\int_{-1}^{+1}P_m(s)P_n(s)ds=\begin{array}{cc}0 & m\pm n\\ \dfrac{2}{2\,n+1} & m=n\end{array}$$

It is thus evident that

$$f(s)=P_1(s)=s.$$

The strength of the source associated with an element hds is

$$\frac{1}{2}\,Ah.\,sds.\,4\pi\rho$$

Multiplying this by $Ux=Uhs$ and integrating with regard to s between -1 and 1, we get

$$\frac{4\pi}{3}\,Ah^2\rho\,U=\frac{4\pi\rho}{3}\,\frac{ah^2U^2}{\dfrac{1}{1-e^2}-\dfrac{1}{2e}\log\dfrac{1+e}{1-e}}$$

The kinetic energy of the fluid plus the kinetic energy of the fluid displaced is, on the other hand

$$\frac{4\pi\rho}{3}ac^2.\frac{1}{2}\,U^2\left[1+\frac{\alpha_0}{2-\alpha_0}\right]$$

and

$$2-\alpha_0=\frac{2(1-e^2)}{e^3}\left[\frac{1}{1-e^2}-\frac{1}{2e}\log\frac{1+e}{1-e}\right]$$

Thus Munk's theorem is again confirmed.

In the case of a prolate spheroid moving broadside on we have

$$\beta_o=\frac{1}{e^2}-\frac{1-e^2}{2\,e^3}\log\frac{1+e}{1-e}$$

and the relation between K and k is

$$K=\frac{lk}{2\pi a}$$

where l is the perimeter of the meridian section. The potential ϕ_b may be expressed in the forms

$$\phi_b=\frac{ab^2Vy}{2-\beta_o}\int_\lambda^\infty\frac{d\lambda}{(a^2+\lambda)^{\frac{1}{2}}(b^2+\lambda)^2}$$

where

$$\frac{x^2}{a^2+\lambda}+\frac{y^2+z^2}{b^2+\lambda}=1$$

$$\phi_b=A(1-\mu^2)^{\frac{1}{2}}(\zeta^2-1)^{\frac{1}{2}}\left\{\frac{1}{2}\log\frac{\zeta+1}{\zeta-1}-\frac{\zeta}{\zeta^2-1}\right\}\cos w$$

where

$$A\left\{\frac{1}{2}\log\frac{1+e}{1-e}-\frac{e(1-2e^2)}{1-e^2}\right\}=-hV$$

$$\phi_b=-\frac{1}{2}\,Ayh\int_{-1}^{+1}\frac{(1-s^2)\,ds}{[(x-hs)^2+y^2+z^2]^{\frac{3}{2}}}$$

At Doctor Munk's suggestion one may interpret these results with the aid of the idea of complete momentum, i. e., the momentum of the fluid plus the momentum which the fluid displaced by the body would have if it moved like a rigid body with the same velocity as the body.

Let M_a and M_b denote the complete masses for motions parallel to the axes of x and y respectively, then

$$M_a=\frac{4}{3}\pi\rho abc\,(1+k_a)\quad M_b=\frac{4}{3}\pi\rho abc\,(1+k_b)$$

and we may write

$$\Phi_a=\frac{3\,M_aU}{8\pi h}\int_{-1}^{+1}\frac{sds}{[(x-hs)^2+y^2+z^2]^{\frac{1}{2}}}$$

$$\Phi_b=\frac{3M_bVy}{16\pi}\int_{-1}^{+1}\frac{(1-s^2)\,ds}{[(x-hs)^2+y^2+z^2]^{\frac{3}{2}}}$$

These equations show that when the complete momentum is given the velocity potential Φ and the sources from which it arises are the same for a series of confocal spheroids.[6] This is true for any angle of attack as is seen by superposition. This result is easily extended to the ellipsoid, for we may write

$$\Phi_a=\frac{3}{8\pi}M_aUx\Gamma,$$

where

$$\Gamma=\int_{\lambda_0}^\infty\frac{d\lambda}{(a^2+\lambda)\,\Delta},$$

$$\frac{x^2}{a^2+\lambda_0}+\frac{y^2}{b^2+\lambda_0}+\frac{z^2}{c^2+\lambda_0}=1.$$

[6] This is an extension to three dimensions of a theorem that has been proved for the elliptic cylinder. Cf. Max. M. Munk, Notes on Aerodynamic Forces. Technical Note No. 104, National Advisory Committee for Aeronautics.

It is easily seen that Γ is the same for a system of confocal ellipsoids. This result may be used to find an appropriate system of singularities distributed over the region bounded by a real confocal ellipse, the result is the same as that already found for the elliptic disk.[7]

It is well known that an ellipsoid has three focal conics, one of which is imaginary, and the question arises whether there is more than one simple distribution of singularities which will produce the potential. This question will be discussed in Section III.

When a prolate spheroid is spinning with angular velocity Ω_y about the axis of y, the velocity potential Φ is given by the formulæ

$$\Phi = A\mu\ (1-\mu^2)^{\frac{1}{2}}\ (\zeta^2-1)^{\frac{1}{2}}\left\{\frac{3}{2}\zeta\log\frac{\zeta+1}{\zeta-1}-3-\frac{1}{\zeta^2-1}\right\}\quad \mathrm{Sin}\ w=-\frac{1}{2}Az\int_{-1}^{+1}\frac{s\ (1-s^2)\ ds}{[(x-hs)^2+y^2+z^2]^{\frac{3}{2}}}$$

where A is a constant to be determined by means of the boundary condition

$$\frac{\delta\Phi}{\delta\zeta}=-\Omega_y\left(z\frac{\delta x}{\delta\zeta}-x\frac{\delta z}{\delta\zeta}\right)$$

It is easily seen that

$$A\left[\frac{3}{2e^3}\ (2-e^2)\ \log\frac{1+e}{1-e}-\frac{8}{e}-\frac{e}{1-e^2}\right]=a^2e^3\Omega_y$$

The energy may be expressed in terms of the mass of the fluid displaced by means of the formula

$$2T=k^1m\left(\frac{a^2}{5}-\frac{c^2}{5}\right)\Omega^2_y$$

(the coefficient k^1 having been tabulated by Lamb) or it may be expressed in terms of other characteristics with the aid of our coefficient K^1. The values of the various coefficients k and K are given in Table I. The suffixes a and c are used to indicate the axis along which the spheriod is moving. The coefficients k^1 and K^1 refer to the case of rotation. It will be seen that the coefficients K vary only slowly and the same remark applies to the product $(1+k_a)(1+k_c)$. One advantage in using the coefficients K_a and K_c is that it is not necessary to compute the volume of the hull of the airship. Since K_c varies very slowly indeed when the fineness ratio a/c is in the neighborhood of 6, it follows that if we take $K_c=0.6$ for an airship hull we shall not be far wrong.

TABLE I.

$\frac{a}{c}$	k_a	k_c	$\frac{(1+k_a)}{(1+k_c)}$	K_a	K_c	k'	K'
1.00	0.500	0.500	2.250	0.500	0.500	0	1
1.155							0.906
1.50	0.305	0.621	2.116	0.457	0.523	0.244	
2.00	0.209	0.702	2.058	0.413	0.541	0.399	0.695
2.065							0.685
2.99	0.122	0.803	2.023	0.365	0.571	0.582	
3.572							0.512
3.99	0.092	0.860	2.012	0.317	0.587	0.689	
4.99	0.059	0.895	2.006	0.294	0.599		
6.01	0.045	0.918	2.004	0.270	0.606	0.807	
6.97	0.036			0.250			
8.01	0.029			0.232			
9.02	0.024			0.215			
9.97	0.021			0.209			
∞	0	1	2	0	0.637	1	0.477

In this table use has been made of the coefficients computed by Lamb. It should be noticed that K_a+2K_c is very nearly constant for values of $\frac{a}{c}$ lying between 1 and 6. This fact may be used to compute K_c when K_a is known using a formula such as

$$K_c=.743-\frac{1}{2}K_a$$

The value thus found is too large for large values of $\frac{a}{c}$ and too small for small values of $\frac{a}{c}$.

[7] Cf. Lamb's Hydrodynamics, 3d ed., ch. V, p. 145.

3. *Oblate spheroid.*—In the case of an oblate spheroid moving with velocity U in the direction of its axis of symmetry, which we take as axis of x, we have

$$\alpha_0=\frac{2}{e^2}\left[1-\frac{\sqrt{1-e^2}}{e}\sin^{-1}e\right]$$

where e is the eccentricity of the meridian section. In this case

$$b=c,\ a=c\sqrt{1-e^2}.$$

The velocity potential is

$$\phi_a=\frac{ac^2Ux}{2-\alpha_0}\int_{\lambda_0}^{\infty}\frac{d\lambda}{(a^2+\lambda)^{\frac{1}{2}}(c^2+\lambda)}$$

where

$$\frac{x^2}{a^2+\lambda_0}+\frac{y^2+z^2}{c^2+\lambda_0}=1.$$

Introducing the spheroidal coordinates

$$x=h\mu\zeta,\ y=\omega\cos w,\ z=\omega\sin w,\ \omega=h\,(1-\mu^2)^{\frac{1}{2}}\,(\zeta^2+1)^{\frac{1}{2}},\ h=ce.$$

we may write

$$\phi_a=A\mu\,(1-\zeta\cot^{-1}\zeta)$$

where

$$A\left\{\frac{a\sqrt{c^2-a^2}}{c^2}-\cos^{-1}\frac{a}{c}\right\}=-h^3U.$$

We also have

$$\phi_a=\frac{Ax}{2\pi}\int_0^1 s\sqrt{1-s^2}\,ds\int_0^{2\pi}\frac{dw}{R^3}$$

$$R^2=(y-hs\cos w)^2+(z-hs\sin w)^2+x^2.$$

When an oblate spheroid moves with velocity W at right angles to its axis of symmetry we have

$$\beta_0=\gamma_0=\frac{\sqrt{1-e^2}}{e^3}\left[\sin^{-1}e-e\sqrt{1-e^2}\right]$$

and the relation between k_0 and K_0 is now

$$K_0=\frac{lk_0}{2\pi a}.$$

The velocity potential ϕ_0 is given by the formulæ

$$\phi_0=\frac{ac^2Wz}{2-\gamma_0}\int_{\lambda_0}^{\infty}\frac{d\lambda}{(a^2+\lambda)^{\frac{1}{2}}(c^2+\lambda)^2}$$

$$=A(1-\mu^2)^{\frac{1}{2}}\,(\zeta^2+1)^{\frac{1}{2}}\left\{\frac{\zeta}{\zeta^2+1}-\cot^{-1}\zeta\right\}\sin w$$

$$=\frac{A}{2\pi}\int_0^1 2s\sqrt{1-s^2}\,ds\int_0^{2\pi}\frac{\partial}{\partial z}\left(\frac{1}{R}\right)$$

$$R^2=(y-hs\cos w)^2+(z-hs\sin w)^2+x^2,\ h=ce=\sqrt{c^2-a^2}$$

$$A\left\{\cos^{-1}\frac{a}{c}-\frac{a^2+2c^2}{ac^2}\sqrt{c^2-a^2}\right\}=h^3W.$$

Some values of the coefficients k_a, k_c, K_a, K_c, are given in Table II.

TABLE II.

$\frac{c}{a}$	k_a	K_a	k_c	K_c	$(1+k_a)(1+k_c)$
1.00	0.500	0.500	0.500	0.500	2.250
1.50	0.621	0.523	0.382	0.4824	2.240
2.00	0.702	0.541	0.310	0.477	2.229
2.99	0.803	0.571	0.223	0.473	2.205
3.99	0.860	0.587	0.174	0.474	2.184
4.99	0.895	0.599	0.145	0.477	2.166
6.01	0.918	0.606	0.1205	0.478	2.149
∞	1.000	0.637	0.000	0.500	2.000

When an oblate spheroid spins with angular velocity ω_y about the axis of y the velocity potential ϕ' is given by the formulæ

$$\phi = Czx \int_{\lambda_0}^{\infty} \frac{d\lambda}{(c^2+\lambda)(a^2+\lambda)\Delta}$$

$$C = \frac{(c^2-a^2)^2 abc\omega_y}{2(c^2-a^2)+(c^2+a^2)(\gamma_0-\alpha_0)}$$

$$\phi' = A\mu(1-\mu^2)^{\frac{1}{2}}(\zeta^2+1)^{\frac{1}{2}}\left\{3\zeta\cot^{-1}\zeta - 3 + \frac{1}{\zeta^2+1}\right\}$$

$$A\left\{3\frac{c^2+a^2}{c^2-a^2}\cos^{-1}\frac{a}{c} - \frac{a}{c^2}\frac{7c^2+a^2}{\sqrt{c^2-a^2}}\right\} = k^5\omega_y.$$

We also have

$$\phi' = -\frac{A}{3\pi}\int_0 s(1-s^2)^{\frac{1}{2}}\,ds \int_0^{2\pi} \frac{\partial^2}{\partial x \partial z}\left(\frac{1}{R}\right)\mathrm{dw}$$

III. THE METHOD BASED ON THE USE OF SOURCES AND SINKS.

It was shown by Stokes [8] that the velocity potential for the irrotational motion of an incompressible nonviscous fluid in the space outside a sphere of radius, a, moving with velocity U, is the same as that of a doublet of moment $2\pi Ua^3$ situated at the center of the sphere. This result has been generalized by Rankine,[9] D. W. Taylor,[10] Fuhrmann,[11] Munk,[12] and others, two sources of opposite signs at a finite distance apart giving stream lines shaped like an airship.

Munk has shown in a recent report that the intensity of the point source near one end of an airship hull may be taken to be $r^2\pi U$, where r is the radius of the greatest section of the ship and $\frac{1}{2}r$ the distance of the point source from the head of the ship. The total energy of the fluid displaced is then

$$T = \frac{1}{6}\pi r^3 \rho U^2$$

and the apparent increment of mass of the airship is equivalent to about $2\frac{1}{2}$ per cent of the mass of fluid displaced.

In this investigation the airship is treated as symmetrical fore and aft, the two sources of opposite signs being equidistant from the two ends and the contributions of the two sources to the kinetic energy being equal. The final result is identical with that for an elongated spheroid with a ratio of axes equal to 9.

[8] Cambr. Phil Trans., vol. 8 (1843). [Math. and Phys. Papers, Vol. I. p. 17.]
[9] Phil. Trans. London (1871), p. 267.
[10] Trans. British Inst. Naval Architects, vol. 35 (1894), p. 385.
[11] Jahrb. der Motorluftschiff-Studiengesellschaft, 1911–12.
[12] National Advisory Committee for Aeronautics, Reports 114 and 117 (1921).

It is thought that a lack of fore and aft symmetry will still further reduce the values of the coefficients k and K. To get an idea of the effect of a lack of symmetry we shall consider the case of a solid bounded by portions of two orthogonal spheres. In this case, as is well known, the velocity potential may be derived from three collinear sources. We may in fact write

$$\phi=\frac{1}{2}a^3\,U\,\frac{\cos\theta}{r^2}+\frac{1}{2}a'^3\,U\,\frac{\cos\theta'}{r'^2}-\frac{1}{2}p^3\,U\,\frac{\cos\Theta}{R^2}$$

$$\psi=\frac{1}{2}a^3\,U\,\frac{\sin^2\theta}{r}+\frac{1}{2}a'^3\,U\,\frac{\sin^2\theta'}{r'}-\frac{1}{2}p^3\,U\,\frac{\sin^2\Theta}{R}$$

where a and a' are the radii of the two spheres (r, θ), $(r'\ \theta')$, (R, Θ) are polar coordinates referred to the three sources as poles, the angles being measured from the line joining the three sources. If Q is a common point of the two spheres R is measured from the foot of the perpendicular from Q on the line of centers, while r and r' are measured from the centers of the two spheres respectively. The quantity p represents the distance of Q from the line of centers and is given by the equation

$$\frac{1}{p^2}=\frac{1}{a^2}+\frac{1}{a'^2}.$$

By means of Munk's theorem we infer that the complete energy is given by the formula

$$2T=2\pi\rho\,[a^3+a'^3-p^3]\,U^2=\rho\,(1+k)\,V\,U^2$$

where

$$V=\frac{\pi}{3}\left[2\,(a^2+a'^2)^{\frac{3}{2}}+2a^3+2a'^3-3\,\frac{a^2a'^2}{(a^2+a'^2)^{\frac{1}{2}}}\right]$$

is the volume of the fluid displaced.

The fineness ratio, i. e., the ratio of the length to the greatest breadth, is

$$f=\frac{a+a'+\sqrt{a^2+a'^2}}{2a}.$$

Some values of k and K are given in Table III and curves have been drawn in Figure 2 to show the effect of a lack of fore and aft symmetry. For a comparison we have given in Table III the values of k and K for a spheroid of the same fineness ratio. The high value of K for the two orthogonal spheres is undoubtedly due to the presence of a narrow waist. The sudden drop in the value of K is probably due to the lack of fore and aft symmetry. The coefficient K shows the effect of a change in shape much more clearly than the coefficient k.

TABLE III.

$\frac{a'}{a}$	k	K	f	k (spheroid).	K(spheroid).
1.0	0.313	0.5897	1.707	0.243	0.440
0.9	0.315	0.5136	1.622	.....	.....
0.8	0.329	0.4708	1.54	.....	.....
0.75	0.334	0.4509	1.5	0.305	0.457
0.66	0.363	0.4603	1.434	.....	.....
0.41	0.448	0.471	1.25	.....	.....
0.29	0.48	0.488	1.166	.....	.....
0	0.5	0.5	1	0.5	0.5

It appears from an examination of the case of the oblate spheroid that the motion of air round a moving surface of revolution can not always be derived from a number of sources at real points on the axis. For the oblate spheroid the sources, or rather doublets, are in the equitorial plane. It is possible, however, to replace these doublets by doublets at imaginary points on the axis as the following analysis will show.

If $F(x, y, z)$ is a potential function, we have the equation [13]

$$\frac{1}{2\pi}\int_0^{2\pi} F[x, y-\sigma\cos\omega, x-\sigma\sin\omega]\,d\omega = \frac{1}{\pi}\int_0^{\pi} F[x+i\sigma\cos X, y, z]\,dX$$

which holds under fairly general conditions. On account of this equation we may write

$$\frac{1}{2\pi}\int_0^h f(\sigma)\,d\sigma\int_0^{2\pi}\frac{\partial}{\partial x}\left(\frac{1}{R}\right)d\omega = \frac{1}{\pi}\int_0^h f(\sigma)\,d\sigma\int_0^{2\pi}\frac{\partial}{\partial x}\left(\frac{1}{R'}\right)dX$$

$$\frac{1}{2\pi}\int_0^h f_1(\sigma)\,d\sigma\int_0^{2\pi}\frac{\partial}{\partial z}\left(\frac{1}{R}\right)d\omega = \frac{1}{\pi}\int_0^h f_1(\sigma)\,d\sigma\int_0^{2\pi}\frac{\partial}{\partial z}\left(\frac{1}{R'}\right)dX$$

$$\frac{1}{2\pi}\int_0^h g(\sigma)\,d\sigma\int_0^{2\pi}\frac{\partial^2}{\partial z\partial x}\left(\frac{1}{R}\right)d\omega = \frac{1}{\pi}\int_0^h g(\sigma)\,d\sigma\int_0^{2\pi}\frac{\partial^2}{\partial z\partial x}\left(\frac{1}{R'}\right)dX$$

where

$$R^2 = x^2+(y-\sigma\cos\omega)^2+(z-\sigma\sin\omega)^2,\quad R'^2 = (x+i\sigma\cos X)^2+y^2+z^2.$$

Putting

$$f(\sigma) = f_1(\sigma) = \sigma(h^2-\sigma^2)^{\frac{1}{2}},\quad g(\sigma) = \sigma(h^2-\sigma^2)^{\frac{1}{2}}$$

making the substitution

$$\sigma\cos X = \xi,\quad dX\sqrt{\sigma^2-\xi^2} = -d\xi,$$

changing the order of integration and making use of the equations

$$\int_\xi^h d\sigma\,\frac{\sigma\sqrt{h^2-\sigma^2}}{\sqrt{\sigma^2-\xi^2}} = \frac{\pi}{4}(h^2-\xi^2),$$

$$\int_\xi^h d\sigma\,\frac{\sigma(h^2-\sigma^2)^{\frac{1}{2}}}{\sqrt{\sigma^2-\xi^2}} = \frac{3\pi}{16}(h^2-\xi^2)^2,$$

which are easily verified by means of the substitution

$$\sigma^2 = \xi^2\cos^2\theta + h^2\sin^2\theta,$$

we find that the potentials for the oblate spheroid in the three types of motion may be written in the forms

$$\phi_a = -\frac{A}{4h^3}\int_{-h}^h (h^2-\xi^2)\,d\xi\,\frac{\partial}{\partial x}\left(\frac{1}{R''}\right) = \frac{iA}{2h^3}\int_{-h}^h \frac{\xi\,d\xi}{R''}$$

$$\phi_c = -\frac{A}{2h^3}\int_{-h}^h (h^2-\xi^2)\,d\xi\,\frac{\partial}{\partial z}\left(\frac{1}{R''}\right)$$

$$\phi' = -\frac{A}{8h^5}\int_{-h}^h (h^2-\xi^2)^2\,d\xi\,\frac{\partial^2}{\partial x\partial z}\left(\frac{1}{R''}\right) = +\frac{iA}{2h^5}\int_{-h}^h \xi\,(h^2-\xi^2)\,d\xi\,\frac{\partial}{\partial z}\left(\frac{1}{R''}\right)$$

where

$$R'' = [(x+i\xi)^2+y^2+z^2]^{\frac{1}{2}}.$$

These formulæ resemble those for the prolate spheroid.

A distribution of sources or doublets over the elliptic area bounded by a focal ellipse of an ellipsoid may be replaced by a system of sources or doublets at imaginary points in one of the other planes of symmetry by making use of the equation.[14]

[13] H. Bateman, Amer. Journ. of Mathematics, vol. 34 (1912), p. 335.
[14] H. Bateman, loc. cit., p. 336.

$$\int_0^{2\pi} F[x-\sigma\cos\theta\cos\alpha, y-\sigma\sin\theta, z]\,d\theta = \int_0^{2\pi} F[x+i\sigma\sin X\sin\alpha, y, z+i\sigma\cos X]\,dX$$

which likewise holds under fairly general conditions when $F(x, y, z)$ is a potential function and α an arbitrary constant.

The theorem relating to the transformation of doublets in a central plane into a series of doublets at imaginary points on the axis of symmetry may be written in the general form

$$\frac{1}{2\pi}\int_0^h f(\sigma)\,d\sigma \int_0^{2\pi} G\left(\frac{\partial}{\partial x}, \frac{\partial}{\partial y}, \frac{\partial}{\partial z}\right)\frac{1}{R}\,d\omega = \frac{1}{\pi}\int_{-h}^{h} G\left(\frac{\partial}{\partial x}, \frac{\partial}{\partial y}, \frac{\partial}{\partial z}\right)\frac{1}{R'}\,F(\xi)\,d\xi$$

where the functions $f(\sigma)$ and $F(\xi)$ are connected by the integral equation

$$F(\xi) = \int_\xi^h \frac{f(\sigma)\,d\sigma}{\sqrt{\sigma^2-\xi^2}}.$$

In order that Munk's theorem may be applicable to doublets at imaginary points as wel as to doublets at real points we must have the equation

$$\frac{1}{\pi}\int_{-h}^{h} F(\xi)\,d\xi = \int_0^h f(\sigma)\,d\sigma.$$

Now

$$\frac{1}{\pi}\int_{-h}^{h} d\xi \int_\xi^h \frac{f(\sigma)\,d\sigma}{\sqrt{\sigma^2-\xi^2}} = \frac{1}{\pi}\int_0^h f(\sigma)\,d\sigma \int_{-\sigma}^{\sigma} \frac{d\xi}{\sqrt{\sigma^2-\xi^2}} = \int_0^h f(\sigma)\,d\sigma$$

hence the formula is verified and the complete mass may be calculated from doublets at imaginary points by adding the moments and using Munk's formula.

IV. CASES IN WHICH THE MASS CAN BE FOUND WITH THE AID OF SPECIAL HARMONIC FUNCTIONS

It is known that the potential problem may be solved in certain cases by using series of spheroidal, toroidal, bipolar, or cylindrical harmonics. Thus it may be solved for the spherical bowl, anchor ring, two spheres,[15] and for the body formed by the revolution of a limaçon about its axis of symmetry. The last case is of some interest, as it indicates the effect of a flattening of the nose of an airship hull. Writing the equation of the limacon in the form

$$r = 2a^2\,\frac{s+\cos\theta}{s^2-1}$$

where r and θ are polar coordinates, we find on making the substitutions

$$r\cos\theta = x = \xi^2-\eta^2. \quad r\sin\theta = y = 2\xi\eta$$

$$\xi = \frac{a\sinh\sigma}{\cosh\sigma-\cos\chi}. \quad \eta = \frac{a\sin\chi}{\cosh\sigma-\cos\chi}$$

that the potential for motion parallel to the axis of symmetry is

$$\phi = \frac{1}{2}a^2U\sum_{m=0}^{\infty}(m+1)\left[(m+2)^2\frac{Q'_{m+1}(s)}{P'_{m+1}(s)} - m^2\frac{Q'_m(s)}{P'_m(s)}\right]$$
$$[P_m(\cosh\sigma)\,P_{m+1}(\cos\chi) - P_{m+1}(\cosh\sigma)\,P_m(\cos\chi)]$$

[15] For references see Lamb's Hydrodynamics, 3d ed., pp. 126, 149; and A. B. Basset, Hydrodynamics, Cambridge, 1888, Vol. I.

where $P_m(s)$ and $Q_m(s)$ are the two types of Legendre functions (zonal harmonics) and $P'_m(s)$, $Q'_m(s)$ are the derivatives of $P_m(s)$ and $Q_m(s)$ respectively. The stream-line function ψ as found by Basset is in our notation.

$$\psi = -\frac{a^4 U}{\cosh\sigma - \cos\chi}\sum_{m=0}^{\infty}(2m+3)\frac{Q'_{m+1}(s)}{P'_{m+1}(s)}P'_{m+1}(\cosh\sigma)\,P'_{m+1}(\cos\chi)\sinh^2\sigma\sin^2\chi$$

At a great distance from the origin we have the approximate expressions

$$\phi = -\frac{1}{2}a^6 U\frac{x}{r^3}S,\ \psi = -\frac{1}{2}a^6 U\frac{y^2}{R^3},\ \frac{2a^2}{R} = \cosh\sigma - \cos\chi,$$

$$S = \sum_{m=0}^{\infty}(2m+3)\,(m+1)^2\,(m+2)^2\frac{Q'_{m+1}(s)}{P'_{m+1}(s)}$$

which give the sum of the moments of the doublets from which the potential arises. The coefficients k amd K may now be calculated with the aid of Doctor Munk's theorem and an incomplete table of spheroidal harmonics which is in the author's possession. We thus obtain the values [16]

TABLE IV.

s	f	k	K	k (spheroid)	K (spheroid)
∞	1	0.500	0.500	0.500	0.500
3	1.05	0.527	0.507	0.512	0.502
2	1.10	0.548	0.513	0.524	0.505
1.2	1.153	0.569	0.518	0.536	0.507
1.1	1.154	0.573	0.523	0.536	0.507
1	1.155	0.578	0.527	0.536	0.507

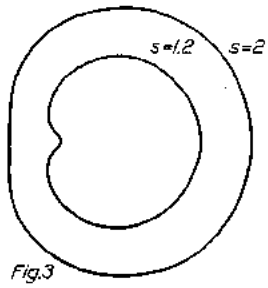

Fig.3

The corresponding values for an oblate spheroid are given for comparison. The case in which $s=2$ is particularly interesting because the limacon then has a point of undulation at the nose. When $s<2$ the limacon curves inward at the front, as may be seen from the diagrams in Figure 3, and the apparent mass is probably increased on account of fluid being confined in the hollow. In calculating the fineness ratio in such a case the length has been measured from the rear to the point where the double tangent meets the axis.

[16] The values for the spheroid have been obtained by interpolation from Table II. The values of k and K for the cardioid $s=1$ have been estimated by extrapolation.

REPORT No. 253

FLOW AND DRAG FORMULAS FOR SIMPLE QUADRICS

By A. F. Zahm

PREFACE

In this text are given the pressure distribution and resistance found by theory and experiment for simple quadrics fixed in an infinite uniform stream of practically incompressible fluid. The experimental values pertain to air and some liquids, especially water; the theoretical refer sometimes to perfect, again to viscid fluids. For the cases treated the concordance of theory and measurement is so close as to make a résumé of results desirable. Incidentally formulas for the velocity at all points of the flow field are given, some being new forms for ready use derived in a previous paper and given in Tables I, III. A summary is given on page 536.

The computations and diagrams were made by Mr. F. A. Louden. The present text is a slightly revised and extended form of Report No. 312, prepared by the writer for the Bureau of Aeronautics in June, 1926, and by it released for publication by the National Advisory Committee for Aeronautics. A list of symbols follows the text.

PRESSURE AND PRESSURE DRAG

We assume the fluid, of constant density and unaffected by weight or viscosity, to have in all the distant field a uniform velocity q_0 parallel to x; in the near field the resultant velocity q. If now the distant pressure is everywhere p_0, and the pressure at any point in the disturbed flow is p_0+p, the superstream pressure p is given by Bernouilli's formula,

$$p/p_n = 1 - q^2/q_0^2, \tag{1}$$

where $p_n = \rho q_0^2/2$, called the "stop" or "stagnation" or "nose" pressure.

At any surface element the superpressure exerts the drag $\int p \, dy \, dz$, whose integral over any zone[1] of the surface is the zonal pressure drag,

$$D = \int p \, dy \, dz. \tag{2}$$

Values of p, D are here derived for various solid forms and compared with those found by experiment.

PRESSURE MEASUREMENTS

The measured pressures here plotted were obtained from some tests by Mr. R. H. Smith and myself in the United States Navy 8-foot wind tunnel at 40 miles an hour. Very accurate models of brass, or faced with brass, had numerous fine perforations, one at the nose, others further aft, which could be joined in pairs to a manometer through fine tubing. Thus the pressure difference between the nose and each after hole could be observed for any wind speed. Then a fine tube with closed tip and static side holes was held along stream at many points abreast of the model, to show the difference of pressure there and at the nose. Next the tube was thrust right through the model, to find the static pressure before and behind it. The method is too well known to require further description.

THE SPHERE

Assume as the fixed body a sphere, of radius a, in a uniform stream of inviscid liquid, as shown in Table I. Then by that table the flow speeds at points on the axis x, y and on the surface are

$$q_x = (1 - a^3/x^3)q_0, \qquad q_y = (1 + a^3/2y^3)q_0, \qquad q_t = 1.5q_0 \sin\theta, \tag{3}$$

where θ is the polar angle. Figure 1 shows plots of these equations.

[1] A zone is a part of the surface bounded by two planes normal to q_0. Usually one plane is assumed tangent to the surface at its upstream end.

To graph p/p_n in Figure 1, we subtract from the line $y=1$, first q_x^2/q_0^2 to show the pressure along x; then q_t^2/q_0^2 to portray the surface pressure. A similar procedure gives the superpressure in the equatorial plane.

The little circles show the actual superpressures found with a 2-inch brass sphere in a tunnel wind at 40 miles an hour. These agree well with the computed pressures except where or near where the flow is naturally turbulent.

By (3) and (1), on the sphere's surface $p/p_n = 1 - 2.25 \sin^2\theta$; hence the zonal pressure drag $\int p.2\pi y dy$ is

$$D = \pi a^2 \sin^2\theta (1 - \frac{9}{8}\sin^2\theta) p_n, \tag{4}$$

for a nose cap whose polar angle is θ. With increase of θ, as in Figure 2, D/p_n increases to a maximum .698 a^2 for $\theta = 41° - 50'$ and $p = 0$; then decreases to zero for $\theta = 70° - 37'$; then to its minimum $-.3927\ a^2$ for $\theta = \pi/2$; then continues aft of the equator symmetrical with its fore part. Thus the drag is decidedly upstream on the front half and equally downstream on the

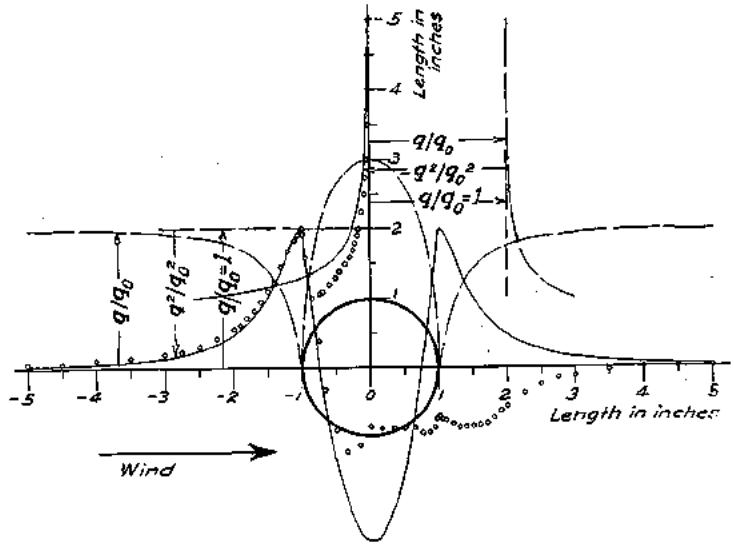

FIG. 1.—Velocity and pressure along axes and over surface of sphere; graphs indicate theoretical values; circles indicate pressures measured at 40 miles per hour in 8-foot wind tunnel, United States Navy

rear half, having zero resultant. The little crosses, giving D/p_n for the measured pressures, show that the total pressure drag in air is downstream, and fairly large for a body so blunt as the sphere.

Figure 3 depicts the whole-drag coefficient [2] $C_D = 2D/\pi\ \rho\ a^2 q_0^2$, of a sphere, for the manifold experimental conditions specified in the diagram, plotted against Reynolds Number $R = 2\ q_0 a/\nu$, ν being the kinematic viscosity. For $0.2 < R < 200000$, the data lie close to the line.

$$C_D = 28R^{-.85} + .48, \tag{5}$$

an empirical formula devised by the writer as an approximation.

For $.5 < R < 2$ (5) fairly merges with Oseen's formula

$$C_D = 24R^{-1} + 4.5, \tag{6}$$

and for $R < .2$ Stokes' equation $C_D = 24/R$ is exactly verified. Both these formulas are theoretical. Stokes treated only viscous resistance at small scale; Oseen added to Stokes' drag coefficient, $24/R$, the term 4.5 due to inertia.

[2] From the drag $D = C_{D_n} S$, where S is the model's frontal area, one derives the drag coefficient $C_D = D/p_n S$.

Over an important R range Figure 3 shows $C_D = .5$, giving as the sphere's whole drag

$$D = .5\, p_n\, S, \tag{7}$$

where $S = \pi\, a^2$ is the frontal area. That is, the sphere's drag equals half its nose pressure times its frontal area. For $R < .2$ Stokes' value, $D = 6\pi\, \mu\, a\, q_0$, has been exactly verified experimentally, as is well known.

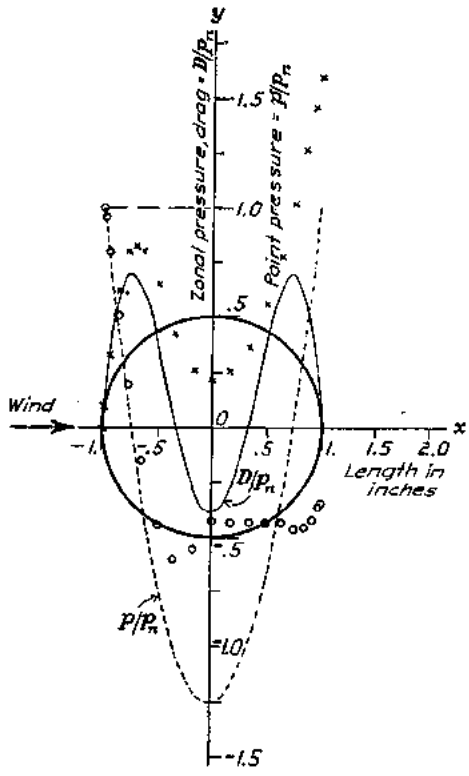

FIG. 2.—Pressure and pressure-drag on sphere. Graphs indicate theoretical values; circles indicate pressure p/p_n measured at 40 miles per hour; crosses indicate pressure-drag D/p_n, computed from measured pressure

THE ROUND CYLINDER

Next assume an endless circular cylinder, of radius a, fixed transverse to the stream, as indicated in Table I. By that table the flow speed at points on the axes x, y and on the surface is

$$q_x = (1 - a^2/x^2)\, q_0,\ q_y = (1 + a^2/y^2)\, q_0, \qquad q_t = 2\, q_0 \sin\theta, \tag{8}$$

where θ is the polar angle. Plots of (8) are shown in Figure 4.

Graphs of p/p_n, made as explained for the sphere, are also given there, together with experimental values, marked by small circles, for an endless 2-inch cylinder in a tunnel wind at 40 miles an hour. The agreement is good for points well within the smooth-flow region.

On the surface $p/p_n = 1 - 4\, \sin^2\theta$. The integral $2\int_0^y p\,dy$ gives, per unit length of cylinder, the zonal pressure-drag formula,

$$D/p_n = 2\, a \sin\theta - \frac{8}{3}\, a \sin^3\theta. \tag{9}$$

42488—27——34

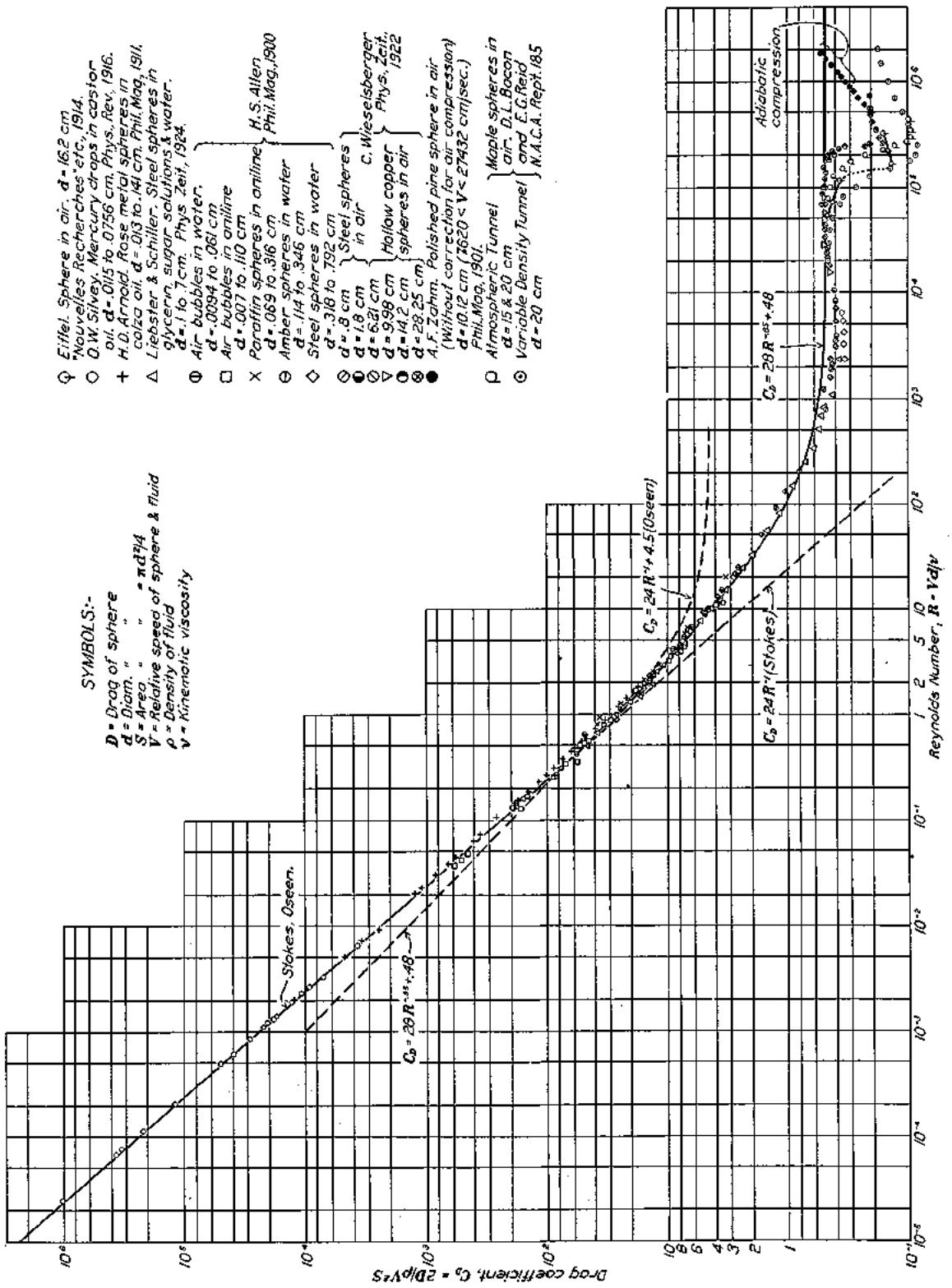

FIG. 3.—Drag coefficient for a sphere in steady translation through a viscous fluid

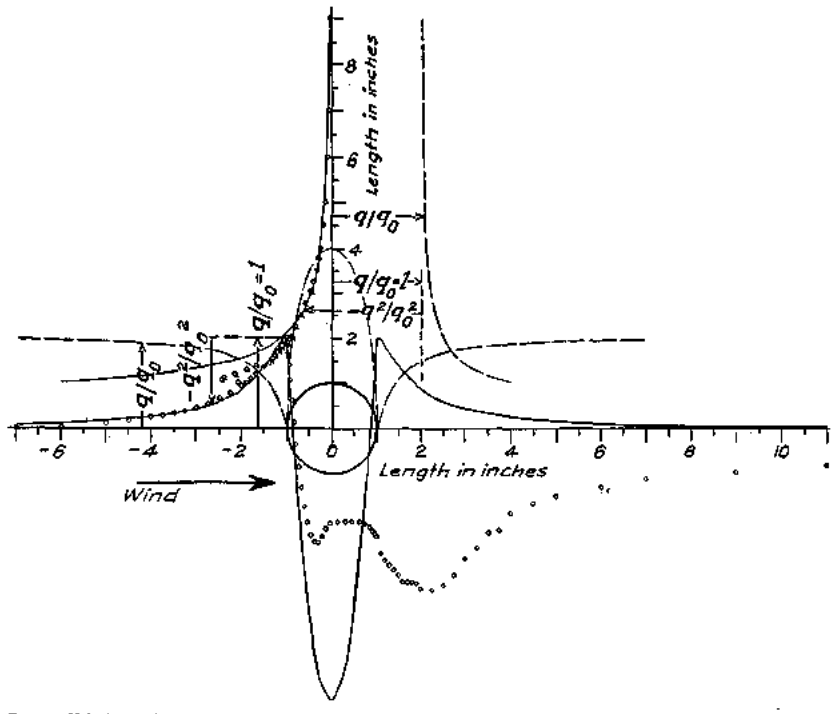

FIG. 4.—Velocity and pressures along axes and over surface of endless cylinder; graphs indicate theoretical values; circles indicate pressures measured at 40 miles per hour in 8-foot wind tunnel, United States Navy

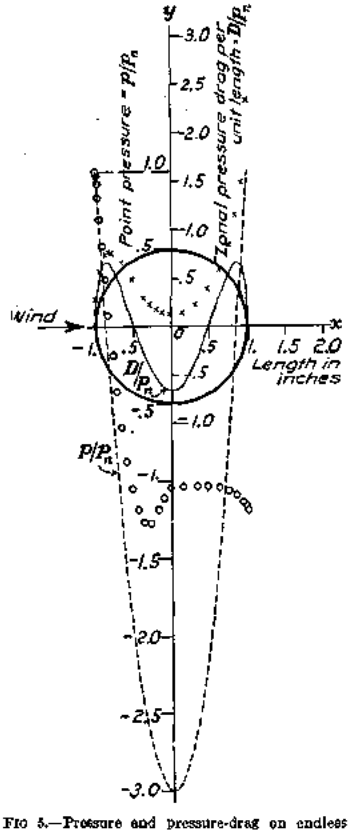

FIG 5.—Pressure and pressure-drag on endless cylinder. Graphs indicate theoretical values; circles indicate pressure p/p_n measured at 40 miles per hour; crosses indicate pressure-drag D/p_n computed from measured pressure

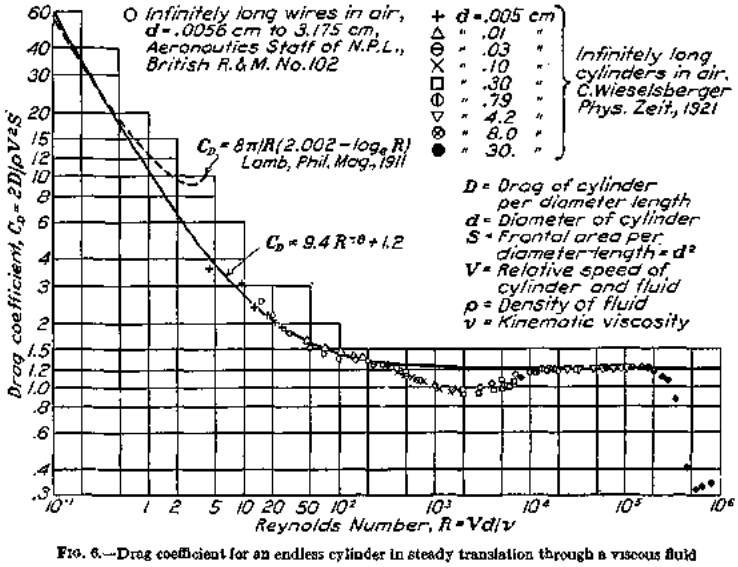

FIG. 6.—Drag coefficient for an endless cylinder in steady translation through a viscous fluid

This is $0, 2a/3$ (max.), $0, -2a/3$, for $\theta = 0°, 30°, 60°, 90°$; and is symmetrical about the equatorial plane $x=0$. In Figure 5, the little crosses give D/p_n for the measured pressures, and show total $D/p_n = 2.33a$.

Figure 6 delineates the drag coefficient C_D plotted against $R = 2\,aq_0/\nu$, from Wieselsberger's (Reference 1) wind tunnel tests of nine endless cylinders held transverse to the steady flow. The faired line is the graph of

$$C_D = 9.4R^{-.6} + 1.2, \tag{10}$$

an empirical equation devised by the present writer.

For very low values of R, Lamb derives the formula

$$C_D = \frac{8}{(2.002 - \log_e R)R}, \tag{11}$$

whose graph in Figure 6 nearly merges with (10) at $R = .3$.

For $15000 < R < 200000$, Figure 6 gives $C_D = 1.2$; hence the drag per unit frontal area is

$$D = 1.2p_n, \tag{12}$$

which is 2.4 times that for the sphere, given by (7).

THE ELLIPTIC CYLINDER

An endless elliptic cylinder held transverse to the stream, as shown in Table I, gives for points on x, y and on its surface,

$$q_x = (1-n)q_0, \qquad q_y = (1+m)q_0, \qquad q_t = (1 + b/a)q_0 \sin\theta, \tag{13}$$

where m, n are as in Table I. Amidships $q_t = (1 + b/a)q_0 = 2q_0$ for $a = b$, as given by (8). Graphs of (13) are given in Figure 7.

To find a', b' for plotting (13), assume a' and with it as radius strike about the focus an arc cutting y. The cutting point is distant b' from the origin. Otherwise, $b' = \sqrt{a'^2 - c^2}$, where $c^2 = a^2 - b^2 = \text{const.}$

With $a/b = 4$ one plots p/p_n in Figure 7, as explained for the sphere. The circles give the experimental p/p_n for an endless 2-inch by 8-inch strut, at zero pitch and yaw, in a tunnel wind at 40 miles an hour. The theoretical and measured pressures agree nicely for all points before, abreast, and well behind the cylinder.

Again, $\sin^2\theta = a^2y^2/(b^4 + c^2y^2)$, if $c^2 = a^2 - b^2$. Hence on the model

$$p/p_n = 1 - q_t^2/q_0^2 = 1 - \frac{(a+b)^2y^2}{b^4 + c^2y^2}. \tag{14}$$

This gives the zonal pressure drag, $D = 2\int_0^y p\,dy$, per unit length of cylinder, or

$$D/p_n = 2y - 2(a+b)^2 \int_0^y \frac{y^2\,dy}{b^4 + c^2y^2} = -4b\frac{a+b}{c^2}y + 2b^2\frac{(a+b)^2}{c^3}\tan^{-1}\frac{cy}{b^2}. \tag{15}$$

whose graph, for $a/b=4$, appears in Figure 8. It rises from 0 at the nose to its maximum where $p=0$, then falls to its minimum amidships.

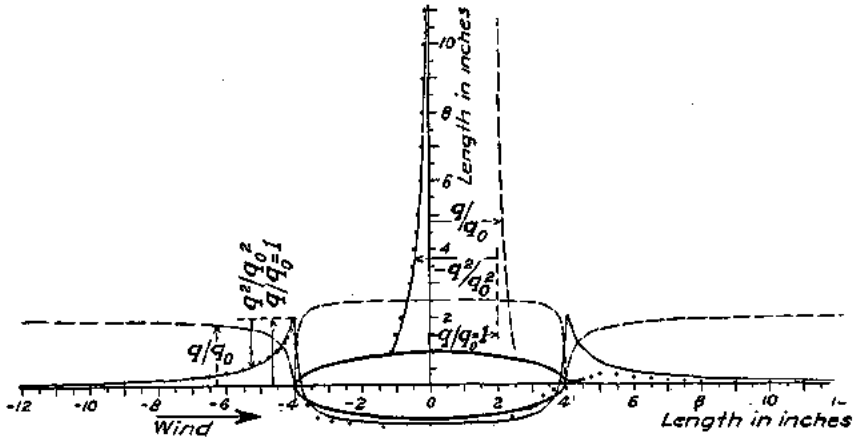

FIG. 7.—Velocity and pressure along axes and over surface of endless elliptic cylinder. Graphs indicate theoretical values; circles indicate pressure measured at 40 miles per hour in 8-foot wind tunnel, United States Navy

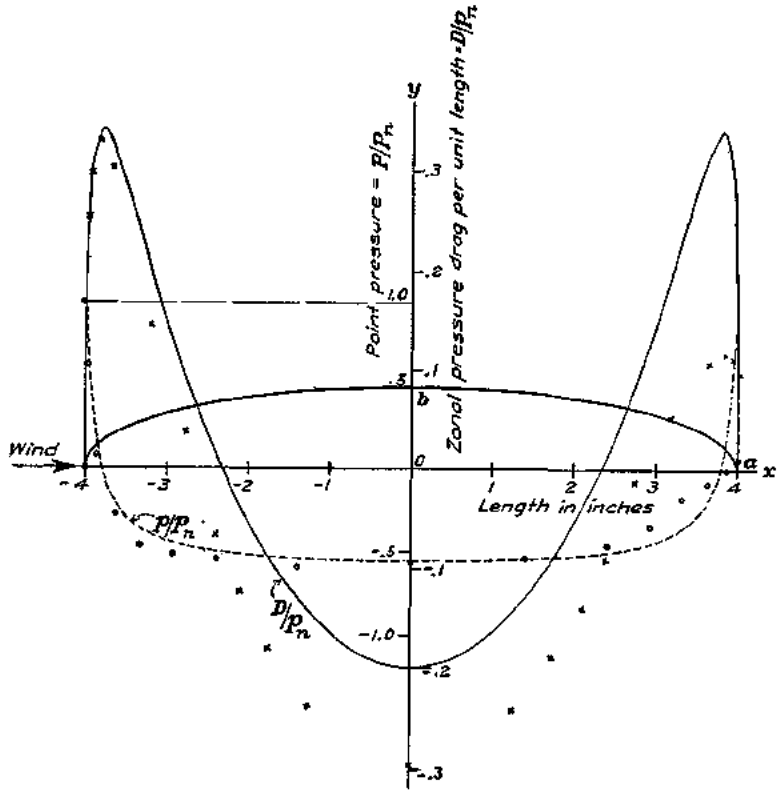

FIG. 8.—Pressure and pressure-drag on endless elliptic cylinder. Graphs indicate theoretical values; circles indicate pressure p/p_n measured at 40 miles per hour; crosses indicate pressure-drag D/p_n computed from measured pressure

Whatever the value of a/b, the whole pressure on the front half is negative or upstream, as for the sphere and round cylinder, and is balanced by the rear drag. For b fixed it decreases indefinitely with b/a.

The crosses marking actual values of D/p_n found in said test show a downstream resultant D. In fact, it is one-third the whole measured drag of pressure plus friction, or one-half the friction drag.

For the cylinder held broadside on, $b>a$ and $a^2-b^2=-c^2$, hence changing c^2 to $-c^2$ under the integral sign of (15), we find

$$D/p_n=-4b\frac{a+b}{c^2}y-b^2\frac{(a+b)^2}{c^3}\log_e\frac{b^2+cy}{b^2-cy}, \tag{16}$$

where now $c^2=b^2-a^2$. With b fixed, the upstream pressure drag on the front half increases with b/a, becoming infinite for a thin flat plate. It is balanced by a symmetrical drag back of the plate.

Such infinite forces imply infinite pressure change at the edges where, as is well known, the velocity can be $q=\sqrt{2p_r/\rho}=\infty$, in a perfect liquid whose reservoir pressure is $p_r=\infty$. Otherwise viewed, the pressure is p_r at the plate's center (front and back) and decreases indefinitely toward the edges, thus exerting an infinite upstream push on the back and a symmetrical downstream push on the front. In natural fluids no such condition can exist.

THE PROLATE SPHEROID

A prolate spheroid, fixed as in Table I, gives for points on x, y and the solid surface, respectively, the flow speeds

$$q_x=(1-n)q_0, \qquad q_y=(1+m)q_0, \qquad q_l=(1+k_a)\,q_0\sin\theta, \tag{16}$$

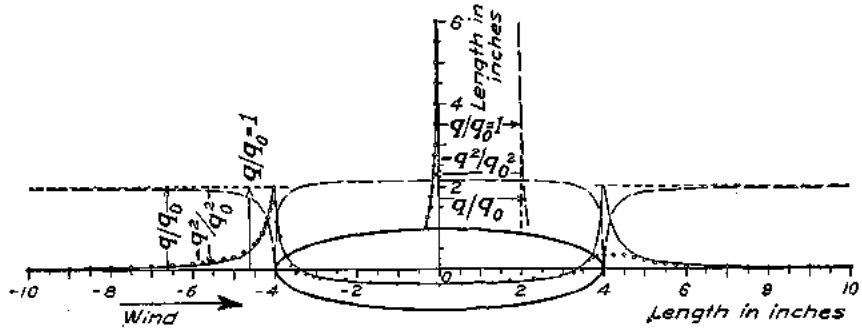

FIG. 9.—Velocity and pressure along axes and over surface of prolate spheroid. Graphs indicate theoretical values; circles indicate pressures measured at 40 miles per hour in 8-foot wind tunnel, United States Navy; dots give pressures found with an equal model in British test, R. and M. No. 600, British Advisory Committee for Aeronautics

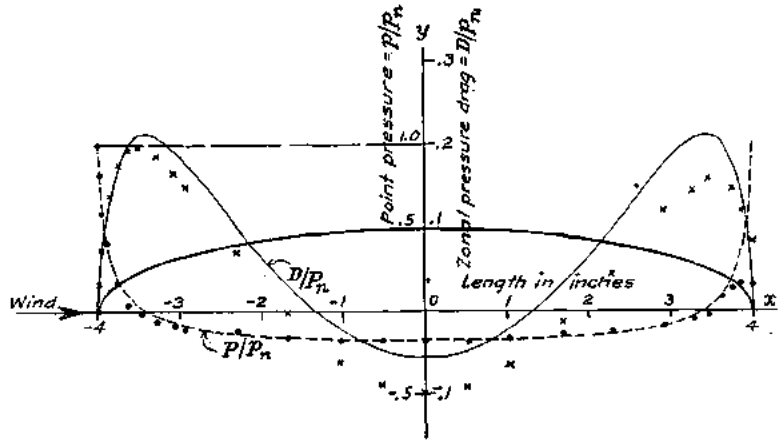

FIG. 10.—Pressure and pressure-drag on prolate spheroid. Graphs indicate theoretical values; dots indicate measured pressure p/p_n from Figure 9; crosses indicate pressure-drag D/p_n computed from measured pressure

where k_a is to be taken from Table II. Graphs of (16) are given in Figure 9, for a model having $a/b = 4$, viz., $k_a = 0.082$.

For this surface p/p_n plots as in Figure 10. For a 2 by 8 inch brass model values of p/p_n are shown by circles for a test at 40 miles an hour in the United States Navy tunnel; by dots for a like test in a British tunnel. (Reference 2.)

By (16), for points on the surface $p/p_n = 1 - q_t^2/q_0^2 = 1 - (1+k_a)^2 \sin^2\theta$. From this, since $\sin^2\theta = a^2y^2/(b^4 + c^2y^2)$, the zonal pressure drag $\int p.\, 2\pi y\, dy$ is found. Thus

$$D/p_n = \pi y^2 - \frac{\pi a^2}{c^2}(1+k_a)^2 y^2 + \frac{\pi a^2 b^4}{c^4}(1+k_a)^2 \log. \frac{b^4 + c^2y^2}{b^4}. \tag{17}$$

Starting from $y=0$, D/p_n increases to its maximum when $p=0$, or $\sin\theta = 1/(1+k_a)$; then diminishes to its minimum for $y=b$. Figure 10 gives the theoretical and empirical graphs of D/p_n for $a/b=4$.

For b fixed the upstream drag on the front half decreases indefinitely with b/a, becoming zero for infinite elongation.

OBLATE SPHEROID

The flow velocity about an oblate spheroid with its polar axis along stream is given by formulas in Table I, and plotted in Figure 11, together with computed values of p/p_n. No determinations of p or D were made for an actual flow. The formula for D/p_n is like (17), except that $c^2 = b^2 - a^2$, and k_a is larger for the oblate spheroid, as seen in Table II. For b fixed the upstream drag on the front half increases indefinitely with b/a.

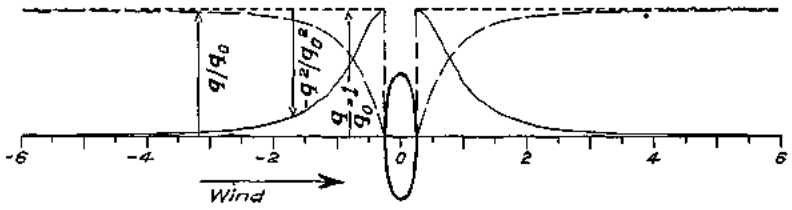

FIG. 11.—Theoretical velocity and pressure along x axis of oblate spheroid. Diameter/thickness = 4

CIRCULAR DISK

The theoretical flow speeds and superpressures for points on the axis of a circular disk fixed normal to a uniform stream of inviscid liquid are plotted in Figure 12, without comparative data from a test. One notes that the formulas are those for an oblate spheroid with eccentricity $e = 1$.

For $1500 < q_0\, a/\nu < 500000$, Wieselsberger (Reference 3) finds for the air drag of a thin normal disk, of area S,

$$D = 1.1\, p_n S, \tag{18}$$

or 2.2 times that for a sphere. For aq_0/ν extremely small, theory gives

$$D = 5.1\, \pi\, \mu\, a\, q_0, \tag{19}$$

as is well known. Test data for a complete graph, including these extremes, are not yet available.

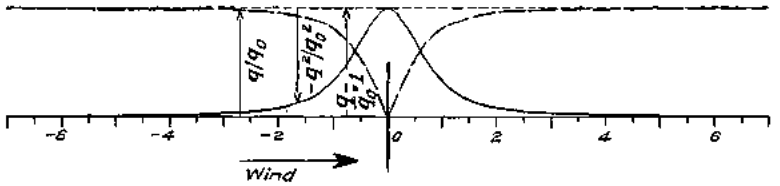

FIG. 12.—Theoretical pressure and velocity along axis of disk

REGIONS OF EQUAL SPEED

In the flow field q, p are constant where $q_t^2 + q_n^2 = \text{constant}$, viz. where

$$q^2/q_0^2 = (1+m)^2 \sin^2\theta + (1-n)^2 \cos^2\theta = \text{const.} \tag{20}$$

In particular for the region $q = q_0$, this becomes

$$\tan^2\theta = \frac{n}{m}\frac{2-n}{2+m} = \frac{a'^4}{b'^4}\tan^2\beta^* \tag{21}$$

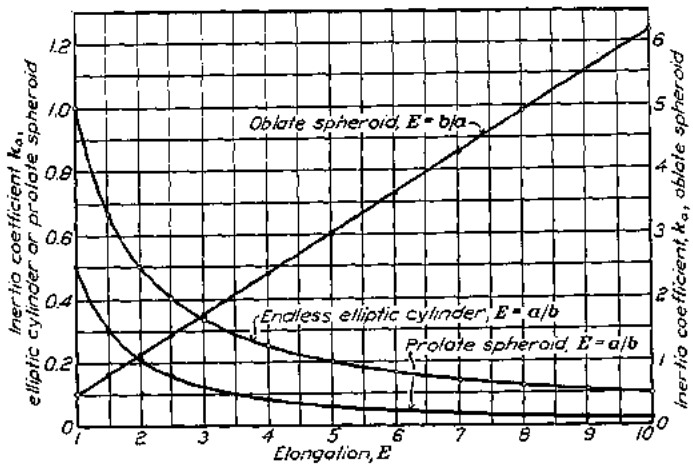

FIG. 13.—Inertia coefficient vs. elongation. Plotted from Table II

which applies to all the quadrics in Table I. Clearly $\tan\theta = 0$ for $n = 2$; $\tan^2\theta = n/m$ for m, $n = 0$, viz. for all distant points of (21). For these points the normal to any confocal ellipse lies along the radius vector and asymptote of (21), as seen in Figures 14 to 17.

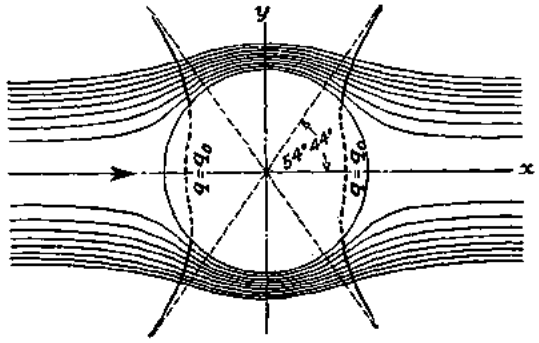

FIG. 14.—Lines of steady flow, lines of constant speed and pressure, for infinite frictionless liquid streaming past a sphere

For the sphere $n = 2m = a^3/r^3$; hence (21) becomes

$$\tan^2\theta = 2\frac{2r^3 - a^3}{2r^3 - .5a^3} \tag{22}$$

where $r = a' = \sqrt{x^2+y^2}$. The form of this is depicted in Figure 14.

* $\tan\beta = y/x$ is the slope of a radial line through the point (x, y) where (21) cuts a confocal curve $a'b'$, of Table I. Knowing a', b', β, to locate (x, y) draw across the radial line an arc of $a'b'$ by sliding along the x, y axes a straightedge subdivided as in the ellipsograph. The operation is rapid and easy.

For a round cylinder $n = m = a^2/r^2$; hence

$$\tan^2\theta = \frac{2r^2 - a^2}{2r^2 + a^2} \text{ or, } 2r^2 = a^2 \sec 2\theta, \tag{23}$$

which is the section of a hyperbolic cylinder, as in Figure 15.

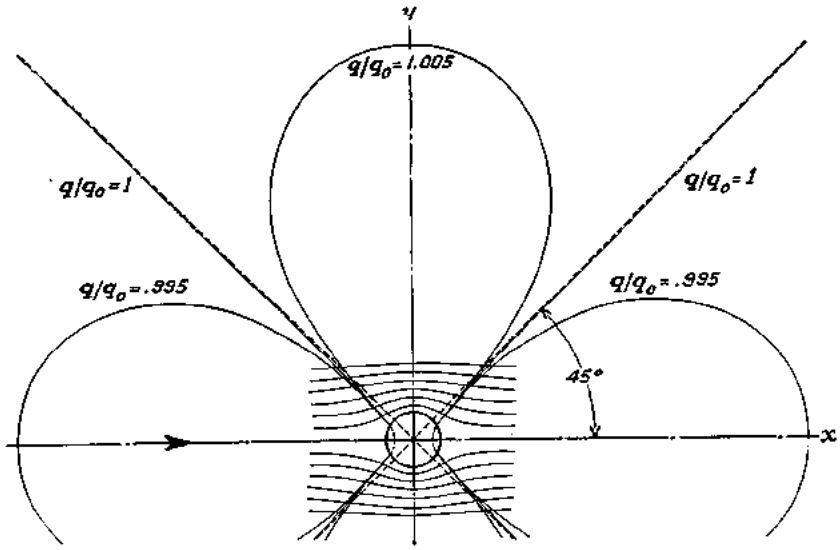

FIG. 15.—Lines of steady flow, lines of constant speed and pressure, for infinite frictionless liquid streaming across endless round cylinder

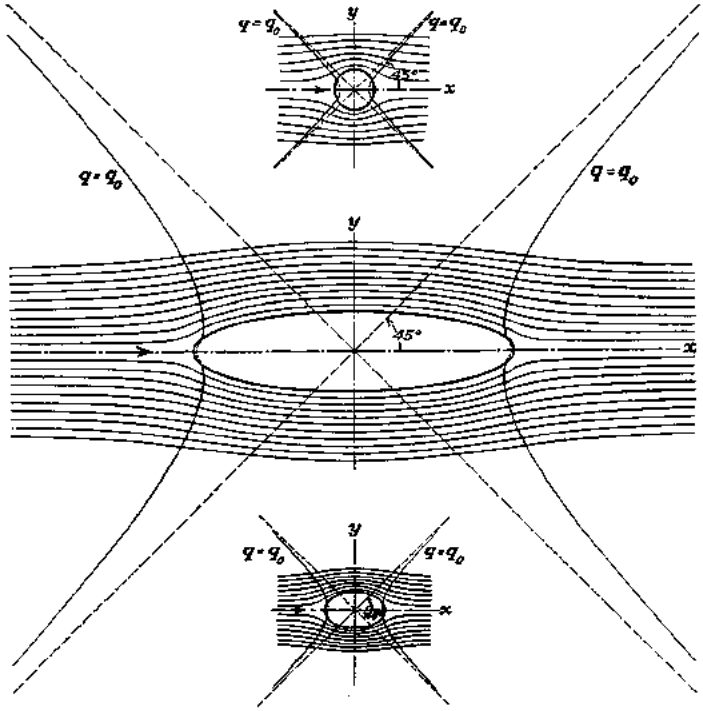

FIG. 16.—Lines of steady flow, lines of constant speed and pressure, for infinite frictionless liquid streaming across endless elliptic cylinder

A plot of (21) for an elliptic cylinder, fixed as shown in Table I, is given in Figure 16; for a prolate spheroid in Figure 17.

Besides the region (21), having $q=q_o$, it is useful to know the limit of perceptible disturbance say where $q^2/q_o^2=1\pm.01$. This in (20) gives

$$(1+m)^2\sin^2\theta+(1-n)^2\cos^2\theta=1\pm.01, \tag{24}$$

which applies to all the quadrics here studied. Hence

$$\tan^2\theta=\frac{n}{m}\frac{2-n}{2+m}\pm\frac{0.01}{m(2+m)\cos^2\theta}, \tag{25}$$

A graph of (25) for a round cylinder is shown in Figure 15. Like plots for the other quadrics

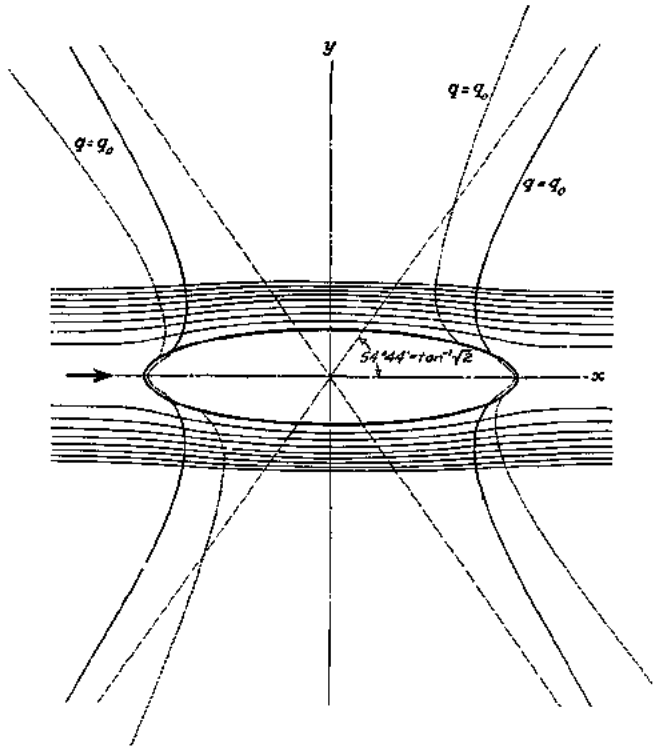

FIG. 17.—Lines of steady flow, lines of constant speed and pressure, for infinite frictionless liquid streaming past a prolate spheroid. Full-line curve $q=q_o$ refers to stream parallel to x; dotted curve $q=q_o$ refers to stream inclined 10° to x

If in (20) a series of constants be written for the right member, the graphs compose a family of lines of equal velocity and pressure, covering the entire flow field. Rotating Figures 14, 17 about x gives surfaces of $q=q_o$.

COMPARISON OF SPEEDS

Before all the fixed models the flow speed is q_o at a great distance and 0 at the nose; abreast of them it is q_o at a distance, and $(1+k_a)q_o$ amidships.

The flux of $q-q_o$ through the equatorial plane obviously must equal q_oS where S is the body's frontal area. Hence two bodies having equal equators have the same flux q_oS, and the same average superspeed or average $q-q_o$. But the longer one has the lesser midship speed;

hence its outboard speed wanes less rapidly with distance along y. A like relation obtains along x from the nose forward. These relations are shown in the velocity graphs of Figures 18 and 19. A figure similar to 18, including many models, is given in Reference 4.

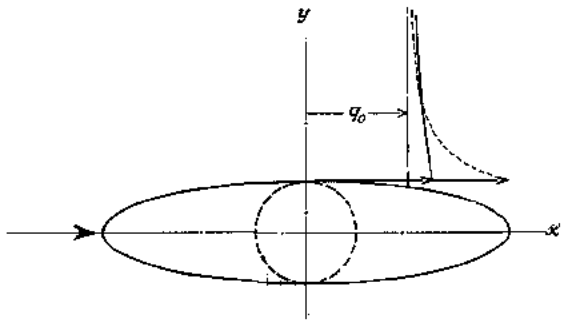

FIG. 18.—*Superposed graphs of flow speed abreast of endless round and elliptic cylinders of same thickness fixed transverse to an infinite stream of inviscid liquid. At great distance flow speed is q_0.*

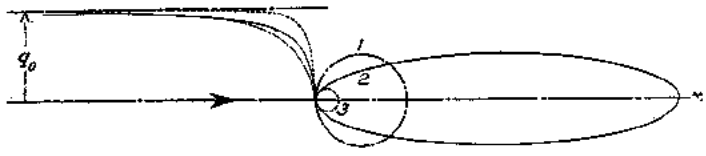

FIG. 19.—*Superposed graphs of axial flow speed before three endless cylinders 1, 2, and 3 (3 osculating 2), each fixed transverse to an infinite stream of inviscid liquid. At great distance flow speed is q_0.*

COMPARISON OF PRESSURES

The foregoing speed relations determine those of the pressures. The nose pressures all are $p_n = \rho q_0^2/2$; the midship ones are $p = p_n - (1+k_a)^2 p_n$. The drag on the front half of the model is upstream for all the quadrics here treated; it increases with the flatness, as one proves by (15), (17), and is infinite for the normal disk and rectangle.

APPLICATION OF FORMULAS

The ready equations here given, aside from their academic interest in predicting natural phenomena from pure theory, are found useful in the design of air and water craft. The formula for nose pressure long has been used. That for pressure on a prolate spheroid, of form suitable for an airship bow, is so trustworthy as to obviate the need for pressure-distribution measurements on such shapes. The same may be said of the fore part of well-formed torpedoes deeply submerged. The computations for stiffening the fore part of airship hulls can be safely based on theoretical estimates of the local pressures. The velocity change, well away from the model, especially forward of the equatorial plane, can be found more accurately by theory than by experiment. The equation (21) of undisturbed speed shows where to place anemometers to indicate, with least correction, the relative speed of model and general stream.

REFERENCES

1. WIESELSBERGER, C.: Physicalische Zeitschrift, vol. 22. 1921.
2. JONES, R., and WILLIAMS, D. H.: The distribution of pressure over the surface of airship model U. 721, together with a comparison with the pressure over a spheroid. Brit. Adv. Com. for Aeron. Reports and Memoranda No. 600. 1919.
3. WIESELSBERGER, C.: Physicalische Zeitschrift, vol. 23. 1922.
4. TAYLOR, D. W.: Speed and Power of Ships, gives a figure similar to 18 but including more models. 1910.

SYMBOLS USED IN TEXT

x, y ..... Cartesian coordinates; also axes of same.
r, β ..... Polar coordinates.
α ..... Angle of attack of uniform stream.
s ..... Length of arc, increasing with β.
θ ..... Inclination to x of normal to confocal curves in Table I.
φ ..... Velocity function.
ψ ..... Stream function.
q ..... Resultant velocity at any point of fluid.
q_o ..... Velocity of distant fluid (parallel to x axis).
q_x, q_y ..... Velocity at points on x and y axes (parallel to x axis).
q_t ..... Velocity along confocal surface or model surface.
q_n ..... Velocity normal to confocal surface.
ρ ..... Density of fluid.
μ ..... Viscosity.
ν ..... Kinematic viscosity.
p_n ..... Nose pressure $=\rho q_o^2/2$.
p_o ..... Pressure in distant fluid.
p ..... Superstream pressure anywhere.
D_x ..... Zonal pressure drag $=\int p\,dy\,dz$.
D ..... Whole drag.
S ..... Frontal area of model.
C_D ..... Drag coefficient $=D/p_nS$.
R ..... Reynolds number.
a ..... Radius of sphere, cylinder.
a, b ..... Semiaxes of ellipse.
a', b' ..... Semiaxes of confocal ellipse.
e ..... Eccentricity of ellipse.
e' ..... Eccentricity of confocal ellipse.
c ..... Focal distance $=ae=a'e'=\sqrt{a^2-b^2}$
k_a ..... Inertia factor (Table II).
m, n, m_s ..... Quantities defined in Tables I, II.
ϵ ..... Colatitude (see equation 30).

TABLE I

Flow functions for simple quadrics fixed in a uniform stream of speed q_o along x positive

Symbol definitions	Form of quadric	Value of functions at any confocal surfaces of semiaxes a', b'		
		Velocity function φ	Stream function ψ	Component velocities q_t, q_n
See diagram A (fig. 20)	Sphere	$\varphi=-(1+m)\,q_o x$, where $m=\frac{a^3}{2a'^3}$	$\psi=-\frac{1}{2}(1-n)\,q_o y^2$, where $n=\frac{a^3}{a'^3}$	Differentiation along arc s of either figure gives: $q_t=\frac{\partial\varphi}{\partial x}\frac{dx}{ds}=(1+m)\,q_o \sin\theta$, valid for all the figures; $q_n=\frac{\partial\psi}{\partial y}\frac{dy}{ds}=-(1-n)\,q_o \cos\theta$, for the cylinders; $q_n=\frac{1}{y}\frac{\partial\psi}{\partial y}\frac{dy}{ds}=-(1-n)\,q_0\cos\theta$, for the axial surfaces; viz., sphere, spheroids, disk. For a', $b'=a$, b, Table II gives m_s; whence $q_t=(1+m_s)\,q_o \sin\theta$, as the flow velocity on a fixed quadric surface. $q_n=\pm 0$ for disk, since $n=1$. *Remark*—both q_t, q_n can be derived from either φ or ψ. If q_t, q_n=max. q_t, q_n on $a'b'$, at any other point thereof $q_t=q_t \sin\theta$, $q_n=\overline{q}_n\cos\theta$
	Circular cylinder	$\varphi=-(1+m)\,q_o x$, $m=\frac{a^2}{a'^2}$	$\psi=-(1-n)\,q_o y$, $n=\frac{a^2}{a'^2}$	
See diagram B (fig. 20)	Elliptic cylinder	$\varphi=-(1+m)\,q_o x$, $m=\frac{b}{a'}\frac{a+b}{a'+b'}$	$\psi=-(1-n)\,q_o y$, $n=\frac{b}{b'}\frac{a+b}{a'+b'}$	
	Prolate spheroid $e=\frac{1}{a}\sqrt{a^2-b^2}$	$\varphi=-(1+m)\,q_o x$, $m=-\frac{\log_e\frac{1+e'}{1-e'}-2e'}{\log_e\frac{1+e}{1-e}-\frac{2e}{1-e^2}}$	$\psi=-\frac{1}{2}(1-n)\,q_o y^2$, $n=\frac{\log_e\frac{1+e'}{1-e'}-\frac{2e'}{1-e'^2}}{\log_e\frac{1+e}{1-e}-\frac{2e^2}{1-e^2}}$	
See diagram C (fig. 20)	Oblate spheroid $e=\frac{1}{b}\sqrt{b^2-a^2}$	$\varphi=-(1+m)\,q_o x$, $m=-\frac{\frac{e'b'}{a'}-\sin^{-1}e'}{\frac{ea}{b}-\sin^{-1}e}$	$\psi=-\frac{1}{2}(1-n)\,q_o y^2$, $n=\frac{\frac{e'a'}{b'}-\sin^{-1}e'}{\frac{ea}{b}-\sin^{-1}e}$	
	Circular disk $a=0$, $e=1$	$\varphi=-(1+m)\,q_o x$, $m=\frac{2}{\pi}\left(\frac{b}{a'}-\sin^{-1}e'\right)$	$\psi=-\frac{1}{2}(1-n)\,q_o y^2$, $n=-\frac{2}{\pi}\left(\frac{a'b}{b'^2}-\sin^{-1}e'\right)$	

φ, ψ, in elliptic coordinates, can be found in textbooks; e. g., §§ 71,105,108, Lamb's Hydrodynamics, 4th Ed.

TABLE II

Inertia factors k_a* for quadric surfaces in steady translation along axis a in Figure 20

Elongation E	Elliptic cylinder, $E=a/b$ $k_a=\frac{b}{a}$	Prolate spheroid $E=a/b$ $k_a=-\frac{\log_e\frac{1+e}{1-e}-2e}{\log_e\frac{1+e}{1-e}-\frac{2e}{1-e^2}}$	Oblate spheroid $E=b/a$ $k_a=-\frac{eE^2-E\sin^{-1}e}{e-E\sin^{-1}e}$
1.00	1.000	0.500	0.500
1.50	.667	.305	.803
2.00	.500	.209	1.118
2.50	.400	.157	1.428
3.00	.333	.121	1.742
4.00	.250	.082	2.379
5.00	.200	.059	3.000
6.00	.167	.045	3.642
7.00	.143	.036	4.279
8.00	.125	.029	4.915
9.00	.111	.024	5.549
10.00	.100	.021	6.183
∞	.000	.000	∞

* In this table $k_a=m_a$ of Table I, viz, the value of m when a', $b'=a$, b. Lamb (R. and M. No. 623, Brit. Adv. Com. Aeron.) gives the numerical values in the third column above. For motion of elliptic cylinder along b axis inertia factor is $k_b=a/b$.

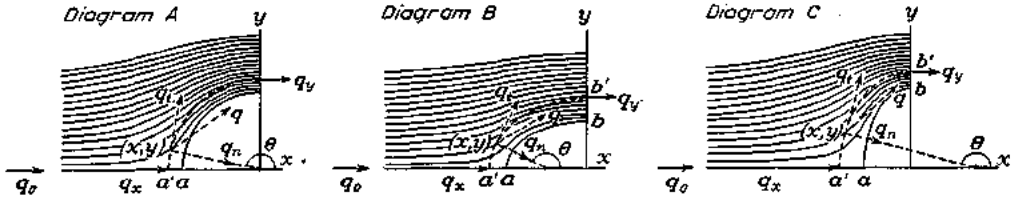

FIG. 20

VELOCITY AND PRESSURE IN OBLIQUE FLOW [2]

PRINCIPLE OF VELOCITY COMPOSITION

A stream q_0 oblique to a model can be resolved in chosen directions into component streams each having its individual velocity at any flow point, as in Figure 21. Combining the individuals gives their resultant, whence p is found.

VELOCITY FUNCTION

Let a uniform infinite stream q_0 of inviscid liquid flowing past a fixed ellipsoid centered at the origin have components U, V, W along x, y, z, taken parallel, respectively, to the semiaxes, a, b, c; then we find the velocity potential φ for q_0 as the sum of the potentials φ_a, φ_b, φ_c for U, V, W.

In the present notation textbooks prove, for any point (x, y, z) on the confocal ellipsoid a' b' c',

$$\varphi_a=-(1+m_a)Ux, \tag{26}$$

and give as constant for that surface

$$m_a=abc\left(1-abc\int_a^\infty\frac{da'}{a'^2\,b'\,c'}\right)^{-1}\int_\lambda^\infty\frac{da'}{a'^2\,b'\,c'}\ * \tag{27}$$

the multiplier of $\int_\lambda^\infty$ being constant for the model, and $\lambda=a'^2-a^2$. Adding to (26) analogous values of φ_b, φ_c gives

$$\varphi=-(1+m_a)Ux-(1+m_b)Vy-(1+m_c)Wz\equiv-(1+m)q_0h, \tag{28}$$

[2] This brief treatment of oblique flow was added by request after the preceding text was finished.

* Simple formulas for this integral and the corresponding b, c ones, published by Greene, R. S. Ed. 1833, are given by Doctor Tuckerman in Report No. 210 of the National Advisory Committee for Aeronautics for 1925. Some ready values are listed in Tables III, IV.

where h is the distance of (x, y, z) from the plane $\varphi=0$, and m_a, m_b, m_c, m are generalized inertia coefficients of $a'\ b'\ c'$ for the respective streams U, V, W, q_0. For the model itself the inertia coefficients usually are written k_a, k_b, k_c, k. The direction cosines of h are

$$L=\frac{1+m_a}{1+m}\frac{U}{q_0},\quad M=\frac{1+m_b}{1+m}\frac{V}{q_0},\quad N=\frac{1+m_c}{1+m}\frac{W}{q_0}, \tag{29}$$

as appears on dividing (28) by $(1+m)q_0$, the resultant of $(1+m_a)U$, $(1+m_b)V$, $(1+m_c)W$.

EQUIPOTENTIALS AND STREAMLINES

On $a'\ b'\ c'$ the plane sections $\varphi=$constant are equipotential ellipses parallel to the major section $\varphi=0$, and dwindling fore and aft to mere points, which we call stream poles, where the plane (28) is tangent to $a'\ b'\ c'$. If ϵ is the angle between any normal to $a'\ b'\ c'$ and the polar

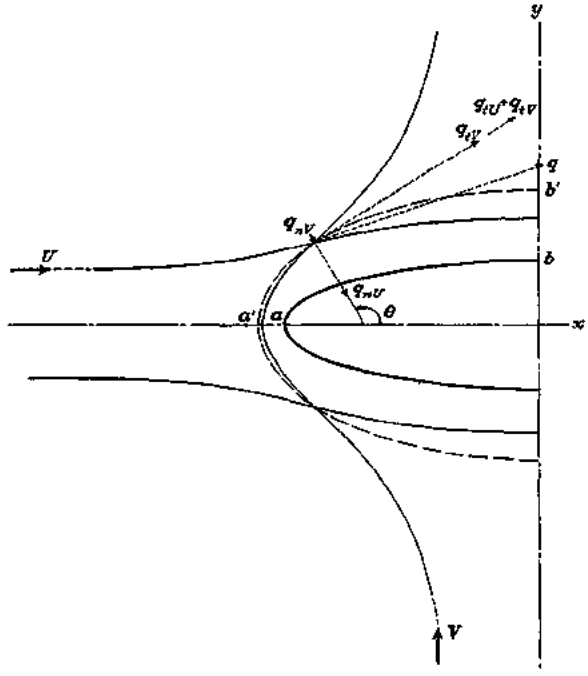

FIG. 21.—Superposition of streamline velocities for component plane flows parallel to axes of elliptic cylinder

normal, whose direction cosines are L, M, N, we call the line $\epsilon=$const. a line of stream latitude. Thus ϵ is the colatitude or obliquity of a surface element of $a'\ b'\ c'$. The line $\epsilon=90°$ is the stream equator. This latter marks the contact of a tangent cylinder parallel to the polar normal, viz, perpendicular to the plane (28), as in Figure 22. If l, m, n are the direction cosines of any normal to $a'\ b'\ c'$

$$\cos\epsilon=lL+mM+nN. \tag{30}$$

Since the streamlines all cut the equipotentials squarely,[3] the polar streamline must run continuously normal to the family of confocal ellipsoids $a'\ b'\ c'$. Hence it forms the intersection of a pair of confocal hyperboloids, and at infinity asymptotes a line parallel to q_0 through the origin. This straight line may be called the stream axis. Its equation is $x:y:z=U:V:W$.

[3] On the model, therefore, the streamlines are longitude lines, viz. orthogonals to the latitude lines.

COMPONENT VELOCITIES

At any point of any confocal surface $a'\ b'\ c'$ the streamline velocity q, perpendicular to the equipotential ellipse there, has components q_n, q_t, respectively, along the surface normal n and the tangent s in the plane of q and n. By (28) we have

$$q_t = \frac{\partial \varphi}{\partial h}\frac{dh}{ds} = \bar{q}_t \sin \epsilon, \tag{31}$$

where $-\partial\varphi/\partial h = (1+m)q_0 \equiv \bar{q}_t = \max.$ q_t, is the equatorial velocity. By (26) the inward normal velocity due to φ_a is

$$-\frac{\partial}{\partial_n}(1+m_a)\,\overline{Ux} = -l(1-n_a)\,U, \tag{32}$$

n_a being constant on $a'\ b'\ c'$, as may be shown. Similarly, φ_b, φ_c contribute $-m(1-n_b)\,V$, $-n(1-n_c)\,W$; hence the whole normal component is

$$q_n = -l(1-n_a)\,U - m(1-n_b)\,V - n(1-n_c)\,W = \bar{q}_n \cos \epsilon, \tag{33}$$

where $\bar{q}_n = [(1-n_a)^2 U^2 + (1-n_b)^2 V^2 + (1-n_c)^2 W^2]^{.5} = \max.$ q_n is the normal velocity at the stream poles. Some values of n_a, n_b are given in Tables I, III. One also may find (33) as the normal derivative of (28).

We now state (28): At any point of $a'\ b'\ c'$ the velocity potential equals $\bar{q}_t h$, the equatorial speed times the distance from the plane of zero potential. Similarly (31) (33) state: At any point of $a'\ b'\ c'$ the tangential speed ($\bar{q}_t \sin \epsilon$) equals the equatorial speed times the sine of the obliquity; the normal speed ($\bar{q}_n \cos \epsilon$) equals the polar speed times the cosine of the obliquity. This theorem applies to all the confocals, even at the model where $q_n = 0$.[4]

Incidentally the normal flux through $a'\ b'\ c'$ is $\int \bar{q}_n \cos \epsilon \cdot dS = \bar{q}_n \int dS_\phi$, where S_ϕ is the projection of S on the plane of $\phi = \text{const.}$ and equals the cross section of the tangent cylinder. The whole flux through $a'\ b'\ c'$ is therefore zero, as should be.

POLAR STREAMLINE

Some of the foregoing relations are portrayed in Figure 22 for a case of plane flow. Noteworthy is the polar streamline or hyperbola. Starting at infinity parallel to q_0, the polar filament runs with waning speed normally through the front poles of the successive confocal surfaces; abuts on the model at its front pole, or stop point; spreads round to the rear pole; then accelerates downstream symmetric with its upstream part. Its equation $q_t = 0 = \partial\phi/\partial s$ can be written from (28)

$$q_t = (1+m_a)\,U \sin \theta - (1+m_b)\,V \cos \theta = 0, \text{ or } \tan \theta = \frac{1+m_b}{1+m_a}\frac{V^*}{U} \tag{34}$$

This asymptotes the stream axis $y/x = V/U$; for at infinity m_a, $m_b = 0$, and $\tan \theta = V/U$. Plane-flow values of m_a, m_b are given in Tables I, III.

All the confocal poles are given by (34); those of the model are at the stops where

$$\tan \theta = \frac{1+k_a}{1+k_b}\frac{V}{U} = \frac{a^2}{b^2}\frac{y}{x}. \tag{37}$$

Thus on an elliptic cylinder they are where $y/x = b^3/a^3$. V/U; on a thin lamina they are at $x = \pm c \cos \alpha$, as given in the footnote. Tables II, IV give values of k_a, k_b.

---

[4] An analogous theorem obtains also for any other uniform steady stream, say of heat or electricity, that has zero normal component at the boundary ellipsoid and zero concentration in the flow field.

[5] To graph (34) we may use the known relations,

$$\tan \theta = \frac{a'^2}{b'^2}\frac{y}{x} = \frac{a'}{b'}\tan \alpha, \tag{35}$$

where $\tan \alpha = V/U$ is the slope of q_0 or the asymptote to (34). Thus (34) becomes $a'/b' = (1+m_b)/(1+m_a)$, which with the tabulated values of m_a, m_b, reduces to

$$\frac{x}{c^2 \cos^2 \alpha} - \frac{y^2}{c^2 \sin^2 \alpha} = 1, \tag{36}$$

a hyperbola whose semiaxes are $c \cos \alpha$, $c \sin \alpha$, c being the focal distance. In this treatment $x = a' \cos \alpha$, $y = b' \sin \alpha$, α being a fixed eccentric angle of the successive confocal ellipses.

Each angle of attack has its own flow pattern; each its polar streamline given by (34). A close-graded family of confocal ellipses and hyperbolas therefore portrays all the poles and polar streamlines in the plane ab for all angles of attack. The family can be written

$$x = a' \cos \alpha, \qquad y = b' \sin \alpha. \tag{38}$$

Thus, giving a', b' a set of fixed values, then α a set, we have the confocal families

$$\frac{x^2}{a'^2} + \frac{y^2}{b'^2} = 1. \qquad \frac{x^2}{c^2 \cos^2 \alpha} - \frac{y^2}{c^2 \sin^2 \alpha} = 1. \tag{39}$$

the first being ellipses, the second hyperbolas like (36) below.

Similarly, the locus $q_n = 0$, or $q = \bar{q}_t$, is written from (33). With $W = 0$,

$$\tan \theta = -\frac{1 - n_a}{1 - n_b} \frac{U}{V}. \tag{40}$$

Its discussion is of minor interest.

DRAG AND MOMENT

Formulas for the pressure p all over the simple quadrics here treated are well known, for oblique as well as axial flow, and serve to find the drag and moment. For uniform flow the resultant drag is zero; its zonal parts can be found as heretofore. The moment about z is the surface integral of $p(y\,dy\,dz - x\,dx\,dz)$, and generally is not zero.

REGIONS OF EQUAL SPEED ABOUT OBLIQUE MODELS

Compounding the velocities (31), (33) at any point in the ab plane, as in Figure 22, gives for q constant

$$q^2 = [(1 + m_a) U \sin \theta - (1 + m_b) V \cos \theta]^2 + [(1 - n_a) U \cos \theta + (1 - n_b) V \sin \theta]^2 = \text{const.} \tag{41}$$

In particular for $q^2 = U^2 + V^2$ (41) gives

$$\tan \theta = \frac{K}{B} (A \pm \sqrt{BC + A^2}) = \frac{a'^2}{b'^2} \tan \beta. \tag{42}$$

where $K = V/U$, and

$$A = (1 + m_a)(1 + m_b) - (1 - n_a)(1 - n_b), B = m_a(2 + m_a) - n_b(2 - n_b) K^2, C_D = \frac{n_a(2 - n_a)}{K^2} - m_b(2 + m_b).$$

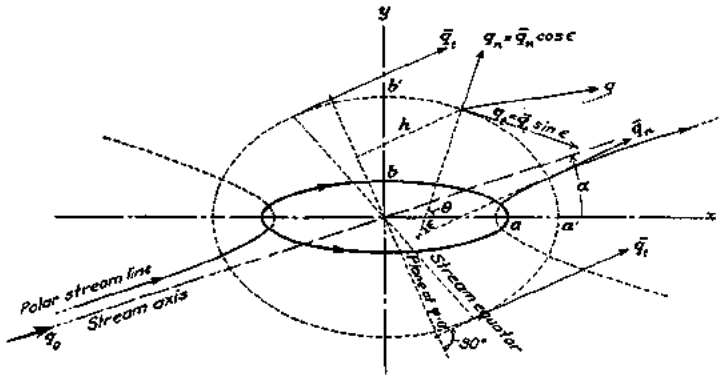

FIG. 22.—Polar streamline and component velocities for uniform stream of inviscid liquid about oblique elliptic cylinder

For an elliptic cylinder, as is well known.

$$m_a = \frac{b}{a'} \frac{a + b}{a' + b'}, \qquad n_a = \frac{b}{b'} \frac{a + b}{a' + b'}, \qquad m_b = \frac{a}{b'} \frac{a + b}{a' + b'}, \qquad n_b = \frac{a}{a'} \frac{a + b}{a' + b'},$$

which determines A, B, C, and thence β in terms of a' b'. Thus, for an endless elliptic cylinder of semiaxes $a = 4$, $b = 1$, yawed 10° to the stream, i. e., $V/U = \tan 10° = .1763$, the graph of (42) has the form shown full line in Figure 23. This graph takes the dotted form when $V = 0$, $q_0 = U$.

For a prolate spheriod of semiaxes $a=4$, $b=1$, yawed 10°, the graph of (42) is shown in Figure 17.

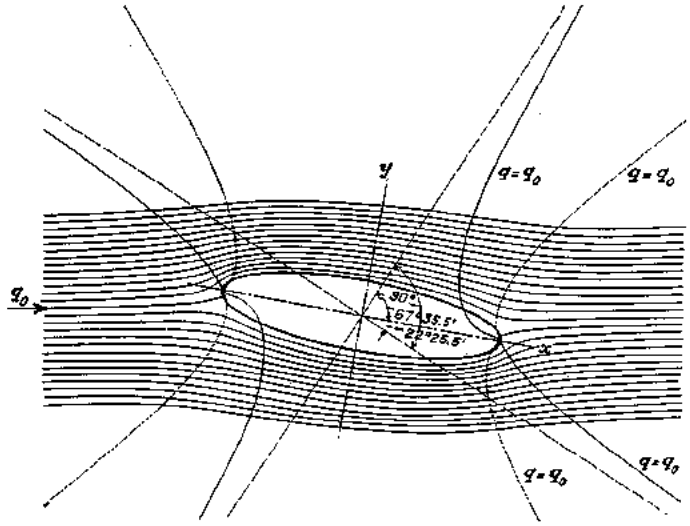

FIG. 23.—Lines of steady flow, lines of constant speed and pressure, for infinite frictionless liquid streaming across endless elliptic cylinder. Dotted curve refers to stream parallel to x; full-line curve $q=q_0$ refers to stream inclined 10° to x

The two values of tan β in (42) are

$$\tan\beta_1=\frac{K}{B}(A+\sqrt{BC+A^2}),\qquad \tan\beta_2=\frac{K}{B}(A-\sqrt{BC+A^2}),\tag{43}$$

from which are readily derived

$$\tan(\beta_1-\beta_2)=\frac{2K\sqrt{BC+A^2}}{B-K^2C},\qquad \tan(\beta_1+\beta_2)=\frac{2KA}{B+K^2}.\tag{44}$$

(43) give the x-ward inclinations β_1, β_2, of the asymptotes of the curves $q=q_0$. As can be proved, the interasymptote angle $\beta_1-\beta_2$ remains constant as $K(=V/U)$ varies and the asymptotes rotate through $\frac{1}{2}(\beta_1+\beta_2)$ about the c axis.

Thus, with an elliptic cylinder, giving A, B, C their values at ∞ makes

$$\tan(\beta_1-\beta_2)=\infty,\qquad \tan(\beta_1+\beta_2)=\frac{K(a+b)}{b-aK^2};\tag{45}$$

hence the asymptotes continue rectangular, as in Figure 23, while with varying angle of attack they rotate through $\frac{1}{2}(\beta_1+\beta_2)$. Or more generally one may show that $\frac{d}{da}(\beta_1-\beta_2)=0\therefore\beta_1-\beta_2=$ const.

A similar treatment applies to the other figures of Table III. For all the cylinders the interasymptote angle is 90°; for the spheroids it is $2\tan^{-1}\sqrt{2}=109°-28'$ in the ab plane. Figure 17 is an example. If the flow past the spheroids is parallel to the bc plane the interasymptote angle for the curves $q=q_0$ in that plane is obviously unaffected by stream direction. It is 90° for infinitely elongated spheroids; 109°−28′ for all others. Excluded from the generalizations of this paragraph are the infinitely thin figures, such as disks and rectangles edgewise to the stream, that cause no disturbance of the flow. Passing to three dimensions, we note that the asymptotic lines form asymptotic cones having their vertex at the origin.

42488—27——35

SUMMARY

For an infinite inviscid liquid streaming uniformly, in any direction, past an ellipsoid or simple quadric:

1. The velocity potential at any confocal surface point equals the greatest tangential speed along that surface times the distance from the point to the surface's zero-potential plane.

2. The tangential flow speed at said surface point equals the greatest tangential speed times the sine of the obliquity, or inclination of the local surface element to the equipotential plane.

3. The normal speed at the point equals the greatest normal speed times the cosine of the obliquity.

4. The locus of $q=q_o$ is a cup-shaped surface asymptoting a double cone with vertex at the center.

5. The vertex angle of this cone is invariant with stream direction; for cylinders it is 90°, for spheroids it is $2\tan^{-1}\sqrt{2}=109°-28'$.

6. The velocity and pressure distribution are closely the same as for air of the same density, except in or near the region of disturbed flow.

7. The zonal drag is upstream on the fore half; downstream on the rear half; zero on the whole. These zones may be bounded by the isobars, ϵ const.

For the same stream, but with kinematic viscosity ν, if the dynamic scale is $R=q_o d/\nu$, d being the model's diameter:

8. The drag coefficient of a sphere is $24/R$ for $R<.2$; $28R^{-.85}+.48$ for $0.2<R<200{,}000$; and 0.5 for $10^4<R<10^5$.

9. The drag coefficient of an endless round cylinder fixed across stream is $8\pi/R(2.002-\log_e R)$ for $R<.5$; approximately $9.4\ R^{-.6}+1.2$ for $0.5<R<200{,}000$; 1.2 for $10^4<R<200{,}000$.

10. For $15{,}000<R<200{,}000$ the drag coefficient of a round cylinder is 2.4 times that for a sphere.

TABLE III

Flow functions for simple quadrics in stream V along y positive

(For all shapes $\phi=-(1+m_b)\,Vy$, $\quad q_t=(1+m_b)\,V\sin\epsilon^*$ $\quad q_n=-(1-n_b)\,V\cos\epsilon$)

Shape	m_b	n_b
Sphere	$\frac{a^3}{2a'^3}$	$\frac{a^3}{a'^3}$
Circular cylinder	$\frac{a^2}{a'^2}$	$\frac{a^2}{a'^2}$
Elliptic cylinder	$\frac{a}{b'}\,\frac{a+b}{a'+b'}$	$\frac{a}{a'}\,\frac{a+b}{a'+b'}$
Prolate spheroid $e=\frac{1}{a}\sqrt{a^2-b^2}$	$-\frac{\log_e\frac{1+e'}{1-e'}-\frac{2e'}{1-e'^2}}{\log_e\frac{1+e}{1-e}-2e\frac{1-2e^2}{1-e^2}}$	$\frac{\log_e\frac{1+e'}{1-e'}-2e'\frac{1-2e'^2}{1-e'^2}}{\log_e\frac{1+e}{1-e}-2e\frac{1-2e^2}{1-e^2}}$
Oblate spheroid $e=\frac{1}{b}\sqrt{b^2-a^2}$	$-\frac{e'\sqrt{1-e'^2}-\sin^{-1}e'}{e\frac{1+e^2}{\sqrt{1-e^2}}-\sin^{-1}e}$	$\frac{e'\frac{1+e'^2}{\sqrt{1-e'^2}}-\sin^{-1}e'}{e\frac{1+e^2}{\sqrt{1-e^2}}-\sin^{-1}e}$

* ϵ is the angle between b' and any normal to the confocal surface.

TABLE IV

Inertia factors k_b for quadric surfaces in steady translation along axis b in Figure 20

Elongation E	Ellip. cyl $E=a/b$ $k_b=\frac{a}{b}$	Prol. spher. $E=a/b$ $k_b=-\frac{\log_e\frac{1+e}{1-e}-\frac{2e}{1-e^2}}{\log_e\frac{1+e}{1-e}-2e\frac{1-2e^2}{1-e^2}}$	Obl. spher. $E=b/a$ $k_b=-\frac{e-E\sin^{-1}e}{eE^2(e^2+1)-E\sin^{-1}e}$
1.00	1.00	0.500	0.500
1.50	1.50	.621	.384
2.00	2.00	.702	.310
2.50	2.50	.763	.260
3.00	3.00	.803	.223
4.00	4.00	.860	.174
5.00	5.00	.895	.140
6.00	6.00	.918	.121
7.00	7.00	.933	.105
8.00	8.00	.945	.092
9.00	9.00	.954	.084
10.00	10.00	.960	.075
∞	∞	1.000	0

The numerical values in column 3 are given in Lamb's paper already cited; those in column 4 are given substantially by Doctor Bateman, Report No. 163 National Advisory Committee for Aeronautics, 1923.

REPORT No. 323

FLOW AND FORCE EQUATIONS FOR A BODY REVOLVING IN A FLUID

By A. F. ZAHM
Aerodynamical Laboratory
Bureau of Construction and Repair, U. S. Navy

104397—30——27

CONTENTS

	Page
SUMMARY	411
PART I. INTRODUCTION	412
Steady-flow method	412
General formulas for velocity components	413
Surface velocity	413
Zonal forces and moments	413
Geometrical formulas	414
Conventions	415
PART II. VELOCITY AND PRESSURE	416
(A) Bodies in Simple Rotation	416
Elliptic cylinder	416
Prolate spheroid	418
Ellipsoid	422
(B) Bodies in Combined Translation and Rotation	422
Most general motion	422
Yawing flight	422
Flow inside ellipsoid	424
Potential coefficients	426
Relative velocity and kinetic pressure	426
PART III. ZONAL FORCE AND MOMENT ON HULL FORMS	427
Pressure loading	427
Zonal force	428
Zonal moment	428
Correction factors	428
PART IV. RESULTANT FORCE AND MOMENT	429
Body in free space	429
Reactions of fluid	429
Combination of applied forces	431
Hydrokinetically symmetric forms	432
Examples	432
Theory *vs.* experiment	433
Correction factors	435
PART V. POTENTIAL COEFFICIENTS—INERTIA COEFFICIENTS	436
Green's integrals	436
Potential coefficients	436
Inertia coefficients	436
Limiting conditions	437
Physical meaning of the coefficients	437
SYMBOLS USED IN THE TEXT	438
REFERENCES	438
TABLES AND DIAGRAMS	439

REPORT No. 323

FLOW AND FORCE EQUATIONS FOR A BODY REVOLVING IN A FLUID

IN FIVE PARTS

By A. F. Zahm

SUMMARY

This report, submitted to the National Advisory Committee for Aeronautics for publication, is a slightly revised form of U. S. Navy Aerodynamical Laboratory Report No. 380, completed for the Bureau of Aeronautics in November, 1928. The diagrams and tables were prepared by Mr. F. A. Louden; the measurements given in Tables 9 to 11 were made for this paper by Mr. R. H. Smith, both members of the Aeronautics Staff.

Part I gives a general method for finding the steady-flow velocity relative to a body in plane curvilinear motion, whence the pressure is found by Bernoulli's energy principle. Integration of the pressure supplies basic formulas for the zonal forces and moments on the revolving body.

Part II, applying this steady-flow method, finds the velocity and pressure at all points of the flow inside and outside an ellipsoid and some of its limiting forms, and graphs those quantities for the latter forms. In some useful cases experimental pressures are plotted for comparison with theoretical.

Part III finds the pressure, and thence the zonal force and moment, on hulls in plane curvilinear flight.

Part IV derives general equations for the resultant fluid forces and moments on trisymmetrical bodies moving through a perfect fluid, and in some cases compares the moment values with those found for bodies moving in air.

Part V furnishes ready formulas for potential coefficients and inertia coefficients for an ellipsoid and its limiting forms. Thence are derived tables giving numerical values of those coefficients for a comprehensive range of shapes.

REPORT No. 323

FLOW AND FORCE EQUATIONS FOR A BODY REVOLVING IN A FLUID

PART I

INTRODUCTION

STEADY-FLOW METHOD.—In some few known cases one can compute the absolute particle velocity q' at any point (x, y, z) of the flow caused by the rotation of a body, say with uniform angular speed Ω, in an infinite inviscid liquid otherwise still. Thence, since q' is unsteady at (x, y, z), the instantaneous pressure there is found by Kelvin's formula $p_v/\rho = -\partial\varphi/\partial t - q'^2/2$, p_v being the supervacuo pressure there, and φ the velocity potential.

Otherwise superposing upon said body and flow field the reverse speed $-\Omega$, about the same axis, gives the same relative velocity q but which now is everywhere a steady space velocity. In the body's absence the circular flow speed at the radial distance R would be $q_0 = -\Omega R$.[1] If the fixed body's presence lowers the speed at (x, y, z) from q_0 to q, it obviously begets there the superstream pressure

$$p = \frac{1}{2}\rho(q_0^2 - q^2) \qquad (1)$$

or in dimensionless form, a being some fixed length in the body,

$$\frac{p}{\frac{1}{2}\rho a^2\Omega^2} = \frac{R^2}{a^2}(1 - q^2/q_0^2) \qquad (1_1)^2$$

The present text finds p by this steady-flow method only, and applies it to streams about various forms of the ellipsoid and its derivatives.

The superposed circular flow, $q_0 = -\Omega R = -\partial\psi/\partial R$, has the stream-function

$$\psi = \frac{1}{2}\Omega R^2 \qquad (2)$$

which, for rotation about the z axis, plots as in Figure 4. This flow has no velocity potential, since $\partial\psi/\partial R \neq 0$.

GENERAL FORMULAS FOR VELOCITY COMPONENTS.—In plane flow,[3] as is known, a particle at any point (x, y) of a line s drawn in the fluid has the tangential and normal velocity components

$$q_t = \frac{\partial\varphi}{\partial s} = -\frac{\partial\psi}{\partial n} \qquad q_n = \frac{\partial\varphi}{\partial n} = \frac{\partial\psi}{\partial s} \qquad (3)$$

[1] This velocity entails the centrifugal pressure $p_c = \rho\Omega^2R^2/2$ at all distances, $R = \sqrt{x^2+y^2}$ from the rotation axis of the circular stream, here assumed to be constrained by a coaxial closed cylinder infinitely large. To the dynamic pressure $p_c + p$ may also be added any arbitrary static pressure such as that due to weight or other impressed force.

[2] At any surface-point of the body q is the velocity of wash or slip, whether the body moves or not; it is $q'_t - q''_t$, the difference of the tangential space velocities of the fluid and surface point. If the body is fixed $q''_t = 0$, $q = q'_t$.

[3] Plane flow, viz two-dimensional flow, literally means flow in a plane; the term applies also to space flow that is the same in all parallel planes.

where δs, δn are elements along the line and its normal. As usual, q_t, q_n are reckoned positive respectively along δs, δn positive; e. g. Figure 2. The components along x, y are

$$u=\frac{\partial\varphi}{\partial x}=\frac{\partial\psi}{\partial y} \qquad v=\frac{\partial\varphi}{\partial y}=-\frac{\partial\psi}{\partial x} \quad \text{---------- (4)}$$

In solid flow (3), (4) still hold for φ, and further $w=\partial\varphi/\partial z$. In general, $q^2=u^2+v^2+w^2=q_t^2+q_n^2$. At any point of a surface drawn in the fluid q_t is taken in the plane of q and q_n. All these velocities are referred to fixed space.

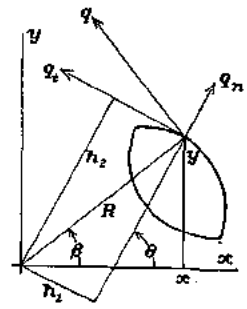

FIGURE 1.—Component velocities q_n, q_t of surface point of any rigid cylinder having angular speed Ω about any axis parallel to its length. $q_n=\Omega h_1$; $q_t=\Omega h_2$. $h_1=R\sin(\theta-\beta)=-R\,dR/ds=mx-ly$, l, m being direction cosines of the normal to the contour element ds at (x, y). If the body rotates in a fluid, $q_n=\partial\phi/\partial s=\partial\varphi/\partial n$. At any surface point q_n is the same for body and fluid; q_t different except at points of no slippage

SURFACE VELOCITY.—A fixed body in any stream, since $q_n=0$, has the surface flow velocity $q=q_t$, which put in (1) determines the surface pressure.

At any surface point of an immersed moving body q_n is the same for body and fluid, hence is known from solid kinematics. Thus, if the body is any cylinder rotating as in Figure 1,

$$q_n=-\Omega R\,dR/ds=\Omega R\sin(\theta-\beta)=\Omega h_1=\Omega(mx-ly) \quad \text{-------- (5)}$$

where the symbols are as defined in Figures 1, 2.

More generally, for any surface with velocities Ω_x, Ω_y, Ω_z about the axes x, y, z,

$$q_n=(ny-mz)\Omega_x+(lz-nx)\Omega_y+(mx-ly)\Omega_z \quad \text{---------- (6)}$$

where l, m, n are the direction cosines of the surface normal, as in (13_1). If at the same time the body has translation components, U, V, W along x, y, z, (6) must be increased by $lU+mV+nW$, giving

$$q_n=l(U+z\Omega_y-y\Omega_z)+m(V+x\Omega_z-z\Omega_x)+n(W+y\Omega_x-x\Omega_y) \quad \text{-- (7)}$$

But (5), (6), (7) express q_n only at the model's surface.

Equations (1) to (7) obtain whether the fluid is inside or outside the body.

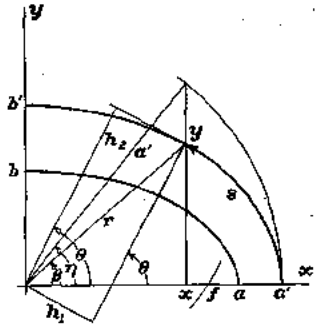

FIGURE 2.—Geometric data for confocal ellipses. $x=a'\cos\eta=r\cos\beta$; $y=b'\sin\eta=r\sin\beta$; $\frac{b'}{a'}\tan\theta=\tan\eta=\frac{a'}{b'}\tan\beta=\frac{a'}{b'}\frac{y}{x}$; $h_1=r\sin(\theta-\beta)$; $h_2=r\cos(\theta-\beta)$. $f=ae=a'\,e'$, $e=\sqrt{1-b^2/a^2}$ being eccentricity of ab

ZONAL FORCES AND MOMENTS.—For *any cylinder* spinning about z, as in Figure 1 or 5, surface integration of p gives, per unit of z-wise length, the zonal[4] forces and moment, respectively,

$$X=\int p\,dy \qquad Y=\int p\,dx \qquad N=\int p\,r\,dr \quad \text{-----(8)}$$

where $p\,dy$, $p\,dx$ are the x, y components of the elementary surface force $p\,ds$, and r is the radius vector of (x, y). To derive N we note that $p\,ds$ has components $p\,r\,d\beta$, $p\,dr$ along and across r. Having no moment, $p\,r\,d\beta$ can be ignored, leaving only $p\,dr$ with arm r. Thus, $2N=\int p\,d(r^2)$, which varies as the area of the graph of p versus r^2.

A *surface of rotation* about x, spinning about its z axis, has zonal forces

$$X=\int\int p\,dy\,dz \qquad Y=\int\int p\,dx\,dz \quad \text{----------(9)}$$

[4] A zone is any part of the surface bounded by two parallel planes; in this text they are assumed normal to x, and the zone has the bounding planes $x=0$, $x=\pm x_1$; in Part III other planes are used; e. g. $x=x_1$, $x=a$.

If ds_η, ds_ω are elements of its lines of meridian and latitude, as in Figure 3, the moment about z of $p\ ds_\eta\ ds_\omega$ is $p\ r\ dr\ ds_\omega$ in the plane $\omega=0$, and $p\ r\ dr\ ds_\omega \cos\omega = p\ r\ dr\ dz = dN$ for any meridian plane; hence the zonal moment is

$$N = \int Pr\ dr \qquad (10)$$

where $P = \int_{-z_0}^{z_0} p\ dz = dY/dx$, is the y-wise pressure-force per unit length x-wise.[5] Thus, as for (8), N varies as the area of the graph of P versus r^2. Also one notes that

$$Y = \int P dx \qquad P = z_0 \int_0^{2\pi} p \cos\omega\ d\omega \qquad (10_1)$$

Since p is symmetrical about the x axis, $Z=0=Y=L=M=N$; viz, the assumed zone is not urged along y, z or about x, y, z. In general, X is not zero for such a zone, but is zero for the whole model. The zonal Y, N are zero for steady rotation about z in a frictionless liquid, because p is symmetrical about the x axis; but are not so in a viscid fluid, nor for accelerated spin in a perfect fluid.

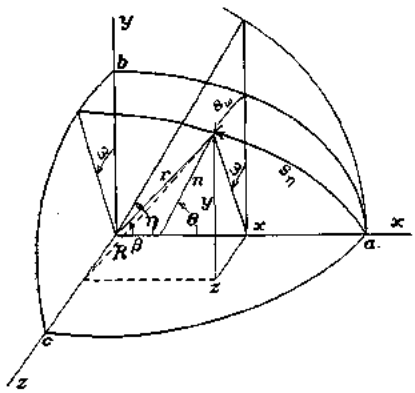

FIGURE 3.—Geometric data for prolate spheroid. $x=a\cos\eta$; $y=b\sin\eta\cos\omega=r\sin\beta\cos\omega$; $z=b\sin\eta\sin\omega=r\sin\beta\sin\omega$; $R=\sqrt{x^2+y^2}$. δ n is positive outward; δs_η, δs_ω positive as indicated by arrows; $z_0=y_0=b\sin\eta$

For trisymmetrical surfaces we note also: If the zones were formed by planes normal to z, zonal X would be zero for motion about z; zonal N in general not zero; e. g., for a viscid fluid. Similarly for zones with faces normal to y.

By (10) the bending moment about the z ordinate in the plane $y=0$ is $\int_{r_1}^{a} P\ r\ dr$. This is zero for a frictionless liquid; for a viscid fluid it increases with length of zone.

In addition to the pressure forces and moments just considered, due to rotation about z, a viscid fluid exerts surface friction symmetrical about the z axis, but not treated here.

For *any surface* S, clearly (9) still holds and (10) can be generalized to the usual form

$$N = \int\int p(x dx - y dy) dz \qquad (10_2)$$

GEOMETRICAL FORMULAS.—Most of the surfaces treated in this text are members of the confocal ellipsoid family

$$\frac{x^2}{a^2+\lambda} + \frac{y^2}{b^2+\lambda} + \frac{z^2}{c^2+\lambda} = 1 = \frac{x^2}{a'^2} + \frac{y^2}{b'^2} + \frac{z^2}{c'^2} \qquad (11)$$

whose semi axes are $a' = \sqrt{a^2+\lambda}$, etc. The following known properties are needed.

The distance from the center to the tangent plane at the point (x, y, z) of $a'b'c'$ is

$$h_2 = \left(\frac{x^2}{a'^4} + \frac{y^2}{b'^4} + \frac{z^2}{c'^4}\right)^{-\frac{1}{2}} \qquad (12)$$

The direction-cosines of the normal to said plane are

$$l,\ m,\ n = \frac{h_2 x}{a'^2},\ \frac{h_2 y}{b'^2},\ \frac{h_2 z}{c'^2} \qquad (13)$$

[5] The radius of the latitude circle is denoted by $z_0=y_0$.

The partial derivatives of λ are

$$\frac{\partial\lambda}{\partial x}=2lh_2 \qquad \frac{\partial\lambda}{\partial y}=2mh_2 \qquad \frac{\partial\lambda}{\partial z}=2nh_2 \qquad \frac{\partial\lambda}{\partial n}=2h_2 \qquad (14)$$

More generally for any surface $f(x, y, z)=0$, one knows

$$l=j\frac{\partial f}{\partial x} \qquad m=j\frac{\partial f}{\partial y} \qquad n=j\frac{\partial f}{\partial z} \qquad j=\left[\left(\frac{\partial f}{\partial x}\right)^2+\left(\frac{\partial f}{\partial y}\right)^2+\left(\frac{\partial f}{\partial z}\right)^2\right]^{-\frac{1}{2}} \qquad (13_1)$$

and the distance from the origin to the tangent plane at (x, y, z) is

$$h_2=lx+my+nz=r\cos\gamma \qquad (12)$$

γ being the angle between the radius vector r and the normal.

Conventions.—In all the text x, y, z have the positive directions shown in Figure 3, as also have the x, y, z components of velocity, acceleration, force, linear momentum. The angular components about x, y, z of velocity, acceleration, moment, momentum are positive in the respective directions y to z, z to x, x to y. The positive direction of a plane closed contour s is that followed by one going round it with the inclosure on his left, as in Figure 2; the positive direction of the normal n is from left to right across s; and δs, δn determine the positive directions of the tangential and normal flow velocities q_t, q_n, as previously stated. For a closed surface δn is positive outward and δs is positive in the direction of one walking on the outer surface with n on his left.

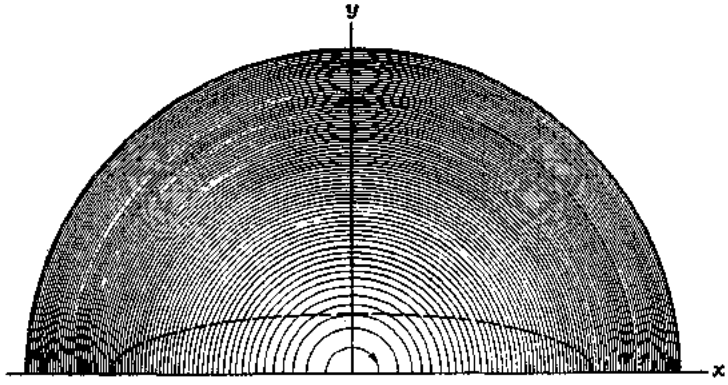

Figure 4.—Streamlines for $\psi=\frac{1}{2}\Omega R^2$, with increments $\Delta\psi=.2$, for fluid rotating with uniform angular velocity $\Omega=-1$

The word "displaced fluid," used in treating the motion of a submerged body, usually means fluid that would just replace the body if the latter were removed.

REPORT No. 323

FLOW AND FORCE EQUATIONS FOR A BODY REVOLVING IN A FLUID

PART II

VELOCITY AND PRESSURE

(A) BODIES IN SIMPLE ROTATION

ELLIPTIC CYLINDER.—For an endless elliptic cylinder, of semiaxes a, b, c ($=\infty$), rotating about c with angular speed Ω_c in an infinite inviscid liquid, otherwise still, one knows [1]

$$\varphi = -m'_c \Omega_c xy = -\frac{1}{2} m'_c \Omega_c a'b' \sin 2\eta \qquad \psi = -\frac{1}{2} m'_c \Omega_c a'b' \cos 2\eta \quad \text{.....(15)}$$

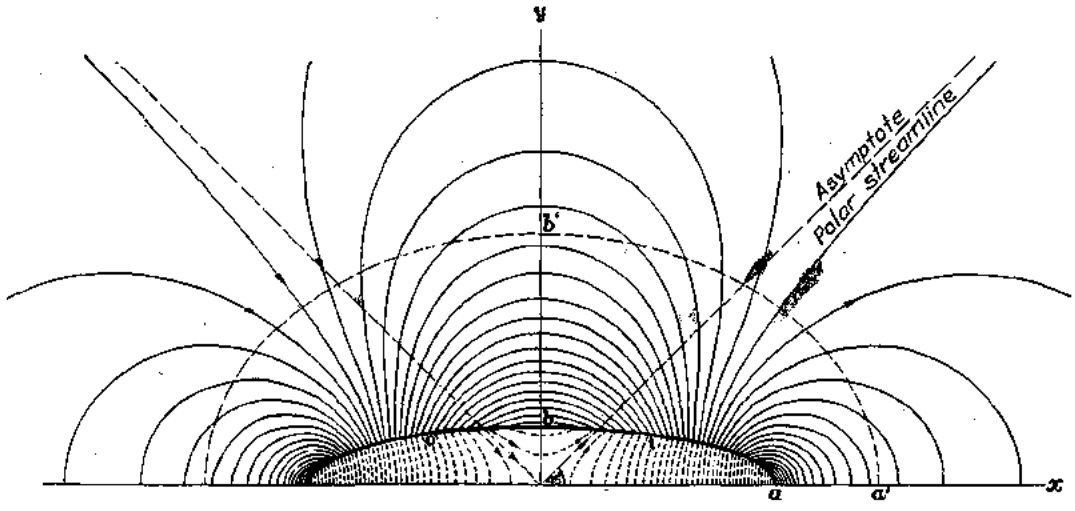

FIGURE 5.—Streamlines for endless elliptic cylinder rotating about its long axis with uniform angular velocity Ω; shows $\psi = -\frac{1}{2} m'_c \Omega a' b' \cos 2\eta$ with increments $\Delta\psi = .2$, $\Omega = 1$. For inside fluid, $\psi = -\frac{1}{2}\frac{a^2-b^2}{a^2+b^2}\Omega(x^2-y^2)$

the geometric symbols being as in Figure 2. For any outer confocal $a'b'$ the potential coefficient has the constant value

$$m'_c = (a+b)^2(a'-b')/2a'b'(a'+b') \quad \text{.....(16)}^2$$

On the model's surface $a'=a$, $b'=b$; $m'_c = (a^2-b^2)/2ab$.

The equipotential lines on either surface ab or $a'b'$ are its intersections with the corresponding family of hyperbolic cylinders $xy = -\varphi/m'_c\Omega = \text{const.}$ Normal to the equipotentials are the streamlines $\psi = \text{const.}$ Graphs for $\psi = 0$, 0.2, 0.4, etc., are shown in Figure 5 for a model having $a/b = 4$. They are instantaneous streamlines, and form with the model a constant pattern in uniform rotation about c in said infinite liquid.

At any outer confocal $a'b'$ the velocity components are, if $\kappa = m'_c a'b'\Omega_c$,

$$q'_t = \frac{\partial\varphi}{\partial s} = -\kappa \cos 2\eta \frac{d\eta}{ds} \qquad q'_n = \frac{\partial\psi}{\partial s} = \kappa \sin 2\eta \frac{d\eta}{ds} = -q'_t \tan 2\eta \quad \text{.....(17)}$$

[1] Proofs of (15), (23), (29), (40) are found in books: e. g., Lamb §§ 72, 106, 110, 115, 5th ed., except that Lamb reverses the sign of φ, ψ.

[2] Equivalent to (16) is $m'_c = \left(\frac{e'}{e}\frac{e'+\sqrt{1-e^2}}{e+\sqrt{1-e'^2}}\right)^2 \frac{e'^2}{2\sqrt{1-e^2}}$, e, e' being the eccentricities of ab, $a'b'$. On ab this becomes $m'_c = e^2/\sqrt{1-e^2}$. See (49) for the six potential coefficients m_a, m_b, m_c, m'_a, m'_b, m'_c, in the value of φ for more general motion.

where $d\eta/ds = 1/a' \sqrt{1-e'^2\cos^2\eta}$, as one easily finds. Alternative to (17) are

$$q'_t = -m'_c\Omega_c \frac{d}{ds}xy = -m'_c\Omega_c r\cos(\theta+\beta) \qquad q'_n = -q'_t \tan 2\eta \quad \ldots\ldots\ldots\ldots (17_1)$$

Thus for $\eta = 0$, 45°, 90° (17) and (17$_1$) give $q'_t/\Omega_c = -m'_c a'$, o, $m'_c b'$. At the model's surface, where $m'_c = (a^2-b^2)/2ab$, (17$_1$) become

$$q'_t = -\frac{a^2-b^2}{2ab}\Omega_c r\cos(\theta+\beta) \qquad q'_n = \Omega_c r\sin(\theta-\beta) \quad \ldots\ldots\ldots\ldots\ldots (17_2)$$

the latter being $h_1\Omega_c$, as in (5).

Where $q'_t = 0$, or $\cos\eta = 1/\sqrt{2}$, viz, at the stream poles, clearly $x = a'/\sqrt{2}$, $y = b'/\sqrt{2}$,

$$x^2 - y^2 = a^2e^2/2 \quad \ldots\ldots\ldots\ldots\ldots\ldots\ldots\ldots\ldots\ldots\ldots\ldots\ldots\ldots (18)$$

a rectangular hyperbola. (18) is the instantaneous polar streamline, e. g., Figure 5, orthogonal to all the confocal ellipses. Its asymptotes are $y = \pm x$; its vertices are at $x = \pm ae/\sqrt{2}$; it cuts each ellipse where $x/y = a'/b'$, viz, on the diagonals of the circumscribed rectangle. For an endless thin plate of width $2a$ the poles are at $y = 0$, $x = \pm a/\sqrt{2}$.

Superposing $-\Omega_c$ on the body and fluid, and using (2), changes (15) to

$$\psi = \frac{1}{2}(r^2 - m'_c a'b'\cos 2\eta)\Omega_c \quad \ldots\ldots\ldots\ldots\ldots\ldots\ldots\ldots\ldots\ldots\ldots\ldots (19)$$

Its graph, with $\Delta\psi = 0.2$, gives the streamlines in Figure 6 for the flow $\Omega_c = -1$ round a fixed cylinder having $a/b = 4$. About the point (0, 1.45) in Figure 6, is a whirl separated from the outer flow by the streamline $\psi = 4.25$. This line abuts on the model at the inflow points i, i; spreads round it and emerges at the outflow points o, o.[3] The streamlines for an endless thin rectangle having $b = 0$, $e = 1$, are similar to those of Figure 6, but infinitely crowded at the edges.

The superposed particle velocity $-\Omega_c r$ contributes to (17$_1$)

$$q''_t = -\Omega_c r\cos(\theta-\beta) = -h_2\Omega_c \qquad q''_n = -\Omega_c r\sin(\theta-\beta) = -h_1\Omega_c \quad \ldots\ldots\ldots\ldots (20)$$

also $q''_n = q''_t \tan(\theta-\beta)$. Adding (17$_1$) and (20) gives the components $q_t = q'_t + q''_t$, $q_n = q'_n + q''_n$, of the resultant flow velocity at any field point. One notes that (20) are the reverse of q_t, q_n in Figure 1.

In particular $q_n = 0$ on the fixed model and x, y axes; hence there

$$q/a\Omega_c = -\frac{r}{a}[m'_c\cos(\theta+\beta) + \cos(\theta-\beta)] \qquad q/q_o = m'_c\cos(\theta+\beta) + \cos(\theta-\beta) \quad \ldots\ldots (21)$$

Thus $q/q_o = 1 + m'_c$ on the x axis; $1 - m'_c$ on the y axis; and 1 at ∞ where $m'_c = 0$. The dashed line in Figure 6 gives $q/a\Omega_c = -(1-m'_c)y/a$ for points on the y axis; it crosses y at the whirl center where $q = 0$, viz, where $m'_c = 1$. By (16) $m'_c \geqq 1$ for the surface of any model having $a/b \geqq 1+\sqrt{2}$; and there is no whirl if $a/b < 1+\sqrt{2}$. Figure 7 shows $q/a\Omega_c$ for the surface of a model having $a/b = 4$, $m'_c = (a^2-b^2)/2ab = 15/8$.

Putting q^2/q^2_0 of (21) in (1$_1$), where $r^2/a^2 = \cos^2\eta/\cos^2\beta$, gives

$$p/\frac{1}{2}\rho a^2\Omega^2_c = (1 - [m'_c\cos(\theta+\beta) + \cos(\theta-\beta)]^2)\cos^2\eta/\cos^2\beta \quad \ldots\ldots\ldots\ldots (22)$$

which is graphed in Figure 7 for a model having $a/b = 4$.

Integrating $p/\frac{1}{2}\rho a^2\Omega^2_c$, as in (8), gives for an inviscid liquid $Y = 0 = N$; $X \neq 0$. Figure 7 delineates X for this case.

[3] The points i, o are identical with those in Figure 5; viz, where the slip speed q in (21) is zero; they are called stop points, stagnation points, etc.

For the surface of an endless flat plate ($b=0$, $c=\infty$) fixed in the stream $-\Omega_c$, clearly $m'_c=a/2b$ and generally $r\cos(\theta-\beta)=0$; hence (21) gives

$$q/a\Omega_c=-\frac{r}{2b}\cos(\theta+\beta)=-\sin\theta\cos\eta\cot 2\eta \qquad (21_1)$$

which equals $-\infty$, 0, 1/2 for $\eta=0°$, 45°, 90°. The flow resembles that in Figure 6; it has twin whirls abreast its middle, stop points at $x=\pm a/\sqrt{2}$, and infinite velocity at the edges.

Putting in (1_1) $r=x$ and $q_0=-x\Omega_c$ gives the plate's surface pressure

$$p/\tfrac{1}{2}\rho a^2\Omega_c{}^2=\frac{x^2}{a^2}-\frac{q^2}{a^2\Omega^2{}_c}=(1-\cot^2 2\eta)\cos^2\eta \qquad (22_1)$$

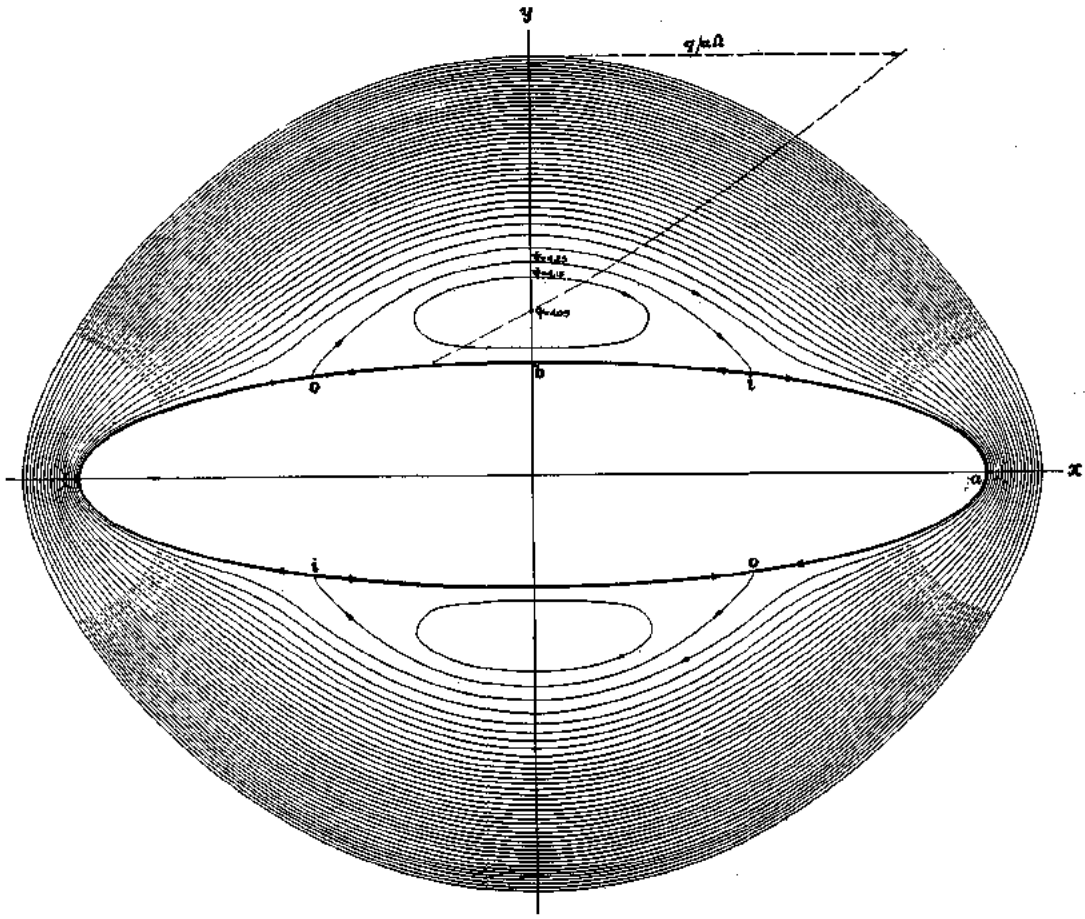

FIGURE 6.—Streamlines about endless elliptic cylinder fixed in infinite inviscid liquid rotating about its long axis with uniform angular speed $-\Omega$; shows $\psi=\frac{1}{2}\Omega(r^2-m'_c a' b'\cos 2\eta)$ with increments $\Delta\psi=.1$, $\Omega=-1$. Dotted line portrays x-wise speed on y axis

which equals $-1/4$, $1/2$, $-\infty$ for $x=0$, $\pm a/\sqrt{2}$, $\pm a$; viz, for $\eta=90°$, 45°, 0, etc.

PROLATE SPHEROID.—For a prolate spheroid, of semiaxes a, b, c, rotating about c with speed Ω_c in an infinite inviscid liquid,

$$\varphi=-m'_c\Omega_c xy=-\frac{1}{2}m'_c\Omega_c a' b'\sin 2\eta\cos\omega \qquad (23)$$

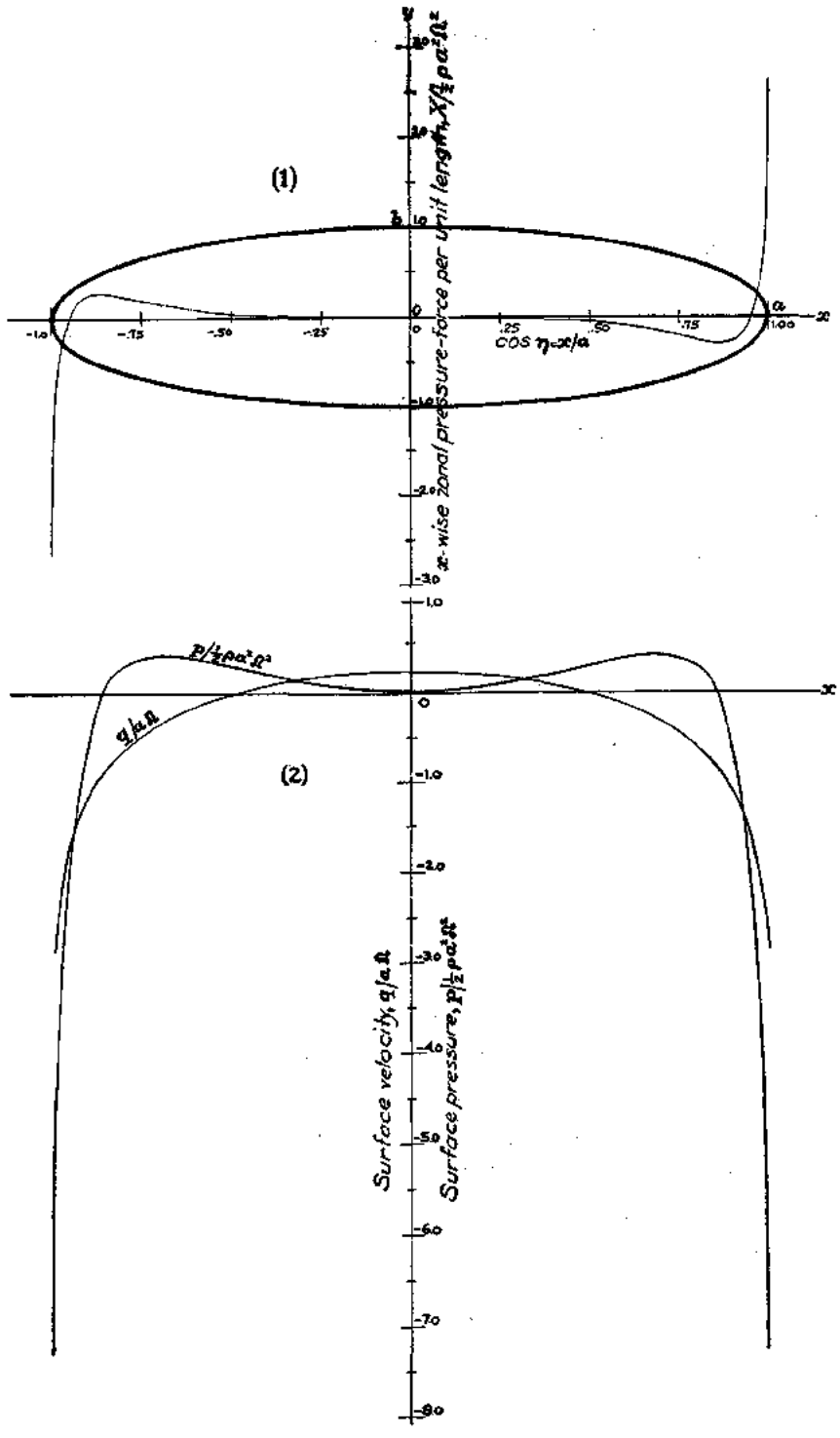

FIGURE 7.—Endless elliptic cylinder fixed in infinite inviscid liquid uniformly rotating about it; shows (1) x-wise zonal pressure-force, $X/\frac{1}{2}\rho a^2\Omega^2$; (2) surface velocity $q/a\Omega$ and surface pressure, $p/\frac{1}{2}\rho a^2\Omega^2$, above or below undisturbed local pressure in uniform stream, $-\Omega$

the geometric symbols being as in Figure 3. For any outer confocal spheroid $a'b'c'$ (23) has the known constant potential coefficient

$$m'_c = \frac{\frac{3}{2e'}\log\frac{1+e'}{1-e'} - 3 - \frac{e'^2}{1-e'^2}}{\frac{3}{2e}(2-e^2)\log\frac{1+e}{1-e} - 6 + \frac{e^2}{1-e^2}}\, ee' \qquad (24)$$

e, e' being the eccentricities of ab, $a'b'$. Table IV gives surface values of m'_c for various shapes of prolate spheroid.

In the yz, zx planes $\varphi = 0$; in the xy plane, where $\cos\omega = 1$

$$\varphi = -\frac{1}{2}m'_c\Omega_c a'b' \sin 2\eta \qquad \psi = -\frac{1}{2}m'_c\Omega_c a'b' \cos 2\eta \qquad (23_1)$$

which, except for m'_c, have the same values as (15), entailing the same polar streamlines (18). The equipotentials on $a'b'c'$ are its intersections with the family $xy = -\varphi/m'_c\Omega_c = \text{const.}$

At any point (x, y, z) on $a'b'c'$ the orthogonal velocity components are by (23)

$$q'_n = \frac{\partial\varphi}{\partial e'}\frac{de'}{dn} \qquad q'_\eta = \frac{\partial\varphi}{\partial\eta}\frac{d\eta}{ds_\eta} \qquad q'_\omega = \frac{\partial\varphi}{\partial\omega}\frac{d\omega}{ds_\omega} \qquad (25)$$

δn, δs_η, δs_ω denoting line elements along the normal, meridian, and circle of latitude, as in Figure 3. Since q'_n is absent from (1), we shall not need it; we merely note that on the model's surface it is $r\Omega_c \sin(\theta-\beta)\cos\omega$. By geometry $d\eta/ds_\eta = r\cos(\theta+\beta)/a'b'\cos 2\eta$,[4] $d\omega/ds_\omega = 1/b'\sin\eta$; hence

$$q'_\eta = -m'_c\Omega_c r\cos(\theta+\beta)\cos\omega \qquad q'_\omega = m'_c\Omega_c r\cos\beta\sin\omega \qquad (25_1)$$

For $\omega = 0$, $q'_t (= q'_\eta)$ differs only by m'_c from (17_1) for an elliptic cylinder; also $r\cos\beta = x$ $\therefore$ $q'_\omega = m'_c x\Omega_c \sin\omega = 0$, $m'_c x\Omega_c$ for $\omega = 0$, $\pi/2$.

Superposing $-\Omega_c$ on the above system adds to (25_1), as easily appears

$$q''_n = -\Omega_c r\sin(\theta-\beta)\cos\omega \qquad q''_\eta = -\Omega_c r\cos(\theta-\beta)\cos\omega \qquad q''_\omega = \Omega_c r\cos\beta\sin\omega \qquad (26)$$

At the now fixed surface and on the x, y axes $q_n = 0 = q'_n + q''_n$; hence summing (25_1), (26) gives there

$$\left.\begin{aligned} q_\eta &= -[m'_c\cos(\theta+\beta) + \cos(\theta-\beta)]\,\Omega_c r\cos\omega \equiv \overline{q}_\eta\cos\omega \\ q_\omega &= (1+m'_c)\Omega_c r\cos\beta\sin\omega \equiv \overline{q}_\omega\sin\omega \end{aligned}\right\} \qquad 27$$

Thus for $\omega = 0$ clearly $q/q_0 = m'_c\cos(\theta+\beta) + \cos(\theta-\beta)$, differing from (21) only by m'_c; for $\omega = \pi/2$, $q/q_0 = -(1+m'_c)$, a formula like that for a negative flow q_0 across a cylinder; for $\omega = 0°$, 90°, 45°, $q = \overline{q}_\eta$, $\overline{q}_\omega$, $\sqrt{\frac{1}{2}(\overline{q}^2_\eta + \overline{q}^2_\omega)}$. On the x axis $q/q_0 = 1 + m'_c$; on the y axis $q/q_0 = 1 - m'_c > 0$ everywhere, hence no whirl centers on y.

Figure 8 shows $|q/a\Omega_c|$ on the meridians $\omega = 0$, $\pm 45°$, $\pm 90°$ of a fixed spheroid with $a/b = 4$. Distributions symmetrical with these occur on the opposite half of the surface. Noteworthy is q for $\omega = \pm 90°$. By (27) it is $q = \pm(1+m'_c)\Omega_c x$; hence the straight-line graph in Figure 8.

Figure 8 shows also, for these meridians, the pressure computed with the working formula, derived from (1_1), (27).

$$\frac{p}{\frac{1}{2}\rho a^2\Omega^2_c} = A\cos^2\omega + B\sin^2\omega \qquad (28)$$

[4] E. g., by (23) $\frac{d}{ds_\eta}xy = \frac{d}{ds_\eta}\cdot\frac{1}{2}a'b'\sin 2\eta\cos\omega$; viz, $r\cos(\theta+\beta) = a'b'\cos 2\eta\frac{d\eta}{ds_\eta}$, which gives $\frac{d\eta}{ds_\eta}$ in (25). Also directly $q'_\eta = \frac{\partial\phi}{\partial s_\eta} = -m'_c\Omega_c\frac{d}{ds_\eta}xy = -m'_c\Omega_c r\cos(\theta+\beta)\cos\omega$.

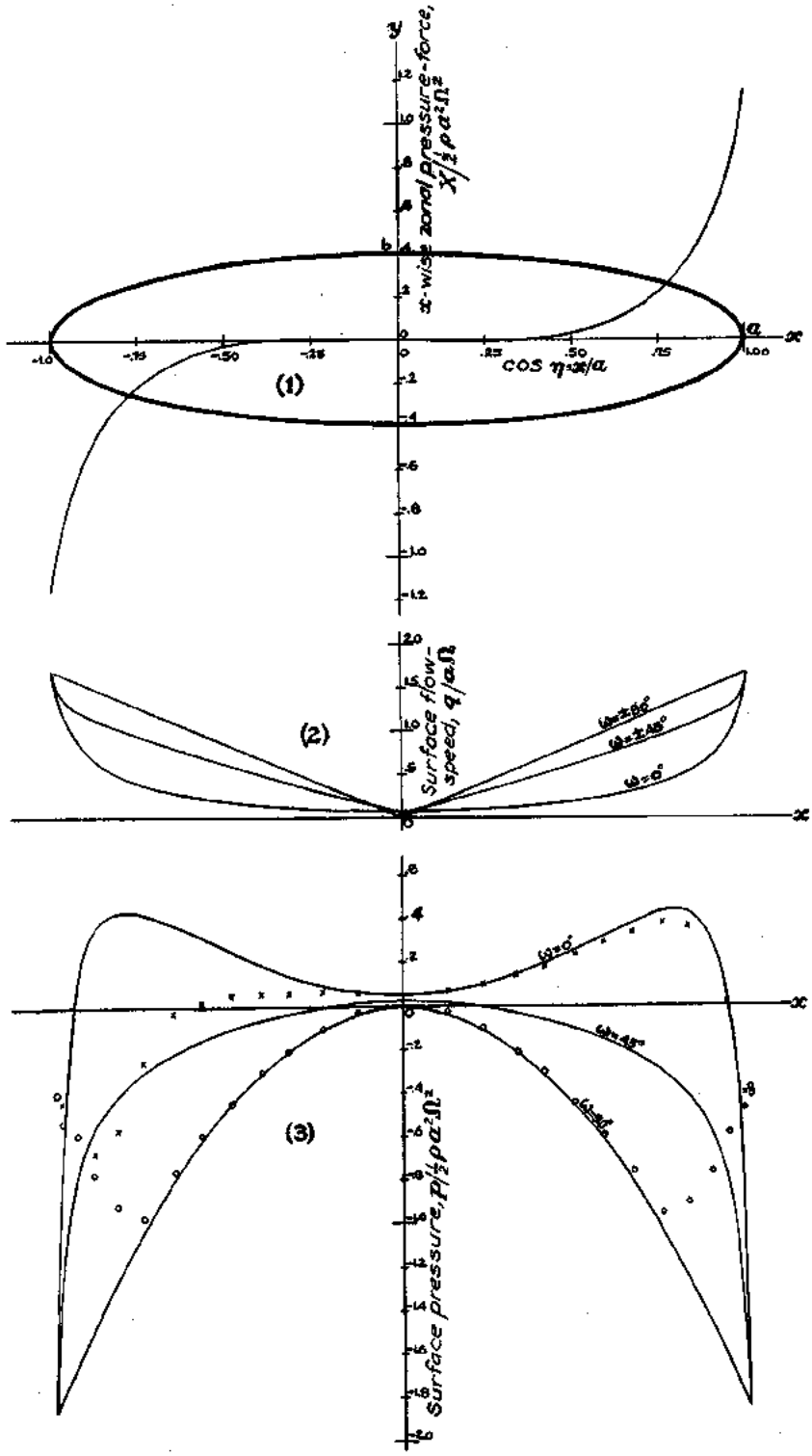

FIGURE 8.—Prolate spheroid fixed in infinite inviscid liquid uniformly rotating about it; shows (1) x-wise zonal pressure-force, $X/\frac{1}{2}\rho a^3\Omega^2$; (2) surface flow-speed, $q/a\Omega$; (3) surface pressure, $p/\frac{1}{2}\rho a^2\Omega^2$, above or below undisturbed local pressure in uniform stream, $-\Omega$. Crosses and circles give measured air pressures for $\Omega=-39.5$ radians per second given in reference 3

where $A=(1-[m'_c\cos(\theta+\beta)+\cos(\theta-\beta)]^2)\cos^2\eta/\cos^2\beta$, $B=-m'_c(2+m'_c)\cos^2\eta$. Here $m'_c=.689$ by Table IV. The crosses and circles, giving experimental values taken from Reference 3, show good agreement with (28) for a considerable part of the surface. For $\cos\omega=0$, $p\propto B\propto x^2$; or the graph is parabolic.

Integrating p, as in (9), (10), gives for an inviscid liquid $Y=0=N$, $X\neq 0$. Figure 8 portrays X computed from theory and experiment.

ELLIPSOID.—For an ellipsoid, of semiaxes a, b, c along x, y, z, rotating about c with speed Ω_c in an infinite inviscid liquid, otherwise still,

$$\varphi=-m'_c\Omega_c xy \qquad (29)$$

which for any outer confocal ellipsoid $a'b'c'$, has the constant potential coefficient

$$m'_c=C(\beta-\alpha) \qquad C=\frac{a^2-b^2}{2(a^2-b^2)-(a^2+b^2)(\beta_0-\alpha_0)} \qquad (30)$$

the Greek letters being as in Part V. Surface values of m'_c are listed in Table IV.

By (29) the equipotential lines on $a'b'c'$ are its intersections with the hyperbolic cylinder family $xy=-\varphi/m'_c\Omega_c=\text{const.}$ The orthogonals to φ const. at the surface $a'b'c'$ are the streamlines there. These by (31) are parallel to x where $x=0$; parallel to y where $y=0$; normal to z where $z=0$. The same obviously holds for spheroids and other ellipsoidal forms.

In the xy plane the flow has the polar streamlines (18); also it has there

$$\varphi=-\frac{1}{2}m'_c\Omega_c a'b'\sin 2\eta \qquad \psi=-\frac{1}{2}m'_c\Omega_c a'b'\cos 2\eta \qquad (29_1)$$

whence the streamlines in that plane are plotted. The form of (29_1) is like those of (15) and (23_1), for the elliptic cylinder and prolate spheroid, entailing similar expressions for the velocity and pressure in the plane-flow field $z=0$.

For the general flow the velocity components at $a'b'c'$ are by (29)

$$u'=-\left(x\frac{\partial m'_c}{\partial x}+m'_c\right)\Omega_c y \qquad v'=-\left(y\frac{\partial m'_c}{\partial y}+m'_c\right)\Omega_c x \qquad w'=-\Omega_c xy\frac{\partial m'_c}{\partial z} \qquad (31)$$

and those due to the superposed velocity $-\Omega_c R=q_0$, are

$$u''=\Omega_c y \qquad v''=-\Omega_c x \qquad w''=0 \qquad (32)$$

whence the resultant velocity and pressure may be derived for all points of the flow field about the ellipsoid fixed in the steady stream $-\Omega_c R$. In forming the x, y, z derivatives of m'_c one may use the relations (14) and (72).

Everywhere in the planes $x=0$, $y=0$, the resultant velocities are respectively, by (31) and (32),

$$q=u=(1-m'_c)\Omega_c y \qquad q=v=-(1+m'_c)\Omega_c x \qquad (33)$$

while in the plane $z=0$, q can be found as indicated for an elliptic cylinder. (33) apply also to the elliptic cylinder and prolate spheroid previously treated, and to all other forms of the ellipsoid fixed in the flow $-\Omega_c$.

(B) BODIES IN COMBINED TRANSLATION AND ROTATION

MOST GENERAL MOTION.—The most general motion of any body through a fluid may have the components U, V, W along, and Ω_a, Ω_b, Ω_c about, three axes, say a, b, c. The entailed resultant particle velocity q' at any flow point is found by compounding there the individual velocities severally due to U, V, W, Ω_a, Ω_b, Ω_c, and computable for an ellipsoid by formulas in Reference 2 and the foregoing text.

YAWING FLIGHT.—In airship study the flow velocity q' caused by a prolate spheroid in steady circular flight is specially interesting. Let the spheroid's center describe about 0,

Figure 9, a circle of radius na, with path speed $na\Omega$. Then if α is the constant yaw angle of attack, the component centroid velocities along a, b, and the steady angular speed about c are, respectively,

$$U = na\Omega \cos \alpha \qquad V = na\Omega \sin \alpha \qquad \Omega_c = \Omega \qquad (34)$$

If, now, velocities the reverse of (34) are imposed on the body and fluid, $q_n = 0$, and the surface velocity q on the fixed spheroid has in longitude and latitude the respective components

$$\left.\begin{aligned} q_\eta &= (1+k_a)U \sin\theta - (1+k_b)V \cos\theta \cos\omega - [m'_c \cos(\theta+\beta) + \cos(\theta-\beta)]\Omega_c r \cos\omega \\ q_\omega &= (1+k_b)V \sin\omega + (1+m'_c)\Omega_c r \cos\beta \sin\omega \end{aligned}\right\} \qquad (35)$$

where positive flows along ds are, respectively, in the directions of increasing η, ω, as in Figure 3. The terms in U, V, are known formulas for translational flow, e. g., Reference 2; the others are from (27). Hence q^2 then p is found for any point (β, ω) on the spheroid.[5] If Ω_c is negligible, $q = \bar{q} \sin \epsilon$, where $\bar{q}^2 = (1+k_a)^2 U^2 + (1+k_b)^2 V^2$, and ϵ is the angle between the local and polar normals, as proved in Reference 2.

Figure 9_2 portrays, for specified conditions, theoretical values of $p/\frac{1}{2}\rho Q^2$, Q being the path speed $\sqrt{U^2+V^2}$ of the spheroid's center; it also portrays $p/\frac{1}{2}\rho Q^2$ for the model in rectilinear motion, with $Q = U$. The difference of $p/\frac{1}{2}\rho Q^2$ for straight and curved paths, though material, is less than experiment gives, as shown by 9_3. Fuller treatment and data are given in Reference 3.

The forces X, Y and moment N, for any zone, may be computed as before; but for the whole model they are more readily found by the method of Part IV. Zonal Y and N for a hull form are found in Part III.

The first of (35) applies also to an elliptic cylinder, with $\cos\omega = 1$, $m'_c = (a^2-b^2)/2ab$. Fixed in a flow $-U$, $-V$, $-\Omega_c$, it has the surface velocity

$$q = (1+b/a)U \sin\theta - (1+a/b)V \cos\theta - \left[\frac{a^2-b^2}{2ab}\cos(\theta+\beta) + \cos(\theta-\beta)\right]\Omega_c r \qquad (36)$$

For an endless flat plate $b = 0$, $\cos\theta = b/a$. $\sin\theta \cot\eta$; and the last term of (36) may be rewritten by (21_1); thus (36) becomes

$$q = (U - V\cot\eta - a\Omega_c \cos\eta \cot 2\eta)\sin\theta \qquad (37)$$

These two values of q with (1_1) give the pressure distribution over an elliptic cylinder or flat plate revolving about an axis parallel to its length or fixed in a fluid rotating about that axis.

Thus an endless plate of width $2a$, revolving with angular speed Ω, path radius na, and incidence α, as in Figure 10_1, has by (37) the relative surface velocity, viz, slip velocity

$$q/a\Omega = (n\cos\alpha - n\sin\alpha\cot\eta - \cos\eta\cot 2\eta)\sin\theta \qquad (38)$$

and since $\sin^2\theta = 1$, $q_0^2 = U^2 + (V+x\Omega)^2 = a^2\Omega^2(n^2 + 2n\sin\alpha\cos\eta + \cos^2\eta)$, (1) gives

$$p/\frac{1}{2}\rho a^2\Omega^2 = \eta^2 + 2n\sin\alpha\cos\eta + \cos^2\eta - n^2(\cos\alpha - \sin\alpha\cot\eta - \frac{1}{n}\cos\eta\cot 2\eta)^2 \qquad (39)$$

For $n = 3$, $\alpha = 30°$, Figure 10_2 delineates the distribution of slip velocity $q/a\Omega$ on both sides of the plate; 10_3 that of the pressure $p/\frac{1}{2}\rho a^2\Omega^2$ on its two faces. This pressure integrated over the plate's double surface gives $Y = 0$, as may be shown. The dashed line in Figure 10_3 is the pressure-difference graph whose integral for $\eta = 0$ to π is also zero. The resultant forces X, Y and moment N for such a plate are found in Part IV by a method simpler than surface integration of the pressure.

[5] Here again q is the slip speed of the flow at any point of the body's surface, and depends only on the relative motion of body and fluid.

FLOW INSIDE ELLIPSOID.—At any point inside an ellipsoid with speeds U, V, W, Ω_a, Ω_b, Ω_c, along and about a, b, c, filled with inviscid liquid otherwise still,

$$\varphi = Ux + Vy + Wz + \frac{b^2-c^2}{b^2+c^2}\Omega_a yz + \frac{c^2-a^2}{c^2+a^2}\Omega_b zx + \frac{a^2-b^2}{a^2+b^2}\Omega_c xy \quad \text{----------} \quad (40)$$

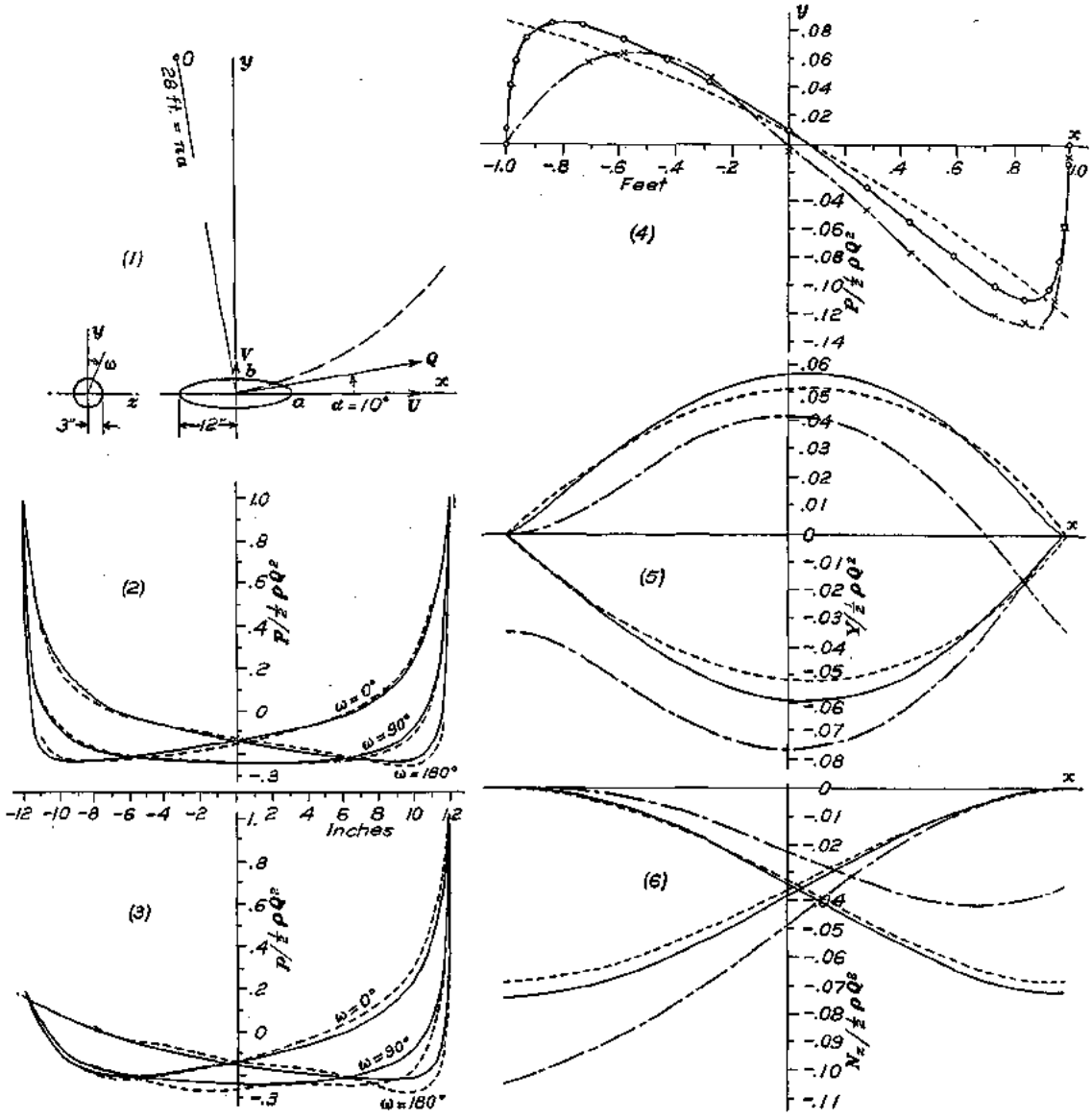

FIGURE 9.—Prolate spheroid in steady yawing flight. (1) Defines velocity conditions; (2) delineates theoretical pressure distribution; (3) experimental pressure distribution for $Q = 40$ feet per second. In (2) and (3), full lines indicate rectilinear, dashed lines curvilinear motion

FIGURE 9 (continued).—For conditions (1), (4) delineates pressure load per unit length; (5) the zonal force; (6) the zonal moment. In (4) the full and dotted lines give theoretical values from equations (a_1), (b_1); the dashed line, experimental values from reference 3. (5) is obtained by planimetring (4); (6) by planimetring (5)

whose coefficients are constant for the whole interior. Hence the components of the particle velocity q are

$$\frac{\partial \varphi}{\partial x} = u = U + \frac{c^2-a^2}{c^2+a^2}\Omega_b z + \frac{a^2-b^2}{a^2+b^2}\Omega_c y \quad \text{----------} \quad (41)$$

and like values for v, w found by permuting the symbols. If the fluid were solidified any particle would have

$$u = U + \Omega_b z - \Omega_c y, \text{ etc., etc} \quad (42)$$

Thus when an ellipsoid full of inviscid still fluid is given any pure translation its content moves as a solid; but when given pure rotation each particle moves with less speed than if the fluid were solidified, since the fractions in (41) are less than unity.

For velocities U, V, Ω_c of the ellipsoid

$$\varphi = Ux + Vy + \frac{a^2 - b^2}{a^2 + b^2}\Omega_c xy \quad (43)$$

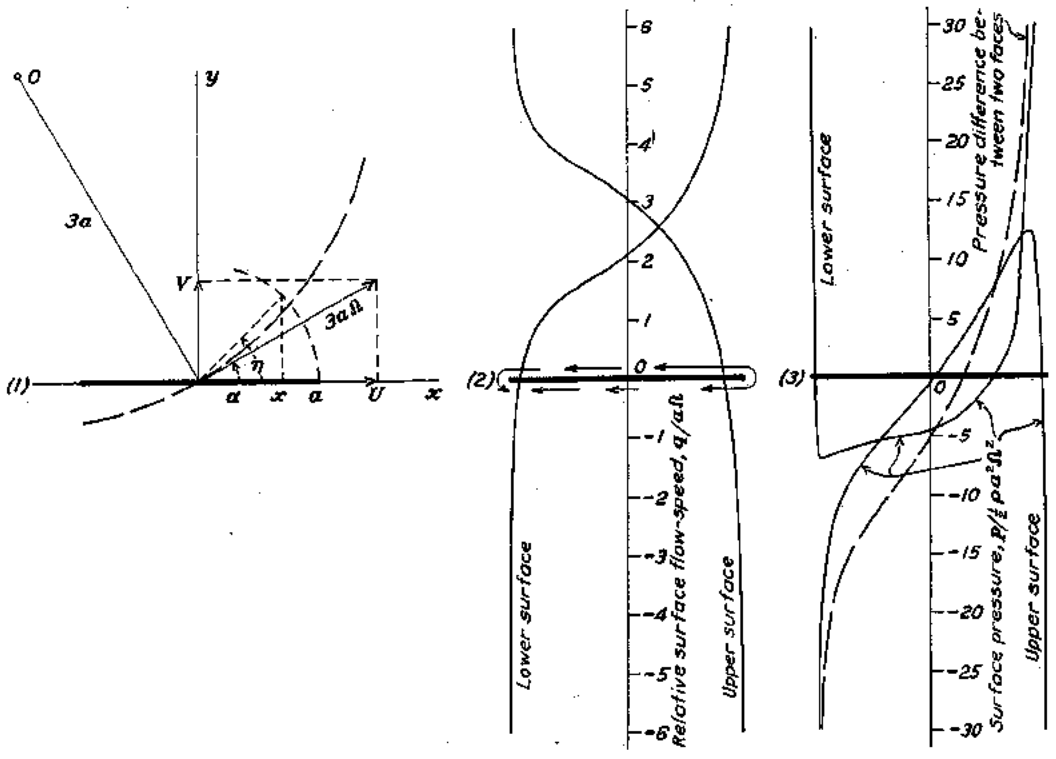

FIGURE 10.—Endless flat plate revolving about axis parallel to its length, in infinite inviscid fluid. (1) Defines conditions; (2) delineates relative velocity $q/a\Omega$ of fluid; (3) pressure $p/\frac{1}{2}\rho a^2\Omega^2$, and pressure difference $\Delta p/\frac{1}{2}\rho a^2\Omega^2$ on two faces of plate

for which $w = \partial\varphi/\partial z = 0$. For this plane flow (4) with (43) gives

$$\psi = Uy - Vx - \frac{1}{2}\Omega_c \frac{a^2 - b^2}{a^2 + b^2}(x^2 - y^2) \quad (44)$$

whence the streamlines may be plotted. In particular if the model has simple rotation Ω_c,

$$x^2 - y^2 = -2\frac{a^2 + b^2}{a^2 - b^2}\psi/\Omega_c = \text{const.} \quad (45)$$

and the interior streamlines are hyperbolas, as in Figure 5.

Adding (2) to ψ in (45) gives the steady flow

$$\psi = \frac{\Omega_c}{a^2 + b^2}(a^2y^2 + b^2x^2) \quad (46)$$

hence the streamlines lie on the elliptic cylinders

$$a^2y^2 + b^2x^2 = (a^2 + b^2)/\Omega_c\psi = \text{const.} \quad (47)$$

104397—30——28

By (46) $q=2\Omega_c(a^4y^2+b^4x^2)^{\frac{1}{2}}/(a^2+b^2)$, which put in (1) gives at (x, y), since $q_0=-\Omega_c R$,

$$p_n-p=\frac{4(a^4y^2+b^4x^2)}{(a^2+b^2)^2(x^2+y^2)}p_n \qquad (48)$$

where $p_n=\rho q_0^2/2$. Here p_n is the centrifugal pressure due to the fluid's peripheral velocity q_0, and p is the pressure change due to q_0-q, q being the relative velocity of fluid and container. In a like balloon hull q would quickly damp out, leaving only p_n as the dynamic pressure. At the ends of a, b, c, respectively, (48) gives

$$\frac{p_n-p}{p_n}=\frac{4b^4}{(a^2+b^2)^2},\ \frac{4a^4}{(a^2+b^2)^2},\ 0.$$

For large a/b the first is negligible, the second approaches 4, giving $p=-3p_n=-1.5\rho\Omega_c^2b^2$ as the temporary dynamic pressure drop inside the hull at the end of b. Experimental proof would be interesting.

Potential Coefficients.—An ellipsoid of semiaxes a, b, c along x, y, z, when moving through an infinite inviscid liquid, otherwise still, with velocities U, V, W, Ω_a, Ω_b, Ω_c along and about the instantaneous lines of a, b, c, begets the known velocity potential

$$\varphi=-m_aUx-m_bVy-m_cWz-m'_a\Omega_ayz-m'_b\Omega_bzx-m'_c\Omega_cxy \qquad (49)$$

the six potential coefficients m being constant over any outer confocal ellipsoid $a'b'c'$. Their values for abc are given in Tables III, IV. Alternatively (49) can be written for this surface

$$\varphi=-k_aUx-k_bVy-k_cWz-\frac{b^2+c^2}{b^2-c^2}k'_a\Omega_ayz-\frac{c^2+a^2}{c^2-a^2}k'_b\Omega_bzx-\frac{a^2+b^2}{a^2-b^2}k'_c\Omega_cxy \qquad (50)$$

the ks being the more familiar inertia coefficients defined and tabulated in Part V. Of the six potential coefficients in (50) the first three are the same as the inertia coefficients k_a, k_b, k_c; the last three are greater except when c/b or a/c or b/a is zero. Thus, if $b/a=0$ the last term of (50) is $-k'_c\Omega_cxy$, which is the potential on the outer surface of an elliptic cylinder ($a=\infty$) rotating about c. Everywhere inside of it the potential is Ω_cxy, as (40) shows.

For the flow (40) textbooks give the inertia coefficients

$$k_a, k_b, k_c=1 \qquad k'_a=\left(\frac{b^2-c^2}{b^2+c^2}\right)^2 \qquad k'_b=\left(\frac{c^2-a^2}{c^2+a^2}\right)^2, \text{ etc} \qquad (51)$$

which are the squares of the potential coefficients. One notes too that the ratios of like terms in (40), (50) equal the ratios of like potential coefficients and like inertia coefficients, which latter in turn are known to equal the ratios of like kinetic energies of the whole outer and inner fluids, if the inner moves as a solid.

Relative Velocity and Kinetic Pressure.—When a body moves steadily through a perfect fluid, otherwise still, the absolute flow velocity it begets at any point (x, y, z), being unsteady, is not a measure of the pressure change there. The relative velocity is such a measure. To find it we superposed on the moving body and its flow field an equal counter velocity, thus reducing the body to rest and making the flow about it steady. The same result would follow from geometrically adding to said absolute flow velocity the reversed velocity of (x, y, z) assumed fixed to the body. In particular this process gives for any point of the body's surface the wash velocity, or slip speed, which with Bernoulli's principle determines the entailed change of surface pressure. Conversely, if the pressure change at a point is known or measured, it determines the relative velocity there. In hydrodynamic books the above reversal is used commonly enough for bodies in translation. In this text it is employed as well for rotation; also for combined translation and rotation. However general its steady motion, the body is steadily accompanied by a flow pattern whose every point, fixed relatively to the body, has constant relative velocity and constant magnitude of instantaneous absolute velocity and pressure.

REPORT No. 323

FLOW AND FORCE EQUATIONS FOR A BODY REVOLVING IN A FLUID

PART III

ZONAL FORCES ON HULL FORMS[1]

PRESSURE LOADING.—For a prolate spheroid abc with speeds U, V, Ω_c, Figure 9_1, or fixed in a stream $-U$, $-V$, $-\Omega_c$, (35) gives at (x, y, z) on abc the relative velocity

$$q^2 = q_s^2 + q_\omega^2 = A - B\cos\omega + C\cos^2\omega$$

A, B, C being constant for any latitude circle. In forming this equation one finds

$$B = 2(1+k_a)U\sin\theta\{(1+k_b)V\cos\theta + [m'_c\cos(\theta+\beta) + \cos(\theta-\beta)]r\Omega_c\},$$

etc., for A, C. In the body's absence said stream has, at said point (x, y, z),

$$q_0^2 = (-U + y\Omega_c)^2 + (-V - x\Omega_c)^2 \equiv A_1 - B_1\cos\omega + C_1\cos^2\omega,$$

where ω alone varies on the latitude circle. Its radius being $y_0 = z_0$, makes $y = y_0\cos\omega$,

$$B_1 = 2Uz_0\Omega_c,$$

etc., for A_1, C_1. Putting q, q_0 in (1) gives the surface pressure

$$p/.5\rho = q_0^2 - q^2 = (A_1 - A) + (B - B_1)\cos\omega + (C_1 - C)\cos^2\omega.$$

By (10_1) the loading per unit length of x is, since $\int_0^{2\pi}\cos\omega = 0 = \int^{2\pi}\cos^3\omega$,

$$P/.5\rho = -\frac{z_0}{.5\rho}\int_0^{2\pi} p\cos\omega\,d\omega = -(B - B_1)z_0\int_0^{2\pi}\cos^2\omega\,d\omega = -\pi(B - B_1)z_0 \qquad \text{(a)}$$

A, A_1, C, C_1 vanishing on integration of p. Thus, finally,

$$P/.5\rho Q^2 = -\pi(B - B_1)z_0/Q^2 \qquad (a_1)$$

P having the direction of the cross-hull component of p at $\omega = 0$.

One notes that $q_\omega^2(\propto \sin^2\omega)$ contributes nothing to B or the integral in (a); viz, the loading P is unaffected by q_ω, and depends solely on q_s, the meridian component of the wash velocity. Also for $\beta = 0$ and π, $B - B_1 = 0 = P$.

In Figure 9_4 the full line depicts (a_1) for the spheroid shown in 9_1, circling steadily at 40 feet per second. The theoretical dots closely agreeing with it are from Jones, Reference 3, as is also the experimental graph. Beside them is a second theoretical graph plotted from Doctor Munk's approximate formula derived in Reference 8 and given in the next paragraph. But that Professor Jones omitted some minor terms in his value of p, his theoretical $P/.5\rho Q^2$ should exactly equal (a_1). His formula, derived by use of Kelvin's $p_s/\rho = \dot{\varphi} - q^2/2$, can best be studied in the detailed treatment of Reference 3.

In Reference 8 Professor Ames derives Munk's airship hull formula

$$\frac{P}{.5\rho Q^2} = \sin 2\alpha\,\frac{dS}{dx} + \frac{2}{R}\frac{d}{dx}(xS),$$

[1] This part was added after Parts I, II, IV, V were typed; hence the special numbering of the equations.

S being the area of a cross-section; R the radius of the path of the ship's center. This was assumed valid for a quite longish solid of revolution; for a short one it was hypothetically changed to

$$\frac{P}{.5\rho Q^2} = (k_b - k_a)\sin 2\alpha \frac{dS}{dx} + 2\frac{k'_c}{R}\frac{d}{dx}(xS) \qquad \text{(b)}$$

Applying this to a prolate spheroid we derive the working formula

$$\frac{P}{.5\rho Q^2} = -Lx - Mx^2 + N \qquad (b_1)$$

where the constants for a fixed angle of attack are [2]

$$L = 2(k_b - k_a)\frac{b^2}{a^2}\cdot\pi\sin 2\alpha, \qquad M = 3k'_c\frac{b^2}{a^2}\cdot\frac{2\pi}{R}\cos\alpha, \qquad N = k'_c b^2\cdot\frac{2\pi}{R}\cos\alpha.$$

Plotting (b_1) for the conditions in 9_1 gives the dotted curve in 9_4. It shows large values of $P/.5\rho Q^2$ for the ends of the spheroid, where (a_1) gives zero. To that extent it fails, though with little consequent error in the zonal force and moment at the hull extremities. It has the merit of being convenient and applicable to any round hull whose equation may be unknown or difficult to use.

ZONAL FORCE.—An end segment of the prolate spheroid, say beyond the section $x = x_1$, bears the resultant cross pressure

$$Y = \int_{x_1}^{a} P\,dx \qquad \text{(c)}$$

which with the resisting shear at x_1 must balance the cross-hull acceleration force on the segment in yawing flight. For the whole model (b_1) with (c) gives $Y = 0$, which is not strictly true for curvilinear motion; but (a_1) with (c) gives the correct theoretical value of Y, and agrees with (67).

In Figure 9_5 graphs of $Y/.5\rho Q^2$, for the values (a_1) and (b_1) of P, are shown beside those derived from Jones' experimental pressure curve. Since Y is proportional to the area of a segment of the graph of P, it can be found by planimetering the segment or by integrating Pdx.

ZONAL MOMENT.—The loading P exerts on any end segment, say of length $a-x$, the moment about its base diameter z

$$N_z = \int_x^a Y\,dx$$

which can be found by planimetering the graph of Y. Figure 9_6 delineates N_z so derived from the three graphs of Y. They show the moment on the right hand segment varying in length from 0 to $2a$; also on the left segment of length from 0 to $2a$. The resisting moment of the cross section must balance N_z and the acceleration moment of the segment.

CORRECTION FACTORS.—No attempt is here made to deduce theoretically a correction factor to reconcile the computed and measured p. In Reference 3 Jones shows that the theoretical and experimental graphs of $P/.5\rho Q^2$ have, for any given latitude $x_1 > a/2$, the same difference of ordinate whatever the incidence $0 < \alpha < 20°$. Thus the ordinate difference found for the zero-incidence graphs, when applied to the theoretical graph for any fixed $0 < \alpha < 20°$, determines the experimental one with good accuracy. Such established agreement in loading favorably affects, in turn, the graphs of Y, N_z the transverse force and moment on any end segment of the spheroid.

[2] From the meridian curve $\frac{x^2}{a^2} + \frac{y_0^2}{b^2} = 1$, $\frac{dy_0}{dx} = -\frac{b^2}{a^2}\frac{x}{y_0}$, $S = \pi y_0^2$; hence $\frac{dS}{dx} = 2\pi y_0\frac{dy_0}{dx} = -2\pi\frac{b^2}{a^2}x$, which put in (b) leads to (b_1).

REPORT No. 323

FLOW AND FORCE EQUATIONS FOR A BODY REVOLVING IN A FLUID

PART IV

RESULTANT FORCE AND MOMENT

BODY IN FREE SPACE.—Let a homogeneous ellipsoid of semiaxes a, b, c move freely with component velocities u, v, w, p, q, r[1] respectively along and about instantaneous fixed space axes x, y, z coinciding at the instant with a, b, c. Then the linear and angular momenta referred to x, y, z are

$$m_1u \qquad m_1v \qquad m_1w \qquad A_1p \qquad B_1q \qquad C_1r \qquad \text{----------(52)}$$

m_1 being the body's mass, A_1, B_1, C_1 its moments of inertia about a, b, c. If, now, forces X_1, Y_1, Z_1 and moments L_1, M_1, N_1 are applied to the body along and about x, y, z, they cause in the vectors (52) the well-known change rates

$$\left.\begin{aligned} m_1(\dot{u}-rv+qw)&=X_1 \qquad & A_1\dot{p}-(B_1-C_1)qr&=L_1\\ m_1(\dot{v}-pw+ru)&=Y_1 \qquad & B_1\dot{q}-(C_1-A_1)rp&=M_1\\ m_1(\dot{w}-qu+pv)&=Z_1 \qquad & C_1\dot{r}-(A_1-B_1)pq&=N_1 \end{aligned}\right\} \text{----------(53)}$$

which apply to any homogeneous solid symmetrical about the planes ab, bc, ca.

For motion in the ab plane; viz, for w, p, $q=0$; (53) give

$$X_1=m_1(\dot{u}-rv) \qquad Y_1=m_1(\dot{v}+ru) \qquad N_1=C_1\dot{r} \text{----------(54)}$$

and for uniform revolution about an axis parallel to z, as in Figure 11, viz, for $\dot{u}$, $\dot{v}$, $\dot{r}=0$, (54) become

$$X_1=-m_1rv \qquad Y_1=m_1ru \qquad N_1=0 \text{----------(55)}$$

where now X_1, Y_1 are merely components of the centripetal force $m_1r\sqrt{u^2+v^2}$, whose slope is $Y_1/X_1=-u/v$. Also if $Q=\sqrt{u^2+v^2}$ is the path velocity of the body's centroid, h its path radius, $r=Q/h$ is the angular velocity of h and of vector m_1Q.

REACTIONS OF FLUID.—If external forces impel the ellipsoid from rest in a quiescent frictionless infinite liquid, with said velocities u, v, w, p, q, r, they beget in the fluid the corresponding linear and angular momenta

$$k_am_1u \qquad k_bmv \qquad k_cmw \qquad k'_aAp \qquad k'_bBq \qquad k'_cCr \text{----------(56)}$$

where m is the mass of the displaced fluid, and A, B, C its moments of inertia about a, b, c.

One calls k_am, k_bm, k_cm the "apparent additional masses"; k'_aA, k'_bB, k'_cC the "apparent additional moments of inertia," of the body for its axial directions; because the fluid's resistance to its linear and angular acceleration gives the appearance of such added inertia in the body. The six k's are called "inertia coefficients," and are shape constants. Values of them are given in Tables III, VI, VIII for various simple quadrics.

The component flow momenta (56), like (52), are vectors along the instantaneous directions of a, b, c; viz, along x, y, z; hence their time rates of change must equal the forces and moments which the body exerts on the fluid; viz,

$$\left.\begin{aligned} X&=m(k_a\dot{u}-k_brv+k_cqw) \qquad & L&=k'_aA\dot{p}-(k'_bB-k'_cC)qr-(k_b-k_c)mvw\\ Y&=m(k_b\dot{v}-k_cpw+k_aru) \qquad & M&=k'_bB\dot{q}-(k'_cC-k'_aA)rp-(k_c-k_a)mwu\\ Z&=m(k_c\dot{w}-k_aqu+k_bpv) \qquad & N&=k'_cC\dot{r}-(k'_aA-k'_bB)pq-(k_a-k_b)muv \end{aligned}\right\} \text{----(57)}$$

[1] These new meanings of u, v, w, p, q, r are assigned for convention's sake and for convenience.

all written from (53) on replacing its momenta by those of (56), and adding vector-shift terms. Thus the vector $k_c mw$ shifts with speed v entailing the change rate $k_c mw.v$ of angular momentum about x, while $k_b mv$ shifts with speed w entailing the opposite rate—$k_b mv.w$. Their sum is $(k_c - k_b)mvw$. Permuting these gives for the y, z axes $(k_a - k_c)mwu$, $(k_b - k_a)muv$. When the k's are equal the vector-shift terms vanish, as for said free body, or for a sphere, cube, etc., in a fluid. The fluid reactions are (57) reversed. (57) apply also to fluid inside the trisymmetrical surface.

If the angle of attack is $\alpha = \tan^{-1} v/u$, we may write in (53), (57)

$$r = Q/h \qquad u = Q\cos\alpha \qquad v = Q\sin\alpha \qquad uv = \frac{1}{2}Q^2 \sin 2\alpha \qquad (58)$$

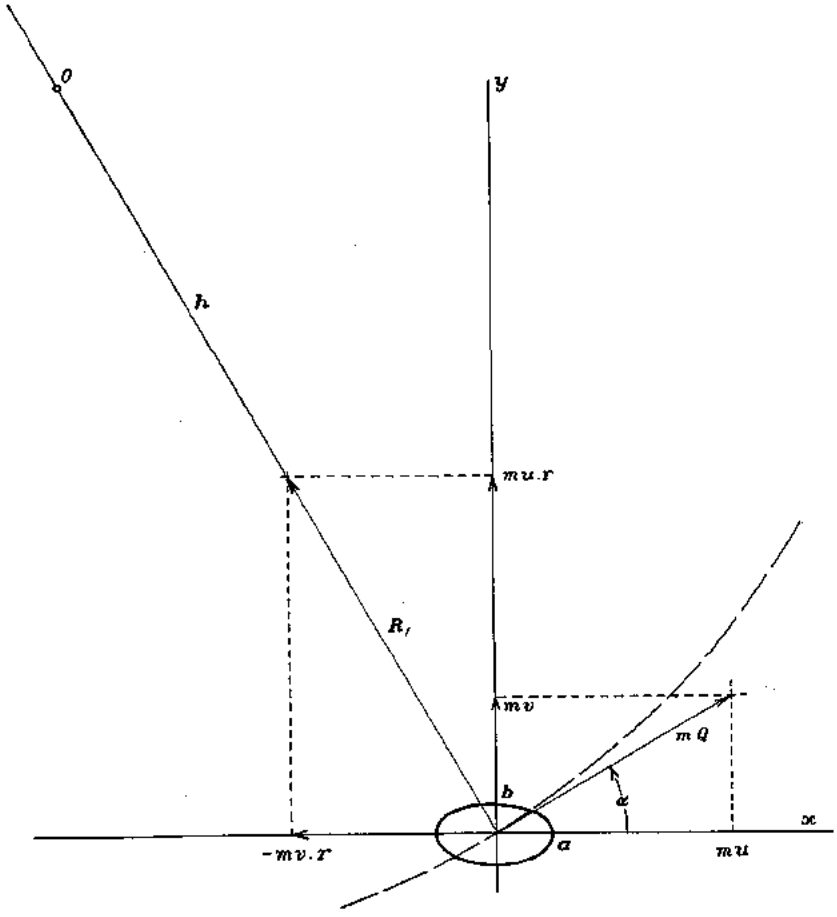

FIGURE 11.—Momenta and forces for free body in uniform circular motion. Centripetal force, $R_r = mQr = mQ^2/h$, has slope $-u/v$, r being angular speed about O

Of special aeronautic interest are (57) for plane motion, such as in yawing airship flight. for which $w, p, q = 0$, giving

$$X = m(k_a \dot{u} - k_b rv) \qquad Y = m(k_b \dot{v} + k_a ru) \qquad N = k'_c C\dot{r} + (k_b - k_a)muv \qquad (59)$$

Thus for uniform circular flight

$$X = -k_b mrv \qquad Y = k_a mru \qquad N = (k_b - k_a)muv \qquad (60)$$

which are the analogues of (55) for the free body. Or in notation (58)

$$X = -\frac{k_b \tau}{h}\rho Q^2 \sin\alpha \qquad Y = \frac{k_a \tau}{h}\rho Q^2 \cos\alpha \qquad N = (k_b - k_a)\tau \frac{\rho Q^2}{2}\sin 2\alpha \qquad (61)$$

τ being the volume of the model.

As shown in Figure 12 (60) give the resultant force and slope

$$R^2 = mr\sqrt{k_a^2u^2 + k_b^2v^2} \qquad Y/X = -\frac{k_a}{k_b}\cot\alpha = -\cot\beta \qquad (62)$$

also R and N at the origin are equivalent to a parallel force R through the path center 0, along a line (called the central axis of the force system) whose arm and intercepts are

$$l = N/R = h\sin(\beta-\alpha) \qquad x = l\sec\beta \qquad y = l\operatorname{cosec}\beta \qquad (63)$$

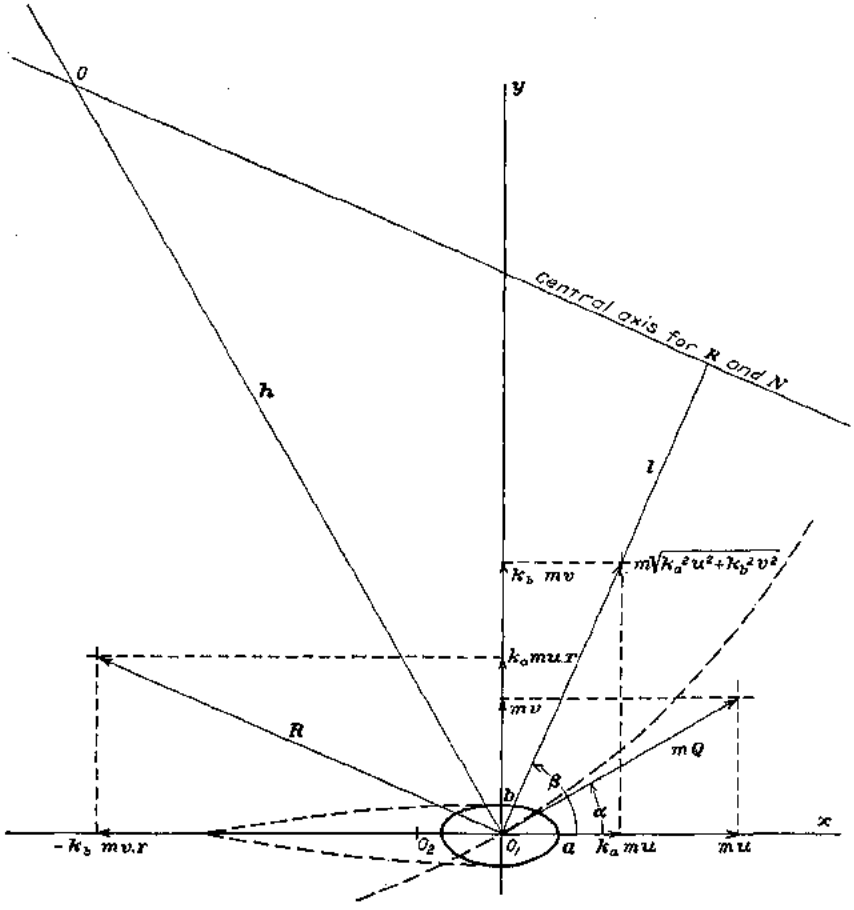

FIGURE 12.—Momenta and forces for symmetrical body in uniform circular motion through frictionless infinite liquid otherwise at rest. Whole hydrodynamic force, $R = mr\sqrt{k_a^2u^2+k_b^2v^2}$, has slope $-k_a u/k_b v$. Yaw moment $N = (k_b - k_a)\, muv = (k_b - k_a)\, \tau\frac{\rho Q^2}{2}\sin 2\alpha$, τ being volume

For steady motion (60) show that the body sustains no force in pure translation ($r = 0$); no force nor moment in pure rotation (u, $v = 0$); no moment in revolution about a point on x or y; viz, for $u = 0$, or $v = 0$. For given u, v the moment is the same for revolution as for pure translation. The forces result from combined translation and rotation; the moment from translation oblique to the axes a, b, irrespective of rotational speed.

COMBINATION OF APPLIED FORCES.—To find the whole applied force constraining a body to uniform circular motion in a perfect fluid (55), (60) may be added, or graphs like those of Figures 11, 12, may be superposed. For an airship having $m_1 = m$, (55), (60) give

$$\overline{X} = -(1+k_b)mvr \qquad \overline{Y} = (1+k_a)mur \qquad \overline{N} = (k_b - k_a)muv \qquad (64)$$

[1] Writing $R = rQ.m\sqrt{k_a^2\cos^2\alpha + k_b^2\sin^2\alpha}$ we may call it the centripetal force of the apparent mass $m\sqrt{k_a^2\cos^2\alpha + k_b^2\sin^2\alpha}$ for the body direction of Q.

where $\overline{X} = X_1 + X$, etc. Figure 13, compounded of Figures 11, 12, shows that a submerged plane-force model, revolving uniformly about its path center, may have as sole constraint a single force $\overline{R}$ through that center, and outside itself; that is attached to an extension of the model. Such conditions appear commonly in vector diagrams of aircraft. The line of $\overline{R}$, so defined, is the central axis of the force system.

HYDROKINETICALLY SYMMETRIC FORMS.—Equations (56), (57), for trisymmetrical shapes, apply also to others having hydrokinetic symmetry. Examples of these are: All surfaces of revolution, axially symmetric surfaces whose cross sections are regular polygons; torpedo forms symmetrically finned, etc. All these figures, as has been known many decades,[3] have three

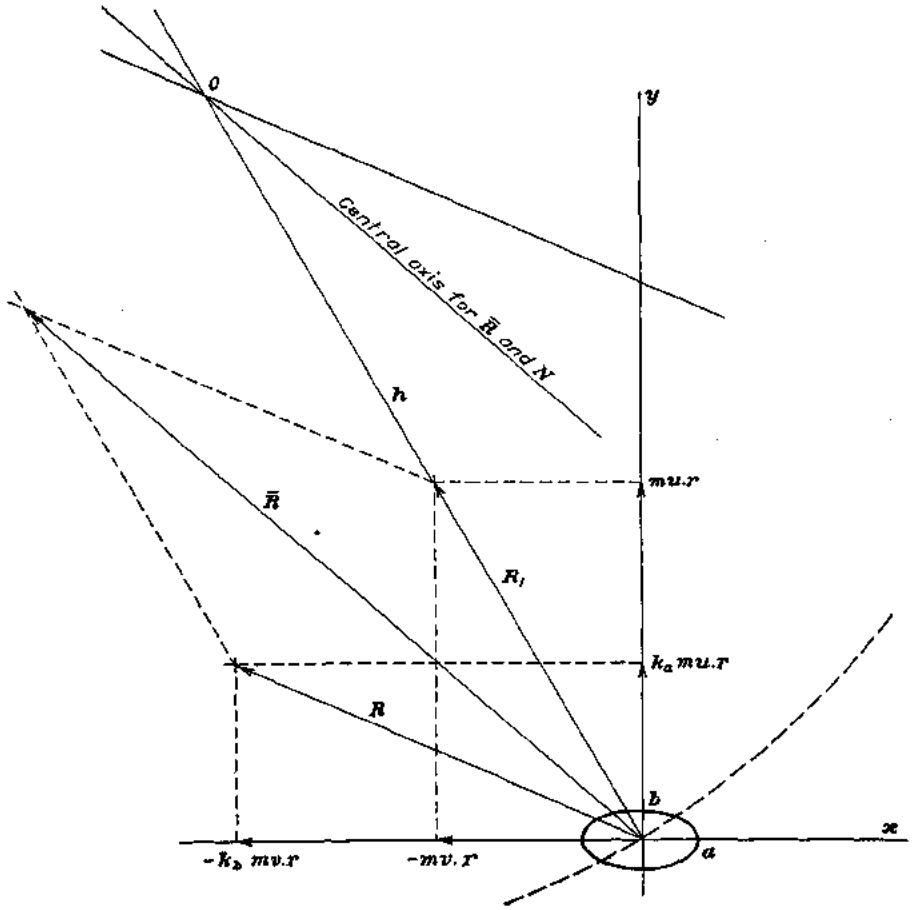

FIGURE 13.—Composition of forces on symmetrical body in uniform circular motion through frictionless infinite liquid otherwise at rest. Resultant of centripetal and hydrodynamic forces, $\overline{R} = m\,r\,\sqrt{(1+k_a)^2\,u^2 + (1+k_b)^2\,v^2}$, has slope $-\frac{1+k_a}{1+k_b}\frac{u}{v}$. Figure 13 is 11 and 12 compounded

orthogonal axes with origin at the body's impulse center,[4] such that if the body, resting in a quiet sea of perfect fluid, is impelled along or about either axis it begets in the fluid a linear or angular momentum expressible by a vector along that axis.

EXAMPLES.—We may apply (60) to some simple cases interesting to the aeronautical engineer.

(1) For an endless elliptic cylinder in uniform yawing flight, as in Figure 12, $m = \pi\rho ab$ per unit length, and by comparison with Table VIII $k_a = b/a$, $k_b = a/b$; hence by (60)

[3] See Reference 7.

[4] I. e., the point of intersection of $k_a m\,U$, $k_b m\,V$, $k_c m\,W$; it may be found as in the last paragraph of Part V.

$$X=-\pi a^2\rho rv \qquad Y=\pi b^2\rho ru \qquad N=\pi(a^2-b^2)\rho.uv=\pi(a^2-b^2)\frac{\rho Q^2}{2}\sin 2\alpha \text{ ------- (65)}$$

The resultant force $\pi\rho r\sqrt{a^4v^2+b^4u^2}$ has the slope $-b^2u/a^2v=-b^2/a^2.\cot\alpha$; the central axis is through the path center; X is the same as for a round cylinder of radius a; Y the same as for one of radius b. For a good elliptic aircraft strut $a/b=3$; hence $X/Y=-9v/u=-9\tan\alpha$; $N=8\pi b^2\rho uv=8\pi b^2.\frac{\rho Q^2}{2}.\sin 2\alpha$. By (65) N is the same for all confocal elliptic cylinders, since a^2-b^2 is so.

If $a=b$, as for a round strut, $N=0$, $R=\pi a^2\rho rQ^2$ and coincides with the body's previously found centripetal force to which it bears the ratio m/m_1.

If $b=0$, as for a flat plate, (65) become

$$X=-\pi a^2\rho rv \qquad Y=0 \qquad N=\pi a^2\rho uv=\pi a^2\frac{\rho Q^2}{2}\sin 2\alpha \text{ ---------- (66)}^5$$

The equivalent resultant force $\pi a^2\rho rv$, with slope $Y/X=-0$, runs through the path center parallel to x. If $r=0$, the plate has pure translation, with forces X, $Y=0$, and moment $N=\pi a^2\rho uv$, a well known result. X in (66), being the same as in (65), is independent of the strut thickness b.

(2) For a prolate spheroid, of semiaxes a, b, b, in uniform yawing flight, $m=4/3.\pi\rho ab^2$, and k_a, k_b are as given in Table III. Thus for $a/b=4$, k_a, $k_b=0.082$, 0.860; hence by (60)

$$X=-3.6ab^2\rho rv \qquad Y=0.3434ab^2\rho ru \qquad N=3.26ab^2\rho uv \text{ - (67)}$$

(3) For an elliptic disk of semiaxes a, b, c, moving as in Figure 14, Table VIII gives $k_cm=\frac{4}{3}\pi\rho ab^2/E$; hence by (57) the forces and moment are

$$Y=-k_cmpw=-\frac{4}{3}\frac{a}{E}.\pi\rho b^2.pw \qquad Z=0$$

$$L=k_cm.vw=\frac{4}{3}\frac{a}{E}.\pi\rho b^2.vw \text{ -------- (68)}$$

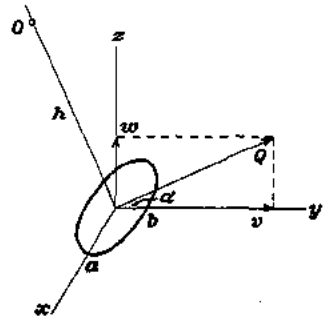

FIGURE 14.—Thin elliptic wing moving parallel to its plane of symmetry through a perfect fluid

the other pertinent terms in (57) vanishing, as appears on numerical substitution. Here $E=E\left(\theta,\frac{\pi}{2}\right)$, $\sin^2\theta=(a^2-b^2)/a^2$; also $L=\frac{4}{3}\frac{a}{E}\pi b^2\frac{\rho Q^2}{2}\sin 2\alpha$. Compare (68) with (66), calling b the width in both.

THEORY VERSUS EXPERIMENT.—In favorable cases the moment formulas of Part IV accord fairly well with experiment, as the following instances show. For lack of available data the force formulas for curvilinear motion are not compared with experiment.

(1) By (65) an endless elliptic strut with $a=1/3$ foot, $b=1/12$ foot, $c=5$ feet, held at α degrees incidence in a uniform stream of standard air at 40 miles an hour, for which $\rho Q^2/2=4.093$ pounds per square foot, sustains the yawing moment per foot length

$$N=\pi(a^2-b^2).\frac{\rho Q^2}{2}.\sin 2\alpha=1.3392\sin 2\alpha \text{ lb. ft} \text{ ---------- (69)}$$

This compares with the values found in the Navy 8 by 8 foot tunnel, as shown in Table IX faired from Figure 15. The agreement is approximate for small angles of attack. The model was of varnished mahogany, and during test was held with its long axis c level across stream, and with two closely adjacent sheet metal end plates, 2 feet square, to give the effect of plane flow.

---

[5] Equations (66) were published in Reference 5 as the result of a special research to determine the fluid forces and moment on a revolving plate. In the present text they follow as corollaries from more general formulas.

(2) By (66) an endless thin flat plate of width $2a = 5/12$ feet, similarly held in the same air stream, has per unit length the moment

$$N = \pi a^2 \frac{\rho Q^2}{2} \sin 2\alpha = 0.5581 \sin 2\alpha \text{ lb. ft.} \qquad (70)$$

This is compared in Table X and Figure 16 with the values found in the Navy 8 by 8 foot tunnel. The flat plate was of polished sheet aluminum 3/32 inch thick, with half round edges front and rear.

Again for an endless flat steel plate 5.95 inches wide by 0.178 inch thick at the center, with its front face flat and back face V-tapered to sharp edges, Fage and Johansen, Reference 6,

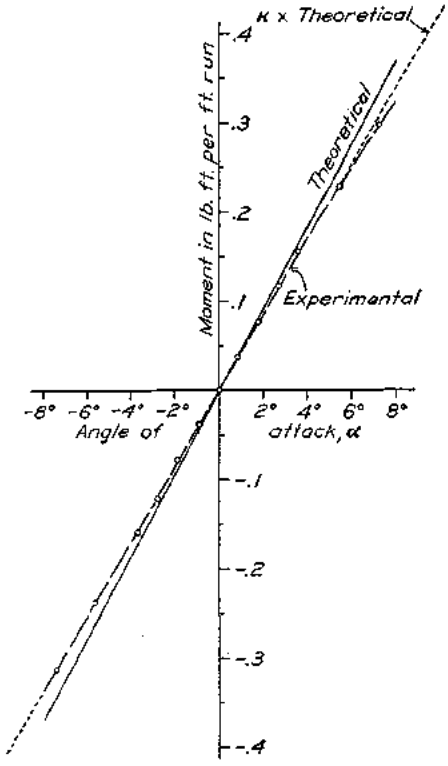

FIGURE 15.—Theoretical and experimental moment about long axis of endless elliptic cylinder. Width 8 inches, thickness 2 inches, air speed 40 miles per hour. Correction factor $\kappa = 0.912$

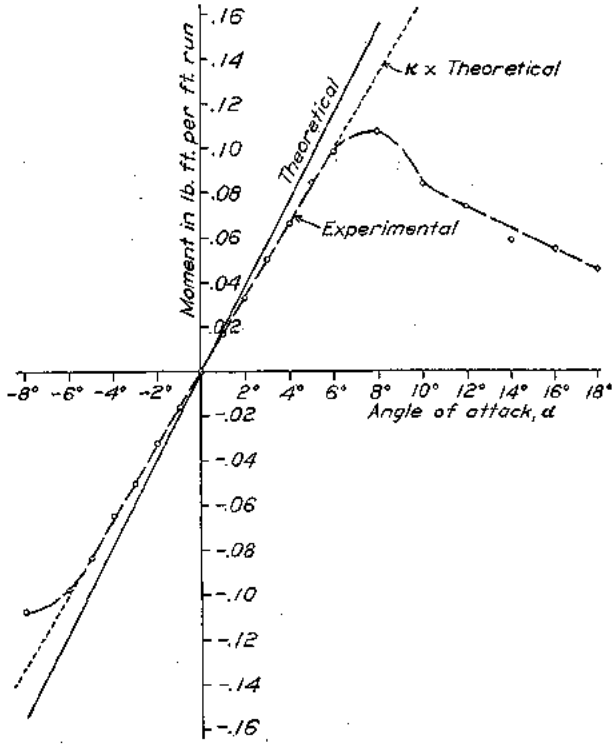

FIGURE 16.—Theoretical and experimental moment about long axis of endless rectangular plate. Width 5 inches, air speed 40 miles per hour. Correction factor $\kappa = 0.860$

found, at 50 feet per second and 5.85° angle of attack, $N = 0.125$ pound foot as the moment per foot run about the long axis, computed from the measured pressure over the median section. By (66), a thin flat plate would have

$$N = \pi a^2 \cdot \frac{\rho Q^2}{2} \cdot \sin 2\alpha = 0.1931 \times 2.9725 \times 0.2028 = 0.116 \text{ lb. ft.}$$

which is 7 per cent less than 0.125 found with their slightly cambered plate.

(3) An elliptic disk 3/32 inch thick with a, $b = 15$, 2.5 inches, when held as a wing in the Navy 40-mile-an-hour stream, had the moment L versus angle of attack α shown in Figure 17 and Table XI. For this case

$$\sin^2\theta = (a^2 - b^2)/a^2 = 875/900, \qquad \theta = 80° - 24', \qquad E = 1.03758.$$

Also in (68) $a = 5/4$ feet, $b = 5/24$ feet, $Q^2 = 4.093$; hence

$$L = \frac{4}{3} \frac{a}{E} \cdot \pi b^2 \cdot \frac{\rho Q^2}{2} \cdot \sin 2\alpha = 0.8963 \sin 2\alpha \text{ lb. ft.} \qquad (71)$$

which gives the theoretical values in Figure 17 and Table XI. The agreement is fair at small incidences. The disk as tested was of sheet aluminum cut square at the edges without any rounding or sharpening.

(4) For a wooden prolate spheroid 24 inches long by 6 inches thick, carried as in Figure 12 round a circle of radius $h=27.96$ feet to the model's center, Jones, Reference 3, found at 40 feet per second the values of N listed in Table XII. For this case Table III gives $k_b-k_a=0.778$, and (61) gives

$$N=(k_b-k_a)\tau\cdot\frac{\rho Q^2}{2}\cdot\sin 2\alpha=0.388\sin 2\alpha.$$

These values appear from Table XII not to accord closely with the experimental ones.

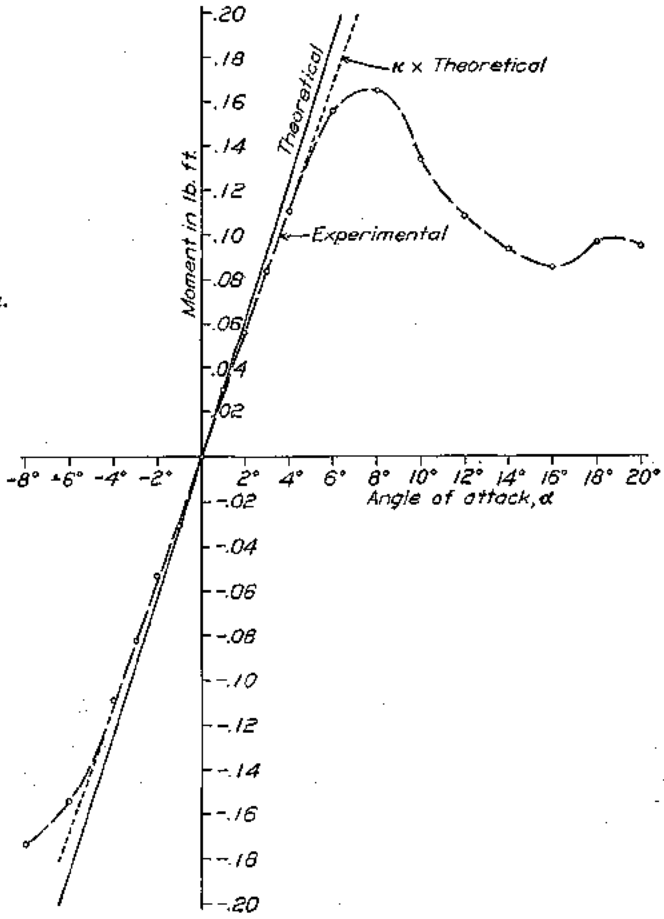

FIGURE 17.—Theoretical and experimental moment about long axis of elliptic disk. Length 30 inches, width 5 inches, air speed 40 miles per hour. Correction factor $\kappa=0.887$

CORRECTION FACTORS.—Figures 15, 16, 17 portray experimental moments, at small angles, as accurately equal to the theoretical times an empirical correction factor κ. Thus amended (61) gives for the experimental moment

$$N_e=\kappa N=\kappa(k_b-k_a)\tau\cdot\frac{\rho Q^2}{2}\cdot\sin 2\alpha.$$

For the given elliptical cylinder $\kappa=0.912$ with $-8°<\alpha<6°$; for the endless plate $\kappa=0.860$ with $-6°<\alpha<6°$; for the elliptic disk $\kappa=0.887$ with $-5°<\alpha<4°$. In such cases one should expect to find the actual air pressure nearly equal to the theoretical over the model's forward part, but so deficient along the rear upper surface as to cause a defect of resultant moment. No effort is made here to estimate it theoretically, nor to determine it empirically for a wide range of conditions.

The measurements shown in Table X, for the flat plate, were repeated at 50 and 60 miles an hour without perceptible scale effect.

REPORT No. 323

FLOW AND FORCE EQUATIONS FOR A BODY REVOLVING IN A FLUID

PART V

POTENTIAL COEFFICIENTS, INERTIA COEFFICIENTS

GREEN'S INTEGRALS.—The foregoing text employs Green's well-known integrals, which for the ellipsoid abc may be symbolized thus:

$$\alpha = abc\int_\lambda^\infty \frac{d\lambda}{a'^3b'c'} \qquad \beta = abc\int_\lambda^\infty \frac{d\lambda}{a'b'^3c'} \qquad \gamma = abc\int_\lambda^\infty \frac{d\lambda}{a'b'c'^3} \quad \text{-------(72)}$$

where $a' = \sqrt{a^2+\lambda}$, $b' = \sqrt{b^2+\lambda}$, etc., are semiaxes of the confocal ellipsoid $a'b'c'$. The integrals have the following values, Reference 4:

$$\left.\begin{aligned} \alpha &= A(b^2-c^2)[F(\theta,\varphi) - E(\theta,\varphi)] \\ \beta &= A(c^2-a^2)\left[\frac{b^2-c^2}{a^2-c^2}F(\theta,\varphi) + \frac{a^2-b^2}{\sqrt{a^2-c^2}}\frac{c'}{a'b'} - E(\theta,\varphi)\right] \\ \gamma &= A(a^2-b^2)\left[\sqrt{a^2-c^2}\frac{b'}{a'c'} - E(\theta,\varphi)\right] \end{aligned}\right\} \text{----------(73)}^1$$

where

$$A = \frac{2abc}{(a^2-b^2)(b^2-c^2)\sqrt{a^2-c^2}} \qquad \sin^2\theta = \frac{a^2-b^2}{a^2-c^2} \qquad \sin^2\varphi = \frac{a^2-c^2}{a^2+\lambda} \text{----------(74)}$$

and the elliptic integrals are

$$F(\theta,\varphi) = \int (1-\sin^2\theta\,\sin^2\varphi)^{-\frac{1}{2}}d\varphi \qquad E(\theta,\varphi) = \int (1-\sin^2\theta\,\sin^2\varphi)^{\frac{1}{2}}d\varphi \text{----------(75)}$$

Numerical values of $F(\theta,\varphi)$, $E(\theta,\varphi)$, α, β, γ are given in Tables I, II for $\lambda=0$ and various ratios a/b, b/c; viz, for various shapes of the ellipsoid abc. For $\varphi=\pi/2$ one writes $F(\theta,\varphi)=K$, $E(\theta,\varphi)=E$, by convention.

POTENTIAL COEFFICIENTS.—For motion (49) the ellipsoid abc has the potential coefficients known from textbooks.

$$\left.\begin{aligned} m_a &= \frac{\alpha}{2-\alpha_0} & m'_a &= \frac{G(\gamma-\beta)}{2G-(\gamma_0-\beta_0)} \text{ where } G=\frac{b^2-c^2}{b^2+c^2} \\ m_b &= \frac{\beta}{2-\beta_0} & m'_b &= \frac{H(\alpha-\gamma)}{2H-(\alpha_0-\gamma_0)} \text{ where } H=\frac{c^2-a^2}{c^2+a^2} \\ m_c &= \frac{\gamma}{2-\gamma_0} & m'_c &= \frac{I(\beta-\alpha)}{2I-(\beta_0-\alpha_0)} \text{ where } I=\frac{a^2-b^2}{a^2+b^2} \end{aligned}\right\} \text{----------(76)}$$

m_a, m_b, m_c being for translation along a, b, c and m'_a, m'_b, m'_c for rotation about them, and α_0, β_0, γ_0 being (73) for $\lambda=0$; viz, for a', b', $c'=a$, b, c. Surface values of (76), viz, for α, β, $\gamma=\alpha_0$, β_0, γ_0 are given in Tables III, IV. For fluid inside the ellipsoid the potential coefficients are as in (40) and given numerically in Table V.

INERTIA COEFFICIENTS.—From (76) are derived the conventional linear and angular inertia coefficients

$$k_a,\ k_b,\ k_c = m_a,\ m_b,\ m_c \qquad k'_a,\ k'_b,\ k'_c = Gm'_a,\ Hm'_b,\ Im'_c \text{----------(77)}$$

for the ellipsoid moving through or containing liquid, as in (40), (49). Surface values are given in Tables III, VI, VII.

[1] (73) satisfy the known relation $\alpha+\beta+\gamma=2abc/a'b'c'$, as appears on adding.

LIMITING CONDITIONS.—In some limiting cases, as for $c=0$, or $a=b$, etc., (73) may become indeterminate and require evaluation, as in Reference 4. In such cases the formulas in Table VIII may be used. For $c=0$, entailing zero mass and infinite k_c, k'_a, k'_b, one may use in (57) the values of $k_c m$, $k'_a A$, $k'_b B$ given at the bottom of Table VIII.

PHYSICAL MEANING OF THE COEFFICIENTS.—The tabulated potential coefficients, put in (40) or (49), serve to find the numerical value of the potential φ, or impulse $-\rho\varphi$ per unit area, at any point (x, y, z) of an ellipsoid surface.[2] Integration of $\rho\varphi$ over any surface, as explained for p in Part I, gives the component linear and angular zonal impulses. So, too, integration of $-\rho\varphi q_n/2$, where q_n is the normal surface velocity at (x, y, z), gives the kinetic energy imparted to the fluid; and integration of the impulsive pressure $-\rho\partial\varphi/\partial t$ gives the impulsive zonal forces and moments. One finds $\rho\partial\varphi/\partial t$ for (40), (49) by using with them the specified density ρ, accelerations $\dot{U}$, $\dot{V}$, $\dot{W}$, $\dot{\Omega}_a$, $\dot{\Omega}_b$, $\dot{\Omega}_c$, and tabulated potential coefficients for the given semiaxes a, b, c.

Thus putting $-\rho\varphi_c$, $-\rho\varphi'_c$ for p in (9), (10_1), and integrating over the whole ellipsoid surface, easily gives the fluid's linear and angular momenta

$$k_c.mW \qquad k'_c.C\Omega_c \qquad\qquad (78)$$

where mW, $C\Omega_c$ are respectively the linear and angular momenta of the displaced fluid moving as a solid with velocities W, Ω_c. The like surface integration of $-\rho\varphi_c q_n/2$ gives, as is well known,

$$k_c.mW^2/2 \qquad k'_c.C\Omega^2_c/2 \qquad\qquad (79)$$

where $mW^2/2$, $C\Omega^2_c/2$ are the kinetic energies of the displaced fluid so moving. Each inertia coefficient therefore is a ratio of the body's apparent inertia, due to the field fluid, to the like inertia of the displaced fluid moving as a solid.

By (49) the potential coefficients due to velocities W, Ω_c are

$$m_c = -\varphi_c/Wz \qquad m'_c = -\varphi'_c/\Omega_c xy$$

The first is the ratio of the outer and inner surface potentials due to W at any point z on the ellipsoid abc; the second is the ratio of the potentials due to Ω_c at (x, y), respectively on the outer surface of that ellipsoid and inside the cylinder of semiaxes ∞, b, c.

One notes that the momenta (78) times half the velocities give (79); also that the time derivatives of (78) are the force and moment Z, $N=k_c m\dot{W}$, $k'_c C\dot{\Omega}_c$, as in (57) for the simple z-wise motions, $\dot{W}$, $\dot{\Omega}$.

For any axial surface, say of torpedo form, moving as in Figure 12, the ratio $-k'_c C\Omega_c/k_b mV$ is the distance from the arbitrary origin 0_1 to the impulse center 0_2, or center of virtual mass. This may be taken as origin, and if the body's center of mass also is there Figures 11, 12 can still be superposed as in Figure 13. In the same way are related the acceleration force and moment $k_b m\dot{V}$, $k'_c C\dot{\Omega}_c$, thus illustrating the doctrine that the motion of a hydrokinetically symmetric form in a boundless perfect fluid, without circulation, obeys the ordinary dynamic equations for a rigid body.

AERODYNAMICAL LABORATORY,
BUREAU OF CONSTRUCTION AND REPAIR, U. S. NAVY,
WASHINGTON, D. C., *December 17, 1928.*

[2] This impulse is imparted by the moving surface to the fluid, otherwise still; the fluid in turn tends to impart to the body the impulse $\rho\varphi$ per unit area at (x, y, z).

CHIEF SYMBOLS USED IN THE TEXT

GEOMETRICAL

a, b, c ..... Semiaxes of ellipsoid abc.
a', b', c' ..... Semiaxes of confocal ellipsoid $a'b'c'$.
e, e' ..... Eccentricities of ellipse ab and its confocal $a'b'$; $ae=a'e'=\sqrt{a^2-b^2}$.
n; h_1, h_2 ..... Normal to ellipse ab; distances from origin to normal and tangent.
l, m, n ..... Direction cosines of normal n to any surface.
s; s_φ, s_ω ..... Length along any line; lengths along meridian and circle of latitude.
x, y, z ..... Cartesian coordinates; also coordinate axes.
r, β, ω ..... Polar coordinates of prolate spheroid abc.
η, θ ..... Eccentric angle of ab, inclination to x of normal to ab.

KINEMATICAL

u, v, w ..... Component velocities of fluid parallel to x, y, z axes.
q_t, q_n ..... Component velocities of fluid parallel to tangent and normal.
q_o, q ..... Resultant velocity of fluid before and after disturbance.
u, v, w ..... Component translation velocities of abc parallel to a, b, c
U, V, W ..... Component translation velocities of abc parallel to a, b, c
p, q, r ..... Component rotation velocities of abc about a, b, c ..... } Alternative symbols.
$\Omega_a, \Omega_b, \Omega_c$ ..... Component rotation velocities of abc about a, b, c .....
φ, ψ ..... Velocity potential, stream function.
m_a, m_b, m_c ..... Potential coefficients for abc with velocities u, v, w or U, V, W.
m'_a, m'_b, m'_c ..... Potential coefficients for abc with velocities p, q, r or $\Omega_a, \Omega_b, \Omega_c$.
$Q=\sqrt{U^2+V^2+W^2}$ .. Resultant velocity of abc.

DYNAMICAL

A_1, B_1, C_1 ..... Moments of inertia of rigid body about its axes a, b, c.
A, B, C ..... Moments of inertia of displaced fluid moving as a solid.
m_1, m ..... Mass of body, mass of displaced fluid.
ρ, τ ..... Density of fluid, volume of model or displaced fluid.
p, p_n ..... Pressure of fluid moving, pressure on coming to rest.
X_1, Y_1, Z_1; R_1 ..... Component forces applied to free rigid body; resultant force.
X, Y, Z; R ..... Component forces exerted by body on fluid; resultant force.
L_1, M_1, N_1 ..... Component moments about a, b, c applied to rigid body.
L, M, N ..... Component moments about a, b, c exerted by body on fluid.
k_a, k_b, k_c ..... Inertia coefficients for abc moving parallel to a, b, c in fluid.
k'_a, k'_b, k'_c ..... Inertia coefficients for abc rotating about a, b, c in fluid.

REFERENCES

Reference 1. Lamb, H.: Hydrodynamics, 5th ed., 1924. On the Forces Experienced by a Solid Moving Through a Liquid. Qart. Journ. Math.-t. XIX (1883).

Reference 2. Zahm, A. F.: Flow and Drag Formulas for Simple Quadrics. Report No. 253, National Advisory Committee for Aeronautics, 1927.

Reference 3. Jones, R.: The Distribution of Normal Pressures on a Prolate Spheroid. R. & M. No. 1061, British Aeronautical Research Committee, 1925.

Reference 4. Tuckerman, L. B.: Inertia Factors of Ellipsoids for Use in Airship Design. Report No. 210, National Advisory Committee for Aeronautics, 1925.

Reference 5. Cardonazzo, B.: Uber die gleichförmige Rotation eines festen Körpers in einer unbegrenzten Flussigkeit. In Vorträge, etc., edited by Karman & Levi-Civita, 1924.

Reference 6. Fage and Johansen: On the Flow of Air Behind an Inclined Flat Plate of Infinite Span. R. & M. No. 1104, British Aeronautical Research Committee, 1927.

Reference 7. Larmor, J.: On Hydrokinetic Symmetry. Quart. Journ. Math. t. XX (1920).

Reference 8. Ames, J. S.: A Résumé of the Advance in Theoretical Aeronautics made by Max M. Munk. Report No. 213, National Advisory Committee for Aeronautics, 1925.

TABLE I

ELLIPTIC INTEGRALS $F(\vartheta, \varphi)$, $E(\vartheta, \varphi)$[1]

[Defined in eq. (75), Part V]

a/c	b/c										
	1	2	3	4	5	6	7	8	9	10	∞
	$F(\vartheta, \varphi)$										
1	0.00000										
2	1.31696	1.04720									
3	1.76305	1.43870	1.23095								
4	2.06412	1.71874	1.48399	1.31814							
5	2.29319	1.92798	1.68471	1.50687	1.36940						
6	2.47903	2.10413	1.85138	1.66560	1.52053	1.40332					
7	2.63508	2.25400	1.99520	1.80281	1.65204	1.52959	1.42745				
8	2.77024	2.38432	2.12075	1.92379	1.76856	1.64194	1.53595	1.44550			
9	2.89035	2.49971	2.23255	2.03191	1.87318	1.74321	1.63405	1.54065	1.45948		
10	2.99638	2.60288	2.33303	2.12855	1.96804	1.83634	1.72357	1.62768	1.54419	1.47063	
∞	∞	∞	∞	∞	∞	∞	∞	∞	∞	∞	
	$E(\vartheta, \varphi)$										
1	0.00000										
2	.86603	1.04720									
3	.94277	1.07024	1.23095								
4	.96822	1.06091	1.18103	1.31814							
5	.97975	1.05019	1.14337	1.25126	1.36940						
6	.98597	1.04146	1.11604	1.20294	1.29096	1.40332					
7	.98972	1.03472	1.09589	1.16833	1.24893	1.33574	1.42745				
8	.99214	1.02946	1.08071	1.14185	1.21083	1.28461	1.36317	1.44550			
9	.99378	1.02529	1.06894	1.12136	1.18040	1.24464	1.31304	1.38453	1.45948		
10	.99496	1.02195	1.05966	1.10516	1.15569	1.21297	1.27316	1.33642	1.40240	1.47063	
∞	1.00000	1.00000	1.00000	1.00000	1.00000	1.00000	1.00000	1.00000	1.00000	1.00000	

[1] The integrals in this table are culled from L. Potin's Formules et Tables Numerique.

TABLE II

GREEN'S INTEGRALS α_0, β_0, γ_0

[Defined in eq. (73), Part V]

a/c	b/c										
	1	2	3	4	5	6	7	8	9	10	∞
	α_0										
1	0.66667										
2	.34713	0.47280									
3	.21751	.31265	0.36460								
4	.15092	.22474	.26820	0.29636							
5	.11171	.17064	.20719	.23189	0.24951						
6	.086527	.13471	.16584	.18769	.20336	0.21541					
7	.069266	.10950	.13629	.15541	.16970	.18079	0.18950				
8	.056894	.091037	.11435	.13135	.14426	.15440	.16254	0.16914			
9	.047710	.077071	.097571	.11276	.12448	.13378	.14132	.14757	0.15271		
10	.040637	.066203	.084381	.097957	.10872	.11728	.12428	.13010	.13500	0.13920	
∞	0	0	0	0	0	0	0	0	0	0	0
	β_0										
1	0.66667										
2	.82643	0.47280									
3	.89127	.53423	0.36460								
4	.92459	.59964	.39662	0.29636							
5	.94418	.59182	.41804	.31587	0.24951						
6	.95678	.60693	.43307	.32965	.26365	0.21541					
7	.96538	.61775	.44413	.34083	.27275	.22477	0.18950				
8	.97154	.62577	.45280	.34912	.28071	.23234	.19654	0.16914			
9	.97619	.63184	.45913	.35569	.28709	.23847	.20237	.17458	0.15271		
10	.97972	.63659	.46437	.36109	.29253	.24354	.20725	.17927	.15712	0.13920	
∞	1.00000	.66667	.50000	.40000	.33333	.28572	.25000	.22222	.20000	.18182	0
	γ_0										
1	0.66667										
2	.82643	1.05440									
3	.89127	1.15312	1.27078								
4	.92459	1.20572	1.35518	1.40726							
5	.94418	1.23752	1.37478	1.45223	1.50098						
6	.95678	1.25835	1.40110	1.48267	1.53401	1.56918					
7	.96538	1.27273	1.41956	1.50377	1.55754	1.59442	1.62100				
8	.97154	1.28320	1.43306	1.51953	1.57504	1.61326	1.64091	1.66172			
9	.97619	1.29109	1.44329	1.53154	1.58844	1.62775	1.65630	1.67784	1.69467		
10	.97972	1.29720	1.45125	1.54094	1.59895	1.63917	1.66846	1.69062	1.70787	1.72160	
∞	1.00000	1.33333	1.50000	1.60000	1.66667	1.71429	1.75000	1.77778	1.80000	1.81818	2.00000

TABLE III

POTENTIAL COEFFICIENTS m_a, m_b, m_c* FOR ELLIPSOIDS IN TRANSLATION

(For outer surface of $a\ b\ c$)

[Defined in eq. (76)]

a/c	b/c										
	1	2	3	4	5	6	7	8	9	10	∞
	m_a										
1	0.5000										
2	.2100	0.3096									
3	.1220	.1853	0.2229								
4	.08162	.1266	.1549	0.1740							
5	.05916	.09328	.1156	.1312	0.1425						
6	.04522	.07222	.09042	.1036	.1132	0.1207					
7	.03583	.05792	.07313	.08425	.09272	.09938	0.1047				
8	.02923	.04769	.06054	.07029	.07774	.08366	.08846	0.09238			
9	.02444	.04008	.05129	.05975	.06637	.07169	.07603	.07966	0.08257		
10	.02074	.03423	.04405	.05150	.05748	.06229	.06626	.06958	.07239	0.07481	
∞	0	0	0	0	0	0	0	0	0	0	0
	m_b										
1	0.5000										
2	.7042	0.3096									
3	.5039	.3845	0.2229								
4	.3598	.3933	.2474	0.1740							
5	.3943	.4203	.2643	.1876	0.1425						
6	.9171	.4357	.2764	.1974	.1512	0.1207					
7	.9331	.4459	.2855	.2054	.1579	.1266	0.1047				
8	.9447	.4554	.2925	.2115	.1633	.1314	.1090	0.09238			
9	.9535	.4619	.2980	.2163	.1676	.1354	.1126	.09564	0.08257		
10	.9603	.4669	.3024	.2203	.1712	.1387	.1156	.09846	.08526	0.07481	
∞	1.0000	.5000	.3333	.2500	.2000	.1667	.1429	.12500	.11111	.10000	0
	m_c										
1	0.5000										
2	.7042	1.115									
3	.5039	1.362	1.743								
4	.3598	1.518	2.008	2.374							
5	.3943	1.622	2.199	2.651	3.008						
6	.9171	1.697	2.339	2.866	3.292	3.642					
7	.9331	1.750	2.446	3.030	3.520	3.931	4.277				
8	.9447	1.790	2.528	3.163	3.706	4.171	4.570	4.912			
9	.9535	1.821	2.593	3.269	3.860	4.373	4.819	5.208	5.548		
10	.9603	1.846	2.645	3.357	3.987	4.543	5.032	5.465	5.846	6.194	
∞	1.0000	2.000	3.000	4.000	5.000	6.000	7.000	8.000	9.000	10.000	∞

* These have the same values as the inertia coefficients k_a, k_b, k_c.

TABLE IV

POTENTIAL COEFFICIENTS m'_a, m'_b, m'_c FOR ELLIPSOIDS IN ROTATION

(For outer surface of $a\ b\ c$)

[Defined in eq. (76)]

a/c	b/c										
	1	2	3	4	5	6	7	8	9	10	∞
	m'_a										
1	0										
2	0	0.5643									
3	0	.6390	1.045								
4	0	.6768	1.135	1.499							
5	0	.6989	1.190	1.596	1.943						
6	0	.7125	1.225	1.663	2.042	2.380					
7	0	.7211	1.249	1.705	2.113	2.481	2.813				
8	0	.7270	1.266	1.738	2.165	2.556	2.915	3.245			
9	0	.7315	1.278	1.762	2.206	2.615	2.995	3.348	3.675		
10	0	.7348	1.288	1.780	2.235	2.660	3.058	3.430	3.778	4.103	
∞	0	.7500	1.333	1.875	2.400	2.917	3.429	3.937	4.444	4.950	∞
	m'_b										
1	0										
2	−0.3990	−0.5643									
3	−.5819	−.8853	−1.045								
4	−.6885	−1.104	−1.349	−1.499							
5	−.7581	−1.264	−1.558	−1.800	−1.943						
6	−.8058	−1.384	−1.750	−2.052	−2.243	−2.380					
7	−.8402	−1.476	−1.935	−2.264	−2.504	−2.680	−2.813				
8	−.8659	−1.548	−2.062	−2.445	−2.732	−2.948	−3.114	−3.245			
9	−.8857	−1.607	−2.168	−2.600	−2.931	−3.188	−3.338	−3.547	−3.675		
10	−.9013	−1.654	−2.257	−2.734	−3.107	−3.402	−3.657	−3.825	−3.978	−4.103	
∞	−1.0000	−2.000	−3.000	−4.000	−5.000	−6.000	−7.000	−8.000	−9.000	−10.000	−∞
	m'_c										
1	0										
2	0.2990	0									
3	.5819	0.1556	0								
4	.6885	.2420	0.08332	0							
5	.7581	.2969	.1359	0.05193	0						
6	.8058	.3350	.1719	.08705	0.03549	0					
7	.8402	.3627	.1981	.1134	.06127	0.02569	0				
8	.8659	.3836	.2181	.1330	.08081	.04529	0.01951	0			
9	.8857	.3998	.2336	.1484	.09610	.06058	.04056	0.01527	0		
10	.9013	.4127	.2460	.1608	.1084	.07291	.04721	.02770	0.01238	0	
∞	1.0000	.5000	.3333	.2500	.2000	.16667	.14286	.12500	.11111	0.10000	0

104397—30——29

TABLE V

POTENTIAL COEFFICIENTS m'_a, m'_b, m'_c FOR ELLIPSOIDS IN ROTATION

(For all points inside of $a\ b\ c$)

[Defined in eq. (40)]

a/c	b/c										
	1	2	3	4	5	6	7	8	9	10	∞
	$m'_c = G$										
0 to ∞	0	0.60000	0.80000	0.88235	0.92308	0.94595	0.96000	0.96923	0.97561	0.98020	1.00000
	$m'_b = H$										
1	0	Same for all values of b/c									
2	−0.60000										
3	−.80000										
4	−.88235										
5	−.92308										
6	−.94595										
7	−.96000										
8	−.96923										
9	−.97561										
10	−.98020										
∞	−1.00000										
	$m'_a = I$										
1	0										
2	0.60000	0									
3	.80000	0.33462	0								
4	.88235	.60000	0.28000	0							
5	.92308	.72414	.47059	0.21951	0						
6	.94595	.80000	.60000	.33462	0.18033	0					
7	.96000	.84906	.68966	.50769	.32432	0.15294	0				
8	.96923	.88235	.75342	.60000	.42820	.28000	0.13274	0			
9	.97561	.90588	.80000	.67010	.52380	.33462	.24615	0.11724	0		
10	.98020	.92308	.83486	.72414	.60000	.47059	.34228	.21951	0.10497	0	
∞	1.00000	1.00000	1.00000	1.00000	1.00000	1.00000	1.00000	1.00000	1.00000	1.00000	.....

TABLE VI

INERTIA COEFFICIENTS [1] k'_a, k'_b, k'_c FOR ELLIPSOIDS IN ROTATION

(For outer surface of a b c)

[Defined in eq. (77)]

a/c	b/c										
	1	2	3	4	5	6	7	8	9	10	∞
	$k'_a = Gm'_a$										
1	0										
2	0	0.3386									
3	0	.3834	0.8359								
4	0	.4051	.9051	1.323							
5	0	.4194	.9519	1.408	1.793						
6	0	.4275	.9803	1.468	1.885	2.251					
7	0	.4328	.9995	1.505	1.950	2.347	2.701				
8	0	.4362	1.013	1.533	1.999	2.418	2.799	3.145			
9	0	.4389	1.023	1.556	2.035	2.473	2.876	3.245	3.585		
10	0	.4409	1.030	1.571	2.064	2.516	2.936	3.324	3.686	4.022	
∞	0	.4500	1.067	1.654	2.215	2.759	3.291	3.816	4.336	4.852	∞
	$k'_b = Hm'_b$										
1	0										
2	0.2394	0.3386									
3	.4655	.7082	0.8359								
4	.6078	.9745	1.191	1.323							
5	.6998	1.167	1.466	1.662	1.793						
6	.7622	1.309	1.683	1.941	2.122	2.251					
7	.8066	1.417	1.857	2.174	2.403	2.573	2.701				
8	.8393	1.501	1.999	2.370	2.648	2.857	3.019	3.145			
9	.8641	1.567	2.115	2.536	2.860	3.110	3.305	3.460	3.585		
10	.8834	1.622	2.213	2.679	3.045	3.335	3.565	3.749	3.900	4.022	
∞	1.0000	2.000	3.000	4.000	5.000	6.000	7.000	8.000	9.000	10.000	∞
	$k'_c = Im'_c$										
1	0										
2	0.2394	0									
3	.4655	0.05985	0								
4	.6078	.1452	0.02333	0							
5	.6998	.2150	.06393	0.01140	0						
6	.7622	.2690	.1031	.03348	0.00640	0					
7	.8066	.3079	.1367	.05758	.01987	0.00293	0				
8	.8393	.3385	.1643	.07982	.03541	.01268	0.00259	0			
9	.8641	.3622	.1869	.09941	.05077	.02330	.00858	0.00179	0		
10	.8834	.3810	.2054	.1164	.06503	.03431	.01616	.00608	0.00130	0	
∞	1.0000	.5000	.3333	.2500	.20000	.16667	.14286	.12500	.11111	0.10000	0

[1] For translation k_a, k_b, k_c are given in Table III.

TABLE VII

INERTIA COEFFICIENTS k'_a, k'_b, k'_c FOR ELLIPSOIDS IN ROTATION.

(Inner surface of $a\ b\ c$)

[Defined in eq. (77)]

a/c	b/c										
	1	2	3	4	5	6	7	8	9	10	∞
	$k'_a = Gm'_a$										
0 to ∞	0	0.36000	0.64000	0.77854	0.85208	0.89482	0.92160	0.93941	0.95181	0.96079	1.00000
	$k'_b = Hm'_b$										
1	0	Same for all values of b/c.									
2	0.36000										
3	.64000										
4	.77854										
5	.85208										
6	.89482										
7	.92160										
8	.93941										
9	.95181										
10	.96079										
∞	1.00000										
	$k'_c = Im'_c$										
1	0										
2	0.36000	0									
3	.64000	0.14793	0								
4	.77854	.36000	0.07840	0							
5	.85208	.52438	.22145	0.04818	0						
6	.89482	.64000	.36000	.14793	0.03252	0					
7	.92160	.72000	.47563	.25775	.10618	0.02239	0				
8	.93941	.77854	.56764	.36000	.19202	.07840	0.01752	0			
9	.95181	.82062	.64000	.44903	.27910	.14793	.06059	0.01375	0		
10	.96079	.85208	.69699	.52438	.36000	.22145	.11716	.04818	0.01102	0	
∞	1.00000	1.00000	1.00000	1.00000	1.00000	1.00000	1.00000	1.00000	1.00000	1.00000	------

TABLE VIII

INERTIA VALUES FOR LIMITING FORMS OF ELLIPSOIDS $a>b>c$

INERTIA COEFFICIENTS FOR TRANSLATION AND ROTATION

a/b	Shape	k_a	k_b	k_c	k'_a	k'_b	k'_c
			$c=0$				
1	Circular disk	0	0	∞	∞	∞	0
1+	Elliptical disk	0	0	∞	∞	∞	0
∞	Long rectangle	0	0	∞	∞	∞	0
			$b>c>0$				
1	Oblate spheroid $e^2=1-c^2/a^2$	$-\frac{c}{a}\frac{ce-a\sin^{-1}e}{ae(e^2+1)-c\sin^{-1}e}$		$\frac{a}{c}\frac{ae-c\sin^{-1}e}{ce-a\sin^{-1}e}$	$\frac{e^4(\gamma_0-\beta_0)}{(2-e^2)[2e^2-(2-e^2)(\gamma_0-\beta_0)]}$‡		0
1+	Ellipsoid						
∞	Elliptical cylinder	0	c/b	b/c	$\frac{1}{2bc}\frac{(b^2-c^2)^2}{b^2+c^2}$	b/c	c/b
			$c=b$				
1	Sphere	½	½	½	0	0	0
1+	Prolate spheroid $e^2=1-c^2/a^2$	$-\frac{\log\frac{1+e}{1-e}-2e}{\log\frac{1+e}{1-e}-\frac{2e}{1-e^2}}$	$-\frac{\log\frac{1+e}{1-e}-\frac{2e}{1-e^2}}{\log\frac{1+e}{1-e}-2e\frac{1-2e^2}{1-e^2}}$		0	$\frac{e^4(\beta_0-\alpha_0)}{(2-e^2)[2e^2-(2-e^2)(\beta-\alpha)}$‡	
∞	Round cylinder	0	1	1	0	1	1

APPARENT MASSES AND MOMENTS OF INERTIA WHEN $c=0$

a/b	Shape	$k_a m$	$k_b m$	$k_c m$	$k'_a A$	$k'_b B$	$k'_c C$
1	Circular disk	0	0	$\frac{8}{3}\rho a^3$	$\frac{16}{45}\rho a^5$		0
1+	Elliptical disk	0	0	$\frac{4}{3}\pi\rho ab^2/E$	$\frac{4\pi\rho}{15}\frac{ab^3(a^2-b^2)}{(2a^2-b^2)E-b^2K}$	$\frac{4\pi\rho}{15}\frac{a^3b^2(a^2-b^2)}{(a^2-2b^2)E+b^2K}$	0
∞	Long rectangle $a=\infty$	0	0	$\pi\rho b^2$*	$\frac{4}{3}\pi\rho b^4$*	$\pi\rho b^2$*	0

‡ $\gamma_0-\beta_0=-1+\frac{3}{e^2}-\frac{3}{e^3}\sqrt{1-e^2}\sin^{-1}e.$ $\beta_0-\alpha_0=-2+\frac{3}{e^2}-\frac{3}{2}\frac{1-e^2}{e^3}\log_e\frac{1+e}{1-e}.$

* Per unit length of model.

TABLE IX

LIFT, DRAG, AND MOMENT ON ENDLESS ELLIPTIC CYLINDER

[Width 8 inches, thickness 2 inches, air speed 40 miles per hour]

Angle of attack α,* degrees	Lift	Drag	Moment about long axis pound foot per foot run	
	Pound per foot run		Experimental	Theoretical $N=1.3392 \sin 2\alpha$
−8	−2.30	0.160	−0.335	−0.3691
−6	−1.94	.139	−.254	−.2784
−4	−1.42	.122	−.170	−.1864
−3	−1.11	.116	−.127	−.1400
−2	−.76	.111	−.084	−.0934
−1	−.40	.108	−.042	−.0467
0	0	.106	0	0
+1	+.41	.108	+.044	+.0467
2	.80	.111	.085	.0934
3	1.13	.116	.129	.1400
4	1.44	.123	.171	.1864
6	1.90	.140	.249	.2784
+8	+2.16	.165	+.325	+.3691

*As the test angles α were in part fractional, all measurements in Table IX are faired from the original graphs of lift, drag, and moment versus α, in fig. 15.

TABLE X

LIFT, DRAG, AND MOMENT ON ENDLESS THIN FLAT PLATE

[Width 5 inches, air speed 40 miles per hour]

Angle of attack α, degrees	Lift	Drag	Moment about long axis pound foot per foot run	
	Pound per foot run		Experimental	Theoretical $N=0.5581 \sin 2\alpha$
−8	−1.345	0.190	−0.107	−0.1538
−6	−.980	.112	−.097	−.1160
−5	−.827	.0916	−.083	−.0984
−4	−.614	.0596	−.064	−.0777
−3	−.471	.0464	−.050	−.0583
−2	−.315	.0360	−.032	−.0389
−1	−.157	.0324	−.016	−.0195
0	0	.0312	0	0
+1	+.155	.0328	+.017	+.0195
2	.311	.0360	.033	.0389
3	.471	.0472	.050	.0583
4	.639	.0648	.066	.0777
5	.831	.0900	.085	.0984
6	1.018	.124	.098	.1160
8	1.346	.206	.107	.1538
10	1.538	.291	.084	+.1909
12	1.594	.360	.074	
14	1.582	.422	.059	
16	1.531	.480	.055	
+18	+1.530	.542	+.046	

TABLE XI

LIFT, DRAG, AND MOMENT ON THIN ELLIPTIC WING

[Length 30 inches, width 5 inches, air speed 40 miles per hour]

Angle of attack α degrees	Lift	Drag	Moment about long axis, pound foot	
	Pounds		Experimental	Theoretical $L=0.5963 \sin 2\alpha$
−8	−2.415	0.426	−0.173	−0.2471
−6	−1.835	.266	−.154	−.1863
−4	−1.136	.169	−.109	−.1247
−3	−.836	.133	−.062	−.0937
−2	−.567	.116	−.053	−.0625
−1	−.294	.105	−.031	−.0313
0	+.005	.103	0	0
+1	.303	.106	+.030	+.0313
2	.590	.118	.056	.0625
3	.890	.136	.084	.0937
4	1.195	.168	.111	.1247
6	1.861	.265	.166	.1863
8	2.474	.422	.165	.2471
10	2.865	.567	.134	+.3068
12	2.958	.696	.109	
14	2.892	.798	.094	
15	2.859	.897	.086	
18	2.769	.974	.097	
+20	+2.725	1.065	+.095	

TABLE XII

MOMENT ON PROLATE SPHEROID [1]

[Length 24 inches, diameter 5 inches, through-air speed 40 feet per second]

Angle of attack α, degrees	Moment about minor axis, pound foot			
	Measured on balance	Found by pressure integration		Theoretical $N=0.383 \sin 2\alpha$
	Rectilinear motion	Rectilinear motion	Curvilinear motion	
−20	−0.179	−0.207	−0.157	−0.249
−10	−.106	−.122	−.073	−.133
−4	−.045	−.052	−.018	−.054
0	0	0	+.021	0
+10	+.106	+.122	.127	+.133
+20	+.179	+.207	+.177	+.249

[1] Data taken from Reference 3.

NATIONAL ADVISORY COMMITTEE FOR AERONAUTICS

TECHNICAL MEMORANDUM NO. 713

BEHAVIOR OF VORTEX SYSTEMS*

By A. Betz

Progressive application of the Kutta-Joukowsky theorem to the relationship between airfoil lift and circulation affords a number of formulas concerning the conduct of vortex systems. The application of this line of reasoning to several problems of airfoil theory yields an insight into many hitherto little observed relations.

The report is confined to plane flow, hence all vortex filaments are straight and mutually parallel (perpendicular to the plane of flow).

I. GENERAL THEOREMS

1. Kutta-Joukowsky theorem.- When a body, about which the line integral of the flow is other than zero, i.e., with a circulation Γ, is in motion relative to this fluid with speed v, it is impressed by a force perpendicular to the direction of motion, which per unit length is

$$P = \rho v \Gamma \tag{1}$$

(Kutta-Joukowsky theorem, fig. 1). If there is no motion in the fluid other than the circulatory flow, then v is the speed at infinity relative to the fluid. But, if the fluid executes still other motions aside from the circulation, say, when several vortices, or sources and sinks are existent, it is not forthwith clear which is to be considered as the relative speed. On the other hand, we do know that v should be the speed of the body relative to that flow which would prevail in the place of the body in its absence. The body is thereby assumed as infinitely small, otherwise different speeds could prevail at different places of the body. (This case can be worked up by integration from infinitely small bodies.) This finer distinction of the Kutta-Joukowsky theorem is readily understood when bearing in mind that a free vortex, upon which no force can act, moves at the same speed as the flow in the place of the vortex if the latter were nonexistent. Consequently, the Kutta-Joukowsky theorem must afford the force zero for the motion at this speed, that is, the speed in the Kutta-Joukowsky theorem must be measured relative to this motion. But this may also be shown direct by appropriate

*"Verhalten von Wirbelsystemen." Z.f.a.M.M., vol. XII, no. 3, June 1932, pp. 164-174.

derivation of the Kutta-Joukowsky theorem. The general rule for this derivation consists of computing those pressures in a coordinate system, in which the body rests (steady motion), which as result of superposition of circulation and translation act upon a control area enveloping the body and the momentums which enter and leave through it. Thus when we choose as control area a cylinder enveloping the body so closely that the speed of translation in the whole region of the control area can be considered as constant, this selfsame translatory speed contiguous to the body becomes the speed v in the Kutta-Joukowsky theorem, although it is the speed which would prevail at this point if the body were nonexistent.

2. The center of gravity of finite vortex zones.- If there are a number of vortices in a fluid, each individual one is within a flow which as field of all other vortices is determined by their magnitude and arrangement, and each vortex moves with this flow. Visualizing these vortices replaced by individual solid bodies with the same circulation as the vortices (say, rotating cylinders), the flow also is the same. Preventing these bodies from moving with the flow without effecting a change in their circulation, each cylinder is impressed according to Kutta-Joukowsky by a force and we must, in order to hold it, exert an opposite force upon it. For a body with circulation Γ_n, existing at a point with speed v_n, this force is

$$P_n = \rho\, v_n\, \Gamma_n \tag{2}$$

and is at right angles to v_n. The resultant of the forces exerted on the cylinders must be taken up by the walls at the boundaries of the fluid, i.e., it must be equal to the resultant from the pressures of the fluid onto the boundary wall.*

*By restraining the vortices the flow becomes steady (provided that there are no singularities other than those vortices, and that the boundary walls are rigid and quiescent). For which reason the pressures can be computed by the simple Bornoulli equation $p + \frac{\rho}{2} = v^2 = \text{constant}$. For free vortices the type of flow within a stated time interval is the same as for restrained vortices, but it is usually no longer steady, for the vortices travel, that is, change their arrangement in space. Therefore the pressures change also, because for nonsteady flow the generalized Bornoulli equation $p + \frac{\rho}{2} v^2 + \rho \frac{\partial \Phi}{\partial t} = \text{constant}$ is applicable (Φ = flow potential, for steady flow $\frac{\partial \Phi}{\partial t} = 0$). With free vortices there is no force as is in the restrained vortices, so that the resultant force on the boundary walls must disappear. This is precisely obtained by the accelerating forces $\rho \frac{\partial \Phi}{\partial t}$. Consequently, the forces on the fluid boundaries used here and in the following are those forces which would occur if the vortices were restrained, i.e., by steady flow.

Now, if the fluid is very much extended so that its assumedly rigid and quiescent boundaries are everywhere far removed from the vortices (or bodies with circulation), the resultant of the pressures onto the boundary walls approaches zero when the vortices are restrained. For the flow velocity v produced by the vortices decreases inversely proportional to the first power of the distance, while the relevant pressure differences (Bornoulli's equation $p - p_o = -\frac{\rho}{2} v^2$) drop inversely proportional to the square of the distance; the surface of the boundary increases linearly with the distance, so that the force produced as sum of pressure difference and surface is a decrease inversely proportional to the distance.

But when this force on the boundary walls vanishes, the resultant force on our body must disappear also, or in other words,

$$\sum_n P_n = \rho \sum_n v_n \Gamma_n = 0 \tag{3}$$

As the forces P_n or the speeds v_n may assume any direction, Σ is considered a vectorial addition of the forces or speeds, respectively. Instead of that the components in the X and Y direction may be added separately, in which case

$$\sum_n P_{nx} = \rho \sum_n v_{ny} \Gamma_n = 0 \tag{3a}$$

and

$$\sum_n P_{ny} = \rho \sum_n v_{nx} \Gamma_n = 0 \tag{3b}$$

with x and y as components along X and Y of the respective vectors. If we release the bodies, whereby they can be replaced again by common vortices, they move at the speed v_n, and our preceding equations constitute a general prediction as to the displacement of the vortices within a fluid without extraneous forces, especially in a fluid extended to infinity. To illustrate: visualize the vortices replaced by mass points (material system) whose mass is proportional to the vortex intensities. Admittedly, we must also include negative masses, in which the vortices with one sense of rotation correspond to positive masses and those with opposite sense of rotation correspond to negative masses. Then we may speak of a center of gravity of a vortex system, while meaning the center of gravity of the corresponding mass system. Applying this interpretation, the vortex motion can be expressed as follows:

Theorem 1.- The motion of vortices in a fluid upon which no extraneous forces can act (fluid extended to infinity), is such that their center of gravity relative to the rigid fluid boundaries or relative to the fluid at rest at infinity remains unchanged. This theorem has already been developed, although in a different way, by Helmholtz, in his well-known work (reference 1). The premise is, of course, the absence of further singular points in the fluid other than the stipulated vortices.

If the fluid is bounded by rigid walls and it is possible to make some prediction as to the resultant force on the boundary walls by restrained vortices (steady flow), then equation (2) gives an account of motion of the center of gravity of the vortex.

If the resultant force on the walls is P, then

$$\rho \Sigma v_n \Gamma_n = P \tag{4}$$

with v_o = velocity in center of gravity relative to the rigid walls, we have

$$\rho v_o \Sigma \Gamma_n = \rho \Sigma v_n \Gamma_n = P$$

hence,

$$v_o = \frac{P}{\rho \Sigma \Gamma_n} \tag{5}$$

which is at right angles to the force P. Thus,

Theorem 2.- When, by restrained vortices (steady flow), the pressures exerted by the fluid onto the boundary walls produce a resultant force, then the movement of the center of gravity of the free vortices is such as an airfoil whose circulation equals the sum of the circulations of the vortices would need to have an quiescent, infinitely extended fluid to make its lift equal to this resultant force.

As a rule the pressures on the boundary walls and thus their resultant force are not summarily known, although it is possible to make at least certain predictions in many cases. For example, if the fluid is bounded on one side by a flat wall or enclosed between two parallel walls, the resultant force can only be perpendicular to those boundary walls. Since the center of gravity of the vortices moves perpendicularly to this force.

Theorem 3 reads as follows: If there are vortices between two flat, parallel walls or on one side of a flat boundary wall, the distance of the center of gravity of the vortex from these walls remains unchanged (it moves parallel to the walls). This result has already been obtained for a small number of vortices by numerical calculation of the vortex paths.*

3. Inertia moment of finite vortex zones.- Again visualize the vortices as being held fast in a fluid and decompose the speeds on each vortex into a component radially toward or away from the center of gravity and one at right angles thereto. If r is the distance of a vortex with circulation Γ away from the center of gravity, and v_r the radial (outwardly directed) speed component, this vortex is impressed with a force

*W. Muller's report before the meeting of the members of the Ges. f. angew. Math. u. Mech., at Göttingen, 1929; and of physicists, at Prague, 1929.

$$T = \rho \Gamma v_r$$

which is perpendicular to r and therefore forms a moment $T r$ with respect to the center of gravity. The tangential component v_t (perpendicular to r) produces a force along r which does not set up a moment about the center of gravity. The sum of the forces impressed upon the vortices can be divided into a resultant passing through the center of gravity (radial force component due to v_t) and a moment

$$M = \rho \Sigma \Gamma v_r r.$$

They must be equal and opposite to the forces and moments acting on the fluid boundaries. Releasing the vortices, the center of gravity moves conformably to the laws of the individual force. Moreover, the vortices move also in radial direction at speed v_r. Since

$$v_r = \frac{\partial r}{\partial t}$$

we obtain

$$\rho \Sigma \Gamma r \frac{\partial r}{\partial t} = \frac{\rho}{2} \frac{\partial}{\partial t} \Sigma \Gamma r^2 = M \qquad (6)$$

where M = moment of extraneous forces, by restrained vortices, with respect to the center of gravity. If this is zero,* we have

$$\Sigma \Gamma r^2 = \text{constant} \qquad (7)$$

$\Sigma \Gamma r^2$ is a quantity which corresponds to the polar mass moment of inertia $\Sigma m r^2$ relative to the center of gravity. Consequently, it may be designated as inertia moment of the vortex system and we obtain

Theorem 4.- When, by restrained vortices, the extraneous forces acting on a fluid have no moment with respect to the center of gravity of the vortex system within this fluid, the inertia moment of this system of vortices remains constant.

If the moment of the extraneous forces is in the same sense as the chosen positive vortex rotation, this inertia moment increases according to equation (6) and vice versa.

4. Vortex systems whose total circulation is zero.- The kinetic energy of a potential vortex in infinitely extended flow in a circular ring between r and dr and thickness layer 1 is

*Whether or not there is an extraneous moment in a given case requires a more careful analysis than the problem of extraneous forces, since, for example, the forces decrease toward zero with $1/r$ when the boundary surfaces are enlarged, whereas the moments may remain finite because of the added factor r as lever arm.

$$\frac{\rho}{2}\left(\frac{\Gamma}{2r\pi}\right)^2 2\,r\,\pi\,dr = \frac{\rho}{2}\frac{\Gamma^2}{2\pi}\frac{dr}{r}.$$

Integration over the whole fluid (from $r = 0$ to $r = \infty$) yields by approximation to $r = 0$ as well as to $r = \infty$, the energy as ∞. For which reason it is physically impossible to realize such vortices. The difficulty with $r = 0$ is obviated because the physical vortices always have a nucleus of finite diameter, in which the speed no longer rises with $1/r$ toward ∞, but remains finite. But by $r = \infty$ the difficulty remains (apart from the energy the rotary momentum likewise = ∞). As a result, the production of vortices in an infinitely extended fluid can only be effected by pairs, so that the sum of the circulations is zero. The velocity field of such a doublet drops at great distances inversely as the square of the distance so that the fluid energy remains finite for any extension. Hence,

Theorem 5.- The total circulation ot all vortices in an infinitely extended fluid is zero. No vortex system with finite total circulation can occur unless the fluid is finitely limited. And of course, a part of the vortices in an infinitely extended fluid can also be at such a remote distance as to be of no account for the flow at that particular point. There may then be vortex systems with one-sided total circulation, in which the very vortices which supplement the total circulation to zero are very remote from it. Since, however, energy and momentum of two opposite vortices increase with the distance, very great distances are encountered only in cases of very great energy input. The case of a vortex system with zero total circulation is consequently relatively frequent and deserves special consideration, since the center of gravity of such a system lies, as we know, at infinity, so that the preceding theorems are not summarily applicable in part.

Combining one part of the vortices into one group and the others into another group, we can analyze each group by itself, as, for instance, the clockwise rotating vortices in one, and the anticlockwise vortices in another, although this is not necessary. The only condition is that the total circulation of the one group be equal and opposite to that of the other group and other than zero.

In the absence of forces and moments on the fluid,* as, say, by infinitely extended fluid, the forces and moments on restrained vortices must be zero or, in other words, the resultant force on one group must be equal and opposite to the force on the other and be on the same line with it. But these forces need not necessarily pass through the center of gravity of each of the two groups. When the vortices are released the center of gravity of each of the two groups moves perpendicularly to this onesided force and at the same speed. This is expressed in

*In such vortex systems the moments also are forthwith small when pushing beyond the rigid boundary walls. (Compare footnote on page 8.)

Theorem 6, as follows: The motion of the centers of gravity of two groups of vortices with equal and opposite total circulation is mutually parallel and has the same speed, hence constant distance.

Knowing at first absolutely nothing about the direction of the opposite force, we can make no prediction as to the direction of motion. When this opposite force passes through the center of gravity of a group, this group is without extraneous moments and its inertia moment is then constant (theorem 4).* As a rule this force does not exactly go through the center of gravity of the two groups. But when they are separate to a certain extent and closed in themselves, the force almost always passes very close to the center of gravity, in which case we can then consider the inertia moments at least approximately as constant.

If the force does not pass through the centers of gravity of the groups, their inertia moment changes. But if the force is parallel to the line connecting the two centers of pressure (S_1, S_2, fig. 2), which is manifested by their perpendicular motion to the connecting line, the moment of the force relative to the two centers of gravity is equal and opposite. The result is that the inertia moment of one group increases at the same rate as that of the other group decreases. (One inertia moment is usually positive, the other negative; their absolute values thus increase or decrease to the same extent.)

Theorem 7.- If the motion of the centers of gravity of two groups of vortices of equal and opposite total circulation within an infinitely extended quiescent fluid is perpendicular to the line connecting the gravity centers, the algebraic sum of the inertia moments of the groups remains unchanged.

When the force forms an angle with this connecting line (S_1 S_2, fig. 3), that is, when one velocity component v_x is along its connecting line, the inertia moment of one group increases more than that of the other decreases or vice versa. In any case, the sum of the inertia moments of the two groups is changed. It amounts, in fact, to

$$\frac{\partial}{\partial t}\left(\Sigma\, r_1^2\, \Gamma_1 + \Sigma\, r_2^2\, \Gamma_2\right) = 2\, v_x\, a\, \Sigma\, \Gamma \tag{8}$$

according to equation (6) and figure 3. ($\Sigma\, r_1^2\, \Gamma_1$ is the inertia moment of one group, $\Sigma\, r_2^2\, \Gamma_2$ that of the other, a is the distance of the two centers of gravity, and $\Sigma\, \Gamma$ the total circulation of one group.)

*It was always assumed that no singularity other than the vortex system existed. But with the two groups and each considered by itself, the assumption ceases to hold. However, the previous considerations can be generalized so that the forces needed to restrain the vortices of the momentarily disregarded group, become the extraneous forces on the fluid. It is readily seen that theorem 4 is equally applicable in this sense to a group of vortices in the presence of further vortices.

The sum of the inertia moments increases when the motion of the centers of gravity in direction of the group with positive circulation is toward the group with negative circulation. It decreases for opposite direction. Thus $\Sigma\,\Gamma$ in equation (8) denotes the total circulation of that group, which moves toward the other.

II. APPLICATION

In the practical application of these theorems, it frequently is not so much a case of a number of individual vortices, but rather of continuously distributed vortices. But that presents no difficulty; it merely means substituting terms for Σ terms. It is, however, something else when the vortex systems extend to infinity and at the same time have infinitely large circulation. But with some care, they also are amenable to solution by these theorems.

1. Vortices back of an airplane wing.- According to airfoil theory (see Handb. d. Phys., vol. VII, p. 239 ff), an area of discontinuity is formed behind a wing by optimum lift distribution (minimum by given lift), which has the same speed of downwash at every point. Thus the flow behind an airfoil may be visualized as if a rigid plate, the area of discontinuity, were downwardly displaced at constant speed and thereby sets the fluid in motion (fig. 4). This, however, is applicable only in first approximation when the interference velocities (foremost of which is the speed of displacement w) are small compared to the flight speed. For this motion would only be possible for any length of time if the area of discontinuity actually were rigid. By flowing around the edges, laterally directed suction forces P occur, which only could be taken up by a rigid plate. These forces are absent when the area of discontinuity is other than rigid, as a result of which the suction P effects other motions; starting at the edges, it unrolls and gradually forms two distinct vortices (fig. 5).

With l = wing span, the circulation per unit length of $\frac{d\Gamma}{dx}$ for such an area of discontinuity is distributed across the span conformably to the following equation

$$\frac{d\Gamma}{dx} = \Gamma_o\left(\frac{2}{l}\right)^2 \frac{x}{\sqrt{1 - \left(2\,\frac{x}{l}\right)^2}} \tag{9}$$

with Γ_o = circulation about the wing in its median plane. The downward velocity of the area of discontinuity prior to development is

$$w = \frac{\Gamma_o}{l} \,. \tag{10}$$

The area of discontinuity may be regarded as a continuously distributed system of vortices with zero total circulation. The distribution of the

vortices is given in equation (9). Combining the two symmetrical halves ($-\frac{l}{2} \leq x \leq 0$ and $0 \leq x \leq \frac{l}{2}$) into one group each, the distance of the center of gravity of the two groups must remain the same, according to theorem 6. The center of gravity of a system of vortices conformable to equation (9) from 0 to 1/2 lies, as is readily computable, at a distance.

$$x_o = \frac{\pi}{4} \frac{l}{2} \tag{11}$$

from the center, so that the distance of the centers of gravity of the two groups becomes

$$a = 2\, x_o = \frac{\pi}{4}\, l \tag{12}$$

This, then, is accordingly also the distance of the centers of gravity of the two formative individual vortices (fig. 5). The steady symmetry of the process in the present case is indicative of the consistently parallel displacement of the centers of gravity and consequently, that the individual vortices are also symmetrical to the original plane of symmetry.

The process of convolution or development with respect to time can also be followed by similar considerations, although this calls for considerable mathematical work. Up to the present the course of the process has been explored very accurately in its first stages, during which the developed part was still small compared to the whole area of discontinuity (reference 3).

In the present report an attempt is made to gain approximate information regarding the magnitude of the tip vortices and the circulatory distribution within them. The vortices of the area of discontinuity are divided at some point x and those lying to the left are grouped into one; these to the right of it (full line in fig. 6) into another. Then it is assumed that the opposite forces on the two groups - the vortices being restrained - pass through the center of gravity of both groups, which actually proves fairly correct, because of the comparatively strong concentration of the vortices toward the tips and the ensuing distinct separation of both groups. Now the inertia moment of one vortex group must remain approximately constant during development. The total circulation of one group of the undeveloped area of discontinuity from x to $l/2$ is

$$\Gamma_x = \int_x^{l/2} \frac{\partial \Gamma}{\partial x}\, dx = \Gamma_o \sqrt{1 - \left(\frac{2x}{l}\right)^2} \tag{13}$$

For the ensuing calculation the angle ϕ is used in place of the variable x, which is bound up with x through

$$\cos \phi = \frac{2x}{l} \quad \text{and} \quad \sin \phi = \sqrt{1 - \left(\frac{2x}{l}\right)^2} \tag{14}$$

Thus the vortex distribution (equation 9) becomes:

$$\frac{\partial \Gamma}{\partial x} = \Gamma_o \left(\frac{2}{l}\right)^2 \frac{x}{\sqrt{1 - \left(\frac{2x}{l}\right)^2}} = \Gamma_o \frac{2}{l} \cot \phi \tag{9a}$$

$$\Gamma_x = \Gamma_o \sqrt{1 - \left(\frac{2x}{l}\right)^2} = \Gamma_o \sin \phi \tag{13a}$$

The distance of the center of gravity of this group is:

$$x_1 = \frac{1}{\Gamma_x} \int_x^{l/2} \frac{\partial \Gamma}{\partial x} x dx = \frac{1}{\sin \phi} \frac{l}{2} \int_0^{\phi} \cos^2 \phi d\phi = \frac{l}{4 \sin \phi} \left[\phi + \frac{1}{2} \sin^2 \phi\right] \tag{15}$$

The inertia moment of the group with respect to the center of the area of discontinuity ($x = 0$) is:

$$J_o = \int_x^{l/2} \frac{\partial \Gamma}{\partial x} x^2 dx = \Gamma_o \left(\frac{l}{2}\right)^2 \int_0^{\phi} \cos^3 \phi d\phi = \Gamma_o \left(\frac{l}{2}\right)^2 \sin\phi \left(1 - \frac{1}{3} \sin^2 \phi\right) \tag{16}$$

The inertia moment of the group with respect to its center of gravity is:

$$J_x = J_o - \Gamma_x x_1^2 = \Gamma_o \left\{ \left(\frac{l}{2}\right)^2 \sin\phi \left(1 - \frac{1}{3} \sin^2\phi\right) - \left(\frac{l}{4}\right)^2 \frac{1}{\sin\phi} \left[\phi + \frac{1}{2} \sin 2\phi\right]^2 \right\} \tag{17}$$

This inertia moment must be present again after the convolution.

Now the coiled-up group is assumed to be circular; that is, the asymmetry stipulated by the mutual interference of the two coiled-up vortices is disregarded, so that the circulation may be presented as a pure function of radius ($\Gamma = f(r)$). The vortex group from x to $l/2$ is coiled up into a spiral which fills the circle with radius r. Then the circulation Γ_r must be equal to the circulation of the original vortex group

$$\Gamma_r = \Gamma_x \tag{18}$$

and likewise, the inertia moment of the vortices coiled up in this circle must be equal to the original inertia moment of the vortex group

$$J_r = \int_o^r \frac{\partial \Gamma}{\partial r} r^2 \, dr = J_x \, . \tag{19}$$

Permitting r to increase by dr, then decreases x by dx and increases ϕ by $d\phi$ under these premises. The result is an increase of

$$\frac{\partial \Gamma_r}{\partial r} dr = \frac{\partial \Gamma_x}{\partial \phi} d\phi = \Gamma_o \cos \phi \, d\phi \tag{20}$$

in circulation, and of

$$\frac{\partial \Gamma_r}{\partial r} r^2 \, dr = \frac{\partial J_x}{\partial \phi} d\phi \tag{21}$$

in inertia moment.

Then the differentiation of (17) yields

$$\frac{\partial J_x}{\partial \phi} = \Gamma_o \left(\frac{l}{2}\right)^2 \left[\cos^3\phi + \frac{\cos\phi}{4 \sin^2 \phi} \left(\phi + \frac{1}{2} \sin 2\phi\right)^2 - \frac{1}{2 \sin\phi} \left(\phi + \frac{1}{2} \sin 2\phi\right)\left(1 + \cos 2\phi\right)\right]$$

which, written into (21) and with regard to (20) gives

$$\left(\frac{2r}{l}\right)^2 = \cos^2\phi + \frac{1}{4 \sin^2\phi} \left(\phi + \frac{1}{2} \sin 2\phi\right)^2 - \frac{\cos\phi}{\sin\phi} \left(\phi + \frac{1}{2} \sin 2\phi\right) \tag{22}$$

Since $\sin\phi = \sqrt{1 - \left(\frac{2x}{l}\right)^2}$, (equation 22) connotes the relationship between r and x, that is, it gives the size of the circle into which a piece of the original area of discontinuity has changed. And, knowing the circulation $\Gamma = \Gamma_o \sin \phi$, the equation also discloses the distribution of the circulation in the coiled-up tip vortex. Figure 7 shows the respective values of Γ and x versus r, and also the distribution of the vortex density $\frac{d\Gamma}{d(r^2\pi)} \frac{l^2}{20 \Gamma_o}$. When forming the pertinent boundary transitions, equation (22) yields

$$\left(\frac{2r}{l}\right)^2 = \frac{1}{9} \sin^4\phi \tag{23}$$

for very small values of ϕ, so that

$$\frac{r}{\frac{l}{2} - x} = \frac{2}{3} \tag{24}$$

In other words, a small boundary piece of the area of discontinuity coils up into a circle, whose radius is 2/3 of the length of the original piece.

For $\phi = \frac{\pi}{2}$ we have $\frac{2r}{l} = \frac{\pi}{4}$, which means that the radius of the tip vortices is $\frac{\pi}{4}\frac{l}{2}$. Since the center of the tip vortices is $\frac{\pi}{4}\frac{l}{2}$ distant from the plane of symmetry, it would indicate that the two tip vortices precisely touch each other. But for such close proximity, our assumption that the individual tip vortices shall be symmetrical circles, ceases to hold: the speed between the two vortices is substantially greater than it is outside, with the result that the individual streamlines are outwardly displaced. So in reality the vortices should not touch each other. The established approximate result however, may, because of its simplicity, give a ready picture of the order of magnitude of the vortices. According to figure 7, the relalationship between r and x is fairly linear. Hence $r = \frac{2}{3}\left(\frac{l}{2} - x\right)$ in the greater part of the vortex conformable to (24), and it is only in the outer edge of the vortex that the factor $2/3$ changes to $\pi/4$. The curve for the distribution of the vortex density shows the main part of the vortices to be very much concentrated around the center despite their comparatively great extent.

2. Phenomena behind cascades of airfoils.- Cascades of airfoils also form areas of discontinuity aft of the airfoils (fig. 8), and whose motion relative to the undisturbed flow would, by optimum lift distribution, be as for rigid surfaces, if the edges could absorb the suction. But in reality they develop with respect to time. (See Handb. d. Phys., vol. VII, p. 272 ff.)

Let us analyze the practically always existing case wherein the distance a' of the surfaces is small compared to their span. Assuming the areas of discontinuity to be actually rigid, the flow around the rigid surfaces far behind the airfoils would, near the edge, be as shown in figure 9, when choosing a system of coordinates within which these surfaces rest. The motion in this system of coordinates being steady, Bernoulli's equation can be employed. Inasmuch as the interference velocity between the surfaces far removed from the edge is evanescently small relative to the surfaces, whereas outside in the undisturbed flow the relative velocity is equal and opposite to the velocity of displacement w, Bernoulli's equation yields

$$p = \rho \frac{w^2}{2} \tag{25}$$

positive pressure between the surfaces with respect to the pressure in the undisturbed flow on the side of the surfaces.* This positive pressure balances the suction at the plate edges. For an analysis of the horizontal forces acting upon a fluid strip of the height of the surface spacing a', reveals on one side a force $a' \rho \frac{w^2}{2}$, as result of the pressure difference within and without, and on the other the suction at one plate edge. No momentums are transmitted by the boundary surfaces, therefore the suction must be

$$P = a' \rho \frac{w^2}{2} \tag{26}$$

In such a system of surfaces the vortices are very much concertrated at the boundaries, at great distance from the edge, that is, in the entire middle part of the surfaces the relative velocities are practically zero and with it, of course, the velocity differences on both sides of the surfaces, i.e., the vortices. As a result, the effects of the developed and of the undeveloped areas of discontinuity are equal at distances which are great compared to spacing a', since the spatial transformation of the vortices during development is subordinate as against the great distance. Nevertheless, there is a fundamental difference as far as the flow is concerned between the theoretical process with undeveloped rigid surfaces and the actual process with developed individual vortices, a fact which up to now has never been pointed out, to my knowledge.

The vortex group at one side is in the velocity field of the vortices of the other. Owing to its remoteness, this field does not change appreciably during the development. Thus assuming the vortices as restrained before and after development, the mutual force exerted by the vortices, remains the same, and with it the velocity in the center of gravity of the developed and the undeveloped vortices. But when visualizing the areas of discontinuity as rigid, they are then no longer exempt from forces because of the suction P, and in that case the velocity is greater by an amount

$$\Delta w = \frac{P}{\rho \Gamma} \tag{27}$$

*Directly behind the cascades the pressures and velocities are different. By contraction or expansion of the lateral edges of the areas of discontinuity (positive or negative contraction) equilibrium is, however, established with the pressure of the lateral undisturbed flow, resulting in a correspondingly different speed. (see Handb. d. Phys., vol. VII, p. 259 ff.) Here and in the following the conditions subsequent to this balance are considered only. For many purposes it should be noted that owing to the width changes of the hypothetical rigid area of discontinuity the suction at the edges has a component along the direction of flow.

than with the free vortices. Γ is herein the circulation about the part of the area of discontinuity lying on one side of the plane of symmetry, respectively, about the single vortex developed therefrom (for the rest equal to the circulation about the airfoil in its median part). Following the line integral in figure 9, it is readily seen that

$$\Gamma = a' w \tag{28}$$

hence, with due regard to (26):

$$\Delta w = \frac{w}{2} \tag{29}$$

Then the velocity of the free vortices is:

$$w' = w - \Delta w = \frac{w}{2} \tag{30}$$

As a matter of fact, the process of development is such that the center of gravity of the vortices clustered around each edge, lags behind the velocity of the central main part of the surfaces. Whereas the latter moves at velocity w, the center of gravity of the vortices moves at a speed $w/2$ and it maintains this speed in the final attitude after development.

However, this speed $w/2$ can also be deduced direct from the field of the opposite vortices. At great distance it is identical with that of a vertical row of concentric vortices (fig. 10). But at medium distance the field of such a vortex row is a constant speed $\pm w' = \pm\frac{\Gamma}{2a'}$ downward on one side and upward on the other. Between the two rows the fields of the two rows add up to speed w, so that

$$w = 2 w' \tag{31}$$

The signs for the fields outside of the rows are contrary, hence the speed is zero. Each vortex row itself moves under the effect of the momentary other row, that is, its speed is

$$w' = \frac{w}{2} \tag{32}$$

But there is yet another result which is not as readily conceived as the change in vortex velocity. For the rigid surfaces we had within the deflected flow a positive pressure $q = \rho \frac{w^2}{2}$ which balanced the suction at the edges. After development the suction is absent, so that there is also no more positive pressure within between the vortex rows, as can be proved from the Bernoulli equation. In the chosen system of coordinates of figure 10, w is the speed of the inside flow, 0 that of the outside flow, and $w/2$ that of the vortices. To insure steady conditions, we must select a coordinate system in which the vortices rest. Then the speed of the inside flow is $w/2$ and that of the

outside flow $-w/2$ (fig. 11). Both are of equal absolute magnitude, hence of equal pressure within and without the vortex rows.

Now this change of pressure during development is not without influence on the flow inside. Analyzing a cut through the airfoil cascades (figs. 8 and 12) while applying Bernoulli's equation to the speeds in front of and behind the cascades, reveals by pressure balance (developed vortices, fig. 12).

$$c_3 = c_1 \tag{33}$$

and by $p = \rho \frac{w^2}{2}$ (undeveloped vortices)

$$c_2^2 + w^2 = c_1^2 \tag{34}$$

Therefore the speed is greater after development than before ($c_3 > c_2$).

This result, while at first sight perhaps somewhat peculiar, can also be elucidated in a different fashion. Looking at the cascades from the side, once with undeveloped vortex surfaces (fig. 8), and then with developed vortices (fig. 12), the direction of the detached vortices is manifestly different because their own speed relative to the undisturbed flow is different (w and $w/2$). The interference velocity w, which may be considered as vortex field, is perpendicular to the vortices, and has therefore a somewhat different position in both cases. For nondeveloped vortices, the vortices lie in the direction of c_2, w is perpendicular to c_2 (fig. 8), and since c_2 is composed of undisturbed velocity c_1 and interference velocity w, we have

$$c_2^2 = c_1^2 - w^2 \ .$$

In the developed state the vortices move with natural speed $w/2$, that is, they are between c_1 and c_3. Since w and therefore $w/2$ in turn are perpendicular to the vortices, the velocity vectors c_1, c_3, and w form a triangle in which the vortex line is the median line (fig. 12). But this implies that $c_3 = c_1$.

Translation by J. Vanier,
National Advisory Committee for Aeronautics.

REFERENCES

1. Helmholtz: Über die Integrale der hydrodynamischen Gleichungen, welche den Wirbelbewegungen entsprechen. Jour. f. d. reine und angew. Math. 55, 1918, pp. 25-55.

2. Kaden, H.: Aufwicklung einer unstabilen Unstetigkeitsfläche (Göttinger Dissertation). Ing.-Arch. 2 (1931), p. 140.

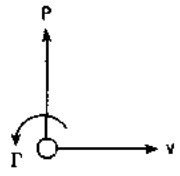

Figure 1.-Kutta-Joukowsky theorem.

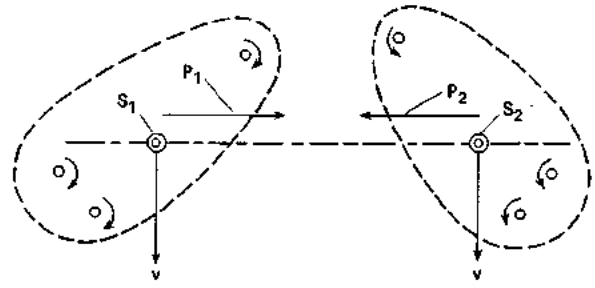

Figure 2.-Two groups of vortices whose centers of gravity move perpendicular to their connecting line.

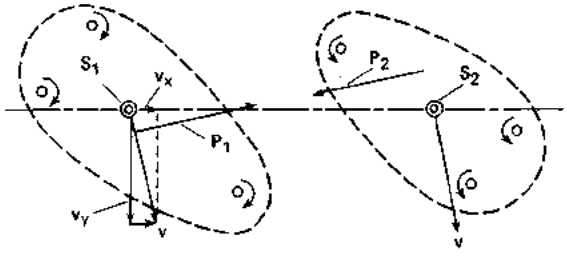

Figure 3.-Two groups of vortices whose centers of gravity move obliquely to their connecting line.

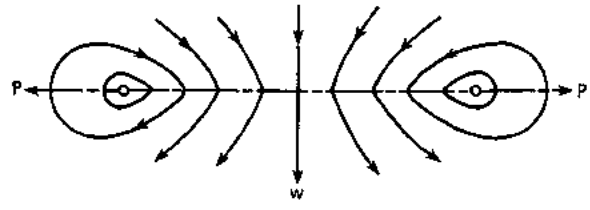

Figure 4.-Displacement of a rigid plate in a fluid.

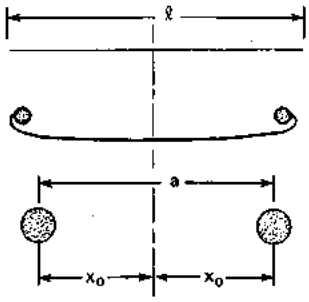

Figure 5.-Development of area of discontinuity behind an airplane wing.

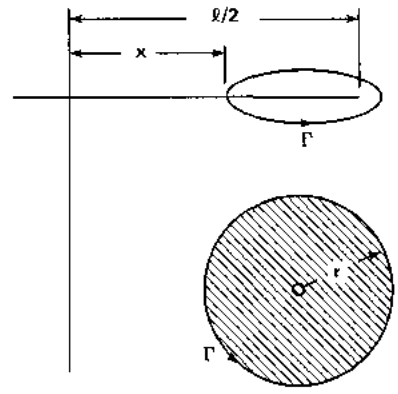

Figure 6.-Part of area of discontinuity and circle over which it is distributed after development.

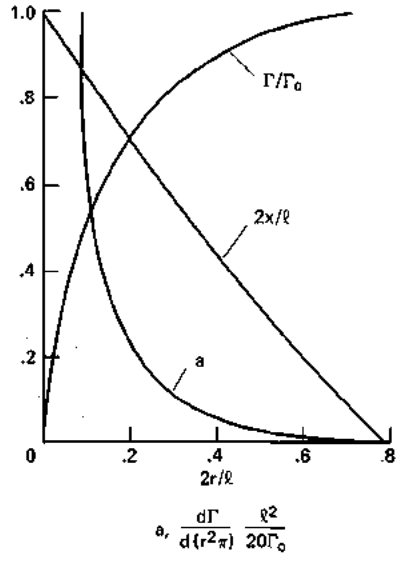

Figure 7.-Relationship between developed and non-developed area of discontinuity.

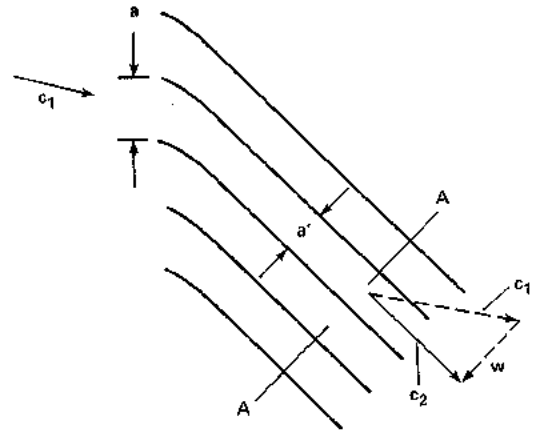

Figure 8.-Flow past cascades of airfoils with hypothetical rigid areas of discontinuity.

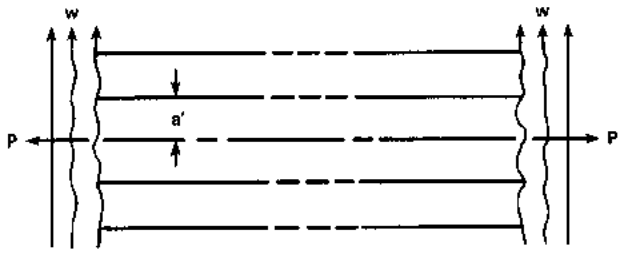

Figure 9.-Flow about the theoretical non-developed areas of discontinuity in cut A-A.

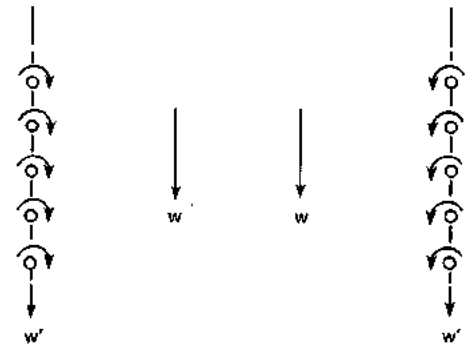

Figure 10.-Velocities relative to undisturbed flow.

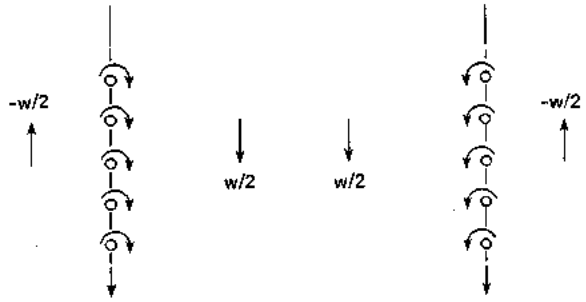

Figure 11.-Velocities relative to vortices after development (steady flow).

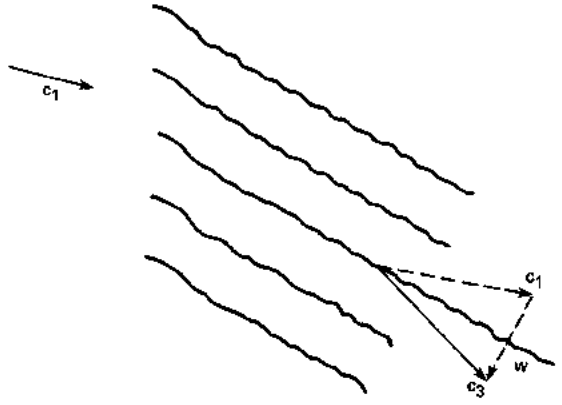

Figure 12.-Composition of velocity after development.

REPORT No. 452

GENERAL POTENTIAL THEORY OF ARBITRARY WING SECTIONS

By T. Theodorsen and I. E. Garrick

SUMMARY

This report gives an exact treatment of the problem of determining the 2-dimensional potential flow around wing sections of any shape. The treatment is based directly on the solution of this problem as advanced by Theodorsen in N. A. C. A. Technical Report No. 411. The problem condenses into the compact form of an integral equation capable of yielding numerical solutions by a direct process.

An attempt has been made to analyze and coordinate the results of earlier studies relating to properties of wing sections. The existing approximate theory of thin wing sections and the Joukowsky theory with its numerous generalizations are reduced to special cases of the general theory of arbitrary sections, permitting a clearer perspective of the entire field. The method not only permits the determination of the velocity at any point of an arbitrary section and the associated lift and moments, but furnishes also a scheme for developing new shapes of preassigned aerodynamical properties. The theory applies also to bodies that are not airfoils, and is of importance in other branches of physics involving potential theory.

INTRODUCTION

The solution of the problem of determining the 2-dimensional potential flow of a nonviscous incompressible fluid around bodies of arbitrary shape can be made to depend on a theorem in conformal representation stated by Riemann almost a century ago, known as the fundamental theorem of conformal representation. This theorem is equivalent to the statement that it is possible to transform the region bounded by a simple curve into the region bounded by a circle in such a way that all equipotential lines and stream lines of the first region transform respectively into those of the circle. The theorem will be stated more precisely in the body of this report and its significance for wing section theory shown—suffice it at present to state that if the analytic transformation by which the one region is transformed conformally into the region bounded by the circle is known, the potential field of this region is readily obtained in terms of the potential field of the circle.

A number of transformations have been found by means of which it is possible to transform a circle into a contour resembling an airfoil shape. It is obviously true that such *theoretical* airfoils possess no particular qualities which make them superior to the types of more empirical origin. It was probably primarily because of the difficulty encountered in the inverse problem, viz, the problem of transforming an airfoil into a circle (which we shall denote as the direct process) that such artificial types came into existence. The 2-dimensional theoretical velocity distribution, or what is called the flow pattern, is known only for some special symmetrical bodies and for the particular class of Joukowsky airfoils and their extensions, the outstanding investigators [1] being Kutta, Joukowsky, and von Mises. Although useful in the development of airfoil theory these theoretical airfoils are based solely on special transformations employing only a small part of the freedom permitted in the general case. However, they still form the subject of numerous isolated investigations.

The direct process has been used in the theory of thin airfoils with some success. An approximate theory of thin wing sections applicable only to the mean camber line has been developed [2] by Munk and Birnbaum, and extended by others. However, attempts [3] which have been made to solve the general case of an arbitrary airfoil by direct processes have resulted in intricate and practically unmanageable solutions. Lamb, in his "Hydrodynamics" (reference 1, p. 77), referring to this problem as dependent upon the determination of the complex coefficients of a conformal transformation, states: "The difficulty, however, of determining these coefficients so as to satisfy given boundary conditions is now so great as to render this method of very limited application. Indeed, the determination of the irrotational motion of a liquid subject to given boundary conditions is a problem whose exact solution can be effected by direct processes in only a very few cases. Most of the cases for which we know the solution have been obtained by an inverse process; viz, instead of trying to find a value of ϕ or ψ which satisfies [the Laplacian] $\nabla^2\phi = 0$ or $\nabla^2\psi = 0$ and given boundary conditions, we take some known solution of these differential equations

[1] See bibliography given in reference 9, pp. 24, 84, and 583.
[2] Cf. footnote 1.
[3] See Appendix II of this paper.

and inquire what boundary conditions it can be made to satisfy."

In a report (reference 2) recently published by the National Advisory Committee for Aeronautics a general solution employing a direct method was briefly given. It was shown that the problem could be stated in a condensed form as an integral equation and also that it was possible to effect the practical solution of this equation for the case of any given airfoil. A formula giving the velocity at any point of the surface of an arbitrary airfoil was developed. The first part of the present paper includes the essential developments of reference 2 and is devoted to a more complete and precise treatment of the method, in particular with respect to the evaluation of the integral equation.

In a later part of this paper, a geometric treatment of arbitrary airfoils, coordinating the results of earlier investigations, is given. Special airfoil types have also been studied on the basis of the general method and their relations to arbitrary airfoils have been analyzed. The solution of the inverse problem of creating airfoils of special types, in particular, types of specified aerodynamical properties, is indicated.

It is hoped that this paper will serve as a step toward the unification and ultimate simplification of the theory of the airfoil.

TRANSFORMATION OF AN ARBITRARY AIRFOIL INTO A CIRCLE

Statement of the problem.—The problem which this report proposes to treat may be formulated as follows. Given an arbitrary airfoil[4] inclined at a specified angle in a nonviscous incompressible fluid and translated with uniform velocity V. To determine the theoretical 2-dimensional velocity and pressure distribution at all points of the surface for all orientations, and to investigate the properties of the field of flow surrounding the airfoil. Also, to determine the important aerodynamical parameters of the airfoil. Of further interest, too, is the problem of finding shapes with given aerodynamical properties.

Principles of the theory of fluid flow.—We shall first briefly recall the known basic principles of the theory of the irrotational flow of a frictionless incompressible fluid in two dimensions. A flow is termed "2-dimensional" when the motion is the same in all planes parallel to a definite one, say xy. In this case the linear velocity components u and v of a fluid element are functions of x, y, and t only.

The differential equation of the lines of flow in this case is

$$v\,dx - u\,dy = 0$$

and the equation of continuity is

$$\frac{\partial u}{\partial x} + \frac{\partial v}{\partial y} = 0 \text{ or } \frac{\partial u}{\partial x} = \frac{\partial (-v)}{\partial y}$$

which shows that the above first equation is an exact differential.

If $Q = c$ is the integral, then

$$u = \frac{\partial Q}{\partial y} \text{ and } v = -\frac{\partial Q}{\partial x}$$

This function Q is called the stream function, and the lines of flow, or streamlines, are given by the equation $Q = c$, where c is in general an arbitrary function of time.

Furthermore, we note that the existence of the stream function does not depend on whether the motion is irrotational or rotational. When rotational its vorticity is

$$\zeta = \frac{\partial v}{\partial x} - \frac{\partial u}{\partial y} = \frac{\partial^2 Q}{\partial x^2} + \frac{\partial^2 Q}{\partial y^2}$$

which is twice the mean angular velocity or "rotation" of the fluid element. Hence, in irrotational flow the stream function has to satisfy

$$\frac{\partial^2 Q}{\partial x^2} + \frac{\partial^2 Q}{\partial y^2} = 0 \qquad (2')$$

Then there exists a velocity potential P and we have

$$\left.\begin{aligned} \frac{\partial P}{\partial x} &= u = \frac{\partial Q}{\partial y} \\ \frac{\partial P}{\partial y} &= v = -\frac{\partial Q}{\partial x} \end{aligned}\right\} \qquad (1)$$

The equation of continuity is now

$$\frac{\partial^2 P}{\partial x^2} + \frac{\partial^2 P}{\partial y^2} = 0 \qquad (2)$$

Equations (1) show that

$$\frac{\partial P}{\partial x}\frac{\partial Q}{\partial x} + \frac{\partial P}{\partial y}\frac{\partial Q}{\partial y} = 0$$

so that the family of curves

$$P = \text{constant},\ Q = \text{constant}$$

cut orthogonally at all their points of intersection.

For steady flows, that is, flows that do not vary with time, the paths of the particles coincide with the streamlines so that no fluid passes normal to them. The Bernoulli formula then holds and the total pressure head H along a streamline is a constant, that is

$$\tfrac{1}{2}\rho v^2 + p' = H$$

where p' is the static pressure, v the velocity, and ρ the density. If we denote the undisturbed velocity at infinity by V, the quantities $p' - p'_\infty$ by p, and $\tfrac{1}{2}\rho V^2$ by q, the Bernoulli formula may be expressed as

$$\frac{p}{q} = 1 - \left(\frac{v}{V}\right)^2 \qquad (3)$$

[4] By an airfoil shape, or wing section, is roughly meant an elongated smooth shape rounded at the leading edge and ending in a sharp edge at the rear. All practical airfoils are characterized by a lack of abrupt change of curvature except for a rounded nose and a small radius of curvature at the tail.

The solutions of equations (2) and (2′), infinite in number, represent all possible types of irrotational motion of a nonviscous incompressible fluid in two dimensions. For a given problem there are usually certain specified boundary conditions to be satisfied which may be sufficient to fix a unique solution or a family of solutions. The problem of an airfoil moving uniformly at a fixed angle of incidence in a fluid field is identical with that of an airfoil fixed in position and fluid streaming uniformly past it. Our problem is then to determine the functions P and Q so that the velocity at each point of the airfoil profile has a direction tangential to the surface (that is, the airfoil contour is itself a streamline) and so that at infinite distance from the airfoil the fluid has a constant velocity and direction.

The introduction of the complex variable, $z=x+iy$, simplifies the problem of determining P and Q. Any analytic function $w(z)$ of a complex variable z, that is, a function of z possessing a unique derivative in a region of the complex plane, may be separated into its real and imaginary parts as $w(z)\equiv w(x+iy)=P(x, y)+iQ(x, y)$, determining functions P and Q which may represent the velocity potential and stream function of a possible fluid motion. Thus, analytic functions of a complex variable possess the special property that the component functions P and Q satisfy the Cauchy-Riemann equations (eq. (1)), and each therefore also satisfies the equation of Laplace (eq. (2)). Conversely, any function $P(x, y)+iQ(x, y)$ for which P and Q satisfy relations (1) and (2) may be written as $w(x+iy)\equiv w(z)$. The essential difficulty of the problem is to find the particular function $w(z)$ which satisfies the special boundary-flow conditions mentioned above for a specified airfoil.

The method of conformal representation, a geometric application of the complex variable, is well adapted to this problem. The fundamental properties of transformations of this type may be stated as follows: Consider a function of a complex variable $z=x+iy$, say $w(z)$ analytic in a given region, such that for each value of z, $w(z)$ is uniquely defined. The function $w(z)$ may be expressed as $w=\xi+i\eta$ where ξ and η are each real functions of x and y. Suppose now in the xy complex plane there is traced a simple curve $f(z)$. (Fig. 1.) Each value of z along the curve defines a point w in the w plane and $f(z)$ maps into a curve $f(w)$ or $F(z)$. Because of the special properties of analytic functions of a complex variable, there exist certain special relations between $f(z)$ and $F(z)$.

The outstanding property of functions of a complex variable analytic in a region is the existence of a unique derivative at every point of the region.

$$\frac{dw}{dz}=\lim_{z\to z'}\frac{w-w'}{z-z'}=\rho e^{i\gamma}$$

or

$$dw=\rho e^{i\gamma}dz$$

This relation expresses the fact that any small curve zz' through the point z is transformed into a small curve ww' through the point w by a magnification ρ and a rotation γ; i. e., in Figure 1 the tangent t will coincide in direction with T by a rotation $\gamma=\beta-\alpha$.

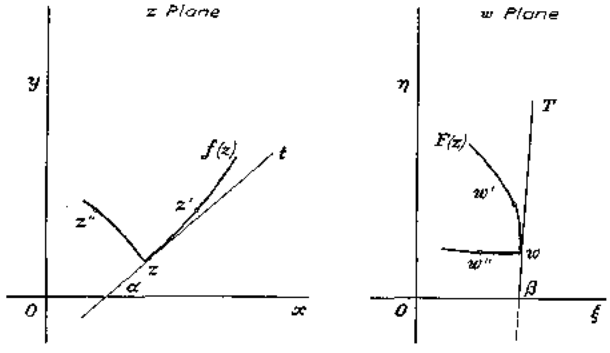

FIGURE 1.—Conformal property of analytic functions

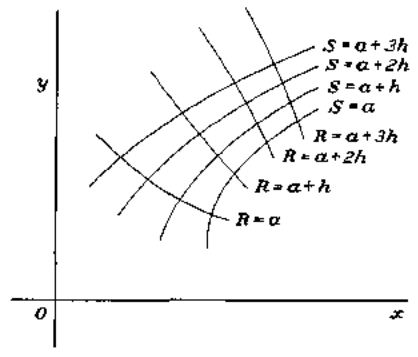

FIGURE 2.—Orthogonal network obtained by a conformal transformation

This is also true for any other pair of corresponding curves through z and w, so that in general, angles between corresponding curves are preserved. In particular, a curve zz'' orthogonal to zz' transforms into a curve ww'' orthogonal to ww'.

It has been seen that an analytic function $f(z)$ may be written $P(x, y)+iQ(x, y)$ where the curves $P=$ constant and $Q=$ constant form an orthogonal system. If then $f(z)$ is transformed conformally into $f(w)=P(\xi, \eta)+iQ(\xi, \eta)$ that is into $f[w(z)]\equiv F(z)=R(x, y)+iS(x, y)$, the curves $P(x, y)=$ constant, $Q(x, y)=$ constant map into the orthogonal network of curves $R(x, y)=$ constant, $S(x, y)=$ constant. (Fig. 2.) If the magnification $\left|\frac{dw}{dz}\right|=\rho$ is zero at a point w, the transformation at that point is singular and ceases to be conformal.

We may use the method of conformal transformations to find the motion about a complicated boundary from that of a simpler boundary. Suppose $w(z)$ is a function which corresponds to any definite fluid motion in the z plane, for instance, to that around a circle. Now if a new variable ζ is introduced and z set equal

to any analytic function of ζ, say $z=f(\zeta)$, then $w(z)$ becomes $w[f(\zeta)]$ or $W(\zeta)$ representing a new motion in the ζ plane. This new motion is, as has been seen, related to that in the z plane in such a way that the streamlines of the z plane are transformed by $z=f(\zeta)$ into the streamlines of the ζ plane. Thus, the contour into which the circle is transformed represents the profile around which the motion $W(\zeta)$ exists. The problem of determining the flow around an airfoil is now reduced to finding the proper conformal transformation which maps a curve for which the flow is known into the airfoil. The *existence* of such a function was first shown by Riemann.

We shall first formulate the theorem for a simply connected region [5] bounded by a closed curve, and then show how it is readily applied to the region external to the closed curve. The guiding thought leading to the theorem is simple. We have seen that an analytic function may transform a given closed region into another closed region. But suppose we are given two separate regions bounded by closed curves—does there exist an analytic transformation which transforms one region conformally into the other? This question is answered by Riemann's theorem as follows:

Riemann's theorem.—The interior T of any simply connected region (whose boundary contains more than one point, but we shall be concerned only with regions having closed boundaries, the boundary curve being composed of piecewise differentiable curves [Jordan curve], corners at which two tangents exist being permitted) can be mapped in a one-to-one conformal manner on the interior of the unit circle, and the analytic [6] function $\zeta=f(z)$ which consummates this transformation becomes *unique* when a given interior point z_0 of T and a direction through z_0 are chosen to correspond, respectively, to the center of the circle and a given direction through it. By this transformation the boundary of T is transformed uniquely and continuously into the circumference of the unit circle.

The unit circle in this theorem is, of course, only a convenient normalized region. For suppose the regions T_1 in the ζ plane and T_2 in the w plane are transformed into the unit circle in the z plane by $\zeta=f(z)$ and $w=F(z)$, respectively, then T_1 is transformed into T_2 by $\zeta=\Phi(w)$, obtained by eliminating z from the two transformation equations.

In airfoil theory it is in the region external to a closed curve that we are interested. Such a region can be readily transformed conformally into the region internal to a closed curve by an inversion. Thus, let us suppose a point z_0 to be within a closed curve B whose external region is Γ, and then choose a constant k such that for every point z on the boundary of Γ, $|z-z_0|>k$. Then the inversion transformation $w=\frac{k}{z-z_0}$ will transform every point in the external region Γ into a point internal to a closed region Γ' lying entirely within B, the boundary B mapping into the boundary of Γ', the region at infinity into the region near z_0. We may now restate Riemann's theorem as follows:

One and only one analytic function $\zeta=f(z)$ exists by means of which the region Γ external to a given curve B in the ζ plane is transformed conformally into the region external to a circle C in the z plane (center at $z=0$) such that the point $z=\infty$ goes into the point $\zeta=\infty$ and also $\frac{df(z)}{dz}=1$ at infinity. This function can be developed in the external region of C in a uniformly convergent series with complex coefficients of the form

$$\zeta-m=f(z)-m=z+\frac{c_1}{z}+\frac{c_2}{z^2}+\frac{c_3}{z^3}+\cdots \qquad (4)$$

by means of which the radius R and also the constant m are completely determined. Also, the boundary B of Γ is transformed continuously and uniquely into the circumference of C.

It should be noticed that the transformation (4) is a normalized form of a more general series

$$\zeta-m=a_0+a_{-1}z+\frac{a_1}{z}+\frac{a_2}{z^2}+\cdots\cdots$$

and is obtained from it by a finite translation by the vector a_0 and a rotation and expansion of the entire field depending on the coefficient a_{-1}. The condition $a_{-1}=1$ is necessary and sufficient for the fields at infinity to coincide in magnitude and direction.

The constants c_i of the transformation are functions of the shape of the boundary curve alone and our problem is, really, to determine the complex coefficients defining a given shape. With this in view, we proceed first to a convenient intermediate transformation.

The transformation $\zeta=z'+\frac{a^2}{z'}$.—This initial transformation, although not essential to a purely mathematical solution, is nevertheless very useful and important, as will be seen. It represents also the key transformation leading to Joukowsky airfoils, and is the basis of nearly all approximate theories.

Let us define the points in the ζ plane by $\zeta=x+iy$ using rectangular coordinates (x, y), and the points in the z' plane by $z'=ae^{\psi+i\theta}$ using polar coordinates (ae^{ψ}, θ). The constant a may conveniently be considered unity and is added to preserve dimensions. We have

$$\zeta=z'+\frac{a^2}{z'} \qquad (5)$$

[5] A region of the complex plane is simply connected when any closed contour lying entirely within the region may be shrunk to a point without passing out of the region. Cf. reference 3, p. 367, where a proof of the theorem based on Green's function is given.

[6] Attention is here directed to the fact that an analytic function is developable at a point in a power series convergent in any circle about the point and entirely within the region.

and substituting $z' = ae^{\psi+i\theta}$

we obtain $\zeta = 2a \cosh(\psi + i\theta)$

or $\zeta = 2a \cosh\psi \cos\theta + 2ia \sinh\psi \sin\theta$

Since $\zeta = x + iy$, the coordinates (x, y) are given by

$$\left.\begin{aligned} x &= 2a \cosh\psi \cos\theta \\ y &= 2a \sinh\psi \sin\theta \end{aligned}\right\} \tag{6}$$

If $\psi = 0$, then $z' = ae^{i\theta}$ and $\zeta = 2a \cos\theta$. That is, if P and P' are corresponding points in the ζ and z' planes, respectively, then as P traverses the x axis from $2a$ to $-2a$, P' traverses the circle $ae^{i\theta}$ from $\theta = 0$ to $\theta = \pi$, and as P retraces its path to $\zeta = 2a$, P' completes the circle. The transformation (5) then may be seen to map the entire ζ plane external to the line $4a$ uniquely into the region external (or internal) to the circle of radius a about the origin in the z' plane.

Let us invert equations (6) and solve for the elliptic coordinates ψ and θ. (Fig. 3.) We have

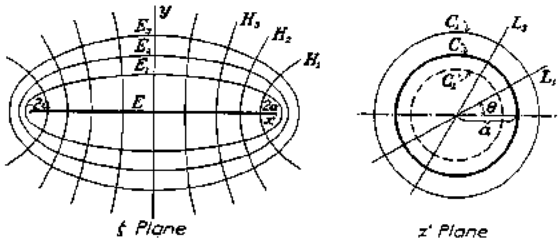

FIGURE 3.—Transformation by elliptic coordinates

$$\cosh\psi = \frac{x}{2a\cos\theta}$$

$$\sinh\psi = \frac{y}{2a\sin\theta}$$

and since $\cosh^2\psi - \sinh^2\psi = 1$

$$\left(\frac{x}{2a\cos\theta}\right)^2 - \left(\frac{y}{2a\sin\theta}\right)^2 = 1$$

or solving for $\sin^2\theta$ (which can not become negative),

$$2\sin^2\theta = p + \sqrt{p^2 + \left(\frac{y}{a}\right)^2} \tag{7}$$

where $$p = 1 - \left(\frac{x}{2a}\right)^2 - \left(\frac{y}{2a}\right)^2$$

Similarly we obtain

$$\left(\frac{x}{2a\cosh\psi}\right)^2 + \left(\frac{y}{2a\sinh\psi}\right)^2 = 1$$

or solving for $\sinh^2\psi$

$$2\sinh^2\psi = -p + \sqrt{p^2 + \left(\frac{y}{a}\right)^2} \tag{8}$$

We note that the system of radial lines $\theta = \text{constant}$ become confocal hyperbolas in the ζ plane. The circles $\psi = \text{constant}$ become ellipses in the ζ plane with major axis $2a\cosh\psi$ and minor axis $2a\sinh\psi$. These orthogonal systems of curves represent the potential lines and streamlines in the two planes. The foci of these two confocal systems are located at $(\pm 2a, 0)$.

Equation (8) yields two values of ψ for a given point (x, y), and one set of these values refers to the correspondence of (x, y) to the point (ae^{ψ}, θ) external to a curve and the other set to the correspondence of (x, y) to the point $(ae^{-\psi}, -\theta)$ internal to another curve. Thus, in Figure 3, for every point external to the ellipse E_1 there is a corresponding point external to the circle C_1, and also one internal to C_1'.

The radius of curvature of the ellipse at the end of the major axis is $\rho = 2a\dfrac{\sinh^2\psi}{\cosh\psi}$ or for small values of ψ, $\rho \cong 2a\psi^2$. The leading edge is at

$$2a\cosh\psi \cong 2a\left(1 + \frac{\psi^2}{2}\right) \cong 2a + \frac{\rho}{2}.$$

Now if there is given an airfoil in the ζ plane (fig. 4), and it is desired to transform the airfoil profile into a curve as nearly circular as possible in the z' plane by using only transformation (5), it is clear that the axes of coordinates should be chosen so that the airfoil appears as nearly elliptical as possible with respect to the chosen axes. It was seen that a focus of an elongated ellipse very nearly bisects the line joining the end of the major axis and the center of curvature of this point; thus, we arrive at a convenient choice of origin for the airfoil as the point bisecting the line of length $4a$, which extends from the point midway between the leading edge and the center of curvature of the leading edge to a point midway between the center of curvature of the trailing edge and the trailing edge. This latter point practically coincides with the trailing edge.

The curve B, defined by $ae^{\psi+i\theta}$, resulting in the z' plane, and the inverse and reflected curve B', defined by $ae^{-\psi-i\theta}$, are shown superposed on the ζ plane in Figure 4. The convenience and usefulness of transformation (5) and the choice of axes of coordinates will become evident after our next transformation.

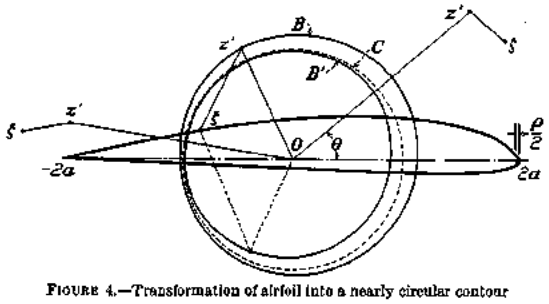

FIGURE 4.—Transformation of airfoil into a nearly circular contour

The transformation $z' = ze^{\sum_0^\infty \frac{c_n}{z^n}}$.—Consider the transformation $z' = ze^{f(z)}$ where $f(z) = \sum_0^\infty \frac{c_n}{z^n}$. Each exponential term $e^{\frac{c_n}{z^n}}$ represents the uniformly convergent series

$$1 + \frac{c_n}{z^n} + \frac{1}{2!}\left(\frac{c_n}{z^n}\right)^2 + \cdots \frac{1}{m!}\left(\frac{c_n}{z^n}\right)^m + \cdots \tag{9}$$

where the coefficients $c_n = A_n + iB_n$ are complex numbers. For $f(z)$ convergent at all points in a region external to a certain circle, z' has a unique real absolute value $|z|e^{U(\alpha)}$ in the region and its imaginary part is definitely defined except for integral multiples of $2\pi i$. When $z = \infty$, $z' = ze^{\psi_0}$. The constant $c_0 = A_0 + Bi_0$ is then the determining factor at infinity, for the afield t infinity is magnified by e^{A_0} and rotated by the angle B_0. It is thus clear that if it is desired that the regions at infinity be identical, that is, $z' = z$ at infinity, the constant c_0 must be zero. The constants c_1 and c_2 also play important rôles, as will be shown later.

We shall now transform the closed curve [7] $z' = ae^{\psi+i\theta}$ into the circle $z = ae^{\psi_0+i\varphi}$ (radius ae^{ψ_0}, origin at center) by means of the general transformation (reference 2)

$$z' = ze^{\sum_1^\infty \frac{c_n}{z^n}} \tag{10}$$

which leaves the fields at infinity unaltered, and we shall obtain expressions for the constants A_n, B_n, and ψ_0. The justification of the solution will be assured by the actual convergence of $\sum_1^\infty \frac{c_n}{z^n}$, since if the solution exists it is unique.

By definition, for the correspondence of the boundary points, we have

$$z' = ze^{\psi-\psi_0+i(\theta-\varphi)} \tag{10'}$$

Also $$z' = ze^{\sum_1^\infty (A_n+iB_n)\frac{1}{z^n}}$$

Consequently

$$\psi - \psi_0 + i(\theta-\varphi) = \sum_1^\infty (A_n + iB_n)\frac{1}{z^n}$$

where $$z = ae^{\psi_0+i\varphi}$$

On writing $z = R(\cos\ \varphi + i\ \sin\ \varphi)$ where $R = ae^{\psi_0}$, we have

$$\psi - \psi_0 + i(\theta-\varphi) = \sum_1^\infty (A_n + iB_n)\frac{1}{R^n}(\cos n\varphi - i \sin n\varphi)$$

Equating the real and imaginary parts of this relation, we obtain the two conjugate Fourier expansions:

$$\psi - \psi_0 = \sum_1^\infty \left[\frac{A_n}{R^n}\cos n\varphi + \frac{B_n}{R^n}\sin n\varphi\right] \tag{11}$$

$$\theta - \varphi = \sum_1^\infty \left[\frac{B_n}{R^n}\cos n\varphi - \frac{A_n}{R^n}\sin n\varphi\right] \tag{12}$$

From equation (11), the values of the coefficients $\frac{A_n}{R^n}$, $\frac{B_n}{R^n}$, and the constant ψ_0 are obtained as follows:

$$\frac{A_n}{R^n} = \frac{1}{\pi}\int_0^{2\pi} \psi \cos n\varphi\ d\varphi \tag{a}$$

$$\frac{B_n}{R^n} = \frac{1}{\pi}\int_0^{2\pi} \psi \sin n\varphi\ d\varphi \tag{b}$$

[7] Unless otherwise stated, ψ and θ will now be used in this restricted sense, i. e., as defining the boundary curve itself, and not all points in the z' plane.

$$\psi_0 = \frac{1}{2\pi}\int_0^{2\pi} \psi d\varphi \tag{c}$$

The evaluation of the infinite number of constants as represented by equations (a) and (b) can be made to depend upon an important single equation, which we shall obtain by eliminating these constants from equation (12).

Substitution of (a) and (b) for the coefficients of equation (12) gives

$$(\theta-\varphi)' = \frac{1}{\pi}\sum_1^\infty \left[\cos n\varphi' \int_0^{2\pi} \psi(\varphi)\sin n\varphi\ d\varphi - \sin n\varphi' \int_0^{2\pi} \psi(\varphi)\cos n\varphi\ d\varphi\right]$$

where $\psi(\varphi) = \psi$ and $(\theta-\varphi)'$ represents $\theta-\varphi$ as a function of φ', and where φ' is used to distinguish the angle kept constant while the integrations are performed. The expression may be readily rewritten as

$$(\theta-\varphi)' = \frac{1}{\pi}\sum_1^\infty \int_0^{2\pi} \psi(\varphi)(\sin n\varphi\cos n\varphi' - \cos n\varphi \sin n\varphi')d\varphi$$

$$= \frac{1}{\pi}\sum_1^\infty \int_0^{2\pi} \psi(\varphi)\sin n(\varphi-\varphi')\ d\varphi$$

But

$$\sum_1^n \sin n(\varphi-\varphi') = \frac{1}{2}\cot\frac{\varphi-\varphi'}{2} - \frac{\cos(2n+1)\frac{(\varphi-\varphi')}{2}}{2\sin\frac{\varphi-\varphi'}{2}}$$

Then

$$(\theta-\varphi)' = \lim_{n\to\infty}\left\{\frac{1}{2\pi}\int_0^{2\pi}\psi(\varphi)\cot\frac{\varphi-\varphi'}{2}\,d\varphi - \frac{1}{2\pi}\int_0^{2\pi}\psi(\varphi)\frac{\cos(2n+1)\frac{(\varphi-\varphi')}{2}}{\sin\frac{\varphi-\varphi'}{2}}\,d\varphi\right\}$$

The first integral is independent of n, while the latter one becomes identically zero.

Then finally, representing $\varphi-\theta$ by a single quantity ϵ, viz $\varphi-\theta \equiv \epsilon \equiv \epsilon(\varphi)$, we have

$$\epsilon(\varphi') = -\frac{1}{2\pi}\int_0^{2\pi}\psi(\varphi)\cot\frac{\varphi-\varphi'}{2}\,d\varphi \tag{13}$$

By solving for the coefficients in equation (12) and substituting these in equation (11) it may be seen that a similar relation to equation (13) holds for the function $\psi(\varphi)$.

$$\psi(\varphi') = \frac{1}{2\pi}\int_0^{2\pi}\epsilon(\varphi)\cot\frac{\varphi-\varphi'}{2}\,d\varphi + \frac{1}{2\pi}\int_0^{2\pi}\psi(\varphi)d\varphi \tag{14}$$

The last term is merely the constant ψ_0, which is, as has been shown, determined by the condition of mag-

nification of the z and z' fields at infinity. The corresponding integral $\frac{1}{2\pi}\int_0^{2\pi}\epsilon(\varphi)\,d\varphi$ does not appear in equation (13), being zero as a necessary consequence of the coincidence of directions at infinity and, in general, if the region at infinity is rotated, is a constant different from zero.

Investigation of equation (13).—This equation is of fundamental importance. A discussion of some of its properties is therefore of interest. It should be first noted that when the function $\psi(\varphi)$ is considered known, the equation reduces to a definite integral. The function [8] $\epsilon(\varphi)$ obtained by this evaluation is the "conjugate" function to $\psi(\varphi)$, so called because of the relations existing between the coefficients of the Fourier expansions as given by equations (11) and (12). For the existence of the integral it is only necessary that $\psi(\varphi)$ be piecewise continuous and differentiable, and may even have infinities which must be below first order. We shall, however, be interested only in continuous single-valued functions having a period 2π, of a type which result from continuous closed curves with a proper choice of origin.

If equation (13) is regarded as a definite integral, it is seen to be related to the well-known Poisson integral which solves the following boundary-value problem of the circle. (Reference 3.) Given, say for the z plane a single-valued function $u(R,\tau)$ for points on the circumference of a circle $w=Re^{i\tau}$ (center at origin), then the single-valued continuous potential function $u(r,\sigma)$ in the external region $z=re^{i\sigma}$ of the circle which assumes the values $u\ (R,\ \tau)$ on the circumference is given by

$$u(r,\sigma)=\frac{1}{2\pi}\int_0^{2\pi}u(R,\tau)\frac{r^2-R^2}{R^2+r^2-2Rr\cos\ (\sigma-\tau)}\,d\tau$$

and similarly for the conjugate function $v(r,\sigma)$

$$v(r,\sigma)=\frac{1}{2\pi}\int_0^{2\pi}v(R,\tau)\frac{r^2-R^2}{R^2+r^2-2Rr\cos\ (\sigma-\tau)}\,d\tau$$

These may be written as a single equation

$$u(r,\sigma)+iv(r,\sigma)=f(z)=\frac{1}{2\pi i}\int_C f(w)\frac{z+w}{z-w}\,dw$$

where the value $f(z)$ at a point of the external region $z=re^{i\sigma}$ is expressed in terms of the known values $f(w)$ along the circumference $w=Re^{i\tau}$. In particular, we may note that at the boundary itself, since $i\frac{e^{i\sigma}+e^{i\tau}}{e^{i\sigma}-e^{i\tau}}=\cot\frac{(\sigma-\tau)}{2}$, we have

$$u(R,\sigma)+iv(R,\sigma)=-\frac{i}{2\pi}\int_0^{2\pi}[u(R,\tau)+iv(R,\tau)]\cot\frac{(\sigma-\tau)}{2}\,d\tau,$$

which is a special form of equations (13) and (14).

The quantity ψ is immediately given as a function of θ when a particular closed curve is preassigned, and this is our starting point in the direct process of transforming from airfoil to circle. We desire, then, to find the quantity ψ as a function of φ from equation (13), and this equation is no longer a definite integral but an integral equation whose process of solution becomes more intricate. It would be surprising, indeed, if anything less than a functional or integral equation were involved in the solution of the general problem stated. The evaluation of the solution of equation (13) is readily accomplished by a powerful method of successive approximations. It will be seen that the nearness of the curve $ae^{\psi+i\epsilon}$ to a circle is very significant, and in practice, for airfoil shapes, one or at most two steps in the process is found to be sufficient for great accuracy.

The quantities ψ and ϵ considered as functions of φ have been denoted by $\psi(\varphi)$ and $\epsilon(\varphi)$, respectively. When these quantities are thought of as functions of θ they shall be written as $\bar{\psi}(\theta)$ and $\bar{\epsilon}(\theta)$, respectively.

Then, by definition

$$\left.\begin{aligned}\bar{\psi}(\theta)&\equiv\psi[\varphi(\theta)]\\ \bar{\epsilon}(\theta)&\equiv\epsilon[\varphi(\theta)]\end{aligned}\right\}\qquad(15)$$

and

Since $\varphi-\theta=\epsilon$, we have

$$\left.\begin{aligned}\theta(\varphi)&=\varphi-\epsilon(\varphi)\\ \varphi(\theta)&=\theta+\bar{\epsilon}(\theta)\end{aligned}\right\}\qquad(16)$$

We are seeking then two functions, $\psi(\varphi)$ and $\epsilon(\varphi)$, conjugate in the sense that their Fourier series expansions are given by (11) and (12), such that $\psi[\varphi(\theta)]=\bar{\psi}(\theta)$ where $\bar{\psi}(\theta)$ is a *known* single-valued function of period 2π.

Integrating equation (13) by parts, we have

$$\epsilon(\varphi')=\frac{1}{\pi}\int_0^{2\pi}\log\sin\frac{\varphi-\varphi'}{2}\frac{d\psi(\varphi)}{d\varphi}\,d\varphi\qquad(13')$$

The term $\log\sin\frac{\varphi-\varphi'}{2}$ is real only in the range $\varphi=\varphi'$ to $\varphi=2\pi+\varphi'$, but we may use the interval 0 to 2π for φ with the understanding that only the real part of the logarithm is retained.

Let us write down the following identity:

$$\begin{aligned}\log\sin\frac{\varphi-\varphi'}{2}\equiv&\log\sin\frac{\theta-\theta'}{2}\\ &+\log\frac{\sin\frac{(\theta+\bar{\epsilon}_1)-(\theta+\bar{\epsilon}_1)'}{2}}{\sin\frac{\theta-\theta'}{2}}+\log\frac{\sin\frac{(\theta+\bar{\epsilon}_2)-(\theta+\bar{\epsilon}_2)'}{2}}{\sin\frac{(\theta+\bar{\epsilon}_1)-(\theta+\bar{\epsilon}_1)'}{2}}\\ &+\ldots+\log\frac{\sin\frac{(\theta+\bar{\epsilon}_k)-(\theta+\bar{\epsilon}_k)'}{2}}{\sin\frac{(\theta+\bar{\epsilon}_{k-1})-(\theta+\bar{\epsilon}_{k-1})'}{2}}+\ldots\qquad(17)\\ &+\log\frac{\sin\frac{(\theta+\bar{\epsilon}_n)-(\theta+\bar{\epsilon}_n)'}{2}}{\sin\frac{(\theta+\bar{\epsilon}_{n-1})-(\theta+\bar{\epsilon}_{n-1})'}{2}}+\log\frac{\sin\frac{(\theta+\bar{\epsilon})-(\theta+\bar{\epsilon})'}{2}}{\sin\frac{(\theta+\bar{\epsilon}_n)-(\theta+\bar{\epsilon}_n)'}{2}}\end{aligned}$$

where in the last term we recall that $\theta+\bar{\epsilon}(\theta)=\varphi(\theta)$; and where it may be noted that each denominator is the

[8] This function will be called "conformal angular distortion" function, for reasons evident later.

numerator of the preceding term. The symbols $\bar{\epsilon}_k$ ($k=1, 2, \ldots, n$) represent functions of θ, which thus far are arbitrary.[9]

Since by equation (15) $\bar{\psi}(\theta)\equiv\psi[\varphi(\theta)]$ we have for corresponding elements $d\theta$ and $d\varphi$

$$\frac{d\psi(\varphi)}{d\varphi}\,d\varphi=\frac{d\bar{\psi}(\theta)}{d\theta}\,d\theta$$

Then multiplying the left side of equation (17) by $\frac{1}{\pi}\frac{d\psi(\varphi)}{d\varphi}\,d\varphi$ and the right side by $\frac{1}{\pi}\frac{d\bar{\psi}(\theta)}{d\theta}\,d\theta$ and integrating over the period 0 to 2π we obtain

$$\epsilon[\varphi(\theta')]\equiv\bar{\epsilon}(\theta')=\frac{1}{\pi}\int_0^{2\pi}\log\sin\frac{\theta-\theta'}{2}\,\frac{d\psi(\theta)}{d\theta}\,d\theta+\ \ldots$$

$$+\frac{1}{\pi}\int_0^{2\pi}\log\frac{\sin\dfrac{(\theta+\bar{\epsilon}_k)-(\theta+\bar{\epsilon}_k)'}{2}}{\sin\dfrac{(\theta+\bar{\epsilon}_{k-1})-(\theta+\bar{\epsilon}_{k-1})'}{2}}\,\frac{d\bar{\psi}(\theta)}{d\theta}\,d\theta+\ \ldots$$

$$+\frac{1}{\pi}\int_0^{2\pi}\log\frac{\sin\dfrac{(\theta+\bar{\epsilon}(\theta))-(\theta+\bar{\epsilon}(\theta))'}{2}}{\sin\dfrac{(\theta+\bar{\epsilon}_n)-(\theta+\epsilon_n)'}{2}}\,\frac{d\bar{\psi}(\theta)}{d\theta}\,d\theta \qquad (18)$$

where $k=1, 2, \ldots, n$.

We now choose the arbitrary functions $\bar{\epsilon}_k(\theta')$ so that

$$\bar{\epsilon}_o(\theta')=0$$

and

$$\bar{\epsilon}_k(\theta')=\frac{1}{\pi}\int_0^{2\pi}\log\sin\frac{(\theta+\bar{\epsilon}_{k-1})-(\theta+\bar{\epsilon}_{k-1})'}{2}\,\frac{d\bar{\psi}(\theta)}{d\theta}\,d\theta \qquad (19)$$

where $k=1, 2, \ldots, n$.

Equation (18) may then be written

$$\bar{\epsilon}(\theta')=\bar{\epsilon}_0+\bar{\epsilon}_1+(\bar{\epsilon}_2-\bar{\epsilon}_1)+\ \ldots\ +(\bar{\epsilon}_n-\bar{\epsilon}_{n-1})+(\bar{\epsilon}-\bar{\epsilon}_n) \qquad (20)$$

or $$\bar{\epsilon}(\theta')=\lambda_1+\lambda_2+\ \ldots\ \lambda_n+\lambda$$

where $\lambda_k(\theta')=\bar{\epsilon}_k-\bar{\epsilon}_{k-1}$ and is in fact the k^{th} term of equation (18). The last term we denote by λ.

From equation (19) we see that the function $\bar{\epsilon}_k(\theta')$ is obtained by a knowledge of the preceding function $\bar{\epsilon}_{k-1}(\theta')$. For convenience in the evaluation of these functions, say

$$\bar{\epsilon}_{k+1}(\theta')=\frac{1}{\pi}\int_0^{2\pi}\log\sin\frac{(\theta+\bar{\epsilon}_k)-(\theta+\bar{\epsilon}_k)'}{2}\,\frac{d\bar{\psi}(\theta)}{d\theta}\,d\theta$$

we introduce a new variable φ_k defined by

$$\varphi_k(\theta)=\theta+\bar{\epsilon}_k(\theta) \qquad (k=1, 2, \ldots, n)$$

Then

$$\bar{\epsilon}_{k+1}[\theta(\varphi'_{k+1})]\equiv\epsilon^*_{k+1}(\varphi'_k)$$

$$=\frac{1}{\pi}\int_0^{2\pi}\log\sin\frac{(\varphi_k-\varphi'_k)}{2}\,\frac{d\bar{\psi}[\theta(\varphi_k)]}{d\varphi_k}\,d\varphi_k \qquad (21)$$

From the definition of φ_k as

$$\varphi_k(\theta)=\theta+\bar{\epsilon}_k(\theta)$$

we may also define the symbol $\epsilon_k(\varphi_k)$ by

$$\theta(\varphi_k)=\varphi_k-\epsilon_k(\varphi_k)$$

where

$$\bar{\epsilon}_k(\theta)\equiv\epsilon_k[\varphi_k(\theta)]$$

It is important to note that the symbols $\bar{\epsilon}_k$, ϵ_k, ϵ_k^* denote the same quantity considered, however, as a function of θ, φ_k, φ_{k-1}, respectively.

The quantities $(\bar{\epsilon}_k-\bar{\epsilon}_{k-1})$ in equation (20) rapidly approach zero for wide classes of initial curves $\bar{\psi}(\theta)$, i. e., $\bar{\psi}[\theta(\varphi_k)]$ very nearly equals $\bar{\psi}[\theta(\varphi_{k+1})]$ for even small k's. The process of solution of our problem is then one of obtaining successively the functions $\bar{\psi}(\theta)$, $\bar{\psi}[\theta(\varphi_1)]$, $\bar{\psi}[\theta(\varphi_2)]$, ... $\bar{\psi}[\theta(\varphi_n)]$ where $\bar{\psi}[\theta(\varphi_n)]$ and $\bar{\epsilon}_n[\theta(\varphi_n)]$ become more and more "conjugate." The process of obtaining the successive conjugates in practice is explained in a later paragraph. We first pause to state the conditions which the functions φ_k are subject to, necessary for a one-to-one correspondence of the boundary points, and for a one-to-one correspondence of points of the external regions, i. e., the conditions which are necessary in order that the transformations be conformal.

In order that the correspondence between boundary points of the circle in the z plane and boundary points of the contour in the z' plane be one-to-one, it is necessary that $\theta(\varphi)$ be a monotonic increasing function of its argument. This statement requires a word of explanation. We consider only values of the angles between 0 and 2π. For a point of the circle boundary, that is, for one value of φ there can be only one value of θ, i. e., $\theta(\varphi)$ is always single valued. However, $\varphi(\theta)$, in general, does not need to be, as for example, by a poor choice of origin it may be many valued, a radius vector from the origin intersecting the boundary more than once; but since we have already postulated that $\bar{\psi}(\theta)$ is single valued this case can not occur, and $\varphi(\theta)$ is also single valued. If we decide on a definite direction of rotation, then the inequality $\frac{d\theta}{d\varphi}\geqq 0$ expresses the statement that as the radius vector from the origin sweeps over the boundary of the circle C, the radius vector in the z' plane sweeps over the boundary of B and never retraces its path.

The inequality

$$\frac{d\theta}{d\varphi}=1-\frac{d\epsilon(\varphi)}{d\varphi}\geqq 0$$

corresponds to

$$\frac{d\epsilon(\varphi)}{d\varphi}\leqq 1$$

Also, the condition

$$\frac{d\varphi}{d\theta}=1+\frac{d\bar{\epsilon}(\theta)}{d\theta}\geqq 0$$

corresponds to

$$\frac{d\bar{\epsilon}(\theta)}{d\theta}\geqq -1$$

[9] The symbol $(\theta+\epsilon_k)'$ represents $\theta'+\epsilon_k(\theta')$ and is used to denote the same function of θ' that $\theta+\epsilon_k(\theta)$ is of θ. The variables θ and θ' are regarded as independent of each other.

Multiplying $\frac{d\theta}{d\varphi}$ by $\frac{d\varphi}{d\theta}$ we get

$$\left(1-\frac{d\epsilon(\varphi)}{d\varphi}\right)\left(1+\frac{d\bar{\epsilon}(\theta)}{d\theta}\right)=1$$

This relation is shown in Figure 5 as a rectangular

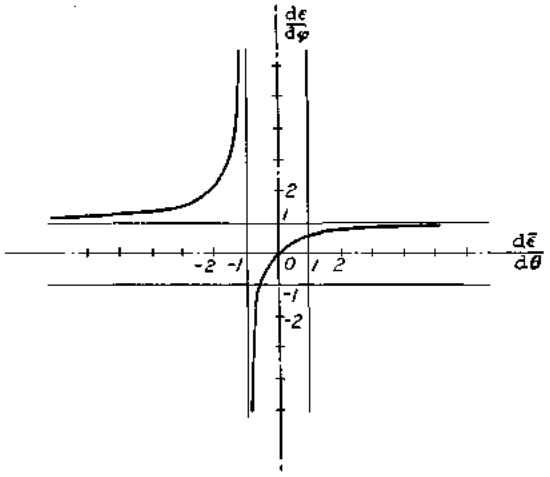

FIGURE 5.—The quantity $\frac{d\epsilon}{d\varphi}$ as a function of $\frac{d\bar{\epsilon}}{d\theta}$

hyperbola. We may notice then that the monotonic behavior of $\varphi(\theta)$ and $\theta(\varphi)$ requires that $\frac{d\epsilon}{d\varphi}$ remain on the *lower* branch [10] of the hyperbola, i. e.,

$$-\infty \leqq \frac{d\epsilon}{d\varphi} \leqq 1 \tag{22}$$

It will be seen later that the limiting values

$$\frac{d\epsilon(\varphi)}{d\varphi}=1, \frac{d\epsilon(\varphi)}{d\varphi}=-\infty \left(\text{i. e., } \frac{d\bar{\epsilon}}{d\theta}=\infty, \frac{d\bar{\epsilon}}{d\theta}=-1\right)$$

correspond to points of infinite velocity and of zero velocity, respectively, arising from sharp corners in the original curve.

The condition for a one-to-one conformal correspondence between points of the external region of the circle and of the external region of the contour in the z' plane may be given (reference 5, p. 98 and reference 6, Part II) as follows: There must be a one-to-one boundary point correspondence and the derivative of the analytic function $z'=ze^{\sum_1^\infty \frac{c_n}{z^n}}$ given by equation (10) must not vanish in the region. That is, writing $g(z)$ for $\sum_1^\infty \frac{c_n}{z^n}$ we have

$$\frac{dz'}{dz}=e^{g(z)}\left(1+z\frac{dg(z)}{dz}\right)\neq 0 \text{ for } |z|>R \text{ or since}$$

the integral transcendental function $e^{g(z)}$ does not vanish in the entire plane, the condition is equivalent to

$$z\frac{dg(z)}{dz}\neq -1 \text{ for } |z|>R$$

By equation (10′) we have on the boundary of the circle, $g(Re^{i\varphi})=\psi-\psi_0-i\epsilon$, and

$$z\frac{dg(z)}{dz}=Re^{i\varphi}\frac{d[\psi(\varphi)-i\epsilon(\varphi)]}{iRe^{i\varphi}\,d\varphi}$$

$$=-\frac{d\epsilon(\varphi)}{d\varphi}-i\frac{d\psi(\varphi)}{d\varphi}$$

the first term on the right-hand side being real and the last term a pure imaginary. We have already postulated the condition

$$-\infty \leqq \frac{d\epsilon}{d\varphi} \leqq 1$$

as necessary for a one-to-one boundary point correspondence. Now by writing $z=\xi+i\eta$ and $z\frac{dg(z)}{dz}=P(\xi,\eta)+iQ(\xi,\eta)$, we note that $\frac{d\epsilon(\varphi)}{d\varphi}$ gives the boundary values of a harmonic function $P(\xi,\eta)$ and therefore this function assumes its maximum and minimum values on the boundary of the circle itself. (Reference 3, p. 223.) Hence $z\frac{dg(z)}{dz}$ can never become -1 in the external region, i. e., $\frac{dz'}{dz}$ can never vanish in this region.

At each step in the process of obtaining the successive conjugates we desire to maintain a one-to-one correspondence between θ and φ_k, i. e., the functions $\theta(\varphi_k)$ and $\varphi_k(\theta)$ should be monotonic increasing and are hence subject to a restriction similar to equation (22), viz,

$$-\infty \leqq \frac{d\epsilon_k}{d\varphi_k} \leqq 1 \tag{22′}$$

The process may be summed up as follows: We consider the function $\bar{\psi}(\theta)$ as known, where $\bar{\psi}(\theta)$ is the functional relation between ψ and θ defining a closed curve $ae^{\bar{\psi}+i\theta}$. The conjugate of $\bar{\psi}(\theta)$ with respect to θ is $\bar{\epsilon}_1(\theta)$. We form the variable $\varphi_1=\theta+\bar{\epsilon}_1(\theta)$ and also the function $\bar{\psi}[\theta(\varphi_1)]$. The conjugate of $\bar{\psi}[\theta(\varphi_1)]$ with respect to φ_1 is $\epsilon^*_2(\varphi_1)$ which expressed as a function of θ is $\bar{\epsilon}_2(\theta)$. We form the variable $\varphi_2=\theta+\bar{\epsilon}_2(\theta)$ and the function $\bar{\psi}[\theta(\varphi_2)]$. The conjugate of $\bar{\psi}[\theta(\varphi_2)]$ is $\epsilon^*_3(\varphi_2)$, which as a function of θ is $\bar{\epsilon}_3(\theta)$, etc. The graphical criterion for convergence is, of course, reached when the function $\bar{\psi}[\theta(\varphi_n)]$ is no longer altered by the process. The following figures illustrate the method and exhibit vividly the rapidity of convergence. The numerical calculations of the various conjugates are obtained from formula I of the appendix.

In Figure 6, the $\bar{\psi}(\theta)$ curve represents a circle referred to an origin which bisects a radius (obtained from an extremely thick Joukowsky airfoil) (see p. 200) and has numerical values approximately five times greater than occur for common airfoils. The $\psi(\varphi)$ curve is known independently and is represented by the dashed curve. The process of going from $\bar{\psi}(\theta)$ to $\psi(\varphi)$ assuming $\psi(\varphi)$ as unknown is as follows: The function $\bar{\epsilon}_1(\theta)$, the conjugate function of $\bar{\psi}(\theta)$, is found.

[10] The values of the upper branch of the hyperbola arise when the region internal to the curve $ae^{\bar{\psi}+i\theta}$ is transformed into the external region of a circle, but may also there be avoided by defining $\epsilon=\varphi+\theta$ instead of $\varphi-\theta$.

The quantity ψ is then plotted against the new variable $\varphi_1 = \theta + \bar{\epsilon}_1(\theta)$ (i. e., each point of $\bar{\psi}(\theta)$ is displaced horizontally a distance $\bar{\epsilon}_1$) and yields the curve $\bar{\psi}[\theta(\varphi_1)]$. (Likewise, $\bar{\epsilon}_1(\theta)$ is plotted against φ_1 yielding $\epsilon_1(\varphi_1)$.) is drawn at P'. This process yields the function $\bar{\epsilon}_2(\theta)$. The quantity ψ is now plotted against the new variable $\varphi_2 = \theta + \bar{\epsilon}_2(\theta)$ (i. e., each point of $\bar{\psi}(\theta)$ is displaced horizontally a distance $\bar{\epsilon}_2$) giving the function $\bar{\psi}[\theta(\varphi_2)]$.

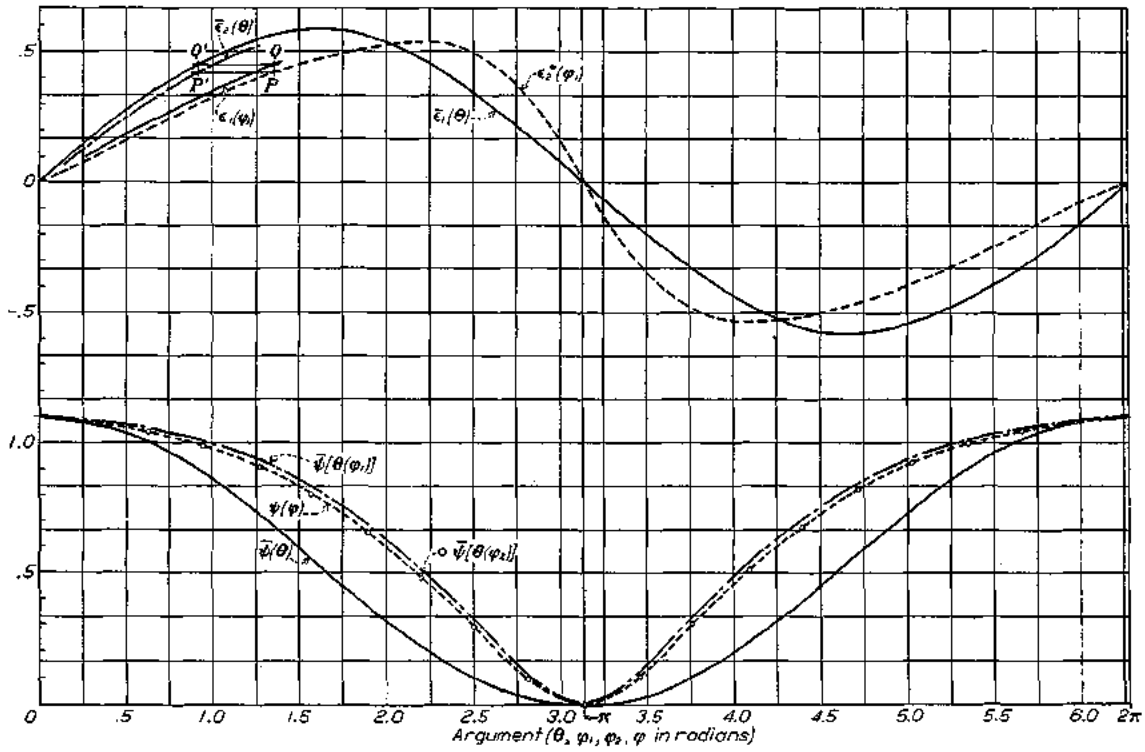

FIGURE 6.—The process of obtaining successive conjugates

The function $\epsilon^*_2(\varphi_1)$ is now determined as the conjugate function of $\psi[\theta(\varphi_1)]$. This function expressed as a function of θ is $\epsilon^*_2[\varphi_1(\theta)] \equiv \bar{\epsilon}_2(\theta)$. It is plotted as follows: This curve is shown with small circles and coincides with $\psi(\varphi)$. Further application of the process can yield no change in this curve. It may be remarked

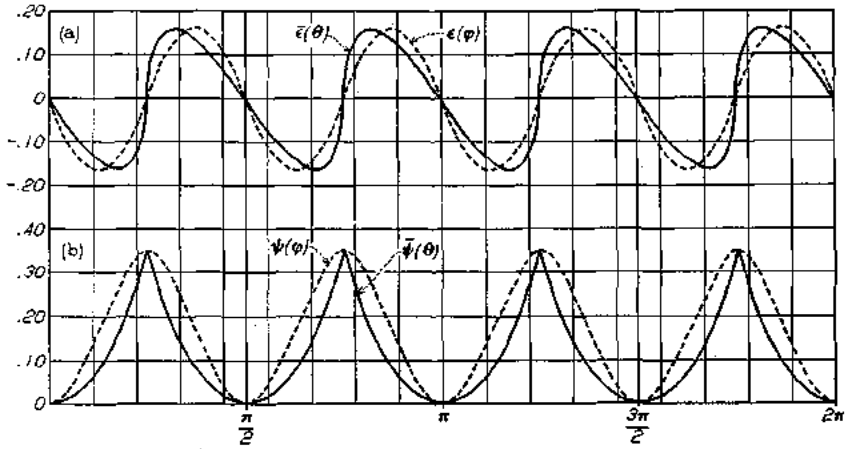

FIGURE 7.—Process applied to transforming a square into a circle

At a point P of $\epsilon^*_2(\varphi_1)$ and Q of $\epsilon_1(\varphi_1)$ corresponding to a definite value of φ_1 one finds the value of θ which corresponds to φ_1 by a horizontal line through Q meeting $\bar{\epsilon}_1(\theta)$ in Q'; for this value of θ, the quantity ϵ_2 at P here that for nearly all airfoils used in practice one step in the process is sufficient for very accurate results.

As another example we shall show how a square (origin at center) is transformed into a circle by the

method. In Figure 7 the $\bar{\psi}(\theta)$ curve is shown, and in Figure 8 it is reproduced for one octant.[11] The value is $\bar{\psi}(\theta) = \log \sec \theta$. The function $\bar{\psi}[\theta(\varphi_1)]$ is shown dashed; the function $\bar{\psi}[\theta(\varphi_2)]$ is shown with small crosses; and $\bar{\psi}[\theta(\varphi_3)]$ is shown with small circles. The solution $\psi(\varphi)$ is represented by the curve with small triangles and is obtained independently by the known transformation (reference 3, p. 375) which transforms the external region of a square into the external region of the unit circle, as follows:

$$w(z) = \int_{z_0}^{z} \frac{\sqrt{z^4-1}}{z^2} dz = z\left[1 + P\left(\frac{1}{z}\right)\right]$$

where $P\left(\frac{1}{z}\right)$ denotes a power series. Comparing this with equation (10), we find that $\psi(\varphi)$ except for the constant ψ_0 is given as the real part of $\log\left[1 + P\left(\frac{1}{z}\right)\right]$ evaluated for $z = e^{i\varphi}$, and that $\epsilon(\varphi)$ is given as the negative of the imaginary part. It may be observed in Figure 8 that the function $\bar{\psi}[\theta(\varphi_3)]$ very nearly

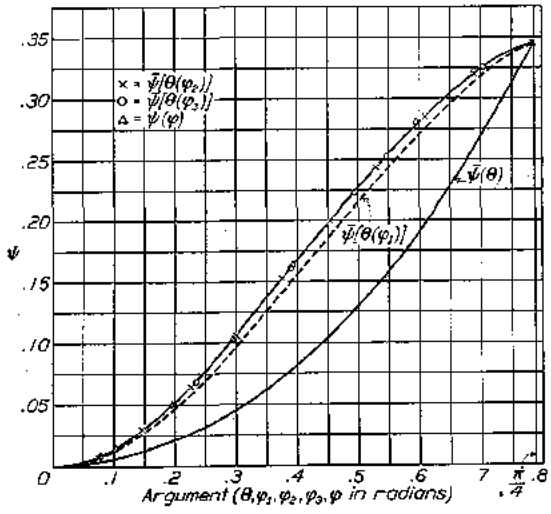

FIGURE 8.—Process applied to transforming a square into a circle

equals $\psi(\varphi)$. The functions $\epsilon(\varphi)$ and $\bar{\epsilon}(\theta)$ are shown in Figure 7 (a); we may note that at $\varphi = \frac{\pi}{4}$, which corresponds to a corner of the square, $\frac{d\epsilon}{d\varphi} = 1$ or also, $\frac{d\bar{\epsilon}}{d\theta} = \infty$.

[11] Because of the symmetry involved only the interval 0 to $\frac{\pi}{4}$ need be used. The integral in the appendix can be treated as

$$\epsilon(\varphi') = -\frac{1}{2\pi}\int_0^{2\pi} \psi(\varphi) \cot\frac{\varphi-\varphi'}{2} d\varphi$$

$$= -\frac{2}{\pi}\int_0^{\frac{\pi}{4}} \psi(\varphi)[\cot 2(\varphi-\varphi') - \cot 2(\varphi+\varphi')]d\varphi$$

It may be remarked that the rapidity of convergence is influenced by certain factors. It is noticeably affected by the initial choice of $\bar{\epsilon}_0(\theta)$. The choice $\bar{\epsilon}_0(\theta) = 0$ implies that θ and φ are considered to be very nearly equal, i. e., that $ae^{\varphi+i\theta}$ represents a nearly circular curve. The initial transformation given by equation (5) and the choice of axes and origin were adapted for the purpose of obtaining a nearly circular

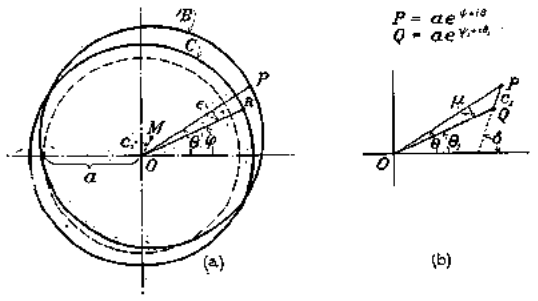

FIGURE 9.—Translation by the distance OM

curve for airfoil shapes.[12] If we should be concerned with other classes of contours, more appropriate initial transformations can be developed. If, however, for a curve $ae^{\varphi+i\theta}$ the quantity $\epsilon = \varphi - \theta$ has large values, either because of a poor initial transformation or because of an unfavorable choice of origin, it may occur that the choice $\bar{\epsilon}_0(\theta) = 0$ will yield a function $\epsilon_1(\varphi_1)$ for which $\frac{d\epsilon_1}{d\varphi_1}$ may exceed unity at some points, thus violating condition (22′). Such slopes can be replaced by slopes less than unity, the resulting *function* chosen as $\bar{\epsilon}_0(\theta)$ and the process continued as before.[12] Indeed, the closer the choice of the function $\bar{\epsilon}_0(\theta)$ is to the final solution $\bar{\epsilon}(\theta)$, the more rapid is the convergence. The case of the square illustrates that even the relatively poor choice $\bar{\epsilon}_0(\theta) = 0$ does not appreciably defer the convergence.

The translation $z_1 = z + c_1$.—Let us divert our attention momentarily to another transformation which will prove useful. We recall that the initial transformation (eq. (5)) applied to an airfoil in the ζ plane gives a curve B in the z' plane shown schematically in Figure 9(a). Equation (10) transforms this curve into a circle C about the origin 0 as center and yields in fact small values of the quantity $\varphi - \theta$. We are, however, in a position to introduce a convenient transformation, namely, to translate the circle C into a most favorable position with respect to the curve B (or vice versa). These qualitative remarks admit of a mathematical formulation. It is clear that if the curve B itself happens to be a circle [13] the vector by which the circle C should be translated is exactly the distance between centers. It is readily shown that

[12] The first step in the process is now to define $\varphi_0 = \theta + \epsilon_0(\theta)$ and form the function $\bar{\psi}[\theta(\varphi_0)]$. The conjugate function of $\bar{\psi}[\theta(\varphi_0)]$ is $\epsilon_0(\varphi_0)$ which expressed as a function of θ is $\bar{\epsilon}_1(\theta)$, etc.

[13] See p. 200.

then equation (10) should contain no constant term. We have

$$z' = ze^{\sum_1^\infty \frac{c_n}{z^n}} \tag{10}$$

$$= z\left(1+\frac{c_1}{z}+\frac{1}{2!}\left(\frac{c_1}{z}\right)^2+\cdots\right)\left(1+\frac{c_2}{z^2}+\cdots\right)\times \left(1+\frac{c_3}{z^3}+\cdots\right) etc.$$

$$= z\left(1+\frac{k_1}{z}+\frac{k_2}{z^2}+\cdots\right) \tag{10a}$$

where [14]

$$k_1 = c_1$$
$$k_2 = c_2+\frac{c_1^2}{2}$$
$$k_3 = c_3+c_2c_1+\frac{c_1^3}{6}$$
$$\cdots\cdots\cdots$$

It is thus apparent that if equation (10) contains no first harmonic term, i. e., if

$$c_1 = A_1+iB_1 = \frac{R^2}{\pi}\int_0^{2\pi}\psi e^{i\varphi}d\varphi = 0,$$

the transformation is obtained in the so-called normal form

$$z' = z_1+\frac{d_1}{z_1}+\frac{d_2}{z_1^2}+\cdots \tag{23}$$

This translation can be effected either by substituting a new variable $z_1 = z+c_1$, or a new variable $z_1' = z'-c_1$.

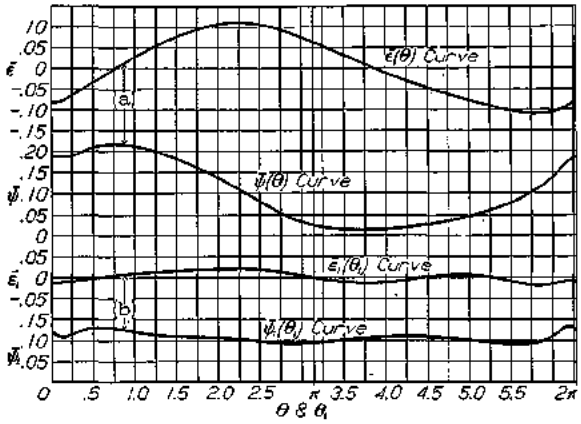

FIGURE 10.—The $\bar{\psi}(\theta)$ and $\bar{\psi}_1(\theta_1)$ curves (for Clark Y airfoil)

This latter substitution will be more convenient at this time. Writing

$$z_1' = ae^{\psi_1+i\theta_1},\ c_1 = ae^{\gamma+i\delta},\ \text{and}\ z' = ae^{\psi+i\theta}$$

we have

$$ae^{\psi_1+i\theta_1} = ae^{\psi+i\theta}-ae^{\gamma+i\delta}$$

The variables ψ_1, and θ_1, can be expressed in terms of ψ, θ, γ, and δ. In Figure 9(b), P is a point on the B curve, i. e., $OP = ae^{\psi}$, PQ represents the translation vector $c_1 = ae^{\gamma+i\delta}$, OQ is $ae^{\psi_1+i\theta_1}$, and angle POQ is denoted by μ. Then by the law of cosines

$$e^{2\psi_1} = e^{2\psi}+e^{2\gamma}-2e^{\psi}e^{\gamma}\cos(\theta-\delta) \tag{a}$$

and by the law of sines

$$\sin\mu = \frac{e^{\gamma}\sin(\theta-\delta)}{e^{\psi_1}}$$

or
$$\theta_1 = \theta+\mu = \theta+\tan^{-1}\frac{e^{\gamma-\psi}\sin(\theta-\delta)}{1-e^{\gamma-\psi}\cos(\theta-\delta)} \tag{b}$$

In Figure 10 are shown the $\bar{\psi}(\theta)$ and $\bar{\epsilon}(\theta)$ curves for the Clark Y airfoil (shown in fig. 4) and the $\bar{\psi}_1(\theta_1)$ and $\bar{\epsilon}_1(\theta_1)$ curves which result when the origin is moved from 0 to M. It may be noted that $\bar{\epsilon}_1(\theta_1)$ is indeed considerably smaller than $\bar{\epsilon}(\theta)$. It is obtained from

$$(\varphi-\theta_1)' = -\frac{1}{2\pi}\int_0^{2\pi}\psi_1(\varphi)\cot\frac{\varphi-\varphi'}{2}\,d\varphi$$

and the constant ψ_0 is given [15] by

$$\psi_0 = \frac{1}{2\pi}\int_0^{2\pi}\psi_1(\varphi)d\varphi$$

The combined transformations.—It will be useful to combine the various transformations into one. We obtain from equations (5) and (10) an expression as follows:

$$\zeta = 2a\cosh\left(\log\frac{z}{a}+\sum_1^\infty\frac{c_n}{z^n}\right) \tag{24}$$

or we can also obtain a power series development in z

$$\zeta = c_1+z+\frac{a_1}{z}+\frac{a_2}{z^2}+\frac{a_3}{z^3}+\cdots \tag{25}$$

where [16] $a_n = k_{n+1}+a^2h_{n-1}$

The constants k_n may be obtained in a convenient recursion form as

$$k_1 = c_1$$
$$2k_2 = k_1c_1+2c_2$$
$$3k_3 = k_2c_1+2k_1c_2+3c_3$$
$$4k_4 = k_3c_1+2k_2c_2+3k_1c_3+4c_4$$
$$\cdots\cdots\cdots$$

The constants h_n have the same form as k_n but with *each* c_i replaced by $-c_i$ (and $h_0 = 1$). It will be re-

[14] These constants can be obtained in a recursion form. See footnote 16.

[15] The constant ψ_0 is invariant to change of origin. (See p. 290.) It should be remarked that the translation by the vector c_1 is only a matter of convenience and is especially useful for very irregular shapes. For a study of the properties of airfoil shapes we shall use only the original $\epsilon(\varphi)$ curve. (Fig. 10(a).)

[16] By equations (5) and (10) we have

$$\zeta = ze^{\sum_1^\infty\frac{c_n}{z^n}}+\frac{a^2}{z}e^{-\sum_1^\infty\frac{c_n}{z^n}}$$

The constant k_n is thus the coefficient of $\frac{1}{z^n}$ in the expansion of $e^{\sum_1^\infty\frac{c_n}{z^n}}$ and the constant h_n the coefficient of $\frac{1}{z^n}$ in the expansion of $e^{-\sum_1^\infty\frac{c_n}{z^n}}$. For the recursion form for k_n see Smithsonian Mathematical Formulæ and Tables of Elliptic Functions, p. 120.

called that the values of c_n are given by the coefficients of the Fourier expansion of $\psi(\varphi)$ as

$$\frac{c_n}{R^n}=\frac{1}{\pi}\int_0^{2\pi}\psi(\varphi)e^{in\varphi}d\varphi \text{ where } R=ae^{\psi_0}$$

and

$$\psi_0=\frac{1}{2\pi}\int_0^{2\pi}\psi(\varphi)d\varphi$$

The first few terms of equation (25) are then as follows:

$$\zeta=z+c_1+\frac{c_2+\frac{c_1^2}{2}+a^2}{z}+\frac{c_3+c_2c_1+\frac{c_1^3}{6}-c_1a^2}{z^2}+\ldots \quad (25')$$

By writing $z_1=z+c_1$, equation (25) is cast into the normal form

$$\zeta=z_1+\frac{b_1}{z_1}+\frac{b_2}{z_1^2}+\ldots \quad (26)$$

The constants b_n may be evaluated directly in terms of a_n or may be obtained merely by replacing $\psi(\varphi)$ by $\psi_1(\varphi)$ in the foregoing values for a_n.

The series given by equations (25) and (26) may be inverted and z or z_1 developed as a power series in ζ. Then

$$z(\zeta)=\zeta-c_1-\frac{a_1}{\zeta}-\frac{a_2+a_1c_1}{\zeta^2}-\frac{a_1c_1^2+2a_2c_1+a_3+a_1^2}{\zeta^3}\ldots \quad (27)$$

and

$$z_1(\zeta)=\zeta-\frac{b_1}{\zeta}-\frac{b_2}{\zeta^2}-\frac{b_3+b_1^2}{\zeta^3}\ldots \quad (28)$$

The various transformations have been performed for the purpose of transforming the flow pattern of a

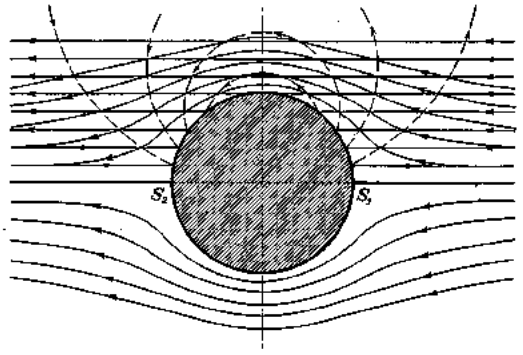

FIGURE 11.—Streamlines about circle with zero circulation (shown by the full lines) $Q=-V\sinh\mu\sin\varphi=$constant

circle into the flow pattern of an airfoil. We are thus led immediately to the well-known problem of determining the most general type of irrotational flow around a circle satisfying certain specified boundary conditions.

The flow about a circle.—The boundary conditions to be satisfied are: The circle must be a streamline of flow and, at infinity, the velocity must have a given magnitude and direction. Let us choose the ξ axis as corresponding to the direction of the velocity at infinity. Then the problem stated is equivalent to that of an infinite circular cylinder moving parallel to the ξ axis with velocity V in a fluid at rest at infinity.

The general complex flow potential [17] for a circle of radius R, and velocity at infinity V parallel to the x axis is

$$w(z)=-V\left(z+\frac{R^2}{z}\right)-\frac{i\Gamma}{2\pi}\log\frac{z}{R} \quad (29)$$

where Γ is a real constant parameter, known as the

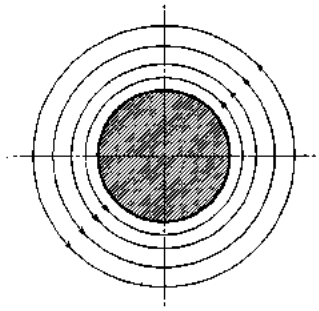

FIGURE 12.—Streamlines about circle for $V=0$ $Q=-\frac{\Gamma}{2\pi}\mu=$constant

circulation. It is defined as $\oint v_s ds$ along any closed curve inclosing the cylinder, v_s being the velocity along the tangent at each point.

Writing $z=Re^{\mu+i\varphi}$ and $w=P+iQ$, equation (29) becomes

$$w=-V\cosh(\mu+i\varphi)-\frac{i\Gamma}{2\pi}(\mu+i\varphi) \quad (29')$$

or

$$\left.\begin{aligned}P&=-V\cosh\mu\cos\varphi+\frac{\Gamma}{2\pi}\varphi\\ Q&=-V\sinh\mu\sin\varphi-\frac{\Gamma}{2\pi}\mu\end{aligned}\right\}$$

For the velocity components, we have

$$\frac{dw}{dz}=u-iv=-V\left(1-\frac{R^2}{z^2}\right)-\frac{i\Gamma}{2\pi z} \quad (30)$$

In Figures 11 and 12 are shown the streamlines for the cases $\Gamma=0$, and $V=0$, respectively. The cylinder experiences no resultant force in these cases since all streamlines are symmetrical with respect to it.

The stagnation points, that is, points for which u and v are both zero, are obtained as the roots of $\frac{dw}{dz}=0$. This equation has two roots.

$$z_0=\frac{i\Gamma\pm\sqrt{16\pi^2R^2V^2-\Gamma^2}}{4\pi V}$$

and we may distinguish different types of flow according as the discriminant $16\pi^2R^2V^2-\Gamma^2$ is positive, zero, or negative. We recall here that a conformal transformation $w=f(z)$ ceases to be conformal at points where $\frac{dw}{dz}$ vanishes, and at a stagnation point the flow divides and the streamline possesses a singularity.

[17] Reference 4, p. 56 or reference 5, p. 118. The log term must be added because the region outside the infinite cylinder (the point at infinity excluded) is doubly connected and therefore we must include the possibility of cyclic motion.

The different types of flow that result according as the parameter $\Gamma^2 \gtrless 16\pi^2R^2V^2$ are represented in Figure 13. In the first case (fig. 13 (a)), which will not interest us later, the stagnation point occurs as a double point in the fluid on the η axis, and all fluid within this streamline circulates in closed orbits around the circle, while the rest of the fluid passes downstream. In the second case (fig. 13 (b)), the stagnation points are together at S on the circle $Re^{i\varphi}$ and in the third case (fig. 13 (c)) they are symmetrically located on the circle. We have noted then that as Γ increases from 0 to $4\pi RV$ the stagnation points move downward on the circle $Re^{i\varphi}$ from the ξ axis toward the η axis. Upon further increase in Γ they leave the circle and are located on the η axis in the fluid.

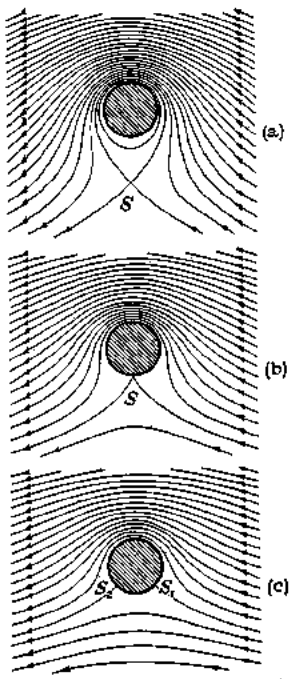

FIGURE 13.—Streamlines about circle [from Lagally—Handbuch der Physik Bd. VIII] $Q = V\sin\varphi - \frac{\Gamma}{2\pi}\varphi = \text{constant}$ (a) $\Gamma^2 > 16\pi^2R^2V^2$ (b) $\Gamma^2 = 16\pi^2R^2V^2$ (c) $\Gamma^2 < 16\pi^2R^2V^2$

Conversely, it is clear that the position of the stagnation points can determine the circulation Γ. This fact will be shown to be significant for wing-section theory. At present, we note that when both Γ and $V \neq 0$ a marked dissymmetry exists in the streamlines with respect to the circle. They are symmetrical about the η axis but are not symmetrical about the ξ axis. Since they are closer together on the upper side of the circle than on the lower side, a resultant force exists perpendicular to the motion.

We shall now combine the transformation (27) and the flow formula for the circle equation (29) and obtain the general complex flow potential giving the 2-dimensional irrotational flow about an airfoil shape, and indeed, about any closed curve for which the Riemann theorem applies.

The flow around the airfoil.—In Figure 14 are given, in a convenient way, the different complex planes and transformations used thus far. The complex flow potential in the z plane for a circle of radius R origin at the center has been given as

$$w(z) = -V\left(z + \frac{R^2}{z}\right) - \frac{i\Gamma}{2\pi}\log z \qquad (29)$$

where V, the velocity at infinity, is in the direction of the negative ξ axis. Let us introduce a parameter to permit of a change in the direction of flow at infinity by the angle α which will be designated *angle of attack* and defined by the direction of flow at infinity with respect to a fixed axis on the body, in this case the axis $\varphi = 0$. This flow is obtained simply by writing $ze^{i\alpha}$ for z in equation (29) and represents a rotation of

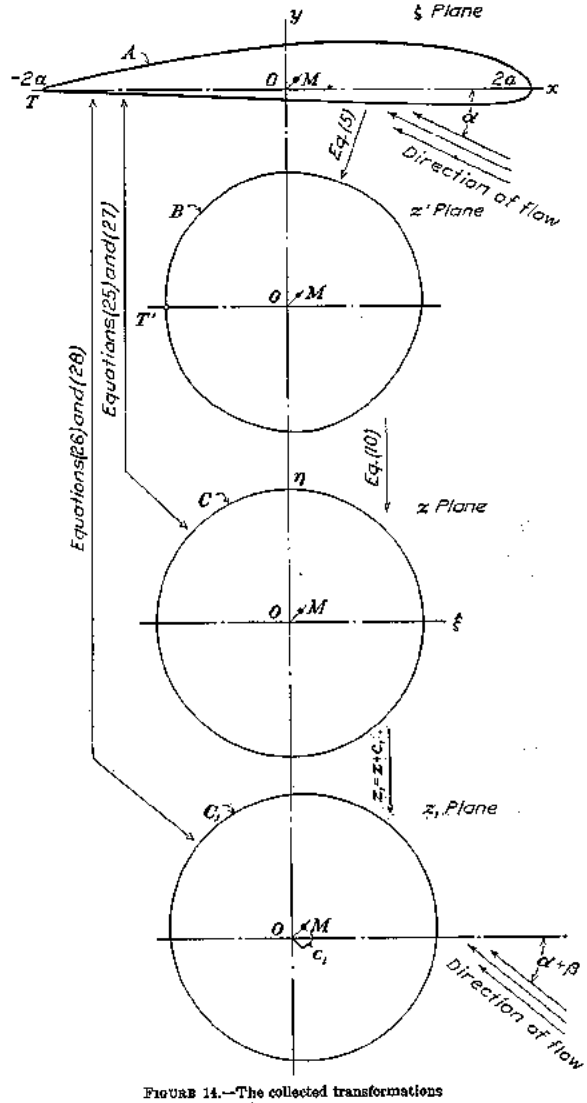

FIGURE 14.—The collected transformations

the entire flow field about the circle by angle α. We have

$$w(z) = -V\left(ze^{i\alpha} + \frac{R^2}{z}e^{-i\alpha}\right) - \frac{i\Gamma}{2\pi}\log z \qquad (31)$$

$$\frac{dw}{dz} = u - iv = -Ve^{i\alpha}\left(1 - \frac{R^2}{z^2}e^{-2i\alpha}\right) - \frac{i\Gamma}{2\pi z} \qquad (32)$$

Since a conformal transformation maps streamlines and potential lines into streamlines and potential lines,

we may obtain the complex flow potentials in the various planes by substitutions. For the flow about the circle in the z_1 plane, z is replaced by $z_1 - c_1$

$$w(z_1) = -V\left[(z_1-c_1)e^{i\alpha}+\frac{R^2e^{-i\alpha}}{(z_1-c_1)}\right]-\frac{i\Gamma}{2\pi}\log(z_1-c_1) \quad (31')$$

$$\frac{dw}{dz_1} = -Ve^{i\alpha}\left[1-\frac{R^2e^{-2i\alpha}}{(z_1-c_1)^2}\right]-\frac{i\Gamma}{2\pi(z_1-c_1)} \quad (32')$$

For the flow about the B curve in the z' plane, z is replaced by $z(z')$ (the inverse of eq. (10a)) and for the flow about the airfoil in the ζ plane z is replaced by $z(\zeta)$ from equation (27)

$$W(\zeta) = -V[z(\zeta)e^{i\alpha}+\frac{R^2}{z(\zeta)}e^{-i\alpha}] \ -\frac{i\Gamma}{2\pi}\log\, z(\zeta) \quad (33)$$

$$\frac{dW}{d\zeta} = \left[-Ve^{i\alpha}\left(1-\frac{R^2e^{-2i\alpha}}{[z(\zeta)]^2}\right)-\frac{i\Gamma}{2\pi[z(\zeta)]}\right]\frac{dz(\zeta)}{d(\zeta)} \quad (34)$$

The flow fields at infinity for all these transformations have been made to coincide in magnitude and direction.

At this point attention is directed to two important facts. First, in the previous analysis the original closed curve may differ from an airfoil shape. The formulas, when convergent, are applicable to any closed curve satisfying the general requirements of the Riemann theorem. However, the peculiar ease of numerical evaluations for streamline shapes is noteworthy and significant. The second important fact is that the parameter Γ which as yet is completely undetermined is readily determined for airfoils and to a discussion of this statement the next section is devoted. It will be seen that airfoils may be regarded as fixing their own circulation.

Kutta-Joukowsky method for fixing the circulation.—All contours used in practice as airfoil profiles possess the common property of terminating in either a cusp or sharp corner at the trailing edge (a point of two tangents). Upon transforming the circle into an airfoil by $\zeta = f(z)$, we shall find that $\left|\frac{dz}{d\zeta}\right|$ is infinite at the trailing edge if the tail is perfectly sharp (or very large if the tail is almost sharp). This implies that the numerical value of the velocity $\left|\frac{dw}{dz}\right|\left|\frac{dz}{d\zeta}\right| = |v|$ is infinite (or extremely large) provided the factor $\left|\frac{dw}{dz}\right|$ is not zero at the tail. There is but one value of the circulation that avoids infinite velocities or gradients of pressure at the tail and this fact gives a practical basis for fixing the circulation.

The concept of the ideal fluid in irrotational potential flow implies no dissipation of energy, however large the velocity at any point. The circulation being a measure of the energy in a fluid is unaltered and inde pendent of time. In particular, if the circulation is zero to begin with, it can never be different from zero.

However, since all real fluids have viscosity, a better physical concept of the ideal fluid is to endow the fluid with infinitesimal viscosity so that there is then no dissipation of energy for finite velocities and pressure gradients, but for infinite velocities, energy losses would result. Moreover, by Bernoulli's principle the pressure would become infinitely negative, whereas a real fluid can not sustain absolute negative pressures and the assumption of incompressibility becomes invalid long before this condition is reached. It should then be postulated that nowhere in the ideal fluid from the physical concept should the velocity become infinite. It is clear that the factor $\left|\frac{dw}{dz}\right|$ must then be zero at the trailing edge in order to avoid infinite velocities. It is then precisely the sharpness of the trailing edge which furnishes us the following basis for fixing the circulation.

It will be recalled that the equation $\frac{dw}{dz} = 0$ determines two stagnation points symmetrically located on the circle, the position of which varies with the value of the circulation and conversely the position of a stagnation point determines the circulation. In this paper the x axis of the airfoil has been chosen so that the negative end ($\theta = \pi$) passes through the trailing edge. From the calculation of $\epsilon = \varphi - \theta$ (by eq. (13)) the value of φ corresponding to any value of θ is determined as $\varphi = \theta + \epsilon$, in particular at $\theta = \pi$, $\varphi = \pi + \beta$, where β is the value of ϵ at the tail and for a given airfoil is a geometric constant (although numerically it varies with the choice of axes). This angle β is of considerable significance and for good reasons is called the angle of zero lift. The substance of the foregoing discussion indicates that the point $z = Re^{i(\pi+\beta)} = -Re^{i\beta}$ is a stagnation point on the circle. Then for this value of z, we have by equation (32)

$$\frac{dw}{dz} = -Ve^{i\alpha}\left(\frac{1-R^2e^{-2i\alpha}}{z^2}\right)-\frac{i\Gamma}{2\pi z} = 0$$

or

$$\Gamma = -2\pi RVie^{i(\alpha+\beta)}\ (1-e^{-2i(\alpha+\beta)})$$

$$= 4\pi RV\left(\frac{e^{i(\alpha+\beta)}-e^{-i(\alpha+\beta)}}{2i}\right)$$

$$= 4\pi RV\sin\,(\alpha+\beta) \quad (35)$$

This value of the circulation is then sufficient to make the trailing edge a stagnation point for any value of α. The airfoil may be considered to equip itself with that amount of circulation which enables the fluid to flow past the airfoil with a minimum energy loss, just as electricity flowing in a flat plate will distribute itself so that the heat loss is a minimum. The final justification for the Kutta assumption is not only its plausibility, but also the comparatively good agreement with experimental results. Figure 15 (b) shows the streamlines around an airfoil for a flow satisfying the Kutta condition, and Figures 15 (a) and 15 (c) illus-

trate cases for which the circulation is respectively too small and too large, the stagnation point being then on the upper and lower surfaces, respectively. For these latter cases, the complete flow is determinable only if, together with the angle of attack, the circulation or a stagnation point is specified.

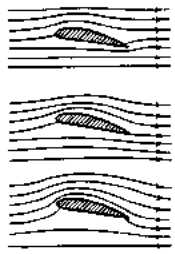

FIGURE 15.—(a) Flow with circulation smaller than for Kutta condition; (b) flow satisfying Kutta condition; (c) flow with circulation greater than for Kutta condition

Velocity at the surface.—The flow formulas for the entire field are now uniquely determined by substituting the value of Γ in equations (33) and (34). We are, however, in a position to obtain much simpler and more convenient relations for the boundary curves themselves. Indeed, we are chiefly interested in the velocity at the surface of the airfoil, which velocity is tangential to the surface, since the airfoil contour is a streamline of flow. The numerical value of the velocity at the surface of the airfoil is

$$v=\sqrt{v_x^2+v_y^2}=|v_x-iv_y|=\left|\frac{dw}{d\zeta}\right|=\left|\frac{dw}{dz}\right|\cdot\left|\frac{dz}{dz'}\right|\cdot\left|\frac{dz'}{d\zeta}\right|$$

We shall evaluate each of these factors in turn. From equations (32 and (35)

$$\frac{dw}{dz}=-Ve^{i\alpha}\left(1-\frac{R^2}{z^2}e^{-2i\alpha}\right)-\frac{i4\pi RV\sin(\alpha+\beta)}{2\pi z}$$

At the boundary surface $z=Re^{i\varphi}$, and

$$\frac{dw}{dz}=-Ve^{i\alpha}(1-e^{-2i(\alpha+\varphi)})-2iVe^{-i\varphi}\sin(\alpha+\beta)$$

or

$$\frac{dw}{dz}=-Ve^{-i\varphi}[(e^{i(\alpha+\varphi)}-e^{-i(\alpha+\varphi)})+2i\sin(\alpha+\beta)]$$

$$=-2iVe^{-i\varphi}[\sin(\alpha+\varphi)+\sin(\alpha+\beta)]$$

and

$$\left|\frac{dw}{dz}\right|=2V[\sin(\alpha+\varphi)+\sin(\alpha+\beta)] \tag{36}$$

In general, for arbitrary Γ we find that

$$\left|\frac{dw}{dz}\right|=2V\sin(\alpha+\varphi)+\frac{\Gamma}{2\pi R} \tag{36'}$$

To evaluate $\left|\frac{dz}{dz'}\right|$ we start with relation (10)

$$z'=ze^{\sum_1^\infty \frac{c_n}{z^n}}.$$

At the boundary surface

$$z'=ze^{\psi-\psi_0-i\epsilon} \text{ where } \epsilon=\varphi-\theta \text{ and } z=ae^{\psi_0+i\varphi}$$

$$\frac{dz'}{dz}=\frac{z'}{z}\left(1+z\frac{d(\psi-i\epsilon)}{dz}\right)$$

$$=\frac{z'}{z}\left(1+\frac{d(\psi-i\epsilon)}{id\varphi}\right) \tag{37'}$$

$$=\frac{z'}{z}\left(\frac{\frac{d\varphi}{d\theta}-\frac{d\bar{\epsilon}}{d\theta}-i\frac{d\bar{\psi}}{d\theta}}{\frac{d\varphi}{d\theta}}\right)=\frac{z'}{z}\left(\frac{1-i\frac{d\bar{\psi}}{d\theta}}{1+\frac{d\bar{\epsilon}}{d\theta}}\right)$$

Then $$\left|\frac{dz'}{dz}\right|=e^{\psi-\psi_0}\sqrt{\frac{1+\left(\frac{d\bar{\psi}}{d\theta}\right)^2}{1+\frac{d\bar{\epsilon}}{d\theta}}} \tag{37}$$

By equation (5)

$$\zeta=z'+\frac{a^2}{z'} \text{ and at the boundary } z'=ae^{\psi+i\theta}, \text{ or}$$

$$\zeta=2a\cosh(\psi+i\theta)$$

$$\frac{d\zeta}{dz'}=2a\sinh(\psi+i\theta)\frac{d(\psi+i\theta)}{dz'}$$

$$=2\sinh(\psi+i\theta)e^{-(\psi+i\theta)}.$$

Then $$\left|\frac{d\zeta}{dz'}\right|^2=4e^{-2\psi}(\sinh^2\psi\cos^2\theta+\cosh^2\psi\sin^2\theta)$$

$$=4e^{-2\psi}(\sinh^2\psi+\sin^2\theta)$$

and $$\left|\frac{d\zeta}{dz'}\right|=2e^{-\psi}\sqrt{\sinh^2\psi+\sin^2\theta)} \tag{38}$$

Then finally

$$v=\left|\frac{dw}{d\zeta}\right|=\left|\frac{dw}{dz}\right|\cdot\left|\frac{dz}{dz'}\right|\cdot\left|\frac{dz'}{d\zeta}\right|$$

$$=\frac{V[\sin(\alpha+\varphi)+\sin(\alpha+\beta)]\left(1+\frac{d\bar{\epsilon}}{d\theta}\right)e^{\psi_0}}{\sqrt{(\sinh^2\psi+\sin^2\theta)\left(1+\left(\frac{d\bar{\psi}}{d\theta}\right)^2\right)}} \tag{39}$$

In this formula the circulation is given by equation (35). In general, for an arbitrary value of Γ (see equation (36')), the equation retains its form and is given by

$$v=\frac{V\left[\sin(\alpha+\varphi)+\frac{\Gamma}{4\pi RV}\right]\left(1+\frac{d\bar{\epsilon}}{d\theta}\right)e^{\psi_0}}{\sqrt{(\sinh^2\psi+\sin^2\theta)\left(1+\left(\frac{d\bar{\psi}}{d\theta}\right)^2\right)}} \tag{40}$$

For the special case $\Gamma=0$, we get

$$v=\frac{V\sin(\alpha+\varphi)\left(1+\frac{d\bar{\epsilon}}{d\theta}\right)e^{\psi_0}}{\sqrt{(\sinh^2\psi+\sin^2\theta)\left(1+\left(\frac{d\bar{\psi}}{d\theta}\right)^2\right)}} \tag{41}$$

Equation (40) is a general result giving the velocity at any point of the surface of an arbitrary airfoil section, with *arbitrary* circulation for any angle of attack α. Equation (39) represents the important special case in which the circulation is specified by the Kutta condition. The various symbols are functions only of the coordinates (x, y) of the airfoil boundary and expressions for them have already been given. In Tables

I and II are given numerical results for different airfoils, and explanation is there made of the methods of calculation and use of the formulas developed.

We have immediately by equation (3) the value of the pressure p at any point of the surface in terms of the pressure at infinity as

$$\frac{p}{q}=1-\left(\frac{v}{V}\right)^2$$

Some theoretical pressure distribution curves are given at the end of this report and comparison is there made with experimental results. These comparisons, it will be seen, within a large range of angles of attack, are strikingly good.[18]

GENERAL WING-SECTION CHARACTERISTICS

The remainder of this report will be devoted to a discussion of the parameters of the airfoil shape affecting aerodynamic properties with a view to determining airfoil shapes satisfying preassigned properties. This discussion will not only furnish an illuminating sequel

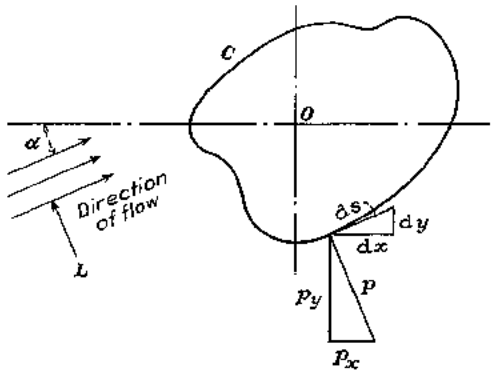

FIGURE 16.

to the foregoing analysis leading to a number of new results, but will also unify much of the existing theory of the airfoil. In the next section we shall obtain some expressions for the integrated characteristics of the airfoil. We start with the expressions for total lift and total moment, first developed by Blasius.

Blasius' formulas.—Let C in Figure 16 represent a closed streamline contour in an irrotational fluid field. Blasius' formulas give expressions for the total force and moment experienced by C in terms of the complex velocity potential. They may be obtained in the following simple manner. We have for the total forces in the x and y directions

$$P_x=-\int_C p_x ds=-\int_C p\,dy$$

$$P_y=\int_C p_y ds=\int_C p\,dx$$

$$P_x-iP_y=-\int_C p(dy+i\,dx)$$

[18] A paper devoted to more extensive applications to present-day airfoils is in progress.

The pressure at any point is

$$p=p_0-\tfrac{1}{2}\rho v^2$$

Then,

$$P_x-iP_y=\frac{\rho}{2}\int_C v^2(dy+i\,dx)$$

$$=\frac{i\rho}{2}\int_C \frac{dw}{dz}\frac{\overline{dw}}{\overline{dz}}\,\overline{dz}$$

where the bar denotes conjugate complex quantities. Since C is a streamline, $v_x dy-v_y dx=0$. Adding the quantity

$$i\rho\int_C (v_y+iv_x)(v_x dy-v_y dx)=0$$

to the last equation, we get. [19]

$$P_x-iP_y=\frac{i\rho}{2}\int_C (v_x-iv_y)^2(dx+i\,dy)$$

$$=\frac{i\rho}{2}\int_C\left(\frac{dw}{dz}\right)^2 dz \qquad (42)$$

The differential of the moment of the resultant force about the origin is,

$$dM_0=p(x\,dx+y\,dy)$$
$$=R.\ P.\ \text{of}\ p[x\,\overline{dx}+y\,dy+i(y\,dx-x\,dy)]$$
$$=R.\ P.\ \text{of}\ p\,z\,\overline{dz}$$

where "$R.\ P.$ of" denotes the real part of the complex quantity. We have from the previous results

$$d(P_x-iP_y)=-i\,p\,\overline{dz}=\frac{i\rho}{2}\left(\frac{dw}{dz}\right)^2 dz$$

Then $$dM_0=-R.\ P.\ \text{of}\ \frac{\rho}{2}\left(\frac{dw}{dz}\right)^2 z\,dz$$

and $$M_0=-R.\ P.\ \text{of}\ \frac{\rho}{2}\int_C\left(\frac{dw}{dz}\right)^2 z\,dz \qquad (43)$$

Let us now for completeness apply these formulas to the airfoil A in the ζ plane (fig. 14) to derive the Kutta-Joukowsky classical formula for the lift force. By equation (32) we have

$$\frac{dw}{dz}=-Ve^{i\alpha}-\frac{i\Gamma}{2\pi z}+\frac{R^2Ve^{-i\alpha}}{z^2}$$

and by equation (25)

$$\frac{d\zeta}{dz}=1-\frac{a_1}{z^2}-\frac{a_2}{z^3}-\ \cdots$$

Then

$$\frac{dw}{d\zeta}=\frac{dw}{dz}\cdot\frac{dz}{d\zeta}$$

$$=-Ve^{i\alpha}-\frac{i\Gamma}{2\pi}\frac{1}{z}+(R^2Ve^{-i\alpha}-a_1Ve^{i\alpha})\frac{1}{z^2}+\ \cdots$$

[19] Cf. Blasius, H: Zs. f. Math. u. Phys. Bd. 58 S. 93 and Bd. 59 S. 43, 1910. Similarly,

$$P_x+iP_y=-\frac{i\rho}{2}\int_C\left(\frac{\overline{dw}}{dz}\right)^2\overline{dz},$$

a less convenient relation to use than (42).

Note that when the region about C is regular the value of the integral (42) remains unchanged by integrating about any other curve enclosing C.

and

$$\left(\frac{dw}{d\zeta}\right)^2 = A_0 + \frac{A_1}{z} + \frac{A_2}{z^2} + \cdots$$

where

$$A_0 = V^2 e^{2i\alpha}$$

$$A_1 = iVe^{i\alpha}\frac{\Gamma}{\pi}$$

$$A_2 = -2R^2V^2 + 2a_1V^2e^{2i\alpha} - \frac{\Gamma^2}{4\pi^2}$$

Then

$$P_x - iP_y = \frac{i\rho}{2}\int_A \left(\frac{dw}{d\zeta}\right)^2 d\zeta$$

$$= \frac{i\rho}{2}\int_C \left(\frac{dw}{d\zeta}\right)^2 \frac{d\zeta}{dz}dz$$

$$= \frac{i\rho}{2}(2\pi i A_1)$$

$$= -ie^{i\alpha}\rho V\Gamma$$

Therefore

$$\left.\begin{aligned} P_x &= \rho V\Gamma \sin\alpha \\ P_y &= \rho V\Gamma \cos\alpha \end{aligned}\right\}$$

and are the components of a force $\rho V\Gamma$ which is perpendicular to the direction of the stream at infinity. Thus the resultant lift force experienced by the airfoil is

$$L = \rho V\Gamma \tag{44}$$

and writing for the circulation Γ the value given by equation (35)

$$L = 4\pi R\rho V^2 \sin(\alpha+\beta) \tag{45}$$

The moment of the resultant lift force about the origin $\zeta = 0$ is obtained as

$$M_0 = R.\ P.\ \text{of} -\frac{\rho}{2}\int_A \left(\frac{dw}{d\zeta}\right)^2 \zeta\, d\zeta$$

$$= R.\ P.\ \text{of} -\frac{\rho}{2}\int_C \left(\frac{dw}{d\zeta}\right)^2 \zeta \frac{d\zeta}{dz}dz$$

$$= R.\ P.\ \text{of} -\frac{\rho}{2}\int_C \left(A_0 + \frac{A_1}{z} + \frac{A_2}{z^2} + \cdots\right)\times \left(c_1 + z + \frac{a_1}{z} + \frac{a_2}{z^2} + \cdots\right)\left(1 - \frac{a_1}{z^2} + \cdots\right)dz$$

$$= R.\ P.\ \text{of} -\frac{\rho}{2}2\pi i\ (\text{coefficient of } z^{-1})$$

$$= R.\ P.\ \text{of} -\frac{\rho}{2}2\pi i\,(A_2 + A_1c_1)$$

or, M_0 is the imaginary part of $\pi\rho(A_2 + A_1c_1)$. After putting [20] $c_1 = me^{i\delta}$ and $a_1 = b^2e^{2i\gamma}$ we get

$$M_0 = 2\pi\rho V^2b^2 \sin 2(\alpha+\gamma) + \rho V\Gamma m\cos(\alpha+\delta) \tag{46}$$

The results given by equations (44) and (46) have physical significance and are invariant to a transformation of origin as may be readily verified by employing equations (26) and (32′) and integrating around the C_1 circle in the z_1 plane. It is indeed a remarkable fact that the total integrated characteristics, lift and location of lift, of the airfoil depend on so few parameters of the transformation as to be almost independent of the shape of the contour. The parameters R, β, a_1, and c_1 involved in these relations will be discussed in a later paragraph.

We shall obtain an interesting result [21] by taking moments about the point $\zeta = c_1$ instead of the origin. (M in fig. 17.) By equation (25) we have,

$$\zeta - c_1 = z + \frac{a_1}{z} + \frac{a_2}{z^2} + \cdots$$

and by equation (43)

$$M_M = R.\ P.\ \text{of} -\frac{\rho}{2}\int_A \left[\frac{dw}{d(\zeta - c_1)}\right]^2 (\zeta - c_1)d\zeta$$

$$= R.\ P.\ \text{of} -\frac{\rho}{2}\int_C \left(A_0 + \frac{A_1}{z} + \frac{A_2}{z^2} + \cdots\right)\times \left(z + \frac{a_1}{z} + \frac{a_2}{z^2} + \cdots\right)\left(1 - \frac{a_1}{z^2} + \cdots\right)dz$$

$$= R.\ P.\ \text{of} -i\pi\rho A_2$$

or

$$M_M = 2\pi b^2\rho V^2 \sin 2(\alpha+\gamma) \tag{47}$$

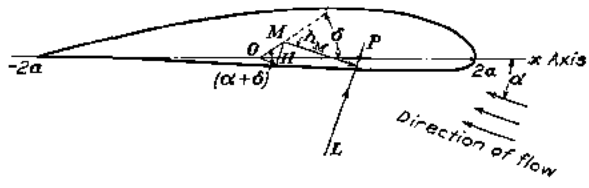

FIGURE 17.—Moment arm from M onto the lift vector

This result could have been obtained directly from equation (46) by noticing that $\rho V\Gamma$ in the second term is the resultant lift force L and that $Lm\cos(\alpha+\delta)$ represents a moment which vanishes at M for all values of α. (In fig. 17 the complex coordinate of M is $\zeta = me^{i\delta}$, the arm OH is $m\cos(\alpha+\delta)$.) The perpendicular h_M from M onto the resultant lift vector is simply obtained from $M_M = Lh_M$, as

$$h_M = \frac{b^2\sin 2(\alpha+\gamma)}{2R\sin(\alpha+\beta)} \tag{48}$$

The intersection of the resultant lift vector with the chord or axis of the airfoil locates a point which may be considered the center of pressure. The amount of travel of the center of pressure with change in angle of attack is an important characteristic of airfoils, especially for considerations of stability, and will be discussed in a later paragraph.

[20] It may be recalled that $c_1 = \frac{R}{\pi}\int_0^{2\pi}\psi(\varphi)e^{i\varphi}d\varphi$ and $a_1 = a^2 + \frac{c_1^2}{2} + c_1$. (See eq. (25′).)

[21] First obtained by R. von Mises. (Reference 6.) The work of von Mises forms an elegant geometrical study of the airfoil.

The lift force has been found to be proportional to $\sin(\alpha+\beta)$ or writing $\alpha+\beta=\alpha_1$

$$L=4\pi\rho RV^2\sin\alpha_1 \tag{49}$$

where α_1 may be termed the absolute angle of attack. Similarly writing $\alpha+\gamma=\alpha_2$

$$M_M=2\pi b^2\rho V^2\sin 2\alpha_2 \tag{50}$$

With von Mises (reference 6, Pt. II) we shall denote the axes determined by passing lines through M at angles β and γ to the x axis as the first and second axes of the airfoil, respectively. (Fig. 18.) The directions of these axes alone are important and these are fixed with respect to a given airfoil. Then the lift L is proportional to the sine of the angle of attack with respect to the first axis and the moment about M to the sine of twice the angle of attack with respect to the second axis.

From equation (47) we note that the moment at any point Q whose radius vector from M is $re^{i\sigma}$, is given by

$$M_Q=2\pi\rho b^2V^2\sin 2(\alpha+\gamma)-Lr\cos(\alpha+\sigma)$$

Let us determine whether there exist particular values of r and σ for which M_Q is independent of the angle of attack α. Writing for L its value given by equation (45),

$$M_Q=2\pi\rho b^2V^2\sin 2(\alpha+\gamma)-4\pi\rho Rr V^2\sin(\alpha+\beta)\cos(\alpha+\sigma)$$

And separating this trigonometrically

$$M_Q=2\pi\rho V^2[(b^2\cos 2\gamma-Rr\cos(\beta+\sigma))\sin 2\alpha + (b^2\sin 2\gamma-Rr\sin(\beta+\sigma))\cos 2\alpha - Rr\sin(\beta-\sigma)]$$

If this moment is to be independent of α, the coefficients of $\sin 2\alpha$ and $\cos 2\alpha$ must vanish.

Then

$$b^2\cos 2\gamma=Rr\cos(\beta+\sigma)$$

and

$$b^2\sin 2\gamma=Rr\sin(\beta+\sigma)$$

Hence,

$$r=\frac{b^2}{R}\text{ and }\sigma=2\gamma-\beta$$

Then if we move the reference point of the moment to a point F whose radius vector from M is $\frac{b^2}{R}e^{i(2\gamma-\beta)}$, the moment existing at F is for all angles of attack constant, and given by

$$M_F=2\pi\rho b^2V^2\sin 2(\gamma-\beta) \tag{51}$$

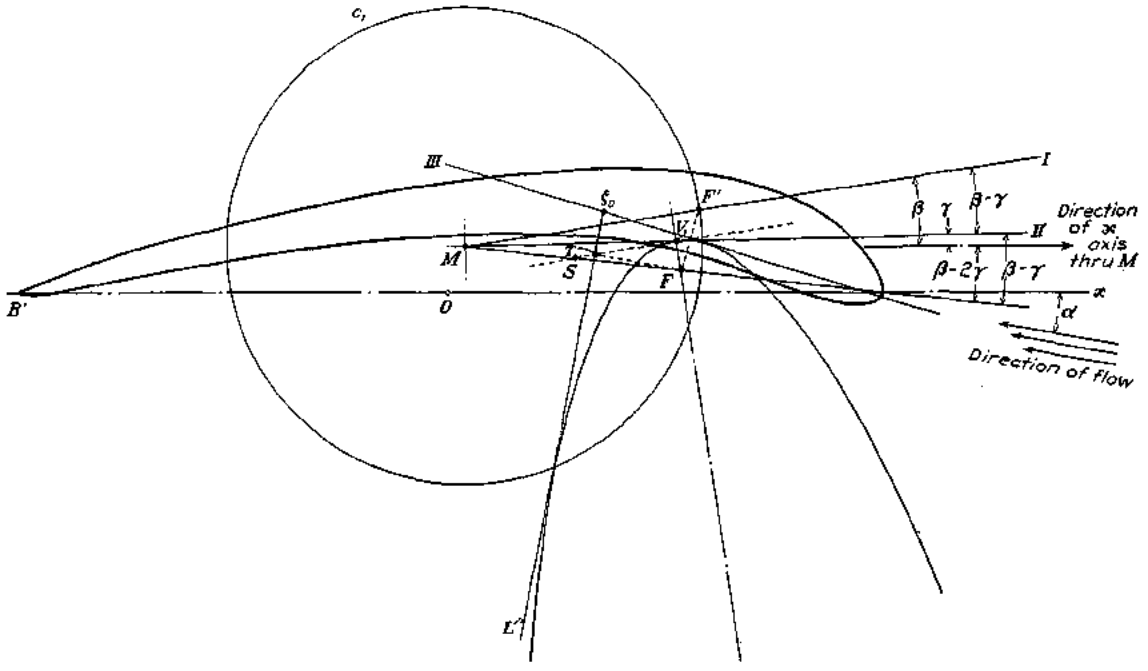

FIGURE 18.—Illustrating the geometrical properties of an airfoil (axes and lift parabola of the R. A. F. 19 airfoil)

It has thus been shown that with every airfoil profile there is associated a point F for which the moment is independent of the angle of attack. A change in lift force resulting from a change in angle of attack distributes itself so that its moment about F is zero.

From equation (47) it may be noted that at zero lift (i. e., $\alpha=-\beta$) the airfoil is subject to a moment couple which is, in fact, equal to M_F. This moment is often termed "diving moment" or "moment for zero lift." If M_F is zero, the resultant lift force must pass through F for all angles of attack and we thus have the statement that the airfoil has a constant center of pressure, if and only if, the moment for zero lift is zero.

The point F, denoted by von Mises as the focus of the airfoil, will be seen to have other interesting properties. We note here that its construction is very

simple. It lies at a distance $\frac{b^2}{R}$ from M on a line making angle $2\gamma-\beta$ with respect to the x axis. From Figure 18 we see that the angle between this line and the first axis is bisected by the second axis.

The arm h_F from F onto the resultant lift vector L (h_F is designated FT in Figure 18; note also that FT, being perpendicular to L, must be parallel to the direction of flow; the line TV is drawn parallel to the first axis and therefore angle $VTF=\alpha+\beta$) is obtained as

$$h_F=\frac{M_F}{L}=\frac{-b^2\sin 2(\beta-\gamma)}{2R\sin(\alpha+\beta)}$$

or setting $$h=\frac{b^2}{2R}\sin 2(\beta-\gamma)$$

$$h_F=-\frac{h}{\sin(\alpha+\beta)} \tag{52}$$

But h_F is parallel to the direction of α, and the relation $h=-h_F\sin(\alpha+\beta)$ states then that the projection of h_F onto the line through F perpendicular to the first axis is equal to the constant h (h is designated FV in the figure) for all angles of attack. In other words, the pedal points T determined by the intersection of h_F and L for *all* positions of the lift vector L lie on a straight line. (The line is determined by T and V in fig. 18.) The parabola is the only curve having the property that pedal points of the perpendiculars dropped from its focus onto any tangent lie on a straight line, that line being the tangent at the vertex. This may be shown analytically by noting that the equation of L for a coordinate system having F as origin and FV as negative x axis is

$$x\sin\alpha_1+y\cos\alpha_1=h_F=-\frac{h}{\sin(\alpha+\beta)}$$

By differentiating with respect to $\alpha_1=\alpha+\beta$ and eliminating α_1 we get the equation of the curve which the lines L envelop as $y^2=4h(x+h)$. From triangle FVS in Figure 18, it may be seen that the distance $MF=\frac{b^2}{R}$ is bisected at S by the line TV; for, since $FV=h=\frac{b^2}{2R}\sin 2(\gamma-\beta)$ and angle $FSV=2(\beta-\gamma)$, then $SF=\frac{b^2}{2R}$. It has thus been shown that the resultant lift vectors envelop, in general, a parabola whose focus is at F and whose directrix is the first axis. The second axis and its perpendicular at M, it may be noted, are also tangents to the parabola being, by definition, the resultant lift vectors for $\alpha=-\gamma$ and $\alpha=\frac{\pi}{2}-\gamma$, respectively.

If the constant h reduces to zero, the lift vectors reduce to a pencil of lines through F. Thus a constant center of pressure is given by $h=0$ or $\sin 2(\beta-\gamma)=0$ which is equivalent to stating that the first and second axes coincide. The lift parabola opens downward when the first axis is above the second axis ($\beta>\gamma$); it reduces to a pencil of lines when the two axes are coincident ($\beta=\gamma$) and opens upward when the second axis is above the first ($\beta<\gamma$).

W. Müller [23] introduced a third axis which has some interesting properties. Defining the complex coordinate ζ_0 as the centroid of the circulation by

$$\Gamma\zeta_0=\int_A\zeta\left(\frac{dw}{d\zeta}\right)d\zeta$$

and using equations (25) and (32) one obtains

$$\zeta_0-c_1=x_0+iy_0$$

where

$$\left.\begin{aligned}x_0&=\frac{1}{2\sin(\alpha+\beta)}\left[R\sin\alpha+\frac{b^2}{R}\sin(\alpha+2\gamma)\right]\\ y_0&=\frac{1}{2\sin(\alpha+\beta)}\left[R\cos\alpha-\frac{b^2}{R}\cos(\alpha+2\gamma)\right]\end{aligned}\right\} \tag{53}$$

The equation of the lift vector lines referred to the origin at M and x axis drawn through M is

$$x\cos\alpha-y\sin\alpha=\frac{b^2\sin(\alpha+\gamma)}{2R\sin(\alpha+\beta)} \tag{54}$$

and it may be seen that the point (x_0, y_0) satisfies this equation. The centroid of the circulation then lies on the lift vectors. By elimination of α from equation (53) one finds as the locus of (x_0, y_0)

$$2x_0\left[R\cos\beta-\frac{b^2}{R}\cos(\beta-2\gamma)\right]+2y_0\left[R\sin\beta+\frac{b^2}{R}\sin(\beta-2\gamma)\right]=R^2-\frac{b^4}{R^2} \tag{55}$$

which is the equation of a line, the third axis, and proves to be a tangent to the lift parabola. Geometrically, it is the perpendicular bisector of the line FF' joining the focus to the point of intersection of the first axis with the circle. (Fig. 18.)

The conformal centroid of the contour.—It has already been seen that the point M has special interesting properties. The transformation from the airfoil to the circle having M as center was expressed in the normal form and permitted of a very small $\epsilon(\varphi)$ curve. (See p. 188.) It was also shown that the moment with respect to M is simply proportional to the sine of twice the angle of attack with respect to the second axis. We may note, too, that in the presentation of this report the coordinate of M, $\zeta=c_1=\frac{R}{\pi}\int_0^{2\pi}\psi e^{i\varphi}d\varphi$, is a function only of the first harmonic of the $\psi(\varphi)$ curve.

We shall now obtain a significant property of M invariant with respect to the transformation from airfoil to circle. We start with the evaluation of the integral

$$\int_A\zeta\left|\frac{dz}{d\zeta}\right|ds$$

[23] Reference 7, p. 169. Also Zs. für Ang. Math. u. Mech. Bd. 3 S. 117, 1923.

Airfoils having the same first, second, and third axes are alike theoretically in total lift properties and also in travel of the center of pressure, i. e., they have the same lift parabola.

where A is the airfoil contour, ds the differential of arc along A, and $\left|\frac{dz}{d\zeta}\right|$, as will be recalled, is the magnification factor of the transformation $\zeta=f(z)$ mapping airfoil into circle; i. e., each element ds of A when magnified by $\left|\frac{dz}{d\zeta}\right|$ gives dS the differential of arc in the plane of the circle, i. e., $|dz|$. Then we have,

$$\int_A \zeta\left|\frac{dz}{d\zeta}\right|ds=\int_C \zeta(z)\,|dz| \text{ and by equation (25),}$$

$$=\int_C\left(c_1+z+\frac{a_1}{z}+\frac{a_2}{z^2}+\ \ldots\right)|dz|$$

$$=\int_0^{2\pi}\left(c_1+Re^{i\varphi}+\frac{a_1}{R}e^{-i\varphi}+\frac{a_2}{R^2}e^{-2i\varphi}+\ \ldots\right)Rd\varphi$$

$$=2\pi R\,c_1$$

$$=c_1\int_C dS=c_1\int_A\left|\frac{dz}{d\zeta}\right|ds$$

Then

$$c_1=\frac{\int_A \zeta\left|\frac{dz}{d\zeta}\right|ds}{\int_A\left|\frac{dz}{d\zeta}\right|ds} \tag{56}$$

The point M of the airfoil is thus the conformal centroid obtained by giving each element of the contour a weight equal to the magnification of that element, which results when the airfoil is transformed into a circle, the region at infinity being unaltered. It lies within any convex region enclosing the airfoil contour.[23]

ARBITRARY AIRFOILS AND THEIR RELATION TO SPECIAL TYPES

The total lift and moment experienced by the airfoil have been seen to depend on but a few parameters of the airfoil shape. The resultant lift force is completely determined for a particular angle of attack by only the radius R and the angle of zero lift β. The moment about the origin depends, in addition, on the complex constants c_1 and a_1 or, what is the same, on the position of the conformal centroid M and the focus F. The constants c_1 and a_1 were also shown (see footnote 20) to depend only on the first and second harmonics of the $\epsilon(\varphi)$ curve. Before studying these parameters for the case of the arbitrary airfoil, it will be instructive to begin with special airfoils and treat these from the point of view of the "conformal angular distortion" [$\epsilon(\varphi)$] curve.

Flow about the straight line or flat plate.—As a first approximation to the theory of actual airfoils, there is the one which considers the airfoil section to be a straight line. It has been seen that the line of length $4a$ is obtained by transforming a circle of radius a, center at the origin, by $\zeta=z+\frac{a^2}{z}$. The region external to the line $4a$ in the ζ plane maps uniquely into the region external to the circle $|z|=a$. A point Q of the line corresponding to a point P at $ae^{i\theta}$ is obtained by simply adding the vectors $a(e^{i\theta}+e^{-i\theta})$ or completing the parallelogram $OPQP'$.

For $\psi=0$, we have from equation (6)

$$x=2a\cosh\psi\cos\theta=2a\cos\theta$$
$$y=2a\sinh\psi\sin\theta=0$$

Then the parameters for this case are $R=a$, $\beta=0$, $a_1=a^2$ (i. e., $b=a$, $\gamma=0$), and M is at the origin O. Taking the Kutta assumption for determining the circulation we have,

$$\left.\begin{array}{ll}\text{the circulation,} & \Gamma=4\pi aV\sin\alpha\\ \text{the lift,} & L=4\pi a\rho V^2\sin\alpha\\ \text{moment about } M, & M_M=2\pi a^2\rho V^2\sin 2\alpha\\ \text{position of } F \text{ is at } z_F & =c_1+\frac{b^2}{R}e^{i(2\gamma-\beta)}=a\end{array}\right\} \tag{57}$$

Since $\beta=\gamma$, we know that the travel of the center of pressure vanishes and that the center of pressure is at

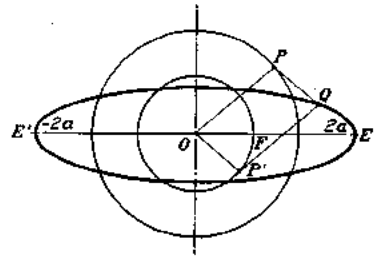

FIGURE 19.

F or at one-fourth the length of the line from the leading edge. The complex flow potential for this case is

$$w(\zeta)=-V[z(\zeta)e^{i\alpha}+\frac{a^2}{z(\zeta)}e^{-i\alpha}]+\frac{i\Gamma}{2\pi}\log z(\zeta) \tag{58}$$

where $z(\zeta)=\frac{\zeta}{2}\pm\sqrt{\left(\frac{\zeta}{2}\right)^2-a^2}$ is the inverse of equation (5). Since $\psi(\varphi)=\epsilon(\varphi)=0$ for this case, equation (39) giving the velocity at the surface reduces to

$$v=V\left[\frac{\sin\left(\frac{\varphi}{2}+\alpha\right)}{\sin\frac{\varphi}{2}}\right]\text{for } \Gamma=4\pi aV\sin\alpha,$$

and by equation (41) $v=V\left(\frac{\sin(\varphi+\alpha)}{\sin\varphi}\right)$ for $\Gamma=0$.

Flow about the elliptic cylinder.—If equation (5) is applied to a circle with center at the origin and radius ae^{ψ}, the ellipse (fig. 19)

$$\frac{x^2}{(2a\cosh\psi)^2}+\frac{y^2}{(2a\sinh\psi)^2}=1$$

is obtained in the ζ plane and the region external to this ellipse is mapped uniquely into the region external to the circle. The same transformation also transforms this external region into the region internal to the inverse circle, radius $ae^{-\psi}$. We note that a point

[23] Cf. P. Frank and K. Lowner, Math. Zs. Bd. 3, S. 78, 1919. Also reference 5, p. 146.

Q of the ellipse corresponding to P at $ae^{\psi+i\theta}$ is obtained by simply completing the parallelogram $OPQP'$ (fig. 19) where P' now terminates on the circle $ae^{-\psi}$. The parameters are obtained as $R=ae^{\psi}$, $\beta=0$, $a_1=a_2$, M is at the origin O. Then, assuming the rear stagnation point at the end of the major axis,

$$\Gamma=4\pi ae^{\psi}V\sin\alpha$$
$$L=4\pi\rho ae^{\psi}V^2\sin\alpha$$
$$M_M=2\pi a^2\rho V^2\sin 2\alpha$$

Since $\beta=\gamma$, the point F is the center of pressure for all angles of attack and is located at $z_F=ae^{-\psi}$ from O or a distance ae^{ψ} from the leading edge. The quantity

$$\frac{EF}{EE'}=\frac{ae^{\psi}}{2a(e^{\psi}+e^{-\psi})}=\frac{\cosh\psi+\sinh\psi}{4\cosh\psi}=\frac{1}{4}(1+\tanh\psi)$$

represents the ratio of the distance of F from the leading edge to the major diameter of the ellipse.

The complex flow potential is identical with that given by equation (58) for the flat plate, except that the quantity a^2 in the numerator of the second term is replaced by the constant $a^2e^{2\psi}$. Since $\psi(\varphi)=$constant, $\epsilon(\varphi)=0$ and equation (39) giving the velocity at each point of the surface for a stagnation point at end of major axis becomes

$$v=V\frac{[\sin(\varphi+\alpha)+\sin\alpha]e^{\psi}}{\sqrt{\sinh^2\psi+\sin^2\varphi}} \qquad (59)$$

and for zero circulation by equation (41)

$$v=V\frac{\sin(\varphi+\alpha)e^{\psi}}{\sqrt{\sinh^2\psi+\sin^2\varphi}} \qquad (59')$$

Circular arc sections.—It has been shown that the transformation $\zeta=z+\frac{a^2}{z}$ applied to a circle with center at $z=0$ and radius a gives a straight line in the ζ plane, and when applied to a circle with center $z=0$ and radius different from a gives an ellipse in the ζ plane. We now show that if it is used to transform a circle with center at $z=is$ (s being a real number) and radius $\sqrt{a^2+s^2}$, a circular arc results. The coordinates of the transform of the circle C in the ζ plane are given by equation (6) as

$$x=2a\cosh\psi\cos\theta$$
$$y=2a\sinh\psi\sin\theta$$

A relation between ψ and θ can be readily obtained. In right triangle OMD (fig. 20), $OM=s$, angle $OMD=\theta$, and recalling that the product of segments of any chord through O is equal to a^2, $OD=\frac{1}{2}(OP-OP_1)=a\frac{(e^{\psi}-e^{-\psi})}{2}=a\sinh\psi$. Then $s\sin\theta=a\sinh\psi$, and from the equation for y, $y=2s\sin^2\theta$. Eliminating both θ and ψ in equation (6) we get

$$x^2+\left(y+\left(\frac{a^2-s^2}{s}\right)\right)^2=\left(\frac{a^2+s^2}{s}\right)^2 \qquad (60)$$

the equation of a circle; but since y can have only positive values, we are limited to a circular arc. In fact, as the point P in Figure 20 moves from A' to A on the circle, the point Q traverses the arc $A_1'A_1$ and as P completes the circuit AA' the arc is traversed in the opposite direction. As in the previous cases, we note that the point Q corresponding to either P or to the inverse and reflected point P' is obtained by completing the parallelogram $OPQP'$. We may also note

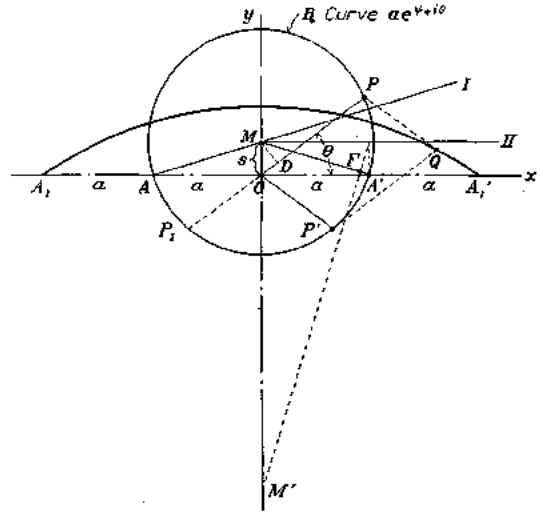

FIGURE 20.—The circular arc airfoil

that had the arc A_1A_1' been preassigned with the requirement of transforming it into the circle, the most convenient choice of origin of coordinates would be the midpoint of the line, length $4a$, joining the end points. The curve B then resulting from using transformation (5) would be a circle in the z' plane, center at $z'=is$, and the theory developed in the report could be directly applied to this continuous closed B curve.

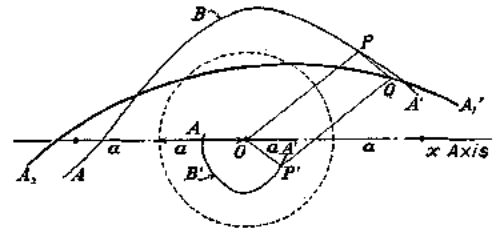

FIGURE 21.—Discontinuous B curve

Had another axis and origin been chosen, e. g., as in Figure 21, the B curve resulting would have finite discontinuities at A and A', although the arc A_1A_1' is still obtained by completing the parallelogram $OPQP'$.

The parameters of the arc A_1A_1' of chord length $4a$, and maximum height $2s$ are then, $R=\sqrt{a^2+s^2}$, $\beta=\tan^{-1}\frac{s}{a}$. The focus F may be constructed by erecting a perpendicular to the chord at A' of length s

and projecting its extremity on MA'. The center M' of the arc also lies on this line.

The infinite sheet having the circular arc as cross section contains as a special case the flat plate, and thus permits of a better approximation to the mean camber line of actual airfoils. The complex flow potential and the formulas for the velocity at the surface for the circular arc are of the same form as those given in the next section for the Joukowsky airfoil, where also a simple geometric interpretation of the parameters ϵ and ψ are given.

Joukowsky airfoils.—If equation (5) is applied to a circle with center at $z=s$, s being a real number, and with radius $R=a+s$, a symmetrical Joukowsky airfoil (or strut form) is obtained. The general Joukowsky airfoil is obtained when the transformation $\zeta=z+\frac{a^2}{z}$ is applied to a circle C passing through the point $z=-a$ and containing $z=a$ (near the circumference usually), and whose center M is not limited to either the x or y axes, but may be on a line OM inclined to the axes. (Fig. 22.) The parametric equations of the shape are as before

$$\left.\begin{aligned} x&=2a\cosh\psi\cos\theta\\ y&=2a\sinh\psi\sin\theta\end{aligned}\right\} \tag{6}$$

Geometrically a point Q of the airfoil is obtained by adding the vectors $ae^{\psi+i\theta}$ and $ae^{-\psi-i\theta}$ or by completing the parallelogram $OPQP'$ as before, but now P' lies on another circle B' defined as $z=ae^{-\psi-i\theta}$, the inverse and reflected circle of B with respect to the circle of radius a at the origin (obtained by the transformation of reciprocal radii and subsequent reflection in the x axis). Thus $OP\cdot OP'=a^2$ for all positions of P, and OP' is readily constructed. The center M_1 of the circle B' may be located on the line AM by drawing OM_1 symmetrically to OM with respect to the y axis. Let the coordinate of M be $z=is+de^{i\beta}$, where d, s, and β are real quantities. The circle of radius a, with center M_0 at $z=is$, is transformed into a circular arc through A_1A_1' which may be considered the mean camber line of the airfoil. At the tail the Joukowsky airfoil has a cusp and the upper and lower surfaces include a zero angle. The lift parameters are $R=\sqrt{a^2+s^2}+d$, $\beta=\tan^{-1}\frac{s}{a}$, $a_1=a^2=b^2e^{2i\gamma}$ or $b=a$ and $\gamma=0$. Since $\gamma=0$, the second axis has the direction of the x axis. The focus F is determined by laying off the segment $MF=\frac{a^2}{R}$ on the line MA'. This quantity, it may be noted, is obtained easily by the following construction. In triangle MDC', $MD=R$, MC' and MC are made equal to a, then CF drawn parallel to DC' determines $MF=\frac{a^2}{R}$. The lift parabola may be now determined uniquely since its directrix AM and focus F are known.

It may be observed that if it is desired to transform a preassigned Joukowsky profile into a circle, there exists a choice of axis and origin for the airfoil such that the inverse of transformation (5) will map the airfoil directly into a circle. This axis is very approximately given by designating the tail as $(-2a, 0)$ and the point midway between the leading edge and the center of curvature of the leading edge as $(+2a, 0)$ the origin then bisecting the line joining these points.

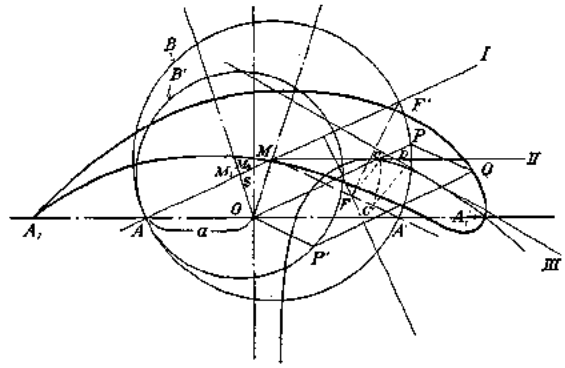

FIGURE 22.—The Joukowsky airfoil

The complex potential flow function for the Joukowsky airfoil is

$$w(\zeta)=-V\left[g(\zeta)e^{i\alpha}+\frac{R^2e^{-i\alpha}}{g(\zeta)}\right]+\frac{i\Gamma}{2\pi}\log g(\zeta) \tag{61}$$

where

$$g(\zeta)=\frac{\zeta}{2}\pm\sqrt{\left(\frac{\zeta}{2}\right)^2-a^2}-m$$

By equation (39) we have for the velocity at the surface

$$v=\frac{V[\sin(\alpha+\varphi)+\sin(\alpha+\beta)]\left(1+\frac{d\bar{\epsilon}}{d\theta}\right)e^{\psi_0}}{\sqrt{(\sinh^2\psi+\sin^2\theta)\left(1+\left(\frac{d\bar{\psi}}{d\theta}\right)^2\right)}}$$

This formula was obtained by transforming the flow around C into that around B and then into that around A. Since we know that B is itself a circle for this case, we can simply use the latter two transformations alone.

We get

$$v=\frac{V[\sin(\alpha+\varphi)+\sin(\alpha+\beta)]e^{\psi}}{\sqrt{\sinh^2\psi+\sin^2\theta}} \tag{62}$$

That these formulas are equivalent is immediately evident since the quantity

$$\frac{e^{\psi_0-\psi}\left(1+\frac{d\bar{\epsilon}}{d\theta}\right)}{\sqrt{1+\left(\frac{d\bar{\psi}}{d\theta}\right)^2}}$$

is unity being the ratio of the magnification of each arc element of C to that of B. (See eq. (37).)

A very simple geometrical picture of the parameters ϵ and ψ, exists for the cases discussed. In Figure 23 the value of ϵ or $\varphi-\theta$ at the point P is simply

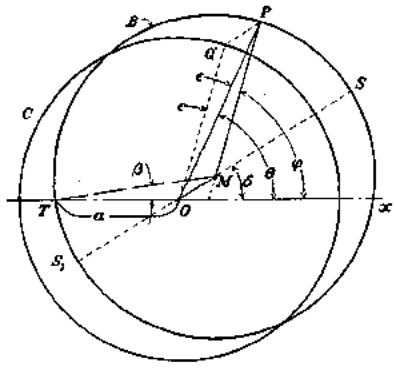

FIGURE 23.—Geometrical representation of ϵ and ψ for Joukowsky airfoils

angle OPM, i. e., the angle subtended at P by the origin O and the center M. The angle of zero lift is the value of ϵ for $\theta=\pi$; i. e., $\epsilon_{Tail}=\beta=OTM$. In particular, we may note that $\epsilon=0$ at S and S_1 which are on the straight line OM. Consider the triangle OMP, where $OP=ae^{\psi}$, $MP=R=ae^{\psi_0}$, $\frac{OM}{MP}=\rho$, angle $OPM=\epsilon$; also, $MOX=\delta$, $MOP=\theta-\delta$, $OMP=\pi-(\varphi-\delta)$. Then by the law of cosines, we have

$$e^{2(\psi-\psi_0)}=1+2\rho\cos(\varphi-\delta)+\rho^2$$

or

$$\psi-\psi_0=\frac{1}{2}\log\,(1+2\rho\cos(\varphi-\delta)+\rho^2) \qquad (63)$$

$$=\sum_1^\infty(-1)^{n-1}\frac{\cos\,n(\varphi-\delta)}{n}\rho^n$$

and by the law of sines

$$\sin\epsilon=\frac{\rho\sin(\varphi-\delta)}{(1+2\rho\cos(\varphi-\delta)+\rho^2)^{1/2}}$$

or

$$\epsilon(\varphi)=\tan^{-1}\frac{\rho\sin(\varphi-\delta)}{1+\rho\cos(\varphi-\delta)}$$

$$=\sum_1^\infty(-1)^{n-1}\frac{\sin\,n(\varphi-\delta)}{n}\rho^n \qquad (64)$$

We see that, as required, the expressions for the "radial distortion" $\psi(\varphi)$ and the "angular distortion" $\epsilon(\varphi)$ are conjugate Fourier series and may be expressed as a single complex quantity

$$(\psi-\psi_0)-i\epsilon=\sum_1^\infty\frac{(-1)^{n-1}}{n}\rho^n e^{-in(\varphi-\delta)}$$

$$=\log\,[1+\rho e^{-i(\varphi-\delta)}]$$

It is evident also that the coefficient for $n=1$ or the "first harmonic term" is simply $\rho e^{i\delta}$ and a translation by this quantity brings the circle C into coincidence with B as was pointed out on page 187.

The constant $\psi_0=\frac{1}{2\pi}\int_0^{2\pi}\psi d\varphi$ is readily shown to be invariant to the choice of origin O, as long as O is within B. We have

$$\frac{1}{2\pi}\int_0^{2\pi}\psi d\varphi=\frac{1}{2\pi}\int_0^{2\pi}\frac{1}{2}\log\,(1+2\rho\cos\,(\varphi-\delta)+\rho^2)e^{2\psi_0}d\varphi$$

$$=\frac{1}{2\pi}\int_0^{2\pi}\left(\psi_0+\sum_1^\infty(-1)^{n-1}\frac{\cos\,n(\varphi-\delta)}{n}\rho^n\right)d\varphi=\psi_0$$

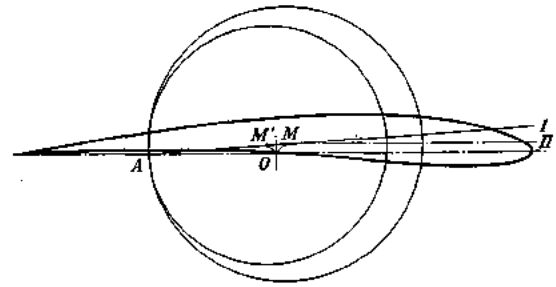

FIGURE 24.—The Joukowsky airfoil $\rho=0.10$, $\delta=45°$

Figure 24 shows the Joukowsky airfoil defined by $\rho=0.10$ and $\delta=45°$, and Figure 25 shows the $\bar{\psi}(\theta)$, $\psi(\varphi)$, $\bar{\epsilon}(\theta)$, and $\epsilon(\varphi)$ curves for this airfoil.

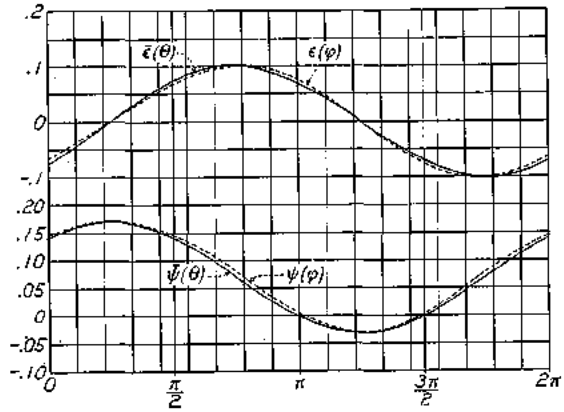

FIGURE 25.—The $\epsilon(\theta)$ and $\bar{\psi}(\theta)$ curves for the airfoil in Figure 24

Arbitrary sections.—In order to obtain the lift parameters of an arbitrary airfoil, a convenient choice of coordinate axes is first made as indicated for the Joukowsky airfoil and as stated previously. (Page 181.) The curve resulting from the use of transformation (5) will yield an arbitrary curve $ae^{\psi+i\theta}$ which will, in general, differ very little from a circle. The inverse and reflected curve $ae^{-\psi-i\theta}$ will also be almost circular. The transition from the curve $ae^{\psi+i\theta}$ to a circle is reached by obtaining the solution $\epsilon(\varphi)$ of equation (13). The method of obtaining this solution as already given converges with extreme rapidity for nearly circular curves.

The geometrical picture is analogous to that given for the special cases. In Figure 26 it may be seen that a point Q on the airfoil (N. A. C. A. –M6) corresponding to P on the B curve (or P' on the B' curve) is obtained by constructing parallelogram $OPQP'$. The $\bar{\psi}(\theta)$ and $\bar{\epsilon}(\theta)$ curves are shown in Figure 27 for this airfoil. The complex velocity potential and the expression for velocity at the surface are given respectively by equations (33) and (39). The lift parameters are

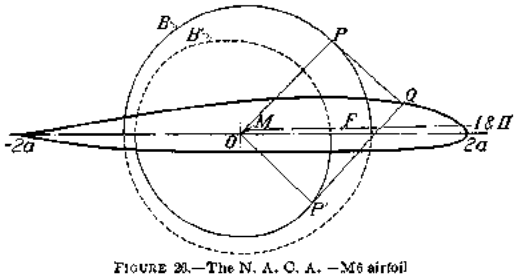

FIGURE 26.—The N. A. C. A. –M6 airfoil

$$R = ae^{i\gamma_0},\ \beta = \epsilon_{Tail}\ (\text{at } \theta = \pi),\ M \text{ is at } z = c_1 = \frac{R}{\pi}\int_0^{\pi} \psi(\varphi)e^{i\varphi}d\varphi$$

and F is at $z = c_1 + \frac{a_1}{R}$ where a_1 is given in equation (25′).

The first and second axes for the N. A. C. A. –M6 airfoil are found to coincide and this airfoil has then a constant center of pressure at F. Figures 28 (a) to 28 (l) give the pressure distribution (along the x axis) for a series of angles of attack as calculated by this theory and as obtained by experiment.[24] Table I contains the essential numerical data for this airfoil.

[24] The experimental results are taken from test No. 323 of the N. A. C. A. variable-density wind tunnel. The angle of attack α substituted in equation (39) has been modified arbitrarily to take account of the effects of finite span, tunnel-wall interference, and viscosity, by choosing it so that the theoretical lift is about 10 per cent more than the corresponding experimental value. The actual values of the lift coefficients are given in the figures.

The method used for arbitrary airfoils is readily applied to arbitrary thin arcs or to broken lines such as the sections of tail surfaces form approximately. In Figure 26 the part of the airfoil boundary above the x axis transforms by equation (5) into the two discontinuous arcs shown by full lines, while the lower boundary transforms into the arcs shown by dashed lines. If the upper boundary surface is alone given (thin airfoil) we may obtain a closed curve $ae^{\psi+i\theta}$ only by joining the end points by a chord of length $4a$ and choosing the origin at its midpoint.[25] The resulting curve has two double points for which the first derivative is not uniquely defined and, in general, it may be seen that infinite velocities correspond to such points.

At a point of the $\bar{\psi}(\theta)$ curve corresponding to a mathematically sharp corner, there exist two tangents, that is, the slope $\frac{d\bar{\psi}(\theta)}{d\theta}$ is finitely discontinuous. The curve $\bar{\epsilon}(\theta)$ must have an infinite slope at such a point for according to a theorem in the theory of Fourier series, at a point of discontinuity of a F. S., the conjugate F. S. is properly divergent. This manifests itself in the velocity-formula equation (39) in the factor $\left(1+\frac{d\bar{\epsilon}}{d\theta}\right)$ which is infinite at these sharp corners. For practical purposes, however, a rounding of the sharp edge, however small, considerably alters the slope $\frac{d\bar{\epsilon}(\theta)}{d\theta}$ at this point.

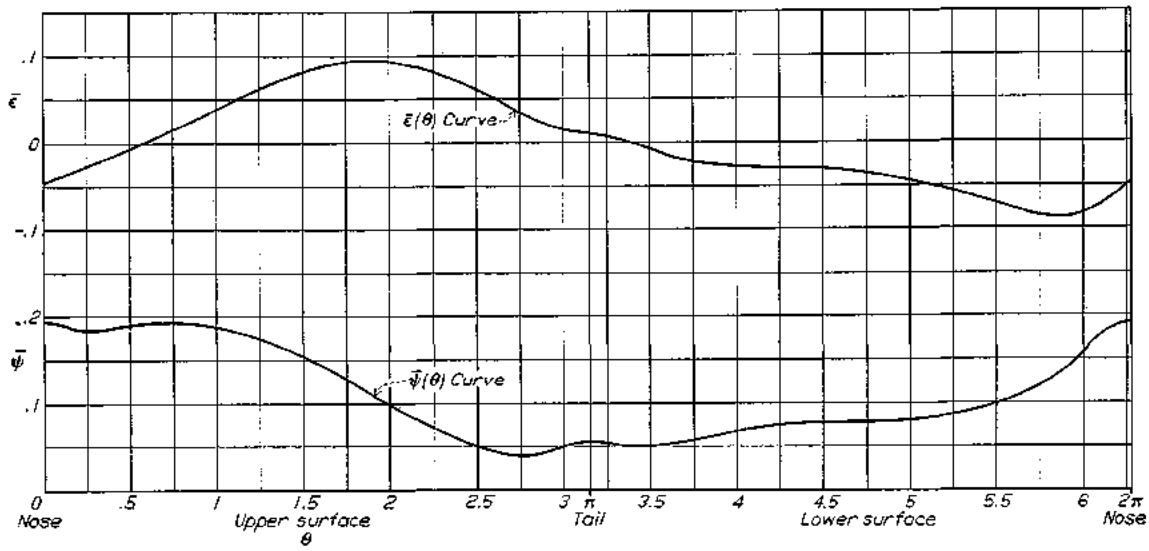

FIGURE 27.—The $\bar{\epsilon}(\theta)$ and $\bar{\psi}(\theta)$ curves for the N. A. C. A. –M6 airfoil

Ideal angle of attack.—A thin airfoil, represented by a line arc, has both a sharp leading edge and a sharp trailing edge. The Kutta assumption for fixing the circulation places a stagnation point at the tail for all angles of attack. At the leading edge, however,

[25] Note that $\bar{\psi}(\theta+\pi) = -\bar{\psi}(\theta)$ for this case.

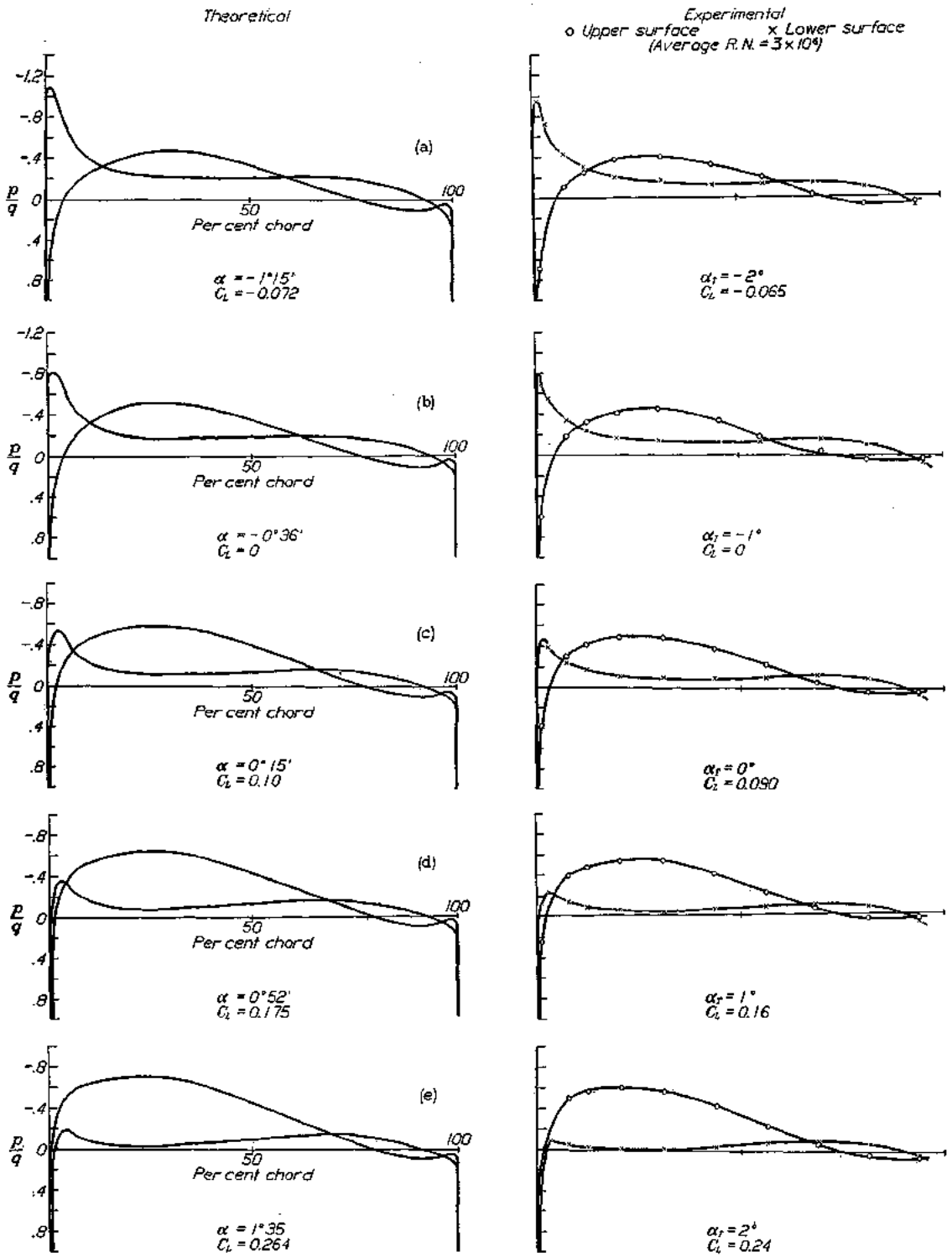

FIGURES 28 a to e.—Theoretical and experimental pressure distribution for the M6 airfoil at various angles of attack

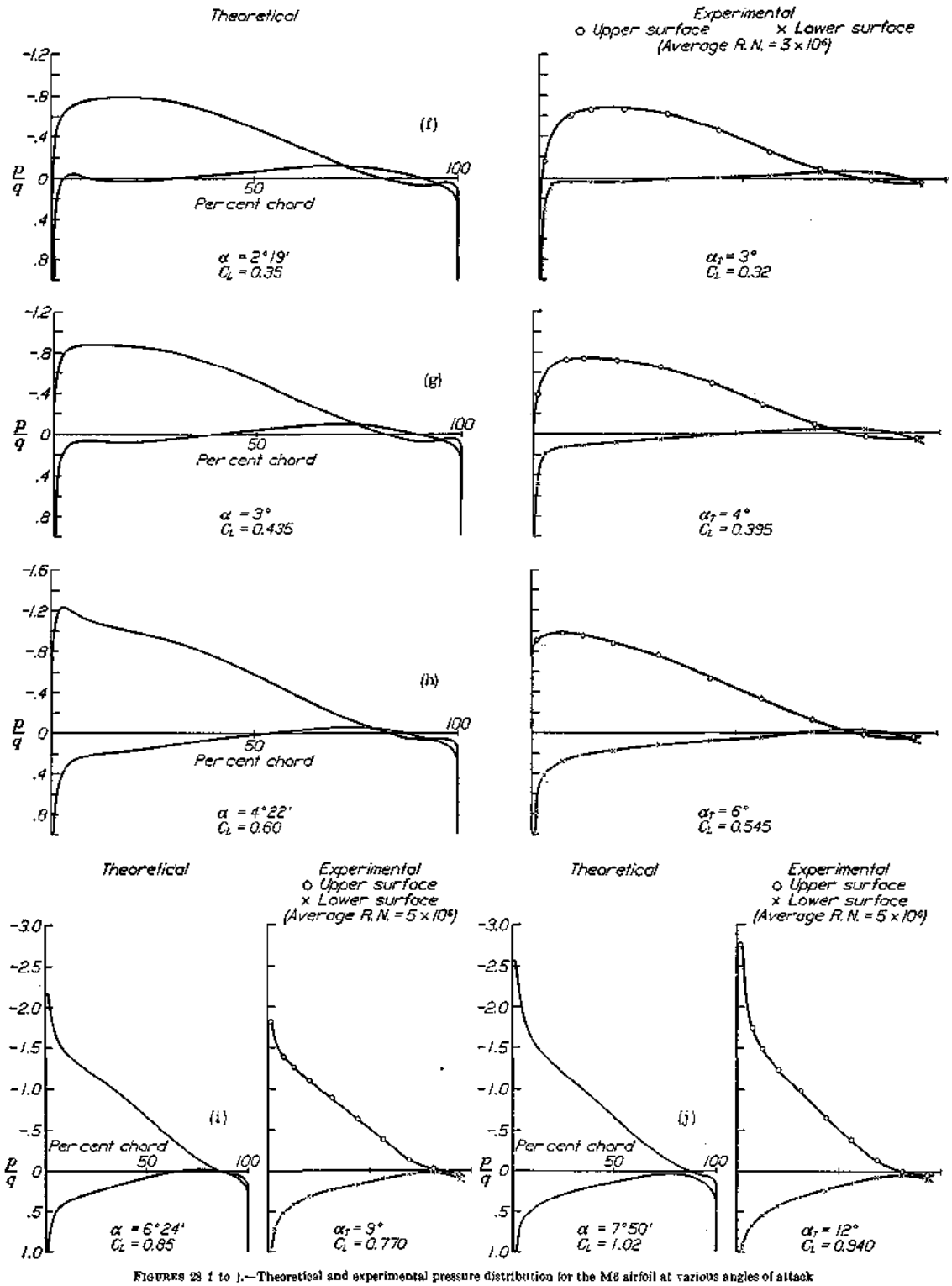

FIGURES 23 f to j.—Theoretical and experimental pressure distribution for the M6 airfoil at various angles of attack

the velocity is infinite at all angles of attack except one, namely, that angle for which the other stagnation point is at the leading edge. It is natural to expect that for this angle of attack in actual cases the frictional losses are at or near a minimum and thus arises the concept of "ideal" angle of attack introduced by Theodorsen (reference 8) and which has also been designated "angle of best streamlining." The definition for the ideal angle may be extended to thick airfoils, as that angle for which a stagnation point occurs directly at the foremost point of the mean camber line.

The lift at the leading edge vanishes and the change from velocity to pressure along the airfoil surface is usually more gradual than at any other angle of attack.

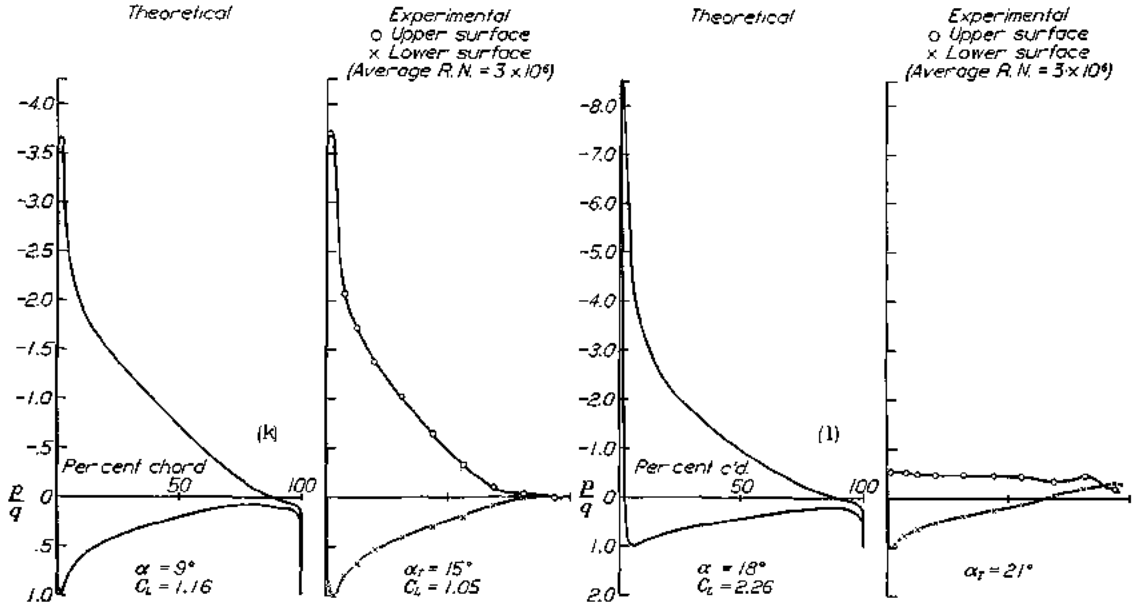

FIGURES 28 k to l.—Theoretical and experimental pressure distribution for the M6 airfoil at various angles of attack

The minimum profile drag of airfoils actually occurs very close to this angle. At the ideal angle, which we denote by α_I, the factor $[\sin(\alpha+\varphi)+\sin(\alpha+\beta)]$ in equation (39) is zero not only for $\theta=\pi$ or $\epsilon=\epsilon_T=\beta$ but also for $\theta=0$ or $\epsilon=\epsilon_N$. We get

$$\alpha_I+\epsilon_N=-(\alpha_I+\epsilon_T) \text{ or}$$

$$\alpha_I=-\frac{(\epsilon_N+\epsilon_T)}{2} \tag{65}$$

CREATION OF FAMILIES OF WING SECTIONS

The process of transforming a circle into an airfoil is inherently less difficult than the inverse process of transforming an airfoil into a circle. By a direct application of previous results we can derive a powerful and flexible method for the creation of general families of airfoils. Instead of assuming that the $\bar{\psi}(\theta)$ curve is preassigned (that is, instead of a given airfoil), we assume an arbitrary $\psi(\varphi)$ or $\epsilon(\varphi)$ curve [26] as given. This is equivalent to assuming as known a boundary-value function along a circle and, by the proper choice of this function, one can determine airfoil shapes of definite properties. The $\epsilon(\varphi)$ function, which we have designated conformal angular distortion function, will be seen to determine not only the shape but also to give easily all the theoretical aerodynamic characteristics of the airfoil.

An arbitrary $\epsilon(\varphi)$ curve is chosen, single valued, of period 2π, of zero area, and such that $-\infty \leqq \frac{d\epsilon}{d\varphi} \leqq 1$. These limiting values of $\frac{d\epsilon}{d\varphi}$ are far beyond values yielding airfoil shapes.[27] The $\psi(\varphi)$ function, except for the constant ψ_0, is given by the conjugate of the Fourier expansion of $\epsilon(\varphi)$ or, what is the same, by evaluating equation (14) as a definite integral. The constant ψ_0 is an important arbitrary [28] parameter which permits of changes in the shape and for a certain range of values may determine the sharpness of the trailing edge.

We first obtain the variable θ as $\theta(\varphi)=\varphi-\epsilon(\varphi)$, so that the quantity ψ considered as a function of θ is $\bar{\psi}(\theta)=\psi[\varphi(\theta)]$. The coordinates of the airfoil surface are then

$$x=2a\cosh\psi\cos\theta$$

$$y=2a\sinh\psi\sin\theta. \tag{6}$$

[26] Subject to some general restrictions given in the next paragraph.

[27] For common airfoils, with a proper choice of origin, $\left|\frac{d\epsilon}{d\varphi}\right| << 0.30$.

[28] For common airfoils ψ_0 is usually between 0.05 and 0.15. The constant ψ_0 is not, however, completely arbitrary. We have seen that the condition given by equation (33) is sufficient to yield a contour free from double points in the z' plane. We may also state the criterion that the inverse of equation (5) applied to this contour shall yield a contour in the ζ plane free from double points. Consider the function $\bar{\psi}(\theta)$ for θ varying from 0 to π only. The negative of each value of $\bar{\psi}(\theta)$ in this range is considered associated with $-\theta$, i. e., $\pi \leqq \theta \leqq 2\pi$. Designate the function thus formed from $\theta=0$ to 2π by $\bar{\psi}(\theta)^*$. Then $\bar{\psi}(\theta)^*$ represents a line arc in the ζ plane, i. e., the upper surface of a contour. [See footnote 25.] Then for the entire contour to be free from double points it is necessary that the lower surface should not cross the upper, that is, the *original* $\bar{\psi}(\theta)$ curve for θ varying from π to 2π must not cross below $\bar{\psi}(\theta)^*$.

The velocity at the surface is

$$v = V\frac{[\sin(\alpha+\varphi)+\sin(\alpha+\beta)]\,e^{\psi_0}}{\sqrt{(\sinh^2\psi+\sin^2\theta)\left[\left(1-\frac{d\epsilon}{d\varphi}\right)^2+\left(\frac{d\psi}{d\varphi}\right)^2\right]}} \qquad (39')$$

and is obtained by using equation (37') instead of (37) in deriving (39). The angle of zero lift β is given by

$$\varphi(\theta) = \theta + \bar{\epsilon}(\theta) \text{ for } \theta = \pi, \text{ i. e., } \varphi(\pi) = \pi + \beta.$$

The following figures and examples will make the process clear. We may first note that the most natural method of specifying the $\epsilon(\varphi)$ function is by a Fourier series expansion. In this sense then the elementary types of $\epsilon(\varphi)$ functions are the individual terms of this expansion.

29(h) to 29(t). In particular, the second harmonic term may yield S shapes, and by a proper combination of first and second harmonic terms, i. e., by a proper choice of the constants A_1, A_2, δ_1, and δ_2 in the relation

$$\epsilon(\varphi) = A_1 \sin(\varphi-\delta_1) + A_2 \sin(2\varphi-\delta_2)$$

it is possible to fix the focus F of the lift parabola as the center of pressure for all angles of attack.[29] The equation

$$\epsilon(\varphi) = 0.1 \sin(\varphi-60°) + 0.05 \cos 2\varphi$$

represents such an airfoil and is shown in Figure 29(u).

The general process will yield infinite varieties of contours by superposition of sine functions; in fact, if the process is thought of as a boundary-value problem of the circle, it is seen that it is sufficiently general to yield every closed curve for which Riemann's theorem applies.

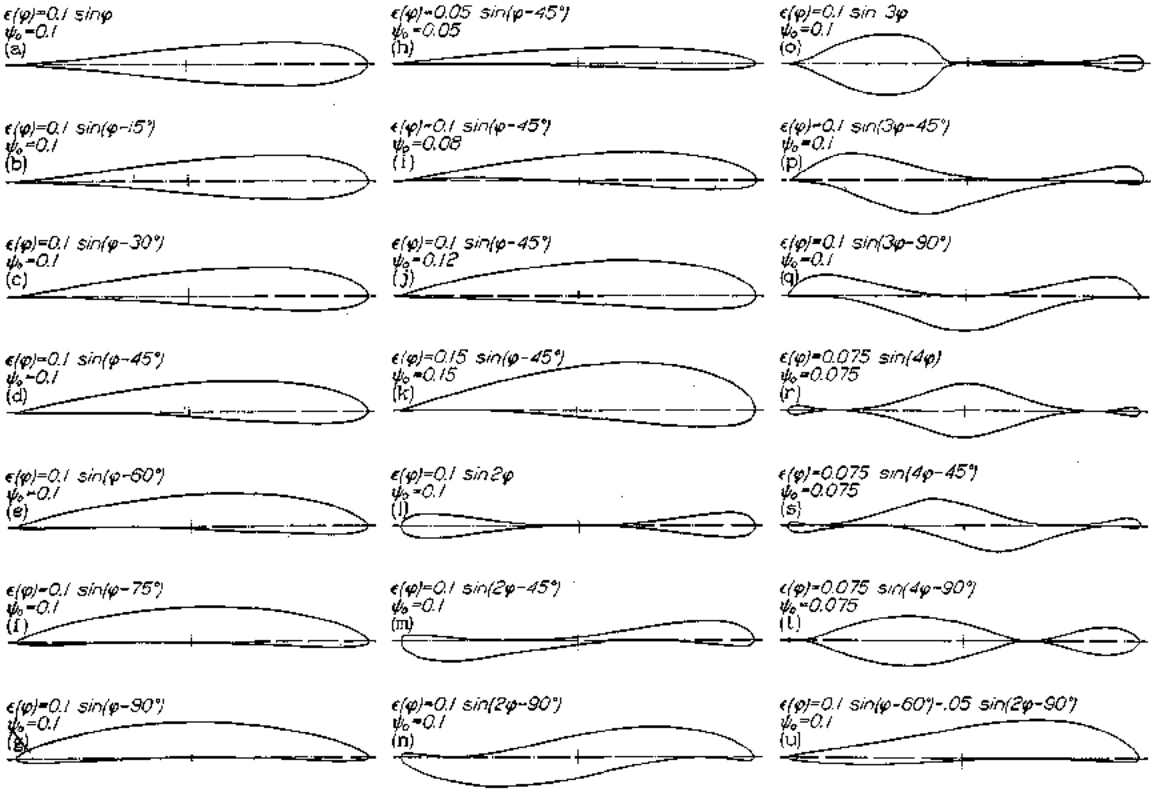

FIGURE 29.—Airfoils created by varying $\epsilon(\varphi)$

Consider first the effect of the first harmonic term

$$\epsilon(\varphi) = A_1 \sin(\varphi-\delta_1),\ \psi_0 = c$$

In Figures 29(a) to 29(g) may be seen the shapes resulting by displacing δ_1 successively by intervals of 15° and keeping the constants $A_1 = 0.10$ and $\psi_0 = 0.10$. The first harmonic term is of chief influence in determining the airfoil shape. The case $\epsilon(\varphi) = 0.1 \sin(\varphi - 45°)$ is given detailed in Table II. (This airfoil is remarkably similar to the commonly used Clark Y airfoil.) The entire calculations are characterized by their simplicity and, as may be noted, are completely free from the necessity of any graphical evaluations or constructions.

The effect of the second and higher harmonics as well as the constant ψ_0 may be observed in Figures

LANGLEY MEMORIAL AERONAUTICAL LABORATORY,
NATIONAL ADVISORY COMMITTEE FOR AERONAUTICS,
LANGLEY FIELD, VA., *November 4, 1932.*

[29] This is accomplished as follows: We seek to determine the constants A_1, A_2, δ_1, and δ_2 so that $\beta = \gamma$, where γ is obtained from equation (25') as $a_1 = be^{2i\gamma} = a^2 + \frac{c_l^2}{2} + c_2$ and we may note that $\frac{c_1}{\pi e^{\psi_0}} = A_1 e^{i\delta_1}$ and $\frac{c_1}{2^2 e^{2\psi_0}} = A_2 e^{i\delta_2}$. These relations are transcendental; however, with but a few practice trials, solutions can be obtained at will. Addition of higher harmonics will yield further shapes having the same center of pressure properties if β is kept unchanged.

APPENDIX

I. EVALUATION OF THE INTEGRAL.

$$\epsilon(\varphi') = -\frac{1}{2\pi}\int_0^{2\pi} \psi(\varphi)\cot\frac{\varphi-\varphi'}{2}\,d\varphi \qquad (13)$$

$$= \frac{1}{\pi}\int_0^{2\pi} \frac{d\psi(\varphi)}{d\varphi}\log\left|\sin\frac{\varphi-\varphi'}{2}\right| d\varphi \qquad (13')$$

The function $\psi(\varphi)$ is of period 2π and is considered known. (Note that the variables φ and φ' are replaced by θ and θ', φ_1 and φ_1', φ_2 and φ_2', etc., in equation (21) and that the following formula is applicable for all these cases.)

A 20-point method for evaluating equation (13) as a definite integral gives

$$\epsilon(\varphi') \cong -\frac{1}{\pi}\left[a_0\frac{d\psi(\varphi)}{d\varphi} + a_1(\psi_1-\psi_{-1}) + a_2(\psi_2-\psi_{-2}) + \ldots\ldots\ldots + a_9(\psi_9-\psi_{-9})\right]_{\varphi=\varphi'} \qquad (I)$$

where

ψ_1 = value of $\psi(\varphi)$ at $\varphi = \varphi' + \frac{\pi}{10}$

. . . . . .

ψ_n = value of $\psi(\varphi)$ at $\varphi = \varphi' + \frac{n\pi}{10}$

$(n = 1, -1, 2, -2, \ldots . 9, -9)$.

and the constants a_n are as follows: $a_0 = \frac{\pi}{10} = 0.3142$; $a_1 = 1.091$; $a_2 = 0.494$; $a_3 = 0.313$; $a_4 = 0.217$; $a_5 = 0.158$; $a_6 = 0.115$; $a_7 = 0.0884$; $a_8 = 0.0511$; and $a_9 = 0.0251$.

This formula may be derived directly from the definition of the definite integral. The 20 intervals[1] chosen are $\varphi - \frac{\pi}{20}$ to $\varphi + \frac{\pi}{20}$, $\varphi + \frac{\pi}{20}$ to $\varphi + \frac{3\pi}{20}$, etc.

It is only necessary to note that by expanding $\psi(\varphi)$ in a Taylor series around $\varphi = \varphi'$ we get

$$\tfrac{1}{2}\int_{\varphi'-s}^{\varphi'+s} \psi(\varphi)\cot\frac{\varphi-\varphi'}{2}d\varphi \cong -2s\left[\frac{d\psi(\varphi)}{d\varphi}\right]_{\varphi=\varphi'}$$

where the interval $\varphi' - s$ to $\varphi' + s$ is small. And, in general,

$$\tfrac{1}{2}\int_{\varphi_1}^{\varphi_2} \psi(\varphi)\cot\frac{\varphi-\varphi'}{2}\,d\varphi$$

is very nearly

$$-\psi_A \log\left|\frac{\sin\frac{\varphi-\varphi_2}{2}}{\sin\frac{\varphi-\varphi_1}{2}}\right|$$

where the range $\varphi_2 - \varphi_1$ is small and ψ_A is the average value of $\psi(\varphi)$ in this range. The constants a_n for the 20 divisions chosen above are actually

$$a_n = \log\left|\frac{\sin\pi\frac{2n+1}{40}}{\sin\pi\frac{2n-1}{40}}\right| (n = -9, \ldots +9)$$

As an example of the calculation of $\bar{\epsilon}(\theta)$ we may refer to Table I and Figures 26 and 27 for the N. A. C. A. —M6 airfoil. From the $\bar{\psi}(\theta)$ curve (fig. 27) we obtain the 20 values of ψ and $\frac{d\bar{\psi}}{d\theta}$ for 20 equal intervals of θ. For the airfoil (fig. 26) we get the following values:

(Upper surface) θ	ψ	$\frac{d\bar{\psi}}{d\theta}$	(Lower surface) θ	ψ	$\frac{d\bar{\psi}}{d\theta}$
0 (nose)	0.192	0.000	$\frac{11\pi}{10}$	0.049	−0.002
$\frac{\pi}{10}$	.185	.027	$\frac{12\pi}{10}$	.057	.050
$\frac{2\pi}{10}$	.192	.000	$\frac{13\pi}{10}$	.071	.030
$\frac{3\pi}{10}$	.189	−.030	$\frac{14\pi}{10}$	.077	.011
$\frac{4\pi}{10}$	.174	−.064	$\frac{15\pi}{10}$	.079	.000
$\frac{5\pi}{10}$	.146	−.095	$\frac{16\pi}{10}$	.082	.016
$\frac{6\pi}{10}$	.110	−.114	$\frac{17\pi}{10}$	.090	.039
$\frac{7\pi}{10}$	.077	−.086	$\frac{18\pi}{10}$	.111	.091
$\frac{8\pi}{10}$	.052	−.066	$\frac{19\pi}{10}$	.150	.154
$\frac{9\pi}{10}$	.041	.025	2π (nose)	.192	.000
π (tail)	.055	.000			

The value of ϵ at the tail (i. e., the angle of zero lift) is, for example, using formula I

$$\epsilon = -\frac{1}{\pi}\Big[\frac{\pi}{10}\times 0 + 1.091(.049-.041) + .494(.057-.052) + .313(.071-.077) + .217(.077-.110) + .158(.079-.146) + .115(.082-.174) + .0884(.090-.189) + .0511(.111-.192) + .0251(.150-.185)\Big] = .0105$$

[1] Reference 2, p. 11, gives a 10-point method result.

The value of ϵ for $\theta=\frac{3\pi}{10}$, for example, is obtained by a cyclic rearrangement. Thus,

$$\epsilon=-\frac{1}{\pi}\Big[\frac{\pi}{10}(-.030)$$
$$+1.091(.174-.192)$$
$$+.494(.146-.185)$$
$$+.313(.110-.192)$$
$$+.217(.077-.150)$$
$$+.158(.052-.111)$$
$$+.115(.041-.090)$$
$$+.0884(.055-.082)$$
$$+.0511(.049-.079)$$
$$+.0251(.057-.077)]=.0347$$

The 20 values obtained in this way form the $\bar{\epsilon}_1(\theta)$ curve, which for all practical purposes for the airfoil considered, is actually identical with the final $\bar{\epsilon}(\theta)$ curve.

II. NOTES ON THE TRANSFORMATION.

$$\zeta=f(z)=c_1+z+\frac{a_1}{z}+\frac{a_2}{z^2}+\ \ldots \qquad (4')$$

There exist a number of theorems giving general limiting values for the coefficients of the transformation equation (4), which are interesting and to some extent useful. If $\zeta=f(z)$ transforms the external region of the circle C of radius R in the z plane, into the external region of a contour A in the ζ plane in a one-to-one conformal manner and the origin $\zeta=0$ lies *within* the contour A (and $f'(\infty)=1$) then the area S inclosed by A is given by the Faber-Bieberbach theorem as [2]

$$S=R^2\pi-\sum_{n=1}^{\infty}\frac{n|a_n|^2}{R^{2(n+1)}}$$

Since all members of the above series term are positive, it is observed that the area of C is greater than that inclosed by any contour A in the ζ plane (or, at most, equal to the area inclosed by A if A is a circle).

This theorem leads to the following results

$$|a_1|\leqq R^2 \qquad \text{(a)}$$
$$|c_1|\leqq 2R \qquad \text{(b)}$$

Let us designate the circle of radius R about the conformal centroid M as center as C_1 (i. e., the center is at $\zeta=c_1$; this circle has been called the "Grundkreis" or "basic" circle by von Mises). Then since $\frac{|a_1|}{R}$ represents the distance of the focus F from M, the relation (a) states that the focus is always within C_1. In fact, a further extension shows that if r_0 is the radius of the largest circle that can be inclosed within A, then F is removed from C_1 by at least $\frac{r_0^2}{R}$.

From relation (b) may be derived the statement that if any circle within A is concentrically doubled in radius it is contained entirely within a circle about M as center of radius $2R$. Also, if we designate by c the largest diameter of A (this is usually the "chord" of the airfoil) then the following limits can be derived:

$$R\geqq\frac{1}{4}c$$

$$R\leqq\frac{1}{2}c$$

These inequalities lead to interesting limits for the lift coefficient. Writing the lift coefficient as

$$C_L=\frac{L}{\frac{1}{2}\rho V^2 c}$$

where by equation (45) the lift force is given by

$$L=4\pi R\rho V^2\sin(\alpha+\beta)$$

we have

$$2\pi\sin(\alpha+\beta)\leqq C_L=\frac{8\pi R}{c}\sin(\alpha+\beta)\leqq 4\pi\sin(\alpha+\beta) \qquad \text{(II)}$$

The flat plate is the only case where the lower limit is reached, while the upper limit is attained for the circular cylinder only. We may observe that a curved thin plate has a lift coefficient which exceeds $2\pi\sin(\alpha+\beta)$ by a very small amount. In general, the thickness has a much greater effect on the value of the lift coefficient than the camber. For common airfoils the lift coefficient is but slightly greater than the lower limit and is approximately $1.1\times 2\pi\sin(\alpha+\beta)$.

Another theorem, similar to the Faber-Bieberbach area theorem, states that if the equation $\zeta=f(z)$ transforms the internal region of a circle in the z plane into the internal region of a contour B in the ζ plane in a one-to-one conformal manner and $f'(0)=1$ (the origins are within the contours) then the area of the circle is less than that contained by any contour B. This theorem, extended by Bieberbach, has been used in an attempt to solve the arbitrary airfoil.[3] The process used is one in which the area theorem is a criterion as to the direction in which the convergence proceeds. Although theoretically sound, the process is, when applied, extremely laborious and very slowly convergent. It can not be said to have yielded as yet really satisfactory results.

III. LOCATION OF THE CENTER OF PRESSURE FOR AN ARBITRARY AIRFOIL

It is of some interest to know the exact location of the center of pressure *on the x axis* as a function of the angle of attack. In Figure 30, O is the origin, M the conformal centroid, L the line of action of the lift force for angle of attack α. Let us designate the

[2] For details of this and following statements see reference 5, p. 100 and p. 147, and also reference 6, Part II.

[3] Müller, W., Zs. f. angew. Math. u. Mech. Bd. 5 S. 397, 1925.
Höhndorf, F., Zs. f. angew. Math. u. Mech. Bd. 6 S. 265, 1926.
Also reference 5, p. 135.

intersection of L with the x axis of the airfoil as the center of pressure P.

In the right ΔONM we have,

$$OM = c_1 = me^{i\delta} = A_1 + iB_1$$

$$ON = m \cos \delta = A_1$$

$$MN = m \sin \delta = B_1$$

and in right ΔJKM, $KM = \frac{MJ}{\sin \alpha} = \frac{h_M}{\sin \alpha}$

Then $$KN = \frac{h_M}{\sin \alpha} - B_1$$

and $$NP = KN \tan \alpha = h_M \sec \alpha - B_1 \tan \alpha$$

By equation (48)

$$h_M = \frac{M_M}{L} = \frac{b^2}{2R} \frac{\sin 2(\alpha+\gamma)}{\sin (\alpha+\beta)}$$

Then the distance from the origin to the center of pressure P is

$$OP = ON + NP = A_1 - B_1 \tan \alpha + \frac{b^2}{2R} \frac{\sin 2 (\alpha+\gamma)}{\cos \alpha \sin (\alpha+\beta)} \qquad \text{(III)}$$

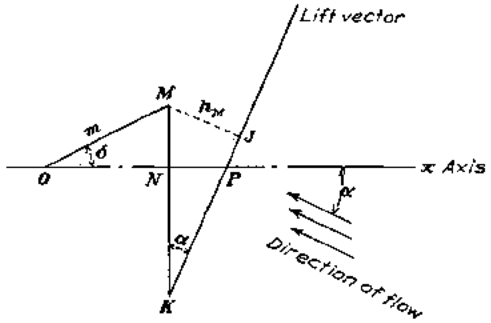

FIGURE 30.—Center of pressure location on the x axis

EXPLANATION OF THE TABLES

Table I gives the essential data for the transformation of the N. A. C. A. –M6 airfoil (shown in fig. 26) into a circle, and yields readily the complete theoretical aerodynamical characteristics. Columns (1) and (2) define the airfoil surface in per cent chord; (3) and (4) are the coordinates after choosing a convenient origin (p. 181); (5) and (6) are obtained from equations (7) and (8) of the report; (9) is the evaluation of equation (13) (see Appendix); (10) and (11) are the slopes, obtained graphically, of the ψ against θ, and ϵ against θ curves, respectively; (12) is given by

$$\frac{\left(1+\frac{d\epsilon}{d\theta}\right)e^{\psi_0}}{\sqrt{(\sinh^2\psi+\sin^2\theta)\left(1+\left(\frac{d\psi}{d\theta}\right)^2\right)}}$$

where $\psi_0 = \frac{1}{2\pi}\int_0^{2\pi} \psi(\varphi)\, d\varphi$ and may be obtained graphically or numerically; column (13) gives $\varphi = \theta + \epsilon$. The velocity v, for any angle of attack, is by equation (39)

$$v = Vk [\sin (\alpha+\varphi) + \sin (\alpha+\beta)]$$

and the pressure is given by equation (3). The angle of zero lift β is the value of ϵ at the tail; i. e., the value of ϵ for $\theta = \pi$.

Table II gives numerical data for the inverse process to that given in Table I; viz, the transformation of a circle into an airfoil. (See fig. 29.) The function $\epsilon(\varphi) = 0.1 \sin (\varphi - 45°)$ and constant $\psi_0 = 0.10$ are chosen for this case. Then $\psi(\varphi) = 0.1 \cos (\varphi - 45°) + 0.10$. It may be observed that columns (11) and (12) giving the coordinates of the airfoil surface are obtained from equations (6) of the report. Column (13) is given by

$$k = \frac{e^{\psi_0}}{\sqrt{(\sinh^2\psi+\sin^2\theta)\left[\left(1-\frac{d\epsilon}{d\varphi}\right)^2+\left(\frac{d\psi}{d\varphi}\right)^2\right]}}$$

and the velocity at the surface is by equation (39′)

$$v = Vk [\sin (\alpha+\varphi) + \sin (\alpha+\beta)]$$

REFERENCES

1. Lamb, H.: Hydrodynamics. Fifth Edition. Cambridge University Press, 1924.
2. Theodorsen, Theodore.: Theory of Wing Sections of Arbitrary Shape. T. R. No. 411, N. A. C. A., 1931.
3. Kellogg, O. D.: Foundations of Potential Theory. J. Springer, Berlin, 1929.
4. Glauert, H.: The Elements of Aerofoil and Airscrew Theory. Cambridge University Press, 1926.
5. Schmidt, H.: Aerodynamik des Fluges. W. de Gruyter, Berlin, 1929.
6. von Mises, R.: Zur Theorie des Tragflächenauftriebs. Zeitschr. f. Flugtechn. u. Motorluftschiffahrt. First Part: (23–24) Bd. 8, 1917. Second Part: (5–6) Bd. 11, 1920.
7. Müller, W.: Mathematische Strömungslehre. J. Springer, Berlin, 1928.
8. Theodorsen, Theodore.: Theory of Wing Sections with Particular Reference to the Lift Distribution. T. R. No. 383, N. A. C. A., 1931.
9. Dryden, Murnaghan, and Bateman: Hydrodynamics. National Research Council, Washington, 1932.

TABLE I

N. A. C. A.—M6

UPPER SURFACE

Per cent c	y in per cent c	x	y	$\sin\frac{\theta}{2}$	$\sinh\frac{\psi}{2}$	θ radians	ψ	ϵ	$\frac{d\bar{\psi}}{d\theta}$	$\frac{d\epsilon}{d\theta}$	k	$\varphi=\theta+\epsilon$
												° ′
0	0	2.037	0.000	0.000	0.0373	0.000	0.192	−0.0457	0.000	0.085	6.280	−2 37
1.25	1.97	1.988	.0796	.0465	.0341	.217	.184	−.0276	−.010	.080	4.249	10 52
2.50	2.81	1.935	.1135	.0941	.0342	.312	.184	−.0205	.009	.080	3.308	16 41
5.0	4.08	1.835	.163	.187	.0354	.447	.187	−.0098	.022	.080	2.557	25 4
7.5	4.94	1.734	.200	.275	.0363	.551	.189	−.0015	.022	.080	2.168	31 31
10	5.71	1.633	.231	.357	.0373	.640	.192	.0003	.020	.085	1.929	37 3
15	6.92	1.431	.276	.507	.0375	.792	.193	.0188	−.009	.095	1.660	46 27
20	7.85	1.229	.305	.636	.0366	.923	.190	.0310	−.031	.100	1.498	54 38
30	8.22	.825	.322	.835	.0330	1.153	.181	.0549	−.066	.107	1.324	69 11
40	8.05	.421	.325	.957	.0276	1.361	.165	.0717	−.085	.088	1.220	82 7
50	7.26	.017	.293	1.000	.0215	1.571	.146	.0856	−.100	.060	1.156	94 55
60	6.03	−.387	.244	.963	.0154	1.764	.124	.0932	−.100	.025	1.152	106 25
70	4.58	−.791	.185	.845	.0101	1.975	.100	.0920	−.100	−.029	1.167	113 28
80	3.06	−1.195	.124	.645	.0059	2.209	.077	.0828	−.088	−.056	1.302	131 19
90	1.55	−1.599	.063	.363	.0027	2.495	.052	.0617	−.067	−.065	1.687	146 30
95	.93	−1.801	.036	.191	.0016	2.690	.040	.0410	−.035	−.080	2.340	156 28
100	.26	−2.003	.000	.000	.0030	3.142	.055	.0105	.000	−.027	19.83	180 36

LOWER SURFACE

0	0	2.037	0.000	0.000	0.0373	6.283	0.192	−0.0457	0.000	0.085	6.280	−2 37
1.25	1.78	1.988	−.071	.0425	.0297	6.075	.172	−.0781	.133	.120	4.615	−16 21
2.50	2.20	1.936	−.089	.0644	.0284	5.989	.153	−.0859	.160	.050	3.625	−21 43
5.0	2.73	1.835	−.110	.173	.0176	5.855	.132	−.0892	.133	−.010	2.510	−29 35
7.5	3.03	1.734	−.122	.259	.0144	5.749	.120	−.0850	.109	−.045	2.025	−35 28
10	3.24	1.633	−.131	.342	.0125	5.659	.112	−.0811	.080	−.057	1.764	−40 24
15	3.47	1.431	−.140	.494	.0099	5.505	.099	−.0723	.069	−.067	1.466	−48 44
20	3.62	1.229	−.146	.626	.0085	5.371	.092	−.0637	.057	−.097	1.307	−55 54
30	3.79	.825	−.153	.831	.0070	5.136	.084	−.0516	.026	−.052	1.156	−68 39
40	3.90	.421	−.158	.956	.0065	4.924	.081	−.0421	.006	−.036	1.098	−80 17
50	3.94	.017	−.159	1.000	.0063	4.712	.079	−.0350	.000	−.029	1.091	−91 59
60	3.82	−.387	−.154	.963	.0062	4.518	.0785	−.0310	.010	−.013	1.120	−102 53
70	3.48	−.791	−.141	.845	.0068	4.307	.076	−.0300	.019	.000	1.211	−114 55
80	2.83	−1.195	−.114	.645	.0050	4.074	.071	−.0295	.036	−.011	1.370	−123 14
90	1.77	−1.599	−.072	.363	.0035	3.788	.059	−.0235	.044	−.040	1.769	−144 16
95	1.08	−1.801	−.044	.191	.0025	3.594	.050	−.0140	.020	−.067	2.368	−154 50
100	.26	−2.003	.009	.000	.0030	3.142	.055	.0105	.000	−.027	19.83	−179 24

TABLE II

$\epsilon(\varphi)=0.1\sin(\varphi-45°)$ $\psi_0=0.10$ $\beta=\bar{\epsilon}(\pi)=0.0857=3°\,47'$

UPPER SURFACE

φ		ϵ	θ		ψ	$\frac{d\epsilon}{d\phi}$	$\frac{d\psi}{d\phi}$	$\cosh\psi$	$\sinh\psi$	$\cos\theta$	$\sin\theta$	$\frac{x}{2}$	$\frac{y}{2}$	k
Degrees	Radians		Radians	Degrees										
				° ′										
0	0.0000	−0.0707	0.0707	4 3	0.1707	0.0707	0.0707	1.0146	0.1715	0.9975	0.0706	1.0121	0.0121	6.3941
5	.0873	−.0643	.1516	8 41	.1766	.0766	.0643	1.0156	.1775	.9885	.1510	1.0039	.0288	5.1215
10	.1745	−.0574	.2319	13 17	.1819	.0819	.0574	1.0166	.1826	.9735	.2298	.9895	.0420	4.0960
15	.2618	−.0500	.3118	17 52	.1866	.0866	.0500	1.0175	.1877	.9518	.3068	.9655	.0576	3.3602
20	.3491	−.0423	.3914	22 26	.1906	.0906	.0423	1.0182	.1918	.9243	.3816	.9411	.0732	2.8421
25	.4363	−.0342	.4705	26 57	.1940	.0940	.0342	1.0189	.1952	.8914	.4532	.9082	.0885	2.4704
30	.5236	−.0259	.5495	31 29	.1966	.0966	.0259	1.0194	.1979	.8528	.5223	.8693	.1034	2.1892
35	.6109	−.0174	.6283	36 0	.1985	.0985	.0174	1.0198	.1998	.8090	.5878	.8250	.1174	1.9746
45	.7854	.0000	.7854	45 0	.2000	.1000	.0000	1.0201	.2013	.7071	.7071	.7213	.1423	1.6689
55	.9599	.0174	.9425	54 0	.1985	.0985	−.0174	1.0198	.1998	.5878	.8090	.5994	.1616	1.4709
70	1.2217	.0423	1.1794	67 35	.1906	.0906	−.0423	1.0182	.1918	.3813	.9244	.3882	.1773	1.2859
80	1.3963	.0574	1.3389	76 43	.1819	.0819	−.0574	1.0166	.1826	.2298	.9733	.2336	.1777	1.2138
90	1.5708	.0707	1.5001	85 57	.1707	.0707	−.0707	1.0146	.1715	.0706	.9975	.0716	.1711	1.1717
100	1.7453	.0819	1.6634	95 18	.1574	.0574	−.0819	1.0124	.1581	−.0924	.9957	−.0935	.1574	1.1536
110	1.9199	.0906	1.8293	104 49	.1423	.0423	−.0906	1.0101	.1428	−.2857	.9568	−.2883	.1351	1.1756
125	2.1817	.0986	2.0832	119 22	.1174	.0174	−.0985	1.0069	.1177	−.4904	.8715	−.4938	.1028	1.2727
135	2.3562	.1000	2.2562	129 16	.1000	.0000	−.1000	1.0050	.1002	−.6329	.7742	−.6361	.0776	1.4038
150	2.6180	.0966	2.5214	144 28	.0741	−.0259	−.0966	1.0028	.0742	−.8138	.5812	−.8161	.0431	1.8306
160	2.7925	.0906	2.7019	154 48	.0577	−.0423	−.0906	1.0017	.0577	−.9048	.4268	−.9063	.0246	2.4584
170	2.9671	.0819	2.8852	165 19	.0426	−.0574	−.0819	1.0009	.0426	−.9673	.2538	−.9682	.0108	4.0496
180	3.1416	.0707	3.0709	175 57	.0293	−.0707	−.0707	1.0004	.0293	−.9975	.0706	−.9979	.0021	13.4411

LOWER SURFACE

0	0.0000	−0.0707	0.0707	4 3	0.1707	0.0707	.0707	1.0146	0.1715	0.9975	0.0706	1.0121	0.0121	6.3941
−5	−.0873	−.0766	−.0107	−0 37	.1643	.0643	.0766	1.0135	.1650	.9899	−.0103	1.0134	−.0018	7.1236
−10	−.1745	−.0819	−.0926	−5 18	.1574	.0574	.0819	1.0124	.1581	.9957	−.0924	1.0090	−.0146	6.3827
−15	−.2618	−.0856	−.1752	−10 2	.1500	.0500	.0866	1.0113	.1505	.9847	−.1742	.9958	−.0252	5.0338
−20	−.3491	−.0906	−.2585	−14 49	.1423	.0423	.0906	1.0101	.1428	.9668	−.2557	.9766	−.0365	3.9225
−25	−.4363	−.0940	−.3423	−19 37	.1342	.0342	.0940	1.0090	.1346	.9420	−.3357	.9503	−.0452	3.1489
−30	−.5236	−.0966	−.4270	−24 28	.1259	.0259	.0966	1.0079	.1262	.9102	−.4142	.9174	−.0523	2.6077
−35	−.6109	−.0985	−.5124	−29 21	.1174	.0174	.0985	1.0069	.1177	.8716	−.4901	.8776	−.0577	2.2203
−45	−.7854	−.1000	−.6854	−39 16	.1000	.0000	.1000	1.0050	.1002	.7742	−.6329	.7781	−.0634	1.7161
−55	−.9599	−.0985	−.8614	−49 21	.0826	−.0174	.0985	1.0034	.0827	.6614	−.7587	.6536	−.0627	1.4163
−70	−1.2217	−.0906	−1.1311	−64 48	.0577	−.0423	.0906	1.0017	.0577	.4268	−.9048	.4225	−.0522	1.1650
−80	−1.3963	−.0819	−1.3144	−75 19	.0426	−.0574	.0819	1.0009	.0426	.2535	−.9673	.2537	−.0412	1.0768
−90	−1.5708	−.0707	−1.5001	−85 57	.0293	−.0707	.0707	1.0004	.0293	.0706	−.9975	.0705	−.0292	1.0322
−100	−1.7453	−.0574	−1.6879	−96 43	.0181	−.0819	.0574	1.0002	.0181	−.1170	−.9931	−.1170	−.0180	1.0270
−110	−1.9199	−.0423	−1.8776	−107 3	.0094	−.0906	.0423	1.0000	.0094	−.3021	−.9533	−.3021	−.0090	1.0616
−125	−2.1817	−.0174	−2.1643	−124 1	.0015	−.0985	.0174	1.0000	.0015	−.5594	−.8289	−.5594	−.0012	1.2138
−135	−2.3562	.0000	−2.3562	−135 0	.0000	−.1000	.0000	1.0000	.0000	−.7071	−.7071	−.7071	.0000	1.4209
−150	−2.6180	.0259	−2.6439	−151 29	.0034	−.0966	−.0259	1.0000	.0034	−.8787	−.4774	−.8787	−.0018	2.1106
−160	−2.7925	.0423	−2.8348	−162 25	.0094	−.0906	−.0423	1.0000	.0094	−.9533	−.3021	−.9533	−.0028	3.3501
−170	−2.9671	.0574	−3.0245	−173 18	.0181	−.0819	−.0574	1.0002	.0181	−.9932	−.1167	−.9934	−.0021	8.6641
−180	−3.1416	.0707	−3.2123	−184 3	.0293	−.0707	−.0707	1.0004	.0293	−.9975	+.0706	−.9979	+.0021	13.4411

REPORT No. 496

GENERAL THEORY OF AERODYNAMIC INSTABILITY AND THE MECHANISM OF FLUTTER

By THEODORE THEODORSEN

SUMMARY

The aerodynamic forces on an oscillating airfoil or airfoil-aileron combination of three independent degrees of freedom have been determined. The problem resolves itself into the solution of certain definite integrals, which have been identified as Bessel functions of the first and second kind and of zero and first order. The theory, being based on potential flow and the Kutta condition, is fundamentally equivalent to the conventional wing-section theory relating to the steady case.

The air forces being known, the mechanism of aerodynamic instability has been analyzed in detail. An exact solution, involving potential flow and the adoption of the Kutta condition, has been arrived at. The solution is of a simple form and is expressed by means of an auxiliary parameter k. The mathematical treatment also provides a convenient cyclic arrangement permitting a uniform treatment of all subcases of two degrees of freedom. The flutter velocity, defined as the air velocity at which flutter starts, and which is treated as the unknown quantity, is determined as a function of a certain ratio of the frequencies in the separate degrees of freedom for any magnitudes and combinations of the airfoil-aileron parameters.

For those interested solely or particularly in the numerical solutions Appendix I has been prepared. The routine procedure in solving numerical examples is put down detached from the theoretical background of the paper. It first is necessary to determine a certain number of constants pertaining to the case, then to perform a few routine calculations as indicated. The result is readily obtained in the form of a plot of flutter velocity against frequency for any values of the other parameters chosen. The numerical work of calculating the constants is simplified by referring to a number of tables, which are included in Appendix I. A number of illustrative examples and experimental results are given in Appendix II.

INTRODUCTION

It has been known that a wing or wing-aileron structurally restrained to a certain position of equilibrium becomes unstable under certain conditions. At least two degrees of freedom are required to create a condition of instability, as it can be shown that vibrations of a single degree of freedom would be damped out by the air forces. The air forces, defined as the forces due to the air pressure acting on the wing or wing-aileron in an arbitrary oscillatory motion of several degrees of freedom, are in this paper treated on the basis of the theory of nonstationary potential flow. A wing-section theory and, by analogy, a wing theory shall be thus developed that applies to the case of oscillatory motion, not only of the wing as a whole but also to that of an aileron. It is of considerable importance that large oscillations may be neglected; in fact, only infinitely small oscillations about the position of equilibrium need be considered. Large oscillations are of no interest since the sole attempt is to specify one or more conditions of instability. Indeed, no particular type or shape of airfoil shall be of concern, the treatment being restricted to primary effects. The differential equations for the several degrees of freedom will be put down. Each of these equations contains a statement regarding the equilibrium of a system of forces. The forces are of three kinds: (1) The inertia forces, (2) the restraining forces, and (3) the air forces.

There is presumably no necessity of solving a general case of damped or divergent motion, but only the border case of a pure sinusoidal motion, applying to the case of unstable equilibrium. This restriction is particularly important as the expressions for the air force developed for oscillatory motion can thus be employed. Imagine a case that is unstable to a very slight degree; the amplitudes will then increase very slowly and the expressions developed for the air forces will be applicable. It is of interest simply to know under what circumstances this condition may obtain and cases in which the amplitudes are decreasing or increasing at a finite rate need not be treated or specified. Although it is possible to treat the latter cases, they are of no concern in the present problem. Nor is the internal or solid friction of the structure of primary concern. The fortunate situation exists that the effect of the solid friction is *favorable*. Knowledge is desired concerning the condition as existing in the absence of the internal friction, as this case constitutes a sort of lower limit, which it is not always desirable to exceed.

Owing to the rather extensive field covered in the paper it has been considered necessary to omit many elementary proofs, it being left to the reader to verify certain specific statements. In the first part of the paper, the velocity potentials due to the flow around the airfoil-aileron are developed. These potentials are treated in two classes: The noncirculating flow potentials, and those due to the surface of discontinuity behind the wing, referred to as "circulatory" potentials. The magnitude of the circulation for an oscillating wing-aileron is determined next. The

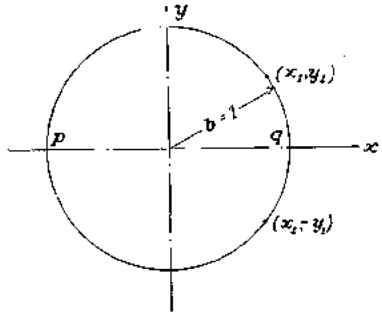

FIGURE 1.—Conformal representation of the wing profile by a circle.

forces and moments acting on the airfoil are then obtained by integration. In the latter part of the paper the differential equations of motion are put down and the particular and important case of unstable equilibrium is treated in detail. The solution of the problem of determining the flutter speed is finally given in the form of an equation expressing a relationship between the various parameters. The three subcases of two degrees of freedom are treated in detail.

The paper proposes to disclose the basic nature of the mechanism of flutter, leaving modifications of the primary results by secondary effects for future investigations.[1] Such secondary effects are: The effects of a finite span, of section shape, of deviations from potential flow, including also modifications of results to include twisting and bending of actual wing sections instead of pure torsion and deflection as considered in this paper.

The supplementary experimental work included in Appendix II similarly refers to well-defined elementary cases, the wing employed being of a large aspect ratio, nondeformable, and given definite degrees of freedom by a supporting mechanism, with external springs maintaining the equilibrium positions of wing or wing-aileron. The experimental work was carried on largely to verify the general shape of and the approximate magnitudes involved in the theoretically predicted response characteristics. As the present report is limited to the mathematical aspects of the flutter problem, specific recommendations in regard to practical applications are not given in this paper.

[1] The effect of internal friction is in some cases essential; this subject will be contained in a subsequent paper.

VELOCITY POTENTIALS, FORCES, AND MOMENTS OF THE NONCIRCULATORY FLOW

We shall proceed to calculate the various velocity potentials due to position and velocity of the individual parts in the whole of the wing-aileron system. Let us temporarily represent the wing by a circle (fig. 1). The potential of a source ϵ at the origin is given by

$$\varphi=\frac{\epsilon}{4\pi}\log\,(x^2+y^2)$$

For a source ϵ at (x_1,y_1) on the circle

$$\varphi=\frac{\epsilon}{4\pi}\log\,\{(x-x_1)^2+(y-y_1)^2\}$$

Putting a double source 2ϵ at (x_1,y_1) and a double negative source -2ϵ at $(x_1,-y_1)$ we obtain for the flow around the circle

$$\varphi=\frac{\epsilon}{2\pi}\log\,\frac{(x-x_1)^2+(y-y_1)^2}{(x-x_1)^2+(y+y_1)^2}$$

The function φ on the circle gives directly the surface potential of a straight line pq, the projection of the circle on the horizontal diameter. (See fig. 1.) In this case $y=\sqrt{1-x^2}$ and φ is a function of x only.

We shall need the integrals:

$$\int_c^1\log\frac{(x-x_1)^2+(y-y_1)^2}{(x-x_1)^2+(y+y_1)^2}dx_1=2(x-c)\log N-2\sqrt{1-x^2}\cos^{-1}c$$

and

$$\int_c^1\log\frac{(x-x_1)^2+(y-y_1)^2}{(x-x_1)^2+(y+y_1)^2}(x_1-c)dx_1=-\sqrt{1-c^2}\sqrt{1-x^2}-\cos^{-1}c(x-2c)\sqrt{1-x^2}+(x-c)^2\log N$$

where $$N=\frac{1-cx-\sqrt{1-x^2}\sqrt{1-c^2}}{x-c}$$

The location of the center of gravity of the wing-aileron x_α is measured from a, the coordinate of the axis of rotation (fig. 2); x_β the location of the center

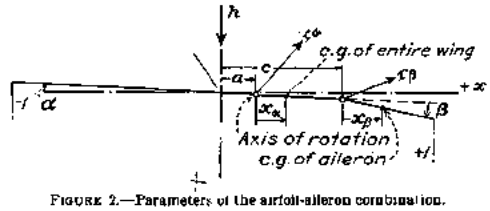

FIGURE 2.—Parameters of the airfoil-aileron combination.

of gravity of the aileron is measured from c, the coordinate of the hinge; and r_α and r_β are the radii of gyration of the wing-aileron referred to a, and of the aileron referred to the hinge. The quantities x_β and r_β are "reduced" values, as defined later in the paper. The quantities a, x_α, c, and x_β are positive toward the rear (right), h is the vertical coordinate of the axis of rotation at a with respect to a fixed reference frame and is positive downward. The angles α and β are positive clockwise (right-hand turn). The wind velocity v is to

the right and horizontal. The angle (of attack) α refers to the direction of v, the aileron angle β refers to the undeflected position and *not* to the wind direction. The quantities r_α and r_β always occur as squares. Observe that the leading edge is located at -1, the trailing edge at $+1$. The quantities a, c, x_α, x_β, r_α, and r_β, which are repeatedly used in the following treatment, are all dimensionless with the half chord b as reference unit.

The effect of a flap bent down at an angle β (see fig. 2) is seen to give rise to a function φ obtained by substituting $-v\beta b$ for ϵ; hence

$$\varphi_\beta = \frac{v\beta b}{\pi}[\sqrt{1-x^2}\cos^{-1}c - (x-c)\log N]$$

To obtain the effect of the flap going down at an angular velocity $\dot\beta$, we put $\epsilon = -(x_1-c)\dot\beta b^2$ and get

$$\varphi_{\dot\beta} = \frac{\dot\beta b^2}{2\pi}[\sqrt{1-c^2}\sqrt{1-x^2} + \cos^{-1}c(x-2c)\sqrt{1-x^2} - (x-c)^2\log N]$$

To obtain the effect of an angle α of the entire airfoil, we put $c=-1$ in the expression for φ_β, hence

$$\varphi_\alpha = v\alpha b\sqrt{1-x^2}$$

To depict the airfoil in downward motion with a velocity $\dot h$ (+ down), we need only introduce $\frac{\dot h}{v}$ instead of α. Thus

$$\varphi_{\dot h} = \dot h b\sqrt{1-x^2}$$

Finally, to describe a rotation around point a at an angular velocity $\dot\alpha$, we notice that this motion may be taken to consist of a rotation around the leading edge $c=-1$ at an angular velocity $\dot\alpha$ plus a vertical motion with a velocity $-\dot\alpha(1+a)b$. Then

$$\varphi_{\dot\alpha} = \frac{\dot\alpha b^2}{2\pi}\pi(x+2)\sqrt{1-x^2} - \dot\alpha(1+a)b^2\sqrt{1-x^2} = \dot\alpha b^2\left(\frac{1}{2}x - a\right)\sqrt{1-x^2}$$

The following tables give in succession the velocity potentials and a set of integrals [2] with associated constants, which we will need in the calculation of the air forces and moments.

VELOCITY POTENTIALS

$$\varphi_\alpha = v\alpha b\sqrt{1-x^2}$$

$$\varphi_{\dot h} = \dot h b\sqrt{1-x^2}$$

$$\varphi_{\dot\alpha} = \dot\alpha b^2\left(\frac{1}{2}x - a\right)\sqrt{1-x^2}$$

$$\varphi_\beta = \frac{1}{\pi}v\beta b[\sqrt{1-x^2}\cos^{-1}c - (x-c)\log N]$$

$$\varphi_{\dot\beta} = \frac{1}{2\pi}\dot\beta b^2[\sqrt{1-c^2}\sqrt{1-x^2} + (x-2c)\sqrt{1-x^2}\cos^{-1}c - (x-c)^2\log N]$$

where $$N = \frac{1-cx-\sqrt{1-x^2}\sqrt{1-c^2}}{x-c}$$

[2] Some of the more difficult integral evaluations are given in Appendix III.

INTEGRALS

$$\int_c^1 \varphi_\alpha dx = -\frac{b}{2}v\alpha T_4 \qquad \int_{-1}^{+1} \varphi_\alpha dx = \frac{b}{2}v\alpha\pi$$

$$\int_c^1 \varphi_{\dot h} dx = -\frac{b}{2}\dot h T_4 \qquad \int_{-1}^{+1} \varphi_{\dot h} dx = \frac{b}{2}\dot h\pi$$

$$\int_c^1 \varphi_{\dot\alpha} dx = \dot\alpha b^2 T_9 \qquad \int_{-1}^{+1} \varphi_{\dot\alpha} dx = -\dot\alpha b^2\frac{\pi a}{2}$$

$$\int_c^1 \varphi_\beta dx = -\frac{b}{2\pi}v\beta T_5 \qquad \int_{-1}^{+1} \varphi_\beta dx = -\frac{b}{2}v\beta T_4$$

$$\int_c^1 \varphi_{\dot\beta} dx = -\frac{b^2}{2\pi}\dot\beta T_2 \qquad \int_{-1}^{+1} \varphi_{\dot\beta} dx = -\frac{b^2}{2}\dot\beta T_1$$

$$\int_c^1 \varphi_\alpha(x-c)dx = -\frac{b}{2}v\alpha T_1 \qquad \int_{-1}^{+1} \varphi_\alpha(x-c)dx = -\frac{b}{2}v\alpha c\pi$$

$$\int_c^1 \varphi_{\dot h}(x-c)dx = -\frac{b}{2}\dot h T_1 \qquad \int_{-1}^{+1} \varphi_{\dot h}(x-c)dx = -\frac{b}{2}\dot h c\pi$$

$$\int_c^1 \varphi_{\dot\alpha}(x-c)dx = \dot\alpha b^2 T_{13} \qquad \int_{-1}^{+1} \varphi_{\dot\alpha}(x-c)dx = \dot\alpha b^2 T_{14}\pi$$

$$\int_c^1 \varphi_\beta(x-c)dx = -\frac{b}{2\pi}v\beta T_2 \qquad \int_{-1}^{+1} \varphi_\beta(x-c)dx = -\frac{b}{2}v\beta T_3$$

$$\int_c^1 \varphi_{\dot\beta}(x-c)dx = -\frac{b^2}{2\pi}\dot\beta T_3 \qquad \int_{-1}^{+1} \varphi_{\dot\beta}(x-c)dx = -\frac{b^2}{2}\dot\beta T_7$$

CONSTANTS

$$T_1 = -\frac{1}{3}\sqrt{1-c^2}(2+c^2) + c\cos^{-1}c$$

$$T_2 = c(1-c^2) - \sqrt{1-c^2}(1+c^2)\cos^{-1}c + c(\cos^{-1}c)^2$$

$$T_3 = -\left(\frac{1}{8}+c^2\right)(\cos^{-1}c)^2 + \frac{1}{4}c\sqrt{1-c^2}\cos^{-1}c(7+2c^2) - \frac{1}{8}(1-c^2)(5c^2+4)$$

$$T_4 = -\cos^{-1}c + c\sqrt{1-c^2}$$

$$T_5 = -(1-c^2) - (\cos^{-1}c)^2 + 2c\sqrt{1-c^2}\cos^{-1}c$$

$$T_6 = T_2$$

$$T_7 = -\left(\frac{1}{8}+c^2\right)\cos^{-1}c + \frac{1}{8}c\sqrt{1-c^2}(7+2c^2)$$

$$T_8 = -\frac{1}{3}\sqrt{1-c^2}(2c^2+1) + c\cos^{-1}c$$

$$T_9 = \frac{1}{2}\left[\frac{1}{3}\left(\sqrt{1-c^2}\right)^3 + aT_4\right] = \frac{1}{2}(-p + aT_4)$$

where $$p = -\frac{1}{3}\left(\sqrt{1-c^2}\right)^3$$

$$T_{10} = \sqrt{1-c^2} + \cos^{-1}c$$

$$T_{11} = \cos^{-1}c\,(1-2c) + \sqrt{1-c^2}\,(2-c)$$

$$T_{12} = \sqrt{1-c^2}\,(2+c) - \cos^{-1}c\,(2c+1)$$

$$T_{13} = \frac{1}{2}[-T_7 - (c-a)T_1]$$

$$T_{14} = \frac{1}{16} + \frac{1}{2}ac$$

FORCES AND MOMENTS

The velocity potentials being known, we are able to calculate local pressures and by integration to obtain the forces and moments acting on the airfoil and aileron.

Employing the extended Bernoulli Theorem for unsteady flow, the local pressure is, except for a constant

$$p_h = -\rho\left(\frac{w^2}{2}+\frac{\partial\varphi}{\partial t}\right)$$

where w is the local velocity and φ the velocity potential at the point. Substituting $w = v+\frac{\partial\varphi}{\partial x}$ we obtain ultimately for the pressure difference between the upper and lower surface at x

$$p = -2\rho\left(v\frac{\partial\varphi}{\partial x}+\frac{\partial\varphi}{\partial t}\right)$$

where v is the constant velocity of the fluid relative to the airfoil at infinity. Putting down the integrals for the force on the entire airfoil, the moment on the flap

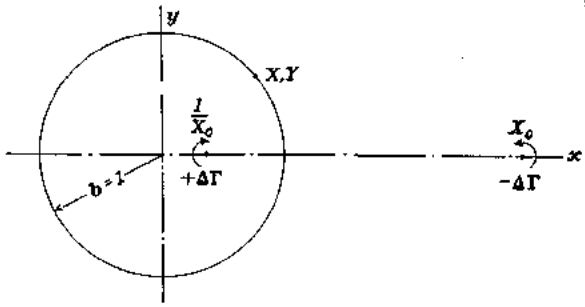

FIGURE 3.—Conformal representation of the wing profile with reference to the circulatory flow.

around the hinge, and the moment on the entire airfoil, we obtain by means of partial integrations

$$P = -2\rho b\int_{-1}^{+1}\dot{\varphi}\,dx$$

$$M_\beta = -.\ b^2\int_c^1\dot{\varphi}(x-c)\,dx+2\rho vb\int_c^1\varphi dx$$

$$M_\alpha = -2\rho b^2\int_{-1}^{+1}\dot{\varphi}\,(x-c)\,dx+2\rho vb\int_{-1}^{+1}\varphi dx$$
$$-2\rho b^2\int_{-1}^{+1}\dot{\varphi}\,(c-a)\,dx$$

Or, on introducing the individual velocity potentials from page 5,

$$P = -\rho b^2[v\pi\dot{\alpha}+\pi\ddot{h}-b\pi a\ddot{\alpha}-vT_4\dot{\beta}-bT_1\ddot{\beta}] \qquad (I)$$

$$M_\beta = -\rho b^3\left[-vT_1\dot{\alpha}-T_1\dot{h}+2T_{13}b\ddot{\alpha}-\frac{1}{\pi}vT_2\dot{\beta}-\frac{1}{\pi}T_8b\ddot{\beta}\right]$$
$$+\rho vb^2\left[-vT_4\alpha-T_4\dot{h}+2T_9b\dot{\alpha}-\frac{1}{\pi}vT_5\beta-\frac{1}{\pi}T_2b\dot{\beta}\right]$$
$$=-\rho b^2\left[T_4v^2\alpha-(2T_9+T_1)bv\dot{\alpha}+2T_{13}b^2\ddot{\alpha}+\frac{1}{\pi}T_5v^2\beta\right.$$
$$\left.+\left(\frac{1}{\pi}T_2-\frac{1}{\pi}T_2\right)bv\dot{\beta}-\frac{1}{\pi}b^2T_9\ddot{\beta}+T_4v\dot{h}-T_1b\ddot{h}\right] \qquad (II)$$

$$M_\alpha = -\rho b^2\left[-\pi v^2\alpha+\pi\left(\frac{1}{8}+a^2\right)b^2\ddot{\alpha}+vT_4\beta+\{T_1^{\dagger}-T_{\cdot}\right.$$
$$-(c-a)\,T_4\}b\dot{\beta}v+\{-T_7-(c-a)\,{}^{\cdot}{}_{\cdot}\}b^2\ddot{\beta}$$
$$\left.-ba\pi\ddot{h}-\pi v\dot{h}\right] \qquad (III)$$

VELOCITY POTENTIALS, FORCES, AND MOMENTS OF THE CIRCULATORY FLOW

In the following we shall determine the velocity potentials and associated forces and moments due to a surface of discontinuity of strength U extending along the positive x axis from the wing to infinity. The velocity potential of the flow around the circle (fig. 3) resulting from the vortex element $-\Delta\Gamma$ at $(X_0, 0)$ is

$$\varphi_\Gamma = \frac{\Delta\Gamma}{2\pi}\left[\tan^{-1}\frac{Y}{X-X_0}-\tan^{-1}\frac{Y}{X-\frac{1}{X_0}}\right]$$
$$=\frac{\Delta\Gamma}{2\pi}\tan^{-1}\frac{\left(-\frac{1}{X_0}+X_0\right)Y}{X^2-\left(X_0+\frac{1}{X_0}\right)X+Y^2+1}$$

where (X, Y) are the coordinates of the variable and X_0 is the coordinate of $-\Delta\Gamma$ on the x axis.

Introducing $X_0+\frac{1}{X_0}=2x_0$

or $X_0 = x_0+\sqrt{x_0^2-1}$ on the x axis

and $X=x$ and $Y=\sqrt{1-x^2}$ on the circle

the equation becomes

$$\varphi_{xx_0} = -\frac{\Delta\Gamma}{2\pi}\tan^{-1}\frac{\sqrt{1-x^2}\sqrt{x_0^2-1}}{1-xx_0}$$

This expression gives the clockwise circulation around the airfoil due to the element $-\Delta\Gamma$ at x_0.

We have: $p = -2\rho\left(\frac{\partial\varphi}{\partial t}+v\frac{\partial\varphi}{\partial x}\right)$

But, since the element $-\Delta\Gamma$ will now be regarded as moving to the right relative to the airfoil with a velocity v

$$\frac{\partial\varphi}{\partial t} = \frac{\partial\varphi}{\partial x_0}v$$

Hence, $p = -2\rho v\left(\frac{\partial\varphi}{\partial x}+\frac{\partial\varphi}{\partial x_0}\right)$

Further

$$\frac{2\pi}{\Delta\Gamma}\frac{\partial\varphi}{\partial x} = \sqrt{x_0^2-1}\,\frac{\frac{x}{(1-xx_0)\sqrt{1-x^2}}+\frac{x_0\sqrt{1-x^2}}{(1-xx_0)^2}}{1+\frac{(1-x^2)(x_0^2-1)}{(1-xx_0)^2}}$$
$$=\frac{\sqrt{x_0^2-1}}{\sqrt{1-x^2}}\frac{1}{(x_0-x)}$$

and

$$\frac{2\pi}{\Delta\Gamma}\frac{\partial\varphi}{\partial x_0} = \sqrt{1-x^2}\,\frac{\frac{1}{(1-xx_0)}\frac{x_0}{\sqrt{x_0^2-1}}+\sqrt{x_0^2-1}\frac{x}{(1-xx_0)^2}}{1+\frac{(1-x^2)(x_0^2-1)}{(1-xx_0)^2}}$$
$$=\frac{\sqrt{1-x^2}}{\sqrt{x_0^2-1}}\frac{1}{(x_0-x)}$$

By addition:

$$\frac{\partial\varphi}{\partial x}+\frac{\partial\varphi}{\partial x_0} = \frac{\Delta\Gamma}{2\pi}\frac{x_0+x}{\sqrt{1-x^2}\sqrt{x_0^2-1}}$$

To obtain the force on the aileron, we need the integral

$$\int_c^1\left(\frac{\partial\varphi}{\partial x}+\frac{\partial\varphi}{\partial x_0}\right)dx=\frac{\Delta\Gamma}{2\pi}\int_c^1\frac{x_0+x}{\sqrt{x_0^2-1}\sqrt{1-x^2}}dx$$
$$=-\frac{\Delta\Gamma}{2\pi}\left[\frac{x_0}{\sqrt{x_0^2-1}}\cos^{-1}x+\frac{\sqrt{1-x^2}}{\sqrt{x_0^2-1}}\right]_c^1$$
$$=\frac{\Delta\Gamma}{2\pi}\left[\frac{x_0}{\sqrt{x_0^2-1}}\cos^{-1}c+\frac{\sqrt{1-c^2}}{\sqrt{x_0^2-1}}\right]$$

Thus, for the force on the aileron

$$\Delta P_{c1}=-\rho vb\frac{\Delta\Gamma}{\pi}\left(\frac{x_0}{\sqrt{x_0^2-1}}\cos^{-1}c+\frac{1}{\sqrt{x_0^2-1}}\sqrt{1-c^2}\right)\text{ or}$$

$$\Delta P_{c1}=-\rho vb\frac{\Delta\Gamma}{\pi}\left[\frac{x_0}{\sqrt{x_0^2-1}}\left(\cos^{-1}c-\sqrt{1-c^2}\right)\right.$$
$$\left.+\sqrt{\frac{x_0+1}{x_0-1}}\sqrt{1-c^2}\right]$$

Integrated, with $\Delta\Gamma=U\mathrm{d}x_0$

$$P_{c1}=-\frac{\rho vb}{\pi}\left[\left(\cos^{-1}c-\sqrt{1-c^2}\right)\int_1^\infty\frac{x_0}{\sqrt{x_0^2-1}}U\mathrm{d}x_0\right.$$
$$\left.+\sqrt{1-c^2}\int_1^\infty\sqrt{\frac{x_0+1}{x_0-1}}U\mathrm{d}x_0\right]$$

for $c=-1$ we obtain the expression for P, the force on the *whole* airfoil

$$P=-\rho vb\int_1^\infty\frac{x_0}{\sqrt{x_0^2-1}}U\mathrm{d}x_0 \qquad \text{(IV)}$$

Since U is considered stationary with respect to the fluid elements

$$U=\mathrm{f}(vt-x_0)$$

where t is the time since the beginning of the motion. U is thus a function of the *distance* from the location of the *first* vortex element or, referred to a system moving with the fluid, U is *stationary* in value.

Similarly we obtain for the moment on the *aileron*

$$\int_c^1\left(\frac{\partial\varphi}{\partial x}+\frac{\partial\varphi}{\partial x_0}\right)(x-c)dx=\frac{\Delta\Gamma}{2\pi}\int_c^1\frac{(x-c)\ (x_0+x)}{\sqrt{1-x^2}\sqrt{x_0^2-1}}dx$$
$$=-\frac{\Delta\Gamma}{2\pi}\frac{1}{\sqrt{x_0^2-1}}\left[x_0\sqrt{1-x^2}+\frac{x\sqrt{1-x^2}}{2}-c\sqrt{1-x^2}\right.$$
$$\left.+\left(\frac{1}{2}-x_0c\right)\cos^{-1}x\right]_c^1$$
$$=+\frac{\Delta\Gamma}{2\pi}\frac{1}{\sqrt{x_0^2-1}}\left[(x_0+\frac{c}{2}-c)\sqrt{1-c^2}\right.$$
$$\left.+\frac{1}{2}\left(1-2x_0c\right)\cos^{-1}c\right]$$
$$=+\frac{\Delta\Gamma}{2\pi}\left[\frac{x_0}{\sqrt{x_0^2-1}}\left(\sqrt{1-c^2}-c\cos^{-1}c\right)\right.$$
$$\left.+\frac{\frac{1}{2}}{\sqrt{x_0^2-1}}\left(\cos^{-1}c-c\sqrt{1-c^2}\right)\right]$$

Finally

$$\Delta M_\beta=-\rho vb^2\frac{\Delta\Gamma}{\pi}\left[\frac{x_0}{\sqrt{x_0^2-1}}\left\{\sqrt{1-c^2}\left(1+\frac{c}{2}\right)\right.\right.$$
$$\left.\left.-\cos^{-1}c\left(c+\frac{1}{2}\right)\right\}+\frac{1}{2}\sqrt{\frac{x_0+1}{x_0-1}}\left(\cos^{-1}c-c\sqrt{1-c^2}\right)\right]$$

Putting $\Delta\Gamma=U\mathrm{d}x_0$ and integrating

$$M_\beta=-\frac{\rho vb^2}{\pi}\left[\left\{\sqrt{1-c^2}\left(1+\frac{c}{2}\right)\right.\right.$$
$$\left.\left.-\cos^{-1}c\left(c+\frac{1}{2}\right)\right\}\int_1^\infty\frac{x_0}{\sqrt{x_0^2-1}}U\mathrm{d}x_0\right.$$
$$\left.+\left(\cos^{-1}c-c\sqrt{(1-c^2)}\right)\frac{1}{2}\int_1^\infty\sqrt{\frac{x_0+1}{x_0-1}}U\mathrm{d}x_0\right] \qquad \text{(V)}$$

Further, for the moment on the entire airfoil around a

$$\int_{-1}^{+1}\left(\frac{\partial\varphi}{\partial x}+\frac{\partial\varphi}{\partial x_0}\right)(x-a)dx=-\frac{\Delta\Gamma}{2\pi}\frac{1}{\sqrt{x_0^2-1}}\left[\left(x_0+\frac{x}{2}-a\right)\sqrt{1-x^2}\right.$$
$$\left.+\left(\frac{1}{2}-x_0a\right)\cos^{-1}x\right]_{-1}^{+1}=+\frac{\Delta\Gamma}{2\pi}\frac{1}{\sqrt{x_0^2-1}}\left(\frac{1}{2}-x_0a\right)\pi$$

and
$$\Delta M_\alpha=-\rho vb^2\Delta\Gamma\frac{\frac{1}{2}-x_0a}{\sqrt{x_0^2-1}}$$

Integrated, this becomes

$$M_\alpha=-\rho vb^2\int_1^\infty\frac{\frac{1}{2}-x_0a}{\sqrt{x_0^2-1}}U\mathrm{d}x_0$$
$$=-\rho vb^2\int_1^\infty\left\{\frac{\frac{1}{2}+\frac{1}{2}x_0}{\sqrt{x_0^2-1}}-\frac{x_0\left(a+\frac{1}{2}\right)}{\sqrt{x_0^2-1}}\right\}U\mathrm{d}x_0$$
$$=-\rho vb^2\int_1^\infty\left\{\frac{1}{2}\sqrt{\frac{x_0+1}{x_0-1}}-\left(a+\frac{1}{2}\right)\frac{x_0}{\sqrt{x_0^2-1}}\right\}U\mathrm{d}x_0 \qquad \text{(VI)}$$

THE MAGNITUDE OF THE CIRCULATION

The magnitude of the circulation is determined by the Kutta condition, which requires that no infinite velocities exist at the trailing edge,
or, at $x=1$

$$\frac{\partial}{\partial x}(\varphi_\Gamma+\varphi_a+\varphi_{\dot h}+\varphi_{\dot\alpha}+\varphi_\beta+\varphi_{\dot\beta})=\text{finite}$$

Introducing the values of φ_a, etc. from page 5 and φ_Γ from $\frac{\partial\varphi}{\partial x}$ page 6 gives the important relation:

$$\frac{1}{2\pi}\int_1^\infty\frac{\sqrt{x_0+1}}{\sqrt{x_0-1}}U\mathrm{d}x_0=v\alpha+\dot h+b\left(\frac{1}{2}-a\right)\dot\alpha$$
$$+\frac{T_{10}}{\pi}v\beta+b\frac{T_{11}}{2\pi}\dot\beta \qquad \text{(VII)}$$

This relation must be satisfied to comply with the Kutta condition, which states that the flow shall leave the airfoil at the trailing edge.

It is observed that the relation reduces to that of the Kutta condition for stationary flow on putting $x_0=\infty$,

and in subsequence omitting the variable parameters $\dot{\alpha}$, $\dot{\beta}$, and $\dot{h}$.

Let us write

$$\frac{1}{2\pi}\int_1^\infty \sqrt{\frac{x_0+1}{x_0-1}}\,U\mathrm{d}x_0 = v\alpha + \dot{h} + b\left(\frac{1}{2}-a\right)\dot{\alpha} + \frac{T_{10}}{\pi}v\beta + b\frac{T_{11}}{2\pi}\dot{\beta} = Q$$

Introduced in (IV)

$$P = -2\pi\rho v b Q\,\frac{\int_1^\infty \frac{x_0}{\sqrt{x_0^2-1}}U\mathrm{d}x_0}{\int_1^\infty \sqrt{\frac{x_0+1}{x_0-1}}U\mathrm{d}x_0}$$

from (V)

$$M_\beta = -2\rho v b^2\left[\left(\sqrt{1-c^2}\left(1+\frac{c}{2}\right)-\cos^{-1}c\left(c+\frac{1}{2}\right)\right)\times \frac{\int_1^\infty \frac{x_0}{\sqrt{x_0^2-1}}U\mathrm{d}x_0}{\int_1^\infty \sqrt{\frac{x_0+1}{x_0-1}}U\mathrm{d}x_0} + \frac{1}{2}\left(\cos^{-1}c - c\sqrt{1-c^2}\right)\right]Q$$

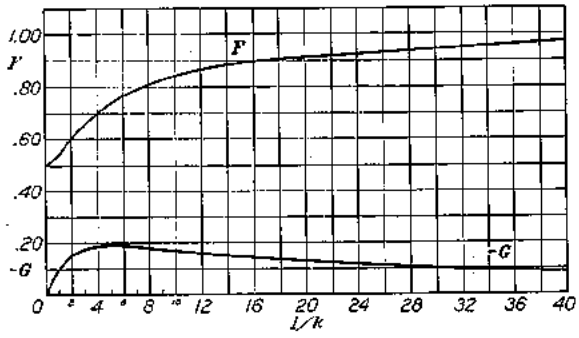

FIGURE 4.—The functions F and G against $\frac{1}{k}$.

and from (VI)

$$M_\alpha = -2\pi\rho v b^2\left[\frac{1}{2}-\left(a+\frac{1}{2}\right)\frac{\int_1^\infty \frac{x_0}{\sqrt{x_0^2-1}}U\mathrm{d}x_0}{\int_1^\infty \sqrt{\frac{x_0+1}{x_0-1}}U\mathrm{d}x_0}\right]Q$$

Introducing

$$C = \frac{\int_1^\infty \frac{x_0}{\sqrt{x_0^2-1}}U\mathrm{d}x_0}{\int_1^\infty \sqrt{\frac{x_0+1}{x_0-1}}U\mathrm{d}x_0}$$

we obtain finally

$$P = -2\rho v b\pi C Q \qquad \text{(VIII)}$$

$$M_\beta = -2\rho v b^2\left[\left(\sqrt{1-c^2}\left(1+\frac{c}{2}\right)-\cos^{-1}c\left(c+\frac{1}{2}\right)\right)C + \frac{1}{2}\left(\cos^{-1}c - c\sqrt{1-c^2}\right)\right]Q = -\rho v b^2(T_{12}C - T_4)Q \qquad \text{(IX)}$$

$$M_\alpha = 2\pi\rho v b^2\left[\left(a+\frac{1}{2}\right)C - \frac{1}{2}\right]Q \qquad \text{(X)}$$

where Q is given above and $C = C(k)$ will be treated in the following section.

VALUE OF THE FUNCTION $C(k)$

Put $U = U_0 e^{i\left[k\left(\frac{s}{b}-x_0\right)+\varphi\right]}$

where $s = vt$ $(s \to \infty)$, the distance from the *first* vortex element to the airfoil, and k a positive constant determining the wave length,

then

$$C(k) = \frac{\int_1^\infty \frac{x_0}{\sqrt{x_0^2-1}}e^{-ikx_0}\mathrm{d}x_0}{\int_1^\infty \frac{x_0+1}{\sqrt{x_0^2-1}}e^{-ikx_0}\mathrm{d}x_0}. \qquad \text{(XI)}$$

These integrals are known, see next part, formulas (XIV)—(XVII) and we obtain [3]

$$C(k) = \frac{-\frac{\pi}{2}J_1 + i\frac{\pi}{2}Y_1}{-\frac{\pi}{2}J_1 - \frac{\pi}{2}Y_0 + i\frac{\pi}{2}Y_1 - i\frac{\pi}{2}J_0} = \frac{-J_1+iY_1}{-(J_1+Y_0)+i(Y_1-J_0)}$$

$$= \frac{(-J_1+iY_1)[-(J_1+Y_0)-i(Y_1-J_0)]}{(J_1+Y_0)^2+(Y_1-J_0)^2}$$

$$= \frac{J_1(J_1+Y_0)+Y_1(Y_1-J_0)}{(J_1+Y_0)^2+(Y_1-J_0)^2}$$

$$-i\frac{Y_1(J_1+Y_0)-J_1(Y_1-J_0)}{(J_1+Y_0)^2+(Y_1-J_0)^2} = F + iG$$

where

$$F = \frac{J_1(J_1+Y_0)+Y_1(Y_1-J_0)}{(J_1+Y_0)^2+(Y_1-J_0)^2} \qquad \text{(XII)}$$

$$G = -\frac{Y_1Y_0+J_1J_0}{(J_1+Y_0)^2+(Y_1-J_0)^2} \qquad \text{(XIII)}$$

These functions, which are of fundamental importance in the theory of the oscillating airfoil are given graphically against the argument $\frac{1}{k}$ in figure 4.

SOLUTION OF THE DEFINITE INTEGRALS IN C BY MEANS OF BESSEL FUNCTIONS

We have

$$K_n(z) = \int_0^\infty e^{-z\cosh t}\cosh nt\,\mathrm{d}t$$

(Formula (34), p. 51—Gray, Mathews & MacRobert: Treatise on Bessel Functions. London, 1922)

where

$$K_n(t) = e^{\frac{in\pi}{2}}G_n(it)$$

(Eq. (28), sec. 3, p. 23, same reference)

and

$$G_n(x) = -\overline{Y_n}(x) + \left[\log 2 - \gamma + \frac{i\pi}{2}\right]J_n(x)$$

but

$$\overline{Y_n}(x) = \frac{\pi}{2}Y_n(x) + (\log 2 - \gamma)J_n(x)$$

(where $Y_n(x)$ is from N. Nielsen: Handbuch der Theorie der Cylinderfunktionen. Leipzig, 1904).

[3] This may also be expressed in Hänkel functions. $C = \frac{H_1^{(2)}}{H_1^{(2)}+iH_0^{(2)}}$

Thus,

$$G_n(x) = -\frac{\pi}{2}[Y_n(x) - iJ_n(x)]$$

We have

$$K_0(-ik) = \int_0^\infty e^{ik\cosh t}\,dt = \int_1^\infty \frac{e^{ikx}}{\sqrt{x^2-1}}\,dx$$

or

$$-\frac{\pi}{2}Y_0(k) + i\frac{\pi}{2}J_0(k) = \int_1^\infty \frac{\cos kx\,dx}{\sqrt{x^2-1}} + i\int_1^\infty \frac{\sin kx\,dx}{\sqrt{x^2-1}}$$

Thus,

$$\int_1^\infty \frac{\cos kx\,dx}{\sqrt{x^2-1}} = -\frac{\pi}{2}Y_0(k) \qquad \text{(XIV)}$$

$$\int_1^\infty \frac{\sin kx\,dx}{\sqrt{x^2-1}} = \frac{\pi}{2}J_0(k) \qquad \text{(XV)}$$

Further,

$$K_1(-ik) = \int_0^\infty e^{ik\cosh t}\cosh t\,dt = \int_1^\infty \frac{e^{kx}\,x\,dx}{\sqrt{x^2-1}}$$

$$iG_1(k) = -i\frac{\pi}{2}Y_1(k) - \frac{\pi}{2}J_1(k)$$

$$= \int_1^\infty \frac{x}{\sqrt{x^2-1}}(\cos kx + i\sin kx)\,dx$$

Thus,

$$\int_1^\infty \frac{x\cos kx\,dx}{\sqrt{x^2-1}} = -\frac{\pi}{2}J_1(k) \qquad \text{(XVI)}$$

$$\int_1^\infty \frac{x\sin kx\,dx}{\sqrt{x^2-1}} = -\frac{\pi}{2}Y_1(k) \qquad \text{(XVII)}$$

TOTAL AERODYNAMIC FORCES AND MOMENTS

TOTAL FORCE

From equations (I) and (VIII) we obtain

$$P = -\rho b^2(v\pi\dot\alpha + \pi\ddot h - \pi ba\ddot\alpha - vT_4\dot\beta - T_1b\ddot\beta)$$
$$-2\pi\rho vbC\left\{v\alpha + \dot h + b\left(\frac12 - a\right)\dot\alpha + \frac{1}{\pi}T_{10}v\beta + b\frac{1}{2\pi}T_{11}\dot\beta\right\} \qquad \text{(XVIII)}$$

TOTAL MOMENTS

From equations (II) and (IX) we obtain similarly

$$M_\beta = -\rho b^2\left[\left\{-2T_3 - T_1 + T_4\left(a - \frac12\right)\right\}vb\dot\alpha + 2T_{13}b^2\ddot\alpha + \frac{1}{\pi}v^2\beta(T_5 - T_4T_{10}) - \frac{1}{2\pi}vb\dot\beta T_4T_{11} - \frac{1}{\pi}T_3b^2\ddot\beta - T_1b\ddot h\right] - \rho vb^2T_{12}C\left\{v\alpha + \dot h + b\left(\frac12 - a\right)\dot\alpha + \frac{1}{\pi}T_{10}v\beta + b\frac{1}{2\pi}T_{11}\dot\beta\right\} \qquad \text{(XIX)}$$

From equations (III) and (X)

$$M_\alpha = -\rho b^2\left[\pi\left(\frac12 - a\right)vb\dot\alpha + \pi b^2\left(\frac18 + a^2\right)\ddot\alpha + (T_4 + T_{10})v^2\beta + \left(T_1 - T_8 - (c-a)T_4 + \frac12T_{11}\right)vb\dot\beta - \left(T_7 + (c-a)T_1\right)b^2\ddot\beta - a\pi b\ddot h\right] + 2\rho vb^2\pi\left(a + \frac12\right)C\left\{v\alpha + \dot h + b\left(\frac12 - a\right)\dot\alpha + \frac{1}{\pi}T_{10}v\beta + b\frac{1}{2\pi}T_{11}\dot\beta\right\} \qquad \text{(XX)}$$

DIFFERENTIAL EQUATIONS OF MOTION

Expressing the equilibrium of the moments about a of the entire airfoil, of the moments on the aileron about c, and of the vertical forces, we obtain, respectively, the following three equations:

α: $\quad -I_\alpha\ddot\alpha - I_\beta\ddot\beta - b(c-a)S_\beta\ddot\beta - S_\alpha\ddot h - \alpha C_\alpha + M_\alpha = 0$

β: $\quad -I_\beta\ddot\beta - I_\beta\ddot\alpha - b(c-a)\ddot\alpha S_\beta - \ddot hS_\beta - \beta C_\beta + M_\beta = 0$

h: $\quad -\ddot hM - \ddot\alpha S_\alpha - \ddot\beta S_\beta - hC_h + P = 0$

Rearranged:

α: $\quad \ddot\alpha I_\alpha + \ddot\beta(I_\beta + b(c-a)S_\beta) + \ddot hS_\alpha + \alpha C_\alpha - M_\alpha = 0$

β: $\quad \ddot\alpha(I_\beta + b(c-a)S_\beta) + \ddot\beta I_\beta + \ddot hS_\beta + \beta C_\beta - M_\beta = 0$

h: $\quad \ddot\alpha S_\alpha + \ddot\beta S_\beta + \ddot hM + hC_h - P = 0$

The constants are defined as follows:

ρ,	mass of air per unit of volume.
b,	half chord of wing.
M,	mass of wing per unit of length.
S_α, S_β,	static moments of wing (in slugs-feet) per unit length of wing-aileron and aileron, respectively. The former is referred to the axis a; the latter, to the hinge c.
I_α, I_β,	moments of inertia per unit length of wing-aileron and aileron about a and c, respectively.
C_α,	torsional stiffness of wing around a, corresponding to unit length.
C_β,	torsional stiffness of aileron around c, corresponding to unit length.
C_h,	stiffness of wing in deflection, corresponding to unit length.

DEFINITION OF PARAMETERS USED IN EQUATIONS

$\kappa = \frac{\pi\rho b^2}{M}$,	the ratio of the mass of a cylinder of air of a diameter equal to the chord of the wing to the mass of the wing, both taken for equal length along span.

$r_\alpha = \sqrt{\frac{I_\alpha}{Mb^2}}$, the radius of gyration divided by b.

$x_\alpha = \frac{S_\alpha}{Mb}$, the center of gravity distance of the wing from a, divided by b.

$\omega_\alpha = \sqrt{\frac{C_\alpha}{I_\alpha}}$, the frequency of torsional vibration around a.

$r_\beta = \sqrt{\frac{I_\beta}{Mb^2}}$, *reduced* radius of gyration of aileron divided by b, that is, the radius at which the entire mass of the airfoil would have to be concentrated to give the moment of inertia of the aileron I_β.

$x_\beta = \frac{S_\beta}{Mb}$, *reduced* center of gravity distance from c.

$\omega_\beta = \sqrt{\frac{C_\beta}{I_\beta}}$, frequency of torsional vibration of aileron around c.

$\omega_h = \sqrt{\frac{C_h}{M}}$, frequency of wing in deflection.

FINAL EQUATIONS IN NONDIMENSIONAL FORM

On introducing the quantities M_α, M_β, and P, replacing T_9 and T_{13} from page 5, and reducing to nondimensional form, we obtain the following system of equations:

$$(A)\quad \ddot{\alpha}\left[r_\alpha^2+\kappa\left(\frac{1}{8}+a^2\right)\right]+\dot{\alpha}\frac{v}{b}\kappa\left(\frac{1}{2}-a\right)+\alpha\frac{C_\alpha}{Mb^2}+\ddot{\beta}\left[r_\beta^2+(c-a)x_\beta-\frac{T_7}{\pi}\kappa-(c-a)\frac{T_1}{\pi}\kappa\right]+\frac{1}{\pi}\dot{\beta}\kappa\frac{v}{b}\left[-2p-\left(\frac{1}{2}-a\right)T_4\right]$$
$$+\beta\kappa\frac{v^2}{b^2}\frac{1}{\pi}(T_4+T_{10})+\ddot{h}\left(x_\alpha-a\kappa\right)\frac{1}{b}-2\kappa\left(a+\frac{1}{2}\right)\frac{vC(k)}{b}\left[\frac{v\alpha}{b}+\frac{\dot{h}}{b}+\left(\frac{1}{2}-a\right)\dot{\alpha}+\frac{T_{10}}{\pi}\frac{v}{b}\beta+\frac{T_{11}}{2\pi}\dot{\beta}\right]=0$$

$$(B)\quad \ddot{\alpha}\left[r_\beta^2+(c-a)x_\beta-\kappa\frac{T_7}{\pi}-(c-a)\frac{T_1}{\pi}\kappa\right]+\dot{\alpha}\left(p-T_1-\frac{1}{2}T_4\right)\frac{v}{b}\frac{\kappa}{\pi}+\ddot{\beta}\left(r_\beta^2-\frac{1}{\pi^2}\kappa T_3\right)-\frac{1}{2\pi^2}\dot{\beta}T_4T_{11}\frac{v}{b}\kappa$$
$$+\beta\left[\frac{C_\beta}{Mb^2}+\frac{1}{\pi^2}\frac{v^2}{b^2}\kappa(T_5-T_4T_{10})\right]+\ddot{h}\left(x_\beta-\frac{1}{\pi}\kappa T_1\right)\frac{1}{b}+\frac{T_{12}}{\pi}\kappa\frac{vC(k)}{b}\left[\frac{v\alpha}{b}+\frac{\dot{h}}{b}+\left(\frac{1}{2}-a\right)\dot{\alpha}+\frac{T_{10}}{\pi}\frac{v}{b}\beta+\frac{T_{11}}{2\pi}\dot{\beta}\right]=0$$

$$(C)\quad \ddot{\alpha}\left(x_\alpha-\kappa a\right)+\dot{\alpha}\frac{v}{b}\kappa+\ddot{\beta}\left(x_\beta-\frac{1}{\pi}T_{1\kappa}\right)-\dot{\beta}\frac{v}{b}T_4\kappa\frac{1}{\pi}+h(1+\kappa)\frac{1}{b}+h\frac{C_h}{M}\frac{1}{b}$$
$$+2\kappa\frac{vC(k)}{b}\left[\frac{v\alpha}{b}+\frac{\dot{h}}{b}+\left(\frac{1}{2}-a\right)\dot{\alpha}+\frac{T_{10}}{\pi}\frac{v}{b}\beta+\frac{T_{11}}{2\pi}\dot{\beta}\right]=0$$

SOLUTION OF EQUATIONS

As mentioned in the introduction, we shall only have to specify the conditions under which an unstable equilibrium may exist, no general solution being needed. We shall therefore introduce the variables at once as sine functions of the distance s or, in complex form with $\frac{1}{k}$ as an auxiliary parameter, giving the ratio of the wave length to 2π times the half chord b:

$$\alpha=\alpha_0 e^{ik\frac{s}{b}}$$

$$\beta=\beta_0 e^{i\left(k\frac{s}{b}+\varphi_1\right)}$$

and
$$h=h_0 e^{i\left(k\frac{s}{b}+\varphi_2\right)}$$

where s is the distance from the airfoil to the *first* vortex element, $\frac{ds}{dt}=v$, and φ_1 and φ_2 are phase angles of β and h with respect to α.

Having introduced these quantities in our system of equations, we shall divide through by $\left(\frac{v}{b}k\right)^2\kappa$.

We observe that the velocity v is then contained in only *one* term of each equation. We shall consider this term containing v as the unknown parameter ΩX. To distinguish terms containing X we shall employ a bar; terms without bars do not contain X.

We shall resort to the following notation, taking care to retain a perfectly cyclic arrangement. Let the letter A refer to the coefficients in the first equation not containing $C(k)$ or X, B to similar coefficients of the second equation, and C to those in the third equation. Let the first subscript α refer to the first variable α, the subscript β to the second, and h to the third. Let the second subscripts 1, 2, 3 refer to the second derivative, the first derivative, and the argument of each variable, respectively. $A_{\alpha 1}$ thus refers to the coefficient in the first equation associated with the second derivative of α and not containing $C(k)$ or

X; C_{h3} to the constant in the third equation attached to h, etc. These coefficients[4] are as follows:

$$A_{\alpha 1}=\frac{r_\alpha^2}{\kappa}+\left(\frac{1}{8}+a^2\right)$$

$$A_{\alpha 2}=\left(\frac{1}{2}-a\right)$$

$$A_{\alpha 3}=0$$

$$A_{\beta 1}=\frac{r_\beta^2}{\kappa}-\frac{T_7}{\pi}+(c-a)\left(\frac{x_\beta}{\kappa}-\frac{T_1}{\pi}\right)$$

$$A_{\beta 2}=\frac{1}{\pi}\left[-2p-\left(\frac{1}{2}-a\right)T_4\right]$$

$$A_{\beta 3}=\frac{1}{\pi}(T_4+T_{10})$$

$$A_{h1}=\frac{x_\alpha}{\kappa}-a$$

$$A_{h2}=0$$

$$A_{h3}=0$$

$$B_{\alpha 1}=\frac{r_\beta^2}{\kappa}-\frac{T_7}{\pi}+(c-a)\left(\frac{x_\beta}{\kappa}-\frac{T_1}{\pi}\right)\qquad(=A_{\beta 1})$$

$$B_{\alpha 2}=\frac{1}{\pi}\left(p-T_1-\frac{1}{2}T_4\right)$$

$$B_{\alpha 3}=0$$

$$B_{\beta 1}=\frac{r_\beta^2}{\kappa}-\frac{1}{\pi^2}T_3$$

$$B_{\beta 2}=-\frac{1}{2\pi^2}T_4T_{11}$$

$$B_{\beta 3}=\frac{1}{\pi^2}(T_5-T_4T_{10})$$

$$B_{h1}=\frac{x_\beta}{\kappa}-\frac{1}{\pi}T_1$$

$$B_{h2}=0$$

$$B_{h3}=0$$

$$C_{\alpha 1}=\frac{x_\alpha}{\kappa}-a\qquad(=A_{h1})$$

$$C_{\alpha 2}=1$$

$$C_{\alpha 3}=0$$

$$C_{\beta 1}=\frac{x_\beta}{\kappa}-\frac{1}{\pi}T_1\qquad(=B_{h1})$$

$$C_{\beta 2}=-\frac{1}{\pi}T_4$$

$$C_{\beta 3}=0$$

$$C_{h1}=\frac{1}{\kappa}+1$$

$$C_{h2}=0$$

$$C_{h3}=0$$

[4] The factor $\frac{1}{k}$ or $\frac{1}{k^2}$ is not included in these constants. See the expressions for the R's and I's on next page.

The solution of the instability problem as contained in the system of three equations A, B, and C is given by the vanishing of a third-order determinant of complex numbers representing the coefficients. The solution of particular subcases of two degrees of freedom is given by the minors involving the particular coefficients. We shall denote the case *torsion-aileron* (α, β) as case 3, *aileron-deflection* (β, h) as case 2, and *deflection-torsion* (h, α) as case 1. The determinant form of the solution is given in the major case and in the three possible subcases, respectively, by:

$$\overline{D}=\begin{vmatrix}\bar{R}_{a\alpha}+iI_{a\alpha}, & R_{a\beta}+iI_{a\beta}, & R_{ah}+iI_{ah}\\ R_{b\alpha}+iI_{b\alpha}, & \bar{R}_{b\beta}+iI_{b\beta}, & R_{bh}+iI_{bh}\\ R_{c\alpha}+iI_{c\alpha}, & R_{c\beta}+iI_{c\beta}, & \bar{R}_{ch}+iI_{ch}\end{vmatrix}=0$$

and

$$\overline{M}_{ch}=\begin{vmatrix}\bar{R}_{a\alpha}+iI_{a\alpha}, & R_{a\beta}+iI_{a\beta}\\ R_{b\alpha}+iI_{b\alpha}, & \bar{R}_{b\beta}+iI_{b\beta}\end{vmatrix}=0\qquad\text{Case 3}$$

$$\overline{M}_{a\alpha}=\begin{vmatrix}\bar{R}_{b\beta}+iI_{b\beta}, & R_{bh}+iI_{bh}\\ R_{c\beta}+iI_{c\beta}, & \bar{R}_{ch}+iI_{ch}\end{vmatrix}=0\qquad\text{Case 2}$$

$$\overline{M}_{b\beta}=\begin{vmatrix}\bar{R}_{ch}+iI_{ch}, & R_{c\alpha}+iI_{c\alpha}\\ R_{ah}+iI_{ah}, & \bar{R}_{a\alpha}+iI_{a\alpha}\end{vmatrix}=0\qquad\text{Case 1}$$

REAL EQUATIONS		IMAGINARY EQUATIONS		
$\begin{vmatrix}\bar{R}_{a\alpha}R_{a\beta}\\ R_{b\alpha}\bar{R}_{b\beta}\end{vmatrix}-\begin{vmatrix}I_{a\alpha}I_{a\beta}\\ I_{b\alpha}I_{b\beta}\end{vmatrix}=0$	$\begin{vmatrix}\bar{R}_{a\alpha}R_{a\beta}\\ I_{b\alpha}I_{b\beta}\end{vmatrix}+\begin{vmatrix}I_{a\alpha}I_{a\beta}\\ R_{b\alpha}\bar{R}_{b\beta}\end{vmatrix}=0$	Case 3
$\begin{vmatrix}\bar{R}_{b\beta}R_{bh}\\ R_{c\beta}\bar{R}_{ch}\end{vmatrix}-\begin{vmatrix}I_{b\beta}I_{bh}\\ I_{c\beta}I_{ch}\end{vmatrix}=0$	$\begin{vmatrix}\bar{R}_{b\beta}R_{bh}\\ I_{c\beta}I_{ch}\end{vmatrix}+\begin{vmatrix}I_{b\beta}I_{bh}\\ R_{c\beta}\bar{R}_{ch}\end{vmatrix}=0$	Case 2
$\begin{vmatrix}\bar{R}_{ch}R_{c\alpha}\\ R_{ah}\bar{R}_{a\alpha}\end{vmatrix}-\begin{vmatrix}I_{ch}I_{c\alpha}\\ I_{ah}I_{a\alpha}\end{vmatrix}=0$	$\begin{vmatrix}\bar{R}_{ch}R_{c\alpha}\\ I_{ah}I_{a\alpha}\end{vmatrix}+\begin{vmatrix}I_{ch}I_{c\alpha}\\ R_{ah}\bar{R}_{a\alpha}\end{vmatrix}=0$	Case 1

NOTE.—Terms with bars contain X; terms without bars do not contain X.

The 9 quantities $R_{a\alpha}$, $R_{a\beta}$, etc., refer to the real parts and the 9 quantities $I_{a\alpha}$, $I_{a\beta}$, etc., to the imaginary parts of the coefficients of the 3 variables α, β, and h in the 3 equations A, B, C on page 10. Denoting the coefficients of $\ddot{\alpha}$, $\dot{\alpha}$, and α in the first equation by p, q, and r,

$$R_{a\alpha}+iI_{a\alpha}=\frac{1}{\kappa}\left[-p+iq\frac{b}{kv}+r\left(\frac{b}{kv}\right)^2\right]$$

which, separated in real and imaginary parts, gives the quantities $R_{a\alpha}$ and $I_{a\alpha}$. Similarly, the remaining quantities R and I are obtained. They are all functions of k or $C(k)$. The terms with bars $\bar{R}_{a\alpha}$, $\bar{R}_{b\beta}$, and $\bar{R}_{ch}$ are seen to be the only ones containing the unknown X. The quantities Ω and X will be defined shortly. The quantities R and I are given in the following list:

$$\begin{cases} \bar{R}_{a\alpha}=-A_{\alpha 1}+\Omega_\alpha X+\frac{1}{k}2\left(\frac{1}{2}+a\right)\left[\left(\frac{1}{2}-a\right)G-\frac{1}{k}F\right] & (1)\\ R_{a\beta}=-A_{\beta 1}+\frac{1}{k^2}A_{\beta 3}+\frac{1}{k}\frac{1}{\pi}\left(a+\frac{1}{2}\right)\left[T_{11}G-2\frac{1}{k}T_{10}F\right] & (2)\\ R_{ah}=-A_{h1}+\frac{1}{k}2\left(a+\frac{1}{2}\right)G & (3)\end{cases}$$

$$\begin{cases} R_{b\alpha}=-B_{\alpha 1}-\frac{1}{k}\frac{T_{12}}{\pi}\left[\left(\frac{1}{2}-a\right)G-\frac{1}{k}F\right] & (4)\\ \bar{R}_{b\beta}=-B_{\beta 1}+\frac{1}{k^2}B_{\beta 3}+\Omega_\beta X-\frac{1}{k}\frac{T_{12}}{2\pi^2}\left[T_{11}G-2T_{10}\frac{1}{k}F\right] & (5)\\ R_{bh}=-B_{h1}-\frac{1}{k}\frac{T_{12}}{\pi}G & (6)\end{cases}$$

$$\begin{cases} R_{c\alpha}=-C_{\alpha 1}-\frac{1}{k}2\left[\left(\frac{1}{2}-a\right)G-\frac{1}{k}F\right] & (7)\\ R_{c\beta}=-C_{\beta 1}-\frac{1}{k}\frac{1}{\pi}\left[T_{11}G-2T_{10}\frac{1}{k}F\right] & (8)\\ \bar{R}_{ch}=-C_{h1}+\Omega_h X-\frac{1}{k}2G & (9)\end{cases}$$

$$\begin{cases} I_{a\alpha}=-\frac{1}{k}\left[2\left(a+\frac{1}{2}\right)\left\{\left(\frac{1}{2}-a\right)F+\frac{1}{k}G\right\}-A_{\alpha 2}\right] & (11)\\ I_{a\beta}=-\frac{1}{k}\left[\frac{1}{\pi}\left(a+\frac{1}{2}\right)\left(T_{11}F+2\frac{1}{k}T_{10}G\right)-A_{\beta 2}\right] & (12)\\ I_{ah}=-\frac{1}{k}2\left(a+\frac{1}{2}\right)F & (13)\end{cases}$$

$$\begin{cases} I_{b\alpha}=\frac{1}{k}\left[\frac{T_{12}}{\pi}\left\{\left(\frac{1}{2}-a\right)F+\frac{1}{k}G\right\}+B_{\alpha 2}\right] & (14)\\ I_{b\beta}=\frac{1}{k}\left[\frac{T_{12}}{2\pi^2}\left(T_{11}F+2\frac{1}{k}T_{10}G\right)+B_{\beta 2}\right] & (15)\\ I_{bh}=\frac{1}{k}\frac{T_{12}}{\pi}F & (16)\end{cases}$$

$$\begin{cases} I_{c\alpha}=\frac{1}{k}\left[2\left\{\left(\frac{1}{2}-a\right)F+\frac{1}{k}G\right\}+C_{\alpha 2}\right] & (17)\\ I_{c\beta}=\frac{1}{k}\left[\frac{1}{\pi}\left(T_{11}F+2\frac{1}{k}T_{10}G\right)+C_{\beta 2}\right] & (18)\\ I_{ch}=\frac{1}{k}2F & (19)\end{cases}$$

The solution as given by the three-row determinant shall be written explicitly in X. We are immediately able to put down for the general case a cubic equation in X with complex coefficients and can easily segregate the three subcases. The quantity D is as before the value of the determinant, but with the term containing X missing. The quantities $M_{a\alpha}$, $M_{b\beta}$, and M_{ch} are the minors of the elements in the diagonal squares $a\alpha$, $b\beta$, and ch, respectively. They are expressed explicitly in terms of R and I under the subcases treated in the following paragraphs.

$$\bar{D}=\begin{vmatrix} A_{a\alpha}+\Omega_\alpha X & A_{a\beta} & A_{ah}\\ A_{b\alpha} & A_{b\beta}+\Omega_\beta X & A_{bh}\\ A_{c\alpha} & A_{c\beta} & A_{ch}+\Omega_h X\end{vmatrix}=0$$

where $A_{a\alpha}=R_{a\alpha}+iI_{a\alpha}$ etc.

Complex cubic equation in X:

$$\Omega_\alpha\Omega_\beta\Omega_h X^3+(\Omega_\alpha\Omega_\beta A_{ch}+\Omega_\beta\Omega_h A_{a\alpha}+\Omega_h\Omega_\alpha A_{b\beta})X^2+(\Omega_\alpha M_{a\alpha}+\Omega_\beta M_{b\beta}+\Omega_h M_{ch})X+D=0 \qquad \text{(XXI)}$$

Case 3, (α, β):

$$\Omega_\alpha\Omega_\beta X^2+(\Omega_\alpha A_{b\beta}+\Omega_\beta A_{a\alpha})X+M_{ch}=0 \qquad \text{(XXII)}$$

Case 2, (β, h):

$$\Omega_\beta\Omega_h X^2+(\Omega_\beta A_{ch}+\Omega_h A_{b\beta})X+M_{a\alpha}=0 \qquad \text{(XXIII)}$$

Case 1, (h, α):

$$\Omega_h\Omega_\alpha X^2+(\Omega_h A_{a\alpha}+\Omega_\alpha A_{ch})X+M_{b\beta}=0 \qquad \text{(XXIV)}$$

$$\Omega_\alpha X=\frac{C_\alpha}{k^2Mv^2\kappa}=\left(\frac{\omega_\alpha r_\alpha}{\omega_\tau r_\tau}\right)^2\frac{1}{\kappa}\left(\frac{br_\tau\omega_\tau}{vk}\right)^2$$

$$\Omega_\beta X=\frac{C_\beta}{k^2Mv^2\kappa}=\left(\frac{\omega_\beta r_\beta}{\omega_\tau r_\tau}\right)^2\frac{1}{\kappa}\left(\frac{br_\tau\omega_\tau}{vk}\right)^2$$

$$\Omega_h X=\frac{C_h b^2}{k^2Mv^2\kappa}=\left(\frac{\omega_h}{\omega_\tau r_\tau}\right)^2\frac{1}{\kappa}\left(\frac{br_\tau\omega_\tau}{vk}\right)^2$$

and finally

$$X=\frac{1}{\kappa}\left(\frac{br_\tau\omega_\tau}{vk}\right)^2$$

We are at liberty to introduce the reference parameters ω_τ and r_τ, and the convention adopted is: ω_τ is the last ω in cyclic order in each of the subcases 3, 2, and 1.

Then $\Omega_n=\left(\frac{\omega_n r_n}{\omega_{n+1}r_{n+1}}\right)^2$ and $\Omega_{n+1}=1$, thus for

Case 3, $\Omega_\alpha=\left(\frac{\omega_\alpha r_\alpha}{\omega_\beta r_\beta}\right)^2$ and $\Omega_\beta=1$

Case 2, $\Omega_\beta=\left(\frac{\omega_\beta r_\beta}{\omega_h}\right)^2$ and $\Omega_h=1$

Case 1, $\Omega_h=\left(\frac{\omega_h}{\omega_\alpha r_\alpha}\right)^2$ and $\Omega_\alpha=1$

To treat the general case of three degrees of freedom (equation (XXI)), it is observed that the real part of the equation is of third degree while the imaginary part furnishes an equation of second degree. The problem is to find values of X satisfying both equations. We shall adopt the following procedure: Plot graphically X against $\frac{1}{k}$ for both equations. The points of intersection are the solutions. We are only concerned with positive values of $\frac{1}{k}$ and positive values of X. Observe that we do not have to solve for k, but may reverse the process by choosing a number of values of k and solve for X. The plotting of X against $\frac{1}{k}$ for the second-degree equation is simple enough, whereas the task of course is somewhat more laborious for the third-degree equation. However, the general case is of less practical importance than are the three subcases. The equation simplifies considerably, becoming of second degree in X.

We shall now proceed to consider these three subcases. By virtue of the cyclic arrangement, we need only consider the first case (α, β). The complex quadratic equations (XXII)-(XXIV) all resolve themselves into two independent statements, which we shall for convenience denote "Imaginary equation" and "Real equation", the former being of first and the latter of second degree in X. All constants are to be resolved into their real and imaginary parts, denoted by an upper index R or I, respectively.

Let $M_{a\alpha}=M^R{}_{a\alpha}+iM^I{}_{a\alpha}$ and let similar expressions denote $M_{b\beta}$ and M_{ch}

Case 3, (α,β). Separating equation (XXII) we obtain.

(1) Imaginary equation:

$$(\Omega_\alpha I_{b\beta}+\Omega_\beta I_{a\alpha})X+M^I{}_{ch}=0$$

$$X=-\frac{M^I{}_{ch}}{\Omega_\alpha I_{b\beta}+\Omega_\beta I_{a\alpha}}$$

(2) Real equation:

$$\Omega_\alpha\Omega_\beta X^2+(\Omega_\alpha R_{b\beta}+\Omega_\beta R_{a\alpha})X+M^R{}_{ch}=0$$

Eliminating X we get

$$\Omega_\alpha\Omega_\beta(M^I{}_{ch})^2-(\Omega_\alpha R_{b\beta}+\Omega_\beta R_{a\alpha})(\Omega_\alpha I_{b\beta}+\Omega_\beta I_{a\alpha})M^I{}_{ch}+M^R{}_{ch}(\Omega_\alpha I_{b\beta}+\Omega_\beta I_{a\alpha})^2=0$$

By the convention adopted we have in this case:

$$\omega_r=\omega_\beta, \qquad \Omega_\alpha=\left(\frac{\omega_\alpha}{\omega_\beta}\right)^2\left(\frac{r_\alpha}{r_\beta}\right)^2, \qquad \text{and } \Omega_\beta=1$$

Arranging the equation in powers of Ω_α we have:

$$\Omega_\alpha{}^2[-M^I{}_{ch}(R_{b\beta}I_{b\beta})+M^R{}_{ch}I_{b\beta}{}^2]+\Omega_\alpha[(M^I{}_{ch})^2-M^I{}_{ch}(R_{a\alpha}I_{b\beta}+I_{a\alpha}R_{b\beta})+2M^R{}_{ch}I_{a\alpha}I_{b\beta}]+[-M^I{}_{ch}R_{a\alpha}I_{a\alpha}+M^R{}_{ch}I_{a\alpha}{}^2]=0$$

But we have

$$(M^I{}_{ch})^2-M^I{}_{ch}(R_{a\alpha}I_{b\beta}+I_{a\alpha}R_{b\beta})$$
$$=M^I{}_{ch}[R_{a\alpha}I_{b\beta}-R_{a\beta}I_{b\alpha}+R_{b\beta}I_{a\alpha}-R_{b\alpha}I_{a\beta}-R_{a\alpha}I_{b\beta}-R_{b\beta}I_{a\alpha}]$$
$$=-M^I{}_{ch}(R_{a\beta}I_{b\alpha}+I_{a\beta}R_{b\alpha})$$

Finally, the equation for Case 3 (α, β) becomes:

$$\Omega_\alpha{}^2(M^R{}_{ch}I_{b\beta}{}^2-M^I{}_{ch}R_{b\beta}I_{b\beta})+\Omega_\alpha[-M^I{}_{ch}(R_{a\beta}I_{b\alpha}+I_{a\beta}R_{b\alpha})+2M^R{}_{ch}I_{a\alpha}I_{b\beta}]+M^R{}_{ch}I_{a\alpha}{}^2-M^I{}_{ch}R_{a\alpha}I_{a\alpha}=0 \quad \text{(XXV)}$$

where

$$M^R{}_{ch}=R_{a\alpha}R_{b\beta}-R_{a\beta}R_{b\alpha}-I_{a\alpha}I_{b\beta}+I_{a\beta}I_{b\alpha}$$
$$M^I{}_{ch}=R_{a\alpha}I_{b\beta}-R_{a\beta}I_{b\alpha}+I_{a\alpha}R_{b\beta}-I_{a\beta}R_{b\alpha}$$

The remaining cases may be obtained by cyclic rearrangement:

Case 2, (β,h) $\quad \omega_r=\omega_h \quad \Omega_\beta=\left(\frac{\omega_\beta}{\omega_h}\right)^2 r_\beta{}^2 \quad \Omega_h=1$

$$\Omega_\beta{}^2(M^R{}_{a\alpha}I_{ch}{}^2-M^I{}_{a\alpha}R_{ch}I_{ch})+\Omega_\beta[-M^I{}_{a\alpha}(R_{bh}I_{c\beta}+I_{bh}R_{c\beta})+2M^R{}_{a\alpha}I_{b\beta}I_{ch}]+M^R{}_{a\alpha}I_{b\beta}{}^2-M^I{}_{a\alpha}R_{b\beta}I_{b\beta}=0 \quad \text{(XXVI)}$$

where $\quad M^R{}_{a\alpha}=R_{b\beta}R_{ch}-R_{bh}R_{c\beta}-I_{b\beta}I_{ch}+I_{bh}I_{c\beta}$
$\quad M^I{}_{a\alpha}=R_{b\beta}I_{ch}-R_{bh}I_{c\beta}+I_{b\beta}R_{ch}-I_{bh}R_{c\beta}$

Case 1, (h,α) $\quad \omega_r=\omega_\alpha \quad \Omega_h=\left(\frac{\omega_h}{\omega_\alpha}\right)^2\frac{1}{r_\alpha{}^2} \quad \Omega_\alpha=1$

$$\Omega_h{}^2(M^R{}_{b\beta}I_{a\alpha}{}^2-M^I{}_{b\beta}R_{a\alpha}I_{a\alpha})+\Omega_h[-M^I{}_{b\beta}(R_{c\alpha}I_{ah}+I_{c\alpha}R_{ah})+2M^R{}_{b\beta}I_{ch}I_{a\alpha}]+M^R{}_{b\beta}I_{ch}{}^2-M^I{}_{b\beta}R_{ch}I_{ch}=0 \quad \text{(XXVII)}$$

where $\quad M^R{}_{b\beta}=R_{ch}R_{a\alpha}-R_{c\alpha}R_{ah}-I_{ch}I_{a\alpha}+I_{c\alpha}I_{ah}$
$\quad M^I{}_{b\beta}=R_{ch}I_{a\alpha}-R_{c\alpha}I_{ah}+I_{ch}R_{a\alpha}-I_{c\alpha}R_{ah}$

Equations (XXV), (XXVI), and (XXVII) thus give the solutions of the cases: *torsion-aileron*, *aileron-deflection*, and *deflection-torsion*, respectively. The quantity Ω may immediately be plotted against $\frac{1}{k}$ for any value of the independent parameters.

The coefficients in the equations are all given in terms of R and I, which quantities have been defined above. Routine calculations and graphs giving Ω against $\frac{1}{k}$ are contained in Appendix I and Appendix II.

Knowing related values of Ω and $\frac{1}{k}$, X is immediately expressed as a function of Ω by means of the first-degree equation. The definition of X and Ω for each subcase is given above. The cyclic arrangement of all quantities is very convenient as it permits identical treatment of the three subcases.

It shall finally be repeated that the above solutions represent the *border case* of unstable equilibrium. The plot of X against Ω gives a boundary curve between the stable and the unstable regions in the $X\Omega$ plane. It is preferable, however, to plot the quantity $\frac{1}{k^2}\frac{1}{X}$ instead of X, since this quantity is proportional to the square of the flutter speed. The stable area can easily be identified by inspection as it will contain the axis $\frac{1}{k^2}\frac{1}{X}=0$, if the combination is stable for zero velocity.

LANGLEY MEMORIAL AERONAUTICAL LABORATORY,
NATIONAL ADVISORY COMMITTEE FOR AERONAUTICS,
LANGLEY FIELD, VA., *May 2, 1934.*

APPENDIX I

PROCEDURE IN SOLVING NUMERICAL EXAMPLES

(1) Determine the R's and I's, nine of each for a major case of three degrees of freedom, or those pertaining to a particular subcase, 4 R's and 4 I's. Refer to the following for the R's and I's involved in each case:

The numerals 1 to 9 and 11 to 19 are used for convenience.

(Major case) Three degrees of freedom

1	$R_{a\alpha}$	$I_{a\alpha}$	11
2	$R_{a\beta}$	$I_{a\beta}$	12
3	R_{ah}	I_{ah}	13
4	$R_{b\alpha}$	$I_{b\alpha}$	14
5	$R_{b\beta}$	$I_{b\beta}$	15
6	R_{bh}	I_{bh}	16
7	$R_{c\alpha}$	$I_{c\alpha}$	17
8	$R_{c\beta}$	$I_{c\beta}$	18
9	R_{ch}	I_{ch}	19

(Case 3) Torsional-aileron (α, β)

1	$R_{a\alpha}$	$I_{a\alpha}$	11
2	$R_{a\beta}$	$I_{a\beta}$	12
4	$R_{b\alpha}$	$I_{b\alpha}$	14
5	$R_{b\beta}$	$I_{b\beta}$	15

(Case 2) Aileron-deflection (β, h)

5	$R_{b\beta}$	$I_{b\beta}$	15
6	R_{bh}	I_{bh}	16
8	$R_{c\beta}$	$I_{c\beta}$	18
9	R_{ch}	I_{ch}	19

(Case 1) Deflection-torsion (h, α)

7	$R_{c\alpha}$	$I_{c\alpha}$	17
9	R_{ch}	I_{ch}	19
1	$R_{a\alpha}$	$I_{a\alpha}$	11
3	R_{ah}	I_{ah}	13

It has been found convenient to split the R's in two parts $R=R'+R''$, the former being independent of the argument $\frac{1}{k}$. The quantities I and R'' are functions of the two independent parameters a and c only.[5] The formulas are given in the following list.

$$R''_{a\alpha}=\frac{1}{k}2\left(a+\frac{1}{2}\right)\left|\left(\frac{1}{2}-a\right)G-\frac{F}{k}\right| \tag{1}$$

$$R''_{a\beta}=\frac{1}{k}\frac{1}{\pi}\left|(T_4+T_{10})\frac{1}{k}+\left(a+\frac{1}{2}\right)\left(T_{11}G-\frac{2}{k}T_{10}F\right)\right| \tag{2}$$

$$R''_{ah}=\frac{1}{k}2\left(a+\frac{1}{2}\right)G \tag{3}$$

$$R''_{b\alpha}=-\frac{1}{k}\frac{T_{12}}{\pi}\left|\left(\frac{1}{2}-a\right)G-\frac{F}{k}\right| \tag{4}$$

$$R''_{b\beta}=-\frac{1}{k}\frac{1}{\pi^2}\left|\frac{T_{12}}{2}\left(T_{11}G-\frac{2}{k}T_{10}F\right)-\frac{1}{k}(T_5-T_4T_{10})\right| \tag{5}$$

$$R''_{bh}=-\frac{1}{k}\frac{T_{12}}{\pi}G \tag{6}$$

$$R''_{c\alpha}=-\frac{1}{k}2\left|\left(\frac{1}{2}-a\right)G-\frac{F}{k}\right| \tag{7}$$

$$R''_{c\beta}=-\frac{1}{k}\frac{1}{\pi}\left(T_{11}G-2T_{10}\frac{F}{k}\right) \tag{8}$$

$$R''_{ch}=-\frac{1}{k}2\,G \tag{9}$$

$$I_{a\alpha}=-2\left(a+\frac{1}{2}\right)\left|\left(\frac{1}{2}-a\right)F+\frac{1}{k}G\right|+\frac{1}{2}-a \tag{11}$$

$$I_{a\beta}=-\frac{1}{\pi}\left|\left(a+\frac{1}{2}\right)\left(T_{11}F+\frac{2}{k}T_{10}G\right)+2p+\left(\frac{1}{2}-a\right)T_4\right| \tag{12}$$

$$I_{ah}=-2\left(a+\frac{1}{2}\right)F \tag{13}$$

$$I_{b\alpha}=\frac{T_{12}}{\pi}\left|\left(\frac{1}{2}-a\right)F+\frac{1}{k}G\right|+\frac{1}{\pi}\left(p-T_1-\frac{1}{2}T_4\right) \tag{14}$$

Where $p=-\frac{1}{3}(1-c^2)^{3/2}$

$$I_{b\beta}=\frac{1}{2\pi^2}\left|T_{12}\left(T_{11}F+\frac{2}{k}T_{10}G\right)-T_4T_{11}\right| \tag{15}$$

$$I_{bh}=\frac{T_{12}}{\pi}F \tag{16}$$

$$I_{c\alpha}=2\left|\left(\frac{1}{2}-a\right)F+\frac{1}{k}G\right|+1 \tag{17}$$

$$I_{c\beta}=\frac{1}{\pi}\left|\left(T_{11}F+\frac{2}{k}T_{10}G\right)-T_4\right| \tag{18}$$

$$I_{ch}=2F \tag{19}$$

[5] The quantities I given in the appendix and used in the following calculations are seen to differ from the I's given in the body of the paper by the factor $\frac{1}{k}$. It may be noticed that this factor drops out in the first-degree equations.

Choosing certain values of a and c and employing the values of the T's given by the formulas of the report (p. 5) or in table I and also using the values of F and G (formulas (XII) and (XIII)) or table II, we evaluate the quantities I and R'' for a certain number of $\frac{1}{k}$ values. The results of this evaluation are given in tables III and IV, which have been worked out for $a=0,-0.2$, and -0.4, and for $c=0.5$ and $c=0$. The range of $\frac{1}{k}$ is from 0 to 40. These tables save the work of calculating the I's and R'''s for almost all cases of practical importance. Interpolation may be used for intermediate values. This leaves the quantities R' to be determined. These, being independent of $\frac{1}{k}$, are as a result easy to obtain. Their values, using the same system of numbers for identification, and referring to the definition of the original independent variables on pages 9 and 10, are given as follows:

$$R'_{a\alpha}=-\frac{r_\alpha^2}{\kappa}-\left(\frac{1}{8}+a^2\right) \tag{1}$$

$$R'_{a\beta}=-\frac{r_\beta^2}{\kappa}-(c-a)\frac{x_\beta}{\kappa}+\frac{T_7}{\pi}+(c-a)\frac{T_1}{\pi} \tag{2}$$

$$R'_{ah}=-\frac{x_\alpha}{\kappa}+a \tag{3}$$

$$R'_{b\alpha}=\text{same as } R'_{a\beta} \tag{4}$$

$$R'_{b\beta}=-\frac{r_\beta^2}{\kappa}+\frac{1}{\pi^2}T_3 \tag{5}$$

$$R'_{bh}=-\frac{x_\beta}{\kappa}+\frac{1}{\pi}T_1 \tag{6}$$

$$R'_{c\alpha}=\text{same as } R'_{ah} \tag{7}$$

$$R'_{c\beta}=\text{same as } R'_{bh} \tag{8}$$

$$R'_{ch}=-\frac{1}{\kappa}-1 \tag{9}$$

Because of the symmetrical arrangement in the determinant, the 9 quantities, are seen to reduce to 6 quantities to be calculated. It is very fortunate, indeed, that all the remaining variables, segregate themselves in the 6 values of R' which are independent of $\frac{1}{k}$, while the more complicated I and R'' are functions solely of c and a. In order to solve any problem it is therefore only necessary to refer to tables III and IV and then to calculate the 6 values of R'.

The quantities (1) to (9) and (11) to (19) thus having been determined, the plot of Ω against $\frac{1}{k}$, which constitutes our method of solution, is obtained by solving the equation $a\Omega^2+b\Omega+c=0$. The constants a, b, and c are obtained automatically by computation according to the following scheme:

Case 3

Find products 1.5 2.4 11.15 12.14

Then $M^R_{ch}=1.5-2.4-\frac{1}{k^2}(11.15-12.14)$

Find products 1.15 2.14 11.5 12.4

Then $M^I_{ch}=1.15-2.14+11.5-12.4$

and $a=M^R_{ch}(15)^2-M^I_{ch}(5.15)$

$b=-M^I_{ch}(2.14+12.4)+M^R_{ch}(11.15)$

$c=M^R_{ch}(11)^2-M^I_{ch}(1.11)$ Find Ω_α

Solution: $\frac{1}{X}=-\frac{\Omega_\alpha(15)+11}{M^I_{ch}}$

Similarly

Case 2

5.9 6.8 15.19 16.18

$M^R_{a\alpha}=5.9-6.8-\frac{1}{k^2}(15.19-16.18)$

5.19 6.18 15.9 16.8

$M^I_{a\alpha}=5.19-6.18+15.9-16.8$

$a=M^R_{a\alpha}(19)^2-M^I_{a\alpha}(9.19)$

$b=-M^I_{a\alpha}(6.18-16.8)-2M^R_{a\alpha}(15.19)$

$c=M^R_{a\alpha}(15)^2-M^I_{a\alpha}(5.15)$ Find Ω_β

$\frac{1}{X}=\frac{\Omega_\beta(19)+15}{M^I_{a\alpha}}$

and

Case 1

9.1 7.3 19.11 17.13

$M^R_{b\beta}=9.1-7.3-\frac{1}{k^2}(19.11-17.13)$

9.11 7.13 19.1 17.3

$M^I_{b\beta}=9.11-7.13+19.1-17.3$

$a=M^R_{b\beta}(11)^2-M^I_{b\beta}(1.11)$

$b=-M^I_{b\beta}(7.13+17.3)+M^R_{b\beta}(19.11)$

$c=M^R_{b\beta}(19)^2-M^I_{b\beta}(9.19)$ Find Ω_h

$\frac{1}{X}=\frac{\Omega_h(11)+19}{M^I_{b\beta}}$

Ω_α is defined as $\left(\frac{\omega_\alpha r_\alpha}{\omega_\beta r_\beta}\right)^2$ for case 3;

Ω_β is defined as $\left(\frac{\omega_\beta r_\beta}{\omega_h}\right)^2$ for case 2; and

Ω_h is defined as $\left(\frac{\omega_h}{\omega_\alpha r_\alpha}\right)^2$ for case 1.

The quantity $\frac{1}{X}$ is $\kappa\left(\frac{vk}{b\omega_\tau r_\tau}\right)^2$ by definition.

Since both Ω and $\frac{1}{X}$ are calculated for each value of $\frac{1}{k}$, we may plot $\frac{1}{k^2}\frac{1}{X}$ directly as a function of Ω. This quantity, which is proportional to the square of the flutter speed, represents the solution.

We shall sometimes use the square root of the above quantity, viz, $\frac{1}{k}\sqrt{\frac{1}{X}}=\frac{\sqrt{\kappa}v}{b\omega_\tau r_\tau}$, and will denote this

quantity by F, which we shall term the "flutter factor" The flutter velocity is consequently obtained as

$$v=F\frac{b\omega_\gamma r_\gamma}{\sqrt{\kappa}}$$

Since F is nondimensional, the quantity $\frac{b\omega_\gamma r_\gamma}{\sqrt{\kappa}}$ must obviously be a velocity. It is useful to establish the significance of this velocity, with reference to which the flutter speed, so to speak, is measured. Observing that $\kappa=\frac{\pi\rho b^2}{M}$ and that the stiffness in case 1 is given by $\omega_\alpha=\sqrt{\frac{C_\alpha}{Mb^2r_\alpha^2}}$ this reference velocity may be written:

$$v_R=\frac{b\omega_\alpha r_\alpha}{\sqrt{\kappa}}=\frac{1}{b}\sqrt{\frac{C_\alpha}{\pi\rho}} \text{ or}$$

$$\pi\rho v_R^2b^2=C_\alpha$$

The velocity v_R is thus the velocity at which the total force on the airfoil $\pi\rho v_R^2 2b$ attacking with an arm $\frac{b}{2}$ equals the torsional stiffness C_α of the wing. This statement means, in case 1, that the reference velocity used is equal to the "divergence" velocity obtained with the torsional axis in the middle of the chord. This velocity is considerably smaller than the usual divergence velocity, which may be expressed as

$$v_D=v_R\frac{1}{\frac{1}{2}+a}$$

where a ranges from 0 to $-\frac{1}{2}$. We may thus express the flutter velocity as

$$v_F=v_RF$$

In case 3 the reference velocity has a similar significance, that is, it is the velocity at which the entire lift of the airfoil attacking with a leverage $\frac{1}{2}b$ equals numerically the torsional stiffness C_β of the aileron or movable tail surface.

In case 2, no suitable or useful significance of the reference velocity is available.

TABLE I.—VALUES OF T

	$c=1$	$c=\frac{1}{2}$	$c=0$	$c=-\frac{1}{2}$	$c=-1$
T_1	0	−0.1259	−0.0607	−1.6967	−3.1416
T_2	0	−0.2103	−1.5707	−4.8356	−9.8697
T_3	0	−.05313	−.9084	−3.8375	−11.1034
T_4	0	−.6142	−1.5708	−2.5274	−3.1416
T_5	0	−.9098	−3.4674	−6.9503	−9.8697
T_6	0	−0.2103	−1.5707	−4.8356	−9.8697
T_7	0	.0132	−.1964	−1.1913	−3.5343
T_8	0	.0903	−.3533	−1.4805	−3.1416
T_{10}	0	1.0132	2.5708	2.9604	3.1416
T_{11}	0	1.2990	3.5708	6.3538	9.4248
T_{12}	0	.07066	.4292	1.2990	3.1416

TABLE II.—TABLE OF THE BESSEL FUNCTIONS J_0, J_1 Y_0, Y_1 AND THE FUNCTIONS F AND G

$$F(k)=\frac{J_1(J_1+Y_0)+Y_1(Y_1-J_0)}{(J_1+Y_0)^2+(Y_1-J_0)^2}$$

$$-G(k)=\frac{Y_1(J_1+Y_0)-J_1(Y_1-J_0)}{(J_1+Y_0)^2+(Y_1-J_0)^2}$$

k	$\frac{1}{k}$	J_0	J_1	Y_0	Y_1	F	$-G$
∞	0					0.5000	0
10	1/10	−0.2459	0.0435	0.0557	0.2490	.5006	0.0126
6	1/6	.1503	−.2767	−.2882	−.1750	.5018	.0207
4	1/4	−.3972	−.0660	−.0170	.3979	.5037	.0305
2	1/2	.2239	.5767	.5104	−.1071	.5129	.0577
1	1	.7652	.4401	.0882	−.7813	.5395	.1003
.8	1 1/4	.8463	.3688	−.0868	−.9780	.5541	.1163
.6	1 2/3	.9120	.2867	−.3085	−1.2604	.5788	.1378
.5	2	.9385	.2423	−.4444	−1.4714	.6030	.151
.4	2 1/2	.9604	.1960	−.6060	−1.7808	.6245	.166
.3	3 1/3	.9776	.1483	−.8072	−2.2929	.6650	.180
.2	5	.9900	.0995	−1.0810	−3.2235	.7276	.1886
.1	10	.9975	.0499	−1.5342	−7.0317	.8457	.1626
.05	20					.911	.132
.025	40					.965	.090
0	∞					1.000	0

TABLE III.—VALUES OF R

$\frac{1}{k}$	c	a	0	1/10	1/5	1/4	1/2	1	1 1/4	1 3/5	2	2 1/2	3 1/3	5	10	20	40
R''_{aa}	(1)	−.2	0	−0.00564	−0.01586	−0.03529	−0.14265	−0.33965	−0.93656	−1.72330	−2.56300	−4.11090	−7.68720	−16.66150	−85.38300	−365.72000	−1,628.2000
		−.4	0	−.00353	−.00981	−.02208	−.06905	−.16886	−.68061	−1.06138	−1.57407	−2.51580	−4.69430	−11.81010	−51.42490	−219.74900	−917.3520
			0	−.00123	−.00341	−.00767	−.03084	−.12595	−.19935	−.36205	−.53676	−.85520	−1.56540	−3.80774	−17.20670	−73.35590	−305.9260
$R''_{a\beta}$	0	−.2	0	−.00163	−.00452	−.01020	−.04175	−.18016	−.20384	−.56223	−.87212	−1.43983	−2.84966	−7.46300	−38.29650	−172.36360	−741.7972
			0	.00030	.00083	.00184	.00679	.01922	.02268	.01629	−.01460	−.06803	−.29517	−1.29480	−10.24590	−52.49020	−241.3664
		−.4	0	.00222	.00617	.01388	.05531	.21861	.33914	.69499	.84414	1.30365	2.25914	4.87340	17.80470	67.38320	259.0648
	0.5	−.2	0	.00083	.00229	.00510	.01932	.00419	.08876	.12176	.12260	.12205	−.02900	−.93535	−10.48970	−69.15180	−268.7236
			0	.00214	.00595	.01336	.05278	.20325	.31085	.53062	.73222	1.10233	1.81135	3.65230	10.14740	31.49620	101.6340
		−.4	0	.00347	.00965	.02170	.08656	.34361	.53463	.94336	1.34762	2.09190	3.66913	8.06235	30.97980	120.89760	475.2592
R''_{ah}	(1)	−.2	0	−.00125	−.00345	−.00763	−.02890	−.10030	−.14560	−.22470	−.30200	−.41500	−.60000	−.94300	−1.62600	−2.64000	−3.6000
			0	−.00075	−.00207	−.00429	−.01734	−.06018	−.08736	−.13482	−.18120	−.24900	−.36000	−.56580	−.97560	−1.58400	−2.1600
		−.4	0	−.00201	−.00334	−.00502	−.01003	−.02006	−.02508	−.03236	−.04012	−.05015	−.06083	−.10080	−.20060	−.40120	−.8024
R''_{ba}	0	−.2	0	.00077	.00214	.00482	.01949	.08055	.12821	.23541	.35010	.56143	1.05008	2.54020	11.66330	49.95700	208.7520
			0	.00080	.00223	.00503	.02027	.08329	.13219	.24169	.35836	.57276	1.06650	2.57490	11.70770	50.03000	208.8500
		−.4	0	.00084	.00233	.00523	.02106	.08603	.13616	.24795	.36661	.58410	1.08286	2.60969	11.75220	50.10160	208.9490
	0.5	−.2	0	.00013	.00035	.00079	.00321	.01327	.02112	.03878	.05767	.09248	.17296	.41988	1.92110	8.22870	34.3850
			0	.00013	.00037	.00083	.00334	.01372	.02177	.03981	.05903	.09434	.17666	.42413	1.92340	8.24060	34.4007
		−.4	0	.00014	.00038	.00086	.00347	.01417	.02243	.04084	.06039	.09621	.17836	.42837	1.93576	8.25246	34.4169
$R''_{b\beta}$	0	.5	0	.00124	.00343	.00772	.03101	.12642	.19830	.35907	.52400	.82930	1.5193	3.54970	15.35120	64.02240	263.2340
	.5	(2)	0	.00031	.00087	.00196	.00783	.03170	.04930	.08935	.13000	.20440	.36940	.84970	3.55050	14.56740	59.3188
R''_{bh}	0	.5	0	.00017	.00047	.00104	.00394	.01370	.01989	.03177	.04125	.05069	.08195	.12881	.22211	.36062	.4918
	.5	(2)	0	.00003	.00008	.00016	.00055	.00226	.00328	.00506	.00680	.00934	.01360	.02122	.03659	.05940	.0810
R''_{ca}	(1)	−.2	0	.01128	.03132	.07058	.28530	1.17930	1.87710	3.44670	5.12600	8.22000	15.37450	37.32300	170.76600	731.44000	3,056.4000
			0	.01178	.03270	.07362	.29684	1.21954	1.93540	3.53860	5.24980	8.38600	15.61440	37.70020	171.41640	732.49600	3,057.8400
		−.4	0	.01228	.03409	.07668	.30838	1.25950	1.99360	3.63050	5.36760	8.55200	15.85440	38.07740	172.06680	733.55200	3,059.2800
R''_{cb}	0	(2)	0	.00063	.00273	.00818	.24266	1.00561	1.58246	2.89371	4.29100	6.85898	15.49965	30.94330	140.26370	599.41300	2,502.3470
	.5		0	.00060	.01340	.04150	.16810	.69850	1.11458	2.05320	3.06224	4.92530	9.24438	22.54400	103.67300	444.86400	1,831.9900
R''_{ch}	(1)	(2)	0	.00260	.00690	.01420	.05780	.20960	.29120	.44940	.60400	.83000	1.20000	1.86600	3.25200	5.28000	7.2000

[1] Independent of c.

[2] Independent of a.

TABLE IV.—VALUES OF I

$\frac{1}{k}$	c	a	0	1/10	1/5	1/4	1/2	1	1 1/4	1 3/5	2	2 1/2	3 1/3	5	10	20	40
I_{aa}	(1)	0	0.25000	0.25096	0.25255	0.25378	0.27240	0.33055	0.36855	0.44030	0.50050	0.60276	0.76750	1.07920	1.70320	2.68450	3.61760
		−.2	.49000	.49050	.49131	.49302	.50189	.53359	.55464	.59472	.62794	.68671	.78070	.99021	1.52040	1.90140	2.45470
		−.4	.81000	.81014	.81037	.81066	.81145	.82395	.82938	.84176	.85186	.87059	.90030	.95763	1.07300	1.26400	1.44630
$I_{a\beta}$	0	0	.17805	.17874	.17985	.18219	.19433	.23768	.26845	.32132	.36064	.44890	.57526	.82035	1.31213	2.10476	2.85983
		−.2	.39170	.39212	.39278	.39418	.40147	.42748	.44474	.47761	.50485	.55300	.63902	.77708	1.07215	1.54773	2.00065
		−.4	.60531	.60545	.60567	.60614	.60857	.61724	.62299	.63395	.64303	.65908	.68475	.73327	.82313	.99065	1.14163
	0.5	0	.13262	.13317	.13425	.13640	.14742	.18544	.20914	.25611	.29514	.35951	.46379	.65973	1.05124	1.65524	2.22869
		−.2	.21297	.21336	.21401	.21530	.22191	.24472	.25894	.28712	.31054	.34916	.41173	.52929	.76420	1.12651	1.47067
		−.4	.29342	.29354	.29376	.29419	.29640	.30400	.30891	.31813	.32604	.33881	.35966	.39884	.47714	.63702	.71260
I_{ah}	(1)	0	−.30000	−.30060	−.30180	−.30370	−.31290	−.33950	−.35410	−.37880	−.39360	−.42450	−.46500	−.72760	−.84570	−.94100	−.96500
		−.2	−.30000	−.30036	−.30108	−.30222	−.30774	−.32370	−.33246	−.34726	−.35780	−.37470	−.39900	−.43656	−.50752	−.56460	−.57900
		−.4	−.10000	−.10012	−.10036	−.10074	−.10258	−.10790	−.11082	−.11576	−.12060	−.12490	−.13300	−.14552	−.16914	−.18220	−.18300
I_{ba}	0	0	.39023	.39010	.38985	.38944	.38717	.37923	.37404	.36424	.35601	.34204	.31954	.27686	.19172	.05766	−.06980
		−.2	.40339	.40378	.40359	.40320	.40119	.39397	.38918	.38005	.37249	.35911	.33771	.29683	.21469	.08255	−.04344
		−.4	.41735	.41746	.41730	.41697	.41520	.40871	.40432	.39586	.38896	.37617	.35598	.31671	.23793	.10744	−.01707
	0.5	0	.07438	.07435	.07433	.07424	.07387	.07256	.07171	.07009	.06874	.06644	.06273	.05572	.04168	.01960	−.00327
		−.2	.07663	.07661	.07658	.07651	.07618	.07499	.07420	.07270	.07145	.06925	.06572	.05599	.04548	.02370	.00295
		−.4	.07887	.07885	.07882	.07877	.07848	.07741	.07668	.07529	.07416	.07205	.06871	.06226	.04928	.02779	.00728
$I_{b\beta}$	0	(2)	.32297	.32288	.32273	.32241	.32075	.31483	.31090	.30342	.29721	.28625	.26872	.23524	.16806	.06979	−.04335
	.5		.04270	.04270	.04270	.04270	.04240	.04160	.04005	.03930	.03904	.03780	.03396	.03090	.02200	.00845	−.00470
I_{bh}	0	(2)	.06830	.06840	.06860	.06880	.07010	.07370	.07570	.07910	.08240	.08530	.09080	.09940	.11550	.12440	.13180
	.5		.01125	.01126	.01129	.01133	.01154	.01214	.01247	.01302	.01357	.01405	.01496	.01637	.01903	.02117	.02171
I_{ca}	(1)	0	1.50000	1.49808	1.49490	1.48849	1.45520	1.33890	1.25290	1.11940	.99900	.74950	.46500	−.15840	−1.40630	−3.30990	−5.23500
		−.2	1.70000	1.69832	1.69562	1.68992	1.66036	1.55470	1.48464	1.35092	1.24020	1.04430	.73100	.13264	−1.06802	−3.00460	−4.84900
		−.4	1.90000	1.89856	1.89634	1.89140	1.86552	1.77650	1.70618	1.58244	1.48410	1.31410	.99760	.42370	−.72974	−2.64020	−4.46300
$I_{c\beta}$	0	(2)	1.06830	1.06690	1.06470	1.06090	1.03580	.94900	.89150	.78190	.69110	.52840	.27380	−.21640	−1.20010	−2.73550	−4.29530
	.5		.40220	.40100	.39880	.39450	.37240	.29640	.24640	.15510	.07610	−.05150	−.26030	−.65220	−1.43520	−2.64380	−3.79010
I_{ch}	(1)	(2)	1.00000	1.00120	1.00360	1.00740	1.02580	1.07900	1.10820	1.15760	1.20600	1.24900	1.33000	1.45520	1.69140	1.82200	1.93000

[1] Independent of c.

[2] Independent of a.

APPENDIX II

NUMERICAL CALCULATIONS

A number of routine examples have been worked out to illustrate typical results. A "standard" case has been chosen, represented by the following constants:

$$\kappa=0.1,\ c=0.5,\ a=-0.4,\ x_a=0.2,$$

$$r_a^2=0.25,\ x_\beta=\frac{1}{80},\ r_\beta^2=\frac{1}{160}$$

$$\omega_\alpha, \omega_\beta, \omega_h \text{ variable.}$$

We will show the results of a numerical computation of the three possible subcases in succession.

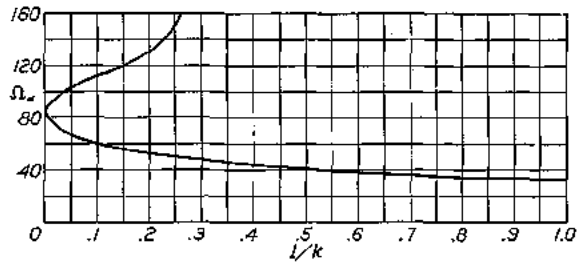

FIGURE 5.—Case 3, Torsion-aileron (α, β): Standard case. Showing Ω_α against $\frac{1}{k}$.

Case 3, Torsion-aileron (α,β): Figure 5 shows the Ω_α against $\frac{1}{k}$ relation and figure 6 the final curve

$$F=\kappa\left(\frac{v}{\omega_\beta r_\beta b}\right)^2 \text{ against } \Omega_\alpha=\left(\frac{\omega_\alpha r_\alpha}{\omega_\beta r_\beta}\right)^2=40\left(\frac{\omega_\alpha}{\omega_\beta}\right)^2$$

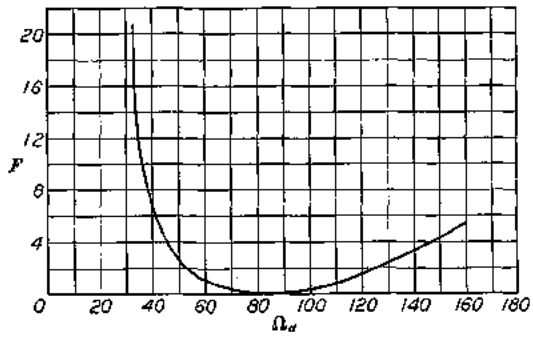

FIGURE 6.—Case 3. Torsion-aileron (α, β): Standard case. Showing flutter factor F against Ω_α.

Case 2, Aileron-flexure (β, h): Figure 7 shows the Ω_β against $\frac{1}{k}$ relation[6] and figure 8 the final curve $\kappa\left(\frac{v}{\omega_h b}\right)^2$ against $\Omega_\beta=\left(\frac{\omega_\beta r_\beta}{\omega_h}\right)^2=\frac{1}{160}\left(\frac{\omega_\beta}{\omega_h}\right)^2$

[6] It is realized that considerable care must be exercised to get these curves reasonably accurate.

The heavy line shows the standard case, while the remaining curves show the effect of a change in the value of x_β to $\frac{1}{40}$ and $\frac{1}{160}$.

Case 1, Flexure-torsion (h, α): Figure 9 shows again

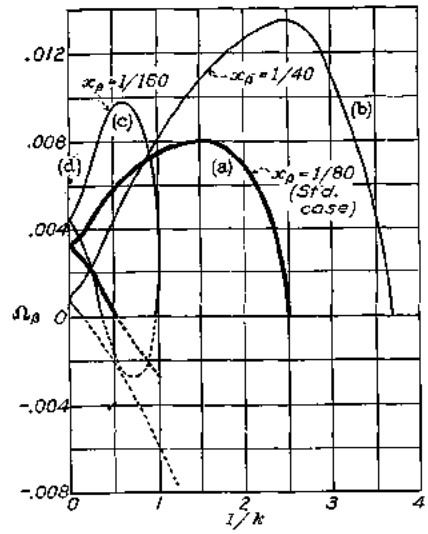

FIGURE 7.—Case 2. Aileron-deflection (β, h): (a) Standard case. (b), (c), (d) Indicate dependency on x_β. Case (d), $x_\beta=-0.004$, reduces to a point.

the Ω_h against $\frac{1}{k}$ relation and figure 10 the final result

$$\kappa\left(\frac{v}{\omega_\alpha r_\alpha b}\right)^2 \text{ against } \Omega_h=\left(\frac{\omega_h}{\omega_\alpha r_\alpha}\right)^2=4\left(\frac{\omega_h}{\omega_\alpha}\right)^2$$

Case 1, which is of importance in the propeller theory, has been treated in more detail. The quantity F shown in the figures is $\sqrt{\kappa}\,\frac{v}{\omega_\alpha r_\alpha b}$.

Figure 11 shows the dependency on $\frac{\omega_h}{\omega_\alpha}=\frac{\omega_1}{\omega_2}$; figure 12 shows the dependency on the location of the axis a; figure 13 shows the dependency on the radius of gyration $r_\alpha=r$; and figure 14 shows the dependency on the location of the center of gravity x, for three different combinations of constants.

EXPERIMENTAL RESULTS

Detailed discussion of the experimental work will not be given in this paper, but shall be reserved for a later report. The experiments given in the following are

restricted to wings of a large aspect ratio, arranged with two or three degrees of freedom in accordance with the

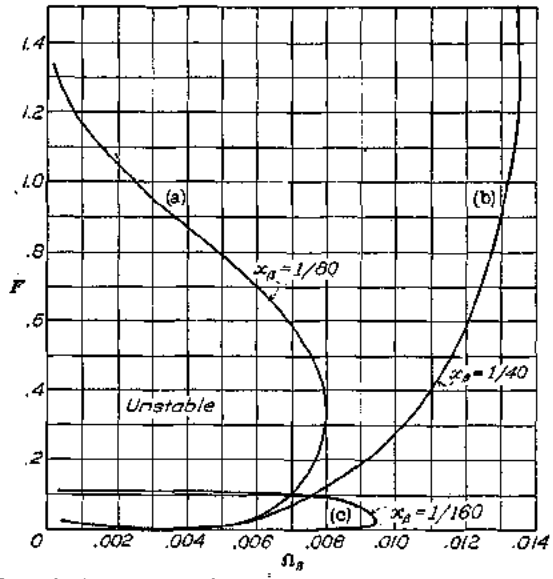

FIGURE 8.—Case 2, Aileron-deflection (β, h): Final curves giving flutter factor F against Ω_β corresponding to cases shown in figure 7.

theoretical cases. The wing is free to move parallel to itself in a vertical direction (h); is equipped with an

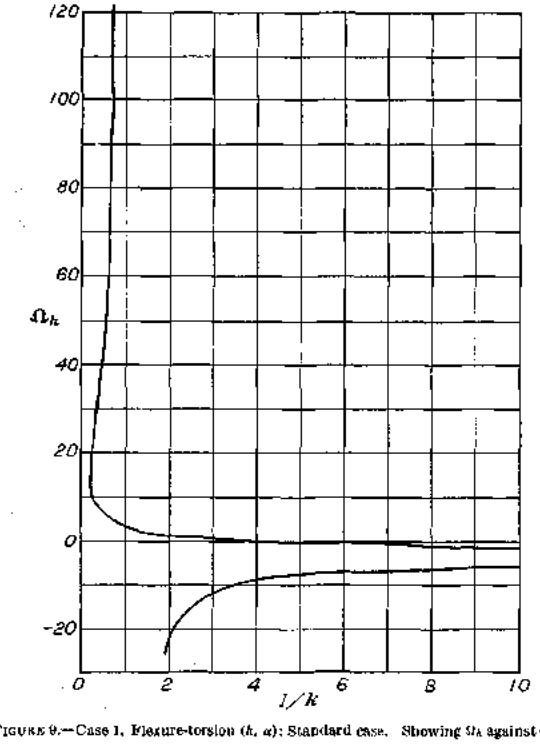

FIGURE 9.—Case 1, Flexure-torsion (h, α): Standard case. Showing Ω_h against $\frac{1}{k}$.

axis in roller bearings at (a) (fig. 2) for torsion, and with an aileron hinged at (c). Variable or exchangeable springs restrain the wing to its equilibrium position.

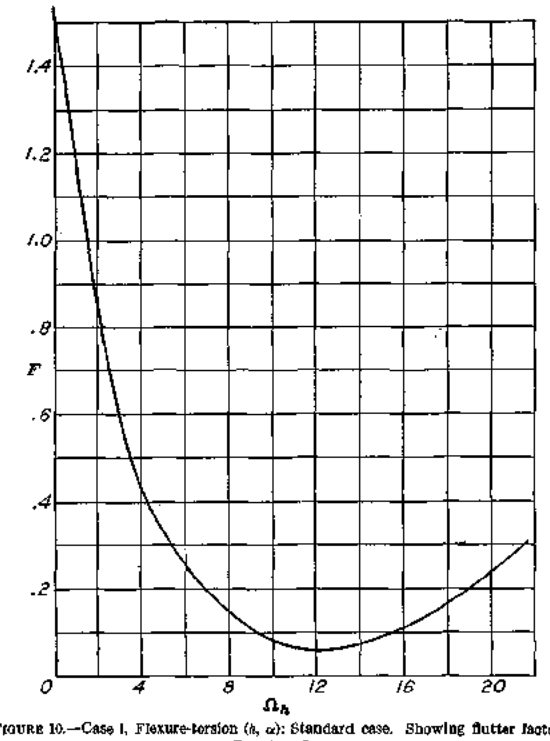

FIGURE 10.—Case 1, Flexure-torsion (h, α): Standard case. Showing flutter factor F against Ω_h.

We shall present results obtained on two wings, both of symmetrical cross section 12 percent thick, and with chord $2b = 12.7$ cm, tested at 0°.

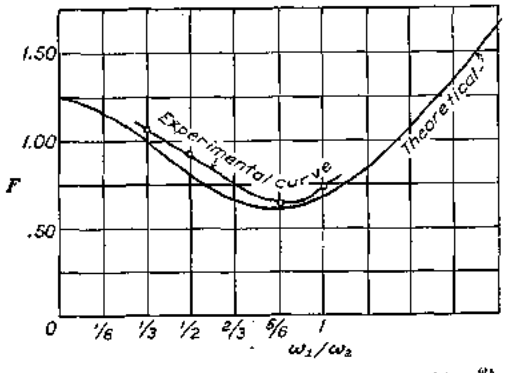

FIGURE 11.—Case 1, Flexure-torsion (h, α): Showing dependency of F on $\frac{\omega_h}{\omega_\alpha}$. The upper curve is experimental. Airfoil with $r = \frac{1}{2}$; $a = -0.4$; $x = 0.2$; $4k = .01$; $\frac{\omega_1}{\omega_2}$ variable.

Wing A, aluminum, with the following constants:

$$\kappa = \frac{1}{416},\ a = -0.4,\ x_\alpha = 0.31,\ 0.173, \text{ and } 0.038,$$

respectively;

$$r_\alpha^2 = 0.33 \text{ and } \omega_\alpha = 7 \times 2\pi$$

Wing B, wood, with flap, and the constants:

$\kappa=\frac{1}{100}$, $c=0.5$, $a=-0.4$, $x_\alpha=0.192$, $r_\alpha^2=0.178$, $x_\beta=0.019$, $r_\beta^2=0.0079$, and ω_α kept constant $=17.6\times 2\pi$

The results for wing A, case 1, are given in figure 15; and those for wing B, cases 2 and 3, are given in figures 16 and 17, respectively. The abscissas are the frequency ratios and the ordinates are the velocities in cm/sec. Compared with the theoretical results calculated for the three test cases, there is an almost perfect

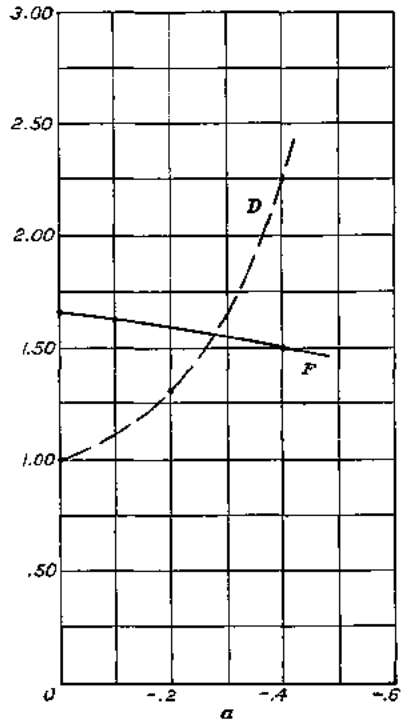

FIGURE 12.—Case 1, Flexure-torsion (h, α): Showing dependency of F on location of axis of rotation a. Airfoil with $r=\frac{1}{2}$; $x=0.2$; $\kappa=\frac{1}{4}$; $\frac{\omega_1}{\omega_2}=\frac{1}{6}$; a variable.

agreement in case 1 (fig. 15). Not only is the minimum velocity found near the same frequency ratio, but the experimental and theoretical values are, furthermore, very nearly alike. Very important is also the fact that the peculiar shape of the response curve in case 2, predicted by the theory, repeats itself experimentally. The theory predicts a *range* of instabilities extending from a small value of the velocity to a definite upper limit. It was very gratifying to observe that the upper branch of the curve not only existed but that it was remarkably definite. A small increase in speed near this upper limit would suffice to change the condition from violent flutter to complete rest, no range of transition being observed. The experimental cases 2 and 3 are compared with theoretical results given by the dotted lines in both figures (figs. 16 and 17).

The conclusion from the experiments is briefly that the general shapes of the predicted response curves re-

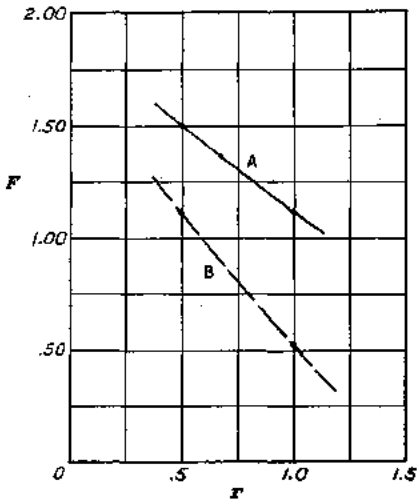

FIGURE 13.—Case 1, Flexure-torsion (h, α): Showing dependency of F on the radius of gyration $r_\alpha=r$.

A, airfoil with $a=-0.4$; $\kappa=\frac{1}{4}$; $x=0.2$; $\frac{\omega_1}{\omega_2}=\frac{1}{6}$; r variable.

B, airfoil with $a=-0.4$; $\kappa=\frac{1}{4}$; $x=0.2$; $\frac{\omega_1}{\omega_2}=1.60$; r variable.

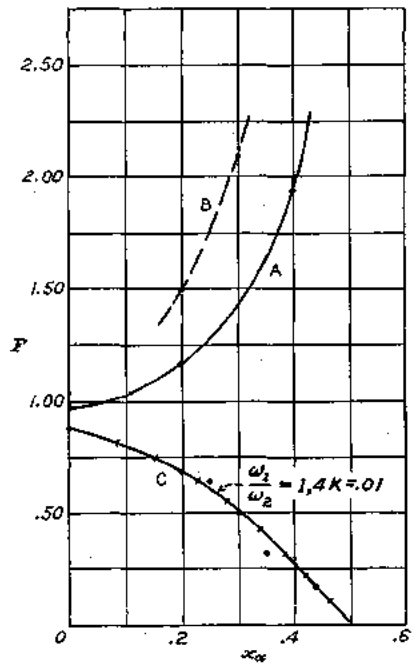

FIGURE 14.—Case 1, Flexure-torsion (h, α): Showing dependency of F on x_α, the location of the center of gravity.

A, airfoil with $r=\frac{1}{2}$; $a=-0.4$; $\kappa=\frac{1}{400}$; $\frac{\omega_1}{\omega_2}=\frac{1}{6}$; x variable.

B, airfoil with $r=\frac{1}{2}$; $a=-0.4$; $\kappa=\frac{1}{4}$; $\frac{\omega_1}{\omega_2}=\frac{1}{6}$; x variable.

C, airfoil with $r=\frac{1}{2}$; $a=-0.4$; $\kappa=\frac{1}{100}$; $\frac{\omega_1}{\omega_2}=1$; x variable.

peat themselves satisfactorily. Next, that the influence of the internal friction[7] obviously is quite appreci-

[7] This matter is the subject of a paper now in preparation.

able in case 3. This could have been expected since the predicted velocities and thus also the air forces on the aileron are very low, and no steps were taken to eliminate the friction in the hinge. The outline of the stable region is rather vague, and the wing is subject

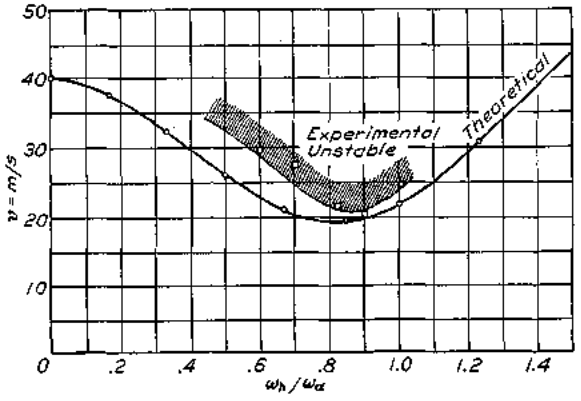

FIGURE 15.—Case 1. Wing A. Theoretical and experimental curves giving flutter velocity v against frequency ratio $\frac{\omega_h}{\omega_\alpha}$. Deflection-torsion.

to temporary vibrations at much lower speeds than that at which the violent flutter starts. The above experiments are seen to refer to cases of exaggerated unbalance, and therefore of low flutter speeds. It is evident that the internal friction is less important at larger velocities. The friction does in all cases *increase* the speed at which flutter starts.

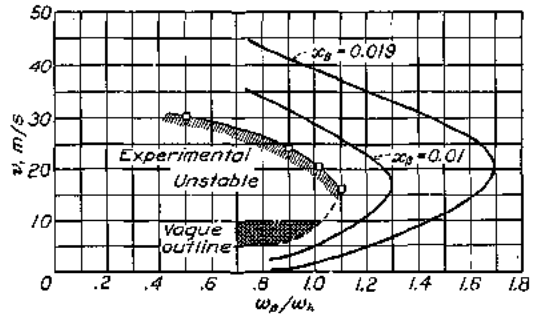

FIGURE 16.—Case 2. Wing B. Theoretical and experimental curves giving flutter velocity v against frequency ratio $\frac{\omega_\beta}{\omega_h}$. Aileron-deflection ($\beta$, h).

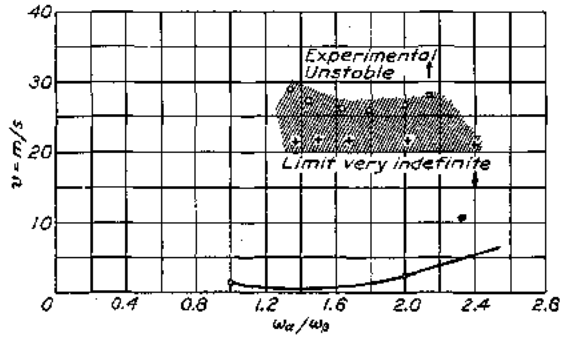

FIGURE 17.—Case 3. Theoretical curve giving flutter velocity against the frequency ratio $\frac{\omega_\alpha}{\omega_\beta}$. The experimental unstable area is indefinite due to the importance of internal friction at very small velocities. Torsion-aileron (α, β)

APPENDIX III

EVALUATION OF φ_β

$$\int_c^1 \log\frac{(x-x_1)^2+(y-y_1)^2}{(x-x_1)^2+(y+y_1)^2}\,dx_1$$

$$=\left[x_1\log\frac{(x-x_1)^2+(y-y_1)^2}{(x-x_1)^2+(y+y_1)^2}\right]_c^1-2y\int_c^1\frac{x_1dx_1}{y_1(x-x_1)}$$

$$=-2c\log\frac{1-xc-y\sqrt{1-c^2}}{(x-c)}-2y\int_c^1\frac{x_1dx_1}{\sqrt{1-x_1^2}(x-x_1)}$$

$$+\int_c^1\frac{x_1dx_1}{\sqrt{1-x_1^2}(x-x_1)}=\int\frac{dx_1}{\sqrt{1-x_1^2}}$$

$$+x\int\frac{dx_1}{(x_1-x)\sqrt{1-x_1^2}}\ [\text{Putting } x_1=\cos\theta]$$

$$=-\theta-\frac{x}{\sqrt{1-x^2}}\log\frac{1-x\cos\theta+\sqrt{1-x^2}\sin\theta}{\cos\theta-x}\Bigg|_{\cos\theta=c}^{\cos\theta=1}$$

$$=\cos^{-1}c+\frac{x}{\sqrt{1-x^2}}\log\frac{1-cx+\sqrt{1-x^2}\sqrt{1-c^2}}{c-x}$$

$$=\cos^{-1}c+\frac{x}{\sqrt{1-x^2}}\log\frac{c-x}{1-cx-\sqrt{1-x^2}\sqrt{1-c^2}}$$

$$\varphi\frac{2\pi}{\epsilon}=-2c\log(1-cx-\sqrt{1-x^2}\sqrt{1-c^2})+2c\log(x-c)$$

$$-2\sqrt{1-x^2}\cos^{-1}c-2x\log(c-x)$$

$$+2x\log(1-cx-\sqrt{1-x^2}\sqrt{1-c^2})$$

$$=2(x-c)\log\left(\frac{1-cx-\sqrt{1-x^2}\sqrt{1-c^2}}{x-c}\right)$$

$$-2\sqrt{1-x^2}\cos^{-1}c$$

EVALUATION OF φ_β

$$\varphi_x=\int_c^1\{\log[(x-x_1)^2+(y-y_1)^2]$$

$$-\log[(x-x_1)^2+(y+y_1)^2]\}(x_1-c)dx_1$$

$$=\frac{(x_1-c)^2}{2}\{\log[(x-x_1)^2+(y-y_1)^2]$$

$$-\log[(x-x_1)^2+(y+y_1)^2]\}]_c^1$$

$$+y\int_c^1(x_1-c)^2\frac{dx_1}{y_1(x-x_1)}$$

$$\int_c^1\frac{(x_1-c)^2dx_1}{y_1(x-x_1)}=\int_c^1\frac{(x_1-c)^2dx_1}{1-x_1^2(x-x_1)}=-\int\frac{(\cos\theta-c)^2d\theta}{x-\cos\theta}$$

$$x_1=\cos\theta,\ y_1=\sin\theta,\ dx_1=-\sin\theta d\theta$$

$$\int_c^1\frac{(x_1-c)^2dx_1}{y_1(x-x_1)}=\sin\theta+(x-2c)\theta-(x-c)^2\int_c^1\frac{d\theta}{x-\cos\theta}$$

$$\int_c^1\frac{d\theta}{x-\cos\theta}=\int_c^1\frac{d(\pi+\theta)}{x+\cos(\pi+\theta)}$$

$$=\frac{1}{\sqrt{1-x^2}}\log\frac{1-x\cos\theta-\sqrt{1-x^2}\sin\theta}{x-\cos\theta}\Bigg|_{\cos\theta=c}^{\cos\theta=1}$$

$$=\frac{1}{\sqrt{1-x^2}}\left[\log\frac{1-x}{x-1}-\log\frac{1-cx-\sqrt{1-x^2}\sqrt{1-c^2}}{x-c}\right]$$

$$=-\frac{1}{\sqrt{1-x^2}}\log(1-cx-\sqrt{1-x^2}\sqrt{1-c^2})$$

$$+\frac{1}{\sqrt{1-x^2}}\log(x-c)$$

$$\frac{2\pi}{\epsilon}\varphi_x=\sqrt{1-x^2}\left[-\sqrt{1-c^2}-(x-2c)\cos^{-1}c\right.$$

$$+\frac{(x-c)^2}{\sqrt{1-x^2}}\log(1-cx-\sqrt{1-x^2}\sqrt{1-c^2})$$

$$\left.-\frac{(x-c)^2}{\sqrt{1-x^2}}\log(x-c)\right]$$

$$\frac{2\pi}{\epsilon}\varphi_x=-\sqrt{1-c^2}\sqrt{1-x^2}-\cos^{-1}c(x-2c)\sqrt{1-x^2}$$

$$+(x-c)^2\log(1-cx-\sqrt{1-x^2}\sqrt{1-c^2})$$

$$-(x-c)^2\log(x-c)$$

EVALUATION OF T_3

$$\int_c^1\frac{2\pi}{\epsilon}\varphi_x(x-c)dx=-\sqrt{1-c^2}\int(x-c)\sqrt{1-x^2}\,dx$$

$$-\cos^{-1}c\int(x-c)(x-2c)\sqrt{1-x^2}\,dx$$

$$+\frac{(x-c)^4}{4}\log(1-cx-\sqrt{1-x^2}\sqrt{1-c^2})$$

$$-\frac{1}{4}\int(x-c)^3dx-\sqrt{\frac{1-c^2}{4}}\frac{(x-c)^3}{\sqrt{1-x^2}}dx$$

$$-\int(x-c)^3\log(x-c)dx;\ x=\cos\theta,\ dx=-\sin\theta d\theta$$

$$\frac{2\pi}{\epsilon}\int_c^1\varphi_x(x-c)dx=\sqrt{1-c^2}\int(\cos\theta-c)\sin^2\theta d\theta$$

$$+\cos^{-1}c\int(\cos\theta-c)(\cos\ -2c)\sin^2\theta d\theta$$

$$+\frac{(x-c)^4}{4}\log(1-cx-\sqrt{1-x^2}\sqrt{1-c^2})$$

$$-\frac{1}{4}\int(x-c)^3dx+\frac{\sqrt{1-c^2}}{4}\int(\cos\theta-c)^3d\theta$$

$$-\frac{(x-c)^4}{4}\log(x-c)+\frac{1}{4}\int(x-c)^3dx$$

$$\frac{2\pi}{\epsilon}\int_c^1\varphi_x(x-c)dx=-\cos^{-1}c\int\cos^4\theta d\theta$$

$$+\left(3c\cos^{-1}c-\sqrt{1-c^2}+\frac{\sqrt{1-c^2}}{4}\right)\int\cos^3\theta d\theta$$

$$+\left(\cos^{-1}c-2c^2\cos^{-1}c+c\sqrt{1-c^2}-\frac{3}{4}c\sqrt{1-c^2}\right)\int\cos^2\theta d\theta$$

$$+\left(-3c\cos^{-1}c+\sqrt{1-c^2}+\frac{3c^2\sqrt{1-c^2}}{4}\right)\int\cos\theta d\theta$$

$$+\left(2c^2\cos^{-1}c-c\sqrt{1-c^2}-\frac{c^3\sqrt{1-c^2}}{4}\right)\int d\theta$$

$$=-\cos^{-1}c\left[\frac{\cos^3\theta\sin\theta}{4}+\frac{3}{4}\left(\frac{\theta}{2}+\frac{\sin\theta\cos\theta}{2}\right)\right]$$
$$+\frac{1}{3}\left(3c\cos^{-1}c-\frac{3}{4}\sqrt{1-c^2}\right)\sin\theta(\cos^2\theta+2)$$
$$+\left(\cos^{-1}c-2c^2\cos^{-1}c+\frac{c\sqrt{1-c^2}}{4}\right)\left(\frac{\theta}{2}+\frac{\sin\theta\cos\theta}{2}\right)$$
$$+\left(-3c\cos^{-1}c+\sqrt{1-c^2}+\frac{3c^2\sqrt{1-c^2}}{4}\right)\sin\theta$$
$$+\left(2c^2\cos^{-1}c-c\sqrt{1-c^2}-\frac{c^3\sqrt{1-c^2}}{4}\right)\theta$$
$$=\cos^{-1}c\left(\frac{3}{8}\pi+\frac{\pi}{2}-3\pi\right)=-\frac{9}{8}\pi\cos^{-1}c$$

$$\frac{2\pi}{\epsilon}\int_c^1\varphi_r(x-c)\,dx$$
$$=\cos^{-1}c\left[\frac{c^3\sqrt{1-c^2}}{4}+\frac{3\cos^{-1}c}{8}+\frac{3c\sqrt{1-c^2}}{8}\right]$$
$$-\left[c\cos^{-1}c-\frac{\sqrt{1-c^2}}{4}\right](c^2\sqrt{1-c^2}+2\sqrt{1-c^2})$$
$$-\left(\cos^{-1}c-2c^2\cos^{-1}c+\frac{c\sqrt{1-c^2}}{4}\right)\left(\frac{\cos^{-1}c+c\sqrt{1-c^2}}{2}\right)$$
$$-\left(-3c\cos^{-1}c+\sqrt{1-c^2}+\frac{3c^2\sqrt{1-c^2}}{4}\right)\sqrt{1-c^2}$$
$$-\left(2c^2\cos^{-1}c-c\sqrt{1-c^2}-\frac{c^3\sqrt{1-c^2}}{4}\right)\cos^{-1}c$$
$$=\cos^{-1}c\left[\frac{3}{8}-\frac{1}{2}+c^2-2c^2\right]$$
$$+\sqrt{1-c^2}\cos^{-1}c\left[\frac{c^3}{4}+\frac{3c}{8}-c^3-2c-\frac{c}{2}+c^3+3c+c\right.$$
$$\left.+\frac{c^3}{4}-\frac{c}{8}\right]+\frac{c^2(1-c^2)}{4}+\frac{(1-c^2)}{2}-\frac{c^2(1-c^2)}{8}$$
$$-(1-c^2)-\frac{3c^2(1-c^2)}{4}=-\left(\frac{1}{8}+c^2\right)(\cos^{-1}c)^2$$
$$+\frac{c\sqrt{1-c^2}\cos^{-1}c}{4}(7+2c^2)-\frac{(1-c^2)}{8}(5c^2+4)\quad(=T_3)$$

EVALUATION OF T_5

$$\int_c^1\left\{2(x-c)\log\frac{1-cx-\sqrt{1-x^2}\sqrt{1-c^2}}{x-c}\right.$$
$$\left.-2\sqrt{1-x^2}\cos^{-1}c\right\}dx=T_5=-2\int(x-c)\log(x-c)dx$$
$$+2\int(x-c)\log(1-cx-\sqrt{1-x^2}\sqrt{1-c^2})dx$$
$$-2\cos^{-1}c\int\sqrt{1-x^2}\,dx=-\frac{2(x-c)^2}{2}\log(x-c)$$
$$+\int(x-c)dx+2\cos^{-1}c\int\sin^2\theta d\theta$$
$$+(x-c)^2\log(1-cx-\sqrt{1-x^2}\sqrt{1-c^2})$$
$$-\int(x-c)^2\frac{-c+x\frac{\sqrt{1-c^2}}{\sqrt{1-x^2}}}{1-cx-\sqrt{1-x^2}\sqrt{1-c^2}}dx$$

Now

$$\int(x-c)^2\frac{-c+x\frac{\sqrt{1-c^2}}{\sqrt{1-x^2}}}{1-cx-\sqrt{1-x^2}\sqrt{1-c^2}}\,dx$$
$$=\int\left\{-c+c^2x-c\sqrt{1-c^2}\sqrt{1-x^2}+x\frac{\sqrt{1-c^2}}{\sqrt{1-x^2}}-cx^2\frac{\sqrt{1-c^2}}{\sqrt{1-x^2}}\right.$$
$$\left.+(1-c^2)x\right\}dx=\int\frac{(x-c)\sqrt{1-x^2}+(x-c)\sqrt{1-c^2}}{\sqrt{1-x^2}}\,dx$$
$$=\int(x-c)dx+\sqrt{1-c^2}\int\frac{(x-c)}{\sqrt{1-x^2}}\,dx$$

$$T_5=-(x-c)^2\log(x-c)+2\cos^{-1}c\int\sin^2\theta d\theta$$
$$+(x-c)^2\log(1-cx-\sqrt{1-x^2}\sqrt{1-c^2})$$
$$+\sqrt{1-c^2}\int(\cos\theta-c)d\theta$$
$$=\frac{2\cos^{-1}c}{2}(\theta-\sin\theta\cos\theta)+\sqrt{1-c^2}\sin\theta$$
$$-c\sqrt{1-c^2}\,\theta\Big|_{\cos\theta=c}^{\cos\theta=1}$$
$$=-(1-c^2)-(\cos^{-1}c)^2+2c\sqrt{1-c^2}\cos^{-1}c$$

1. Report No.	2. Government Accession No.	3. Recipient's Catalog No.
NASA RP-1050		

4. Title and Subtitle	5. Report Date
CLASSICAL AERODYNAMIC THEORY*	December 1979
	6. Performing Organization Code

7. Author(s)	8. Performing Organization Report No.
Compiled by R. T. Jones	A-7556
	10. Work Unit No.
9. Performing Organization Name and Address	010-01-01
Ames Research Center, NASA Moffett Field, Calif. 94035	11. Contract or Grant No.
	13. Type of Report and Period Covered
12. Sponsoring Agency Name and Address	Reference Publication
National Aeronautics and Space Administration Washington, D.C. 20546	14. Sponsoring Agency Code

15. Supplementary Notes

*A Collection of Reports and Notes of Historic and Enduring Value Issued by the U.S. National Advisory Committee for Aeronautics

16. Abstract

A collection of original papers by Prandtl, Munk, Von Karman, and others which laid the foundations for modern theoretical aerodynamics. The collection is limited primarily to theories of incompressible potential flow and to papers which appeared as publications of the U.S. National Advisory Committee for Aeronautics in the 1920's and early 1930's.

17. Key Words (Suggested by Author(s))	18. Distribution Statement
Fundamental aerodynamic theory Prandtl wing theory Incompressible flow theory	Unlimited STAR Category – 02

19. Security Classif. (of this report)	20. Security Classif. (of this page)	21. No. of Pages	22. Price*
Unclassified	Unclassified	318	$11.75

*For sale by the National Technical Information Service, Springfield, Virginia 22161

NASA-Langley, 1979

National Aeronautics and Space Administration

Washington, D.C.
20546

Official Business
Penalty for Private Use, $300

SPECIAL FOURTH CLASS MAIL
BOOK

Postage and Fees Paid
National Aeronautics and
Space Administration
NASA-451

NASA

POSTMASTER: If Undeliverable (Section 158 Postal Manual) Do Not Return